Design and Synthesis of Helically Chiral BODIPY Dyes through Point-to-Helical Chirality Transfer

by

Aminah Ahmed Almarshad

A thesis submitted in partial fulfilment of the requirements for the degree of

Doctor of Philosophy

April 2024

Declaration

I declare that the work presented in this dissertation, titled "Design and Synthesis of Helically Chiral BODIPY Dyes through Point-to-Helical Chirality Transfer," has been carried out by me in the School of Natural and Environmental Sciences, Newcastle University. The information derived from the literature has been duly acknowledged in the text, and a comprehensive list of references has been provided. None of the content of this dissertation has been previously submitted for another degree or professional qualification. Where work is collaborative, this is made clear in the text. Additionally, any assistance received in the course of my project has been fully acknowledged and disclosed within the thesis.

Aminah Ahmed Almarshad

05/04/2024

Acknowledgements

First and foremost, I would like to thank Allah for giving me the strength and perseverance to achieve my goals and ultimately making my success possible (Alhamdulillah).

I would like to express my deepest gratitude to my supervisor, Dr Michael Hall, for his invaluable guidance, exceptional patience, encouragement, and unwavering support throughout my PhD study over the past four years. I have learned a great deal under his supervision and am truly appreciative of his expertise, mentorship, and insightful feedback, all of which have significantly contributed to the completion of this thesis and to shaping me into a confident and capable researcher. I feel incredibly fortunate to have had the opportunity to work under his supervision. Additionally, I would like to extend my thanks to him for his proofreading of this thesis. Thank you, Dr Hall, for everything.

I would also like to thank my second supervisor, Dr Julian Knight, for his willingness to provide advice and support throughout my PhD research.

I would like to thank Dr Paul Waddell for his assistance in X-ray crystallography and his patience in answering my questions.

Furthermore, I would like to thank all past and present members of the MJH research group. Particularly, I would like to thank Dr Damon (Xin) Wen for his encouragement, especially when he says 'Masha Allah Aminah, proper!', and for being like a brother to me. Special thanks to Dr Felicity Frank, with whom I had the pleasure of working on a similar project, supporting each other, and attending conferences together. Lastly, I would like to thank Xiniy Zhang and Dr Lina Mardiana for their support and friendship. I would like to extend my thanks to everyone in the Johnston lab for creating a wonderful place to work.

I would also like to thank all my friends in Bedson building, especially Dr Afkar Alshammari, who has provided assistance since I arrived in Newcastle and helped me achieve a work-life balance outside of the laboratory. I am grateful to Sara Waly (preparative TLC friend), Linah Alqahtani, Dr Albatul Almushayti, and Fatimah Alsalem for their understanding and friendship. I consider them friends for life.

I extend my thank to those who contributed to this thesis. Thanks to Dr Patrycja Brook and Dr Dominic Black for conducting CPL spectroscopy, and to both Prof Wouter Herrebout and Dr Jonathan Bogaerts for performing ECD spectroscopy. I also want to express my appreciation to Dr Corrine Wills and Dr Casey Dixon for their assistance and guidance with NMR spectroscopy, and to Aaron Campbell for his support with HPLC.

I would like to extend my sincerest thanks and appreciation to my sponsor Imam Abdulrahman bin Faisal University for giving me the opportunity to complete my postgraduate studies and I also would like to thank the Saudi Arabian Cultural Bureau in London for their financial support.

I would like to extend my thanks to my close friends, Zainab Alghamdi, Fatimah Alomari, and Dr Aishah Alamri, for their support and encouragement. Throughout both the good times and the challenging moments, they have stood by me, demonstrating the true meaning of friendship.

Finally, I would like to thank my parents, Ahmed Almarshad and Montaha Algharbi, who have always been an important source of wisdom, comfort, and support. I would like to express my gratitude to my siblings, Nourah, Fahad, Aalyah, and Wateen, for their endless support, encouragement, and love. I would also like to thank my beloved grandparents, Aminah Alsaad and Aliaa Almarshad for their boundless love and words of encouragement.

Thank you all again and I hope I have made you all proud.

Abstract

The boron dipyrromethenes (BODIPYs) are a class of fluorescent organic dyes that have found use in numerous applications, due to their excellent photophysical properties including high fluorescence quantum yields. Chiral BODIPYs are of interest as they have the potential to emit circularly polarized light upon irradiation, however the synthesis of such systems is challenging.

In this thesis, we have examined several new methodologies to access chiral BODIPYs. In particular, we have focused on the development of a point-to-helical chirality transfer strategy in which an enantiopure amino alcohol substituent can be used as a chiral auxiliary to control the formation of helical chirality in the target BODIPY. We have applied this point-to-helical chirality approach to the synthesis of a wide range of novel helical chiral BODIPY architectures, including monomeric helically chiral *N*,*N*,*O*,*C*-BODIPYs containing a 7-membered ring, monomeric helically chiral *N*,*N*,*O*,*C*-BODIPYs containing a 6-membered ring, as well extending this approach to dimeric and trimeric helically chiral *N*,*N*,*O*,*C*-BODIPY systems (Scheme **1**).

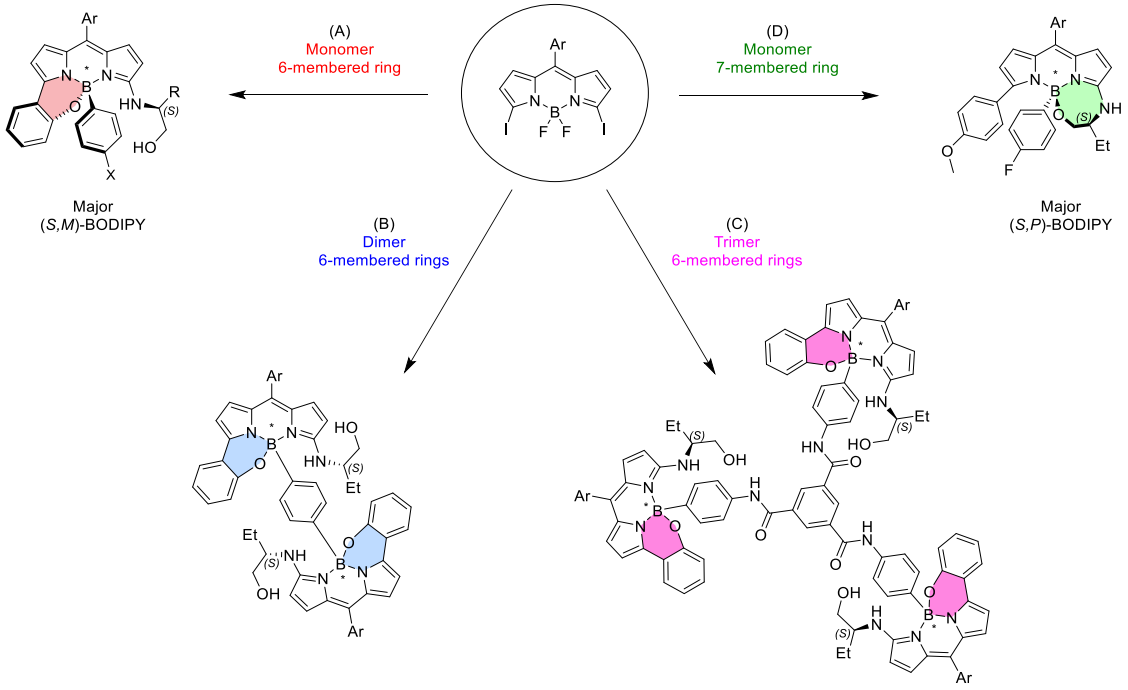

Scheme 1: The synthesis of helically chiral BODIPYs via point-to-helical chirality transfer (Ar = *p*-($MeCO_2$)-C_6H_4-).

Overall, we have shown that our newly developed point-to-helical chirality transfer approach can be applied broadly in the design and synthesis of a wide range of helical chiral BODIPYs, which have potential for further development towards chiroptical materials in the future.

Abbreviation

BINOL	1,1'-bi-2-naphthol
br	broad
B_{CPL}	circularly polarised luminescence brightness
BODIPY	4,4-difluoro-4-bora-3a,4a-diaza-*s*-indacenes
calcd	calculated
CD	circular dichroism
COSY	homonuclear correlation spectroscopy
CPL	circularly polarised luminescence
CPL-SOM	CPL active small organic molecule
d	doublet
DCM	dichloromethane
dd	double doublet
ddd	double double doublet
DDQ	2,3-dichloro-5,6-dicyano-1,4-benoquinone
de	diastereomeric excess
DIPEA	*N*,*N*-diisopropylethylamine
DMF	dimethylformamide
DMSO	dimethyl sulfoxide
ECD	electronic circular dichroism
S_EAr	electrophilic aromatic substitution
ee	enantiomeric excess
eq.	equivalent
G3	third generation
g_{lum}	luminescence dissymmetry factor
HMBC	heteronuclear multiple bond correlation
HPLC	high performance liquid chromatography
HRMS	high resolution mass spectrometry
HSQC	heteronuclear single quantum coherence

IR	Infrared
MBH	Morita–Baylis–Hillman reaction
MeCN	acetonitrile
MeOH	methanol
M	Molar
min	minute
Mp	melting point
NBS	*N*-bromosuccinimide
nm	nanometre
NMR	nuclear magnetic resonance
S_NAr	nucleophilic aromatic substitution
p-chloranil	tetrachloro-1,4-benzoquinone
Ph	phenyl
Ppm	parts per million
Q	Quartet
quant.	Quantitative
R_f	retention factor
RT	room temperature
S	Singlet
SCXRD	single crystal x-ray diffraction
SD	standard deviation
$[\alpha]$	specific rotation
T	triplet
td	triple doublet
TFA	trifluoroacetic acid
THF	tetrahydrofuran
TLC	thin layer chromatography
TMEDA	tetramethylethylenediamine
XPhos	2-dicyclohexylphosphino-2',4',6'-triisopropylbiphenyl
UV/Vis	ultraviolet / visible spectrophotometry

Table of Contents

Chapter 1. Introduction **1**
1.1 Introduction to Luminescence of Organic Molecules 1
1.1.1 Luminescence 1
1.1.2 Fluorescence and Phosphorescence 2
1.1.3 Key Photophysical Properties of an Organic Fluorophore 3
1.1.4 Molar Extinction Coefficient (ε) 3
1.1.5 Stokes Shift 3
1.1.6 Fluorescence Quantum Yield (ϕ_F) 3
1.1.7 Chiroptical Properties of an Organic Fluorophore 4
1.1.8 Circularly Polarised Light 4
1.1.9 Electronic Circular Dichroism (ECD) 5
1.1.10 Circularly Polarised Luminescence (CPL) 6
1.1.11 CPL Quantum Efficiency and CPL Brightness (B_{CPL}) 7
1.1.12 Correlation Between g_{abs} and g_{lum} 7
1.2 Examples of CPL-Active Compounds Including CPL-SOMs 8
1.2.1 Chiral Lanthanide Complexes Capable of CPL 9
1.2.2 Chiral Small Organic Molecules Capable of CPL (CPL-SOMs) 9
1.3 General Introduction of BODIPY Dyes 10
1.3.1 General Approaches to the Synthesis of BODIPYs 12
1.3.2 Modifications on the BODIPY Core 16
1.4 Chirality in BODIPYs 24
1.4.1 Axially Chiral Bis and Tris BODIPYs 25
1.4.2 Axially Chiral SpiroBODIPYs 26
1.4.3 Helical Chirality Mono BODIPYs 27
1.4.4 Helical Chirality Bis BODIPYs 28
1.4.5 Labile Helicity in BODIPYs 29
1.4.6 Propeller Chirality in BODIPYs 29
1.4.7 Chirality at the Boron Centre 30
1.4.8 Conclusions 32
1.5 Chiral Auxiliaries 32
1.5.1 Chirality Transfer in Organic Synthesis 33
1.6 Project Aims 34
Chapter 2. Synthesis of 3,5-Dibromo and 3,5-Diiodo BODIPYs **36**
2.1 Introduction 36

2.2 Regioselective Bromination of Dipyrromethanes and BODIPYs via Electrophilic Aromatic Substitution (S_EAr) 36
2.3 Results and Discussion 38
2.3.1 Synthesis of Common Starting Material 3,5-Dibromo BODIPY (**1.67**) 38
2.3.2 Synthesis of Dipyrromethane (**2.2**) via Acid Catalysed Condensation 38
2.3.3 Synthesis of 3,5-Dibromo BODIPY (**1.67**) 39
2.3.4 Electrophilic Aromatic Substitution (S_EAr) Bromination and Oxidation of Dipyrromethane (**2.2**) 43
2.3.5 Boron Chelation of α,α-Dibromo dipyromethene (**2.14**) 44
2.3.6 Synthesis of 3,5-Diiodo BODIPY via Double S_NAr Reaction (Aromatic Finkelstein reaction) 45
2.4 Nucleophilic Aromatic Substitution (S_NAr) Reaction of Chiral Nucleophiles with 3,5-dihalogenated BODIPYs 47
2.4.1 Synthesis of Chiral 3-Bromo-substituted BODIPY (**2.18**) Followed by Synthesis of Chiral Bis (3-bromo-substituted BODIPY) (**2.3**) 53
2.4.2 Synthesis of Chiral 3-Bromo-substituted BODIPY (**2.18**) via S_NAr Reaction 53
2.4.3 Synthesis of Chiral Bis (3-bromo-substituted BODIPY) (**2.3**) from Chiral 3-Bromo-substituted BODIPY (**2.18**) 55
2.4.4 Synthesis of Chiral Bis (3-iodo-substituted BODIPY) (**2.4**) Followed by Chiral 3-Iodo-substituted BODIPY (**2.19**) 57
2.4.5 Synthesis of Chiral 3-Iodo-substituted BODIPY (**2.19**) via S_NAr Reaction 57
2.4.6 Synthesis of Chiral Bis (3-iodo substituted BODIPY) (**2.4**) from Chiral 3-Iodo-substituted BODIPY (**2.19**) 59
2.5 Synthesis of Di-substituted BODIPY and Cyclic Chiral BODIPY (2.17) 60
2.6 Photophysical Properties of Chiral 3-Halo-substituted BODIPYs and Chiral Bis (3-halo-substituted BODIPYs) 61
2.7 Suzuki Miyaura Cross-Coupling of Chiral 3-Bromo-substituted BODIPY (2.18) 62
2.8 S_NAr Reaction Between 3,5-Dibromo BODIPY (1.67) and Achiral Diamine Linker 65
2.9 Conclusion 66
Chapter 3. Synthesis of Helically Chiral mono BODIPYs via Point-to-Helical Chirality Transfer 68
3.1 Introduction 68
3.2 Synthetic Strategy Towards Helically Chiral mono BODIPYs via Point-to-Helical Chirality Transfer 68
3.3 Synthetic Routes towards Chiral Auxiliary Containing BODIPYs 68
3.3.1 Introduction of Enantiopure Amino Alcohols via S_NAr Reactions 68
3.4 De-chelation Reaction to Remove BF_2 75
3.4.1 De-chelation Reaction to Remove BF_2 by Using Lewis Acids or TFA 75
3.4.2 De-chelation Reaction to Remove BF_2 Centre of 3,5-Dibromo BODIPY (**1.67**) 75
3.4.3 De-chelation Reaction to Remove BF_2 of mono substituted BODIPYs 76

3.5 Suzuki Miyaura Cross-Coupling reaction 79
3.5.1 Suzuki Miyaura Cross-Coupling Reaction with (2-Hydroxyphenyl)boronic acid 79
3.5.2 Chelation Reaction by Using (4-Methoxyphenyl)boronic acid 82
3.6 Suzuki Miyaura Cross-Coupling Reaction and De-chelation Reaction 84
3.6.1 Suzuki Miyaura Cross-Coupling Reaction 84
3.6.2 Suzuki Miyaura Cross-Coupling Reaction Scope 85
3.6.3 De-chelation of (*S*)-3-(1-Hydroxybutan-2-yl)amino)-5-(2-hydroxyphenyl) BODIPY (**3.5**) 91
3.6.4 Purification of (*S*)-α-(1-Hydroxybutan-2-yl)amino)-α'-(2-hydroxyphenyl) dipyrromethene (**3.6**) 92
3.6.5 Reaction Scope of the De-chelation Reaction of 3-Amino alcohol substituted 5-(2-hydroxyphenyl) BODIPYs 95
3.7 Synthesis of Helically Chiral (*S,M/P*)-*N,N,O,C*-3-((1-hydroxybutan-2-yl)amino) BODIPYs 96
3.7.1 Boron Chelation Reactions 96
3.7.2 Absolute Stereochemistry of Helically Chiral (*S,M/P*)-*N,N,O,C*-3-((1-hydroxybutan-2-yl)amino) BODIPYs 98
3.7.3 Optimisation of Diastereoselectivity of Helically Chiral (*S,M*)-*N,N,O,C*-3-((1-hydroxybutan-2-yl)amino) BODIPY (**3.7a**) and (*S,P*)-*N,N,O,C*-3-((1-hydroxybutan-2-yl)amino) BODIPY (**3.7b**) 99
3.7.4 Control Experiment the Epimerisation at Boron Centre in (*S,M*)-*N,N,O,C*-3-((1-hydroxybutan-2-yl)amino) BODIPY (**3.7a**) 101
3.8. Synthesis of Helically Chiral (*R,M/P*)-*N,N,O,C*-3-((1-hydroxybutan-2-yl)amino) BODIPYs 102
3.8.1 Crystal Structures of (*R,P*)-*N,N,O,C*-3-((1-hydroxybutan-2-yl)amino) BODIPY (**3.40a**) and (*R,M*)-*N,N,O,C*-3-((1-hydroxybutan-2-yl)amino) BODIPY (**3.40b**) 103
3.9 Chiral Integrity of Amino Alcohol Moieties in Helically Chiral BODIPYs 106
3.10 Photophysical Properties of Helically Chiral *N,N,O,C*-3-((1-Hydroxybutan-2-yl)amino) BODIPYs (3.7a), (3.7b),(3.40a), and (3.40b) 107
3.10.1 Chiroptical Properties of Helically Chiral BODIPYs 108
3.11 Expansion of the Helically Chiral *N,N,O,C*-3-((1-hydroxybutan-2-yl)amino) BODIPY Series 112
3.11.1 Testing (4-Fluorophenyl)boronic Acid Pinacol Ester in the Chelation Reaction of Helically Chiral (*S,M*)/(*S,P*)-*N,N,O,C*-3-((1-hydroxybutan-2-yl)amino) BODIPYs 112
3.11.2 Expansion of the Helically Chiral *N,N,O,C*-3-((1-hydroxybutan-2-yl)amino) BODIPY Series 113
3.11.3 Expansion of the Helically Chiral *N,N,O,C*-3-Amino alcohol Substituted BODIPY Series 115
3.11.4 Crystal Structures of Helically Chiral BODIPY Series 116
3.11.5 Chiroptical Properties of Helically Chiral *N,N,O,C*-3-Amino Alcohol Substituted BODIPY Series 117
3.12 Conclusion 119
Chapter 4. Synthesis of Helically Chiral BODIPYs including 7-Membred Ring via Point-to-Helical Chirality Transfer 121

4.1 Introduction 121
4.2 Synthetic Strategy Towards Helically Chiral BODIPY Containing 7-Membered Ring 122
4.2.1 Synthesis of Helically Chiral BODIPY Containing 7-Membered Ring 122
4.3 ECD Spectroscopy of Helically Chiral (*S,P*)-*N,N,O,C*-3-(1-hydroxybutan-2-yl)amino)-5-(4-methoxyphenyl) BODIPY (4.2a) and (*S,M*)-*N,N,O,C*-3-(1-hydroxybutan-2-yl)amino)-5-(4-methoxyphenyl) BODIPY (4.2b) 130
4.3.1 Calculated ECD Spectra of Helically Chiral (*S,P*)-*N,N,O,C*-3-(1-hydroxybutan-2-yl)amino)-5-(4-methoxyphenyl) BODIPY (**4.2a**) and (*S,M*)-*N,N,O,C*-3-(1-hydroxybutan-2-yl)amino)-5-(4-methoxyphenyl) BODIPY (**4.2b**) 131
4.4 Solvent Effects on the Diastereoselectivity of Formation of Helically Chiral (*S,P*)-*N,N,O,C*-3-(1-hydroxybutan-2-yl)amino)-5-(4-methoxyphenyl) BODIPY (4.2a) and (*S,M*)-*N,N,O,C*-3-(1-hydroxybutan-2-yl)amino)-5-(4-methoxyphenyl) BODIPY (4.2b) 133
4.5 Conclusions 134
4.6 Synthesis of Helically Chiral BODIPY Containing Double 7-Membered Rings 135
4.6.1 Double S_NAr Reactions on 3,5-Dihalo BODIPYs from the Literature 135
4.6.2 Attempts to Synthesise Disubstituted Chiral BODIPY (**4.9**) 137
4.7 Conclusion 142
4.8 Synthesis of Diastereomeric Helically Chiral *N,N,O,O*-BODIPYs 143
4.8.1 Morita–Baylis–Hillman reaction (MBH) and Boc Protection (Part A) 145
4.8.1.1 Boc Protection of MBH Carbonate compounds 146
4.8.2 Synthesis of Racemic Helically Chiral *meso*-Ethyl-*N,N,O,O*-BODIPY (Part B) 147
4.8.3 Synthesis of diastereomeric helically chiral *N,N,O,O*-BODIPYs (Part C) 154
4.9 Conclusions 158
4.10 Chapter Conclusions 159
Chapter 5: Synthesis of Helically Chiral Di-BODIPYs via Point -to- Helical Chirality Transfer 161
5.1 Introduction 161
5.2 Synthetic Routes Toward Dimeric Helically Chiral BODIPY Arrays 162
5.2.1 Absolute Stereochemistry of Dimeric Helically Chiral BODIPYs 164
5.2.2 Photophysical Properties of Dimeric Helically Chiral (*S,S,P,P*)-*N,N,O,C*-3-(2-aminobutan-1-ol) BODIPY (**5.2a**), Fraction 2 (**5.2b**), and (*S,S,M,M*)-*N,N,O,C*-3-(2-aminobutan-1-ol) BODIPY (**5.2c**) 166
5.2.3 ECD Spectroscopy of Dimeric Helically Chiral (*S,S,P,P*)-*N,N,O,C*-3-(2-aminobutan-1-ol) BODIPY (**5.2a**), Fraction 2 (**5.2b**), and (*S,S,M,M*)-*N,N,O,C*-3-(2-aminobutan-1-ol) BODIPY (**5.2c**) 167
5.2.4 CPL Spectroscopy of Dimeric Helically Chiral (*S,S,P,P*)-*N,N,O,C*-3-(2-aminobutan-1-ol) BODIPY (**5.2a**), Fraction 2 (**5.2b**), and (*S,S,M,M*)-*N,N,O,C*-3-(2-aminobutan-1-ol) BODIPY (**5.2c**) 168
5.3 Expansion of the Dimeric Helically Chiral BODIPY Series 169
5.4 Synthesis of Dimeric Helically Chiral BODIPYs without Chiral axillaries 172

5.4.1 Synthesis of 3-(1*H*-pyrrol-2-yl)-5-bromo BODIPY (**5.13**) and 3-(1*H*-pyrrol-2-yl)-5-iodo BODIPY (**5.14**) via S_NAr reaction 173
5.5 Synthetic Routes Toward Trimeric Helically Chiral BODIPY Arrays 177
5.5.1 Synthesis of Tri-boronic Acid Linker 177
5.5.2 Amide Coupling between Amine and Benzoic Acid (**5.19**) 178
5.5.3 Synthesis of Tri-boronic Acid Linker (**5.3**) 180
5.5.4 Synthesis of Trimeric Helically Chiral BODIPY Arrays 184
5.6 Conclusions 185
5.7 Synthesis of Stacked Helically Chiral Bis BODIPYs 186
5.7.2 Synthesis of 2-(1*H*-pyrrol-2-yl)phenol (**4.35**) (Part B) 187
5.7.3 Synthesis of 2-(2-methoxyphenyl)-1*H*-pyrrole (**5.27**)(Part B) 187
5.7.4 Synthesis of Stacked Helically Chiral Bis BODIPYs from 2-(1*H*-pyrrol-2-yl)phenol (**4.35**)(Prat C) 189
5.7.5 Synthesis of Stacked Helically Chiral Bis BODIPYs from 2-(2-methoxyphenyl)-1*H*-pyrrole (**5.27**) (Prat C) 191
5.8 Conclusion 195
5.9 Chapter Conclusion 195
Chapter 6 Conclusions and Future Work 196
Chapter 7. Experimental Methods and Characterisation 200
7.1 General Experimental Information 200
7.1.1 Analysis 200
7.1.2 Procedures 200
7.2 Experimental Procedures and Characterisation Data 201
7.2.2 Chapter 3 214
7.2.3 Chapter 4 253
7.2.4 Chapter 5 265
7.3 Photophysical and Chiroptical Measurements 285
7.3.1 UV/Vis Absorption and Emission spectra. 285
7.3.2 Molar Extinction Coefficient Measurements and UV/Vis absorption Spectra 292
7.3.3 Fluorescence quantum yields measurements 305
7.4 Chiral HPLC Spectra 310
7.5 X-Ray Crystallography Data 311
References 353

Chapter 1. Introduction

This thesis focuses on developing and investigating new methodologies for the synthesis of helically chiral 4,4-difluoro-4-bora-3a,4a-diaza-*s*-indacene (BODIPY) dyes. In particular, we will explore different strategies for the synthesis of chiral BODIPYs and subsequently measure their chiroptical properties. Chapter 2 shows the use of a chiral flexible linker to connect two non-chiral BODIPY units to synthesize novel chiral bis BODIPYs. In Chapter 3, we will focus on a point-to-helical chirality transfer approach to synthesize a range of helically chiral BODIPYs. Further development of a point-to-helical chirality strategy, including the synthesis of helically chiral BODIPYs containing 7-membered rings will be explored in Chapter 4. In addition, in Chapter 4 we examine the synthesis of enantiopure helically chiral *N,N,O,O*-BODIPYs through a chiral resolution type approach. In the final Chapter, we focus on the development of our point-to-helical chirality approach to access dimeric and trimeric helically chiral BODIPY arrays and we explore the synthesis of stacked helically chiral bis BODIPYs.

This introduction Chapter discusses the theory of luminescence, as well as the photophysical and chiroptical properties (i.e. electronic circular dichroism (ECD) and circularly polarised luminescence (CPL)) of chiral fluorophores, with a particular focus on the BODIPYs. Subsequently, we will explore general methods for the synthesis and modification of BODIPYs. In the final part of this Chapter, we will discuss strategies to introduce chirality into BODIPYs, as well as general approaches for chirality transfer.

1.1 Introduction to Luminescence of Organic Molecules

In this section, we will provide a brief introduction into the photophysics of organic fluorophores, including providing definitions of key concepts and discussing chiroptical properties of chiral organic fluorophores.

1.1.1 Luminescence

Luminescence is the emission of light from a molecule in an electronically excited state. There are several types of luminescence based on the mode of excitation which initiates the luminescence process, i.e. photoluminescence (fluorescence and phosphorescence), electroluminescence, radioluminescence and bioluminescence. This thesis focuses on photoluminescence from small organic fluorophores.[1]

1.1.2 Fluorescence and Phosphorescence

Photoluminescence is the emission of light from electronically excited compound following absorption of light and includes fluorescence and phosphorescence.

Fluorescence is a photon emission process that occurs during relaxation of a molecule from the lowest singlet excited state (S_1) to the ground state (S_0), and happens on a timescale of approximately 10^{-9} - 10^{-6} s. This process is typically fast as there is no change in electron spin multiplicity, and it therefore a spin allowed transition.

Phosphorescence is emission of light from a triplet excited state (T_1) to the ground state (S_0). Following initial photoexcitation to the singlet excited state (typically S_1), the electrons transfer to the triplet excited state (T_1). The transfer to the triplet excited state (T_1) is known as intersystem crossing (ISC) and is spin-forbidden. Finally, the molecule relaxes from the triplet excited state (T_1) to the ground state (S_0) with emission of a photon. This process is also spin-forbidden, resulting in a longer excited state lifetime of 10^{-6} to 10 s. Both fluorescence and phosphorescence processes can be represented in a Jablonski diagram (Figure **1.1**).

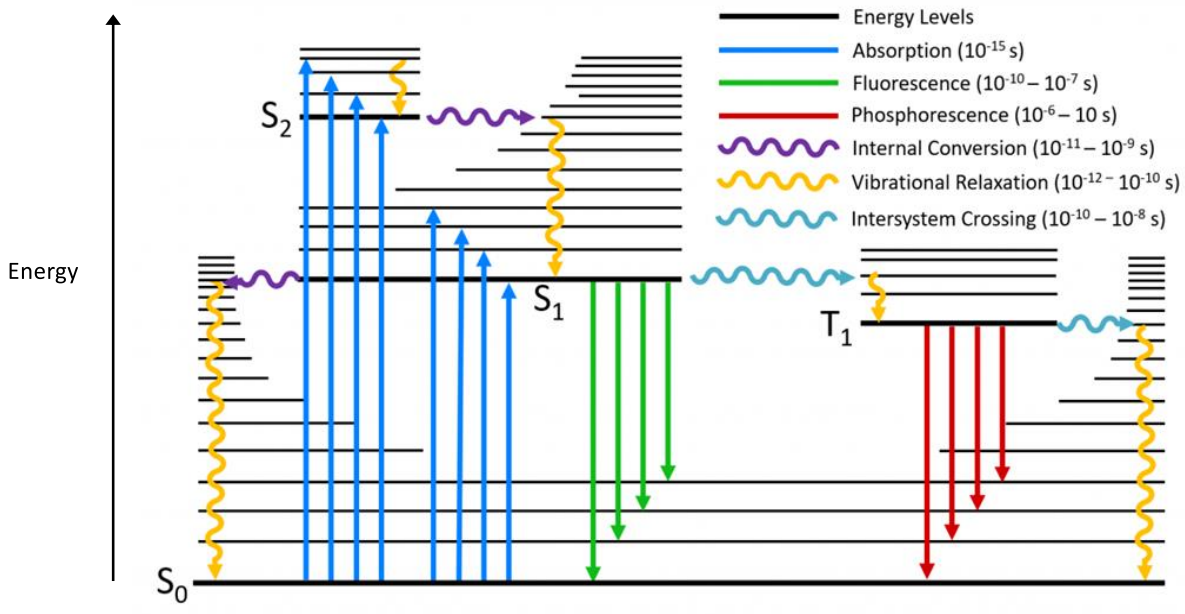

Figure 1.1: Jablonski diagram outlining photoluminescence (fluorescence and phosphorescence) via the absorption and emission of light (photons). Bold and thin horizontal lines denote energy and vibrational levels, respectively. The ground state (S_0) is the lowest line, with the excited singlet (S_1 and S_2), and triplet states labels on all other bold horizonal lines.

1.1.3 Key Photophysical Properties of an Organic Fluorophore

In this section, we will provide of key concepts for photophysical properties exhibited by fluorescent organic compounds and chiroptical properties by chiral organic fluorophores. Several of these properties will be observed across our synthesized chiral BODIPYs.

1.1.4 Molar Extinction Coefficient (ε)

The molar extinction coefficient (also known as the molar absorptivity) measures how strongly a fluorophore absorbs light at a specific wavelength. The molar extinction coefficient can be measured using the Beer-Lambert law in which A = absorption, ε = molar extinction coefficient ($M^{-1}cm^{-1}$), c = concentration (M), and l = path length (cm).[2]

$$A = \varepsilon c l$$

BODIPY dyes typically exhibit high molar extinction coefficients (ε > 40,000 $M^{-1}cm^{-1}$) with absorption in the visible region corresponding to S_0-S_1 transition.

1.1.5 Stokes Shift

Stokes shift is defined as the difference between the wavelength of the maximum absorption (λ_{max}, abs) for the S_0-S_1 transition and the wavelength of the maximum fluorescence emission (λ_{max}, em), and it can be expressed in either wavelength (nm) or wavenumber (cm^{-1}).[1,3] Stokes shifts are caused due to loss of energy during the fluorescence process, typically through vibrational relaxation. BODIPYs normally show small Stokes shifts (~10 nm), although systems have been designed which show large Stokes shifts of up to 11,100 cm^{-1}.[4]

1.1.6 Fluorescence Quantum Yield (ϕ_F)

The fluorescence quantum yield (ϕ_F) is a measure of the efficiency of fluorescence from a system, determined by the ratio of absorbed photons to emitted photons. Fluorescence quantum yield values range from between 0 and 1 or are given as percentages.

There are two main methods to measure fluorescence quantum yields, absolute (or direct) and relative. Absolute methods for the measurement of fluorescence quantum yield involve direct measurement of the incident and emitted photons of the sample. This involves the use of an integrating sphere which allows the collection of all the photons emitted from the sample, which can then be measured directly.[5]

Relative methods are more commonly used in the laboratory to measure the fluorescence quantum yield of the sample. Relative methods involve comparison of the integrated fluorescence intensity of

a sample to that of a known standard reference, for which the quantum yield has been accurately determined, ideally through direct measurement. The fluorescence quantum yield can then be measured using the following equation:

$$QY = QY_{ref} \frac{\eta^2}{\eta_{ref}^2} \frac{I}{A} \frac{A_{ref}}{I_{ref}}$$

In which QY = quantum yield, η = refractive index of solvent, I = peak area (area under emission spectra) and A = absorbance at excitation wavelength.

1.1.7 Chiroptical Properties of an Organic Fluorophore

1.1.8 Circularly Polarised Light

In this section, we will discuss two forms of polarisation of electromagnetic radiation: linear and circular. Firstly, linearly polarised light is electromagnetic radiation in the visible range (~350 - 700 nm) where the electric field component of the photons is all aligned parallel with each other. Linearly polarised light can be generated by passing unpolarized light through a liner polarizer.

Secondly, circularly polarized light occurs when the vector describing the electric field of the photons rotates as the wave propagates, caused when the two electric field components have the same amplitude and are out of phase by 90°. Circularly polarized light can therefore be described as right-handed (clockwise) or left-handed (anticlockwise) when viewed from the point of view of the receiver. Circularly polarized light can be generated by passing linearly polarized light through a birefringent "quarter-wave plate" at a specific angle (Figure **1.2**).

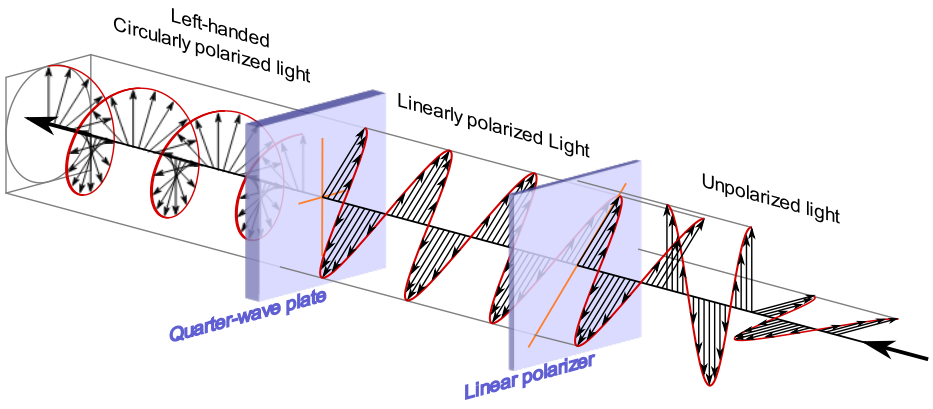

Figure 1.2: Schematic illustration of the transformation of unpolarized light passing the polarizer to create linearly polarized light, followed by passing through quarter-wave plate to create right-handed (clockwise) or left-handed (anticlockwise) circularly polarized light.

Our interest lies in the generation of circularly polarised of light. Circularly polarized light can be created using optical systems (*e.g.*, quarter-wave plates), but can also be seen in nature. Herein, we will explore an example of circularly polarized light observed in nature, specifically focusing on scarab beetles.

Scarab beetles exhibit unique optical properties that involve the reflection of circularly polarized light from their carapaces. Their ability to selectively reflect left-handed circularly polarized light, is attributed to the helical microfibril layers found within the exocuticle (shell). These specialized layers function as multilayer reflectors and allow the beetle to be coloured (Figure **1.3**).[6–8]

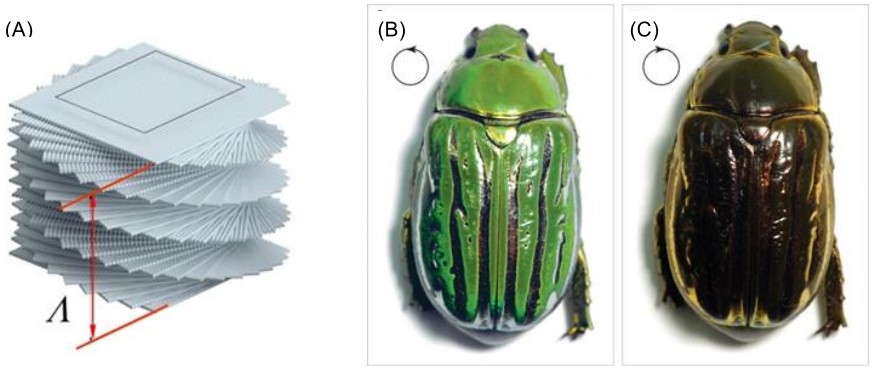

Figure 1.3: (A) Bouligand structure illustrating the twistiness (pitch Λ) of the helix; (B) left-circular polariser; (C) right-circular polariser on scarab beetles (adapted from Srinivasarao *et al.* and Arwin *et al.*).[7,9]

1.1.9 Electronic Circular Dichroism (ECD)

Circular dichroism (CD) is the differential absorption between right- and left-handed circularly polarized light from a chiral molecule. Electronic circular dichroism (ECD) is a spectroscopic technique used to measure the differences in the absorption of right- and left-handed circularly polarised light, associated with the electronic transitions in the S_0-S_1 within the molecular chromophore. The electronic circular dichroism reflects the structural properties of the ground state and can be used in determining the absolute confirmation of an organic compound.[10] The intensity of electronic circular dichroism can be measured by the absorptive dissymmetry factor (g_{abs}) which described by the following equation:

$$g_{abs} = \frac{\varepsilon_L(\lambda) - \varepsilon_R(\lambda)}{\frac{1}{2}\,\varepsilon_L(\lambda) + \varepsilon_R(\lambda)}$$

Where $\varepsilon_L(\lambda)$ and $\varepsilon_R(\lambda)$ are the molar extinction coefficients of left- and right-handed circularly polarised light at a particular wavelength (λ).

In ECD spectroscopy the term "Cotton effect" is commonly used to describe spectra. ECD spectra are typically plotted to show Δε verses wavelength, where $\Delta\varepsilon = \varepsilon_L - \varepsilon_R$. The Cotton effect refers to sign of the differential absorption of left- and right-handed circularly polarized light by chiral molecules. A positive Cotton effect is defined as a positive peak (+Δε) in the ECD spectra for the longest wavelength absorption, whilst a negative Cotton effect is defined as a negative peak (-Δε) in the ECD spectra for the longest wavelength absorption. For instance, Knight *et al.* reported a chiral BODIPY system that showed a positive Cotton effect for the *P*-isomer and a negative for *M*-isomer (Figure **1.4**).[11]

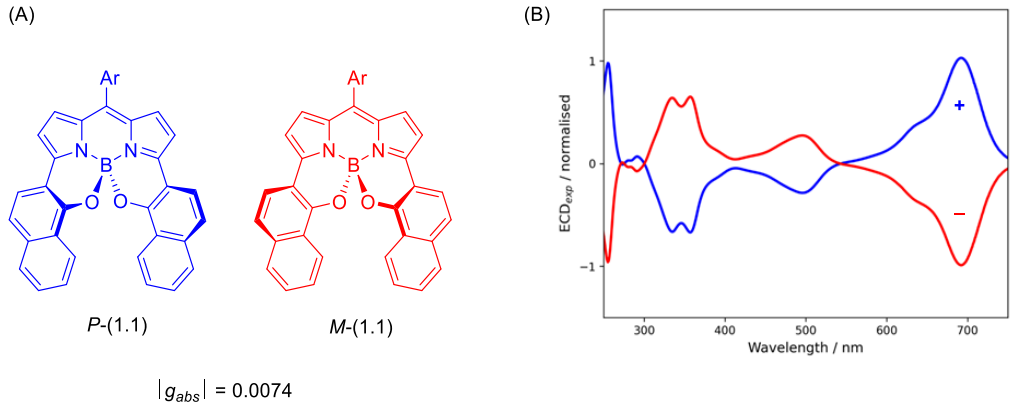

Figure 1.4: (A) Chiral BODIPYs (Ar = *p*-($MeCO_2$)-C_6H_4-); (B) Normalised ECD spectra of both enantiomers (*M*)-(**1.1**) (negative Cotton effect, red) and (*P*)-(**1.1**) (positive Cotton effect, blue).

1.1.10 Circularly Polarised Luminescence (CPL)

Circularly polarized luminescence (CPL) is the differential emission between right- and left-handed circularly polarized light from a chiral molecule. Circularly polarized luminescence reflects the structural properties of the electronic excited state. The circularly polarized luminescence is quantified by the luminescence dissymmetric factor (g_{lum}) using the following equation:

$$g_{lum} = \frac{(I_L - I_R)}{\frac{1}{2}(I_L + I_R)}$$

Where I_L is the intensity of left-handed circularly polarised light and I_R is the intensity of right-handed circularly polarised light.

The value of luminescence dissymmetric factor g_{lum} ranges from -2 to +2, where -2 corresponds to fully right-handed circularly polarized light and +2 corresponds to fully left-handed circularly polarized light. This value is determined by the following theoretical equation, which consider magnetic (m) and electric (μ) transition dipole moment vectors and the angle (τ) between these vectors.

$$g_{lum} = \frac{4(|\boldsymbol{\mu}| \,.\, |\boldsymbol{m}|.\cos(\tau))}{(\boldsymbol{\mu}^2 + \boldsymbol{m}^2)}$$

For example, g_{lum} can be maximised when (τ = 0° or 180°) resulting in a $|g_{lum}|$ = 2.

1.1.11 CPL Quantum Efficiency and CPL Brightness (B_{CPL})

In order to easily compare the chiroptical properties of CPL-active compounds we can define their CPL efficiency by their CPL quantum efficiency ($|g_{lum}|\cdot\phi_F$) or circularly polarized luminescence brightness (B_{CPL}).[12] Circularly polarized luminescence brightness (B_{CPL}) combines the luminescence dissymmetric factor (g_{lum}), molar extinction coefficient (ε) and quantum yields (ϕ) of a CPL-active compound into a single number.[13] In addition, this B_{CPL} quantity help to direct the choice of molecular systems for specific CPL applications. Circularly polarized luminescence brightness is defined by the following equation:

$$B_{\mathrm{CPL}} = \varepsilon_\lambda \times \Phi \times \frac{|g_{lum}|}{2}$$

Where ε_λ is the molar extinction coefficient at excitation wavelength, ϕ is the emission quantum yield, and g_{lum} luminescence dissymmetric factor.[13]

1.1.12 Correlation Between g_{abs} and g_{lum}

The relationship between g_{abs} and g_{lum} in CPL active small organic molecules (CPL-SOMs) was recently examined by Mori *et al*., in which they explored the correlation between g_{abs} and g_{lum} across various molecular systems, including chiral cyclophanes, chiral biaryls and chiral BODIPYs.[14] They discovered a good linear relationship between g_{abs} and g_{lum} for all 12 chiral BODIPYs known in the literature at that time, which showed an observed linear correlation of $|g_{lum}| = 0.77 \times |g_{abs}|$ ($r^2 = 0.49$) (Figure **1.5**).

Examination of the correlation between g_{abs} and g_{lum} for all 12 chiral BODIPYs showed two examples as outliers, BODIPYs (**1.10**) and (**1.12**), which appeared to not fit the trends observed for the other examples. In fact, an improved correlation $|g_{lum}| = 1.02 \times |g_{abs}|$ ($r^2 = 0.90$) was observed when BODIPYs (**1.10**) and (**1.12**) were omitted from the data, suggesting that $|g_{lum}|$ and $|g_{abs}|$ are strongly correlated in chiral BODIPYs. The unusual $|g_{lum}|$ and $|g_{abs}|$ values seen for BODIPYs (**1.10**) and (**1.12**), may arise due to the presence of two BODIPY chromophores in these molecules, thus the g_{abs} / g_{lum} correlation observed by Mori *et al*. may be only true for monomeric chiral BODIPYs, with dimeric BODIPYs showing higher g_{abs} values in comparison to g_{lum}.[14–16]

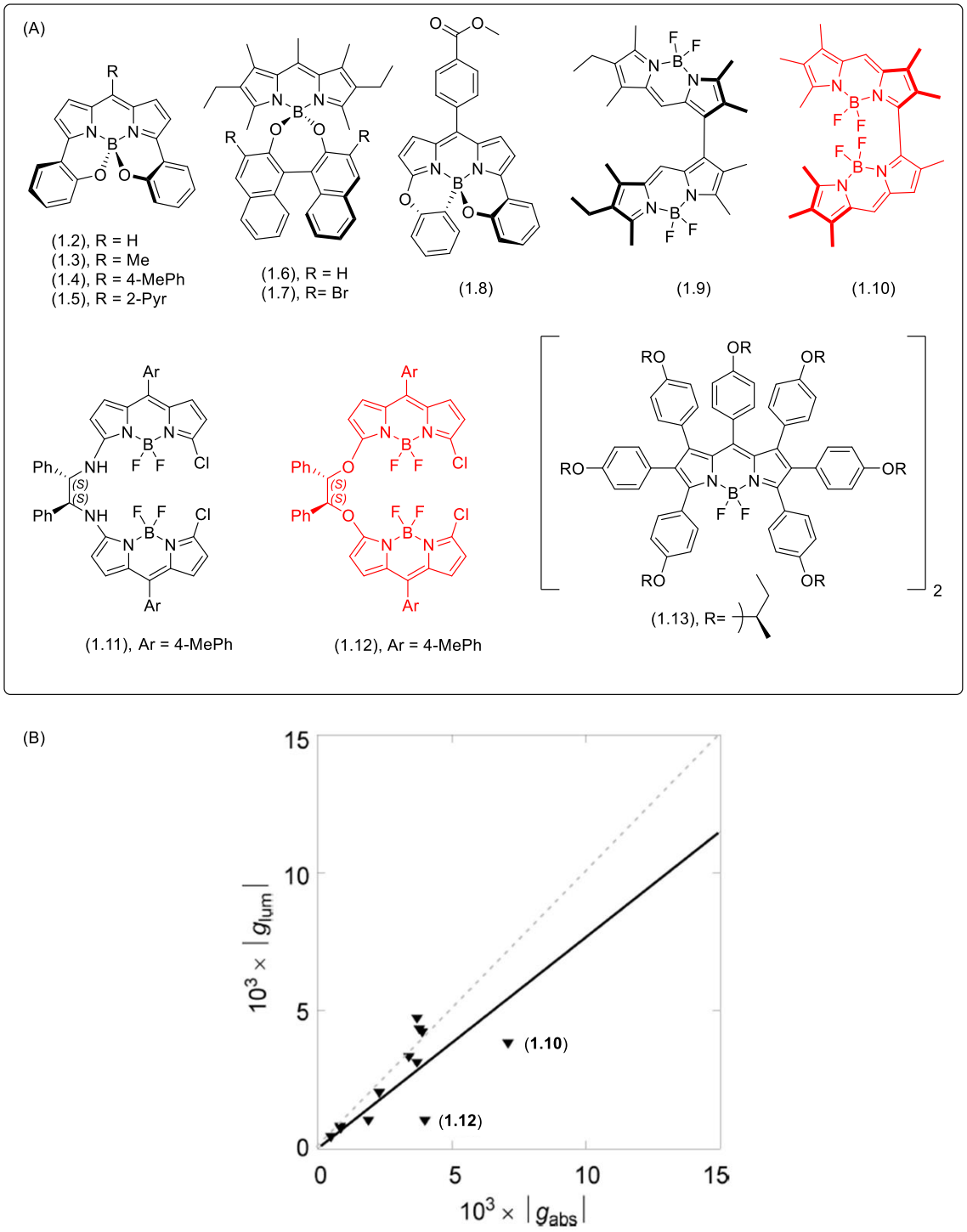

Figure 1.5: (A) Chiral BODIPYs; (B) Correlation between factors of emission and absorption in all 12 chiral BODIPYs and with two omitted BODIPYs, (**1.10**) and (**1.12**), denoted by the solid and dashed line, respectively. (adapted from Mori *et al.*).[14]

1.2 Examples of CPL-Active Compounds Including CPL-SOMs

In this section, we will explore different examples of compounds that are capable of CPL including chiral lanthanide complexes and chiral small organic molecules (CPL-SOMs), including chiral BODIPYs.

1.2.1 Chiral Lanthanide Complexes Capable of CPL

Chiral lanthanide complexes have exhibited the largest value of g_{lum} in the range of (0.05 - 0.5), attributable to electric dipole forbidden and magnetic dipole allowed *f-f* transitions.[17] To date, the highest g_{lum} has been observed in lanthanide (III) coordination complexes reported by Muller *et al*., wherein specifically europium complex (**1.14**) exhibited ($|g_{lum}|$ = 1.38) in visible region at 595 nm for a single complex (Figure **1.6**). However, chiral lanthanide complexes demonstrate very low quantum yield (ϕ_F) and therefore low CPL brightness (B_{CPL}), thus limiting their use in various CPL applications.[18]

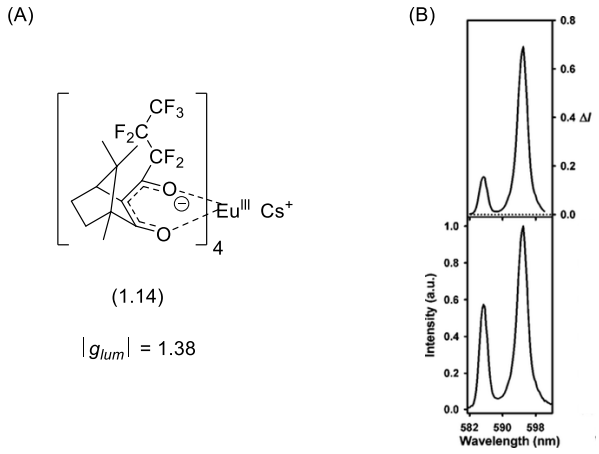

Figure 1.6: (A) Molecular structure of the highest CPL emitter containing Eu(lll); (B) CPL spectra (top) and total luminescence spectra (bottom) of Cs[Eu((+)-hfbc)$_4$] (hfbc = 3-heptafluorobutyryl camphorate) in $CHCl_3$.

1.2.2 Chiral Small Organic Molecules Capable of CPL (CPL-SOMs)

Studying circularly polarized luminescence of small organic molecules (CPL-SOMs) garnered attention in recent years due to their potential for use in a wide range of application areas. For instance, CPL-SOMs could be used in live cell CPL imaging, in which the handedness of the emitted light could be used to examine cellular structure. CPL-SOMs have potential application in this area due to their small molecular size (<1000 MW), to allow uptake into the cell, and low toxicity, in comparison to the metal containing chiral lanthanide (III) complexes.

The first example of small organic molecules capable of CPL was reported by Emeis and Oosterhoff in 1967 for a cyclic chiral ketone.[19] They described the chiroptical properties of (+)-(*S*,*S*)-*trans*-β-hydridanone (**1.15**), upon UV excitation at 313 nm, (+)-(*S*,*S*)-*trans*-β-hydridanone (**1.15**) exhibited high g_{lum} = 0.035 at 361 nm. Later several cyclic chiral ketones have been published as CPL-SOMs optical active emitters, showing g_{lum} values in the range of 10^{-2} - 10^{-5} (Figure **1.7**).[20–22]

(1.15) (1.16) (1.17) (1.18)

g_{lum} = 0.035 g_{lum} = 0.011 g_{lum} = 0.0079 g_{lum} = 0.016

Figure 1.7: First reported example of CPL-SOMs (+)-*trans*-β-hydridanone (**1.15**) and some examples of CPL-SOMs ketones.

Interestingly, cyclic chiral ketones exhibit a relatively high g_{lum} due to the magnetically allowed and electronically forbidden n-π* transition of the distorted carbonyl group, but consequently low fluorescence quantum yields, resulting low overall CPL efficiency.[22] Therefore, the development of chiral SOMs capable of CPL with high overall CPL efficiency (i.e., high luminescence dissymmetric factor g_{lum} and fluorescence quantum yield ϕ_F) is a significant challenge.[23]

Gossauer and co-workers developed chromophores based on CPL-SOMs with π-conjugated systems. In 1997, they reported the ability of chiral BODIPY (*R,R*)-(**1.19**) to emit CPL in the visible region at 546 nm with high luminescence dissymmetric factor and fluorescence quantum yield (g_{lum} = 0.001 , ϕ_F = 0.48) (Figure **1.8**).[24]

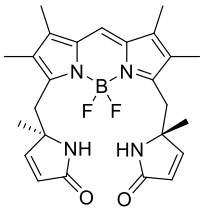

(*R*,*R*)-(1.19)

$|g_{lum}|$ = 0.001
ϕ_F = 0.48

Figure 1.8: First CPL-SOMs based on chiral BODIPY with π-conjugated.

Further discussion of chiral BODIPYs and their CPL will be addressed later in the Chapter, following an introduction to the synthesis of the BODIPY chromophore.

1.3 General Introduction of BODIPY Dyes

In this work, we focused on the development of synthetic routes to helical chiral BODIPYs and the investigation of a new methodology to access different designs of chiral BODIPY systems including chiral dimeric and trimeric BODIPYs. In this section, we will discuss the structure and photophysical

properties of the BODIPY dyes, their potential uses, common synthetic approaches, and strategies to modify their core structure.

The chiral 4,4-difluoro-4-bora-3a,4a-diaza-*s*-indacene (BODIPYs) are a class of fluorescent organic dyes which show highly useful photophysical properties, including high extinction coefficients ($\varepsilon > 40{,}000$ $M^{-1}cm^{-1}$), high fluorescence quantum yields ($\phi_F > 0.8$), high photostability, and the ability to emit light in the longer wavelength visible region ($\lambda > 550$ nm).[25,26] Alongside of these excellent photophysical properties, BODIPY dyes are easy to synthesize and their photophysical properties can be easily tuned through synthetic modifications. BODIPYs have been used in many applications, such as biological imaging,[27] solar cell,[28] and photodynamic therapy.[29]

The core structure of a BODIPY consists of a dipyrromethene unit chelated with a BF_2 moiety. The chelation of the dipyrromethene by BF_2 helps to limit the rotation around the central methylene unit and inhibit the cis/trans isomerisation of dipyrromethene. This increased rigidity also helps to reduce unwanted vibration modes, and thus increase fluorescence quantum yields. The BODIPY core structure has a high degree of symmetry, due to the presence of a C_2 axis and two mirror planes (Figure **1.9**).

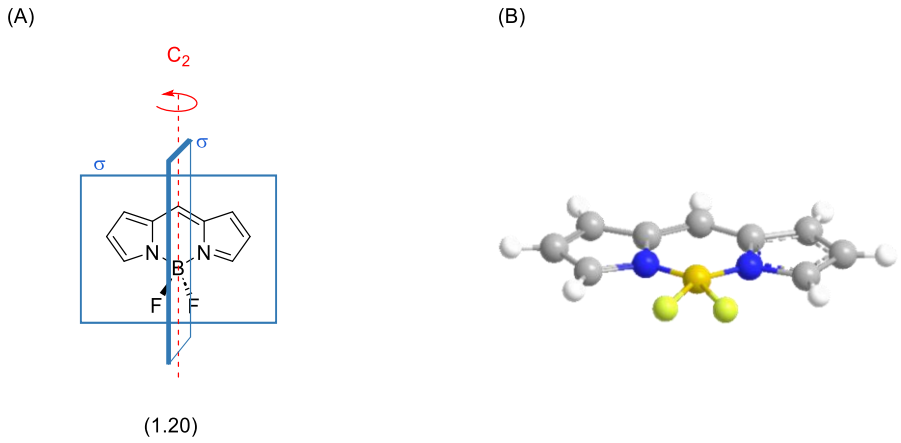

(1.20)

Figure 1.9: Symmetry factors in BODIPY. (A) Shows C_2 axis and two mirror planes; (B) 3D structure of BODIPY, emphasising its planer structure.

BODIPYs and their dipyrromethene precursors have two related numbering systems, common and IUPAC. The numbering systems for BODIPYs and dipyrromethenes are different in IUPAC, but similar in the common system in which the terms *meso*-, α- and β- positions are used the same way for both structures (Figure **1.10**).

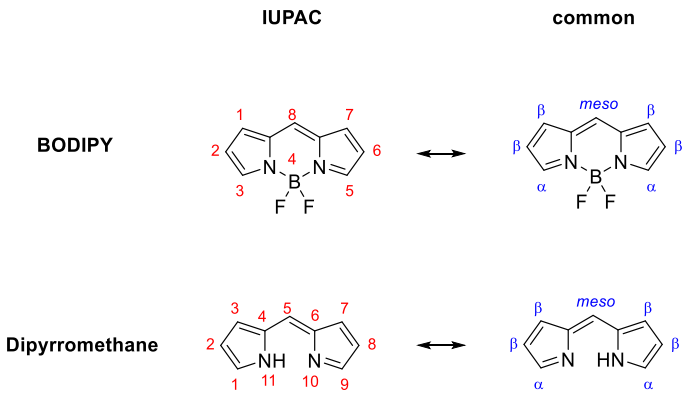

Figure 1.10: BODIPY and dipyrromethene with numbering systems, IUPAC (left) and common (right).

1.3.1 General Approaches to the Synthesis of BODIPYs

Here, we will discuss general methods for the synthesis of BODIPYs, including the first known synthesis of a BODIPY, as well as common oxidative and non-oxidative routes to BODIPYs. Typically, synthetic routes to BODIPYs involve condensation reactions between two equivalent of a pyrrole and an electrophilic carbonyl compound (*e.g*. acid anhydrides, acyl chlorides, or aldehydes) to form a dipyrromethane or dipyrromethene, followed by conversion to the corresponding BODIPY. In addition, we will explore common methodologies for functionalizing the core of a BODIPY.

1.3.1.1 Non-Oxidative Routes to BODIPYs

The first BODIPY was reported by Treibs and Kreuzer in 1968.[30] They reported a one-pot synthetic procedure, involving a Lewis acid mediated condensation between 2,4-dimethylpyrrole (**1.21**) and acetic anhydride to form the intermediate, 1-(3,5-dimethyl-1*H*-pyrrol-2-yl)ethan-1-one (**1.22**). This substituted pyrrole then reacts with another molecule of 2,4-dimethylpyrrole (**1.21**), via another condensation reaction, to form dipyrromethene (**1.23**), which is then chelated by $BF_3.OEt_2$ to form BODIPY (**1.24**). BODIPYs (**1.25** and **1.26**) are then formed in the reaction due to the presence of excess acetic anhydride, via an *in situ* S_EAr acetylation of the intermediate BODIPY (**1.24**) at the reactive β-positions (Scheme **1.1**).

In the same publication, Treibs and Kreuzer improved their procedure by first synthesizing and isolating dipyrromethene , followed by a subsequent chelation reaction using an excess of $BF_3.OEt_2$ in presence of triethylamine as a base.[30] Since this initial work was reported, a large number of groups have continued to use this synthetic approach to BODIPYS, through an acid mediated condensation of two equivalents of a pyrrole with an electrophilic carbonyl at the acid oxidation level (*e.g*. carboxylic acids, acid anhydrides, acyl halides, trialkyl orthoformates).

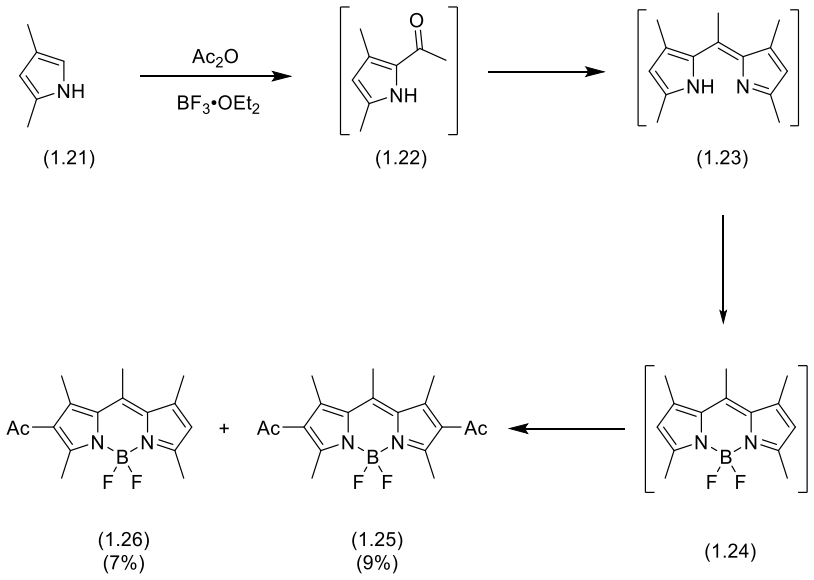

Scheme 1.1: The first synthetic route of BODIPY reported by Treibs and Kreuzer.

1.3.1.2 Oxidative Routes to BODIPYs

An alternative route for the BODIPYs, involves a stepwise synthesis including three main steps: condensation, oxidation, and chelation. The condensation reaction occurs between two equivalents of a pyrrole and an electrophilic carbonyl at the aldehyde level oxidation state to form a dipyrromethane, which is subsequently oxidised to the corresponding dipyrromethene and finally chelated to form the target BODIPY.

One of the most popular methods towards BODIPYs was originally reported by Lindsey *et al.*, an example of which involves a condensation reaction between 4-iodobenzaldehyde (**1.27**) and two equivalents of 2-methylpyrrole (**1.28**) with a catalytic amount of TFA in DCM at room temperature to form dipyrromethane (**1.29**).[31] Subsequently, the resulting dipyrromethane (**1.29**) underwent oxidation by *p*-chloranil to give dipyrromethene (**1.30**), followed by a chelation reaction using $BF_3.OEt_2$ and trimethylamine to produce 3,5-dimethyl-8-aryl substituted BODIPY (**1.31**) (Scheme **1.2**).

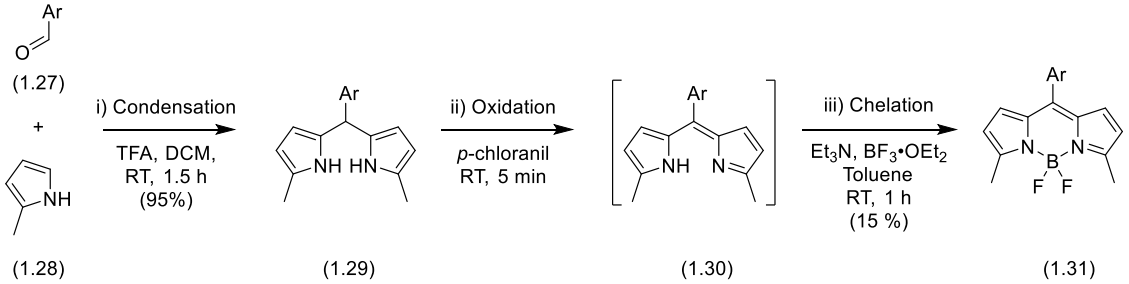

Scheme 1.2: General approach to BODIPYs using a three-step oxidative route (Ar = *p*-(iodo)-C_6H_4-).

1.3.1.3 Routes to α-Unsubstituted BODIPYs

It should be noted that the previous methods are best used for the synthesis of α-substituted BODIPYs. In the case of BODIPYs which do not have an α-substituent, the intermediate dipyrromethanes and dipyrromethenes can react further with any carbonyl containing molecules present (*e.g*. ketones and aldehydes) to form linear and cyclic oligomers. In fact, similar approaches are used in the synthesis of the porphyrins.[32] Alternative methods for the synthesis of α-unsubstituted BODIPYs have therefore been reported in the literature.

In 1994, Lindsey and Lee reported the synthesis of dipyrromethane (**1.34**) through an acid-catalyzed condensation between 1*H*-pyrrole (**1.32**) and an aryl aldehyde (**1.33**).[33] In their procedure, 1*H*-pyrrole is utilized as a solvent, ensuring a large excess is present, to prevent further condensation reaction of the dipyrromethane (**1.34**) by making sure that the rate of reaction between 1*H*-pyrrole and the aldehyde is faster than any subsequent reaction of the product α,α-unsubstituted dipyrromethane (**1.34**) with aldehyde, and ensuring that all the aldehyde is used. However, this approach is inefficient in pyrrole and causes difficulties during work up and product purification due to the need to remove the excess pyrrole at the end of the reaction (Scheme **1.3**).

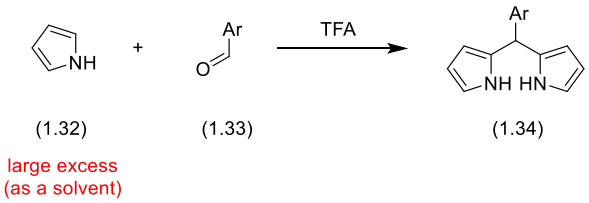

Scheme 1.3: Synthesis of α, α-unsubstituted dipyrromethane (**1.34**) through acid-catalysed condensation using 1*H*-pyrrole as the solvent (Ar = Ph).

Recently, the Dehaen group has developed an alternative synthetic route to α,α-unsubstituted dipyrromethanes without the need to use a large excess of pyrrole. They used an HCl-catalyzed condensation between three equivalents of 1*H*-pyrrole (**1.32**) and one equivalent of aryl aldehyde (**1.33**) in aqueous solution at room temperature (Scheme **1.4**).[34] The use of water as a solvent result in the precipitation of the product α,α-unsubstituted dipyrromethane (**1.34**) during the reaction course. The precipitation of dipyromethane prevents any further condensation reactions, as the dipyrromethane is no longer in solution, and allows for purification by simple filtration at the end of the reaction. However, as a precipitation driven reaction this process can be sensitive to starting material solubility and reaction concentration (Scheme **1.4**).

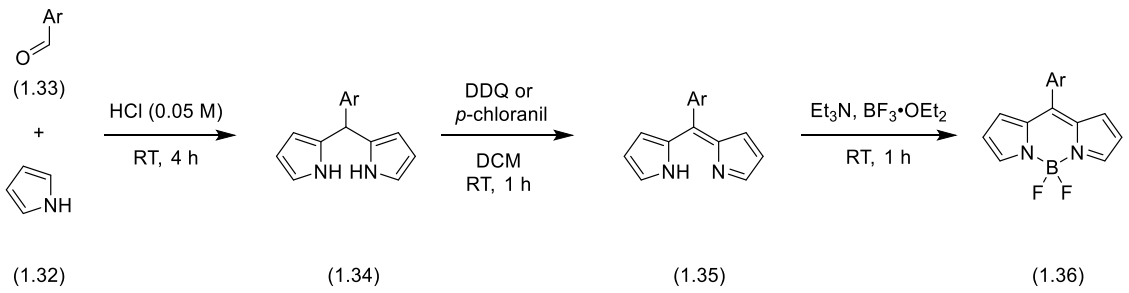

Scheme 1.4: Synthesis of α,α-unsubstituted BODIPYs via Dehaen's method.

Following isolation of the intermediate α,α-unsubstituted dipyrromethane (**1.34**), prepared by Dehaen's methodology, the dipyrromethane (**1.34**) was oxidised to form the corresponding α,α-unsubstituted dipyrromethene (**1.35**) followed by chelation reaction to form the target α,α-unsubstituted BODIPY (**1.36**) (Scheme **1.4**). It should be noted that some dipyrromethanes can be unstable towards air oxidation, consequently it is advisable to use them immediately after preparation.

1.3.1.4 Synthesis of Unsymmetrical BODIPYs

The previous methods only allow direct access to symmetrical BODIPYs formed from two identical pyrrole units. Forming unsymmetrical BODIPYs from two different pyrrole units is more challenging, requiring a more stepwise approach in which one pyrrole would be functionalised with an aldehyde or ketone, followed by condensation with a second pyrrole. For example, the synthesis of an unsymmetrical BODIPY (**1.38**) was reported by Dehaen *et al.*, in which they described such a stepwise approach via a keto-pyrrole intermediate (**1.37**). 2-Acetly-5-chloropyrrole (**1.37**) was first prepared through a one-pot α-chlorination/Vilsmeier-Haack acylation of 1*H*-pyrrole (**1.32**). Subsequently, 2-acetly-5-chloropyrrole (**1.37**) was condensed with 2,4-dimethylpyrrole (**1.21**) in presence of phosphorus oxychloride, followed by chelation reaction under standard conditions to give corresponding unsymmetrical BODIPY (**1.38**) (Scheme **1.5**).[35]

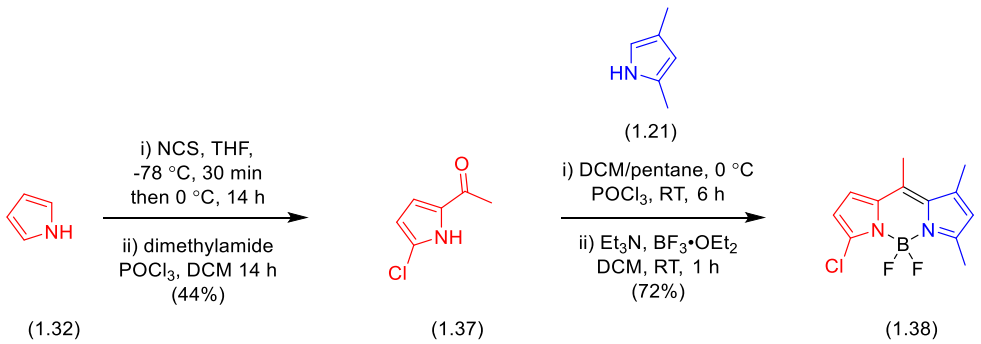

Scheme 1.5: A stepwise synthesis of unsymmetrical BODIPY (**1.38**) via intermediate keto-pyrrole (**1.37**).

1.3.2 Modifications on the BODIPY Core

Functionalisation of BODIPY core can be used to fine tune the photophysical and chiroptical properties. The BODIPY core can be functionalised at the 1,2,3,5,6 and 7 positions of the pyrrolic units (α and β positions), the 8 position (*meso*-position) of the bridging methylene, and at the boron centre. There are many different methods for introducing various functionalities onto the BODIPY core (Figure **1.11**). In this section we will focus mainly on modifications at the 3,5-positions that are most relevant to this work, including electrophilic aromatic substitution (S_EAr), nucleophilic aromatic substitution (S_NAr) and metal cross-coupling reactions (*e.g.*, Stille, Negishi, Heck, Suzuki, and Sonogashira), as well as the 2,6-S_EAr reactions for comparison (highlighted in red).

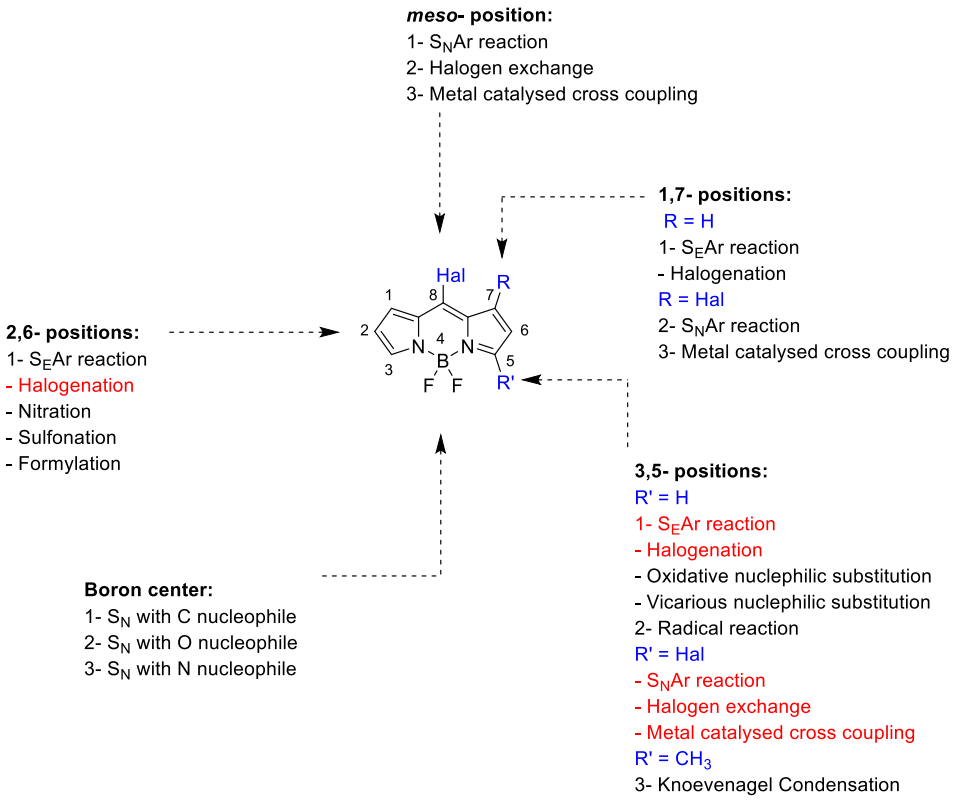

Figure 1.11: Overview of modifications to the BODIPY core. Discussed reactions in this section are highlighted in red.

1.3.2.1 Electrophilic Aromatic Substitution (S_EAr) of BODIPYs

In the literature, electrophilic aromatic substitution is commonly used to halogenate BODIPYs, demonstrating particularly high regioselectivity for the 2- and 6-positions. These positions undergo preferential electrophilic aromatic substitution, mainly due to their higher electron density and more stable transition state. Therefore, these positions are more susceptible to electrophilic attack, in comparison to the 3,5- or 1,7-positions, via S_EAr reaction mechanisms.

This was demonstrated in the work of Ortiz *et al*., where they examined the stepwise chlorination of BODIPYs using an electrophilic chlorination reagent, *N*-chlorosuccinimide (NCS).[36] The reaction between BODIPY (**1.39**) and a slight excess of NCS (2 equivalents) in THF at room temperature for 12 hours resulted in mono-substitution occurring at the 2-postion of BODIPY (**1.39**), to give 2-chloro-BODIPY (**1.40**). Increasing the amount of NCS to 3 equivalents and the time to 24 hours, resulted in 2,6-chloro BODIPY (**1.41**) being obtained as a major product. Further increasing the NCS to 4 equivalents and the reaction time to 72 hours, resulted in the isolation of 2,3,6-trichloro-BODIPY (**1.42**) as the major project, the low yield being due to the formation of other polychlorinated products. Finally, using 10 equivalents of NCS over 48 hours gave 2,3,5,6-tetrachloro-BODIPY (**1.43**). These experiments indicated that chlorination occurs sequentially, first at the 2,6-positions, and then at the 3,5-positions (Scheme **1.6**).

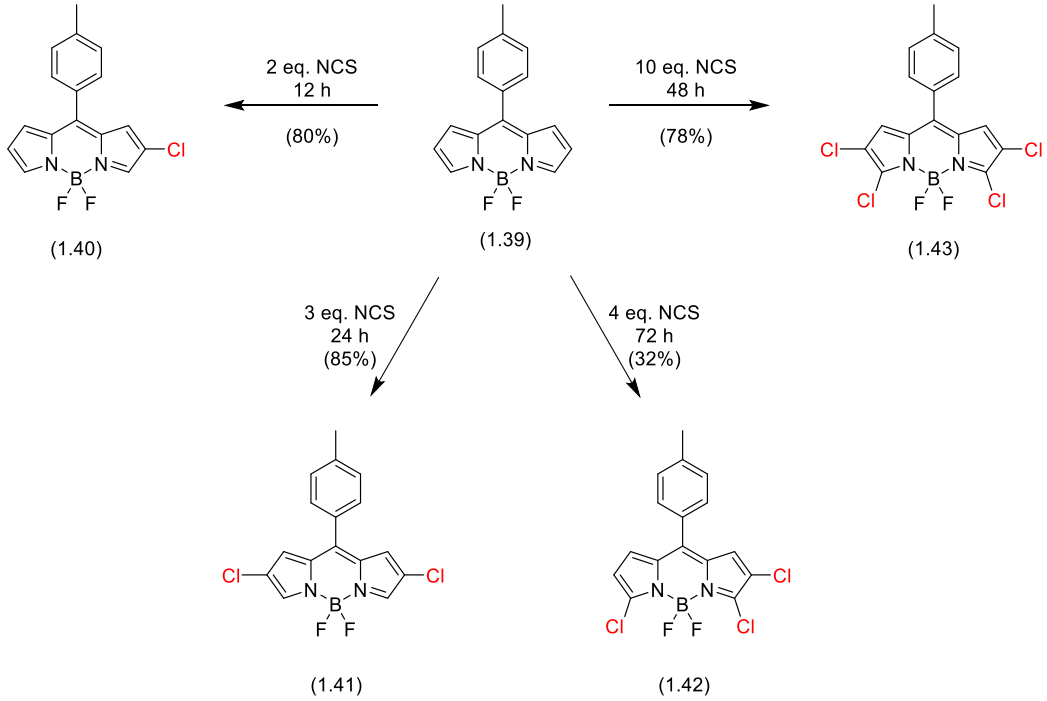

Scheme 1.6: Electrophilic aromatic substitution of BODIPY (**1.39**) with NCS.

Similarly, stepwise bromination of BODIPY was examined by Shinokubo *et al*., in which they treated BODIPY (**1.44**) with 1.2 equivalents of *N*-bromosuccinimide (NBS) at room temperature to give 2-bromo BODIPY (**1.45**) (82%) and 2,6-dibromo-BODIPY (**1.46**) (12%).[37] Increasing the amount of NBS to 2.4 equivalents under similar conditions afforded 2,6-dibromo-BODIPY (**1.46**) as a major product along with a small amount of 2-bromo-BODIPY (**1.45**). Interestingly, the use of excess NBS did not result in any observed bromination of the 3,5-positions under these reaction conditions. Further discussion of the S_EAr bromination of BODIPYs is presented in Chapter 2 (Scheme **1.7**).

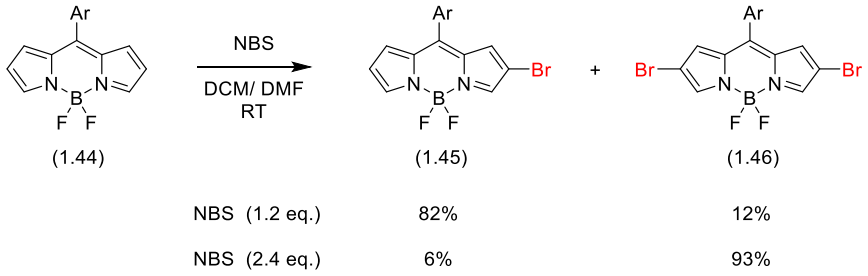

Scheme 1.7: Electrophilic aromatic substitution of BODIPY (**1.44**) with NBS, showing regioselectivity in S_EAr at the 2,6-positions (Ar = Mes).

Despite many studies on chloro- and bromo-substitution of BODIPYs, there are far fewer papers published on the iodination of BODIPYs. For example, a patent was published by the university of Gungdong Technology in 2018 in which BODIPY (**1.47**) was reacted with 10 equivalents of iodine and 2 equivalents of iodic acid in ethanol at 40 °C, giving 2-iodo-BODIPY (**1.48**). Interestingly, using 2.5 equivalents of iodine and 2 equivalents iodic acid in ethanol with an increased reaction temperature of 60 °C, led to the formation of 2,6-diiodo-BODIPY (**1.49**) in good yield. Additionally, increasing the amount of iodine to 25 equivalents in presence of 2 equivalents iodic acid in ethanol at 60 °C for 5 hours afforded 2,3,5,6-tetraiodo-BODIPY (**1.50**) (Scheme **1.8**).[38]

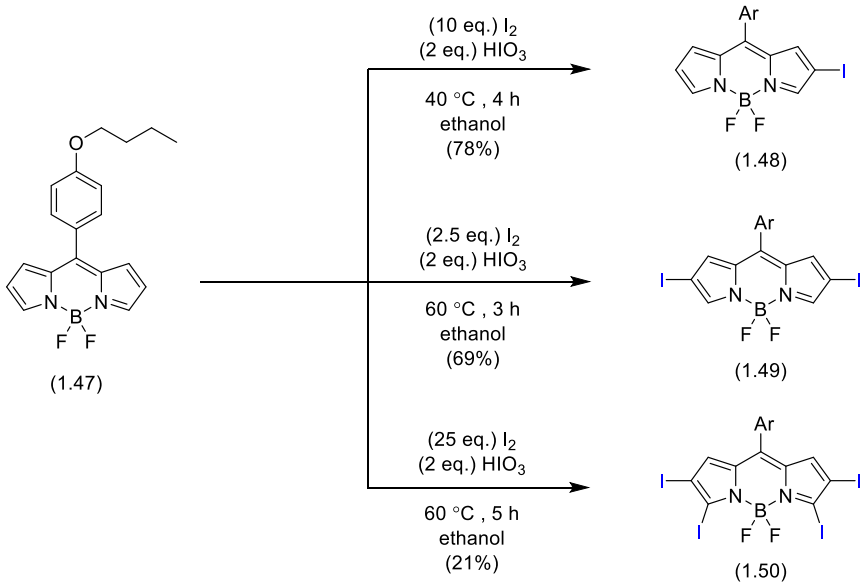

Scheme 1.8: Electrophilic aromatic substitution of BODIPY (**1.47**) with iodine and iodic acid.

Electrophilic aromatic substitution (S_EAr) of unsubstituted BODIPY with halogens therefore shows preferential reaction at the 2- and 6- positions, the 3,5-positions can only be accessed if the 2,6-positions are already substituted. Thus, the selective preparation of 3,5-halogenated-BODIPYs is challenging.

An alternative approach to prepare 3,5-halogenated BODIPYs involves using dipyrromethanes as the key synthetic intermediate, instead of BODIPYs. Dipyrromethanes show a strong preference for S_EAr regioselectivity at the α,α-positions, which correspond to the 3,5-positions of a BODIPY, as dipyrromethanes are more pyrrole-like in their chemistry. The corresponding dipyrromethanes can then undergo to S_EAr, oxidation, and chelation reactions to form 3,5-halogenated BODIPYs.

1.3.2.2 Electrophilic Aromatic Substitution (S_EAr) of Dipyrromethanes

In this section, we will discuss the synthesis of α,α-halogenated dipyrromethanes to access 3,5-halogenated BODIPYs through a three-step method including an S_EAr reaction, oxidation, and boron chelation.

Boens and Dehaen, reported high a regioselective electrophilic aromatic substitution of dipyrromethanes, with halogens.[39,40] They showed that dipyrromethane (**1.51**) could react with NCS at low temperature to give α,α-dichloro dipyrromethane (**1.52**). Following oxidation and boron chelation the desired 3,5-dichloro BODIPY (**1.56**) was the formed in 33% overall yield from dipyrromethane (**1.51**). Similarly, 3,5-dibromo BODIPY (**1.57**) can be synthesized through this three-step method using NBS (Scheme **1.9**).

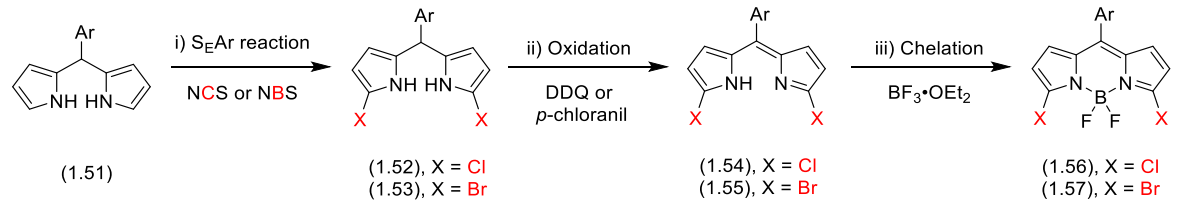

(1.51) (1.52), X = Cl (1.53), X = Br (1.54), X = Cl (1.55), X = Br (1.56), X = Cl (1.57), X = Br

Scheme 1.9: Electrophilic aromatic substitution of dipyrromethane (**1.51**), showing regioselectivity at α,α-positions to access 3,5-dihalo BODIPYs (Ar = *p*-(OH)-C_6H_4-).

The synthesis of 3,5-diiodo BODIPYs via this three-step method has not previously been reported in literature, potentially due to difficulties in controlling S_EAr reactions with NIS verses competing oxidation to the dipyrromethene. However, in 2021 Hall *et al.*, reported a new approach to access 3,5-diiodo BODIPYs via a double aromatic Finkelstein reaction.

1.3.2.3 The Finkelstein or Halex Reaction

The Finkelstein reaction is a halogen exchange reaction, originally discovered in 1910 by Dr Hans Finkelstein.[41] Typically, an alkyl halide (chloride or bromide) reacts with sodium iodide in acetone, via an S_N2 reaction to form the corresponding alkyl iodide, with the formation of sodium chloride or sodium bromide. This reaction would normally be reversible, but the reaction is driven to completion

by the precipitation of sodium chloride or sodium bromide from the reaction mixture, as they are much less soluble in acetone in comparison to sodium iodide (Scheme **1.10**).

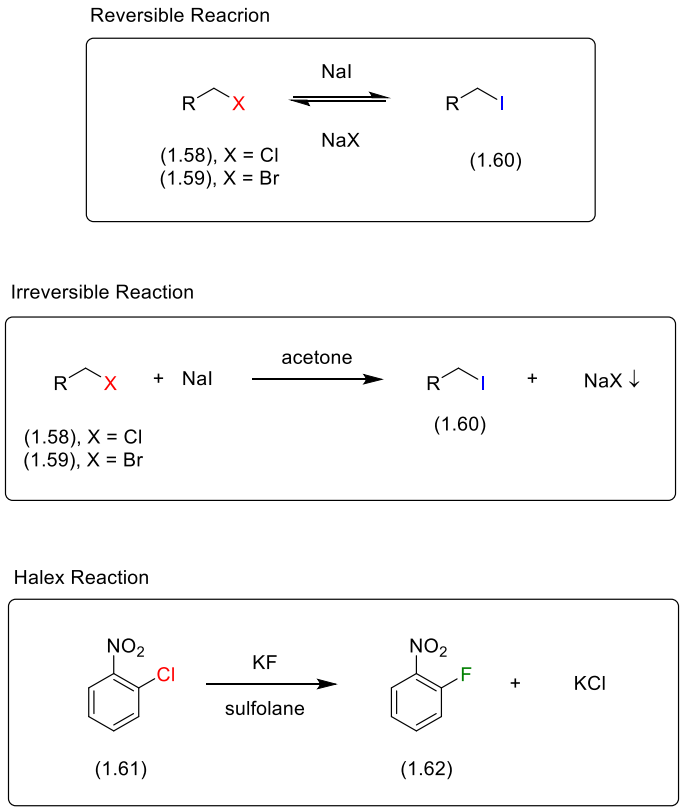

Scheme 1.10: Halogen exchange in aliphatic and aromatic halides using the Finkelstein and Halex reactions.

The Halex reaction, or aromatic Finkelstein, is a related halogen exchange reaction in aromatic compounds, and is primarily used to convert aromatic chlorides to the corresponding aromatic fluorides via an S_NAr reaction process. The Halex reaction is often performed in polar solvents such as DMSO, DMF or sulfolane at high temperatures.[42,43]

While the Halex reaction is traditionally used on aromatic substrates, it can also be applied to non-aromatic substrates, albeit with some modifications. Such an example was reported by Novikov *et al*., in which they described a halogen exchange (Halex) reaction of methyl 2-bromo-3-phenyl-2*H*-azirine-2-carboxylate (**1.63**) with TBAF to give methyl 2-fluoro-3-phenyl-2*H*-azirine-2-carboxylate (**1.64**) alongside a more classical Finkelstein conversion of methyl 2-bromo-3-phenyl-2*H*-azirine-2-carboxylate (**1.63**) to the corresponding methyl 2-iodo-3-phenyl-2*H*-azirine-2-carboxylate (**1.65**) (Scheme **1.11**).[44]

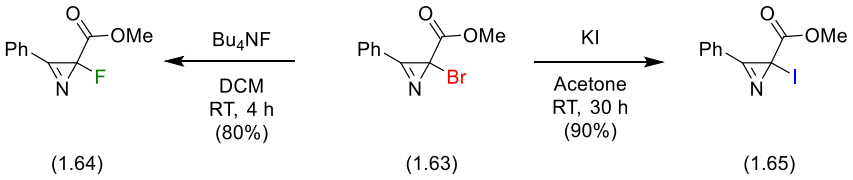

(1.64) (1.63) (1.65)

Scheme 1.11: Halex like reactions in non-aromatic substrates.

1.3.2.4 Double Aromatic Finkelstein Reaction of 3,5-Dichloro/bromo BODIPYs

In this work we will use the term aromatic Finkelstein to define an S_NAr reaction process in which can aromatic chloride or bromide is converted to the corresponding iodide. Such a reaction aromatic Finkelstein has been examined by Hall *et al*. to form 3,5-diiodo BODIPYs, in which they reacted 3,5-dichloro BODIPY (**1.66**) with a saturated solution of NaI in acetone at reflux to give 3,5-diiodo BODIPY (**1.68**) after 11 days. To increase the reaction rate, they examined the aromatic Finkelstein reaction with different high boiling point solvents (Table **1.1**), the best results being obtained using refluxing EtCN for 24 hours to give 3,5-diiodo BODIPY (**1.68**) in an isolated yield of 83%. Following this result, they also examined the aromatic Finkelstein reaction between 3,5-dibromo BODIPY (**1.67**) with a saturated solution of NaI in EtCN at reflux. for 1.5 hours. Surprisingly, the desired 3,5-diiodo BODIPY (**1.68**) was isolated in an excellent yield of 100% under these conditions, suggesting that the aromatic Finkelstein with 3,5-dibromo BODIPY (**1.67**) may occur via a concerted S_NAr mechanism (Table **1.1**).[45]

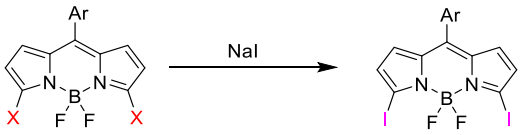

(1.66), X = Cl
(1.67), X = Br

(1.68)

Entry	Starting material	Solvent	Temp./ °C	Time/ h	Yield[a]/%
1	(**1.66**), X = Cl	acetone	Reflux	264	69[b]
2	(**1.66**), X = Cl	DMF	110	24	0
3	(**1.66**), X = Cl	DMSO	100	24	0
4	(**1.66**), X = Cl	MeCN	Reflux	36	84[b][c]
5	(**1.66**), X = Cl	MeCN	Reflux	72	100
6	(**1.66**), X = Cl	EtCN	Reflux	24	83
7	(**1.67**), X = Br	EtCN	Reflux	1.5	100

Table 1.1: Double aromatic Finkelstein reaction of 3,5-dichloro/bromo BODIPYs. [a] Isolated yield of following column chromatography. [b] Conversion by ^{19}F NMR. [c] 5% yield of corresponding 3-chloro-5-iodo-BODIPY.

1.3.2.5 Nucleophilic Aromatic Substitution (S_NAr) of 3,5-halogenated BODIPYs

3,5-Halogenated BODIPYs are useful synthetic intermediates, as they allow for further functionalisation at the 3,5-positions. For example, 3,5-halogenated BODIPYs can react via nucleophilic aromatic substitution reactions (S_NAr), in which a nucleophile displaces a halogen leaving group. Dehaen and coworkers examined the S_NAr reactions of 3,5-dichloro BODIPYs with various nitrogen, oxygen, and sulfur centred nucleophiles to produce 3-substituted or 3,5-disubstituted BODIPYs. The selective formation of 3-substituted BODIPYs or 3,5-disubstituted BODIPYs can be controlled by altering the reaction conditions, with low temperatures, stoichiometric quantities of nucleophile, and short reaction times favouring 3-substituted-BODIPY products, whilst higher temperatures, excess nucleophile, and long reaction times favouring 3,5-disubstituted BODIPY products (Scheme **1.12**).[39]

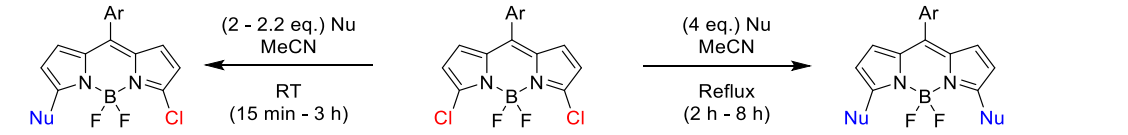

(1.70), Nu = piperidine, (74%)
(1.71), Nu = aniline, (69%)
(1.72), Nu = $EtOOCCH_2SH$/ Et_3N, (65%)
(1.73), Nu = diethyl malonate/ NaH, (67%)

(1.69)

(1.74), Nu = piperidine, (78%)
(1.75), Nu = aniline, (64%)
(1.76), Nu = $EtOOCCH_2SH$/ Et_3N, (70%)
(1.77), Nu = diethyl malonate/ NaH, (71%)

Scheme 1.12: Nucleophilic aromatic substitution of 3,5-dichloro BODIPY (**1.69**) (Ar = *p*-(Me)-C_6H_4-).

A further example of an S_NAr reaction of 3,5-dichloro BODIPYs with *N*-centred nucleophiles was reported by Matano *et al*., in which they examined the reaction between 3,5-dichloro BODIPY (**1.78**) and 10 equivalents of pyrazole in THF under reflux, resulting in the selective formation of 3-substituted BODIPY (**1.79**) as the major product (Scheme **1.13**).[46] They also examined the reaction of 3,5-dichloro BODIPY (**1.78**) with 2 equivalents of pyrazole, which was deprotonated with 2 equivalents of NaH, in THF at room temperature, which resulted in the formation of 3,5-disubstituted BODIPY (**1.80**) in high yield (Scheme **1.13**).

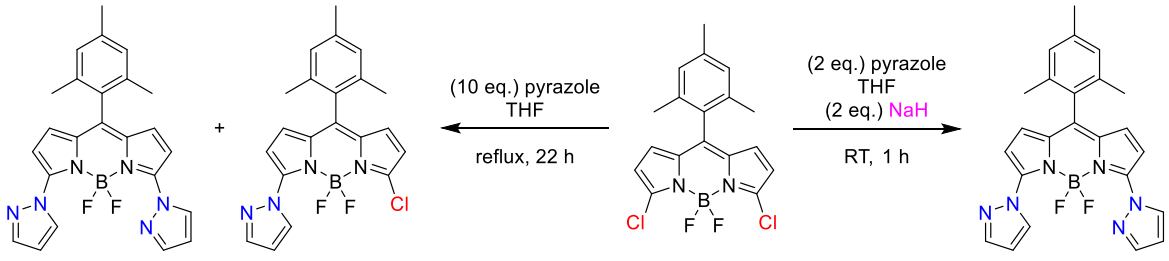

(18%)
(1.80)

(61%)
(1.79)

(1.78)

(87%)
(1.80)

Scheme 1.13: Nucleophilic aromatic substitution of 3,5-dichloro BODIPY (**1.78**) with pyrazole.

Matano and coworkers further expanded the S_NAr reaction of 3,5-dichloro BODIPY (**1.78**) with a range of *N*-heteroaromatic nucleophiles including 3-(2-pyridyl)-pyrazoles, 3-phenylpyrazoles, and carbazoles, in combination with deprotonation by NaH. This resulted in the formation of 3,5-disubstituted BODIPYs in moderate to high yields for all systems (Table **1.2**).

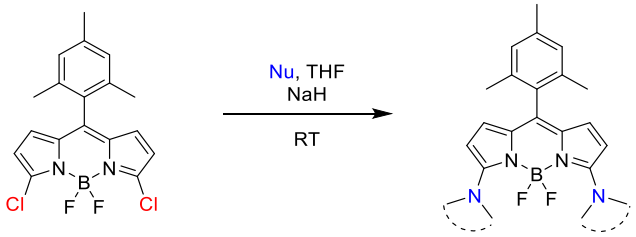

(1.78)

Entry	Nucleophile	Eq. Nu	Eq. NaH	Time/ h	Yield/%
1	2-(1*H*-pyrazol-3-yl)pyridine	4	4	2	42
2	3-phenyl-1*H*-pyrazole	2.5	2.5	2	81
3	9*H*-carbazole	5	5	3	72

Table 1.2: Selected examples S_NAr reaction of 3,5-dichloro BODIPY (**1.78**) with *N*-heteroaromatic nucleophiles.

Further discussion of the S_NAr reactions of 3,5-halogenated BODIPYs with *N*-centred nucleophiles is presented in Chapters 2 and 4.

1.3.2.6 Suzuki Miyaura Cross-Coupling Reactions of 3,5-Dihalogenated BODIPYs

Palladium-catalyzed cross-coupling reactions are widely employed in organic chemistry, due to their reliability, flexibility, particularly for the formation of C-C bonds. Therefore, we can utilize such palladium-catalyzed cross-coupling reactions with halogenated BODIPYs as a method to make substituted systems. In particular, 3,5-dihalogenated BODIPYs are capable of undergoing palladium-catalysed cross-coupling reactions (*e.g.*, Stille, Negishi, Heck, Suzuki, and Sonogashira),[47] facilitating the formation of new C-C bonds from C-halogen bonds. In this work we will focus on the Suzuki Miyaura cross-coupling reaction for BODIPY functionalisation, therefore herein we will explore and compare the performance of 3,5-dichloro-, 3,5-dibromo and 3,5-diiodo BODIPYs in Suzuki Miyaura cross-coupling reactions.

The Suzuki Miyaura cross-coupling reaction has been previously used in BODIPY chemistry, for functionalisation at every possible position including, 3,5-positions,[47,48] 2,6-positions,[49,50] 1,7-positions,[51]and *meso*. More recently, Hall *et al*., examined a double Suzuki Miyaura cross-coupling between 3,5-halogenated BODIPYs and phenyl boronic acid under Suzuki conditions, comparing the

reactivity of dichloro, dibromo, and diiodo-systems. They observed the highest isolated yield of 3,5-diphenyl BODIPY (**1.81**) from 3,5-diiodo BODIPY (**1.68**), with dichloro, dibromo systems giving lower yields of the disubsituted products (90% I > 51% Br > 6% Cl), and in the case of 3,5-dichloro BODIPY (**1.66**) with trace amounts of 3-chloro-5-phenyl BODIPY (**1.82**) (Table **1.3**).

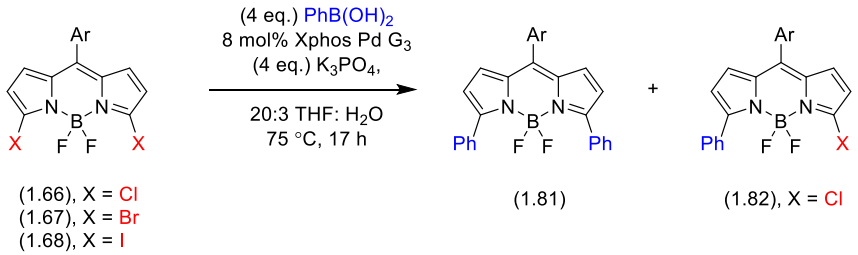

(1.66), X = Cl
(1.67), X = Br
(1.68), X = I

(1.81)

(1.82), X = Cl

Entry	Starting material	Yield (1.81)[a]/ %	Yield (1.82)[a]/ %
1	(**1.66**), X = Cl	6	4
2	(**1.67**), X = Br	51	0
3	(**1.68**), X = I	90	0

Table 1.3: Comparative Suzuki Miyaura cross-coupling reactions of 3,5-dihalogenated BODIPYs.

[a] Isolated yields following column chromatography.

1.3.2.7 Conclusions

In this section, we have presented examples from the literature illustrating the regioselectivity of electrophilic aromatic substitution chemistry (S_EAr) in BODIPYs, resulting in the formation of 3,5-dihalogenated BODIPYs, and then we have highlighted their reactivity potential in nucleophilic aromatic substitution reactions (S_NAr). Furthermore, we have demonstrated their suitability for palladium cross-coupling reactions. Next, the focus of the introduction will shift to introducing various types of chirality into BODIPYs.

1.4 Chirality in BODIPYs

The structure of BODIPY itself is inherently achiral due to its planar structure and high degrees of symmetry. However, introducing chirality to BODIPY molecules is important because it enables them to exhibit chiroptical properties, such as electronic circular dichroism (ECD) and circularly polarized luminescence (CPL), rendering them valuable for diverse applications.

In this section, we will therefore explore strategies which have been used to introduce chirality into BODIPYs and we will provide selected examples from the literatures, along with a discussion of their chiroptical properties. Chiral BODIPYs are known that show axial, helical and propeller-like chirality, as well as labile helicity.

1.4.1 Axially Chiral Bis and Tris BODIPYs

Molecules which possess an axis of chirality, often arising from a restricted rotation about a single bond and known as axially chiral. Bari *et al*., reported the synthesis of axially chiral 3,3′-linked bis(BODIPY)(**1.10**) via an oxidative C-C coupling of two BODIPY units, resulting a racemic mixture which was resolved by preparative chiral HPLC. The two BODIPY units are linked at the 3,3′-positions by a C-C single bond, which due to the adjacent methyl groups shows restricted rotation resulting in a pair of atropisomers.[52] Interestingly, the ECD spectra of axial chiral 3,3′-linked bis(BODIPY)(**1.10**) shows an intense exciton couplet due to strong coupling of the transition dipole moments of the two BODIPY units (Figure **1.12**). In addition, the CPL spectra of two enantiomers of 3,3′-linked bis(BODIPY)(**1.10**) showed mirror image signals with high $|g_{lum}|$= 3.8 x 10^{-3}. This g_{lum} value is similar to the reported values of other chiral BODIPYs systems, and other CPL-SOMs (Figure **1.12**).

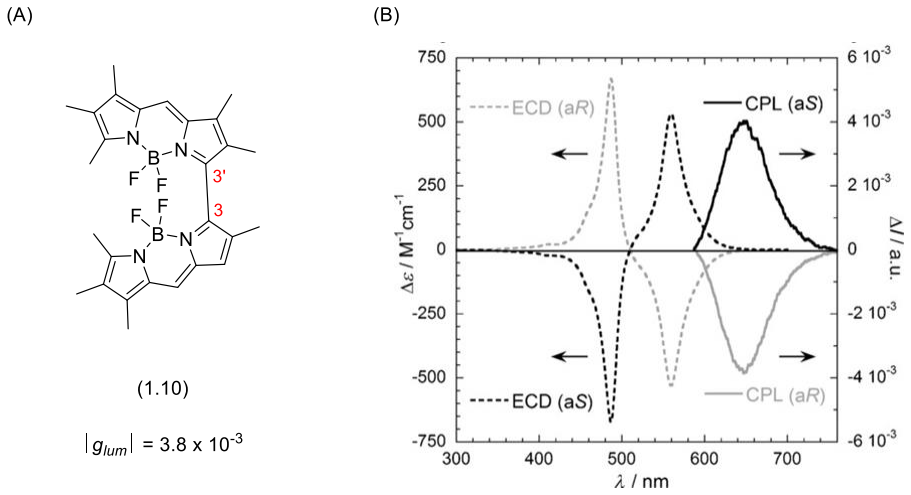

Figure 1.12: (A) Axially chiral 3,3′-linked bis(BODIPY)(**1.10**); (B) ECD and CPL spectra of resolved enantiomers (adapted from Bari *et al*.).[52]

In 2014, Akkaya *et al*. reported more examples of axial chirality within BODIPYs.[53] They described the synthesis of a novel bis BODIPY (**1.83**) which shows rotationally restriction around the *meso*,2'-bond, due to a double methyl-methyl clash, resulting in the generation of a racemic mixture of atropoisomeric bis(BODIPY)(**1.83**) which was subsequently separated by chiral HPLC. ECD spectra were obtained for both enantiomers, showing mirror image spectra. Akkaya also employed a similar strategy to synthesize atropoisomeric tris-BODIPY (**1.84**) (Figure **1.13**).

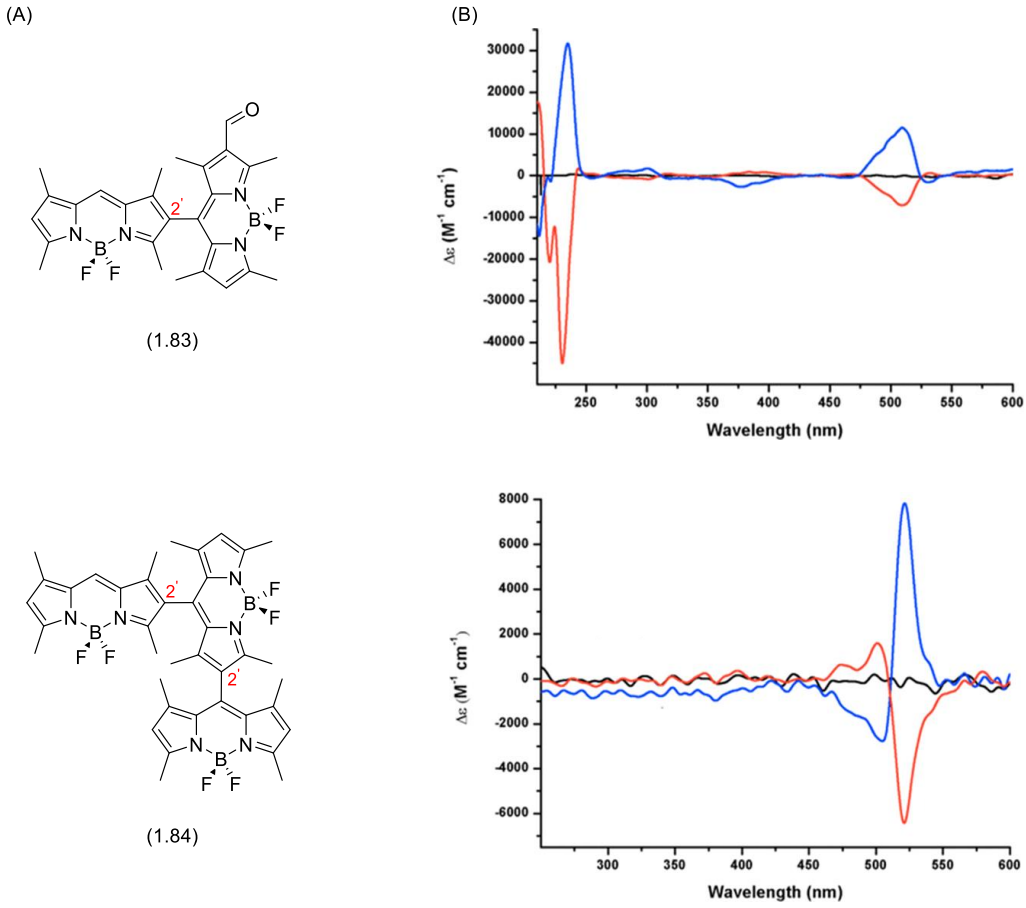

Figure 1.13: (A) Atropoisomeric bis BODIPY (**1.83**) and tris-BODIPY (**1.84**); (B) ECD spectra of resolved enantiomers (red and blue lines) of both bis BODIPY (**1.83**) and tris-BODIPY (**1.84**) (adapted from Akkaya *et al*.).[53]

1.4.2 Axially Chiral SpiroBODIPYs

In an elegant study outlined by de la Moya *et al*., they proposed an approach for inducing axial chirality in BODIPY molecules based on an axially chiral C_2 structure.[54] The strategy presented by de la Moya *et al*. involved attaching an axially chiral 1,1′-binaphthyl (BINOL) moiety to the boron centre of a planar BODIPY chromophore, thereby inducing a chiral perturbation of achiral BODIPY. Initially, an achiral BODIPY was activated with $AlCl_3$, followed by chelation of the boron centre with enantiopure BINOL, to give direct access to the corresponding (*R*)-(**1.6**) and (*S*)-(**1.6**)-BODIPYs. This straightforward synthetic route has access to both enantiomers of the chiral spiroBODIPYs, (*R*)-(**1.6**) and (*S*)-(**1.6**), which exhibited mirror image CPL spectra (Figure **1.14**).

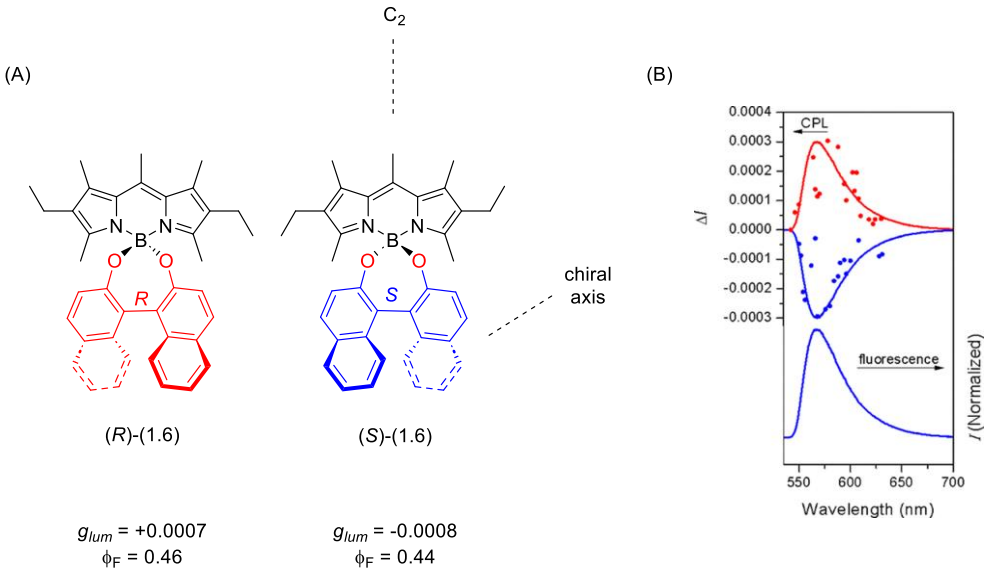

Figure 1.14: (A) Chiral spiroBODIPYs. (B) Upper curves: CPL spectra of single enantiomers ((*R*)-(**1.6**) (red) and (*S*)-(**1.6**) (blue). Lower curve: fluorescence spectra (adapted from de la Moya *et al*).[54]

1.4.3 Helical Chirality Mono BODIPYs

Helically chiral molecules are characterised by an intrinsically helical structure, commonly observed in compounds like helicenes. Helicenes are molecules composed of at least 5 non-linearly fused aromatic rings, where the steric clash of terminal rings causes a helical twist in the structure, resulting in one end of the helicene being positioned below the other. The helical chirality of these molecules can be denoted as *P* and *M,* indicating a clockwise or anti-clockwise direction when moving from the proximal or near component of the structure toward the distal or far component.

Work in 2016 by Hall *et al*. described the synthesis of a series of helically chiral mono *N,N,O,O*-BODIPYs, which were formed as racemates and subsequentially separated by chiral HPLC.[55] The chiroptical properties for the resolved enantiomers (*P*)-(**1.2**) and (*M*)-(**1.2**), displayed mirror image CPL spectra with a high g_{lum} for a CPL-SOM. Interestingly, the degree of helical twist in the molecules appeared to positively influence CPL (Figure **1.15**).

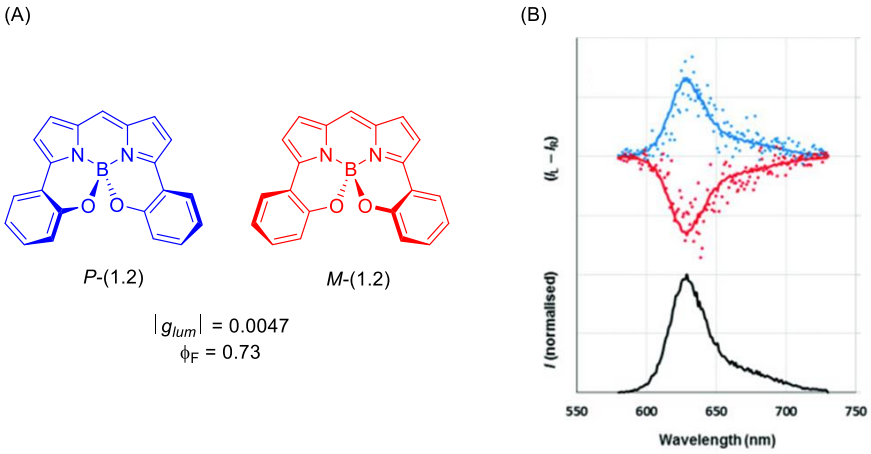

Figure 1.15: (A) Structures of helically chiral mono *N,N,O,O*-BODIPYs (*P*)-(**1.2**) and (*M*)-(**1.2**); (B) Normalised CPL spectra (red and blue) for both enantiomers (*P*)-(**1.2**) (blue) and (*M*)-(**1.2**) (red) and fluorescence spectra (black).[55]

1.4.4 Helical Chirality Bis BODIPYs

Nabeshima *et al.* described the enantioselective synthesis of chiral bis BODIPYs, which showed a figure-of-eight helicity.[56] These chiral bis BODIPYs feature a twisted structure arising from the tetrahedral geometry around the boron centres. Following the successful synthesis of chiral bis BODIPY (**1.85**), the resulting racemic mixture underwent resolution using chiral HPLC. Subsequently, CPL spectra were obtained for both enantiomers, (*P,P*)-and (*M,M*)-BODIPYs, revealing mirror image CPL signals in the red region with a very high luminescence dissymmetry factor (g_{lum}), one of the highest $|g_{lum}|$ recorded for a BODIPY system. Thus, the chiral bis (*P,P*)-and (*M,M*)-BODIPYs show high CPL quantum efficiency of 5.22 x 10^{-3} ($|g_{lum}|$ = 0.009, ϕ_F = 0.58), and are one of the most efficient CPL fluorophores reported in the literature (Figure **1.16**).

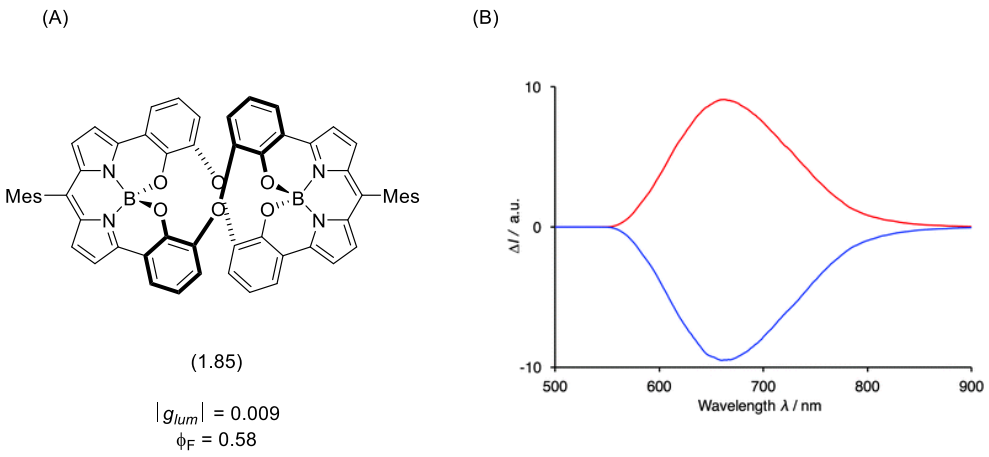

Figure 1.16: (A) Twisted bis BODIPY; (B) CPL spectra of resolved enantiomers (*P,P*)-isomer (red) and (*M,M*)-isomer (blue) (adapted from Nabeshima *et al*).[56]

1.4.5 Labile Helicity in BODIPYs

De la Moya *et al*. described a pioneering approach to designing chiral BODIPYs featuring axial chirality with labile helicity.[16] In this study, they explored the synthesis of chiral bis(haloBODIPY)s and elucidated their chiroptical properties. Chiral bis(haloBODIPY) were synthesised through double S_NAr chemistry, in which 3,5-dichloro BODIPY reacted with an enantiopure chiral diamine linker. CPL spectra of chiral bis(haloBODIPY) (**1.86**) were obtained, showing a preferential helical conformation in chloroform with a good g_{lum} = +0.001, and emission in the visible region (Figure **1.17**).

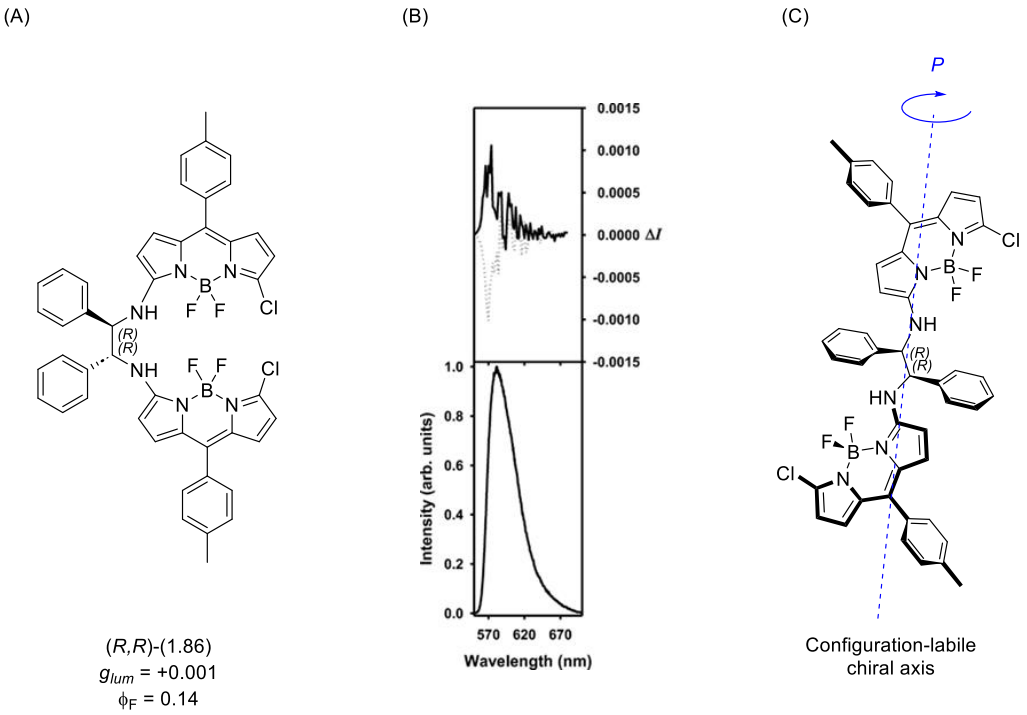

Figure 1.17: (A) Chiral bis(haloBODIPY) (*R,R*)-(**1.86**); (B) Upper curves: CPL spectra of (*R,R*)-(**1.86**) (solid line) and (*S,S*)-(**1.11**) (dashed line). Lower curve: total luminescence; (C) Computed helical structure of (*R,R*)-(**1.86**), showing preferred *P* configuration for the chiral helix (adapted from de la Moya *et al*).[16]

1.4.6 Propeller Chirality in BODIPYs

Propeller chirality emerges when multiple aromatic groups around are arranged around the central axis of a molecule, including twisting or handedness. Mori *et al.* presented an example of a *quasi* propeller chirality within BODIPYs, resulting from a heptaarylBODIPY, and elucidated their chiroptical properties.[57]

In the example presented by Mori *et al*., a BODIPY molecule was functionalised with seven aromatic rings bearing chiral (*R*)-1-methyl-propyloxy groups. The heptaaryl groups around the BODIPY arrange

themselves into an either a *P* or *M* propeller-like structure, due to steric clash. The pendant chiral groups, favour one of the propeller orientations, thus the CPL spectra of (*R*)-heptaarylBODIPY (**1.13**) in methylcyclohexane at 25 °C exhibited a weak signal. The CPL of (*R*)-heptaarylBODIPY (**1.13**) was enhanced at low temperatures, -120 °C, and exhibited a strong positive signal (g_{lum} = +2.0 x 10^{-3}) at 650 nm. These authors attributed the CPL enhancement at low temperature to the formation of head-to-tail propeller dimers in solution (Figure **1.18**).

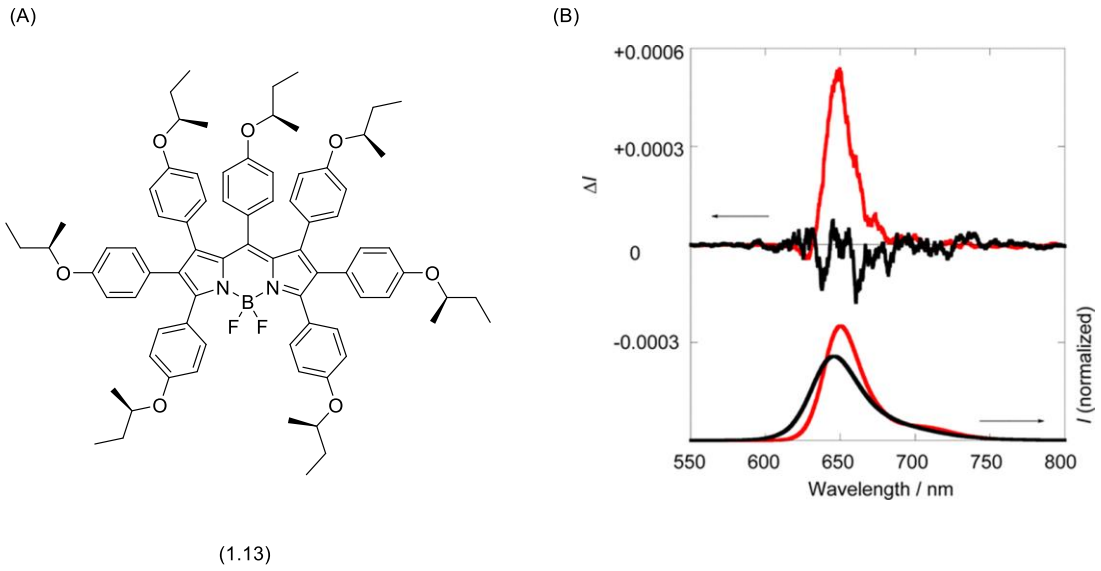

Figure 1.18: (A) (*R*)-HeptaarylBODIPY (**1.13**); (B) Upper curves: CPL spectra of (*R*)-HeptaarylBODIPY (**1.13**) at 25 °C (black) and at –120 °C (red). Lower curve: total luminescence, in methylcyclohexane (adapted from Mori *et al.*).[57]

1.4.7 Chirality at the Boron Centre

Introducing chirality at the boron centre of BODIPYs induces asymmetry through chiral perturbation of the planar fluorophore. In a recent study by Nabeshima *et al*., they described the synthesis of helically chiral *N,N,O,C*-BODIPYs as a racemic mixture, followed by resolution via preparative chiral HPLC.[58] These helically chiral *N,N,O,C*-BODIPYs display absorption and emission in the red to near-infrared region, owing to their extended π-conjugation within their structures. ECD spectra for both enantiomers were obtained, showing mirror image signals with a moderate Cotton effect at 655 nm. Unfortunately no CPL studies that have been conducted on this system to date (Figure **1.19**).

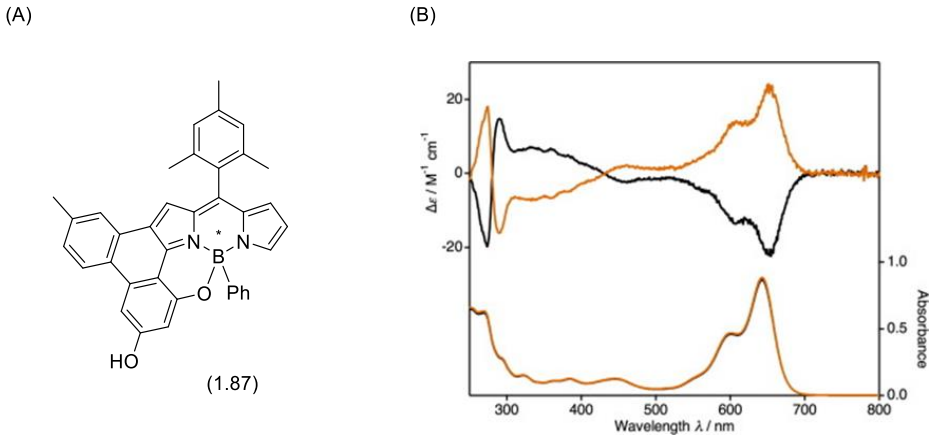

Figure 1.19: (A) Helically chiral *N,N,O,C*-BODIPY (**1.87**); (B) Upper curves: CD spectra of resolved enantiomers ((*R*)-(**1.87**)(orange) and (*S*)-(**1.87**)(black). Lower curve: UV-Vis spectra (adapted from Nabeshima *et al.*).[58]

More recently, He *et al.,* reported on the enantioselective synthesis of chiral BODIPYs containing a boron-stereogenic centre, employing a palladium-catalysed enantioselective intramolecular C-H arylation.[59] In this approach, aryl groups were first tethered to boron via a hydroxyl group, followed by an enantioselective intramolecular Pd catalysed C-C bond formation, using a TADDOL-based phosphonite ligand. This resulted in a series of compounds in which the boron atom was part of a 6, 7, 8 or 9 membered ring systems, in which both enantiomers could be access depending on the choice of ligand stereochemistry. In all cases the enantiomeric BODIPY pairs displayed mirror image ECD spectra in the visible region, however, no CPL studies were reported (Figure **1.20**).

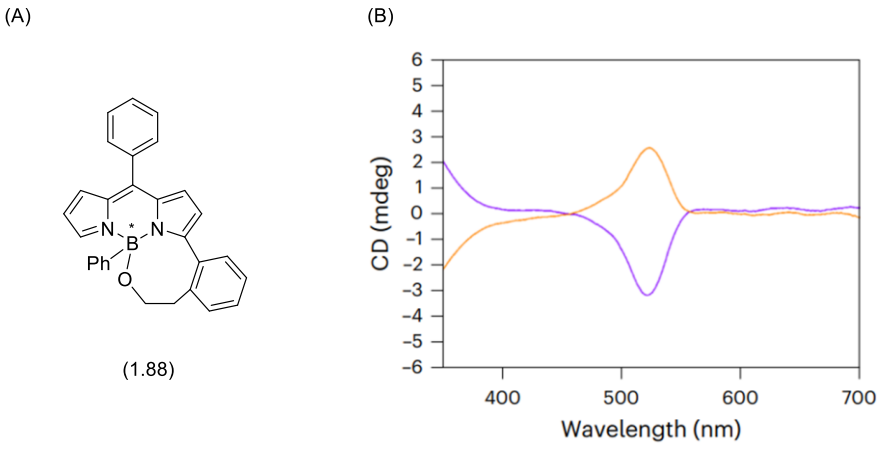

Figure 1.20: (A) Chiral 8 membered ring containing BODIPY containing a boron-stereogenic centre (**1.88**); (B) ECD spectra of (*R*)- (orange) and (*S*)-enantiomers (purple) (adapted from He *et al.*).[59]

1.4.8 Conclusions

The limited research into chiral BODIPYs capable of CPL emission, may be attributable to the challenges associated their synthesis. Although a number of enantioselective syntheses are now known, most approaches result in the generation of racemic mixtures, requiring resolution by chiral HPLC into their individual enantiomers.

A potential approach towards new chiral BODIPYs, which addresses the issue of racemic mixture generation, is through the use of chiral auxiliaries. Incorporating a chiral auxiliary into the synthesis should allow the selective formation of an enantiomer of choice. In addition, chiral auxiliary approaches resulting in the initial formation of diastereomers that can be separated using traditional laboratory techniques such as column chromatography, thereby simplifying the isolation of the desired chiral BODIPY.

1.5 Chiral Auxiliaries

A chiral auxiliary refers to a chiral group temporarily introduced into a molecule to control the stereochemical result during synthesis. Many chiral auxiliaries commonly used are derived from natural products such as amino acids, carbohydrates, and terpenes. Chiral auxiliaries are widely utilised in the synthesis of enantiomerically and diastereomerically compounds. (Figure **1.21**).[60,61]

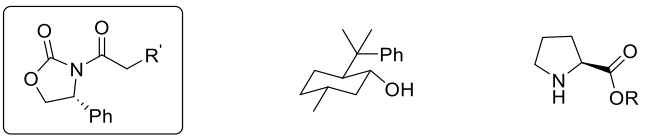

(1.89) (1.90) (1.91)

Evans (1981) Corey (1975) Yamada (1969)

Figure 1.21: Selected chiral auxiliaries that have been used in asymmetric synthesis.

One example of chiral auxiliaries is demonstrated in Evans' utilisation of oxazolidinones in stereoselective aldol reactions.[62] Evans *et al.* showed that chiral oxazolidinone (**1.92**) can be acylated to generate a chiral *N*-acyloxazolidinone (**1.89**). Subsequently, enolization in the presence of a dibutylboron trifate resulted in the formation of the corresponding (*Z*) enolate, which was shown to undergo a subsequent diastereoselective aldol reaction with a range of aldehydes, to form the 1,2-*syn* products (**1.95**) (Scheme **1.14**).[60]

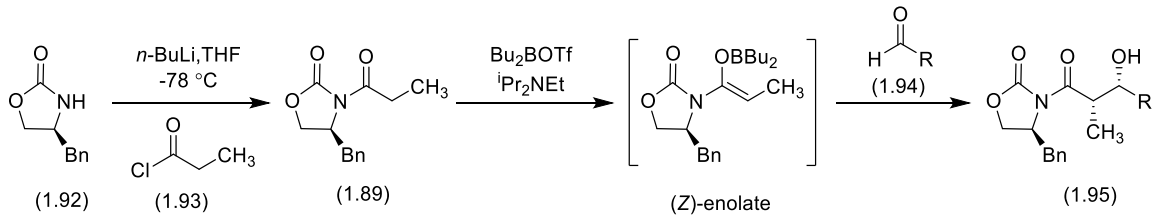

Scheme 1.14: Stereoselective Evans aldol reaction using oxazolidinone chiral auxiliary.

After controlling the diastereoselectivity, the oxazolidinone auxiliary can then be removed under a wide range of conditions, depending on the desired functional group to be generated (Scheme **1.15**).

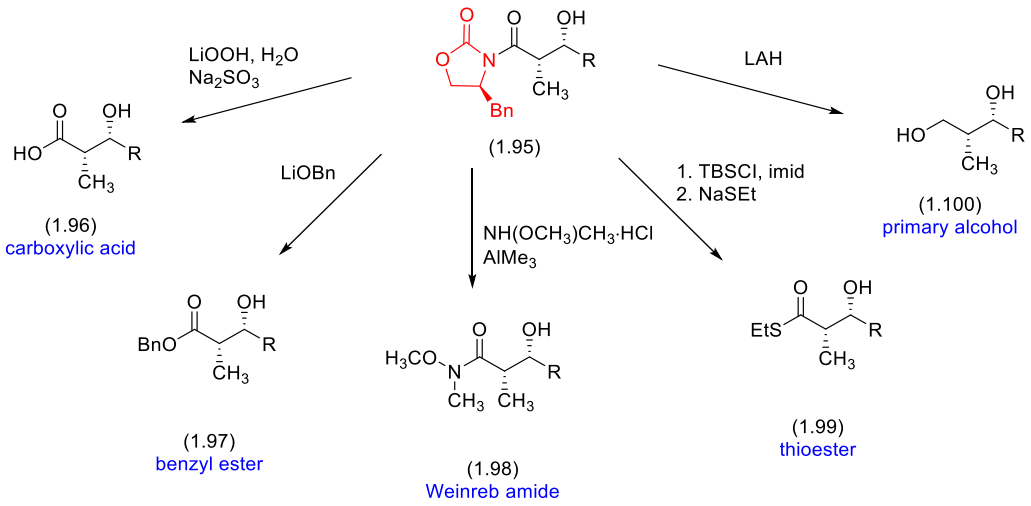

Scheme 1.15: Removal of oxazolidinone auxiliary under various conditions.

1.5.1 Chirality Transfer in Organic Synthesis

A related method to control stereochemistry in organic synthesis is known as chirality transfer, wherein stereochemical information is typically transmitted from type of chirality to another, during the formation of the target molecule.[63]

1.5.1.1 Point-to-Axial Chirality Transfer

A point-to-axial chirality transfer approach was reported by Aggarwal *et al.*, in which they described the enantiodivergent synthesis of allenes.[64] A point-chiral boronic ester (**1.103**) was prepared through the homologation of α-seleno alkenyl boronic ester (**1.101**) with lithiated carbamate (**1.102**). The prepared point-chiral boronic ester (**1.103**) could then be transformed into two different allenes depending on the reaction conditions. Under oxidative conditions using *m*CPBA the (*S*)-point-chirality of the boronic ester was transferred via a *syn* elimination to give a (*P*)-allene, while under basic alkylative conditions using MeOTf *anti* elimination is achieved to give the corresponding (*M*)-allene (Scheme **1.16**).

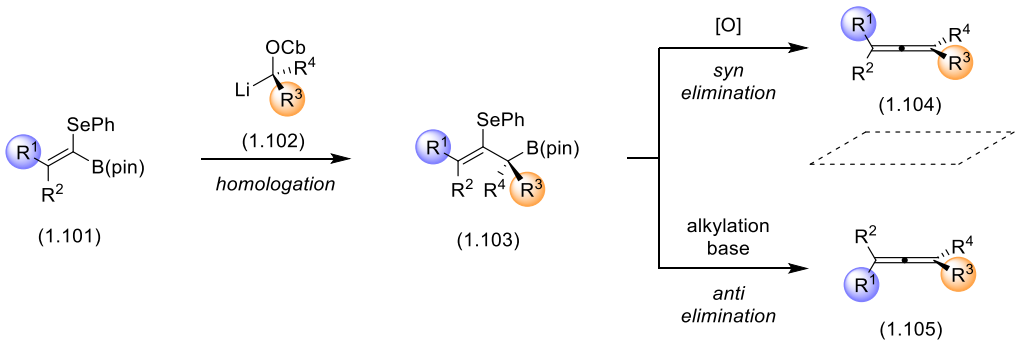

Scheme 1.16: Point-to-axial chirality transfer from point-chiral boronic esters to give allenes.

1.5.1.2 Point-to-Helical Chirality Transfer

Point-to-helical chirality transfer has previously been demonstrated by Carbery *et al*., who demonstrated a highly diastereoselective synthesis of a helicenoidal DMAP organocatalyst.[65] Point chiral (*S*)-pyridyl triyne (**1.106**), undergoes a Rh-catalysed [2 + 2 + 2] triyne cycloisomerisation, thereby controlling the formation of a (*P*)-helical DMAP with a yield of 88% and a high diastereomeric ratio (*dr* = 95:5) (Scheme **1.17**).

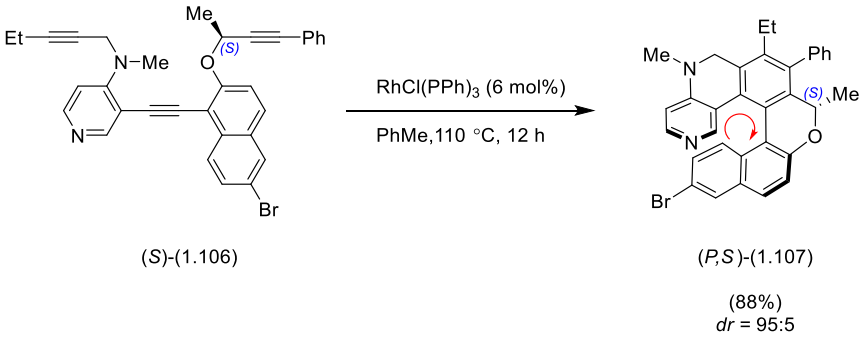

Scheme 1.17: Point-to-helical chirality transfer in the synthesis of helicenoidal DMAP organocatalyst.

1.6 Project Aims

The overall aim of this thesis is to develop new methods to synthesis chiral BODIPY systems, with a focus on the use of a point-to-helical chirality transfer strategy employing chiral auxiliaries to regulate the formation of helical chirality in the targeted BODIPYs.

In chapter 2, the synthesis of 3,5-dibromo and 3,5-diiodo BODIPYs employing methodologies established by the Hall group will be discussed. Our primary aim is to enhance the overall yields of 3,5-dibromo and 3,5-diiodo BODIPYs. We hypothesise that both 3,5-dibromo and 3,5-diiodo BODIPYs will serve as suitable intermediates for both S_NAr chemistry and Suzuki Miyaura cross-coupling. Furthermore, we will analyse our strategies for the synthesis of chiral cyclic bis BODIPYs, while

exploring the synthetic strategy to produce chiral bis BODIPYs utilising the prepared 3,5-dibromo and 3,5-diiodo BODIPYs.

In chapter 3 we will discuss the development of point-to-helical chirality strategies in the diastereoselective synthesis of BODIPYs. We aim to investigate the effectiveness of various enantiopure chiral amino alcohols as chiral auxiliaries in controlling the chirality of the target helically chiral BODIPYs. Additionally, we will present and discuss the photophysical and chiroptical properties of each pair of diastereomeric BODIPYs formed and explore the synthesis of further analogues.

Chapter 4 will utilise data from our point-to-helical chirality approach developed in chapter 3, for extension into the synthesis of helically chiral *N,N,O,C*-BODIPYs containing a 7-membered ring. Furthermore, we will analyse our proposals for synthesising symmetrical helically chiral BODIPYs, including those with two 7-membered rings through a double S_NAr reaction. Through the use of chiral auxiliaries, presented in chapter 3, we aim to control the chirality of the resulting BODIPYs. Moreover, we will discuss novel approaches for accessing enantiopure helically chiral *N,N,O,O*-BODIPYs through a chiral resolution approach, building upon previous work undertaken by the Hall group. Finally, we will explore various methods for separating the final compounds, while also measuring their photophysical and chiroptical properties.

In chapter 5, we will expand use of our point-to helical chirality approach to synthesise a wide range of novel helical chiral BODIPY architectures, including dimeric and trimeric helically chiral *N,N,O,C*-BODIPY systems. Moreover, in this chapter, we will develop synthetic routes for stacked helically chiral bis BODIPYs, with the aim of generating architectures for visible spectrum solution-phase CPL.

Chapter 2. Synthesis of 3,5-Dibromo and 3,5-Diiodo BODIPYs

2.1 Introduction

In this chapter we will discuss the synthetic approach to 3,5-dibromo and 3,5-diiodo BODIPYs as common starting materials in the synthesis of helically chiral BODIPYs. We focused on 3,5-dibromo and 3,5-diiodo BODIPYs as they can be used to introduce functionality at the 3- and 5-positions through both S_NAr chemistry and Suzuki Miyaura cross-coupling (Scheme **2.1**). Additionally, we will explore the synthetic strategy to make chiral bis BODIPYs (Scheme **2.1**).

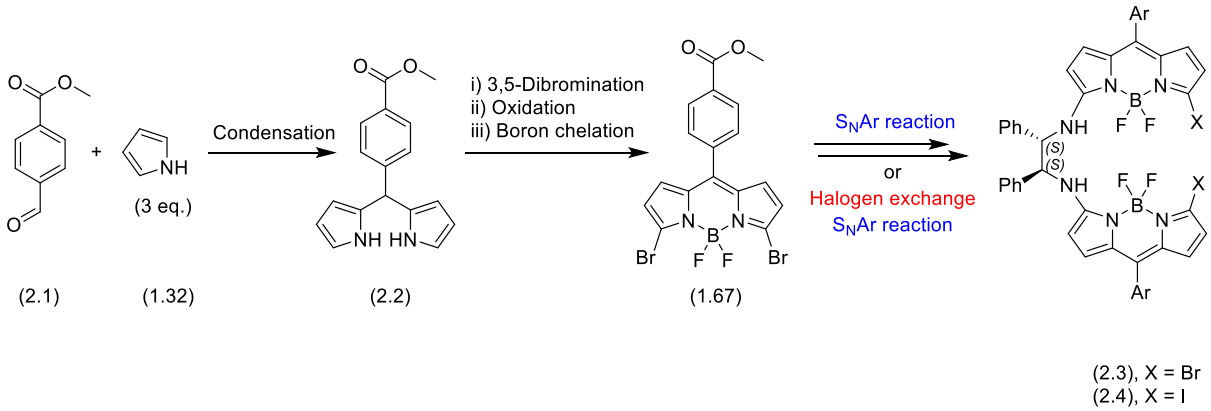

Scheme 2.1: General planned approach to synthesis 3,5-dihalo-BODIPYs to access chiral BODIPYs (Ar = *p*-($MeCO_2$)-C_6H_4-).

2.2 Regioselective Bromination of Dipyrromethanes and BODIPYs via Electrophilic Aromatic Substitution (S_EAr)

Electrophilic aromatic substitution (S_EAr) of BODIPYs is well known as a method for the synthesis of complex BODIPY systems. In particular S_EAr has been shown to result in preferential reaction at the 2,6-positions of a BODIPY. For example, in 2011, the group of Hao *et al.* reported the regioselective bromination of BODIPYs, in which they examined stepwise hexa bromination reactions.[49] When BODIPY (**2.5**) was reacted with two equivalents of bromine in DCM a high yield of 2-bromo BODIPY (**2.6**) was obtained. By sequentially increasing the equivalents of bromine used to 3 equivalents, 2,6-dibromo-BODIPY (**2.7**) became the major product. Subsequentially, 2,3,5,6-tetrabromo-BODIPY (**2.8**) could be formed with 6 eq., and 1,2,3,5,6,7-hexabromo BODIPY (**2.9**) with 300 eq. of bromine. This demonstrates that bromination occurs first at the 2,6-positions, then at the 3,5-, and finally at the 1,7-positions, indicating the order of reactivity towards S_EAr reactions (Scheme **2.2**).

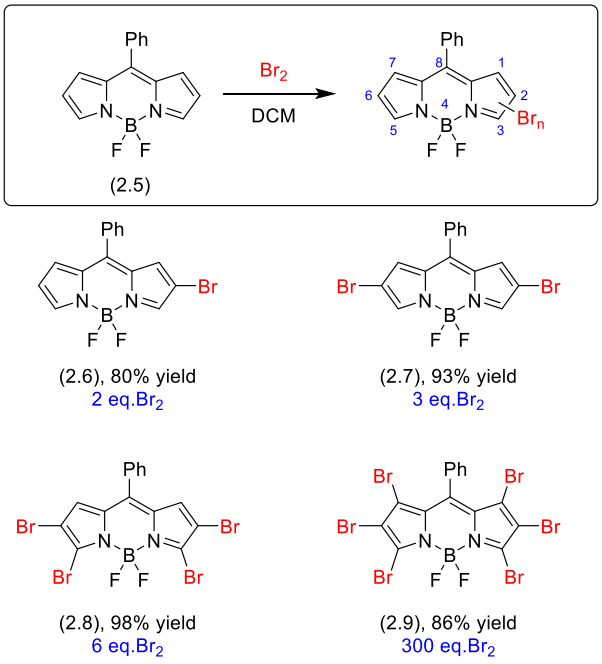

Scheme 2.2: Stepwise bromination of *meso*-phenyl substituted BODIPYs.

Due to the observed regioselectivity, electrophilic bromination at the 3,5-positions of unsubstituted BODIPYs is a challenge, therefore, an alternative synthetic approach is needed. In 2010, the group of Ravikanth reported the synthesis of 3,5-dibromo BODIPY (**2.13**) using dipyrromethane (**2.10**) as a key starting material in a one-pot multistep reaction, followed by chelation. They have examined electrophilic bromination at low temperature between dipyrromethane (**2.10**) and two equivalents of NBS at -78 °C in THF to form the α,α-dibromo dipyrromethane (**2.11**).[66] Following which an oxidation with one equivalent of DDQ at room temperature, was carried out to give the corresponding α,α- or 3,5-dibromo dipyrromethene (**2.12**). The crude mixture was purified by flash chromatography, and the resultant compound was treated with $BF_3.OEt_2$ in presence of a base at room temperature to give desired 3,5-dibromo BODIPY (**2.13**) in a 64% overall yield following purification (Scheme **2.3**).

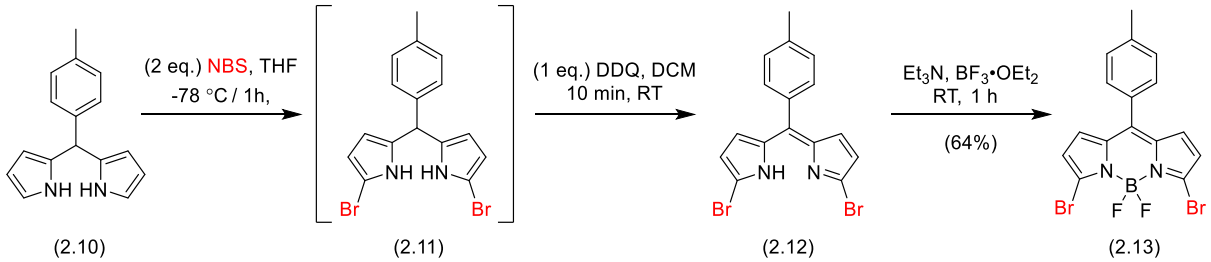

Scheme 2.3: Synthesis of 3,5-dibromo BODIPY (**2.13**) from dipyromethane (**2.10**)

In summary, Ravikanth *et al*. demonstrated that regioselective substitution can be achieved at the 3- and 5- positions, which are the most reactive sites toward S_EAr for the dipyrromethanes. We planned to use Ravikanth's approach as a key route to 3,5-disubsituted BODIPYs.

2.3 Results and Discussion

2.3.1 Synthesis of Common Starting Material 3,5-Dibromo BODIPY (**1.67**)

In this section, we will discuss the proposed synthetic route to access the first target in this project 3,5-dibromo BODIPY (**1.67**). Our synthetic route for the preparation of 3,5-dibropmo-BOIDPY (**1.67**) includes: (i) condensation reaction between methyl 4-formylbenzoate (**2.1**) and 1*H*-pyrrole (**1.32**) to form dipyrromethane (**2.2**), (ii) bromination of dipyrromethane (**2.2**) at the α,α-positions, followed by an oxidation to give α,α-dipyrromethene (**2.14**), and finally (iii) a boron chelation of α,α-dibromo dipyrromethene (**2.14**) give the target 3,5-dibromo BODIPY (**1.67**). This synthetic route was based on the work of Ravikanth *et al*., Dehaen *et al*., and subsequentially that of the Hall's research group (Scheme **2.4**).[34,67]

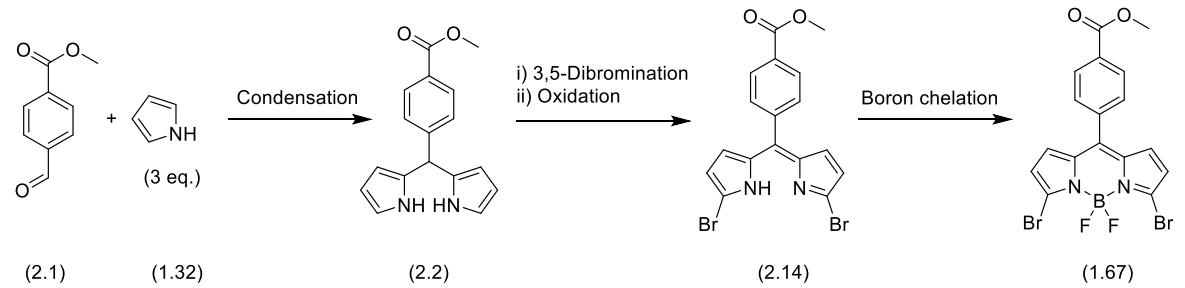

Scheme 2.4: Planned general approach for the synthesis of 3,5-dibromo BODIPY (**1.67**).

2.3.2 Synthesis of Dipyrromethane (**2.2**) via Acid Catalysed Condensation

We planned to synthesize dipyrromethane via an acid-catalysed condensation reaction. Our procedure was based on the work of Dehaen *et al*., in which they reported the synthesis of a range of dipyrromethanes via the condensation between aryl aldehydes and 1*H*-pyrrole in an aqueous acid condition.[68]

Therefore, in our first attempt, we mixed a solution of 0.05 M HCl with three equivalents of 1*H*-pyrrole (**1.32**) and then one equivalent of methyl 4-formylbenzoate (**2.1**), which was crushed into a fine powder using a mortar and pestle to increase surface area and rate of dissolution. The reaction mixture was stirred at room temperature for 4 hours, after which dipyrromethane (**2.2**) precipitated from solution as a pale pink powder. Following a simple filtration, the resulting filter cake was washed with water and petroleum ether to give the desired dipyrromethane (**2.2**) in an excellent yield of 86 % (Scheme **2.5**).

Inspection of the ^{1}H NMR of the dipyrromethane (**2.2**) after filtration showed a very high degree of purity, making it suitable to for use for in the next step without further purification. However, for analysis purposes, we purified a 0.1 g portion of the crude dipyrromethane (**2.2**) by column

chromatography. The structure of dipyrromethane (**2.2**) was confirmed by ^{1}H NMR spectra which showed a distinctive one proton singlet signal at 5.53 ppm, corresponding to proton at the *meso*-position.

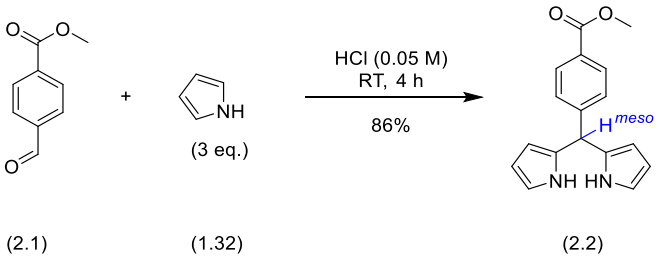

Scheme 2.5: Synthesis of dipyrromethane (**2.2**) via a Dehaen condensation.

As the dipyrromethane (**2.2**) was a key starting material in the project, the condensation reaction was performed many times during the course of the project with different reaction scales (up to 33 mmol) following purification by filtration, giving consistently good yields of dipyrromethane (**2.2**), between 78 % and 93 % and an overall standard deviation of 4.5% (Table **2.1**).

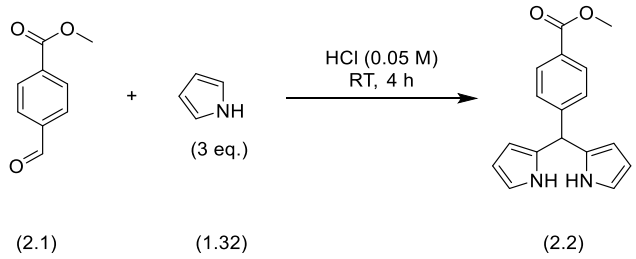

Entry	Scale/ mmol	Yield[c]/% and [standard deviation]/%
1[a]	11.0-12.2	78-88 [3.8]
2[b]	24.4-25.5	87-93 [2.4]
3	33.0	86

Table 2.1: Synthesis of dipyrromethane (**2.2**). [a] The reaction was repeated nine times. [b] The reaction was repeated six times. [c] Isolated yield after filtration.

Following our successful synthesis of dipyrromethane (**2.2**), next we wished to examine the one-pot bromination, oxidation, and boron chelation of dipyrromethane (**2.2**) to give our target 3,5-dibromo BOIDPY (**1.67**).

2.3.3 Synthesis of 3,5-Dibromo BODIPY (**1.67**)

Next, we planned to synthesize 3,5-dibromo BODIPY (**1.67**) via a double S_EAr reaction, following the developed route by the Hall group. In a first attempt, we dissolved dipyrromethane (**2.2**) in THF and stirred at -78 °C for 30 min, after which two equivalents of recrystallised NBS (hot to cold

recrystallisation of 1 g NBS in 10 mL of water) was added in two portions over 30 min. The reaction mixture was stirred at -78 °C for 1 hour. After which, one equivalent of DDQ dissolved in THF was added dropwise under -78 °C and stirred for 10 min. The reaction mixture was left to warm to room temperature before quenching with a saturated solution of Na_2SO_3 to reduce any remaining oxidants. Following an aqueous work up, the organic layer was dried over $MgSO_4$, and the solvent was removed under reduced pressure. Subsequently, under nitrogen atmosphere, the crude α,α-dibromo dipyrromethene (**2.14**) was dissolved in anhydrous DCM and treated with 2.5 equivalents of $BF_3.OEt_2$ and 3.1 equivalents of DIPEA. The reaction mixture was stirred at room temperature for 1 hour. Following an aqueous work up and purification of the resulting crude material by silica gel column chromatography gave the desired 3,5-dibromo BODIPY (**1.67**) in 40% yield over 3 steps (approximately 74% yield per step) (Scheme **2.6**).

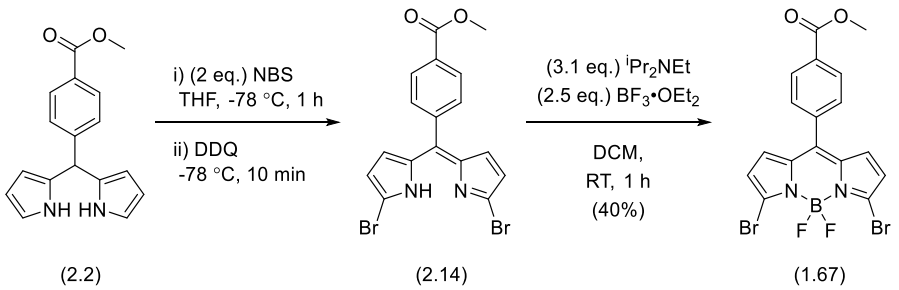

Scheme 2.6: Synthesis of 3,5-dibromo BODIPY (**1.67**) through bromination, oxidation, and boron chelation reaction.

The inspection of the ^{1}H NMR spectrum confirmed the formation of the desired 3,5-dibromo BODIPY (**1.67**) along with residual solvent signals corresponding to petroleum ethers. We attempted to remove the residual petroleum ether under reduced pressure (*e.g*. high vacuum overnight), but this proved difficult. Therefore, DCM was used as the column chromatography solvent for future purifications to facilitate easier solvent removal and helped by removing the need to dry load the sample.

The structure of 3,5-dibromo BODIPY (**1.67**) was confirmed by analysis of NMR spectra. ^{1}H NMR showed two pair of roofed doublet signals at 6.74 ppm (d, *J* = 4.3 Hz, 2H) and 6.55 ppm (d, *J* = 4.3 Hz, 2H) corresponding to the four pyrrolic hydrogen atoms. The ^{11}B NMR showed a triplet at 0.63 ppm (t, *J* = 28.1 Hz) and ^{19}F NMR showed a quartet at -146.8 ppm (q, *J* = 27.6 Hz), that gave us confidence BF_2 moiety had been successfully added. For further confirmation of the structure, crystals were grown by slow evaporation of a DCM solution. A single crystal was analysed by SCXRD, giving a triclinic crystal system with a P-1 space group with 2 molecules in the unit cell (Z = 2). The crystal structure confirms that the presence of two bromine atoms at the 3,5-positions (Figure **2.1**).

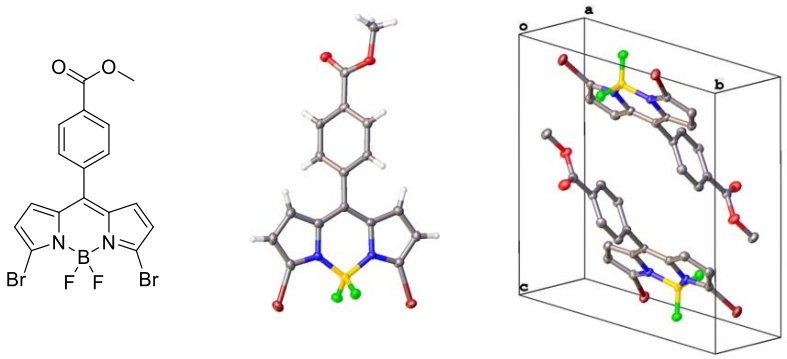

Figure 2.1: 3,5-Dibromo BODIPY (**1.67**); (A) Molecular structure; (B) Single crystal X-ray; (C) Packing of the molecules in the unit cell.

The synthesis of 3,5-dibromo BODIPY (**1.67**) were repeated multiple times during the project with different scales. The synthesis of 3,5-dibromo BODIPY (**1.67**) was successful on scales up 9.0 mmol, although the yields observed were variable from 40 to 62 % (Table **2.2**).

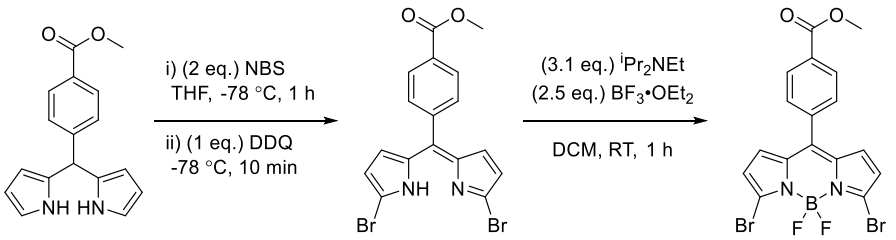

Entry	Scale of dipyrromethane/ mmol	Yield [a]/%
1	5.0	40
2	5.0	44
3	4.0	41
4	5.0	56
5	6.0	62
6	8.0	60
7	9.0	42

Table 2.2: Synthesis of 3,5-dibromo BODIPY (**1.67**) through bromination, oxidation, and boron chelation. [a] Isolated yield of 3,5-dibromo BODIPY (**1.67**) following column chromatography.

In attempts to optimize the conditions for synthesizing 3,5-dibromo BODIPY (**1.67**), several reaction variables were explored for the bromination reaction, including the addition of NBS in two portions over 5 or 10-minute periods, the addition of DDQ either as a solid or in THF solution, and variation in

the reaction atmosphere (air or N_2). In addition, for the boron chelation reaction, we tested different equivalents of $BF_3.OEt_2$ and DIPEA. Unfortunately, a wide range of yields (18-60%) were observed (Table **2.3**), with no clear pattern. We postulate that the inconsistent yields may be due in part to the formation a number of by-products by TLC and crude ^{1}H NMR, which maybe be over brominated BODIPYs or products with alternative bromination patterns, which can occur if the dipyrromethane is oxidised under the reaction conditions, prior to bromination.[51,67]

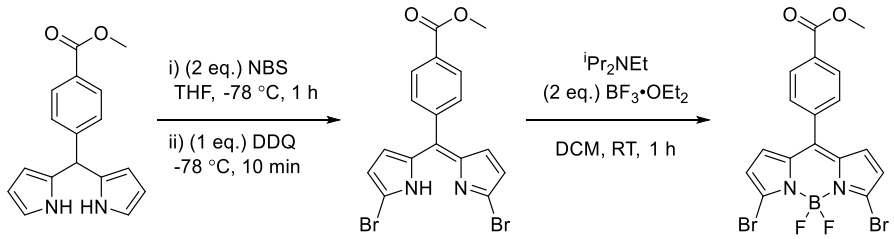

(2.2) (2.14) (1.67)

Entry	Scale of dipyrromethane/ mmol	Atmos.[a]	Eq. DIPEA	DDQ	Chelation Reaction time/h	Yield[b]/%
1	7.1	N_2	2.2	Solid	1	33
2	7.1	N_2	2.5	Solid	1	46
3	7.1	air	2.5	Solid	1	27
4	14.2[c]	N_2	2.2	Solution[d]	18	18
5	8.0	N_2	2.5	Solution[d]	15	55
6	8.0	N_2	2.5	Solid	1	60
7	12.0	air	2.5	Solid	1	41

Table 2.3: Synthesis of 3,5-dibromo BODIPY (**1.67**) through bromination, oxidation, and boron chelation. [a] Atmosphere of bromination and oxidation reaction. [b] Isolated yield of 3,5-dibromo BODIPY (**1.67**) following column chromatography. [c] Reaction was split into two round bottom flasks, each on a 7.1 mmol scale, and combined for chelation reaction. [d] DDQ in THF solution.

As it was difficult to determine the source of the inconsistent overall yield, we decided to focus initially on the investigation of bromination/oxidation step and subsequently on the boron chelation step by separating the process and isolating the intermediate α,α-dibromodipyrromethene (**2.14**).

2.3.4 Electrophilic Aromatic Substitution (S_EAr) Bromination and Oxidation of Dipyrromethane (**2.2**)

Following our plan, we next examined the bromination/oxidation reaction under our standard conditions followed by purification by column chromatography, prior to a separate chelation step.

In the first attempt, a solution of THF and dipyrromethane (**2.2**) was stirred at -78 °C for 30 min, prior to the addition of the reagents. Following the addition of two equivalents of recrystallized NBS in two portions over 10 min, the reaction mixture was stirred for 1 hour at -78 °C. DDQ was then added in small portions, and the reaction was stirred for a further 10 min at -78 °C. The reaction mixture was left to warm to room temperature for 30 min before quenching with saturated solution of Na_2SO_3. Following an aqueous work-up and purification by column chromatography the desired α,α-dibromo dipyrromethene (**2.14**) was isolated in low yield of 17 %.

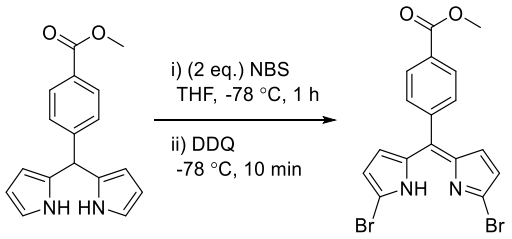

(2.2) (2.14)

Entry	Scale/ mmol	Cooling time/min	Yield [a]/%
1	6.4	30	17
2	5.4	60	Quant.
3	5.4	60	67
4	5.4	60	65
5	21.6[b]	60	59

Table 2.4: Synthesis of α,α-dibromo dipyromethene (**2.14**) by bromination/oxidation. [a] Isolated yield following column chromatography. [b] Reaction was split into four round bottom flasks, each on a 5.4 mmol scale, and combined for work-up and purification.

In a second attempt, we cooled the THF solution of dipyrromethane (**2.2**) to -78 °C for 1 hour prior to the addition of NBS, and the previous procedure was then followed. In this case a quantitative yield was obtained, following column chromatography. The bromination reaction was repeated several times on the same reaction scale and with the same reaction conditions, giving yields between 59-67%. It should be noticed that we used DCM as an eluent for chromatography, despite the high

retention factor (R_f = 0.7), due to the poor solubility of the product in other organic solvents (Table **2.4**).

After successfully optimisation of the regioselective bromination/oxidation step, next we will examine the boron chelation.

2.3.5 Boron Chelation of α,α-Dibromo dipyromethene (**2.14**)

We planned to examine boron chelation reaction, using boron trifluoride diethyl etherate in presence of base. Therefore, under a nitrogen atmosphere, purified α,α-dibromo dipyromethene (**2.14**) was dissolved in dry DCM and treated with 2 equivalents of $BF_3.OEt_2$ and 2.2 equivalents of DIPEA. The reaction mixture was stirred at room temperature for 1 hour. Following an aqueous work up and purification by column chromatography the desired 3,5-dibromo BODIPY (**1.67**) was isolated in a yield of 47 % (Table **2.5**, Entry 1). The lower yield for this reaction was due to the presence of starting material at the end of the reaction, observed by ^{1}H NMR. In a second attempt, we repeated the chelation reaction on a larger scale using 2.5 equivalents of DIPEA. In this case, following work-up and column chromatography, 3,5-dibromo BODIPY (**1.67**) was isolated in a quantitative yield (Table **2.5**, Entry 2). Following these optimised conditions, the chelation reaction was performed many times during the project, with high yields obtained (Table **2.5**, Entry 3-6).

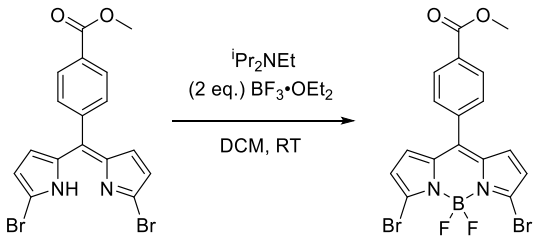

(2.14) (1.67)

Entry	Scale/ mmol	Eq. DIPEA	Reaction time/h	Yield[a]/%
1	1.1	2.2	1	47[b]
2	4.6	2.5	1	100
3	6.2	2.5	1.5	96
4	6.6	2.5	1	Quant.
5	7.2	2.5	1	86
6	7.2	2.5	1	82

Table 2.5: Synthesis of 3,5-dibromo BODIPY (**1.67**). [a] Isolated yield following column chromatography. [b] Crude reaction product still contained starting material (starting material: product, 1:2 ratio by ^{1}H NMR).

Splitting the synthesis of 3,5-dibromo BODIPY (**1.67**) into two parts, bromination/oxidation and boron chelation, provided a clear insight into which steps were more challenging. The poor overall yields, when a previous combined bromination/oxidation/boron chelation reaction was attempted can be attributed to inconsistent bromination/oxidation outcomes, as the chelation step gives reproducibly high yields when performed on purified material.

Both methods to synthesize 3,5-dibromo BODIPY (**1.67**), either one-pot without isolating α,α-dibromo dipyrromethene (**2.14**) or two-pots with an intermediate isolation step, work efficiently. However, we found that isolating α,α-dibromo dipyrromethene (**2.14**) was a more convenient approach to synthesise 3,5-dibromo BODIPY (**1.67**) due to the consistency in the overall yield, despite the solubility issues encountered in purifying the α,α-dibromo dipyrromethene (**2.14**) intermediate by silica gel column chromatography.

Next, we planned to substitute the bromine atoms of 3,5-dibromo BODIPY (**1.67**) with iodine atoms to synthesize 3,5-diiodo BODIPY (**1.68**) via a double aromatic Finkelstein reaction. We wished to access 3,5-diiodo BODIPY (**1.68**) as it has been shown to give improved yields in palladium coupling reactions (*e.g*. Suzuki) in comparison to 3,5-dibromo BODIPY (**1.67**), and we then plan to use both 3,5-dibromo BODIPY (**1.67**) and 3,5-diiodo BODIPY (**1.68**) in future S_NAr reactions and Suzuki Miyaura cross-coupling.

2.3.6 Synthesis of 3,5-Diiodo BODIPY via Double S_NAr Reaction (Aromatic Finkelstein reaction)

Next, we planned to synthesize 3,5-diiodo BODIPY (**1.68**) by replacing bromine of 3,5-dibromo BODIPY (**1.67**) with iodine via a double aromatic Finkelstein reaction, also known as an halex or S_NAr reaction with iodide. We followed a procedure reported by Hall *et al*,. in which they have examined a double Finkelstein reaction of 3,5-dibromo BODIPY (**1.67**) in a refluxing saturated solution of NaI in propionitrile to obtain the desired 3,5-diiodo BODIPY (**1.68**). Interestingly, this reaction is thought to occur via a concerted double S_NAr (Scheme **2.7**).[45]

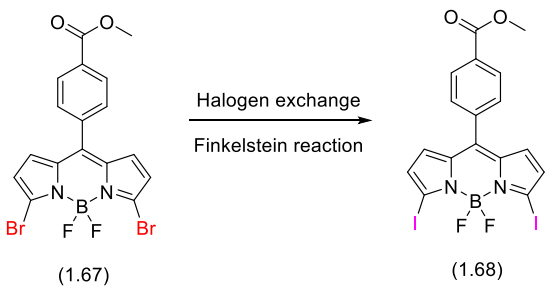

(1.67) (1.68)

Scheme 2.7: Planned halogen exchange via a double aromatic Finkelstein reaction.

Therefore, we reacted 0.4 mmol of 3,5-dibromo BODIPY (**1.67**) in a saturated solution of NaI in propionitrile at reflux for 1.5 hours. During the reaction, the colour of the reaction mixture changed from red to purple. The reaction was monitored by TLC which indicated the disappearance of the starting material and the formation of a new product. Following an aqueous work-up and purification by column chromatography the desired 3,5-diiodo BODIPY (**1.68**) isolated in high yield, 83 % (Table **2.6**).

The double Finkelstein reaction was preformed several times, including the examination of the scale-up of this reaction. High yields ranging from 75% to 91%, were consistently observed up to a 5.9 mmol scale (Table **2.6**).

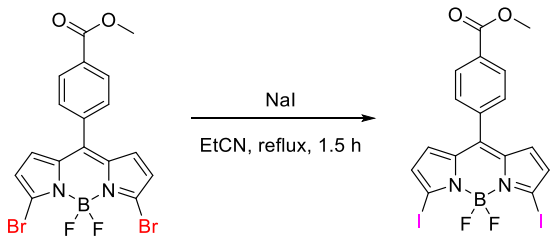

(1.67) (1.68)

Entry	Scale/ mmol	Yield [e]/% and [standard deviation]/%
1[a]	0.4-0.5	83-90 [3.5]
2[b]	1.1-1.6	75-89 [5.8]
3[c]	2.1-2.4	80-90 [7.1]
4[d]	5.9	75-91 [11.3]

Table 2.6: Synthesis of 3,5-diiodo BODIPY (**1.68**) via double Finkelstein reaction. [a] The reaction was repeated three times. [b] The reaction was repeated six times. [c] The reaction was repeated two times. [d] The reaction was repeated two times. [e] Isolated yield following column chromatography.

The structure of 3,5-diiodo BODIPY (**1.68**) was confirmed by ^{1}H NMR spectrum which showed two doublet signals at 6.72 ppm (d, *J* = 4.3 Hz, 2H) and 6.61 ppm (d, *J* = 4.2 Hz, 2H) corresponding to the pyrrolic protons. These are closer in shift, in comparison to the corresponding signals for 3,5-dibromo BODIPY (**1.67**), due to the change in electronegativity of the substituents. For further confirmation, the structure of 3,5-diiodo BODIPY (**1.68**) was validated by HRMS, which showed a peak at 558.8988 *m/z* which is consistent with a formula of $C_{17}H_{11}{}^{10}BFI_2N_2O_2$ $[M\text{-}F]^+$.

For further proof of the structure, crystals were grown by slow evaporation of a DCM solution. A suitable single crystal was submitted to SCXRD analysis, giving a triclinic crystal system with a P-1 space group with 2 molecules in the unit cell (Z = 2). The crystal structure confirmed the replacement of

bromine atoms with iodine (Figure **2.2**). Interestingly, this crystal structure is isostructural with that of 3,5-dibromo BODIPY (**1.68**) and matched a known crystal structure (CCDC: 2075824).

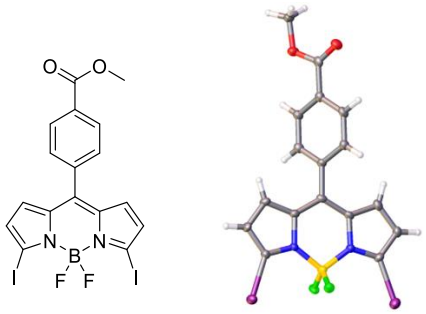

(1.68)

Figure 2.2: Single crystal X-ray structure of 3,5-diiodo BODIPY (**1.68**).

In conclusion, we have successfully synthesized both 3,5-dibromo BODIPY (**1.67**) and 3,5-diiodo BODIPY (**1.68**), in moderate to good yields over four or five synthetic steps respectively. 3,5-Dibromo BODIPY (**1.67**) and 3,5-diiodoBODIPY (**1.68**) have been prepared several times during the project, on scales of up to 12 mmol and 5 mmol or more, providing us with sufficient material to move on to examining the synthesis of chiral BODIPY systems.

2.4 Nucleophilic Aromatic Substitution (S_NAr) Reaction of Chiral Nucleophiles with 3,5-dihalogenated BODIPYs

In the second part of this chapter, we will explore our attempts to synthesize chiral bis BODIPYs linked together by flexible chiral linkers. Such chiral bis BODIPYs have been shown to exhibit interesting chiroptical properties and could be starting points for more complex chiral bis BODIPY systems (Scheme **2.8**)

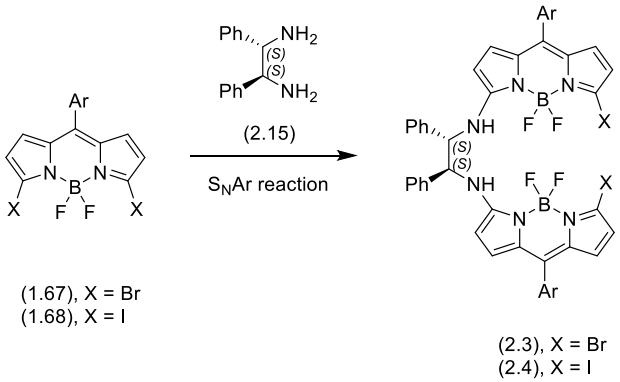

Scheme 2.8: Planned general approach for the synthesis of chiral bis BODIPYs via S_NAr reactions (Ar = *p*-($MeCO_2$)-C_6H_4-).

As a starting point for our work, we decided to synthesise chiral bis (3-halo-substituted BODIPYs) following a similar procedure reported in the literature by de la Moya's group, in which they have examined S_NAr reaction between 3,5-dichloro BODIPY (**1.69**) with (1*S*,2*S*)-1,2-diphenylethane-1,2-diamine (**2.15**) in MeCN, in presence of base. This resulted in the isolation of a major chiral bis (3-chloro-substituted BODIPYs) (**1.11**) and minor a chiral 3-chloro-substituted BODIPY (**2.16**) (Scheme **2.9**).[69]

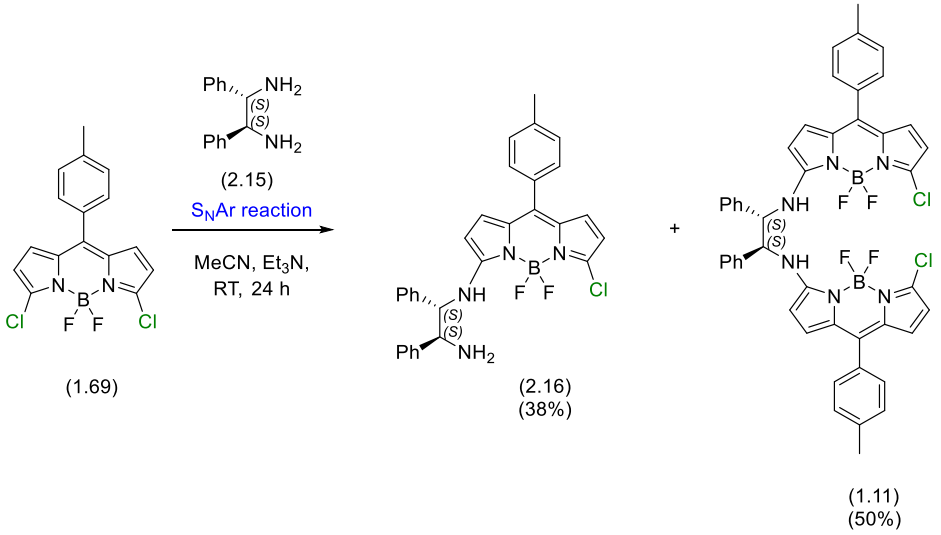

Scheme 2.9: Synthesis of chiral bis (3-chloro-substituted BODIPYs) by using chiral flexible linker by de la Moya.

We therefore planned to examine the S_NAr reaction between 3,5-dibromo BODIPY (**1.67**)/3,5-diiodo BODIPY (**1.68**) and (1*S*,2*S*)-1,2-diphenylethane-1,2-diamine (**2.15**) a chiral linker, to the reaction chemistry and their photophysical and chiroptical properties. We also planned to expand our approach to synthesise cyclic chiral BODIPY systems (**2.17**), as the more rigid motif could have the potential for improving the chiroptical properties (Scheme **2.10**).

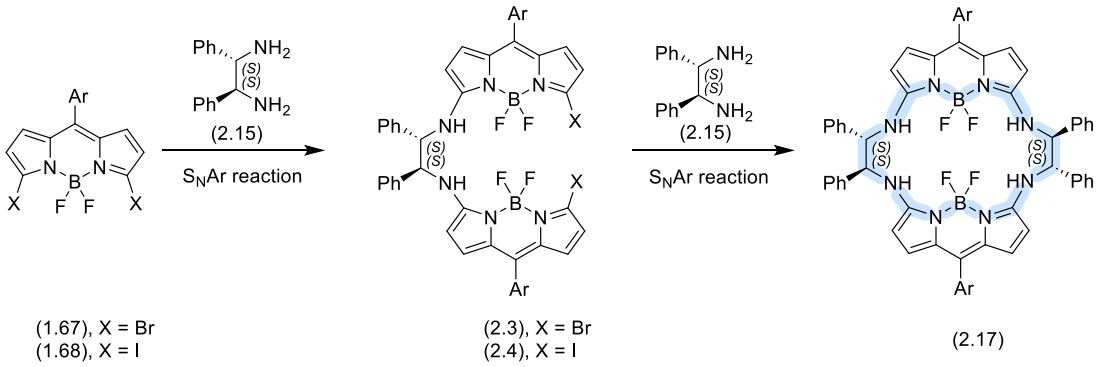

Scheme 2.10: Planned general approach to both chiral bis (3-halo-substituted BODIPYs) and cyclic chiral-BODIPY (Ar = *p*-($MeCO_2$)-C_6H_4-).

In our initial attempt, under nitrogen atmosphere, we reacted 1.8 equivalents of 3,5-dibromo BODIPY (**1.67**), 1 equivalent of (1*S*,2*S*)-1,2-diphenylethane-1,2-diamine (**2.15**) and 2 equivalents of Et_3N in MeCN at room temperature for 24 hours. The solvent was removed under reduced pressure, followed purification by column chromatography. Unexpectedly, only chiral 3-bromo-substituted BODIPY (**2.18**) was isolated in an excellent yield of 73%, with no dimer observed (Table **2.7**, Entry 1).

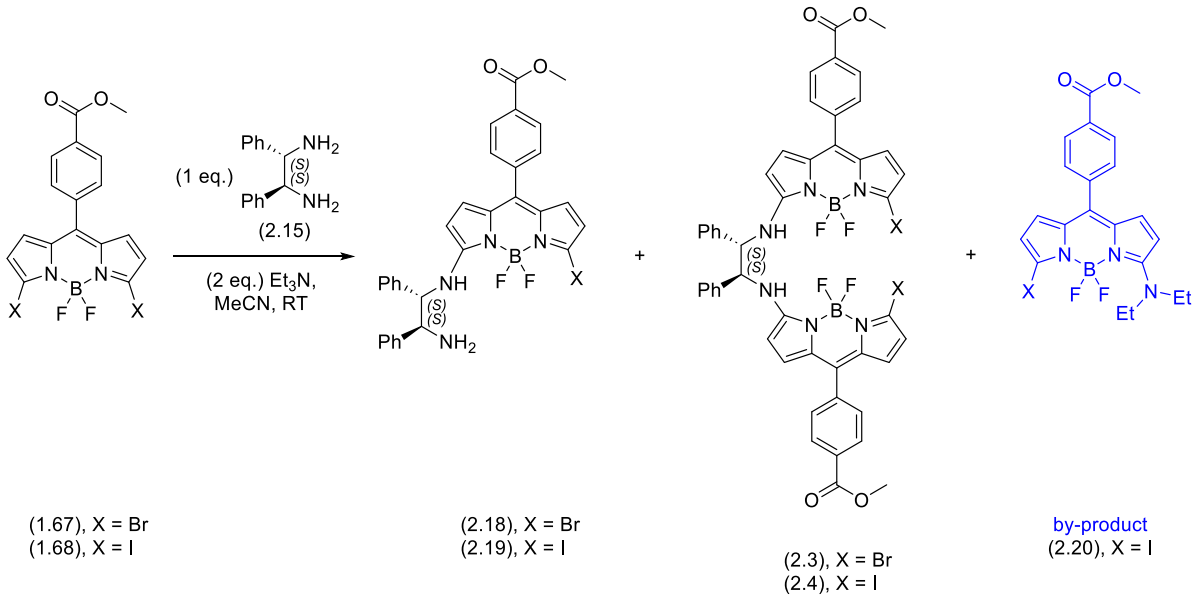

Entry	Starting material	Eq. of BODIPY	Reaction time/ h	Yield chiral mono BODIPY[a]/%	Yield chiral bis BODIPYs[a]/%
1	(**1.67**), X = Br	1.8	24	73 (**2.18**)	0
2	(**1.67**), X = Br	1.8	24	(3.4 (**2.3**):1(**1.67**):4 (**2.18**))[b]	
3	(**1.67**), X = Br	2	24	35 (**2.18**)	31 (**2.3**)
4	(**1.67**), X = Br	1.8	72	29 (**2.18**)	34 (**2.3**)
5	(**1.67**), X = Br	1.8	89	52 (**2.18**)	34 (**2.3**)
6[c]	(**1.68**), X = I	1.8	96	52 (**2.19**)	10 (**2.4**)
7	(**1.68**), X = I	1.8	120	Quant. (**2.19**)	29 (**2.4**)

Table 2.7: Synthesis of both chiral 3-halo-substituted BODIPYs and chiral bis(3-halo-substituted BODIPYs) via S_NAr reaction(s). [a] Isolated yield following column chromatography. [b] The ratio was measured by ^1H NMR of the crude product, isolated yields not obtained. [c] A mixed fraction containing both starting material (16%) and by-product (**2.20**) (10 %) was also isolated following column chromatography (Ar = *p*-($MeCO_2$)-C_6H_4-).

In a second attempt, we repeated the S_NAr reaction as before to validate the previous result. In this case crude ^1H NMR showed a that mixture of both chiral 3-bromo-substituted BODIPY (**2.18**), chiral

bis (3-bromo-substituted BODIPY) (**2.3**) were formed and that starting material 3,5-dibromo BODIPY (**1.67**) was still present, in an approximate ratio of (3.4 (**2.3**):1(**1.67**):4 (**2.18**)), suggesting that dimer formation is possible under these conditions (Table **2.7**, Entry 2). In a third attempt, 3,5-dibromo BODIPY (**1.67**) was increased to 2 equivalents with the other reaction conditions the same, giving chiral 3-bromo-substituted BODIPY (**2.18**) as a major product (35%) after chromatography, and chiral bis (3-bromo-substituted BODIPY) (**2.3**) in a 31% yield (Table **2.7**, Entry 3).

Further attempts to synthesize the chiral bis (3-bromo-substituted BODIPY) (**2.3**) focussed on extending the reaction time to 72 hours with the use of 1.8 equivalents of 3,5-dibromo BODIPY (**1.67**), resulting in chiral bis (3-bromo-substituted BODIPY) (**2.3**) being isolated in 34 % yield, with chiral 3-bromo-substituted BODIPY (**2.18**) in 29% yield (Table **2.7**, Entry 4). Additional extension of the reaction time to 89 hours, resulted in isolation of chiral 3-bromo-substituted BODIPY (**2.18**) as the major product in 52% yield, with chiral bis (3-bromo-substituted BODIPY) (**2.3**) in a slightly improved 34% yield (Table **2.7**, Entry 5).

Next, under our optimised S_NAr reaction conditions, we examined the reaction between 1.8 equivalents of 3,5-diiodo BODIPY (**1.68**) and 1 equivalent of (1*S*,2*S*)-1,2-diphenylethane-1,2-diamine (**2.15**), in MeCN, in presence of 2 equivalents of Et_3N at room temperature for 96 hours. The solvent was removed under reduced pressure. Following purification by column chromatography chiral 3-iodo-substituted BODIPY (**2.19**) and chiral bis (3-iodo-substituted BODIPY)(**2.4**) were isolated in 52% and 10%, respectively, along with a by-product 3-(*N*,*N*-diethylamine)-5-iodo BODIPY (**2.20**) (10%) and remaining starting material (16%) (see section 2.4.3 for further discussion about 3-(*N*,*N*-diethylamine)-5-iodo BODIPY (**2.20**) and 3-(*N*,*N*-diethylamine)-5-bromo BODIPY (**2.21**) by-products. In a final attempt, the rection time was extended to 120 hours, and chiral 3-iodo-substituted BODIPY (**2.19**) was isolated in quantitative yield with chiral bis (3-iodo-substituted BODIPY) (**2.4**) was isolated in improved yield 29% (Table **2.7**, Entry 7).

Since we postulated that chiral 3-halo-substituted BODIPYs (**2.18** and **2.19**) could react with themselves to form the target cyclic chiral-BODIPYs, therefore we kept a sample of chiral 3-bromo-substituted BODIPY (**2.18**) $CDCl_3$ in an NMR tube at room temperature for nine days. There was no observable change in ^1H NMR spectrum, suggesting that chiral 3-bromo-substituted BODIPY (**2.18**) did not reacted with itself under these conditions. Therefore, as a test reaction, we mixed chiral 3-iodo-substituted BODIPY (**2.19**) with base in MeCN under reflux for 48 hours. Following an aqueous work up and analysis of crude ^1H NMR, only starting material was recovered, and again no reaction observed (Scheme **2.11**)

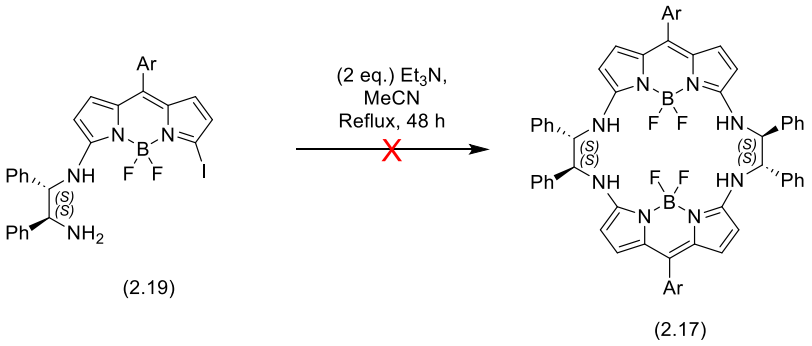

Scheme 2.11: Attempt to synthesis of cyclic chiral-BODIPY (**2.17**) under basic conditions (Ar = *p*-($MeCO_2$)-C_6H_4-).

The structure of both chiral 3-bromo-substituted BODIPY (**2.18**) and chiral bis (3-bromo-substituted BODIPY) (**2.3**) were confirmed by ^{1}H NMR. Along with the expected peaks for the unsymmetrical BODIPY, chiral 3-bromo-substituted BODIPY (**2.18**) showed two signals in the aliphatic range at 4.68 – 4.63 ppm (m, 1H) and 4.46 ppm (d, *J* = 2.7 Hz, 1H) corresponding to two CH group environments of (1*S*,2*S*)-1,2-diphenylethane-1,2-diamine, suggesting unsymmetrically substitution of the diamine.

For further confirmation of the structure, single crystals were grown through liquid-liquid diffusion DCM and hexane (1:3) under nitrogen atmosphere. A suitable single crystal was then examined by SCXRD analysis, giving a triclinic crystal system with P1 space group. A Flack parameter of -0.020(11) was measured, confirming the absolute stereochemistry as (1*S*,2*S*). Interestingly the crystal structure contained two molecules in the unit cell (Z = 2), showing an intramolecular NH---F H-bond interaction and an intermolecular NH---O H-bond between the two molecules (Figure **2.3**).

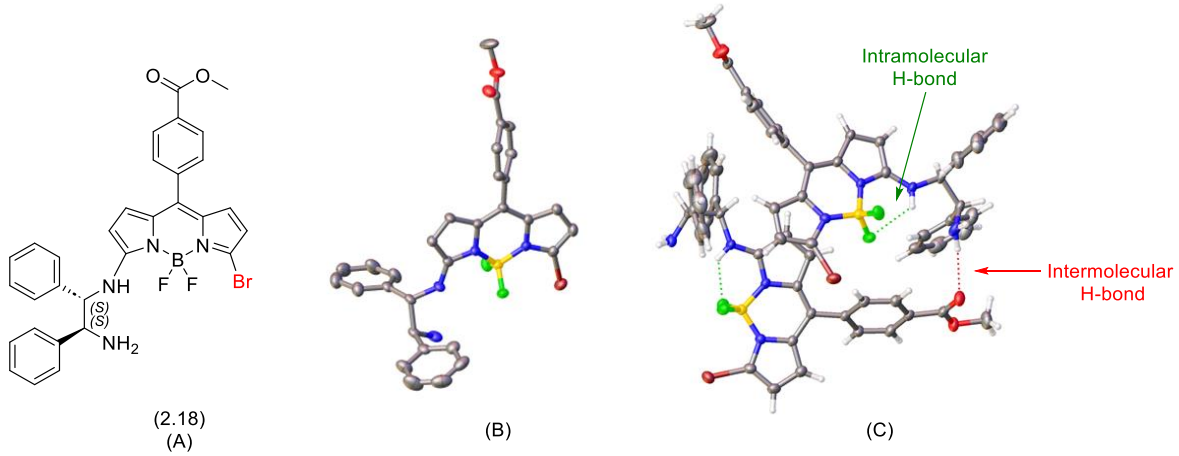

Figure 2.3: Chiral 3-bromo-substituted BODIPY (**2.18**); (A) Molecular structure; (B) Single crystal X-ray structure (hydrogen atoms omitted for clarity); (C) Intramolecular and intermolecular H-bonds within the crystal structure.

The structure of chiral bis (3-bromo-substituted BODIPY)(**2.3**) was confirmed by of ^{1}H NMR spectrum which showed one doublet signal at 5.03 ppm (d, *J* = 6.8 Hz, 2H) corresponding to two CH groups of the linking diamine unit, indicating that the two CH groups are in the same environment due to the presence of a C-2 axis in the molecule. For further confirmation, the structure of chiral bis (3-bromo-substituted BODIPY) (**2.3**) was validated by HRMS, which showed a peak at 999.1263 *m/z* which is consistent with a formula of $C_{48}H_{36}{}^{11}B_2{}^{79}Br^{81}BrF_3N_6O_4$ $[M\text{-}F]^+$, as well as showing an isotope pattern which matched that expected. Similarly, we confirmed the structure of both chiral 3-iodo-substituted BODIPY (**2.19**) and chiral bis (3-iodo-substituted BODIPY) (**2.4**) by NMR. The analysis of ^{1}H NMR of chiral 3-iodo-substituted BODIPY (**2.19**), showing two signals at 4.69 – 4.62 ppm (m, 1H) and 4.46 ppm (d, *J* = 2.9 Hz, 1H) corresponding to CH-groups of the linking diamine unit, whereas the ^{1}H NMR of chiral bis (3-iodo-substituted-BODIPY)(**2.4**) showed a 2H doublet at 5.05 ppm (d, *J* = 6.6 Hz, 2H) (Figure **2.4**). For further confirmation, the structure of chiral bis (3-iodo-substituted BODIPY) (**2.4**) was validated by HRMS, which showed a peak at 1135.0922 *m/z* which is consistent with a formula of $C_{48}H_{36}{}^{11}B_2F_4I_2N_6O_4Na$ $[M+Na]^+$.

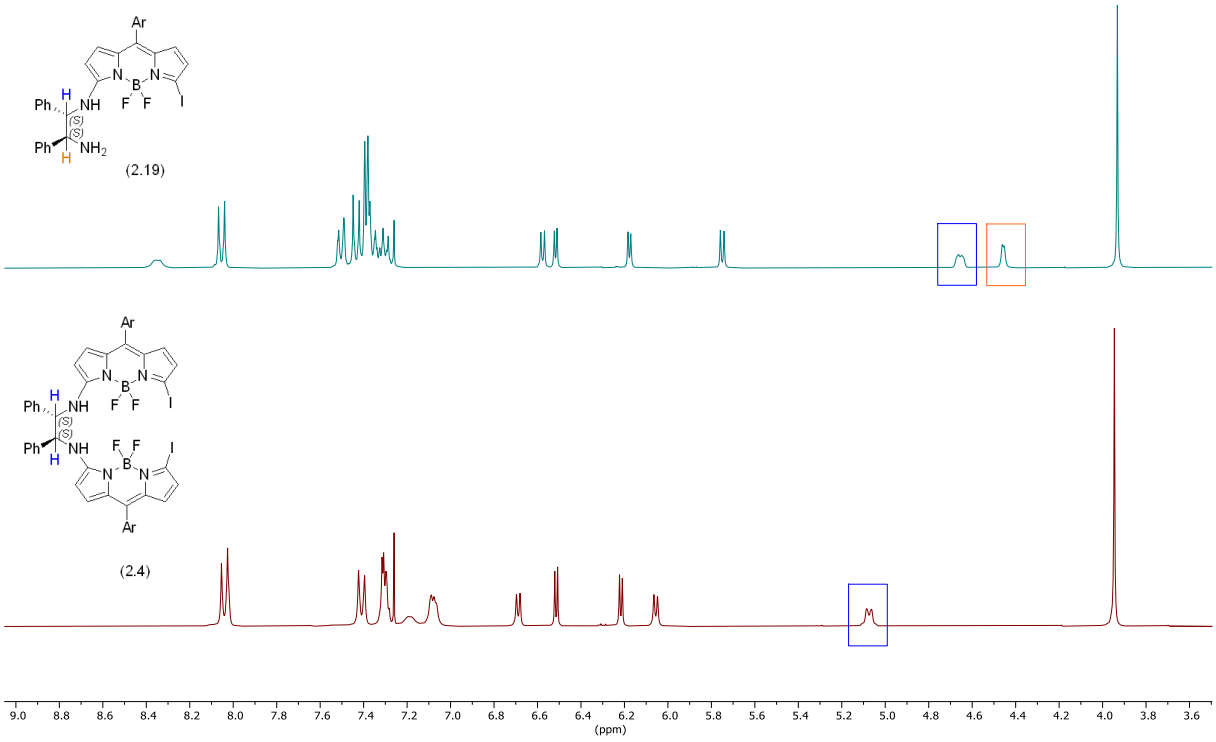

Figure 2.4: ^{1}H NMR spectrum (300 MHz, $CDCl_3$) of the chiral 3-iodo-substituted BODIPY (**2.19**) and chiral bis (3-iodo-substituted BODIPY) (**2.4**). Top: ^{1}H NMR of the chiral 3-iodo-substituted BODIPY (**2.19**) (green) and Bottom: ^{1}H NMR of the chiral bis (3-iodo-substituted BODIPY) (**2.4**)(red) following column chromatography.

In summary, we have been able to access our target chiral bis (3-bromo-substituted BODIPY) (**2.3**), however only as a minor reaction product with chiral 3-bromo-substituted BODIPY (**2.18**) typically being the major product. We have successfully synthesised chiral bis (3-iodo-substituted BODIPY) (**2.19**) albeit in low yields, between 10% to 29%. Note that chiral bis (3-halo-substituted BODIPY) (**2.18** and **2.19**) show poor solubility in organic solvents, which can make purification challenging.

Therefore, to improve our synthesis of chiral 3-halo-bis BODIPYs, we planned to attempt a two-step strategy, synthesis of chiral 3-halo-substituted BODIPYs followed by a second S_NAr reaction with 3,5-dihalo BODIPY to form target chiral bis (3-halo-substituted BODIPY).

2.4.1 Synthesis of Chiral 3-Bromo-substituted BODIPY (**2.18**) Followed by Synthesis of Chiral Bis (3-bromo-substituted BODIPY) (**2.3**)

Therefore, we planned to synthesize chiral bis (3-bromo-substituted BODIPY) (**2.3**) through two synthetic steps, first synthesising chiral 3-bromo-substituted BODIPY (**2.18**) followed by reaction with 3,5-dibromo BODIPY (**1.67**) (Scheme **2.12**).

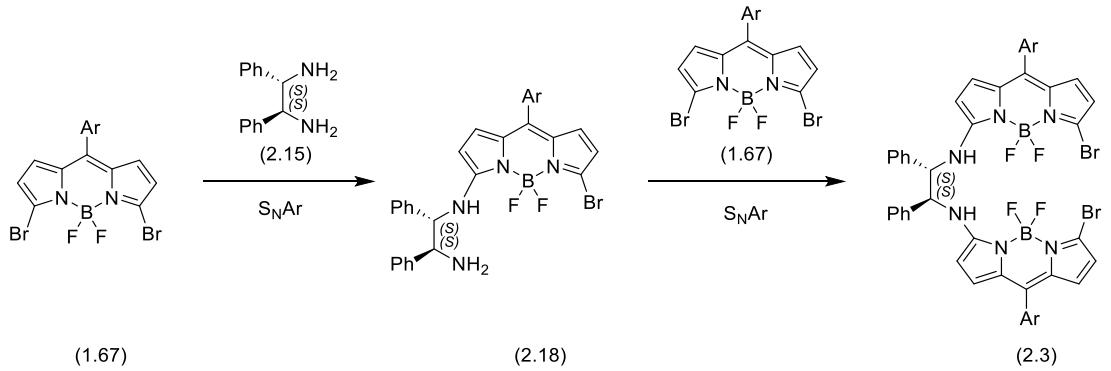

Scheme 2.12: Planned two step approach to chiral chiral bis (3-bromo-substituted BODIPY) (**2.3**) (Ar = *p*-($MeCO_2$)-C_6H_4-).

2.4.2 Synthesis of Chiral 3-Bromo-substituted BODIPY (**2.18**) via S_NAr Reaction

In order to access chiral 3-bromo-substituted BODIPY (**2.18**), we first reacted 1 equivalent of 3,5-dibromo BODIPY (**1.67**), with 1 equivalent of (1*S*,2*S*)-1,2-diphenylethane-1,2-diamine (**2.15**) and 1 equivalent of Et_3N in MeCN at room temperature for 24 hours. Following an aqueous work-up and column chromatography the chiral 3-bromo-substituted BODIPY (**2.18**) was isolated in yield of 42% (Table **2.8**, Entry 1). To improve the target yield, in a second attempt we increased (1*S*,2*S*)-1,2-diphenylethane-1,2-diamine (**2.15**) to 2 equivalents. After 2 hours TLC showed the reaction was complete and, following aqueous work-up, ^1H NMR showed that the desired chiral 3-bromo-substituted BODIPY (**2.18**) had been formed in high purity and quantitative yield, and that no further

purification was required (Table **2.8**, Entry 2). Next, repeating the reaction under the previous conditions with an increase to 2.2 equivalents of Et_3N, gave chiral 3-bromo-substituted BODIPY (**2.18**) in a 90% isolated yield after 2 hours of reaction time following column chromatography (Table **2.8**, Entry 3). Further experiments with a 1 hour reaction time gave quantitative yield after purification (Table **2.8**, Entry 4).

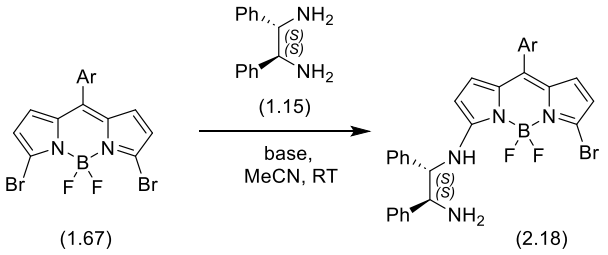

Entry	Scale /mmol	Eq. of BODIPY	Eq. of chiral linker	Eq. of base	Reaction time/h	Yield[a]/%
1	0.47	1	1	1 eq. Et_3N	24	42
2	0.20	1	2	1 eq. Et_3N	2	Quant.[b]
3	0.21	1	2	2.2 eq. Et_3N	2	90
4	0.20	1	2	2.2 eq. Et_3N	1	Quant.
5	0.05	1	1	3 eq. K_2CO_3	24	73
6	0.21	1	1	3 eq. K_2CO_3	24	38[c]
7	0.21	1	1	3 eq. K_2CO_3	22	88
8	0.41	1	1	3 eq. K_2CO_3	18	90
9	0.41	1	1	3 eq. K_2CO_3	18	97
10	0.83	1	1	3 eq. K_2CO_3	18	92

Table 2.8: Synthesis of chiral 3-bromo-substituted BODIPY (**2.18**) using different bases, [a] Isolated yield following column chromatography, [b] No column chromatography required, [c] unusually low yield obtained, multiple additional spots observed in TLC (Ar = *p*-($MeCO_2$)-C_6H_4-).

In parallel, we also examined S_NAr reactions using a non-nucleophilic inorganic base, K_2CO_3 in place of Et_3N, to reduce the chances of by-product formation as seen previously. Thus, we reacted 1 equivalent of 3,5-dibromo BODIPY (**1.67**), with 1 equivalent of (1*S*,2*S*)-1,2-diphenylethane-1,2-diamine (**2.15**) and 3 equivalents of K_2CO_3 in MeCN at room temperature for 24 hours. Following aqueous work-up and purification by column chromatography the desired chiral 3-bromo-substituted BODIPY (**2.18**) was isolated in a yield of 73% (Table **2.8**, Entry 5). This S_NAr reaction was repeated several times, on scales up to 0.83 mmol, giving mainly very high yields (Table **2.8**, Entries 7-10).

In summary, we successfully synthesized chiral 3-bromo-substituted BODIPY (**2.18**), using two related procedures (Et_3N or K_2CO_3) both showing high yields and scalability.

2.4.3 Synthesis of Chiral Bis (3-bromo-substituted BODIPY) (**2.3**) from Chiral 3-Bromo-substituted BODIPY (**2.18**)

Our next step was the synthesis of chiral bis (3-bromo-substituted BODIPY) (**2.3**). Therefore, we reacted 1 equivalent of the previously prepared chiral 3-bromo-substituted BODIPY (**2.18**) with 1 equivalent of 3,5-dibromo BODIPY (**1.67**), and three equivalents of K_2CO_3 at 50 °C for 24 hours under nitrogen (Table **2.9**, Entry 1). The inspection of crude ^{1}H NMR showed only starting material was recovered, and no reaction observed. In parallel, we also reacted 1 equivalent of chiral 3-bromo-substituted BODIPY (**2.18**) with 1 equivalent of 3,5-dibromo BODIPY (**1.67**), and two equivalents of Et_3N at 35 °C. After 29 hours TLC showed the presence of a new product. Following aqueous work-up and purification by column chromatography chiral bis (3-bromo-substituted BODIPY) (**2.3**) was isolated in yield of 31% (Table **2.9**, Entry 2). In a third attempt, increasing the reaction temperature to 50 °C and time to 72 hours, resulted in an improved yield of 62% (Table **2.9**, Entry 3). Further increases in the reaction time to 168 hours gave the product in quantitative yield following column chromatography, although in this case we observed difficulty in dissolving the purified product in $CDCl_3$, and DMSO-d_6 solvent was needed for NMR. This is likely due to the poor solubility of the chiral bis (3-bromo-substituted BODIPY) (**2.3**) formed (Table **2.9**, Entry 4).

As a final test reaction, on small scale we reacted 1 equivalent of chiral 3-bromo-substituted BODIPY (**2.18**), 1 equivalent of 3,5-dibromo BODIPY (**1.67**), with a slightly increased 2.2 equivalents of Et_3N at 50 °C for 120 hours under nitrogen in a Schlenk flask. Following work-up and column chromatography, interestingly we isolated an inseparable mixture of chiral bis (3-bromo-substituted BODIPY) (**2.3**) and chiral 3-bromo-substituted BODIPY (**2.18**), along with a by-product 3-(*N*,*N*-diethylamine)-5-bromo BODIPY (**2.21**) (Table **2.9**, Entry 5).

The structure of 3-(*N*,*N*-diethylamine)-5-bromo BODIPY (**2.21**) was confirmed by the analysis of ^{1}H NMR, showing two signals in aliphatic range at 3.86 ppm (q, J = 7.0 Hz, 4H) and 1.38 ppm (t, J = 7.0 Hz, 6H) corresponding to two ethyl substituents of the amino group, and the ^{19}F NMR showing a quartet at -133.3 ppm (q, J = 33.4 Hz) corresponding to two equivalent fluorine atoms in BF_2 group. We postulate that 3-(*N*,*N*-diethylamine)-5-bromo BODIPY (**2.21**), and the previously discussed 3-(*N*,*N*-diethylamine)-5-iodo BODIPY (**2.20**), were formed from an S_NAr reaction between Et_3N and 3,5-dibromo BODIPY (**1.67**) or 3,5-diiodo BODIPY (**1.68**), followed by loss of an ethyl group from an intermediate ammonium salt.

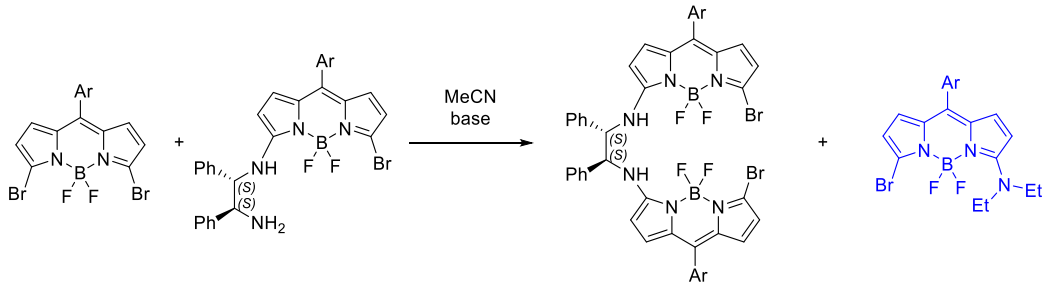

(1.67) (2.18) (2.3) by-product (2.21)

Entry	Scale / mmol	Eq. of BODIPY (1.67)	Eq. of base	Reaction Temp./ °C	Reaction time/h	Yield (2.3)[a]/%	Reaction outcomes
1	0.03	1	3 eq. K_2CO_3	50	24	0	Starting material recovered
2	0.17	1	2 eq. Et_3N	35	29	31	-
3	0.12	1	2 eq. Et_3N	50	72	62	-
4	0.24	1.2	2 eq. Et_3N	50	168	Quant.	-
5	0.04	1	2.2 eq. Et_3N	50	120	10[b]	Starting material (**2.18**) (29z%) [b] and by-product BODIPY (**2.21**) (quant.)[a]

Table 2.9: Synthesis of chiral bis (3-bromo-substituted BODIPY) (**2.3**) via S_NAr reaction, [a] Isolated yield following column chromatography, yield over estimated due to small scale and the presence of solvent by NMR. [b] A mixed fraction containing both chiral bis (3-bromo-substituted-BODIPY) (**2.3**)(12%) and starting material (**2.18**) (29%) was also isolated following column chromatography (Ar = *p*-($MeCO_2$)-C_6H_4-).

Our new strategy to synthesize chiral bis (3-bromo-substituted BODIPY) (**2.3**) through two steps showed promising results. Consequently, we intend to use the same approach for the synthesis of chiral bis (3-iodo-substituted BODIPY) (**2.4**).

2.4.4 Synthesis of Chiral Bis (3-iodo-substituted BODIPY) (**2.4**) Followed by Chiral 3-Iodo-substituted BODIPY (**2.19**)

We plan to use the same synthetic strategy as outlined in section 2.4.1 to access chiral bis (3-iodo-substituted BODIPY) (**2.4**). This strategy involves two synthetic steps, wherein 3,5-diiodo BODIPY (**1.68**) reacts with (1*S*,2*S*)-1,2-diphenylethane-1,2-diamine (**2.15**) to produce chiral 3-iodo-substituted BODIPY (**2.19**). Subsequently, a S_NAr reaction between chiral 3-iodo-substituted BODIPY (**2.19**) and 3,5-diiodo BODIPY (**1.68**) to make chiral bis (3-iodo-substituted BODIPY) (**2.4**) (Scheme **2.13**).

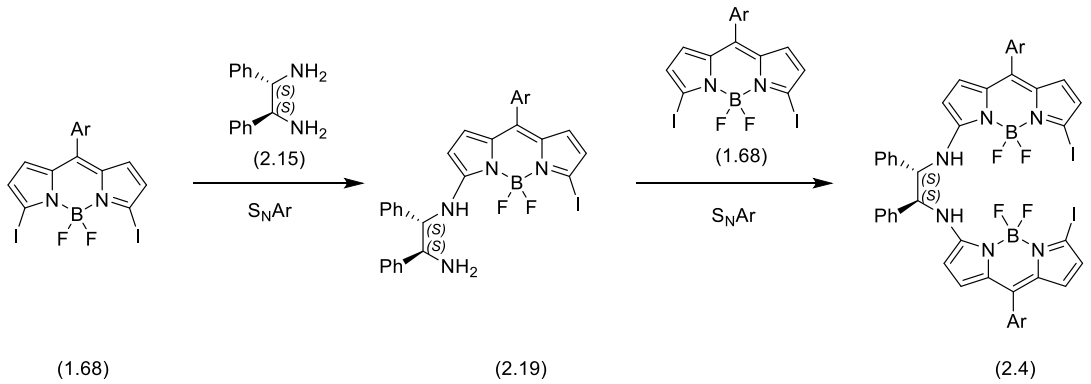

Scheme 2.13: Planned two step approach to chiral bis (3-iodo-substituted BODIPY) (**2.4**) (Ar = *p*-($MeCO_2$)-C_6H_4-).

2.4.5 Synthesis of Chiral 3-Iodo-substituted BODIPY (**2.19**) via S_NAr Reaction

We planned to examine S_NAr reaction between 3,5-diiodo BODIPY (**1.68**) and (1*S*,2*S*)-1,2-diphenylethane-1,2-diamine (**2.15**), under our optimised S_NAr reaction conditions, with the testing of two different bases.

In our initial attempts, we decided to use K_2CO_3 for two reasons: ease of removal during the work-up and to avoid the formation of by-product in which Et_3N could act as nucleophilic base as observed in previous similar reactions (section 2.4.3). Therefore, we reacted 1 equivalent of 3,5-diiodo BODIPY (**1.68**), with 1 equivalent of (1*S*,2*S*)-1,2-diphenylethane-1,2-diamine (**2.15**) and 3 equivalents of K_2CO_3 in MeCN at room temperature for 18 hours. Following an aqueous work-up and purification by column chromatography the desired chiral 3-iodo-substituted BODIPY (**2.19**) was isolated in 33% yield (Table **2.11**, Entry 1). Repeating the reaction under the same conditions for 24 hours showed an improved yield of 83% (Table **2.11**, Entry 2). In a further attempt, we carried out the reaction on a 0.35 mmol scale under similar conditions, with an increase in the reaction temperature to 50 °C to expedite the reaction. TLC showed that starting material had been consumed and new products had formed after 2 hours. The reaction mixture was cooled to room temperature, diluted with DCM, subjected to

aqueous work-up and purified by column chromatography the desired chiral 3-iodo-substituted BODIPY (**2.19**) was isolated in a 47% yield (Table **2.11**, Entry 3).

We also examined the reaction in presence of Et_3N, we reacted 1 equivalent of 3,5-diiodo BODIPY (**1.68**), with 1 equivalent of (1*S*,2*S*)-1,2-diphenylethane-1,2-diamine (**2.15**) and 2.2 equivalents of Et_3N in MeCN at room temperature for 2 hours. Following an aqueous work-up and column chromatography the desired chiral 3-iodo-substituted BODIPY (**2.19**) was obtained in an excellent yield of 97% (Table **2.11**, Entry 4). In parallel, on the same reaction scale using 2 equivalents of Et_3N at room temperature. TLC showed the starting material had fully consumed after 20 hours gave the desired chiral 3-iodo-substituted BODIPY (**2.19**) in a high yield of 85% following column chromatography (Table **2.11**, Entry 5).

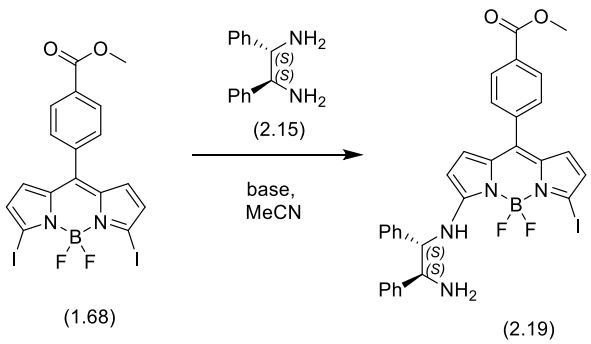

Entry	Scale/ mmol	Eq. of base	Reaction Temp./°C	Reaction time/h	Yield[a]/%
1	0.09	3 eq. K_2CO_3	RT	18	33
2	0.05	3 eq. K_2CO_3	RT	24	83
3	0.35	3 eq. K_2CO_3	50	2	47
4	0.20	2.2 eq. Et_3N	RT	2	97
5	0.20	2 eq. Et_3N	RT	20	85

Table 2.11: Synthesis of chiral 3-iodo-substituted BODIPY (**2.19**) using different bases. [a] Isolated yield following column chromatography.

To confirm the structure and absolute stereochemistry of chiral 3-iodo-substituted BODIPY (**2.19**), single crystals were grown through liquid-liquid diffusion from DCM and hexane (1:3) under a nitrogen atmosphere. A suitable single crystal was then examined by SCXRD analysis, giving a monoclinic crystal system with I2 space group with eight molecules in the unit cell (Z = 8). A Flack parameter of -0.023(3) was measured, confirming the absolute stereochemistry (Figure **2.4**).

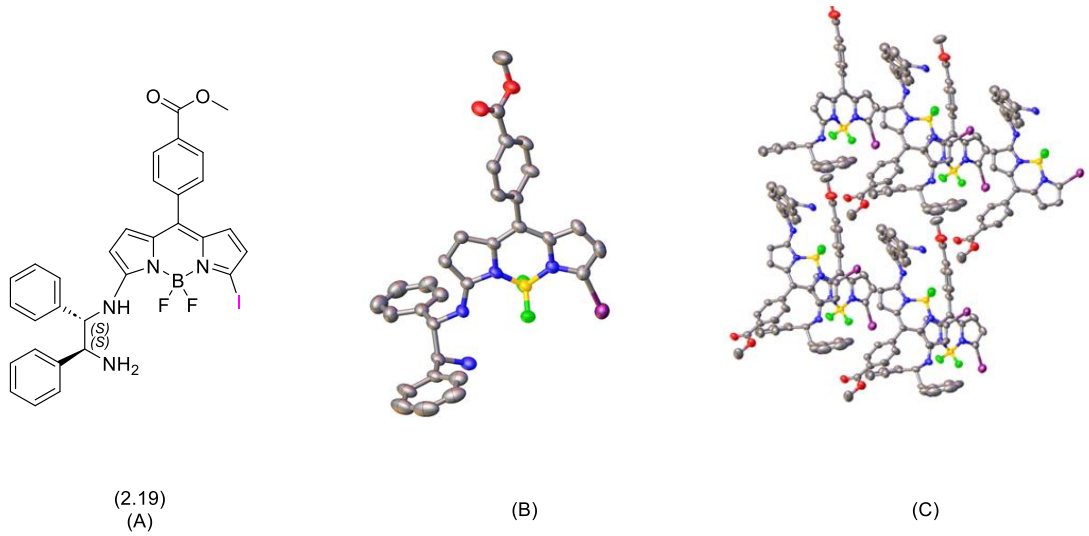

(2.19)
(A)

(B)

(C)

Figure 2.4: Chiral 3-iodo-substituted BODIPY (**2.19**); (A) Molecular structure; (B) Single crystal X-ray structure (hydrogen atoms omitted for clarity); (C) Packing of the molecules in the unit cell.

We have successfully synthesized chiral 3-iodo-substituted BODIPY (**2.19**) in high yield and confirmed the structure and the absolute stereochemistry by SCXRD. Next, we will examine S_NAr reaction between chiral 3-iodo-substituted BODIPY (**2.19**) and 3,5-diiodo BODIPY (**1.68**).

2.4.6 Synthesis of Chiral Bis (3-iodo substituted BODIPY) (**2.4**) from Chiral 3-Iodo-substituted BODIPY (**2.19**)

Our next step was the synthesis of chiral bis (3-iodo-substituted BODIPY) (**2.4**). Thus, we reacted 1 equivalent of chiral 3-iodo-substituted BODIPY (**2.19**) with 1 equivalent of 3,5-diiodo BODIPY (**1.68**), and 2 equivalents of Et_3N under reflux for 18 hours under nitrogen. Following aqueous work-up and purification by column chromatography chiral bis (3-iodo-substituted BODIPY) (**2.4**) was isolated in a 31% yield (Table **2.12**, Entry 1). In a second attempt, in a Schlenk flask, the reaction was carried out in toluene, the reaction was between 1 equivalent of chiral 3-iodo-substituted BODIPY (**2.19**), 1 equivalent of 3,5-diiodo BODIPY (**1.68**), and 2.2 equivalents of Et_3N at 85 °C for 72 hours. The solvent was removed under reduced pressure, followed purification by column chromatography, and three fractions were isolated. Fraction 1 was a mixture of chiral 3-iodo-substituted BODIPY (**2.19**) and 3-(*N*,*N*-diethylamine)-5-iodo BODIPY (**2.20**) and fraction 2 was identified as a pure 3-(*N*,*N*-diethylamine)-5-iodo BODIPY (**2.20**) in a 85% yield, while the analysis of fraction 3 by ^1H NMR showed that the desired chiral bis (3-iodo-substituted BODIPY) (**2.4**) was isolated in trace amount (Table **2.12**, Entry 2).

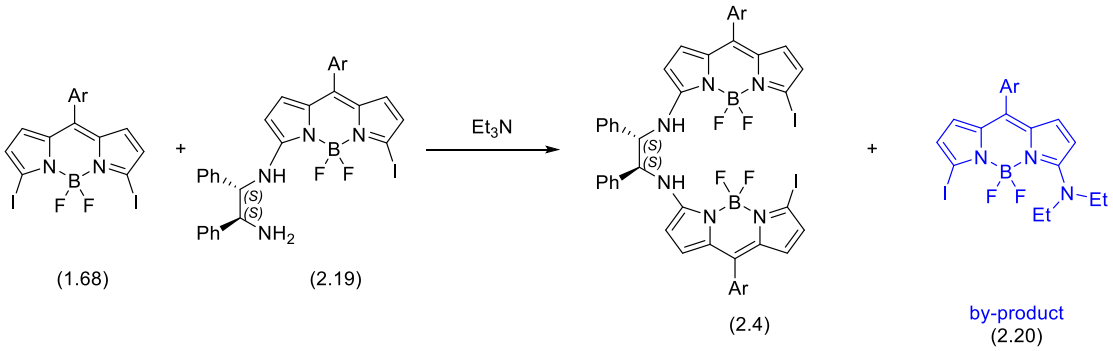

Entry	Scale/ mmol	Eq. of base	Solvent	Reaction Temp./ °C	Reaction time/h	Yield (2.4)[a]/%
1	0.05	2	MeCN	Reflux	18	31
2	0.04	2.2	Toluene	85	72	Trace

Table 2.12: Synthesis of chiral bis (3-iodo-substituted BODIPY) (**2.4**) via S_NAr reaction. [a] Isolated yield following column chromatography (Ar = *p*-($MeCO_2$)-C_6H_4-).

In summary, we have successfully synthesized chiral bis (3-iodo-substituted BODIPY) (**2.4**) in moderated yield of 31% in MeCN through a two steps process. Due to the low solubility of chiral bis (3-bromo-substituted BODIPY) (**2.3**) and chiral bis (3-iodo-substituted BODIPY) (**2.4**) in organic solvents following purification, we were unable to follow the next step which was the synthesis of cyclic chiral BODIPY (**2.17**). Therefore, we planned to use different synthetic route via double S_NAr reactions.

2.5 Synthesis of Di-substituted BODIPY and Cyclic Chiral BODIPY (2.17)

We next planned to examine the synthesis of cyclic chiral-BODIPY (**2.17**) using a new synthetic route that includes two steps. The synthesis of di-substituted BODIPY (**2.22**) through double S_NAr reaction followed by another double S_NAr reaction to form cyclic chiral BODIPY (**2.17**) (Scheme **2.14**).

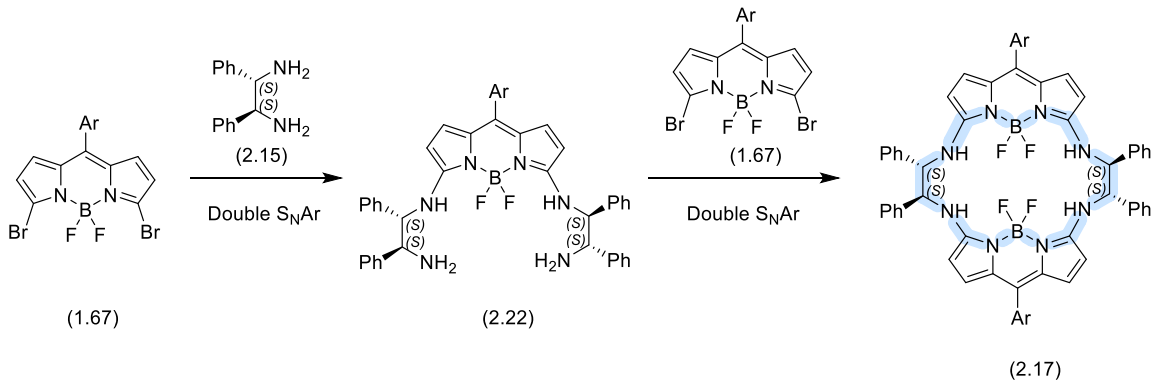

Scheme 2.14: Proposed plan to synthesis cyclic chiral BODIPY (**2.17**) (Ar = *p*-($MeCO_2$)-C_6H_4-).

Therefore, we reacted one equivalent of 3,5-dibromo BODIPY (**1.67**), three equivalents of (1*S*,2*S*)-1,2-diphenylethane-1,2-diamine (**2.15**), and 6 equivalents of K_2CO_3 in MeCN at room temperature for 72 hours. Following an aqueous work-up and column chromatography, unfortunately, the desired di-substituted BODIPY (**2.22**) was not observed, instead chiral 3-bromo-substituted BODIPY (**2.18**) was isolated in a 51% yield (Table **2.13**, Entry 1). In a further attempt, similar conditions were used but increasing the reaction temperature to reflux for 48 hours. Unfortunately, following an aqueous work-up, the inspection of the crude ^{1}H NMR showed a complex mixture with no observation of the desired di-substituted BODIPY (**2.22**). Following purification by column chromatography chiral 3-bromo-substituted BODIPY (**2.18**) was isolated in low yield of 18% (Table **2.13**, Entry 2).

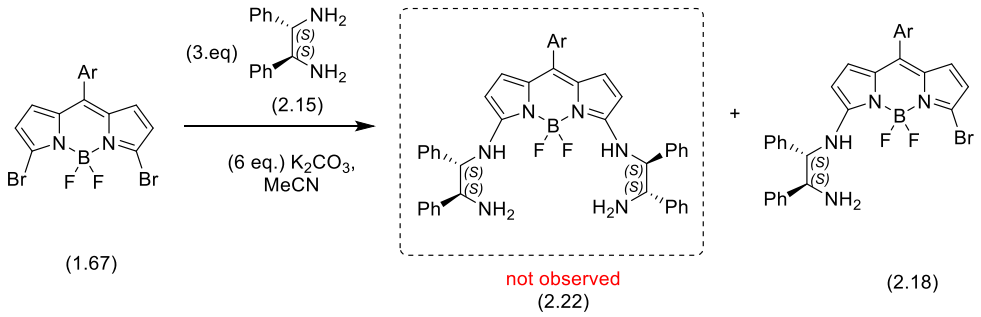

Entry	Scale / mmol	Reaction Temp./ °C	Reaction time/h	Yield (2.18)[a]/%
1	0.21	RT	72	51
2	0.10	Reflux	48	18

Table 2.13: Attempts to synthesis of di-substituted BODIPY (**2.22**) via double S_NAr reaction (Ar = *p*-($MeCO_2$)-C_6H_4-).

We postulated that the synthesis of di-substituted BODIPY (**2.22**) was challenging due to the introduction of an electron-donating amine group in chiral 3-bromo-substituted BODIPY (**2.18**) deactivating the BODIPY for further S_NAr reactions. Therefore, we decided to re-evaluate our synthetic goals, and further focus on examining the photophysical properties of the chiral 3-halo-substituted BODIPY and chiral bis (3-halo-substituted BODIPYs).

2.6 Photophysical Properties of Chiral 3-Halo-substituted BODIPYs and Chiral Bis (3-halo-substituted BODIPYs)

Once we successfully synthesised four compounds chiral 3-bromo-substituted BODIPY (**2.18**), chiral 3-iodo-substituted BODIPY (**2.19**), chiral bis (3-bromo-substituted-BODIPY) (**2.3**), and of chiral bis (3-iodo-substituted-BODIPY) (**2.4**), we turned our attention to measure the photophysical properties including UV-Vis absorption and emission spectra, molar extinction coefficient (ε), the fluorescence quantum yield (ϕ_F).

Hence, we measured the absorption and emission spectra for the four compounds in DCM at room temperature, which exhibited absorption maxima in the range between 505-530 nm and emission maxima between 552-559 nm. The fluorescence quantum yields (ϕ_F) of the for compounds was also measured, using Rhodamine 6G as a standard. Chiral 3-bromo-substituted BODIPY (**2.18**) and chiral 3-iodo-substituted BODIPY (**2.19**) showed quantum yields of 0.20 and 0.35, respectively. Whilst chiral bis (3-bromo-substituted BODIPY) (**2.3**) and chiral bis (3-iodo-substituted BODIPY) (**2.4**) exhibited relatively low quantum yields around 0.03 (Table **2.14**). We postulate that the low fluorescence quantum yield of the chiral bis BODIPYs system is due to intramolecular charge transfer (ICT) in the excited state especially in polar solvents. This phenomenon is known in literature for similar chiral bis BODIPYs system.[70]

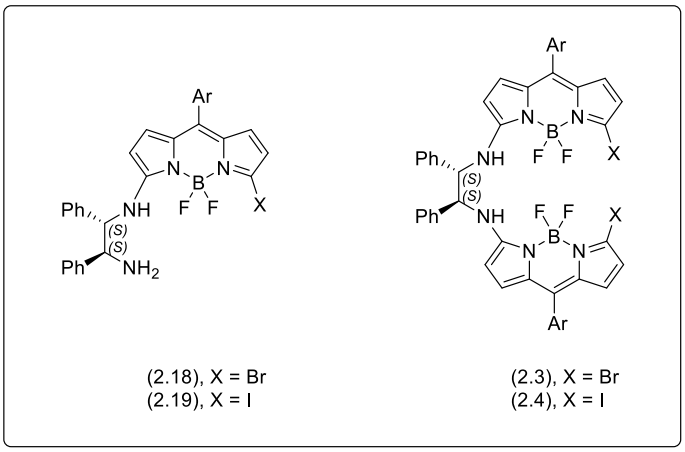

BODIPY	Solvent	λ_{max} (abs)/nm	λ_{max} (em)/nm	ε / mol^{-1} cm^{-1}	Stokes shift (cm^{-1})	ϕ_F[a]
2.18	DCM	505	552	46 128	1686	0.20
2.19	DCM	511	559	65 688	1680	0.35
2.3	DCM	525	554	85 850	997	0.02
2.4	DCM	531	568	42 276	1227	0.03

Table 2.14: Photophysical properties of chiral 3-bromo-substituted BODIPY (**2.18**), chiral 3-iodo-substituted BODIPY (**2.19**), chiral bis (3-bromo-substituted BODIPY) (**2.3**) and chiral bis (3-iodo-substituted BODIPY) (**2.4**). [a] Measured with respect to Rhodamine 6G standard in water (ϕ_F = 0.95), excitation wavelength = 488 nm (Ar = *p*-(MeCO$_2$)-C$_6$H$_4$-).

2.7 Suzuki Miyaura Cross-Coupling of Chiral 3-Bromo-substituted BODIPY (2.18)

In our next approach, we wished to examine the impact on the photophysical properties of chiral 3-bromo-substituted BODIPY (**2.18**) of introducing new groups at that 3-position. To do this we planned to examine a Suzuki Miyaura cross-coupling between chiral 3-bromo-substituted BODIPY (**2.18**) and

(4-methoxyphenyl)boronic acid (**2.23**) (Scheme **2.15**), following a procedure described by Hall *et al,.* in which they reported Suzuki Miyaura cross-coupling reactions with 3,5-dihalo BODIPYs.[45]

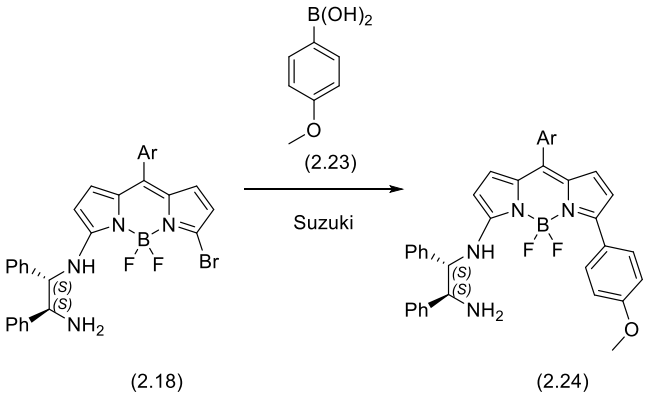

Scheme 2.15: Planned Suzuki Miyaura cross-coupling between chiral 3-bromo-substituted BODIPY (**2.18**) and (4-methoxyphenyl)boronic acid (**2.23**) (Ar = *p*-($MeCO_2$)-C_6H_4-).

Therefore, in a Schlenk flask under an atmosphere of nitrogen (degassed three times), we reacted one equivalent of chiral 3-bromo-substituted BODIPY (**2.18**) on 0.08 mmol scale with two equivalents of (4-methoxyphenyl)boronic acid (**2.23**) in THF/water at 75 °C, with potassium phosphate and 6 mol% XPhos Pd G3 for 20 hours. TLC showed that multiple products had formed. The reaction mixture was diluted with DCM and subjected to aqueous work-up (Table **2.15**, Entry 1). The inspection of crude ^{1}H NMR showed the formation of a complex mixture, in which it was hard to determine if the desired (1*S*,2*S*)-3-(1,2-diphenylethane-1,2-diamine-5-(4-methoxyphenyl)) BODIPY (**2.24**) has been formed. Therefore, we decided to repeat the rection on a larger scale of 0.27 mmol, under the same reaction conditions for 18 hours. Following an aqueous work-up, ^{1}H NMR again showed that a complex mixture had been formed. Purification by column chromatography proved challenging, however the desired (1*S*,2*S*)-3-(1,2-diphenylethane-1,2-diamine-5-(4-methoxyphenyl)) BODIPY (**2.24**) was isolated in an 8% yield, after the three sequential column attempts (Table **2.15**, Entry 2). In the final attempt, the reaction was carried out on a 0.10 mmol scale, under our previous conditions, with a decrease in the reaction time to 5 hours in an attempt to minimise the formation of by-products. Following aqueous work-up ^{1}H NMR again showed that fewer by-products had been formed, and purification by column chromatography gave (1*S*,2*S*)-3-(1,2-diphenylethane-1,2-diamine-5-(4-methoxyphenyl)) BODIPY (**2.24**) in a much improved yield of 41% (Table **2.15**, Entry 3).

We also examined a Suzuki Miyaura cross-coupling between chiral 3-bromo-substituted BODIPY (**2.18**) and two equivalents of (4-fluorophenyl)boronic acid (**2.25**) under our previous conditions for 3.5 hours. Following an aqueous work-up and purification by column chromatography (1*S*,2*S*)-3-(1,2-

diphenylethane-1,2-diamine-5-(4-fluroyphenyl)) BODIPY (**2.26**) was isolated in a low yield of 4 % (Table **2.15**, Entry 4).

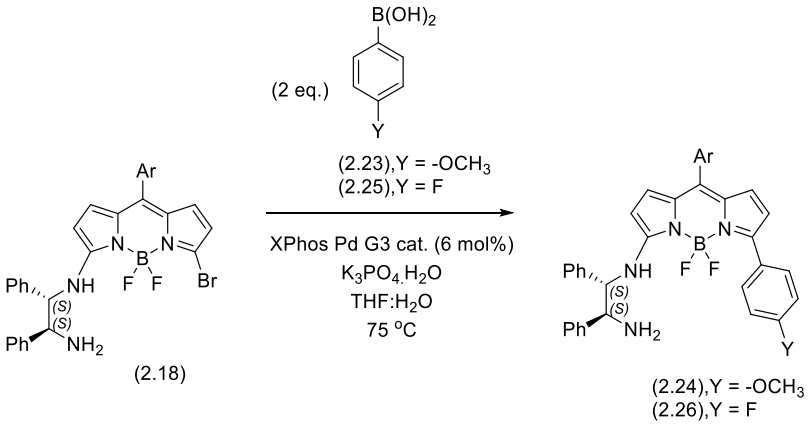

Entry	Scale/mmol	Boronic acid	Reaction time/h	Product	Yield[a]/%
1	0.08	(**2.23**)	20	(**2.24**)	Complex mixture
2	0.27	(**2.23**)	18	(**2.24**)	8
3	0.10	(**2.23**)	5	(**2.24**)	41[b]
4	0.08	(**2.25**)	3.5	(**2.26**)	4

Table 2.15: A Suzuki Miyaura cross-coupling of chiral 3-bromo-substituted BODIPY (**2.18**). [a] Isolated yield following column chromatography. [b] Product contained minor impurities after column chromatography (Ar = *p*-($MeCO_2$)-C_6H_4-).

The structures of both (1*S*,2*S*)-3-(1,2-diphenylethane-1,2-diamine-5-(4-methoxyphenyl)) BODIPY (**2.24**) and (1*S*,2*S*)-3-(1,2-diphenylethane-1,2-diamine-5-(4-fluroyphenyl)) BODIPY (**2.26**) were confirmed by NMR. The ^{1}H NMR of (1*S*,2*S*)-3-(1,2-diphenylethane-1,2-diamine-5-(4-methoxyphenyl)) BODIPY (**2.24**) showed the presence of 3H singlet at 3.89 ppm and two doublets at 7.89 ppm (d, *J* = 9.0 Hz, 2H) and 7.02 (d, *J* = 9.0 Hz, 2H) corresponding to newly added 4-methoxyphenyl ring.

The ^{19}F NMR spectrum of (1*S*,2*S*)-3-(1,2-diphenylethane-1,2-diamine-5-(4-fluroyphenyl)) BODIPY (**2.26**) showed the presence of three different fluorine environments, two multiplets corresponding to the diastereotopic fluorines of the BF_2 group at -140.47 – -141.73 ppm, -141.49 – -142.90 ppm, and a further multiplet at -114.42 – -114.65 ppm for the new aryl fluoride, showing coupling to adjacent aromatic protons.

Due to the low yields, we had observed in the Suzuki Miyaura coupling reactions as shown above (Table **2.15**), we suggest that in the future this problem could be overcome by using a different starting material, 3-substituted-5-iodo BODIPY (**2.19**), as iodo-substituted BODIPYs have been shown to give improved yields in such couplings.[45]

2.8 S_NAr Reaction Between 3,5-Dibromo BODIPY (1.67) and Achiral Diamine Linker

Next, we planned an alternative approach to synthesise dimeric cyclic BODIPY compounds. We wished to examine S_NAr reactions with an achiral diamine linker, followed by a subsequent macrocyclisation with a chiral diamine linker (Scheme **2.16**)

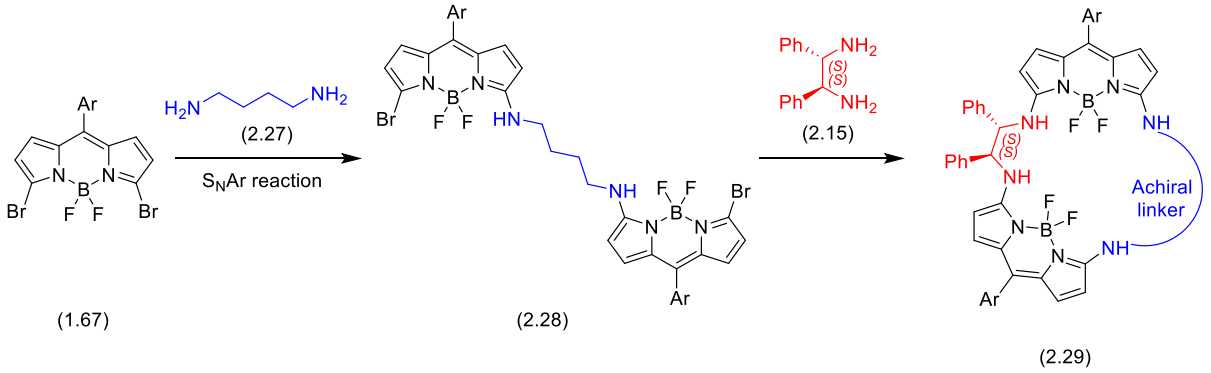

Scheme 2.16: Planned stepwise synthesis of cyclic BODIPY compound (**2.29**) (Ar = *p*-($MeCO_2$)-C_6H_4-).

Therefore, in a first attempt, under nitrogen atmosphere, we reacted 2 equivalents of 3,5-dibromo BODIPY (**1.67**), 1 equivalent of butane-1,4-diamine (**2.27**) and 2.2 equivalents of Et_3N in MeCN at room temperature for 18 hours. Following an aqueous work-up and purification by column chromatography the desired bis (3-bromo-5-butane-1,4-diamine-BODIPY) (**2.28**) was isolated in a 91% yield (Scheme **2.17**). Interestingly, the S_NAr reaction with an achiral linker was a much easier reaction when compared to similar reactions with our chiral linkers, and only the desired bis (3-bromo-5-butane-1,4-diamine-BODIPY) (**2.28**) was formed in high yield.

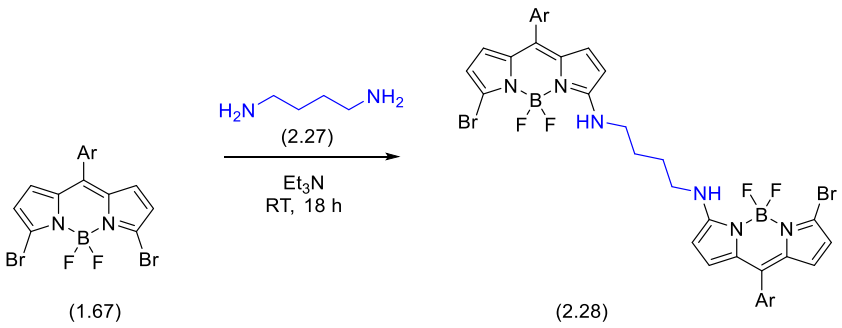

Scheme 2.17: Synthesis of bis (3-bromo-5-butane-1,4-diamine-BODIPY) (**2.28**) via S_NAr reaction (Ar = *p*-($MeCO_2$)-C_6H_4-).

The structure of bis (3-bromo-5-butane-1,4-diamine-BODIPY) (**2.28**) was confirmed by ^1H NMR which showed two, 4H multiplets at 3.54 – 3.42 ppm and 1.86 – 1.79 ppm corresponding to alkyl chain of the newly added butane-1,4-diamine group.

For further confirmation of the structure, crystals were grown by slow evaporation of a DCM solution. A single crystal was analysed by SCXRD, giving a monoclinic crystal system with a $P2_1/c$ space group with 2 molecules in the unit cell (Z = 2) (Figure **2.5**).

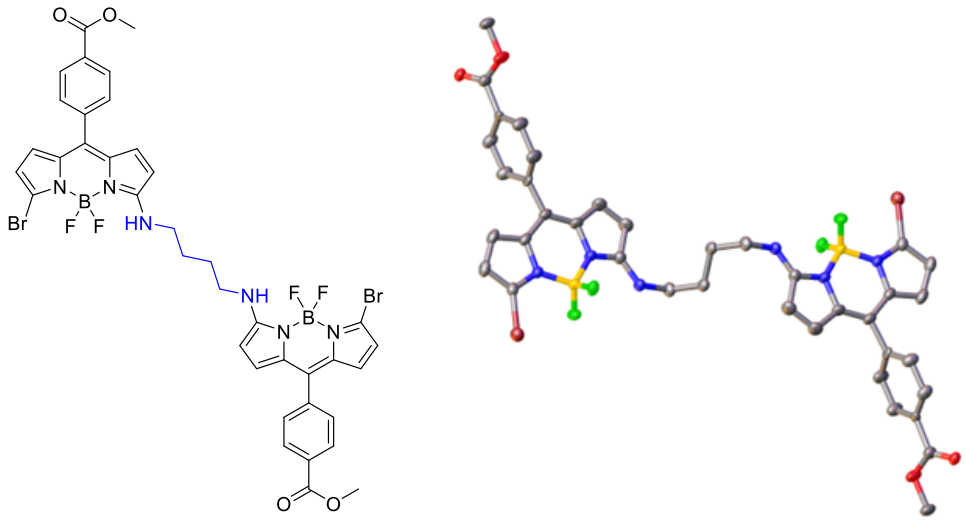

(2.28)

Figure 2.5: Single crystal X-ray structure of bis (3-bromo-5-butane-1,4-diamine-BODIPY) (**2.28**), (Ar = *p*-($MeCO_2$)-C_6H_4-)

2.9 Conclusion

The aim of the first part of this chapter was the synthesis of two key starting materials, 3,5-dibromo BODIPY (**1.67**) and 3,5-diiodo BODIPY (**1.68**). We have successfully optimised the synthetic routes to access both of these molecules. 3,5-Dibromo BODIPY (**1.67**) has been synthesised on scales up to 7.2 mmol with yields up to 86%, and 3,5-diiodo BODIPY (**1.68**) on scales up to 5.9 mmol with high yields between 75 and 91%.

In the second part of this chapter, our aim was to synthesise chiral cyclic BODIPYs. For this aim we have examined S_NAr reactions between both 3,5-dibromo BODIPY (**1.67**) and 3,5-diiodo BODIPY (**1.68**), and (1*S*,2*S*)-1,2-diphenylethane-1,2-diamine (**2.15**). This resulted in the synthesis of four novel chiral BODIPYs, including two chiral monomeric BODIPYs, chiral 3-bromo-substituted BODIPY (**2.18**) and chiral 3-iodo-substituted BODIPY (**2.19**), as well as two chiral dimeric BODIPYS, chiral bis (3-bromo-substituted BODIPY) (**2.3**) and chiral bis (3-iodo-substituted BODIPY) (**2.4**). In the case of our chiral dimeric BODIPYS, we showed that they could be synthesised through two different synthetic approaches, either in a one-pot double S_NAr reaction between two equivalents of 3,5-dihalo BODIPY (**1.67** or **1.68**) and (1*S*,2*S*)-1,2-diphenylethane-1,2-diamine (**2.15**), or via a stepwise sequential S_NAr approach.

However, despite a number of approaches being investigated, we did not manage to find a suitable method to synthesise cyclic chiral BODIPYs, through a macrocyclisation reaction. Macrocyclisations are intrinsically difficult due to the entropic challenges in ring closure, as well as the need for high dilution to avoid polymerisation.[71,72] We believe in our systems, macrocyclisation is also difficult due to the decreased reactivity of systems such as chiral bis (3-halo-substituted BODIPY) (**2.3** and **2.4**) towards further S_NAr reactions. In addition, the formation of a cyclic chiral BODIPYs may also be disfavoured due to issues with steric hindrance, as bringing the two BODIPYs units close together presents a challenge because of the repulsion between fluorine atoms of BF_2 moieties.

Therefore, for future work, we propose a new synthetic route to produce a cyclic chiral BODIPY through the combination of S_NAr and double click-reaction chemistry. Initially, we would begin by preparing a chiral bis (3-chloro-substituted BODIPY) (**2.30**) via a double S_NAr reaction with (1S,2S)-1,2-diphenylethane-1,2-diamine (**2.15**) using conditions outlined previously in this chapter. Subsequently, we would further functionalise chiral bis (3-chloro-substituted BODIPY) (**2.32**) via a second double S_NAr reaction with two equivalents of 3-azidopropan-1-amine (**2.31)**. Finally, we will investigate if the resulting chiral bis (substituted-BODIPY) (**2.32**) can undergo a double click-reaction with the Sondheimer diyne (**2.33**) to form a macrocycle (Scheme **2.18**). This is based on methodology reported by O'Shea *et al*. in which they demonstrated a double click-reaction macrocyclization with Sondheimer diyne with aza-dipyrrins.[73]

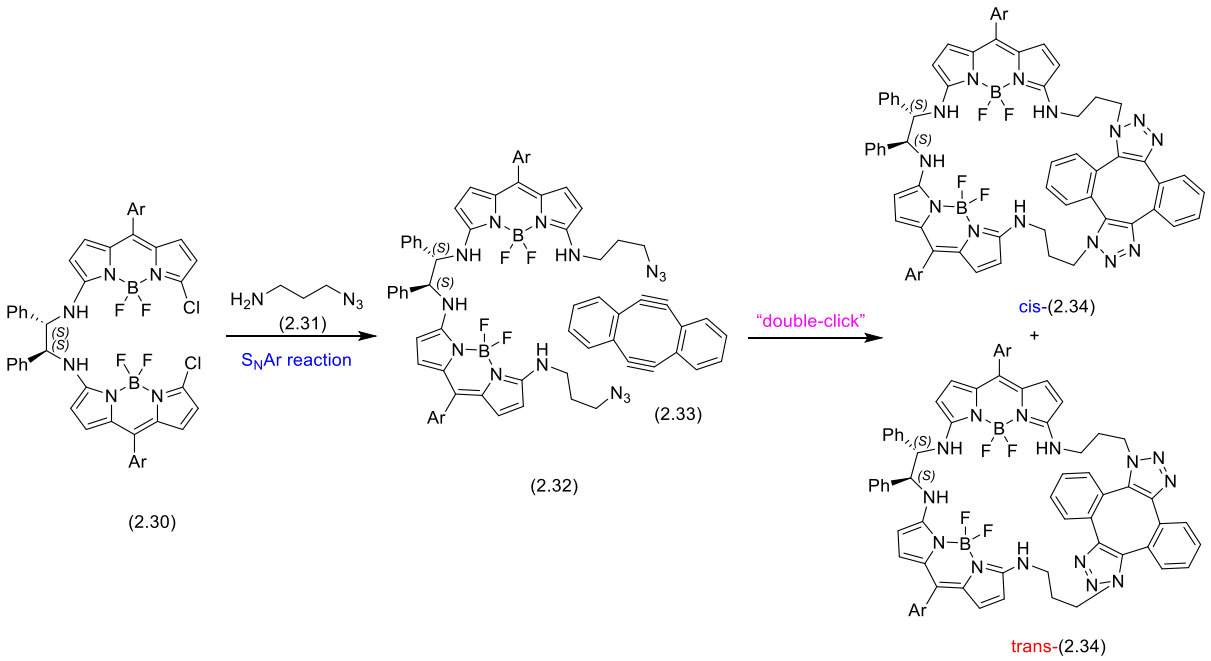

Scheme 2.18: Proposed synthesis of cyclic chiral BODIPYs, via S_NAr reactions and a double click-reaction macrocyclisation with the Sondheimer diyne.

Chapter 3. Synthesis of Helically Chiral mono BODIPYs via Point-to-Helical Chirality Transfer

3.1 Introduction

In this chapter, we will discuss our development of synthetic routes for accessing helically chiral BODIPYs through point-to-helical chirality transfer. Following a discussion of our synthetic strategy towards a series of key advanced intermediates, we will demonstrate the use of enantiopure amino alcohols as point chiral directing groups (chiral auxiliary) to control the helical chirality in the target helically chiral BODIPYs. In addition, we will discuss the chiroptical investigation of these compounds.

3.2 Synthetic Strategy Towards Helically Chiral mono BODIPYs via Point-to-Helical Chirality Transfer

Our planned synthetic toward helically chiral BODIPYs involves four main steps, beginning with the introduction of enantiopure amino alcohols as chiral auxiliaries at the 3-position of a 3,5-dihalo BODIPYs through an S_NAr reaction. We planned to investigate two different routes for the synthesis of helically chiral BODIPYs, going via a key difunctionalised dipyrromethene intermediate (Scheme **3.1**).

Route A will involve de-chelation of BF_2 group by a Lewis acid (step A1), followed by a Suzuki Miyaura cross-coupling reaction to introduce 2-hydroxyphenyl at the 5-position (step A2) and finally re-chelation of the difunctionalised dipyrromethene with 4-fluorophenylboronic acid. Route B will involve Suzuki Miyaura cross-coupling reaction first, to introduce 2-hydroxyphenyl at the 5-position (step B1). Subsequently, the de-chelation of BF_2 group will be achieved using a Lewis acid (step B2), followed by a re-chelation step of the difunctionalised dipyrromethene with 4-fluorophenylboronic acid. We anticipate that during the re-chelation step the formation of the helicity of the BODIPY would be controlled by the point chirality of the amino alcohol group (Scheme **3.1**).

3.3 Synthetic Routes towards Chiral Auxiliary Containing BODIPYs

3.3.1 Introduction of Enantiopure Amino Alcohols via S_NAr Reactions

The first step of our synthetic route was the synthesis of mono substituted-BODIPYs via an S_NAr reaction, starting with 3,5-halo BODIPYs (**1.67** and **1.68**) as previously described (Chapter 2) and chiral amino alcohols. Our procedure was based on the work of Rohand *et al*., in which they showed that a range of *N*-, *C*- and *O*-nucleophiles (*e.g*. aniline, piperidine and NaOMe) could be used in S_NAr reactions with 3,5-dichloroBODIPYs.[39] In parallel with work by Felicity Frank in which (*S*)-serine methyl ester was

used in a similar S_NAr reaction, we decided to start our investigations by introducing (*S*)-2-aminobutan-1-ol, via an S_NAr reaction, at the 3-position of a BODIPY.[74]

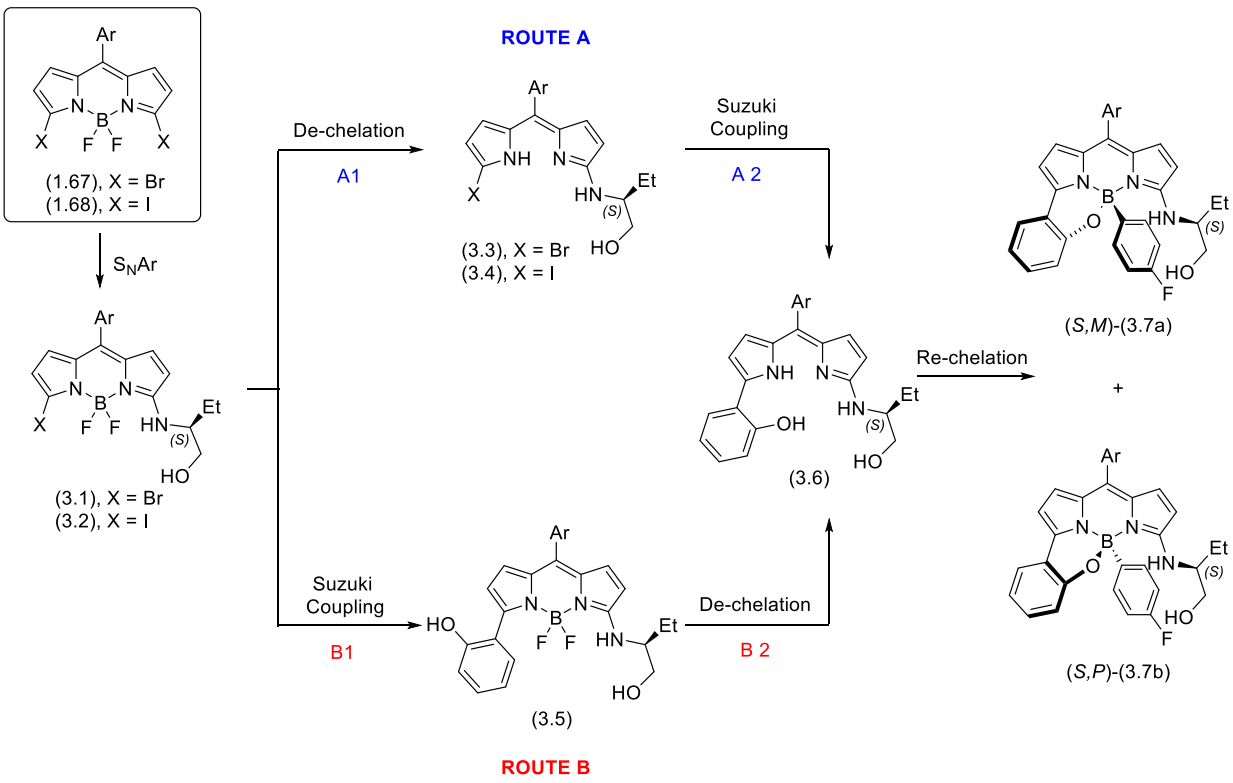

Scheme 3.1: Planned routes to helically chiral BODIPYs via point-to-helical chirality transfer (Ar = *p*-($MeCO_2$)-C_6H_4-).

In our initial attempts, we reacted 2 equivalents of (*S*)-2-aminobutan-1-ol (**3.8**) with 3,5-dibromo BODIPYs (**1.67**) on a 0.4 mmol scale, in the presence of 2.2 equivalents of Et_3N in MeCN at room temperature. The reaction was monitored by TLC, which showed the disappearance of the starting material and the formation of a new product over 4 hours. After aqueous work-up and purification by column chromatography (*S*)-3-(1-hydroxybutan-2-yl)amino)-5-bromo BODIPY (**3.1**) was isolated in a quantitative yield. In order prepare material for further investigation, the S_NAr reaction was repeated on scales up to 1.9 mmol, giving excellent yields in all cases (Table **3.1**, Entries 1-4).

In order to investigate alternative chiral auxiliaries, the S_NAr reaction was repeated using (*S*)-2-amino-2-phenylethan-1-ol (**3.9**), which gave (*S*)-3-(2-hydroxy-1-phenylethyl)amino)-5-bromo BODIPY (**3.10**) in a 91% isolated yield (Table **3.1**, Entry 5).

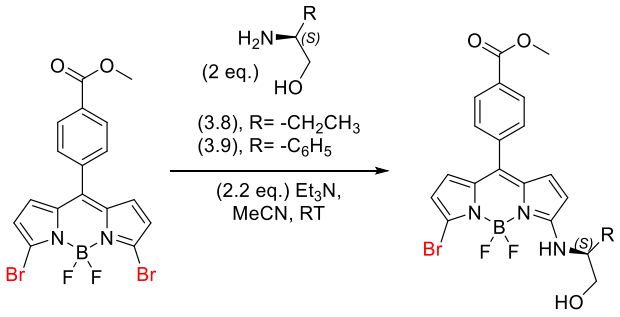

(1.67)

(3.1), R= $-CH_2CH_3$
(3.10), R= $-C_6H_5$

Entry	R	Scale/mmol	Reaction Time/h	Product	Yield[a]/%
1	$-CH_2CH_3$	0.4	4	(**3.1**)	Quant.
2	$-CH_2CH_3$	0.8	4	(**3.1**)	Quant.
3	$-CH_2CH_3$	1.5	4	(**3.1**)	97
4	$-CH_2CH_3$	1.9	4	(**3.1**)	92
5	$-C_6H_5$	0.2	3	(**3.10**)	91

Table 3.1: Synthesis of (*S*)-3-(1-hydroxybutan-2-yl)amino)-5-bromo BODIPY (**3.1**) and (*S*)-3-(2-hydroxy-1-phenylethyl)amino)-5-bromo BODIPY (**3.10**). [a] Isolated yield following column chromatography.

The structure of both (*S*)-3-(1-hydroxybutan-2-yl)amino)-5-bromo BODIPY (**3.1**) and (*S*)-3-(2-hydroxy-1-phenylethyl)amino)-5-bromo BODIPY (**3.10**) were confirmed by ^{1}H NMR. Both molecules showed signals corresponding to four chemically inequivalent pyrrolic protons (*e.g.* (*S*)-3-(1-hydroxybutan-2-yl)amino)-5-bromo BODIPY (**3.1**): δ 6.72 (d, J = 5.1 Hz, 1H), 6.29 (d, J = 5.1 Hz, 1H), 6.22 (d, J = 3.9 Hz, 1H), and 6.15 (d, J = 3.9 Hz, 1H), indicating that a single substitution had occurred to desymmetrise the BODIPY. Interestingly, the ^{19}F NMR spectrum of both molecules showed two double quartets (*e.g.* (*S*)-3-(1-hydroxybutan-2-yl)amino)-5-bromo BODIPY (**3.1**): δ -145.7 (dq, $J_{F\text{-}F}$ = 101.2 Hz, $J_{B\text{-}F}$= 29.5 Hz) and -147.3 (dq, $J_{F\text{-}F}$ = 99.4 Hz, $J_{B\text{-}F}$= 30.7 Hz) corresponding to a pair of diastereotopic fluorine atoms which couple to each other as well as the boron centre. This helped to confirm the introduction of a chiral centre into both molecules.

To further confirm the structure of (*S*)-3-(1-hydroxybutan-2-yl)amino)-5-bromo BODIPY (**3.1**), crystals were grown via slow evaporation of a DCM solution, kept in the fridge for approximately one month. A suitable single crystal was analysed by single crystal X-ray diffraction (SCXRD), showing that (*S*)-3-(1-hydroxybutan-2-yl)amino)-5-bromo BODIPY (**3.1**) had crystallised in the monoclinic C2 space group. Interestingly the crystal structure contained eight molecules in the unit cell, showing an unusual

OH---F H-bond between two molecules. A Flack parameter of -0.015(15) was measured, confirming the absolute stereochemistry (Figure **3.1**).

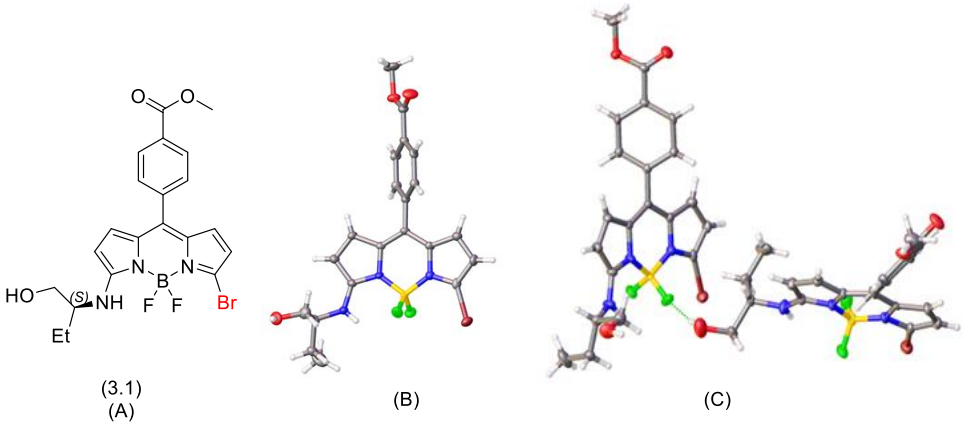

Figure 3.1: (*S*)-3-(1-hydroxybutan-2-yl)amino)-5-bromo BODIPY (**3.1**); (A) Molecular structure; (B) Single crystal X-ray structure; (C) The crystal structure including H-bonding. Note that the (*S*)-2-aminobutan-1-ol group shows disorder in the crystal structure, only the major conformer is shown for clarity.

In our subsequent steps, for both routes A and B, we plan to use a Suzuki Miyaura cross-coupling reaction. 3,5-Diiodo BODIPYs have been previously shown to be good substrates for Suzuki Miyaura reactions, often giving better yields than the corresponding 3,5-dibromo BODIPYs.[45] Therefore, we planned to prepare alternative substrates via the S_NAr reaction of (*S*)-2-aminobutan-1-ol with 3,5-diiodo BODIPY (**1.68**) under our previously described conditions.

Thus, we reacted 3,5-diiodo BODIPY (**1.68**) on a 0.2 mmol scale, with 2 equivalents of (*S*)-2-aminobutan-1-ol (**3.8**) and 2.2 equivalents of Et_3N in MeCN, at room temperature. After 3 hours TLC showed the appearance of a new product, although the starting material was still present, therefore, we decided to leave the reaction to continue overnight at room temperature. After a further 15 hours TLC showed that the starting material had been fully consumed and a new product formed. Following aqueous work-up and column chromatography, the desired (*S*)-3-(1-hydroxybutan-2-yl)amino)-5-iodo BODIPY (**3.2**) was isolated in a quantitative yield (Table **3.2**, Entry 1). Interestingly, we also isolated trace amounts of a by-product, which we have identified as 3-(*N*,*N*-diethylamine)-5-iodo BODIPY (**2.20**), likely arising from an S_NAr reaction between Et_3N and 3,5-diiodo BODIPY (**1.68**) followed by loss of an ethyl group, similar to that seen in the reaction of 3,5-dibromo BODIPY (**1.67**) and Et_3N (see Chapter 2).

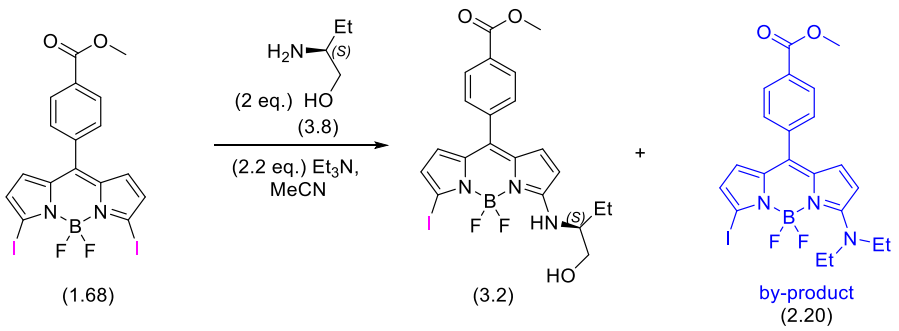

Entry	Scale/mmol	Reaction Temp./°C	Reaction Time/h	Yield (3.2)[a]/%
1	0.2	RT	18	Quant.[b]
2	0.3	50	3	80[c]
3	0.5	50	3	100
4	0.8	50	3	Quant.
5	0.9	50	3	98[c]
6	1.2	50	3	94[c]
7	1.4	50	3	91[c]
8	3.2	50	3	100
9	3.9	50	3	97[c]

Table 3.2: Synthesis of (*S*)-3-(1-hydroxybutan-2-yl)amino)-5-iodo BODIPY (**3.2**). [a] Isolated yield following column chromatography. [b] Trace amount of by-product (**2.20**) confirmed by NMR. [c] Trace amount of by-product (**2.20**) confirmed by TLC.

In order to obtain sufficient amounts of (*S*)-3-(1-hydroxybutan-2-yl)amino)-5-iodo BODIPY (**3.2**) for subsequent steps, we carried out the scale-up of the S_NAr reaction between 3,5-diiodo BODIPY (**1.68**) and (S)-2-aminobutan-1-ol (**3.8**). First, we attempted to reduce the reaction time, by increasing the temperature to 50 °C on a 0.3 mmol scale. After 3 hours the reaction was complete by TLC, and following work-up and purification by column chromatography (*S*)-3-(1-hydroxybutan-2-yl)amino)-5-iodo BODIPY (**3.2**) was obtained in a 80 % yield (Table **3.2**, Entry 2). Further reactions were undertaken up to a 3.9 mmol scale, in all cases reactions were carried out at 50 °C and gave consistently high yields (Table **3.2**).

The structure of (*S*)-3-(1-hydroxybutan-2-yl)amino)-5-iodo BODIPY (**3.2**) was confirmed by the analysis of ^{1}H NMR spectra, which showed four signals corresponding to four pyrrolic proton environments, similar to that previously seen with the corresponding (*S*)-3-(1-hydroxybutan-2-yl)amino)-5-bromo BODIPY (**3.1**). In addition, a broad signal at 6.41 ppm (d, J = 9.1 Hz, 1H) corresponding to the NH proton could also been seen.

In order to assess the absolute stereochemistry of (*S*)-3-(1-hydroxybutan-2-yl)amino)-5-iodo BODIPY (**3.2**), we measured the specific rotation ($[\alpha]_D$) to be 30 (c = 0.1, DCM), taken as an average over 3 measurements. We also successfully crystallised (*S*)-3-(1-hydroxybutan-2-yl)amino)-5-iodo BODIPY (**3.2**) from DCM, though liquid-liquid diffusion with hexane (1:3) in a Schleck flask under nitrogen atmosphere for 2 days. A suitable single crystal was then examined by single crystal X-ray diffraction, giving a monoclinic crystal structure with the C2 space group, with 8 molecules in the unit cell (Z = 8), again showing an unusual OH---F H-bond between two molecules (Figure **3.2**) as seen it before with (*S*)-3-(1-hydroxybutan-2-yl)amino)-5-bromo BODIPY (**3.1**). A Flack parameter of 0.011(4) was measured, confirming the absolute stereochemistry.

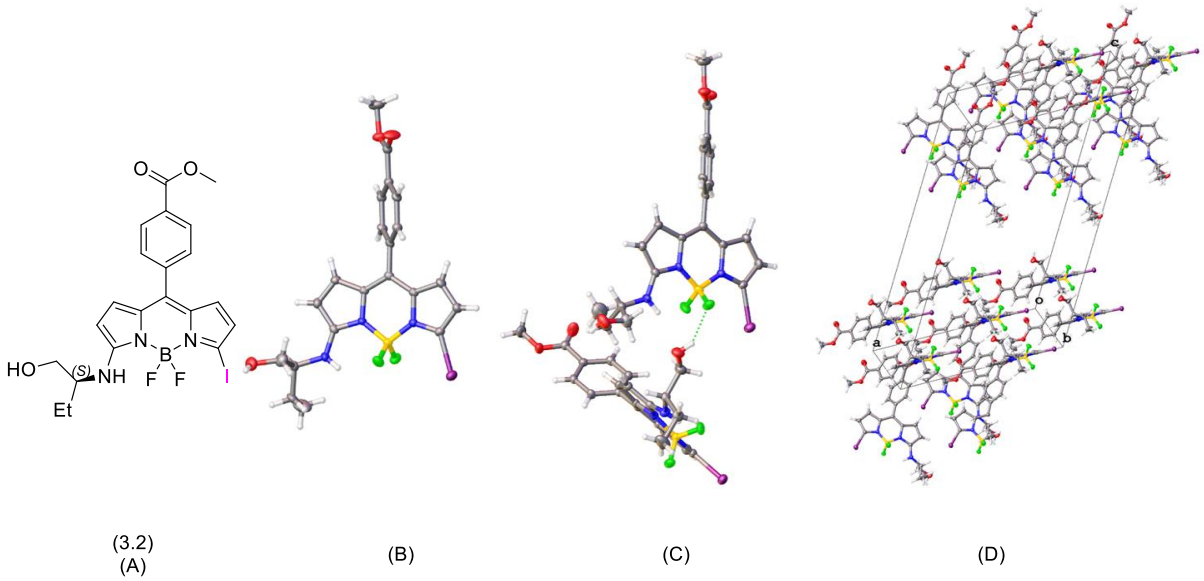

Figure 3.2: (*S*)-3-(1-hydroxybutan-2-yl)amino)-5-iodo BODIPY (**3.2**); (A) Molecular structure; (B) Single crystal X-ray structure; (C)The crystal structure including H-bonding; (D) The packing of the molecules in the unit cell.

In addition, the structure of the minor by-product 3-(*N*,*N*-diethylamine)-5-iodo BODIPY (**2.20**) was confirmed by NMR. The ^{1}H NMR showing signals at 3.87 ppm (q, *J* = 7.0 Hz, 4H, CH_2) and 1.38 ppm (t, *J* = 7.0 Hz, 6H, CH_3) corresponding to two ethyl groups, and the ^{19}F NMR showing a quartet at - 132.1 ppm (q, *J* = 33.5 Hz) corresponding to two equivalent fluorine atoms in BF_2 group.

In conclusion, both 3,5-dibromo BODIPY (**1.67**) and 3,5-diiodo BODIPY (**1.68**) gave good S_NAr reactions with (*S*)-2-aminobutan-1-ol (**3.8**) with high yields. However, we observed that 3,5-dibromo BODIPY (**1.67**) underwent S_NAr reactions with (*S*)-2-aminobutan-1-ol faster than the corresponding 3,5-diiodo BODIPY (**1.68**). We postulate that this is due to the higher electronegativity of bromine over iodine,

which helps in the rate determining step of a stepwise S_NAr mechanism, the addition of nucleophile to the aromatic ring.

After successfully introducing (*S*)-2-aminobutan-1-ol into 3-position of 3,5-diiodo BODIPY (**1.68**) via S_NAr chemistry, our next plan was to synthesize a range of 5-iodo BODIPYs containing enantiopure amino alcohols in the 3-position. These compounds will then be used to investigate the impact of different chiral auxiliaries in controlling the helical chirality in the final target helically chiral BODIPYs (Table **3.3**).

Therefore, using our previous reaction conditions, we synthesised (*R*)-3-(1-hydroxybutan-2-yl)amino)-5-iodo BODIPY (**3.14**) (Table **3.3**, Entry 1). This compound was synthesised as it will be used later to help prove the chiral integrity of the amino alcohol substituent during subsequent synthetic steps, by measuring the enantiomeric excess (*ee*) of the final helically chiral BODIPYs. We also used several other enantiopure (*S*)-amino alcohols with different R groups (*e.g.* CH_3, C_6H_5, and $C(CH_3)_3$) in S_NAr reactions with 3,5-diiodo BODIPY (**1.68**), to give molecules with which we can study the steric effect of the R group on diastereoselectivity of our planned chelation reactions to access helically chiral BODIPYs (Table **3.3**, Entries 2-4). In all cases high yields were obtained, following purification by column chromatography.

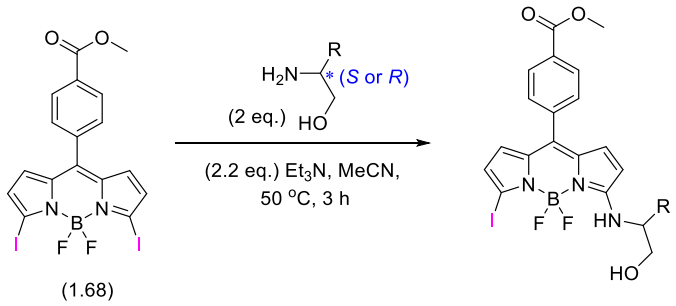

(1.68) (3.14 - 3.17)

Entry	Amino alcohols	Product	Stereochemistry (*R*/*S*)	Yield[a]/%
1	(**3.11**), R = -CH_2CH_3	(**3.14**)	*R*	Quant.
2	(**3.12**)-CH_3	(**3.15**)	*S*	Quant.
3	(**3.9**)-C_6H_5	(**3.16**)	*S*	99
4	(**3.13**)-$C(CH_3)_3$	(**3.17**)	*S*	Quant.

Table 3.3: Synthesis of 3-amino alcohol substituted 5-iodo BODIPYs (R = CH_3 to R = $C(CH_3)_3$). [a] Isolated yield following column chromatography.

In order to check the absolute stereochemistry of (*R*)-3-(1-hydroxybutan-2-yl)amino)-5-iodo BODIPY (**3.11**), we measured the specific rotation ($[\alpha]_D$) to be -19 (c = 0.1, DCM), taken as an average over 3 measurements. This is the opposite sign to that of the corresponding (*S*)-compound, and was of similar magnitude (30), helping to confirm the presence of (*R*)-stereochemistry.

Through the use of S_NAr chemistry we have successfully prepared mono substituted BODIPYs containing different amino alcohols, including examples of both (*S*)- and (*R*)-amino alcohols, as well as a range of R groups, all in high yields. Next, we will examine de-chelation reactions and the introduction of *para*-substituted phenyl boronic acid groups in the 5 position.

3.4 De-chelation Reaction to Remove BF_2

3.4.1 De-chelation Reaction to Remove BF_2 by Using Lewis Acids or TFA

Following our planned route A (Scheme **3.1**), the next step was the removal of the BF_2 group, or de-chelation reaction. Similar de-chelation reactions of BODIPYs are known in the literature, including work by Ravikanth *et al.*, in which they examined a range of different Lewis acids (*e.g*. $ZrCl_4$, $AlCl_3$, and $TiCl_4$) to remove the BF_2 group.[75] Similarly, Rutledge and co-workers have used Brønsted acids (*e.g*. TFA and methanolic hydrogen chloride) at room temperature to remove BF_2 group.[76]

3.4.2 De-chelation Reaction to Remove BF_2 Centre of 3,5-Dibromo BODIPY (**1.67**)

Therefore, we examined the reaction of 3,5-dibromo BODIPY (**1.67**), as a test molecule, with three different Lewis acids in comparison to our previously used TFA/DCM/MeOH de-chelation conditions. In the first attempt, we reacted 3,5-dibromo BODIPY (**1.67**) with five equivalents of $TiCl_4$ in CH_3CN/CH_3OH at reflux for 72 h, however only unreacted 3,5-dibromo BODIPY (**1.67**) was observed (Table **3.4**, Entry 1). Further reactions under the previous conditions, in which $TiCl_4$ was replaced with five equivalents of $ZrCl_4$ or $AlCl_3$, both resulted in loss of the starting material, but with none of the desired product observed following column chromatography (Table **3.4**, Entry 2,3). 3,5-Dibromo BODIPY (**1.67**) could however be de-chelated using TFA/DCM/MeOH (90:5:5) at room temperature for 72 h, which following aqueous work-up gave a 80 % crude yield of α,α-dibromo dipyrromethene (**2.14**) based on the mass recovered and a relatively clean ^{1}H NMR (Table **3.4,** Entry 4).

We have shown that α,α-dibromo-dipyrromethene (**2.14**) can be prepared via de-chelation with TFA/DCM/MeOH. However, since our target dipyrromethenes contain complex substituents are the α,α-positions in the next section we will examine the further use of Lewis acids to attempt de-chelation of these substrates.

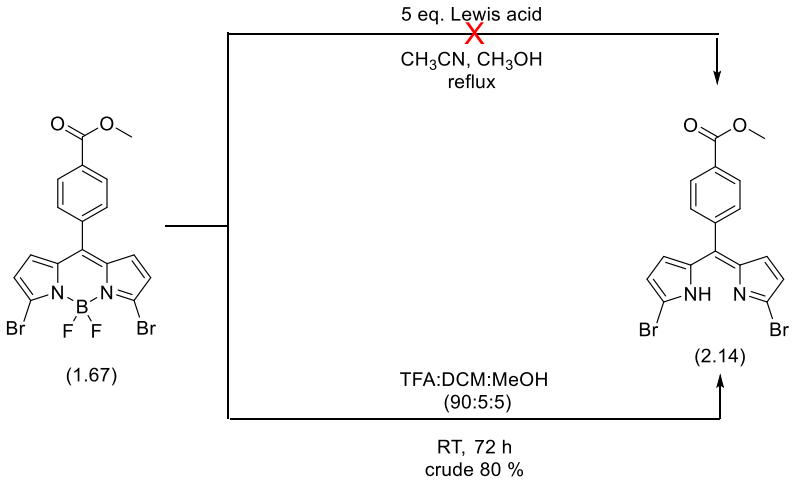

Entry	Reagent	Reaction Temp./°C	Reaction Time/ h	Reaction Outcome
1	$TiCl_4$	Reflux	72	Starting material recovered
2	$ZrCl_4$	Reflux	39	Complex mixture obtained
3	$AlCl_3$	Reflux	18	Complex mixture obtained
4	TFA:DCM:MeOH	RT	72	α,α-dibromo dipyrromethene (**2.14**), 80 %

Table 3.4: Optimisation of de-chelation conditions to prepare α,α-dibromo dipyrromethene (**2.14**)

3.4.3 De-chelation Reaction to Remove BF_2 of mono substituted BODIPYs

Next, we planned to test the de-chelation of mono substituted-BODIPYs. We focussed on the use of both TFA conditions as well $AlCl_3$ as a Lewis acid for the de-chelation (Scheme **3.2**).

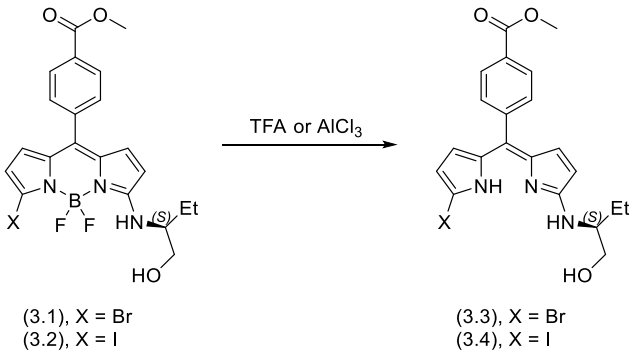

Scheme 3.2: Planned de-chelation reactions of mono substituted-BODIPYs by Brønsted or Lewis acids.

3.4.3.1 De-chelation Reaction to Remove BF_2 of mono substituted BODIPYs by TFA

Our first attempts involved the use of TFA to de-chelate our BODIPYs. Thus, we treated (*S*)-3-(1-hydroxybutan-2-yl)amino)-5-iodo BODIPY (**3.2**) with mixture of TFA:DCM:MeOH (90:5:5) at room

temperature. The reaction was monitored by TLC, which showed the disappearance of the starting material and the formation of multiple new products after 1 hour, after which an aqueous work-up was performed. Analysis of ^{1}H NMR of the crude mixture showed the formation of a highly complex mixture including a trace amount of the desired product α-((*S*)-2-aminobutan-1-ol)-α'-iodo dipyrromethene (**3.4**) (Table **3.5**, Entry 1).

We also examined the de-chelation of (*S*)-3-(1-hydroxybutan-2-yl)amino)-5-bromo BODIPY (**3.1**) under similar conditions with TFA:DCM:MeOH (90:5:5). TLC showed the starting material was consumed and again multiple new products had been formed after 1 hour. Following an aqueous work-up, analysis of ^{1}H NMR showed a complex mixture had formed with only a trace amount of the desired product (*S*)-α-(1-hydroxybutan-2-yl)amino)-α'-bromo dipyrromethene (**3.3**) (Table **3.5**, Entry 2).

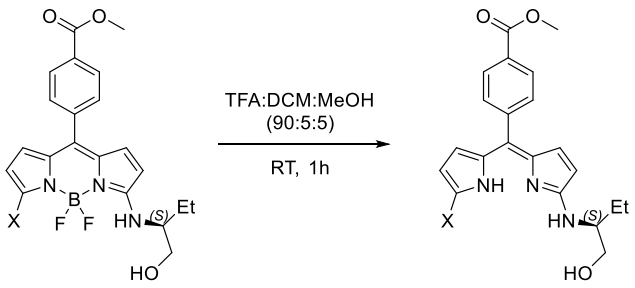

Entry	X	Reaction outcome
1	I	Complex mixture obtained[a]
2	Br	Complex mixture obtained[a]

Table 3.5: Attempted synthesis of α-((*S*)-2-aminobutan-1-ol)-α-halo-dipyrromethene (**3.3** and **3.4**).
[a] including trace amount of the desired product.

Since were unable to isolate the desired products, (*S*)-α-(1-hydroxybutan-2-yl)amino)-α'-bromo dipyrromethene (**3.4**) and (*S*)-α-(1-hydroxybutan-2-yl)amino)-α'-bromo dipyrromethene (**3.3**), due to the presence of a multiple reaction products and low yields, next we examined the use of Lewis acids as alternative de-chelation reagents.

3.4.3.2 De-chelation Reaction to Remove BF_2 of Mono Substituted-BODIPYs by $AlCl_3$

In our next attempts at a de-chelation reaction for our substrates, we decided to use $AlCl_3$ in a mixture of MeOH and MeCN. Therefore, we reacted (*S*)-3-(1-hydroxybutan-2-yl)amino)-5-iodo BODIPY (**3.2**) with five equivalents of $AlCl_3$, in MeOH/MeCN under reflux. After 3 hours we observed the disappearance of starting material and the formation of multiple new compounds including a major product by TLC analysis, which was coloured but non-fluorescent as expected for a dipyrromethene.

Following work-up and purification by column chromatography, the non-fluorescent product was obtained in 64% yield, however examination by NMR showed that the structure did not match that expected for the desired compound (Table **3.6**, Entry 1).

^{19}F NMR and ^{11}B NMR showed that there was no signal present in either spectrum, confirming that BF_2 group had been successfully removed. Interestingly, the ^{1}H NMR spectrum showed a set of five signals corresponding to pyrrolic protons, suggesting the presence of five different pyrrolic proton environments, implying the loss of the iodine group. The loss of iodine was further confirmed by high resolution mass spectrometry (HRMS) which showed a molecular ion at *m/z* = 366.1822 $[M+H]^+$, which corresponded to a molecular formula of $C_{21}H_{24}N_3O_3$. We postulate that this unexpected product (**3.18**) may have been formed through de-chelation followed by an electrophilic aromatic *ipso*-substitution reaction (S_EAr) at the iodine position, with either a proton or $AlCl_3$ followed by proto-demetalation.

Due to the loss of the iodine atom, we decided to repeat the de-chelation reaction with $AlCl_3$ following the reaction progress carefully by TLC in an attempt to isolate the desired de-chelated product before loss of iodine occurs. Thus, we reacted (*S*)-3-(1-hydroxybutan-2-yl)amino)-5-iodo BODIPY (**3.2**) with five equivalents of $AlCl_3$ under our previous conditions, with monitoring by TLC, after 2 h the TLC showed that the starting material had been consumed and new products formed, however the ^{1}H NMR showed that mixture products had been formed (Table **3.6**, Entry 2). We repeated the reaction again under the same conditions, we stopped the reaction after 10 minutes to minimise by-product formation, however a complex mixture was still obtained (Table **3.6**, Entry 3).

Due to the problems with the loss of iodine under the reaction conditions, we next examined the de-chelation reaction (*S*)-3-(1-hydroxybutan-2-yl)amino)-5-bromo BODIPY (**3.1**), with five equivalents of $AlCl_3$, in MeOH/MeCN under reflux. Due to the stronger C-Br bond, in comparison to C-I, we postulated that the bromo-substituted BODIPYs maybe more tolerant to the reaction conditions. The de-chelation reaction was monitored by TLC, which showed the disappearance of the starting material and the formation of new products after 2 hours, however again ^{1}H NMR showed the formation of a complex mixture of products (Table **3.6**, Entry 4). In the final attempt, we repeated the de-chelation reaction with (*S*)-3-(1-hydroxybutan-2-yl)amino)-5-bromo BODIPY (**3.1**) under similar conditions. By TLC analysis, we observed that after 10 min the starting material had been consumed and a new product had been formed. Following aqueous work-up, the desired product (*S*)-α-(1-hydroxybutan-2-yl)amino)-α'-bromo dipyrromethene (**3.3**) was obtained in an 87% crude yield, with acceptable purity by ^{1}H NMR (Table **3.6**, Entry 5). Due to potential problems in purifying de-chelated products, (*S*)-α-(1-hydroxybutan-2-yl)amino)-α'-bromo dipyrromethene (**3.3**) was taken forward for the next steps without additional purification.

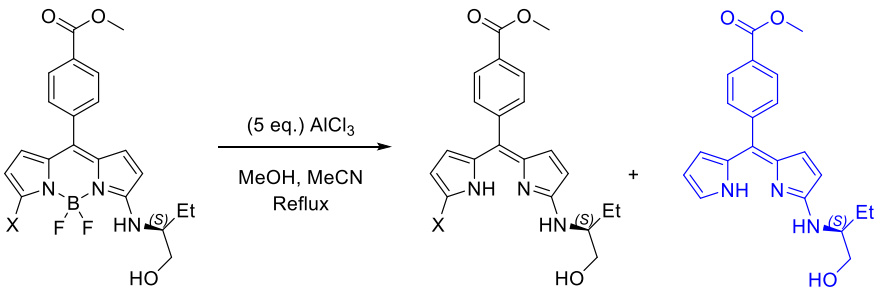

Entry	X	Reaction Time/ min	Reaction outcome and yield
1	I	180	loss of iodine atom, give (**3.18**) 64 %[a]
2	I	120	mixture
3	I	10	mixture
4	Br	120	mixture
5	Br	10	(**3.3**), 87%[b]

Table 3.6: Synthesis of (*S*)-α-(1-hydroxybutan-2-yl)amino)-α'-halo dipyrromethene (**3.3** and **3.4**). [a] isolated yield following column chromatography; [b] crude yield.

The structure of (*S*)-α-(1-hydroxybutan-2-yl)amino)-α'-bromo dipyrromethene (**3.3**) was confirmed by ^{1}H NMR showed a set of signals at 6.65 ppm (d, *J* = 4.7 Hz, 1H), 6.18 ppm (d, *J* = 4.7 Hz, 1H), 6.11 ppm (d, *J* = 3.8 Hz, 1H), and 5.93 ppm (d, *J* = 3.8 Hz, 1H) corresponding to the four pyrrolic proton environments. There were no signals in the ^{19}F NMR and ^{11}B NMR spectra corresponding to a BODIPY, which gave us confidence that the BF_2 group had been removed.

As we had successfully removed the BF_2 group from (*S*)-3-(1-hydroxybutan-2-yl)amino)-5-bromo BODIPY (**3.1**), by using $AlCl_3$, we next planned to examine the second step in our synthetic route, a Suzuki Miyaura cross-coupling reaction between (*S*)-α-(1-hydroxybutan-2-yl)amino)-α'-bromo dipyrromethene (**3.3**) and (2-hydroxyphenyl)boronic acid (**3.19**).

3.5 Suzuki Miyaura Cross-Coupling reaction

3.5.1 Suzuki Miyaura Cross-Coupling Reaction with (2-Hydroxyphenyl)boronic acid

We planned to examine Suzuki Miyaura cross-coupling reaction between (*S*)-α-(1-hydroxybutan-2-yl)amino)-α'-bromo dipyrromethene (**3.3**) and (2-hydroxyphenyl)boronic acid (**3.19**). Following a procedure described by Hall *et al.* in which they reported Suzuki Miyaura cross-coupling reactions with 3,5-dibromo BODIPYs (Scheme **3.3**).[45]

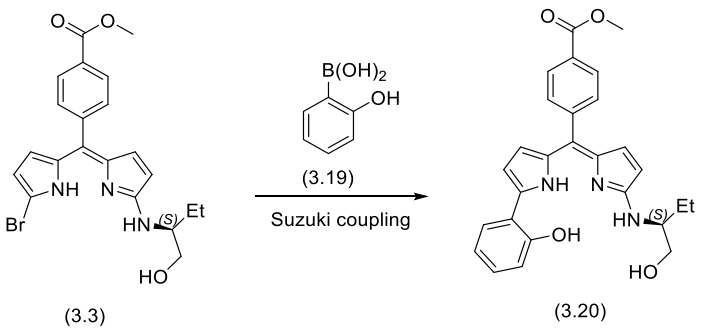

Scheme 3.3: Planned Suzuki Miyaura Cross-Coupling reaction between difunctionalised (*S*)-α-(1-hydroxybutan-2-yl)amino)-α'-bromo dipyrromethene (**3.3**) and (2-hydroxyphenyl)boronic acid (**3.19**).

Thus, for our planned Suzuki cross coupling reaction, we first prepared our catalyst, XPhos Pd G3. Based on a literature procedure reported by Buchwald, we reacted 2-aminobiphenyl (**3.20**) dissolved in diethyl ether with a solution of methanesulfonic acid in diethyl ether at room temperature for 30 min. The resulting reaction mixture was filtered and washed with diethyl ether to afford mesylate salt (**3.22**) as a white solid.[77] In the next step, in a Schlenk flask, the mesylate salt (**3.22**) was coupled with palladium acetate in dry toluene at 50 °C for 45 min. After which the suspension was filtered and washed with toluene and diethyl ether to give μ-OMs dimer (**3.23**). In the last step, a mixture of μ-OMs dimer (**3.23**) and XPhos, as a ligand, was stirred at room temperature for 30 min in THF. About 90% of the solvent was removed under vacuum resulting in an oily solution, followed by addition of pentane to precipitate the product. Following trituration with pentane, the desired XPhos Pd G3 (**3.24**) was obtained in an excellent yield of 81 % (Scheme **3.4**). The structure of XPhos Pd G3 (**3.24**) was confirmed by comparing our ^{1}H and ^{31}P NMR with the literature, which showed similar results.[77]

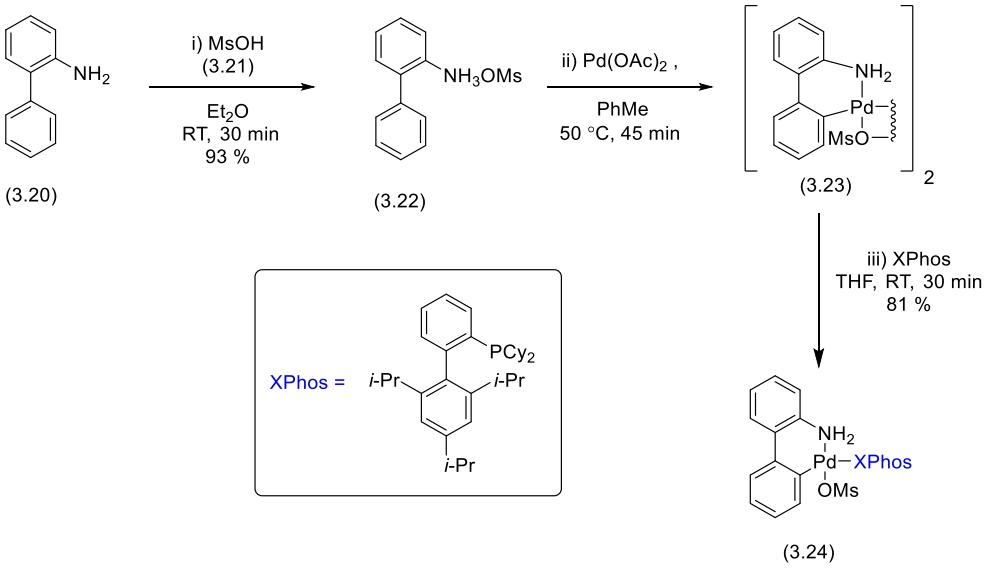

Scheme 3.4: Synthesis of XPhos Pd G3 catalyst (**3.24**).

After we had successfully prepared the XPhos Pd G3 (**3.24**), we next reacted (*S*)-α-(1-hydroxybutan-2-yl)amino)-α'-bromo dipyrromethene (**3.3**), in a Schlenk flask under an atmosphere of nitrogen (degassed three times), with two equivalents of (2-hydroxyphenyl)boronic acid (**3.19**) in THF/water at 75 °C, with potassium phosphate and 6 mol% XPhos Pd G3. The reaction was monitored by TLC, which showed the formation of new products over 96 hours and followed by a simple aqueous work-up (Scheme **3.5**).

Upon an examination of the crude ^{1}H NMR and ^{11}B NMR spectra, ^{1}H NMR showed the formation of a major product, alongside a related minor product. ^{11}B NMR spectra showed that (2-hydroxyphenyl)boronic acid was no longer present, due to the loss of the corresponding boron peak at 28 ppm. However, a new boron centre could be observed by ^{11}B NMR spectra, giving a singlet at 0.90 ppm. Examination of the literature showed that helically chiral *N,N,O,O*-BODIPYs show boron shifts of between -0.90 and 0.10 ppm,[11] *N,N,O,F*-BODIPYs show shifts of approximately 0.2 ppm,[78] "confused" *N,N,O,C*-BODIPYs (in which the boron-chelating aryl group is rotated resulting in a B-C bond in place of the "standard" B-O bond) show shifts in the range -3.26 to -2.39 ppm,[79] whilst "standard" *N,N,O,C*-BODIPYs (including those prepared in Chapter 4 and 5) give a range of 1.30 to 1.64 ppm. Thus we speculate that the unexpected product formed maybe *N,N,O,C*-BODIPY (**3.25**), based on both ^{11}B shift and the presence of possible major and minor diastereomers (Scheme **3.5**).

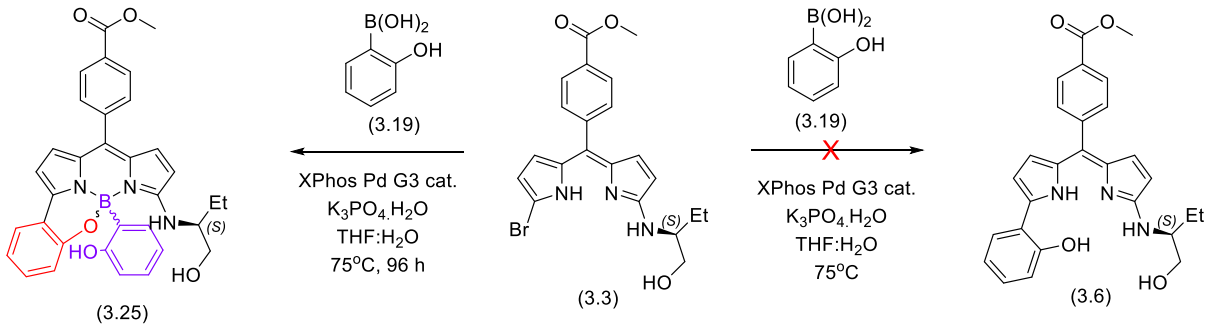

Scheme 3.5: Results of Suzuki Miyaura cross-coupling reaction to give unexpected product *N,N,O,C*-BODIPY (**3.25**).

We propose that *N,N,O,C*-BODIPY (**3.25**) could be formed in the reaction through three reaction steps including the formation of boron centre via boron chelation reaction of one equivalent of (2-hydroxyphenyl)boronic acid (**3.19**), Suzuki coupling with another equivalent of (2-hydroxyphenyl)boronic acid and B-O bond formation in which the boron is chelated with the phenolic hydroxy group (Scheme **3.6**).

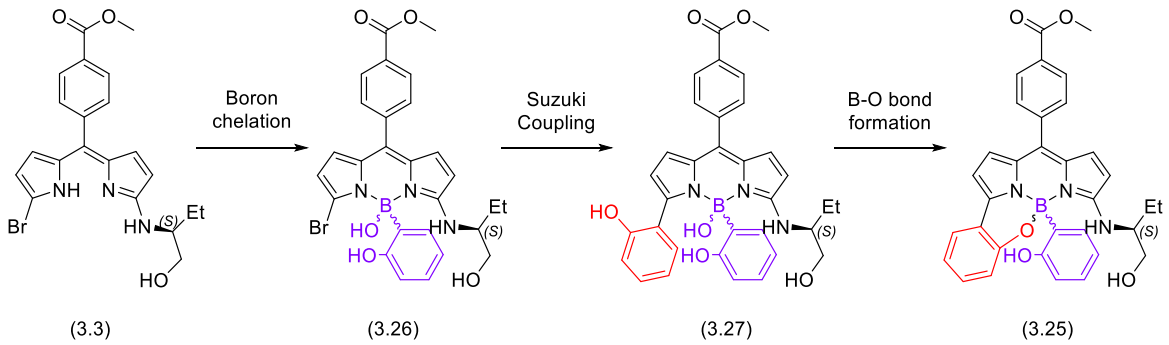

Scheme 3.6: Proposed reaction steps to form *N,N,O,C*-BODIPY (**3.25**)

Unfortunately, attempts to further purify *N,N,O,C*-BODIPY (**3.25**) were unsuccessful due to degradation on silica gel chromatography, thus further study of this reaction was not possible. Due to these unexpected results of the attempted Suzuki Miyaura cross-coupling reaction with (*S*)-α-(1-hydroxybutan-2-yl)amino)-α'-bromo dipyrromethene (**3.3**), we next planned to examine an alternative approach starting with the chelation of (*S*)-α-(1-hydroxybutan-2-yl)amino)-α'-bromo dipyrromethene (**3.3**) with aryl boronic acids under mild conditions.

3.5.2 Chelation Reaction by Using (4-Methoxyphenyl)boronic acid

We planned to examine the chelation of α-((*S*)-2-aminobutan-1-ol)-α'-bromo dipyrromethene (**3.3**) with (4-methoxyphenyl)boronic acid (**2.23**) in chloroform under a mild conditions. Our procedure was based on work of Nabeshima and co-workers, in which they examined the chelation of dipyrromethenes with a range of arylboronic acids, including phenyl boronic acid, naphthalene-1-boronic acid, and (4-methoxyphenyl)boronic acid.[80]

Thus, we reacted one equivalent of α-((*S*)-2-aminobutan-1-ol)-α'-bromo dipyrromethene (**3.3**) with 7.5 equivalents of (4-methoxyphenyl)boronic (**2.23**) in chloroform at room temperature. The reaction was monitored by TLC, and after 17 h showed only the presence of starting material with no other products being formed (Table **3.7**, Entry 1). We then re-examined the reaction focusing on increasing both the temperature and the reaction time. In our first attempt to improve the reaction outcomes, we reacted one equivalent of (*S*)-α-(1-hydroxybutan-2-yl)amino)-α'-bromo dipyrromethene (**3.3**) with 7.5 equivalents of (4-methoxyphenyl)boronic acid (**2.23**) in chloroform as before, but heated the reaction mixture to reflux. The reaction was monitored by TLC and after 48 hours, the formation of multiple products could be observed by crude ^{1}H NMR spectroscopy. The ^{11}B NMR spectrum showed a number of overlapping peaks at around 1.8 ppm, suggesting the formation of chelated *N,N,O,C*-BODIPYs (^{11}B NMR as discussed previously) as well as a large broad singlet signal at 30.8 ppm corresponding to remaining excess (4-methoxyphenyl)boronic acid (**2.23**) (Table **3.7**, Entry 2). Next, we repeated the reaction using only 1 equivalent of (4-methoxyphenyl)boronic acid (**2.23**) in refluxing

chloroform. Monitoring by TLC showed new products had been formed after 127 hours. After removal of the solvent under reduced pressure the crude reaction mixture was purification by column chromatography, two *N,N,O,C*-BODIPYs diastereomers (3.28a) and (3.28b) were obtained in a 48% and 7% isolated yield, giving a *de* of 75% (Table **3.7**, Entry 3).

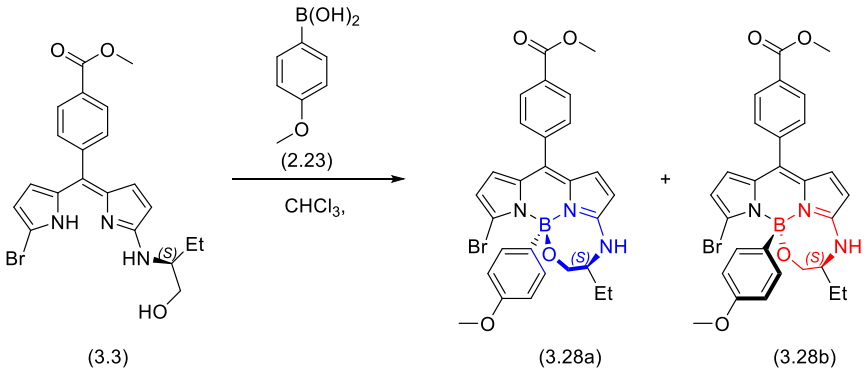

(3.3) (3.28a) (3.28b)

Entry	Eq. of boronic acid	Reaction Temp./°C	Reaction Time/h	Reaction outcome and yield/%
1	7.5	RT	17 h	Starting material recovered
2	7.5	Reflux	48 h	Complex mixture
3	1	Reflux	127 h	48% and 7%

Table 3.7: Synthesis of diastereomeric *N,N,O,C*-BODIPYs (**3.28a**) and (**3.28b**).

The structure of the major isomer of *N,N,O,C*-BODIPYs (**3.28**) was confirmed by the analysis of ^{1}H NMR spectra which showed two singlet signals at 3.96 ppm (s, 3H) and 3.73 (s, 3H) corresponding to methyl ester and methoxy group, respectively. For further confirmation, the major isomer *N,N,O,C*-BODIPY (**3.28**) was analysed by ASAP (Atmospheric Solids Analysis Probe) low resolution mass spectrometry (LRMS) in negative mode, which showed a peak at *m/z* = 560.1 assigned as $[M]^-$ which corresponded to a molecular formula of $C_{28}H_{27}{}^{10}B^{81}BrN_3O_4$. Unfortunately attempts to grow crystals of two diastereomers for further structural analysis and to allow the assignment of absolute stereochemistry by single crystal X-ray diffraction was not successful.

We have shown that the test boron chelation of (*S*)-α-(1-hydroxybutan-2-yl)amino)-α'-bromo dipyrromethene (**3.3**) worked well, and that this substrate can undergo boron chelation reaction under mild conditions with chirality control in the *N,N,O,C*-BODIPYs (**3.28a** and **3.28b**) formed.

Next, due to synthetic difficulties in our originally planned route A (Scheme **3.1**), we decided to examine our planned route B (Scheme **3.1**) approach in which we will change the order of the synthetic

steps. Thus, we will re-examine a route to our target BODIPYS, via an S_NAr, Suzuki Miyaura cross-coupling reaction sequence followed by de-chelation reaction and finally re-chelation.

3.6 Suzuki Miyaura Cross-Coupling Reaction and De-chelation Reaction

Our plan in route B involved following the S_NAr chemistry (as described previously) with a Suzuki Miyaura cross-coupling reaction between (*S*)-3-(1-hydroxybutan-2-yl)amino)-5-iodo BODIPY (**3.2**) and 2-hydroxyphenylboronic acid. A subsequent de-chelation reaction would then afford (*S*)-α-(1-hydroxybutan-2-yl)amino)-α'-(2-hydroxyphenyl) dipyrromethene (**3.6**) (Scheme **3.7**).

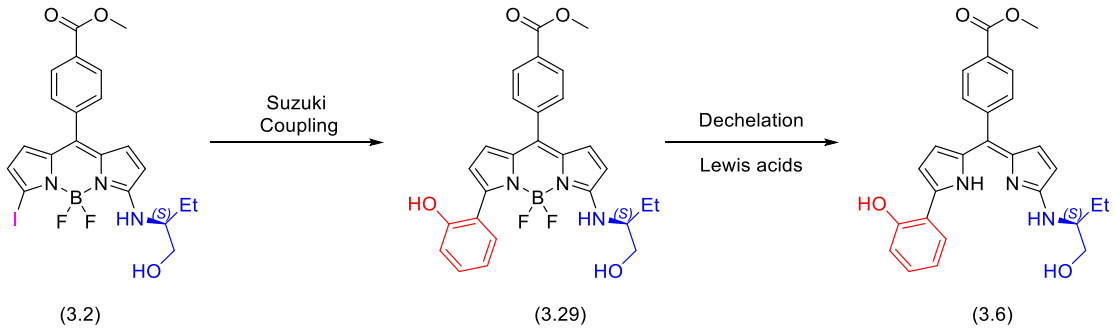

Scheme 3.7: Planned synthetic route to (*S*)-α-(1-hydroxybutan-2-yl)amino)-α'-(2-hydroxyphenyl) dipyrromethene (**3.6**).

3.6.1 Suzuki Miyaura Cross-Coupling Reaction

In our first Suzuki Miyaura cross-coupling reaction, we reacted 1 equivalent of (*S*)-3-(1-hydroxybutan-2-yl)amino)-5-iodo BODIPY (**3.2**) on a 0.10 mmol scale with 2 equivalents of 2-hydroxyphenylboronic acid (**3.19**) catalysed by 6 mol% of XPhos Pd G3. The reaction was monitored by TLC which showed that a new product had been formed after 2 h. After aqueous work-up, the desired (*S*)-3-(1-hydroxybutan-2-yl)amino)-5-(2-hydroxyphenyl) BODIPY (**3.5**) was obtained in a quantitative yield as a red solid without the need for column chromatography (Table **3.8**, Entry 1). The reaction was repeated on scales up to 2.12 mmol, giving good yields in all cases (Table **3.8**, Entries 2-5, 8, and 9), including after purification by column chromatography (Table **3.8**, Entries 6, 7, and 10).

The structure of (*S*)-3-(1-hydroxybutan-2-yl)amino)-5-(2-hydroxyphenyl) BODIPY (**3.5**) was confirmed by the analysis of ^{1}H NMR spectra, which showed new signals at the aromatic range 7.49 ppm (dd, *J* = 7.6, 1.7 Hz, 1H), 7.33 ppm (ddd, *J* = 8.2, 7.3, 1.7 Hz, 1H), 7.05 – 7.02 ppm (m, 1H), 7.00 ppm (dd, *J* = 7.5, 1.2 Hz, 1H) corresponding to the newly included *ortho*-phenolic ring.

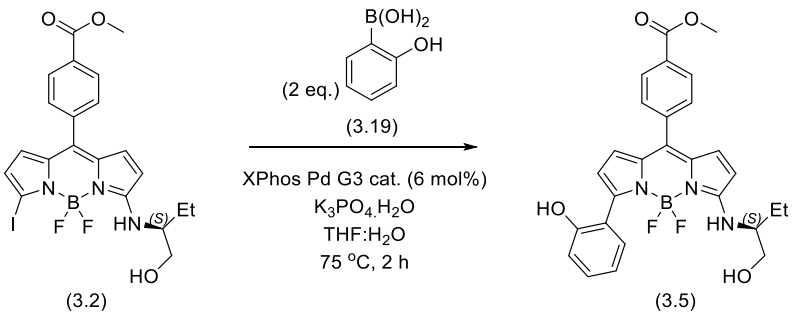

Entry	Scale/mmol	Yield/%
1	0.10	Quant.[b]
2	0.15	Quant.[b]
3	0.21	93[b]
4	0.29	97[b]
5	0.31	Quant.[b]
6	0.50	66[a]
7	0.69	Quant.[a]
8	0.85	Quant.[b]
9	1.20	Quant.[b]
10	2.12	81[a]

Table 3.8: Synthesis of (*S*)-3-(1-hydroxybutan-2-yl)amino)-5-(2-hydroxyphenyl) BODIPY (**3.5**). [a] Isolated yield following column chromatography. [b] crude yield.

After successfully showing that (*S*)-3-(1-hydroxybutan-2-yl)amino)-5-(2-hydroxyphenyl) BODIPY (**3.5**) can undergo a high yielding Suzuki Miyaura cross-coupling reaction. We plan to screen a number of Suzuki Miyaura cross-coupling reactions using different enantiopure amino alcohols for future investigation of the impact of different chiral auxiliaries in controlling the helical chirality in the formation of the final helically chiral BODIPYs.

3.6.2 Suzuki Miyaura Cross-Coupling Reaction Scope

Thus, as a first step, under our previous Suzuki reaction conditions we synthesised the other enantiomer, (*R*)-3-(1-hydroxybutan-2-yl)amino)-5-(2-hydroxyphenyl) BODIPY (**3.29**), in 87 % yield following column chromatography (Table **3.9**, Entry 1). As mentioned previously, this compound will be used to assist in the measurement of the enantiomeric excess (%*ee*) of the final target helically chiral BODIPYs.

We also tested the Suzuki reaction with 2-hydroxyphenylboronic acid (**3.19**) and a number of previously prepared BODIPYs containing enantiopure (*S*)-amino alcohols with different R groups (*e.g.*,

CH_3, C_6H_5, and $C(CH_3)_3$). These molecules will be used to study the steric effects of the R group on the diastereoselectivity of our planned chelation reactions to access helically chiral BODIPYs. In all cases high yields were obtained, following purification by column chromatography (Table **3.9**, Entries 2-4).

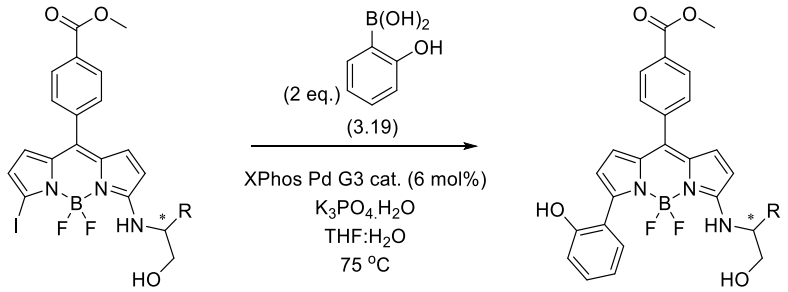

Entry	Stating material	Reaction time/h	Stereochemistry (*R*/*S*)	Product	Yield[a]/%
1	(**3.14**), R = -CH_2CH_3	2	*R*	(**3.29**)	87
2	(**3.15**), R = -CH_3	2	*S*	(**3.30**)	74
3	(**3.16**), R = -C_6H_5	1.5	*S*	(**3.31**)	84
4	(**3.17**), R = -$C(CH_3)_3$	1.5	*S*	(**3.32**)	74

Table 3.9: Synthesis of 3-amino alcohol substituted 5-(2-hydroxyphenyl) BODIPYs (**3.29** – **3.32**). [a] Isolated yield following column chromatography.

The structure of all four of the newly formed 3-amino alcohol substituted 5-(2-hydroxyphenyl)-BODIPYs (**3.29** – **3.32**) was confirmed by NMR. However, in the case of (*R*)-3-(1-hydroxybutan-2-yl)amino)-5-(2-hydroxyphenyl) BODIPY (**3.29**) we observed that the colour of a sample, that was prepared for NMR in $CDCl_3$ following column chromatography, changed from red to purple after being stored at room temperature for one day. Therefore, we decided to re-run NMR analysis to look for any changes to the compound. The analysis of the new ^{1}H NMR spectrum showed that the peak at 3.97 ppm corresponding to the methyl ester of (*R*)-3-(1-hydroxybutan-2-yl)amino)-5-(2-hydroxyphenyl) BODIPY (**3.29**) had disappeared, and two new singlet peaks at 3.96 ppm and 3.93 ppm in a 3:1 ratio had appeared, maybe corresponding to two methyl ester groups of two new molecules. In addition, the presence of multiple new peaks in the aromatic range helped to confirm the formation of mixture of new unknown BODIPYs. Interestingly, further storage of the NMR sample for up to 1 year showed no further change in the spectra, suggesting that the molecules formed were stable (Figure **3.3**).

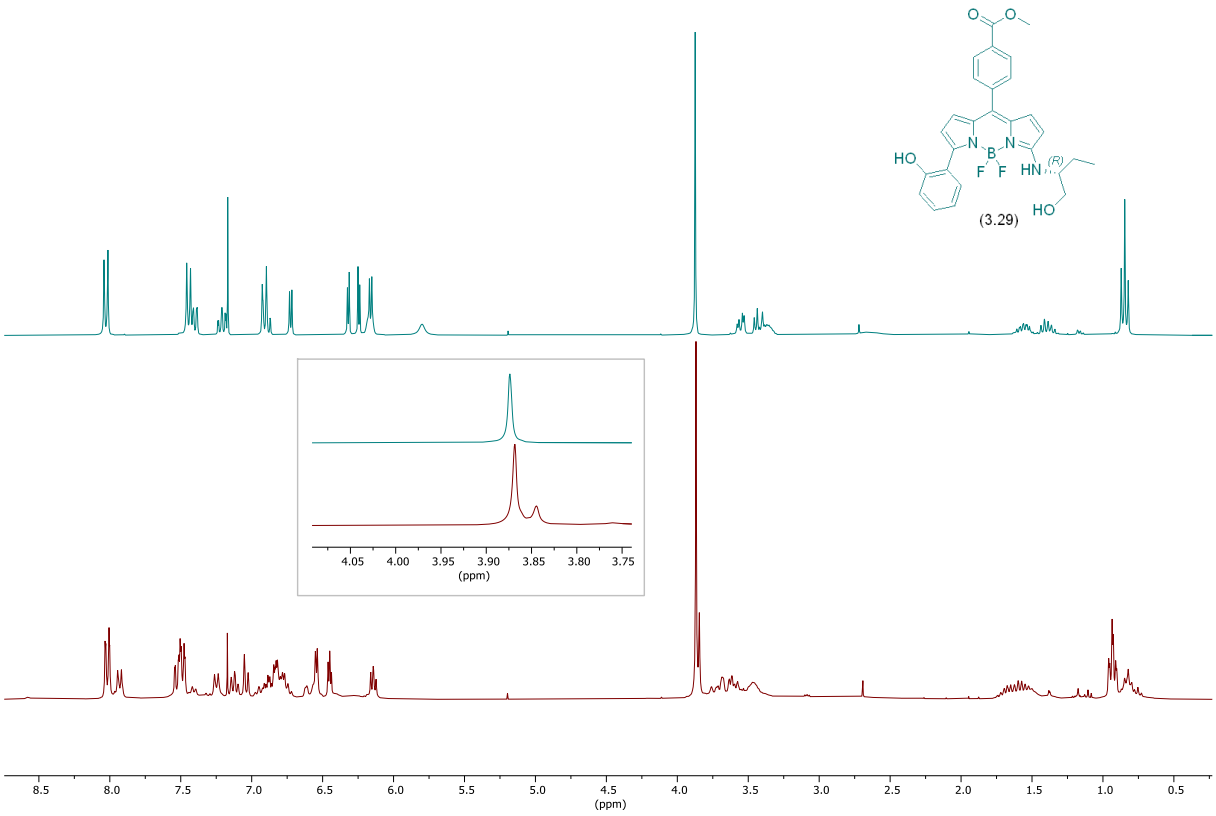

Figure 3.3: ^{1}H NMR spectrum (300 MHz, $CDCl_3$) of (*R*)-3-(1-hydroxybutan-2-yl)amino)-5-(2-hydroxyphenyl) BODIPY (**3.29**). Top: ^{1}H NMR following purification by column chromatography (green), Bottom: ^{1}H NMR following storage in fridge for 1 year (red).

We believe that upon storage in $CDCl_3$, (*R*)-3-(1-hydroxybutan-2-yl)amino)-5-(2-hydroxyphenyl) BODIPY (**3.29**) has undergone further reaction to form two new BODIPYs. We propose that the 2-hydroxyphenyl moiety may have formed a B-O bond, displacing the fluorine, and that this new *N,N,O,F* BODIPY (**3.33**) may have done an addition reaction in which the boron chelated with hydroxyl group of amino alcohol, displacing a second fluorine (Scheme **3.8**).

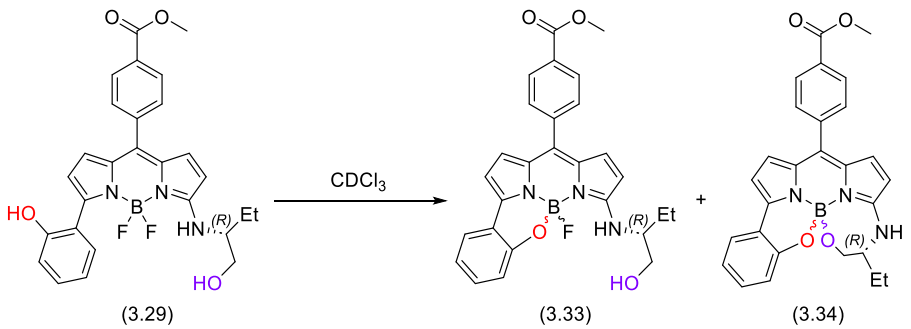

Scheme 3.8: Proposed structures of *N,N,O,F* BODIPY (**3.33**) and *N,N,O,O* BODIPY (**3.34**) formed form (*R*)-3-(1-hydroxybutan-2-yl)amino)-5-(2-hydroxyphenyl) BODIPY (**3.29**)

In order to test our assignment of the proposed structures of *N,N,O,F* BODIPY (**3.33**) and *N,N,O,O* BODIPY (**3.34**), we decided to run ^{11}B NMR. The analysis of the ^{11}B NMR spectrum showed the presence of two boron environments in a 2:1 ratio, a doublet at 0.56 ppm (d, *J* = 51.6 Hz) in which boron was coupled to one fluorine atom with a shift similar to other *N,N,O,F* BODIPYs in the literature (*e.g*. 0.19 ppm (*J* = 46.5 Hz), and a singlet at -0.93 ppm, that consistent with literature values for *N,N,O,O*-BODIPYs (*e.g*. -0.90 to 0.10 ppm) (Figure **3.4**)**.**

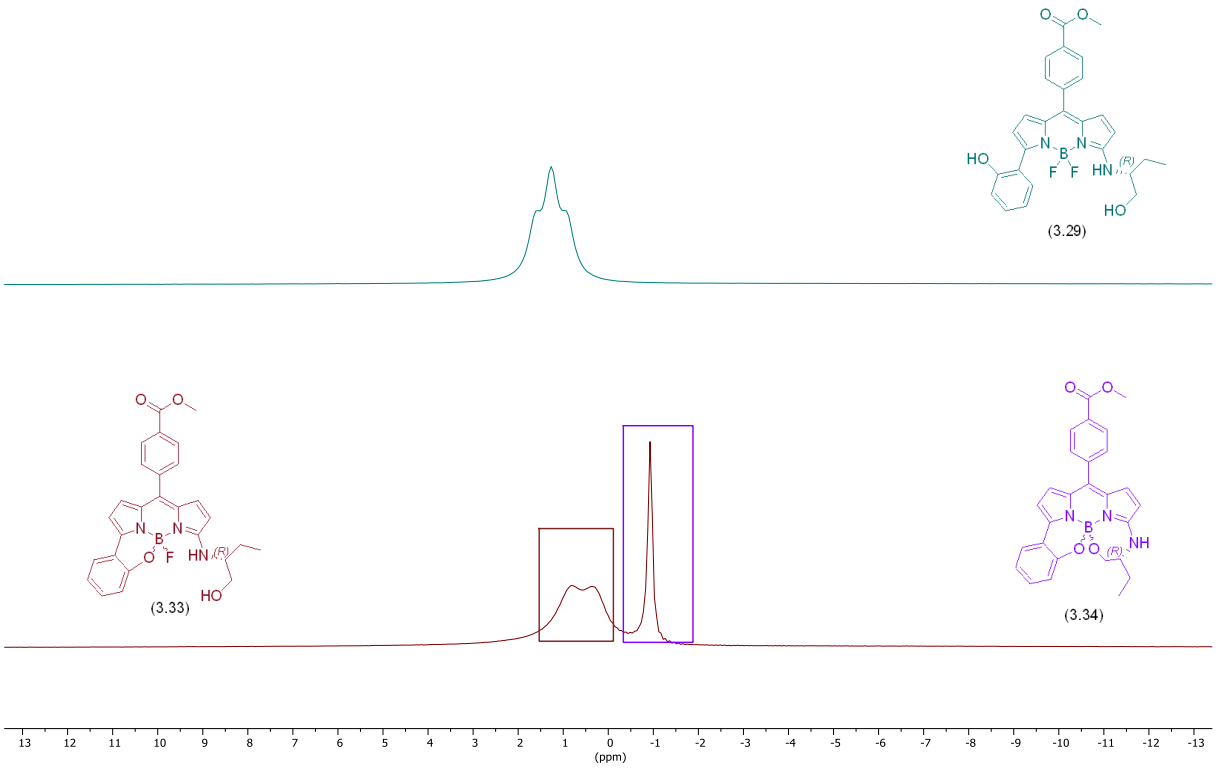

Figure 3.4: ^{1}B NMR spectrum (300 MHz, $CDCl_3$) of (*R*)-3-(1-hydroxybutan-2-yl)amino)-5-(2-hydroxyphenyl) BODIPY (**3.29**). Top: ^{11}B NMR following purification by column chromatography (green), Bottom: ^{11}B NMR following storage in fridge for 1 year (red).

For further confirmation of the proposed *N,N,O,F*-BODIPYs (**3.33**) and *N,N,O,O*-BODIPYs (**3.34**) structures, the analysis by ^{19}F NMR was undertaken. This showed weak signals at -140.8 ppm and -138.8 ppm which may correspond to two diastereomers of *N,N,O,F*-BODIPY (**3.33**). In addition, a singlet at -148.9 ppm was observed that might relate to SiF_4 species formed from the HF evolved during the reaction and the glass of the tube (Figure **3.5**).

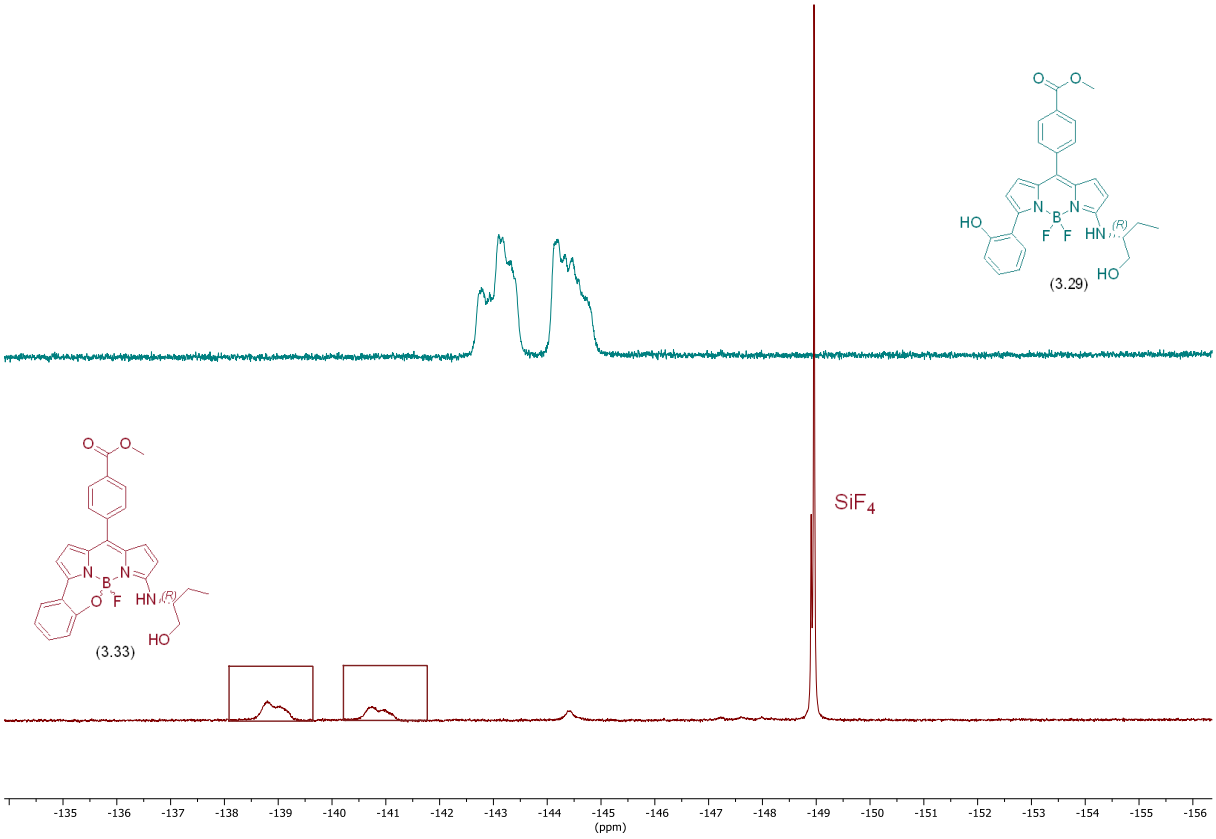

Figure 3.5: ^{19}F NMR spectrum (282 MHz, $CDCl_3$) of (*R*)-3-(1-hydroxybutan-2-yl)amino)-5-(2-hydroxyphenyl) BODIPY (**3.29**). Top: ^{19}F NMR following purification by column chromatography (green), Bottom: ^{19}F NMR following storage in fridge for 1 year (red).

First we tried to separate the two proposed *N,N,O,F*-BODIPYs (**3.33**) and *N,N,O,O*-BODIPYs (**3.34**) by preparative TLC (DCM: Ethyl acetate 100:10), to assist in characterisation of the molecules. Despite considerable streaking on preparative TLC, we were able to achieve separation and isolate one compound (~3 mg) with an R_f = 0.75 (DCM: Ethyl acetate 6:4). Due to the limited quantity of the isolated *N,N,O,F*-BODIPY (**3.33**), the ^{19}F NMR spectrum was too weak to definitively determine which diastereomer was present. However, analysis of the ^{11}B NMR spectrum showed the presence of a doublet at 0.56 ppm (d, *J* = 48.8 Hz) which matched that previously observed, indicating that the boron was coupled to one fluorine, suggesting this compound was *N,N,O,F*-BODIPY (**3.33**) (Figure **3.6**). This was supported by analysis of ^{1}H NMR spectrum, which showed a set of signals at 6.67 ppm (d, *J* = 5.1 Hz, 1H), 6.33 ppm (d, *J* = 3.9 Hz, 1H), 6.24 ppm (d, *J* = 4.0 Hz, 1H), 5.94 ppm (d, *J* = 4.8 Hz, 1H) corresponding to the four pyrrolic proton environments.

Furthermore, the structure of *N,N,O,F*-BODIPY (**3.33**) was confirmed by HRMS (ASAP-ToF) in positive mode which showed a molecular ion at *m/z* = 466.1968 $[M\text{-}F]^+$, which corresponded to a parent molecule with a formula of $C_{27}H_{25}{}^{11}BN_3O_4$.

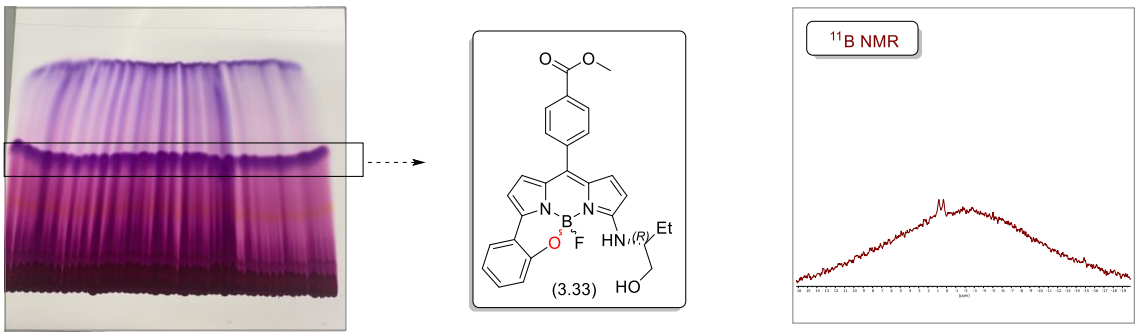

Figure 3.6: (A) Preparative TLC (DCM: Ethyl acetate 100:10), showing purple band of *N,N,O,F*-BODIPY (**3.33**); (B) Structure of *N,N,O,F*-BODIPY (**3.33**); and (C) ^{11}B NMR spectrum (300 MHz, $CDCl_3$) of *N,N,O,F*-BODIPY (**3.33**).

To further understand the formation of *N,N,O,F*-BODIPYs (**3.33**) and *N,N,O,O*-BODIPYs (**3.34**) in our reaction, we attempted a controlled formation of these products from (*S*)-3-(1-hydroxybutan-2-yl)amino)-5-(2-hydroxyphenyl) BODIPY (**3.5**), prepared previously. We followed a procedure reported by the Knight group for the formation of a "Half-Strapped" *N,N,O,F*-BODIPY which used a catalytic quantity of DIPEA and BF_3.OEt to achieved a similar ring closing reaction.[81] Therefore, we treated a solution of (*S*)-3-(1-hydroxybutan-2-yl)amino)-5-(2-hydroxyphenyl) BODIPY (**3.5**) in DCM with 0.12 equivalents of DIPEA and 0.1 equivalent of BF_3.OEt and heated to reflux. TLC showed rapid formation of a new compound, a second compound forming after a few minutes with starting material still present. After 10 min the reaction was quenched with $NaHCO_3$ solution, followed an aqueous work-up and purification by preparative TLC (DCM: Ethyl acetate 80:20). The crude ^{1}H NMR showed the presence of a number of compounds, so a portion of the crude was taken and purified by preparative TLC to obtain an analytically pure sample of the product. Following which we successfully isolated *N,N,O,F*-BODIPY (**3.35**) as a purple solid with the NMR matching that previously observed. This helped to support the formation of *N,N,O,F*-BODIPY (**3.33**) in the presence of catalytic Lewis acid from (*S*)-3-(1-hydroxybutan-2-yl)amino)-5-(2-hydroxyphenyl) BODIPY (**3.5**) (Scheme **3.9**).

Following this observation, we re-examined the NMR spectra for all of the 3-amino alcohol substituted 5-(2-hydroxyphenyl)-BODIPYs, following storage in $CDCl_3$ for a few days. In all cases the formation of similar compounds was observed. However, if the 3-amino alcohol substituted -5-(2-hydroxyphenyl)-BODIPYs were stored as dry solids then they remained stable for long periods of time, up to 1 year.

After successfully synthesising a range of 3-amino alcohol substituted-5-(2-hydroxyphenyl) BODIPYs in high yields, next we planned to examine their de-chelation reactions.

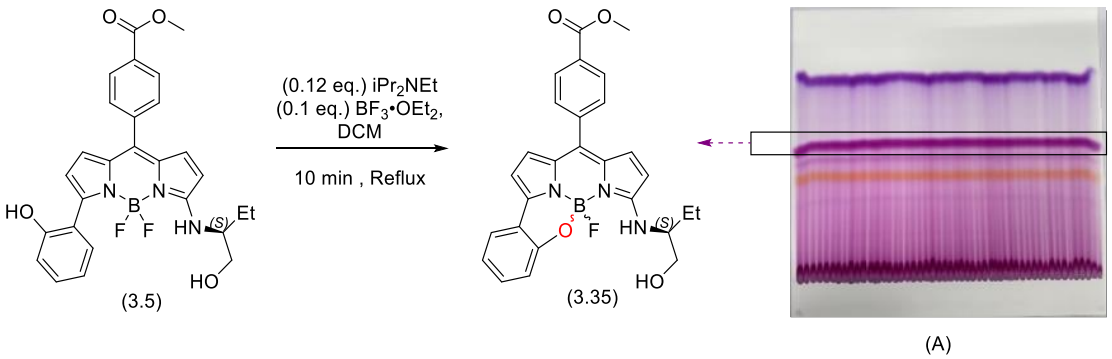

Scheme 3.9: Ring closing reaction of (*S*)-3-(1-hydroxybutan-2-yl)amino)-5-(2-hydroxyphenyl) BODIPY (**3.5**) with catalytic DIPEA and BF_3.OEt to give *N,N,O,F*-BODIPYs (**3.35**); (A) Preparative TLC (DCM: Ethyl acetate 80:20), showing purple band of *N,N,O,F*-BODIPYs (**3.35**)

3.6.3 De-chelation of (*S*)-3-(1-Hydroxybutan-2-yl)amino)-5-(2-hydroxyphenyl) BODIPY (**3.5**)

As discussed previously Ravikanth *et al*., reported that the Lewis acid mediated removal of BF_2 groups can be efficient with sterically crowded BODIPYs. Therefore, we decided to examine the de-chelation reaction of (*S*)-3-(1-hydroxybutan-2-yl)amino)-5-(2-hydroxyphenyl) BODIPY (**3.5**) with $AlCl_3$.[75]

Thus, we reacted one equivalent of (*S*)-3-(1-hydroxybutan-2-yl)amino)-5-(2-hydroxyphenyl) BODIPY (**3.5**) with five equivalents of $AlCl_3$, in MeOH/MeCN under reflux. The reaction was monitored by TLC which showed the starting material had been fully consumed and a new product formed after 2 h, after which an aqueous work-up was performed (Scheme **3.10**).

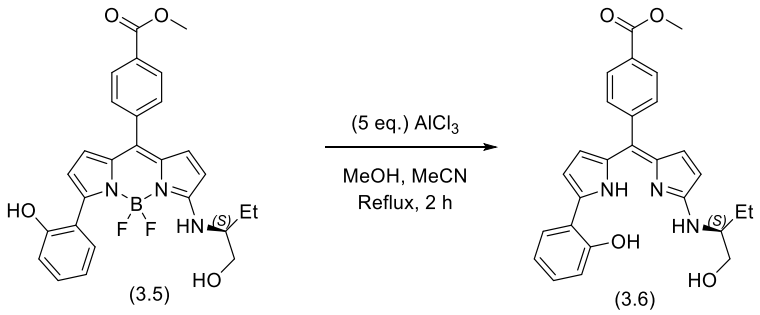

Scheme 3.10: Synthesis of (*S*)-α-(1-hydroxybutan-2-yl)amino)-α'-(2-hydroxyphenyl) dipyrromethene (**3.6**)

Initial attempts to analyse the crude product by NMR in $CDCl_3$ proved unsuccessful, the ^{1}H NMR spectrum showing a number of broad peaks. We postulated that this was due to low solubility of the material in $CDCl_3$, so subsequent NMR spectra were taken in CD_3OD. The analysis of the ^{11}B and ^{19}F NMR spectra in CD_3OD of the crude reaction product gave us confidence that the BF_2 group had been removed as there was no signal in either spectrum. In addition, the crude ^{1}H NMR spectrum showed a set of four signals corresponding to pyrrolic protons and there were signals at 8.08 ppm (d, *J* = 8.1

Hz, 2 H) and 7.54 ppm (d, *J* = 8.2 Hz, 2 H) corresponding to benzene ring that located at *meso*-position. In addition, there were signals at 7.63 ppm (dd, *J* = 8.2, 1.6 Hz, 1H), 7.11-6.97 ppm (m, 1H), and 6.92-6.81 ppm (m, 2H) corresponding to the protons on the phenolic ring.

However, the ^{1}H NMR of the desired product (*S*)-α-(1-hydroxybutan-2-yl)amino)-α'-(2-hydroxyphenyl) dipyrromethene (**3.6**) showed the presence of additional signals at 7.20-7.12 ppm (m, 1H) and 6.84-6.70 ppm (m, 1H) corresponding to the presence of some minor impurities. Thus, we planned to find a suitable purification method to purify the product.

3.6.4 Purification of (*S*)-α-(1-Hydroxybutan-2-yl)amino)-α'-(2-hydroxyphenyl) dipyrromethene (**3.6**)

It turned out that the purification of (*S*)-α-(1-hydroxybutan-2-yl)amino)-α'-(2-hydroxyphenyl) dipyrromethene (**3.6**) was a considerable challenge, in part due to the low solubility in many organic solvents. Thus, we tested a number of different purification methods for this reaction. Recrystallization was reported in literature by Ravikanth *et al*. as a method to purify dipyrromethenes.[75] Therefore, we attempted a range of recrystallization methods. In our initial screening tested small scale recrystallization by slow evaporation from different 12 solvents (dichloromethane, chloroform, acetone, diethyl ether (poor solubility), methanol, ethanol, toluene, acetonitrile, 2-propanol, 1,2-dichloroethane, 1-butanol, hexane (poor solubility)) to see if any solvents might be suitable for large scale purification. However, no crystalline material was obtained from these experiments. Hot to cold recrystallizations using methanol, ethanol, chloroform and a mixture of chloroform and pentane were attempted, but again no suitable crystalline material was obtained. Slow addition of petroleum ether to a chloroform solution did result in precipitation of the product, the ^{1}H NMR showing an improvement in sample purity but still with a number of impurities still present.

Therefore, we decided to use preparative TLC as our purification method. We then attempted to purify 425 mg of the crude (*S*)-α-(1-hydroxybutan-2-yl)amino)-α'-(2-hydroxyphenyl) dipyrromethene (**3.6**) (DCM: MeOH 10:1), which gave around 324 mg of (*S*)-α-(1-hydroxybutan-2-yl)amino)-α'-(2-hydroxyphenyl) dipyrromethene (**3.6**), which was pure by ^{1}H NMR. Preparative TLC was used several times to purify (*S*)-α-(1-hydroxybutan-2-yl)amino)-α'-(2-hydroxyphenyl) dipyrromethene (**3.6**) (see Table **3.10**), however it proved difficult to purify large quantities of material, as preparative TLC is only a useful technique for a small-scale purification < 500 mg. Thus, we decided to use column chromatography instead, based on our methods developed for preparative TLC, to be able to purify large scale of (*S*)-α-(1-hydroxybutan-2-yl)amino)-α'-(2-hydroxyphenyl) dipyrromethene (**3.6**).

We purified (*S*)-α-(1-hydroxybutan-2-yl)amino)-α'-(2-hydroxyphenyl) dipyrromethene (**3.6**) through silica gel using a mixture of DCM: MeOH (100:1). The column chromatography proved to be one of the best methods for purifying (*S*)-α-(1-hydroxybutan-2-yl)amino)-α'-(2-hydroxyphenyl) dipyrromethene (**3.6**), despite a minor issue with some of the product becoming trapped within the column due to poor solubility.

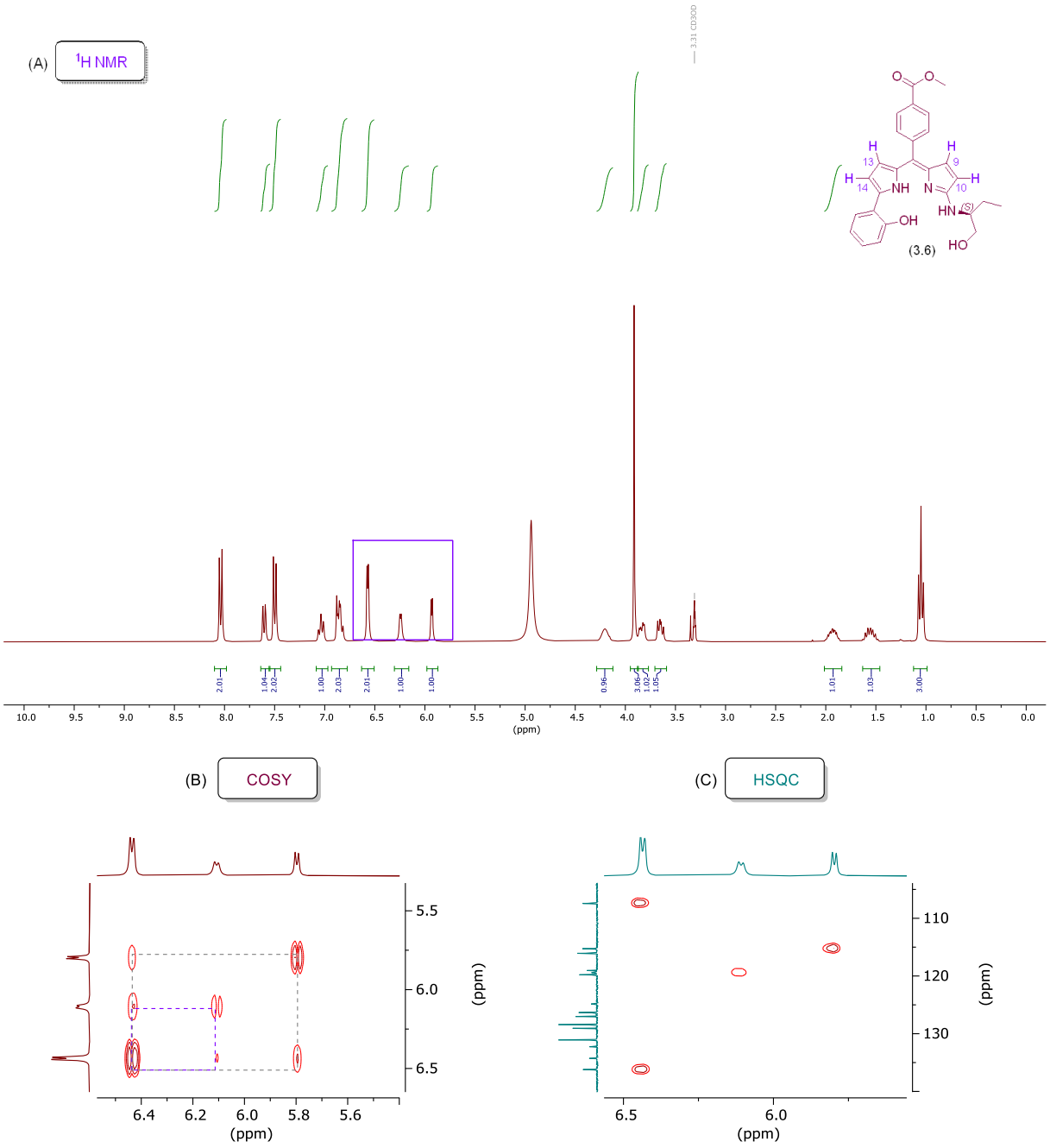

Figure 3.7: (A) ^{1}H NMR spectrum (300 MHz, CD_3OD) of (*S*)-α-(1-hydroxybutan-2-yl)amino)-α'-(2-hydroxyphenyl) dipyrromethene (**3.6**), (B) COSY spectrum of (*S*)-α-(1-hydroxybutan-2-yl)amino)-α'-(2-hydroxyphenyl) dipyrromethene (**3.6**), and (C) HSQC spectrum (*S*)-α-(1-hydroxybutan-2-yl)amino)-α'-(2-hydroxyphenyl) dipyrromethene (**3.6**).

The structure of (*S*)-α-(1-hydroxybutan-2-yl)amino)-α'-(2-hydroxyphenyl) dipyrromethene (**3.6**) was confirmed by ^{1}H NMR spectrum in CD_3OD (due to board signals in $CDCl_3$) which showed signals at 5.93 ppm (d, *J* = 3.9 Hz, 1H, H-13), and 6.24 ppm (d, *J* = 4.6 Hz, 1H, H-9) and two overlapping signals at 6.57 ppm (m, 2H, H-10, H-14) corresponding to a total of four pyrrolic protons. Due to the overlapping pyrrolic signals, the ^{1}H NMR was repeated in DMSO-d_6, which showed four well separated doublets for the four pyrrolic protons. In addition, the structure was confirmed through 2D NMR experiments in CD_3OD, COSY showing (^{3}J) couplings between H-10 and H-9 and the H-14 and H-13 protons of the pyrrolic rings and HSQC allowing assignment of the pyrrolic protons to their corresponding carbon atoms. For further confirmation, high resolution mass spectrometry (HRMS) analysis was conducted in negative mode, which showed a peak at *m/z* = 456.1932 $[M-H]^-$ which corresponded to the correct molecular formula of $C_{27}H_{26}N_3O_4$.

To access enough (*S*)-α-(1-hydroxybutan-2-yl)amino)-α'-(2-hydroxyphenyl) dipyrromethene (**3.6**) for the final step, the de-chelation reaction of (*S*)-α-(1-hydroxybutan-2-yl)amino)-α'-(2-hydroxyphenyl) dipyrromethene (**3.6**) with $AlCl_3$ was performed a number of times, including with scale up to 2.39 mmol, with good to moderate yields (38-75%) depending on purification method (Table **3.10**).

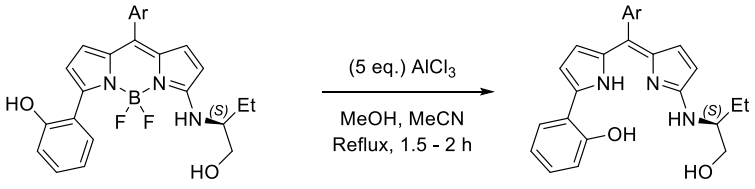

(3.5) (3.6)

Entry	Scale/mmol	Yield/%
1	0.07	59[a]
2	0.23	38[c]
3	0.39	Quant.[b]
4	0.55	69[b]
5	0.58	50[c]
6	0.86	73[d]
7	1.24	57[c]
8	1.73	75[b]
9	2.39	40[b]

Table 3.10: Synthesis of (*S*)-α-(1-hydroxybutan-2-yl)amino)-α'-(2-hydroxyphenyl) dipyrromethene (**3.6**). [a] Crude yield. [b] Isolated yield following column chromatography. [c] Isolated yield following preparative TLC. [d] Isolated yield following precipitation (Ar = *p*-($MeCO_2$)-C_6H_4-).

After we successfully synthesised (*S*)-α-(1-hydroxybutan-2-yl)amino)-α'-(2-hydroxyphenyl) dipyrromethene (**3.6**) and found a suitable method to purify (*S*)-α-(1-hydroxybutan-2-yl)amino)-α'-(2-hydroxyphenyl) dipyrromethene (**3.6**). Next, we planned to examine the de-chelation reactions of a range of 3-amino alcohol substituted-5-(2-hydroxyphenyl) BODIPYs with $AlCl_3$.

3.6.5 Reaction Scope of the De-chelation Reaction of 3-Amino alcohol substituted 5-(2-hydroxyphenyl) BODIPYs

We will follow our previous approach to remove BF_2 group from various 3-amino alcohol substituted 5-(2-hydroxyphenyl) BODIPYs. We tested the de-chelation reaction of (*R*)-3-(1-hydroxybutan-2-yl)amino)-5-(2-hydroxyphenyl) BODIPY (**3.29**) with $AlCl_3$ under our previously described conditions, which gave (*R*)-α-(1-hydroxybutan-2-yl)amino)-α'-(2-hydroxyphenyl) dipyrromethene (**3.36**) in moderate yield 67% following column chromatography (Table **3.11**, Entry 1). We also tested the de-chelation reaction with the previously prepared 3-(*S*)-amino alcohol substituted 5-(2-hydroxyphenyl)-BODIPYs which contain different R group (*e.g.*, CH_3, C_6H_5, and $C(CH_3)_3$), giving moderate to excellent yields across the three molecules examined (46% - 96%) following either column chromatography or preparative TLC (Table **3.11**, Entries 2-4).

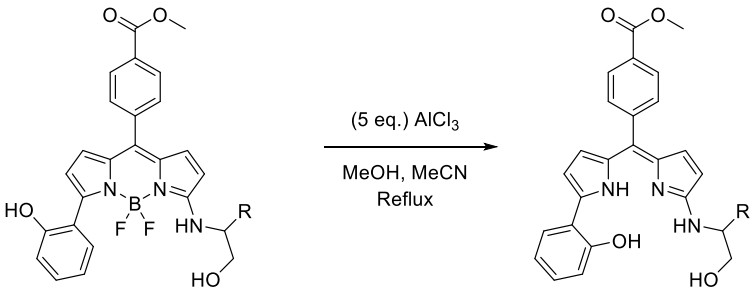

(3.29 - 3.32) (3.36 - 3.39)

Entry	Starting material	Stereochemistry (*R*/*S*)	Reaction Time/h	Product	Yield/%
1	(**3.29**), R = -CH_2CH_3	*R*	1.5	(**3.36**)	67[a]
2	(**3.30**), R = -CH_3	*S*	1.5	(**3.37**)	46[a]
3	(**3.31**), R = -C_6H_5	*S*	2	(**3.38**)	95[a]
4	(**3.32**), R = -$C(CH_3)_3$	*S*	1.5	(**3.39**)	64[b]

Table 3.11: Synthesis of α-amino alcohol substituted α'-(2-hydroxyphenyl)- dipyrromethene (**3.36** – **3.39**), [a] Isolated yield following column chromatography; [b] Isolated yield following preparative TLC.

3.7 Synthesis of Helically Chiral (*S,M/P*)-*N,N,O,C*-3-((1-hydroxybutan-2-yl)amino) BODIPYs

3.7.1 Boron Chelation Reactions

In the final step of our synthetic route, we examined the formation of helically chiral BODIPYs, through the introduction of an aryl boronic acid to our point chiral 3-amino alcohol substituted 5-(2-hydroxyphenyl) BODIPYs. We anticipate that the point chiral 3-amino alcohol will act as a chiral directing group to control the stereochemistry at boron (helical chirality). Therefore, based on a literature chelation procedure, we planned to react (*S*)-α-(1-hydroxybutan-2-yl)amino)-α'-(2-hydroxyphenyl) dipyrromethene (**3.6**) with (4-fluorophenyl)boronic acid (**2.25**) in $CHCl_3$ under mild conditions (Scheme **3.11**).[80] We chose (4-fluorophenyl)boronic acid (**2.25**) for chelation reactions, as we wished to use the fluorine atom as an analytical handle, allowing reaction analysis by ^{19}F NMR. Since we anticipate the formation of two diastereoisomers in the chelation reaction, we will use ^{19}F NMR to estimate diastereoisomeric ratios.

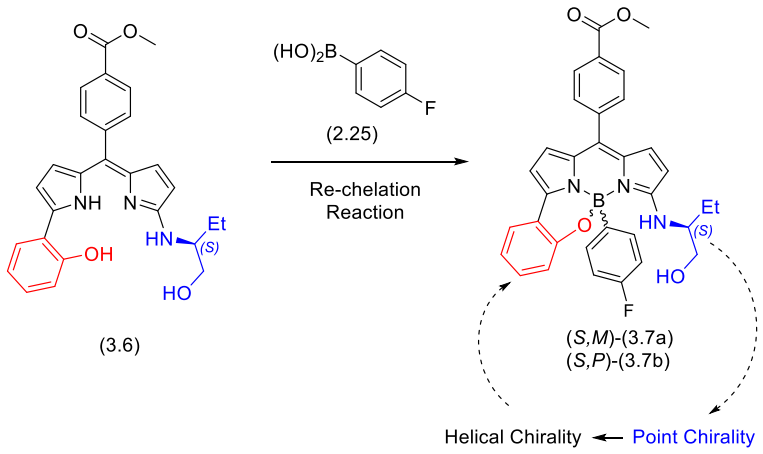

Scheme 3.11: Planned chelation reaction between (*S*)-α-(1-hydroxybutan-2-yl)amino)-α'-(2-hydroxyphenyl) dipyrromethene (**3.6**) and (4-fluorophenyl)boronic acid (**2.25**).

In our first attempt at the chelation reaction, one equivalent of (*S*)-α-(1-hydroxybutan-2-yl)amino)-α'-(2-hydroxyphenyl) dipyrromethene (**3.6**) was dissolved in 15 mL of $CHCl_3$, under a nitrogen atmosphere, and stirred for 30 min at room temperature then 1.5 equivalents of (4-fluorophenyl)boronic acid (dissolved in 5 mL of $CHCl_3$, under N_2) was added dropwise via syringe over 5 min. After all the (4-fluorophenyl)boronic acid (**2.25**) had been added, the reaction was quenched immediately with water. TLC analysis showed that the starting material had been consumed and two new fluorescent products were formed, after which an aqueous work-up was performed. Initial ^{19}F NMR analysis was carried out in CD_3OD, however only one signal was observed in the ^{19}F NMR which did not correlate with the two spots observable by TLC. We postulated the lack of two ^{19}F signals maybe due to a solvent effect with the CD_3OD, causing the signals to overlap. Therefore analysis of

crude ^{19}F NMR was repeated in $CDCl_3$, and showed the expected presence of two signals at -115.8 ppm and -116.7 ppm corresponding to two fluorine environments, indicating that two diastereomers of (*S,M/P*)-*N,N,O,C*-3-((1-hydroxybutan-2-yl)amino) BODIPYs (**3.7a** and **3.7b**) had been formed. The diastereomeric excess (*de*) was measured by integration of the ^{19}F NMR which showed good diastereoselectivity in the reaction (*%de* = 70). In order to allow ^{19}F NMR to be used for the measurement of diastereomeric excess, NMR experiments were performed with an increased relaxation time of 30 seconds for more accurate integration of signals. In addition, the analysis of crude ^{1}H NMR showed two different signals at 1.07 ppm (t, *J* = 7.4 Hz) and 0.65 ppm (t, *J* = 7.4 Hz) corresponding to the two methyl groups of the two diastereomers which integrated in a 3:12 ratio which would correspond to a *%de* = 60%. The crude reaction mixture was purified by column chromatography to isolate each diastereomer of (*S,M/P*)-*N,N,O,C*-3-((1-hydroxybutan-2-yl)amino) BODIPY to give 79% of (*S,M*)-(**3.7a**)(major) and 18% of (*S,P*)-(**3.7b**)(minor) (Figure **3.8**).

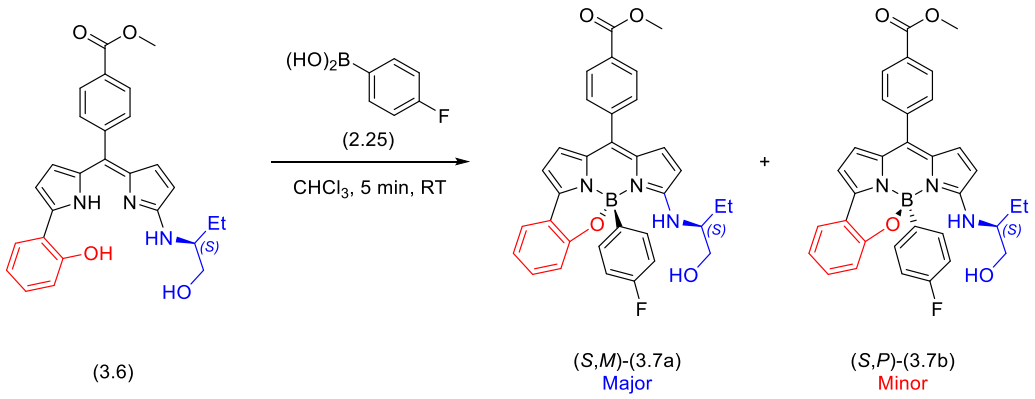

Scheme 3.12: Synthesis of helically chiral (*S,M*)-*N,N,O,C*-3-((1-hydroxybutan-2-yl)amino) BODIPY (**3.7a**) and (*S,P*)-*N,N,O,C*-3-((1-hydroxybutan-2-yl)amino) BODIPY (**3.7b**).

The structures of both (*S,M*)-*N,N,O,C*-3-((1-hydroxybutan-2-yl)amino) BODIPY (**3.7a**) (major) and (**3.7b**)(minor) were confirmed by ^{1}H NMR spectra. The major isomer showed a signal at 0.64 ppm (t, *J* = 7.4 Hz) corresponding to the terminal methyl group of the amino alcohol substituent, while the minor isomer showed a corresponding signal at 1.07 ppm (t, *J* = 7.4 Hz). The ^{19}F NMR of the major *N,N,O,C*-3-((1-hydroxybutan-2-yl)amino) BODIPY showed a singlet signal at -116.7 ppm and the spectrum of the minor *N,N,O,C*-3-((1-hydroxybutan-2-yl)amino) BODIPY showed singlet signal at -115.8 ppm for the 4-fluorophenyl group. In addition, the ^{11}B NMR spectrum of both *N,N,O,C*-3-((1-hydroxybutan-2-yl)amino) BODIPY major and minor diastereomers showed singlets at 2.05 ppm and 1.71 ppm, respectively for the newly introduced boron atom.

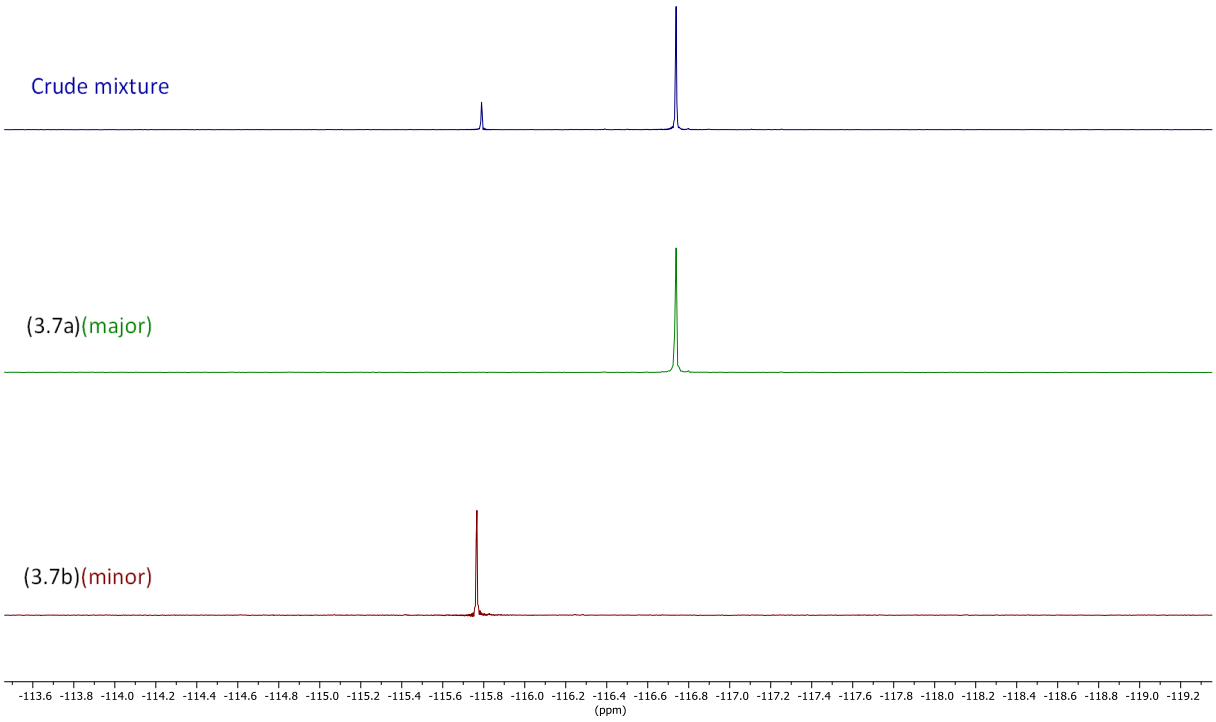

Figure 3.8: ^{19}F NMR spectrum (282 MHz, $CDCl_3$) of the (*S,M/P*)-*N,N,O,C*-3-((1-hydroxybutan-2-yl)amino) BODIPYs (**3.7a** and **3.7b**); Top: ^{19}F NMR of the crude reaction mixture (*S,M/P*)-*N,N,O,C*-3-((1-hydroxybutan-2-yl)amino) BODIPYs (**3.7a** and **3.7b**)(blue); Middle: ^{19}F NMR of the major isomer (green) following column chromatography ; Bottom: ^{19}F NMR of ^{19}F NMR of the minor isomer (red) following column chromatography.

After successfully synthesising our target helically chiral (*S,M/P*)-*N,N,O,C*-3-((1-hydroxybutan-2-yl)amino) BODIPYs via a point-to-helical stereocontrolled reaction, next, we planned to determine the relative stereochemistry of the boron centres of the chiral (*S,M/P*)-*N,N,O,C*-3-((1-hydroxybutan-2-yl)amino) BODIPYs (**3.7a** and **3.7b**).

3.7.2 Absolute Stereochemistry of Helically Chiral (*S,M/P*)-*N,N,O,C*-3-((1-hydroxybutan-2-yl)amino) BODIPYs

To determine the relative stereochemistry of (*S,M/P*)-*N,N,O,C*-3-((1-hydroxybutan-2-yl)amino) BODIPYs (**3.7a** and **3.7b**), particularly at the boron centre, we decided to first focus on the use of single crystal X-ray diffraction (SCXRD). SCXRD allows for the determination of relative stereochemistry in a molecule, which in this case will allow the absolute assignment of the boron centre (or helical chirality of the BODIPY), as the absolute stereochemistry of the chiral auxiliary is known. Thus, we successfully crystallised major (**3.7a**) and minor (**3.7b**) helically chiral (*S,M/P*)-*N,N,O,C*-3-((1-hydroxybutan-2-

yl)amino) BODIPYs through slow evaporation of $CHCl_3$ and CD_3OD solutions, respectively. Their structures were then successfully determined using SCXRD analysis, both molecules crystallising as an orthorhombic crystal structure with a $P2_12_12_1$ space group. For major isomer (**3.7a**) a Flack parameter of 0.00(15) was obtained allowed direct confirmation of the absolute stereochemistry for helically chiral (*S,M*)-*N,N,O,C*-3-((1-hydroxybutan-2-yl)amino) BODIPY (**3.7a**) (Figure **3.9**). The minor product (**3.7b**) showed a Flack parameter of -0.1(2), which is not good enough for direct assignment of absolute stereochemistry. Therefore in this case only relative helical stereochemistry of the BODIPY can be assigned by SCXRD, however since the chiral auxiliary is known to be an *S*-centre, the helicity of the BODIPY can be assigned as *P*, giving the minor product (*S,P*)-*N,N,O,C*-3-((1-hydroxybutan-2-yl)amino) BODIPY (**3.7b**).

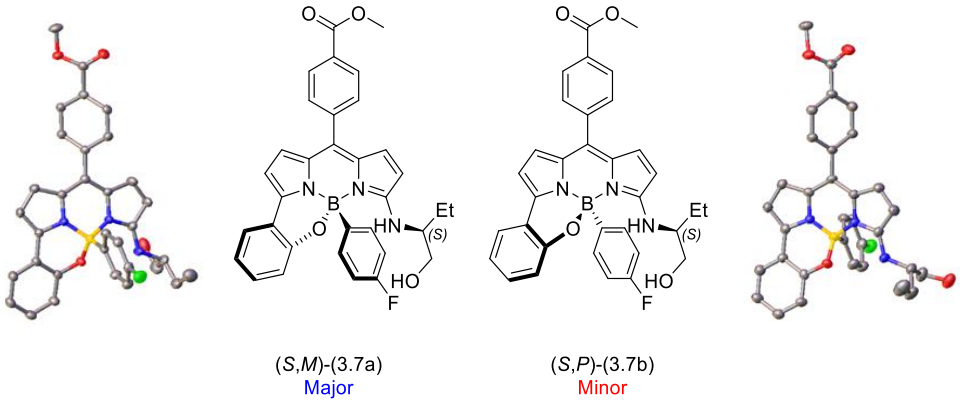

Figure 3.9: Single crystal X-ray structures of the target compounds helically chiral (*S,M*)-*N,N,O,C*-3-((1-hydroxybutan-2-yl)amino) BODIPY (**3.7a**) and (*S,P*)-*N,N,O,C*-3-((1-hydroxybutan-2-yl)amino) BODIPY (**3.7b**).

After successfully determining the structure of (*S,M*)-*N,N,O,C*-3-((1-hydroxybutan-2-yl)amino) BODIPY (**3.7a**) and (*S,P*)-*N,N,O,C*-3-((1-hydroxybutan-2-yl)amino) BODIPY (**3.7b**). Next, we planned to investigate the distereoselectivity of the chelation reaction.

3.7.3 Optimisation of Diastereoselectivity of Helically Chiral (*S,M*)-*N,N,O,C*-3-((1-hydroxybutan-2-yl)amino) BODIPY (**3.7a**) and (*S,P*)-*N,N,O,C*-3-((1-hydroxybutan-2-yl)amino) BODIPY (**3.7b**)

In order to better understand the origins of diastereoselectivity in the chelation reaction, we decided to examine the impact of temperature on the diastereomeric excess (%*de*) of the final products (*S,M*)-*N,N,O,C*-3-((1-hydroxybutan-2-yl)amino) BODIPY (**3.7a**) and (*S,P*)-*N,N,O,C*-3-((1-hydroxybutan-2-yl)amino) BODIPY (**3.7b**).

Therefore, we planned to do examine the chelation reaction under different temperatures, from -41 °C to 65 °C, and to measure the diastereomeric excess (*de*) of the final products by ^{19}F NMR and isolated yields. Thus, each reaction was run on a 0.1 mmol scale, in which (*S*)-α-(1-hydroxybutan-2-yl)amino)-α'-(2-hydroxyphenyl) dipyrromethene (**3.6**) was reacted with 1.5 equivalents of (4-fluorophenyl)boronic (**2.25**) acid in $CHCl_3$ for 5 min. Each reaction was monitored by TLC, followed an aqueous work-up and column chromatography. In each case, the diastereomeric excess (%*de*) was measured by the integration of the ^{19}F NMR for the crude reaction mixture, and after purification by comparing the isolated yields of both diastereomers.

We observed that at low temperature, -41 °C, the reaction showed the lowest *de* (47% by ^{19}F NMR and 44% by isolated yield) (Table **3.12**, Entry 1). The isolated yield of this reaction was also comparatively low (65%), however this was due to purification issues rather than poor conversion. Interestingly, the *de* increased with temperature with the highest *de* (74% by ^{19}F NMR and 64% by isolated yield) achieved at 35 °C (Table **3.12**, Entry 4). However, when the temperature increased above 35 °C, *de* values gradually decreased, although high yields were obtained in all cases (Table **3.12**).

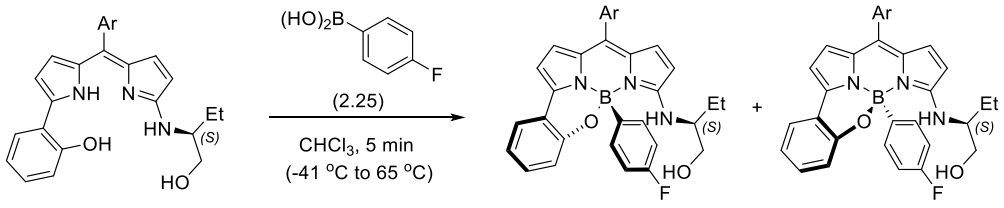

(3.6) (*S*,*M*)-(3.7a) Major (*S*,*P*)-(3.7b) Minor

Entry	Reaction Temp./ °C	*de* ^{19}F NMR[a]/%	*de* after purification[b]/%	Yield[c]/%
1	-41	47	44	65 [d]
2	0	62	41	86
3	RT (25)	70	62	98
4	**35**	**74**	**64**	**100**
5	45	65	50	96
6	55	64	61	87
7	Reflux (65)	61	61	86

Table 3.12: [a] *de* of final helically chiral (*S,M/P*)-*N,N,O,C*-3-((1-hydroxybutan-2-yl)amino) BODIPYs before purification, measured by ^{19}F NMR. [b] *de* after purification by column chromatography. [c] Isolated combined yield following column chromatography. [d] Isolated yield following re-column chromatography (Ar = *p*-($MeCO_2$)-C_6H_4-).

We would have expected that the highest *de* would be obtained at low temperature, however this was not what was observed. We therefore thought that at high temperatures the products may be under equilibrium, resulting in a thermodynamically controlled outcome where the *de* represents the energy difference between the two diastereomers. To examine this, we decided to test the epimerisation at the boron centre of the products via a control experiment.

3.7.4 Control Experiment the Epimerisation at Boron Centre in (*S,M*)-*N,N,O,C*-3-((1-hydroxybutan-2-yl)amino) BODIPY (**3.7a**)

Next we planned to do a control experiment to examine the potential for epimerisation at the boron centre of (*S,M*)-*N,N,O,C*-3-((1-hydroxybutan-2-yl)amino) BODIPY (**3.7a**) in presence and absence of (4-fluorophenyl)boronic acid in $CDCl_3$. The first control experiment was performed in an NMR tube. A single diastereoisomer of (*S,M*)-*N,N,O,C*-3-((1-hydroxybutan-2-yl)amino) BODIPY (**3.7a**) was dissolved in $CDCl_3$, and the solution was heated to 45 ^oC, and monitored by both ^1H NMR and ^{19}F NMR spectroscopy for 500 hours. Analysis of the ^{19}F NMR spectra for (*S,M*)-*N,N,O,C*-3-((1-hydroxybutan-2-yl)amino) BODIPY (**3.7a**) in $CDCl_3$ solution, showed that the ^{19}F signal of (*S,M*)-*N,N,O,C*-3-((1-hydroxybutan-2-yl)amino) BODIPY (**3.7a**) slowly decreased over time and a ^{19}F signal corresponding to the other diastereomer, (*S,P*)-*N,N,O,C*-3-((1-hydroxybutan-2-yl)amino) BODIPY (**3.7b**) slowly increased, appearing after approximately 28 hours (Figure **3.10**, A). After 380 hours, additional $CDCl_3$ was added to the NMR tube, due to solvent loss. At the end of the 500 hours the *de* of the mixture was determined to be 64%. This experiment showed that the major and minor diastereomers can interconvert, which we proposed is due to epimerisation at the boron centre. However, the rate of epimerisation observed is too slow to account for the *de* seen in the reactions at higher temperatures.

We proposed that the epimerisation reaction could be catalysed by the presence of excess boronic acid in the reaction. Thus, to better simulate the reaction conditions, in a second experiment we examined the epimerisation of the major of diastereoisomer of (*S,M*)-*N,N,O,C*-3-((1-hydroxybutan-2-yl)amino) BODIPY (**3.7a**) in the presence of 0.5 equivalents of (4-fluorophenyl)boronic acid (**2.25**). The reaction mixture in $CDCl_3$ was heated to 45 ^oC and monitored by both ^1H NMR and ^{19}F NMR spectroscopy as before, for 500 hours. The ^{19}F NMR spectroscopy analysis showed that the major diastereomer, (*S,M*)-*N,N,O,C*-3-((1-hydroxybutan-2-yl)amino) BODIPY (**3.7a**), slowly epimerised to form (*S,P*)-*N,N,O,C*-3-((1-hydroxybutan-2-yl)amino) BODIPY (**3.7b**), with a final *de* of 50% achieved after 500 hours (Figure **3.10**, B). Overall, this experiment showed that the major and minor diastereomers can interconvert in the presence of excess boronic acid, however the rate of interconversion is not significantly different to experiments without excess boronic acid.

In conclusion, it is clear that the epimerisation of (*S,M*)-*N,N,O,C*-3-((1-hydroxybutan-2-yl)amino) BODIPY (**3.7a**) can occur at 45 °C in $CDCl_3$ with 0.5 equivalents of boronic acid. However, the rate of epimerisation observed does not explain the *de* measured directly from the chelation reactions, which typically occur in a few minutes.

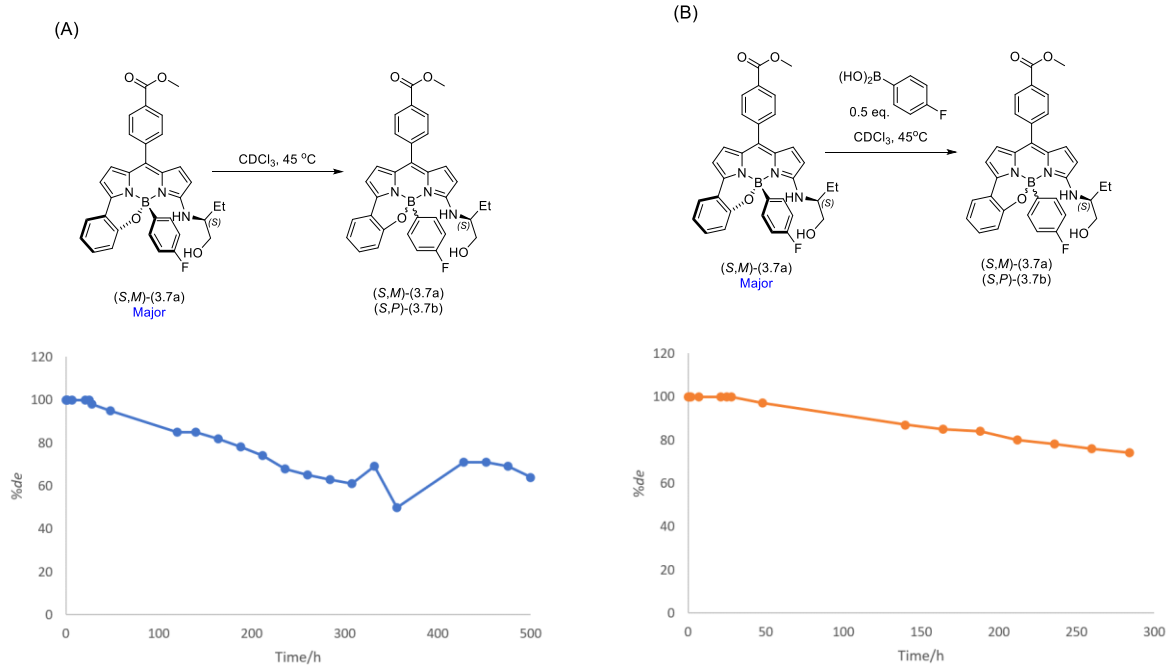

Figure 3.10: (A) Epimerisation of (*S,M*)-*N,N,O,C*-3-((1-hydroxybutan-2-yl)amino) BODIPY (**3.7a**); (B) Epimerisation of (*S,M*)-*N,N,O,C*-3-((1-hydroxybutan-2-yl)amino) BODIPY (**3.7a**) in presence of (4-fluorophenyl)boronic acid.

3.8. Synthesis of Helically Chiral (*R,M/P*)-*N,N,O,C*-3-((1-hydroxybutan-2-yl)amino) BODIPYs

Next we planned to synthesis the opposite enantiomers of (*S,M*)-*N,N,O,C*-3-((1-hydroxybutan-2-yl)amino) BODIPY (**3.7a**) and (*S,P*)-*N,N,O,C*-3-((1-hydroxybutan-2-yl)amino) BODIPY (**3.7b**) to help with later analysis of enantiopurity of products by chiral High-Performance Liquid Chromatography (HPLC). This will be done through the chelation of previously prepared (*R*)-α-(1-hydroxybutan-2-yl)amino)-α'-(2-hydroxyphenyl) dipyrromethene (**3.36**) to give the major (*R,P*)-*N,N,O,C*-3-((1-hydroxybutan-2-yl)amino) BODIPY (**3.40a**) and the minor (*R,M*)-*N,N,O,C*-3-((1-hydroxybutan-2-yl)amino) BODIPY (**3.40b**).

Therefore, under our previous conditions, we reacted one equivalent of (*R*)-α-(1-hydroxybutan-2-yl)amino)-α'-(2-hydroxyphenyl) dipyrromethene (**3.36**) with 1.5 equivalents of (4-fluorophenyl)boronic acid (**2.25**) in chloroform at 35 °C for 5 min. Following an aqueous work-up and column chromatography, the desired products (*R,P*)-*N,N,O,C*-3-((1-hydroxybutan-2-yl)amino) BODIPY

(**3.40a**) (major) and (*R,M*)-*N,N,O,C*-3-((1-hydroxybutan-2-yl)amino) BODIPY (**3.40b**) (minor) were isolated in 44% and 24% yield, respectively (Scheme **3.13**).

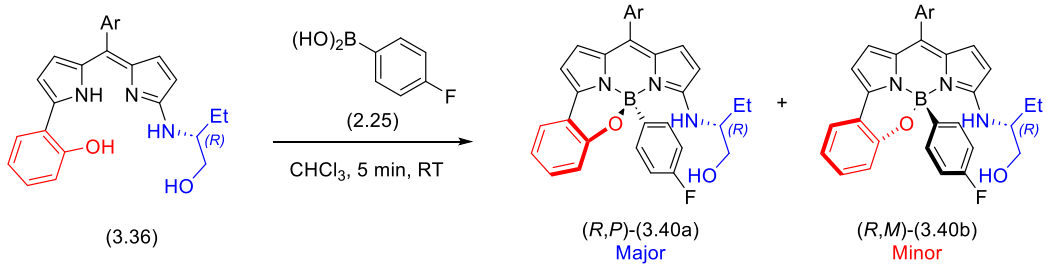

Scheme 3.13: Synthesis of helically chiral (*R,P*)-*N,N,O,C*-3-((1-hydroxybutan-2-yl)amino) BODIPY (**3.40a**) (major) and (*R,M*)-*N,N,O,C*-3-((1-hydroxybutan-2-yl)amino) BODIPY (**3.40b**) (minor) (Ar = *p*-($MeCO_2$)-C_6H_4-).

The structures of both (*R,P*)-*N,N,O,C*-3-((1-hydroxybutan-2-yl)amino) BODIPY (**3.40a**) (major) and (*R,M*)-*N,N,O,C*-3-((1-hydroxybutan-2-yl)amino) BODIPY (**3.40b**) (minor) were confirmed by ^{1}H NMR and ^{19}F NMR spectroscopy, which showed identical signals to the previously isolated enantiomers.

3.8.1 Crystal Structures of (*R,P*)-*N,N,O,C*-3-((1-hydroxybutan-2-yl)amino) BODIPY (**3.40a**) and (*R,M*)-*N,N,O,C*-3-((1-hydroxybutan-2-yl)amino) BODIPY (**3.40b**)

To confirm the structure of both the major and minor isomers (**3.40a**) and (**3.40b**), we attempted to grow crystals suitable for SCXRD by via slow evaporation of a $CDCl_3$ solution. We successfully grew a suitable crystal of the major isomer (*R,P*)-*N,N,O,C*-3-((1-hydroxybutan-2-yl)amino) BODIPY (**3.40a**) and this was analysed by SCXRD. The molecule crystallised to give an orthorhombic crystal system with the $P2_12_12_1$ space group, with four molecules in the unit cell (Z = 4). A Flack parameter of -0.04(4) was measured, confirming the absolute stereochemistry of (*R,P*)-*N,N,O,C*-3-((1-hydroxybutan-2-yl)amino) BODIPY (**3.40a**) (major) (Figure **3.11**).

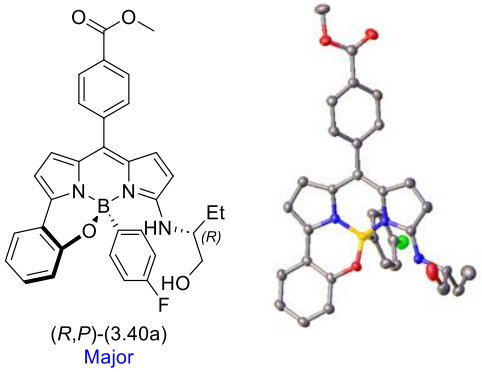

Figure 3.11: Single crystal X-ray structures of the (*R,P*)-*N,N,O,C*-3-((1-hydroxybutan-2-yl)amino) BODIPY (**3.40a**).

Slow evaporation experiments with the minor isomer (*R,M*)-*N,N,O,C*-3-((1-hydroxybutan-2-yl)amino) BODIPY (**3.40b**) were unsuccessful, from $CHCl_3$, DCM and MeOH. Therefore, we attempted vapour diffusion experiments, using DCM as the solvent and hexane as the anti-solvent in a 1:3 ratio over two weeks. A suitable single crystal was obtained and submitted for SCXRD analysis. Interestingly, the results showed that the crystal contained two diastereomers in the crystal structure in a 1:1 ratio. Interestingly the crystal structure obtained was a methanol solvate, the methanol likely to have come from a previous crystallisation attempt. A Flack parameter of 0.07(4) was obtained, allowed absolute stereochemical assignment of the two diastereomers present, which were (*R,P*)-*N,N,O,C*-3-((1-hydroxybutan-2-yl)amino) BODIPY (**3.40a**) and (*R,M*)-*N,N,O,C*-3-((1-hydroxybutan-2-yl)amino) BODIPY (**3.40b**) (Scheme **3.14**).

We postulate that the presence of two diastereomers may be due to the epimerisation at the boron centre during attempted crystallisation. To confirm this, we decided to run ^{1}H and ^{19}F NMR in $CDCl_3$ for the crystals obtained. The ^{19}F NMR showed the presence of two signals, corresponding to the presence of both (*R,P*)-*N,N,O,C*-3-((1-hydroxybutan-2-yl)amino) BODIPY (**3.40a**) and (*R,M*)-*N,N,O,C*-3-((1-hydroxybutan-2-yl)amino) BODIPY (**3.40b**) and in an ~1:2 ratio. This suggests that epimerisation at boron had occurred during crystallisation, and that the dimeric methanol solvate may have been more crystalline than the individual diastereomers under the crystallisation conditions (Scheme **3.14**).

Next we aimed to confirm the structure of (*R,M*)-*N,N,O,C*-3-((1-hydroxybutan-2-yl)amino) BODIPY (**3.40b**) by crystallography. To achieve this, we re-columned the mixture of (*R,M/P*)-*N,N,O,C*-3-((1-hydroxybutan-2-yl)amino) BODIPYs (**3.40a**/**3.40b**) resulting from the crystallisation experiments, and attempted to grow the crystal of (*R,M*)-*N,N,O,C*-3-((1-hydroxybutan-2-yl)amino) BODIPY (**3.40b**) from a pure sample. We successfully crystallised the (*R,M*)-*N,N,O,C*-3-((1-hydroxybutan-2-yl)amino) BODIPY (**3.40b**) via slow evaporation from a MeOH solution. A suitable single crystal was then examined by SCXRD, giving an orthorhombic crystal with the $P2_12_12_1$ space group, and a Flack parameter of -0.02(12), confirming the absolute stereochemistry (Figure **3.12**).

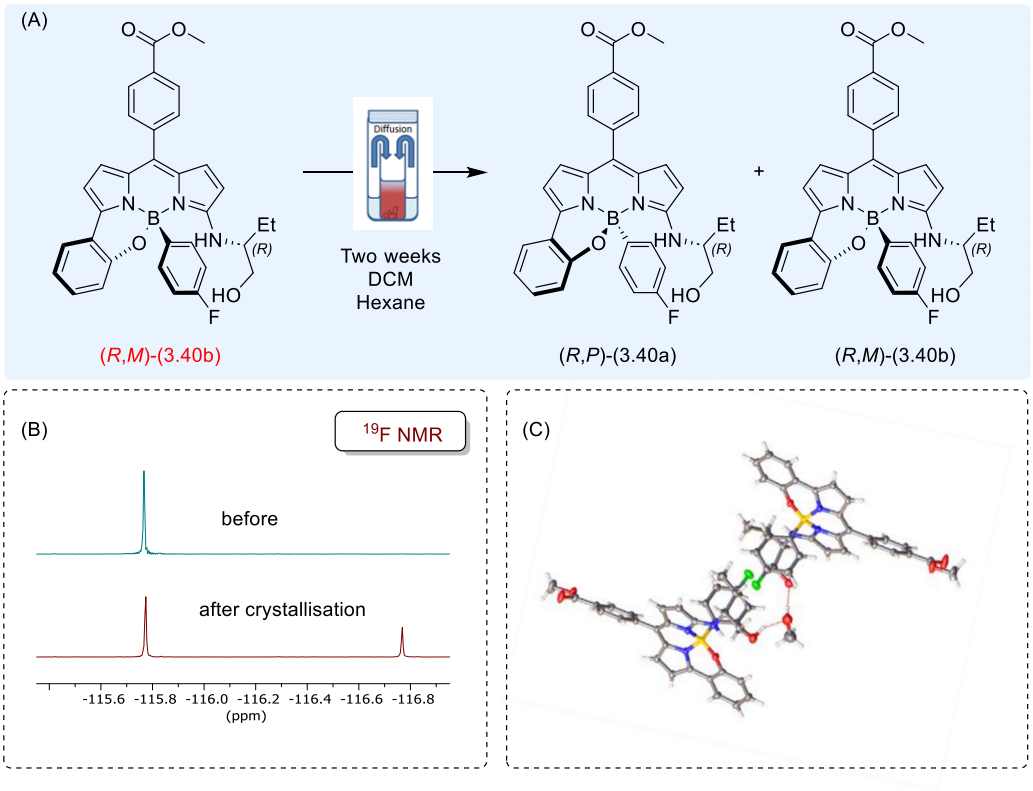

Scheme 3.14: (A) Crystallisation method for (*R,M*)-*N,N,O,C*-3-((1-hydroxybutan-2-yl)amino) BODIPY (**3.40b**); (B) Top: ^{19}F NMR spectrum (282 MHz, $CDCl_3$) of the (*R,M*)-*N,N,O,C*-3-((1-hydroxybutan-2-yl)amino) BODIPY (**3.40b**) before crystallisation (green), Bottom: ^{19}F NMR spectrum (282 MHz, $CDCl_3$) of (*R,M*)-*N,N,O,C*-3-((1-hydroxybutan-2-yl)amino) BODIPY (**3.40b**) after crystallisation (red); and (C) Single crystal X-ray structure of (*R,P*)-*N,N,O,C*-3-((1-hydroxybutan-2-yl)amino) BODIPY (**3.40a**)/ (*R,M*)-*N,N,O,C*-3-((1-hydroxybutan-2-yl)amino) BODIPY (**3.40b**) MeOH solvate.

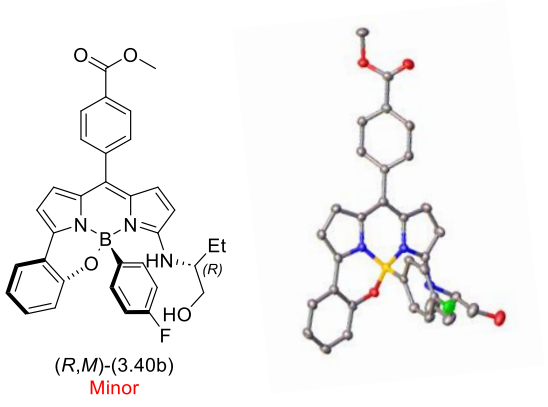

Figure 3.12: Single crystal X-ray structure of (*R,M*)-*N,N,O,C*-3-((1-hydroxybutan-2-yl)amino) BODIPY (**3.40b**).

In conclusion we successfully synthesised (*R,P*)-*N,N,O,C*-3-((1-hydroxybutan-2-yl)amino) BODIPY (**3.40a**) and (*R,M*)-*N,N,O,C*-3-((1-hydroxybutan-2-yl)amino) BODIPY (**3.40b**), and confirmed their

structure and absolute stereochemistry by SCXRD. Next, we planned to examine the chiral integrity of amino alcohol substituent via chiral HPLC.

3.9 Chiral Integrity of Amino Alcohol Moieties in Helically Chiral BODIPYs

The chirality of our target helically chiral BODIPYs comes from the enantiopure amino alcohols that are introduced. It is therefore important to ensure that the chirality of the amino alcohol was retained during the synthesis. Related work in the group by Felicity Frank involved the use of amino acid based chiral auxiliaries, and some evidence suggested potential racemisation of the chiral auxiliary in these cases.[74] Although we expect that amino alcohols would be more stable to racemisation than amino acids, we still wished to evaluate any potential racemisation in our systems (Scheme **3.15**).

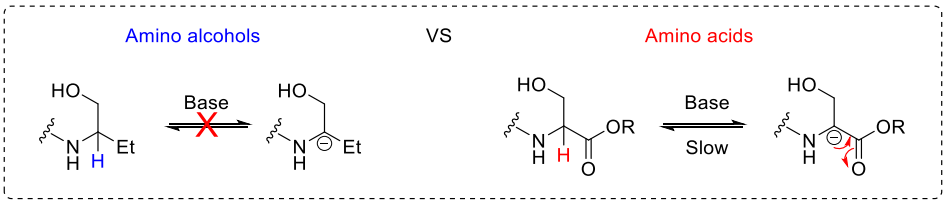

Scheme 3.15: Potential racemisation of amino alcohols and amino acid.

Therefore, we planned to examine the enantiopurity of the amino alcohol moieties in the final target BODIPYs by chiral HPLC. In the first experiments, a ~1:1 mixture of (*S,P*)-*N,N,O,C*-3-((1-hydroxybutan-2-yl)amino) BODIPY (**3.7b**) (minor) and (*R,M*)-*N,N,O,C*-3-((1-hydroxybutan-2-yl)amino) BODIPY (**3.40b**) (minor) prepared previously was formed, to give a racemic mixture to be used as a reference. The racemic reference sample was dissolved in isopropyl alcohol, filtered, and then injected into an analytical chiral HPLC column (CHIRALPAK®IC), and eluted with a mixture of hexane and isopropanol in an 80:20 ratio, to give two well separated peaks. Using the same HPLC conditions, each of the final products, (*S,P*)-*N,N,O,C*-3-((1-hydroxybutan-2-yl)amino) BODIPY (**3.7b**) and (*R,M*)-*N,N,O,C*-3-((1-hydroxybutan-2-yl)amino) BODIPY (**3.40b**) was analysed separately. Comparison of the final products with the racemic standard, allowed the enantiomeric excess (*ee*) of (*S,P*)-*N,N,O,C*-3-((1-hydroxybutan-2-yl)amino) BODIPY (**3.7b**) to be measured as 94% and (*R,M*)-*N,N,O,C*-3-((1-hydroxybutan-2-yl)amino) BODIPY (**3.40b**) was determined to be 96%. These results indicate that the final products exhibit high enantiopurity, with minimal or no presence of the opposite enantiomer, suggesting that no racemisation of the amino alcohol had occurred.

We applied similar methods for the other pair of enantiomers prepared previously, in each case comparing against a prepared racemic sample. (*S,M*)-*N,N,O,C*-3-((1-hydroxybutan-2-yl)amino) BODIPY (**3.7a**) (major) and (*R,P*)-*N,N,O,C*-3-((1-hydroxybutan-2-yl)amino) BODIPY (**3.40a**) (major), both gave good enantiomeric excesses of 77% and 99 %, respectively, again suggesting that no racemisation of

the amino alcohol had occurred (Table **3.13**/appendix 7.4). HPLC measurements were done by Aaron Campbell in Dr Armstrong's group at Newcastle University.

Helically chiral BODIPY	Wavelength detection/nm	Retention time / min	ee/%
(*S,P*)-(**3.7b**) minor	240 nm	6.48	94
(*R,M*)-(**3.40b**) minor	240 nm	8.42	96
(*S,M*)-(**3.7a**) major	290 nm	8.44	77.4
(*R,P*)-(**3.40a**) major	290 nm	12.41	99

Table 3.13: *ee* of each isolated helically chiral *N,N,O,C*-3-((1-hydroxybutan-2-yl)amino) BODIPYs (**3.7a**) (**3.7a**), (**3.7b**),(**3.40a**), and (**3.40b**), with flow rate 1 ml/min.

3.10 Photophysical Properties of Helically Chiral *N,N,O,C*-3-((1-Hydroxybutan-2-yl)amino) BODIPYs (3.7a), (3.7b),(3.40a), and (3.40b)

After successfully isolating and confirming the enantiopurity of each pair of diastereomers (*S,M*)/(*S,P*)-*N,N,O,C*-3-((1-hydroxybutan-2-yl)amino) BODIPY (**3.7a**/**3.7b**) and (*R,M*)/(*R,P*)-*N,N,O,C*-3-((1-hydroxybutan-2-yl)amino) BODIPY (**3.40b**/**3.40a**) by chiral HPLC, we turned our attention to the measurement of the photophysical properties including UV-Vis absorption and emission spectra, molar extinction coefficient (ε), the fluorescence quantum yield (ϕ_F).

Hence, we measured the absorption and emission spectra for two diastereomers (*S,M*)/(*S,P*)-*N,N,O,C*-3-((1-hydroxybutan-2-yl)amino) BODIPY (**3.7a**/**3.7b**) in DCM at room temperature, which exhibited absorption maxima at around 577 nm and emission maxima at around 627 nm. The fluorescence quantum yields (ϕ_F) of each diastereomer (*S,M*)/(*S,P*)-*N,N,O,C*-3-((1-hydroxybutan-2-yl)amino) BODIPY (**3.7a**/**3.7b**) was also measured, using cresyl violet as a standard. These systems showed relatively low quantum yields of around 0.04, compared to standard BODIPYs. We postulate that these low quantum yields are due to the presence of the amino alcohol groups, which could enhance non-radiative decay through vibrational relaxation (Table **3.14**, appendix 7.3.3).

BODIPY	Solvent	λ_{max} (abs)/nm	ε / mol^{-1} cm^{-1}	λ_{max} (em)/nm	ϕ_F[a]
(**3.7a**)	DCM	577	43 212	627	0.04
(**3.7b**)	DCM	578	39 637	627	0.05

Table 3.14: Photophysical properties of (*S,M*)/(*S,P*)-*N,N,O,C*-3-((1-hydroxybutan-2-yl)amino) BODIPY (**3.7a**/**3.7b**). [a] Measured with respect to cresyl violet standard in ethanol (ϕ_F = 0.56), excitation wavelength = 542 nm.[82]

3.10.1 Chiroptical Properties of Helically Chiral BODIPYs

3.10.1.1 ECD Spectroscopy of Helically Chiral BODIPYs *N,N,O,C*-3-((1-Hydroxybutan-2-yl)amino) BODIPYs (**3.7a**), (**3.7b**),(**3.40a**), and (**3.40b**)

Next we wished to measure the chiroptical properties of the four diastereomers (*S,M*)/(*S,P*)-*N,N,O,C*-3-((1-hydroxybutan-2-yl)amino) BODIPY (**3.7a**/**3.7b**) and (*R,M*)/(*R,P*)-*N,N,O,C*-3-((1-hydroxybutan-2-yl)amino) BODIPY (**3.40b**/**3.40a**), namely electronic circular dichroism (ECD) spectroscopy. Electronic circular dichroism (ECD) is the difference in absorption of right- handed and left-handed circularly polarized light by a sample, such as a chiral fluorophore. We planned to use ECD to examine the chirality of our helically chiral BODIPYs, and to determine their absolute stereochemistry by comparison of the experimental ECD spectra with computational predictions.

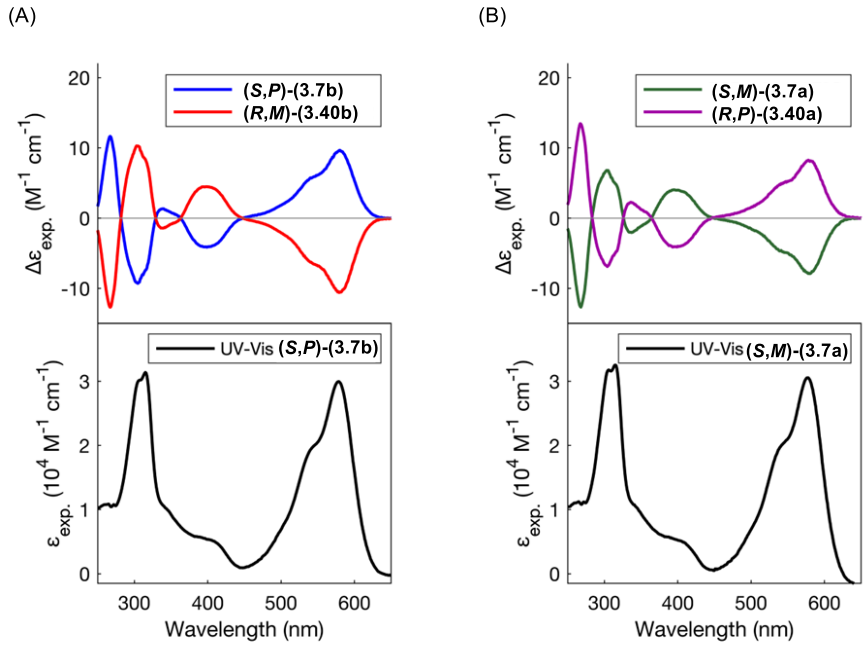

Figure 3.13: Experimental ECD spectra measured in DCM; (A) ECD spectra of (*S,P*)-*N,N,O,C*-3-((1-hydroxybutan-2-yl)amino) BODIPY (**3.7b**) (blue), (*R,M*)-*N,N,O,C*-3-((1-hydroxybutan-2-yl)amino) BODIPY (**3.40b**) (red), and UV-Vis spectrum of (*S,P*)-*N,N,O,C*-3-((1-hydroxybutan-2-yl)amino) BODIPY (**3.7b**) (black); (B) ECD spectra of (*S,M*)-*N,N,O,C*-3-((1-hydroxybutan-2-yl)amino) BODIPY (**3.7a**) (green), (*R,P*)-*N,N,O,C*-3-((1-hydroxybutan-2-yl)amino) BODIPY (**3.40a**) (purple), UV-Vis spectrum of (*S,M*)-*N,N,O,C*-3-((1-hydroxybutan-2-yl)amino) BODIPY (**3.7a**) (black).(Figure **3.13** was created by Dr Jonathan Bogaerts).

Thus, ECD for all four helically chiral *N,N,O,C*-3-((1-Hydroxybutan-2-yl)amino) BODIPYs (**3.7a**), (**3.7b**),(**3.40a**), and (**3.40b**) were measured in DCM by Dr Jonathan Bogaerts and Seppe Verheyen at

the University of Antwerp. Each pair of enantiomers (*S,M*)/(*R,P*)-*N,N,O,C*-3-((1-hydroxybutan-2-yl)amino) BODIPY (**3.7a**/**3.40a**) and (*S,P*)/(*R,M*)-*N,N,O,C*-3-((1-hydroxybutan-2-yl)amino) BODIPY (**3.7b**/**3.40b**) showed mirror image ECD spectra, confirming that they were enantiomeric (Figure **3.13**). The helically chiral BODIPYs all showed Cotton effects with $\Delta\varepsilon_{max} \approx \pm 9$ L mol^{-1} cm^{-1} for the S_0-S_1 transition (λ_{max} = 577 nm).

Interestingly, two sets of diastereomers (*S,M*)/(*S,P*)-*N,N,O,C*-3-((1-hydroxybutan-2-yl)amino) BODIPY (**3.7a**/**3.7b**) and (*R,M*)/(*R,P*)-*N,N,O,C*-3-((1-hydroxybutan-2-yl)amino) BODIPY (**3.40b**/**3.40a**) which differ only in their helical chirality (*P* or *M*), gave ECD spectra that were close to mirror images, which was unexpected as diastereomers would not typically display such spectra. Furthermore, we also observed that the alternative sets of diastereomers (*S,M*)/(*R,M*)-*N,N,O,C*-3-((1-hydroxybutan-2-yl)amino) BODIPY (**3.7a**/**3.40b**) and (*S,P*)/(*R,P*)-*N,N,O,C*-3-((1-hydroxybutan-2-yl)amino) BODIPY (**3.7b**/**3.40a**) which differ only in the stereochemistry of the amino alcohol (*R* or *S*) showed very similar ECD spectra. Therefore, it seems that the ECD spectra of the chiral BODPIYs is dominated by the helical chirality (*P* or *M*) and is relatively unaffected by the amino alcohol stereochemistry (*R* or *S*) (Figure **3.13**).

The measurement of the ECD spectra for the set of helically chiral BODIPYs also allowed the calculation of their anisotropy factors (g_{abs}) at 577 nm or 578 nm (Table **3.15**).

BODIPY	Solvent	λ_{max} (abs)/nm	ε / M^{-1} cm^{-1}	$\lvert g_{abs} \rvert$	Δε / M^{-1} cm^{-1}
(**3.7a**)	DCM	577	43 212[a] (30 091)[b]	2.6x10^{-4}	-7.8
(**3.7b**)	DCM	578	39 637[a] (29 944)[b]	3.2x10^{-4}	+9.5
(**3.40a**)	DCM	577	(30 703)[b]	2.7x10^{-4}	+8.2
(**3.40b**)	DCM	578	(30 144)[b]	3.5x10^{-4}	-10.5

Table 3.15: Chiroptical properties of (*S,M*)/(*S,P*)-*N,N,O,C*-3-((1-hydroxybutan-2-yl)amino) BODIPY (**3.7a**/**3.7b**) and (*R,M*)/(*R,P*)-*N,N,O,C*-3-((1-hydroxybutan-2-yl)amino) BODIPY (**3.40b**/**3.40a**). [a] Measured at the Newcastle University. [b] Measured by Dr Jonathan Bogaerts at the University of Antwerp.

3.10.1.2 CPL Spectroscopy of Helically Chiral *N,N,O,C*-3-((1-Hydroxybutan-2-yl)amino) BODIPYs (**3.7a**), (**3.7b**),(**3.40a**), and (**3.40b**)

Circularly polarized luminescence (CPL) is the emission of an excess of left-or right-handed circularly polarized light from a sample, such as a chiral fluorophore. The intensity of CPL can be expressed by the luminescence dissymmetric factor (g_{lum}). We planned to use the CPL as further assist with assigning

absolute stereochemistry of the final helically chiral *N,N,O,C*-3-((1-Hydroxybutan-2-yl)amino) BODIPYs (**3.7a**), (**3.7b**),(**3.40a**), and (**3.40b**) and to assess their potential for use in CPL applications.

CPL spectra for all four helically chiral (*S,M*)/(*R,P*)-*N,N,O,C*-3-((1-hydroxybutan-2-yl)amino) BODIPY (**3.7a**/**3.40a**) and (*S,P*)/(*R,M*)-*N,N,O,C*-3-((1-hydroxybutan-2-yl)amino) BODIPY (**3.7b**/**3.40b**) were measured (by Dr Patrycja Brook at Durham University). Unfortunately, all the four helically chiral BODIPYs showed very weak CPL spectra, which did not show any measurable emission bands and we were not able to calculate g_{lum} for these systems. We postulate that the difficulties in measuring the CPL spectra may be due to a combination of low g_{abs} and low fluorescence quantum yield (ϕ_F = 0.04) resulting in a low g_{lum} and low circularly polarized luminescence Brightness (B_{CPL}) (Figure **3.14**).[14]

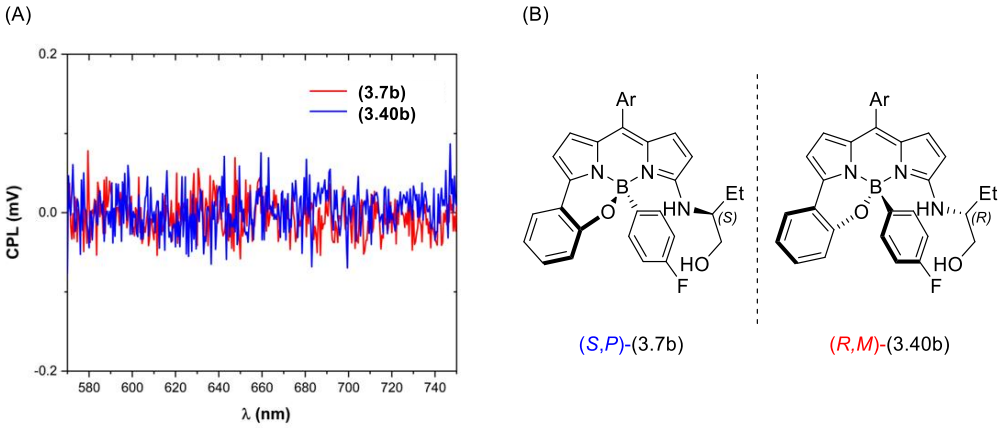

Figure 3.14: Experimental CPL spectra in DCM, excitation wavelength = 542. (A) CPL spectra of (*S,P*)-*N,N,O,C*-3-((1-hydroxybutan-2-yl)amino) BODIPY (**3.7b**) (blue) and (*R,M*)-*N,N,O,C*-3-((1-hydroxybutan-2-yl)amino) BODIPY (**3.40b**) (red); (B) Structure of the enantiomers of (*S,P*)-*N,N,O,C*-3-((1-hydroxybutan-2-yl)amino) BODIPY (**3.7b**) and (*R,M*)-*N,N,O,C*-3-((1-hydroxybutan-2-yl)amino) BODIPY (**3.40b**).

3.10.1.3 Calculated ECD Spectra of Helically Chiral *N,N,O,C*-3-((1-Hydroxybutan-2-yl)amino) BODIPYs (**3.7a**), (**3.7b**) and (**3.40a**), (**3.40b**)

We planned to compare our experimental ECD spectra of helically chiral *N,N,O,C*-3-((1-Hydroxybutan-2-yl)amino) BODIPYs (**3.7a**), (**3.7b**),(**3.40a**), and (**3.40b**) with calculated ECD spectra, in order to help with the assignment of absolute stereochemistry.

ECD spectra were calculated for all four helically chiral BODIPYs by Prof. Wouter Herrebout and their research group at the University of Antwerp. Firstly, the major low-energy conformations of a chosen single enantiomer of each helically chiral BODIPY were identified and their geometries optimised by density functional theory (DFT) to obtain the relative energies of the different conformations. ECD

spectra for each of the low-energy conformations were calculated using TD-DFT at the cam-B3LYP/6-311++G(3df,2pd) level, and the ECD spectra for the sample was calculated by a Boltzmann-weight combination of the individual spectra.

The calculated ECD spectra for each enantiomer agreed with the experimental ECD spectra of the corresponding enantiomer (absolute stereochemistry being determined by SCXRD), providing us with confidence that we had determined the correct absolute stereochemistry for each of the BODIPYs (Figure **3.15**).

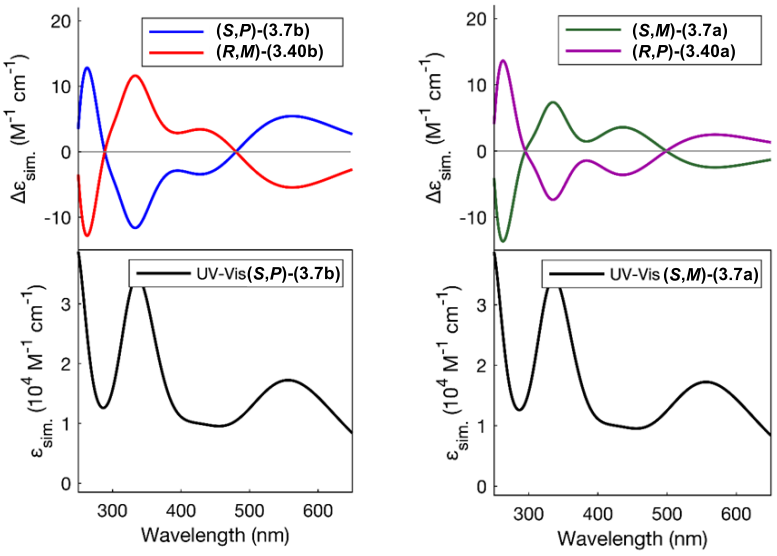

Figure 3.15: Calculated Boltzmann-weighted ECD and UV-Vis spectra (wavelength uncorrected); (A) ECD spectra of (*S,P*)-*N,N,O,C*-3-((1-hydroxybutan-2-yl)amino) BODIPY (**3.7b**) (blue), (*R,M*)-*N,N,O,C*-3-((1-hydroxybutan-2-yl)amino) BODIPY (**3.40b**) (red); and UV-Vis spectrum of (*S,P*)-*N,N,O,C*-3-((1-hydroxybutan-2-yl)amino) BODIPY (**3.7b**) (black); (B) ECD spectra of (*S,M*)-*N,N,O,C*-3-((1-hydroxybutan-2-yl)amino) BODIPY (**3.7a**) (green), (*R,P*)-*N,N,O,C*-3-((1-hydroxybutan-2-yl)amino) BODIPY (**3.40a**) (purple); UV-Vis spectrum of *N,N,O,C*-3-((*S,M*)-2-aminobutan-1-ol) BODIPY (**3.7b**)(black). (Figure **3.15** was created by the team of Prof. Wouter Herrebout).

Once we had successfully studied the photophysical and chiroptical properties of the fist examples of helically chiral *N,N,O,C*-3-((1-Hydroxybutan-2-yl)amino) BODIPYs (**3.7a**), (**3.7b**),(**3.40a**), and (**3.40b**) successfully determined their absolute stereochemistry by SCXRD, calculated ECD Spectra and experimental ECD Spectra , we turned our attention to synthesising a range of (*S,M*)/(*S,P*)-*N,N,O,C*-3-((1-hydroxybutan-2-yl)amino) BODIPYs using different (4-substitted phenyl boronic acid) with an electron withdrawing group or donating group to examine their effect on the diastereoselectivity in the final products.

3.11 Expansion of the Helically Chiral *N,N,O,C*-3-((1-hydroxybutan-2-yl)amino) BODIPY Series

We planned to examine the use of a range of commercially available aryl boronic acids containing an electron-poor or an electron-rich group in the *para*-position, to study how these groups will influence on the diastereoselectivity in the chelation reaction. Initially, we intended to test both aryl boronic acids and aryl boronic acid pinacol esters, to determine suitable starting materials for our experiments.

3.11.1 Testing (4-Fluorophenyl)boronic Acid Pinacol Ester in the Chelation Reaction of Helically Chiral (*S,M*)/(*S,P*)-*N,N,O,C*-3-((1-hydroxybutan-2-yl)amino) BODIPYs

We have previously shown that (4-fluorophenyl)boronic acid can be used in diastereoselective chelation reactions with 3-amino alcohol substituted 5-(2-hydroxyphenyl)-BODIPYs. However, we wished to test a similar chelation reaction with aryl boronic acid pinacol esters, as they are widely commercially available with different substitution patterns, and easier to synthesis than aryl boronic acids, so have the potential for greater reaction scope.

Herein, we tested the reaction of (4-fluorophenyl)boronic acid pinacol ester (**3.41**)with (*S*)-α-(1-hydroxybutan-2-yl)amino)-α'-(2-hydroxyphenyl) dipyrromethene (**3.6**) under the chelation conditions discussed previously. Thus the molecules were reacted in $CHCl_3$ at 35 °C over 16 hours, resulting in the desired (*S,M*)-*N,N,O,C*-3-((1-hydroxybutan-2-yl)amino) BODIPY (**3.7a**) and (*S,P*)-*N,N,O,C*-3-((1-hydroxybutan-2-yl)amino) BODIPY (**3.7b**) in an overall 41 % isolated yield (Table **3.16**, Entry 2), with a *de* of 31% by both ^{19}F NMR and isolated yields. This low yield could be attributed to the observation by crude ^{1}H NMR of both unreacted starting materials. Consequently, we repeated the reaction again under similar conditions, extending the reaction time. The reaction was monitored by TLC which showed that new products had been formed and the starting material had been fully consumed after 72 h. Following aqueous work-up and purification by column chromatography (*S,M*)-*N,N,O,C*-3-((1-hydroxybutan-2-yl)amino) BODIPY (**3.7a**) and (*S,P*)-*N,N,O,C*-3-((1-hydroxybutan-2-yl)amino) BODIPY (**3.7b**) were obtained in an improved yield of 71% with a *de* of 33% and 26% by ^{19}F NMR and isolated yield respectively (Table **3.16**, Entry 3).

Upon comparing the chelation reaction using (4-fluorophenyl)boronic acid (**2.25**) and (4-fluorophenyl)boronic acid pinacol ester (**3.41**), we found that both successfully formed a mixture of the two diastereomeric helically chiral (*S,M*)-*N,N,O,C*-3-((1-hydroxybutan-2-yl)amino) BODIPY (**3.7a**) and (*S,P*)-*N,N,O,C*-3-((1-hydroxybutan-2-yl)amino) BODIPY (**3.7b**). However, chelation reactions with (4-fluorophenyl)boronic acid showed higher yields (up to 100%) and *de* (up to 74%) than the reactions with (4-fluorophenyl)boronic acid pinacol ester (**3.41**), which showed *de* of only ~30%. In addition, the

excess (4-fluorophenyl)boronic acid used in the reactions was easily removed through aqueous work-up, whilst excess (4-fluorophenyl)boronic acid pinacol ester was difficult to remove from the products even after column chromatography. As a result, we decided to select aryl boron acids for further chelation reactions.

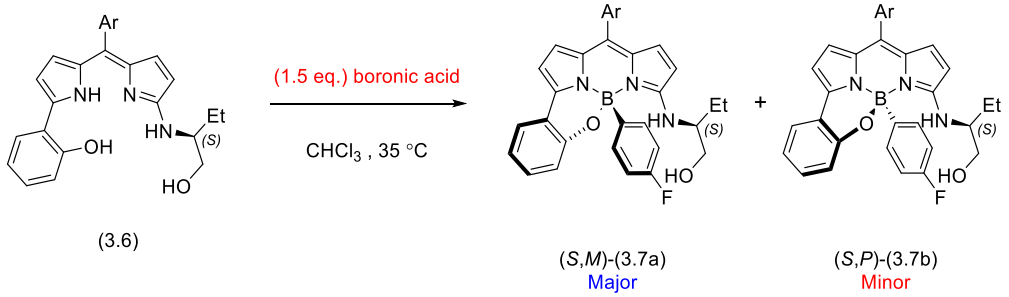

Entry	Boronic acid	Time	*de* ^{19}F NMR/%	*de* after purification/%	Yield[b]/%
1[a]	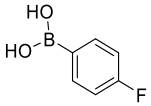	5 min	74	64	100
2	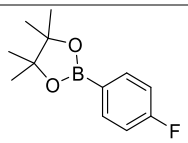	16 h	31	31	41
3	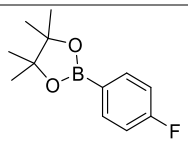	72 h	33	26	71

Table 3.16: Results of testing (4-fluorophenyl)boronic acid pinacol ester (**3.41**). [a] Previously discussed result, included for comparison. [b] Isolated yield following column chromatography (Ar = *p*-($MeCO_2$)-C_6H_4-).

3.11.2 Expansion of the Helically Chiral *N,N,O,C*-3-((1-hydroxybutan-2-yl)amino) BODIPY Series

After selecting boronic acids as our starting material, we planned to examine a range of aryl boronic acids substituted in the *para*- and *ortho*-position with either an electron-donating group or an electron-withdrawing group, to study the impact of these groups on the diastereoselectivity of the chelation reactions (Table **3.17**). Chelation reactions were carried out using our previously optimised conditions for aryl boronic acids (see section 3.7.1).

We found that in each case high combined yields of the two diastereomers following column chromatography were obtained (77 - 85%) (Table **3.17**, Entries 1,2,4,5), with the exception of a moderate yield with (2,4-difluorophenyl) boronic acid (49%) (Table **3.17**, Entry 3). Diastereomeric excess for the crude reaction mixtures were measured by comparative ^{1}H NMR integration of the methyl group of the amino alcohol substituent. In terms of diastereoselectivity, we observed that boronic acids containing electron-withdrawing groups showed only marginally better diastereoselectivity than boronic acids containing electron-donating groups in this series. It should be noted that many of the helically chiral (*S,M*)/(*S,P*)-*N,N,O,C*-3-((1-hydroxybutan-2-yl)amino) BODIPYs formed were successfully crystallised and studied by SCXRD (see section 3.11.4).

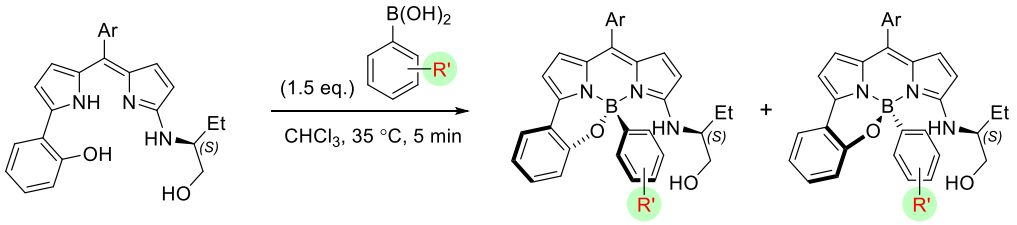

Entry	Boronic acid	Product	Yield[c]/%	*de* crude mixture[a]/%	*de* after purification[b]/%	Crystal Ref
1	(**3.42**), R = CF_3	(**3.46**)	81	27	29	-
2	(**3.43**), R = NO_2	(**3.47**)	85	36	28	mjh220078_fa
3	(**3.44**), R = 2,4-difluoro	(**3.48**)	49	17	28	mjh220070_fa mjh220067_fa
4	(**3.45**), R = CH_3	(**3.49**)	81	22	26	mjh220077_fa
5	(**2.23**), R = OCH_3	(**3.50**)	77	17	31	mjh220061_fa mjh220064_fa

Table 3.17: Results of testing the substrate scope. [a] The *dr* value was determined by ^{1}H NMR analysis of crude mixture. [b] The *dr* value was determined by isolated yields, [c] Isolated combined yield (Ar = *p*-($MeCO_2$)-C_6H_4-).

After successfully investigating the electronic effects of various aryl boronic acids on the diastereomeric excess, we next aimed to examine the influence of the 3-amino alcohol substituents on the diastereoselectivity in the chelation reaction.

3.11.3 Expansion of the Helically Chiral *N,N,O,C*-3-Amino alcohol Substituted BODIPY Series

Next, we planned to study the effects of 3-amino alcohols, varying the R group from the less sterically hindered methyl group to the bulkier tertiary butyl group, on the diastereoselectivity in the formation of helically chiral *N,N,O,C*-3-amino alcohol substituted-BODIPYs (Table **3.18**). Thus, we tested the chelation reaction under our previously optimised conditions, of (4-fluorophenyl)boronic acid with a range of previously prepared of α-amino alcohol substituted-α'-(2-hydroxyphenyl) dipyrromethenes (**3.37**),(**3.38**) and (**3.39**).

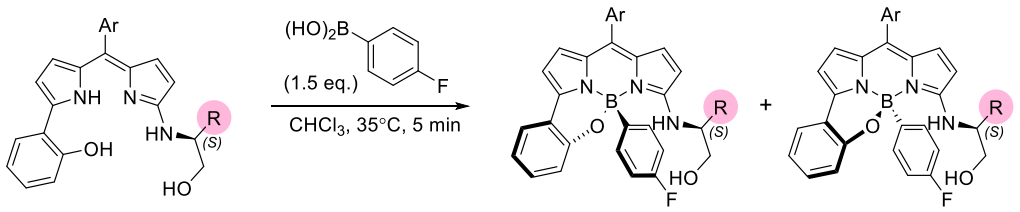

(3.37 - 3.39)

(*S*,*M*)-(3.51 - 3.53a) Major

(*S*,*P*)-(3.51 - 3.53b) Minor

Entry	Starting material	Product	Yield[b]/ %	*de* crude mixture[c]/%	*de* after purification[d]/%	Crystal Ref
1[a]	(**3.6**), R = CH_2CH_3	(**3.7**)	100	74	64	mjh220005_fa mjh220014_fa
2	(**3.37**), R = CH_3	(**3.51**)	96	61	38	mjh220050_fa mjh220052_fa
3	(**3.38**), = C_6H_5	(**3.52**)	100	37	33	mjh220046_fa
4	(**3.39**), R = $C(CH_3)_3$	(**3.53**)	90	24	23	mjh230082_fa

Table 3.18: Results of testing the substrate scope. [a] Previously discussed result, included for comparison. [b] Isolated combined yield. [c] The *dr* was determined by ^{19}F NMR analysis of crude mixture. [d] The *dr* was determined by isolated yields (Ar = *p*-($MeCO_2$)-C_6H_4-).

We observed that, in each case, high combined yields of the two diastereomers were obtained following column chromatography (90 -100 %) (Table **3.18**). Interestingly, the chelation reaction of (**3.37**) containing a methyl group showed high *de* (61%) as calculated by ^{19}F NMR, similar to that seen for the ethyl case. However low *de* (38%) was measured by isolated yield after purification by column chromatography, either due to possible issues with separation or potential epimerisation (Table **3.18**, Entry 2). On the other hand, the formation of BODIPY (**3.38**) and (**3.39**) containing phenyl group and tertiary butyl groups resulted in lower *de* values (24 -37%) as determined by both ^{19}F NMR and isolated yields (Table **3.18**, Entries 3 and 4). These finding suggest that steric effect of the R group of the amino alcohol may significantly impact on the diastereoselectivity of the chelation reactions. It should be

noted that the helically chiral *N,N,O,C*-3-amino alcohol substituted-BODIPYs formed were successfully crystallised and studied by SCXRD (see section 3.11.4).

3.11.4 Crystal Structures of Helically Chiral BODIPY Series

The previously described chemistry gave a total of 16 helically chiral BODIPYs, including variation of the aryl boronic acid or the amino alcohol substituent, all requiring the assignment of their absolute stereochemistry. To achieve this, we attempted to grow crystals of each of the 16 helically chiral BODIPYs by slow evaporation of either a MeOH or a DCM solution. Subsequently, suitable single crystals for 9 of the helically chiral BODIPYs were obtained, including at least one from 6 different diastereomeric pairs. Crystals were analysed by SCXRD (Table **3.19**), and the absolute stereochemistry was assigned using anomalous dispersion (Flack parameter). In the cases where no Flack parameter was seen, absolute stereochemistry was assigned by comparison to the known amino alcohol stereocentre. Interestingly, all of the major diastereomers were shown to have (*S,M*) absolute stereochemistry and the minor diastereomers were assigned as (*S,P*).

Comp.	Crystal Ref.	Solvent	Crystal system	Space group	Flack	Abso-lute	Absolute stereochem.
(**3.47a**)	mjh220078_fa	MeOH	monoclinic[a]	$P2_1$	-0.06(6)	Y	(*S,M*)
(**3.48a**)	mjh220067_fa	MeOH	Orthorhombic	$P2_12_12_1$	-0.09(5)	Y	(*S,M*)
(**3.48b**)	mjh220070_fa	MeOH	Orthorhombic	$P2_12_12_1$	0.00(8)	Y	(*S,P*)
(**3.49a**)	mjh220077_fa	MeOH	monoclinic[a]	$P2_1$	-0.03(5)	Y	(*S,M*)
(**3.50a**)	mjh220064_fa	MeOH	Triclinic	*P-1*	-	N	(*S,M*)[b]
(**3.50b**)	mjh220061_fa	MeOH	Orthorhombic	$P2_12_12_1$	-0.06(9)	Y	(*S,P*)
(**3.51a**)	mjh220052_fa	MeOH	Orthorhombic	$P2_12_12_1$	0.08(5)	Y	(*S,M*)
(**3.51b**)	mjh220050_fa	MeOH	Orthorhombic	$P2_12_12_1$	-0.05(8)	Y	(*S,P*)
(**3.52b**)	mjh220046_fa	DCM	orthorhombic[a]	$P2_12_12$	0.11(5)	Y	(*S,P*)
(**3.53a**)	mjh230082_fa	MeOH	Triclinic	*P1*	0.00(4)	Y	(*S,M*)

Table 3.19: Crystal data of helically chiral BODIPY series, [a] Crystal formed as a hemihydrate; [b] Absolute stereochemistry determined by relative stereochemistry vs existing amino alcohol stereocentre (Ar = *p*-($MeCO_2$)-C_6H_4-).

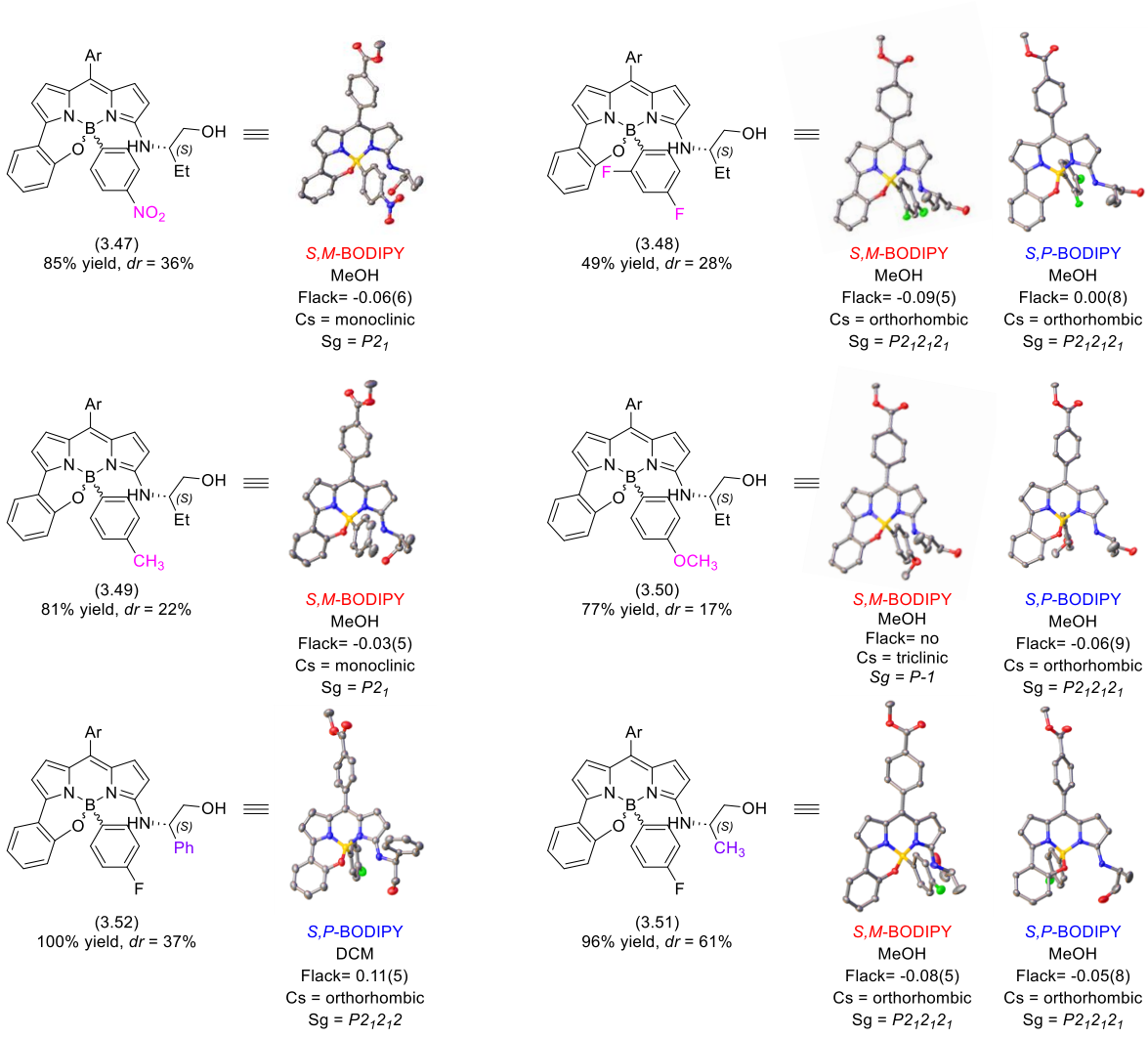

Figure 3.16: Single crystal X-ray structures of helically chiral BODIPY series (Ar = *p*-($MeCO_2$)-C_6H_4-)

3.11.5 Chiroptical Properties of Helically Chiral *N,N,O,C*-3-Amino Alcohol Substituted BODIPY Series

Once we have determined the absolute stereochemistry of our set of helically chiral BODIPYs by SCXRD, next we planned to measure their ECD spectra. This will allow us to correlate the ECD spectra to helically chiral BODIPYs for which we know the stereochemistry and compare against helically chiral BODIPYs for which we do not know the absolute stereochemistry as we were not able to grow crystals.

ECD spectra were measured by Dr Jonathan Bogaerts. Similar what was observed previously, each pair of diastereomers showed almost mirror image ECD spectra, with a range of Cotton effects ($\Delta\varepsilon_{max} \approx \pm5$ - ±17 L mol^{-1} cm^{-1}) for the S_0-S_1 transition (λ_{max} = 578 nm).

From the ECD spectra, we observed that these helically chiral BODIPYs which have the (*S,P*) absolute stereochemistry showed a positive Cotton effect for the BODIPY S_0-S_1 transition, while, the helically

chiral BODIPYs with the (*S,M*) configuration showed a negative Cotton effect at the same wavelength. This was consistent with the trends observed in our previous examples (**3.7a**) and (**3.7b**), allowing us to assign absolute helical stereochemistry in the cases where this could not be directly determined by other methods, *eg*. SCXRD.

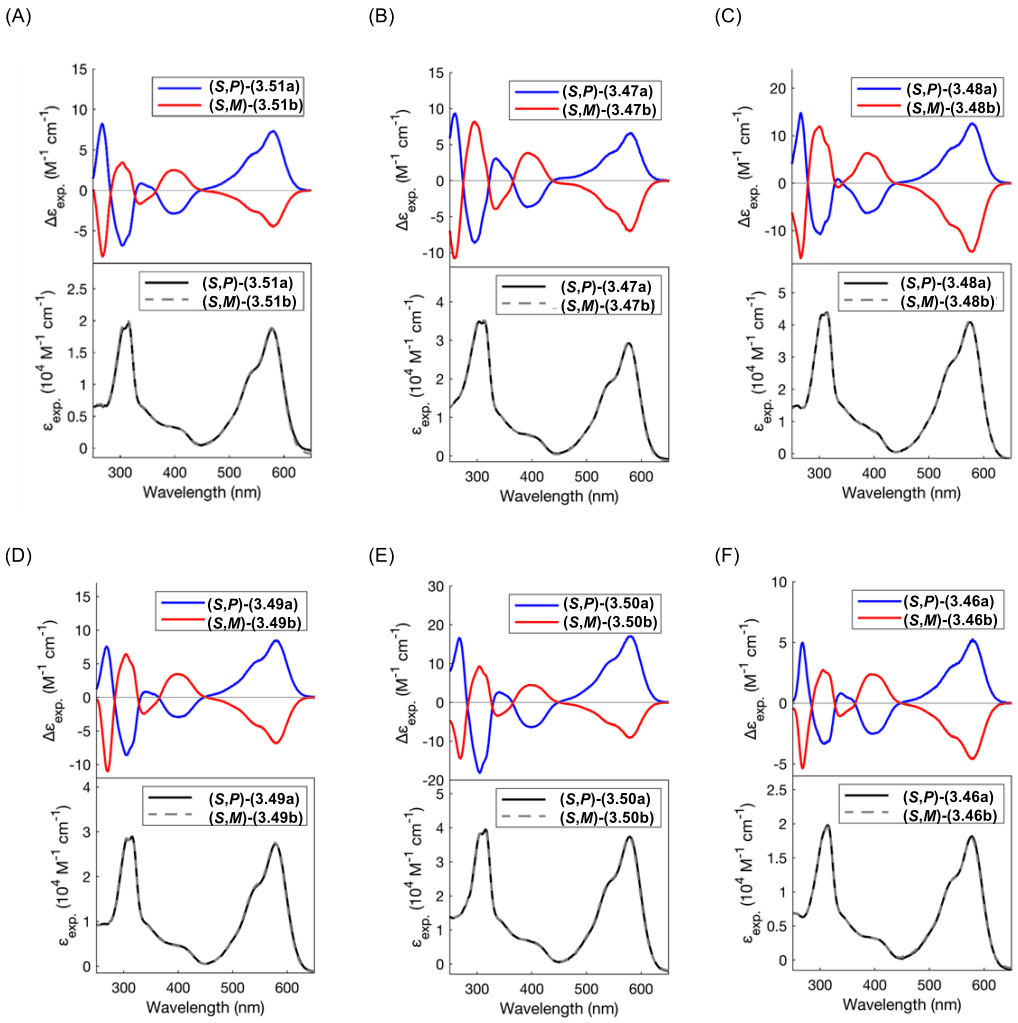

Figure 3.17: Experimental ECD and UV-Vis spectra in DCM, (A) ECD (*S,P*)-BODIPY (**3.51b**) (blue), (*S,M*)-BODIPY (**3.51a**) (red), UV-Vis *N,N,O,C*-3-((*S,P*)-2-aminopropan-1-ol) BODIPY (**3.51**)(black); (B) ECD (*S,P*)-BODIPY (**3.47b**) (blue), ECD (*S,M*)-BODIPY (**3.47a**) (red), UV-Vis BODIPY (**3.47**)(black); (C) ECD (*S,P*)-BODIPY (**3.48b**) (blue), ECD (*S,M*)-BODIPY (**3.48a**) (red), UV-Vis BODIPY (**3.48**)(black); (D) ECD (*S,P*)-BODIPY (**3.49b**) (blue), ECD (*S,M*)-BODIPY (**3.49a**) (red), UV-Vis BODIPY (**3.49**)(black); (E) ECD (*S,P*)-BODIPY (**3.50b**) (blue), ECD (*S,M*)-BODIPY (**3.50a**) (red), UV-Vis BODIPY (**3.50**)(black); (F) ECD (*S,P*)-BODIPY (**3.46b**) (blue), ECD (*S,M*)-BODIPY (**3.46a**) (red), UV-Vis BODIPY (**3.46**)(black); (Figure **3.17** was created by Dr Jonathan Bogaerts).

Interestingly, the only pair of diastereomers that does not behave in this way is (*S,M*)-*N,N,O,C*-3-(2-hydroxy-1-phenylethyl)amino) BODIPY (**3.52a**) and (*S,P*)-*N,N,O,C*-3-(2-hydroxy-1-phenylethyl)amino)

BODIPY (**3.52b**). We postulate that this unexpected result could have a potential explanation the phenyl group in the amino alcohol side chain. We propose that π-stacking interactions between the phenyl group of amino alcohol and 4-flourophenyl group in (*S,P*)-*N,N,O,C*-3-(2-hydroxy-1-phenylethyl)amino) BODIPY (**3.52b**) may be influencing the ECD spectra.

To test this hypothesis, we wished to compare the experimental and calculated ECD calculations for the diastereomers. ECD spectra were therefore calculated for both (*S,M*)-*N,N,O,C*-3-(2-hydroxy-1-phenylethyl)amino) BODIPY (**3.52a**) and (*S,P*)-*N,N,O,C*-3-(2-hydroxy-1-phenylethyl)amino) BODIPY (**3.52b**) by Dr Jonathan Bogaerts (Figure **3.17**). The calculated ECD spectra matched the experimental ECD spectra, confirming that the presence of the phenyl group influences the ECD spectra, resulting in a break to the observed trends.

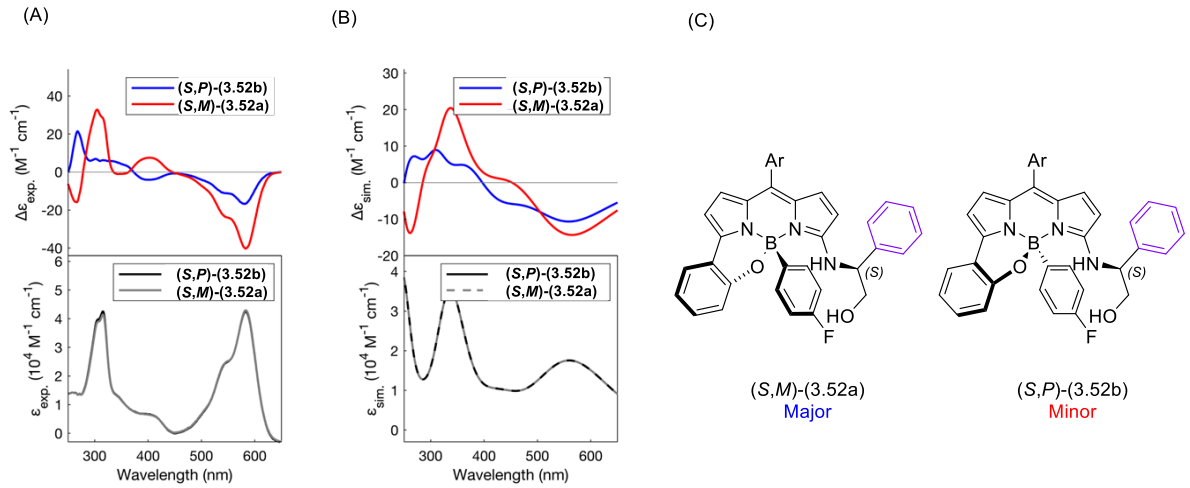

Figure 3.18: (A) Experimental ECD spectra in DCM; ECD (*S,P*)-*N,N,O,C*-3-(2-hydroxy-1-phenylethyl)amino) BODIPY (**3.52b**) (blue), (*S,M*)-*N,N,O,C*-3-(2-hydroxy-1-phenylethyl)amino) BODIPY (**3.52a**) (red), and UV-Vis (*S,P*)-*N,N,O,C*-3-(2-hydroxy-1-phenylethyl)amino) BODIPY (**3.52b**) (black); (B) Calculated Boltzmann-weighted ECD and UV-Vis spectra (wavelength uncorrected), (*S,P*)-*N,N,O,C*-3-(2-hydroxy-1-phenylethyl)amino) BODIPY (**3.52b**) (blue), (*S,M*)-*N,N,O,C*-3-(2-hydroxy-1-phenylethyl)amino) BODIPY (**3.52a**) (red), and UV-Vis (*S,P*)-*N,N,O,C*-3-(2-hydroxy-1-phenylethyl)amino) BODIPY (**3.52b**) (black); (C) The structure of *N,N,O,C*-3-((*S,P/S,M*)-2-amino-2-phenylethan-1-ol) BODIPY (**3.52a** and **3.52b**) (Ar = *p*-($MeCO_2$)-C_6H_4-).

3.12 Conclusion

In this chapter we have successfully developed synthetic routes to access novel helically chiral BODIPY compounds. We have reported the first example of point-to-helical chirality transfer in a BODIPY system, using commercially available amino alcohols as chiral auxiliaries, which resulted in moderate to good diastereoselectivities (17 - 74 %*de*) (Figure **3.19**). We have measured the chiroptical properties

of the helically chiral *N,N,O,C*-3-((1-hydroxybutan-2-yl)amino) BODIPYs (**3.7a**), (**3.7b**),(**3.40a**), and (**3.40b**) synthesised, including ECD and CPL spectra. We were also able to determine the absolute stereochemistry of each pair of diastereomer BODIPYs by a combination of SCXRD and comparison the experimental to calculated ECD spectra.

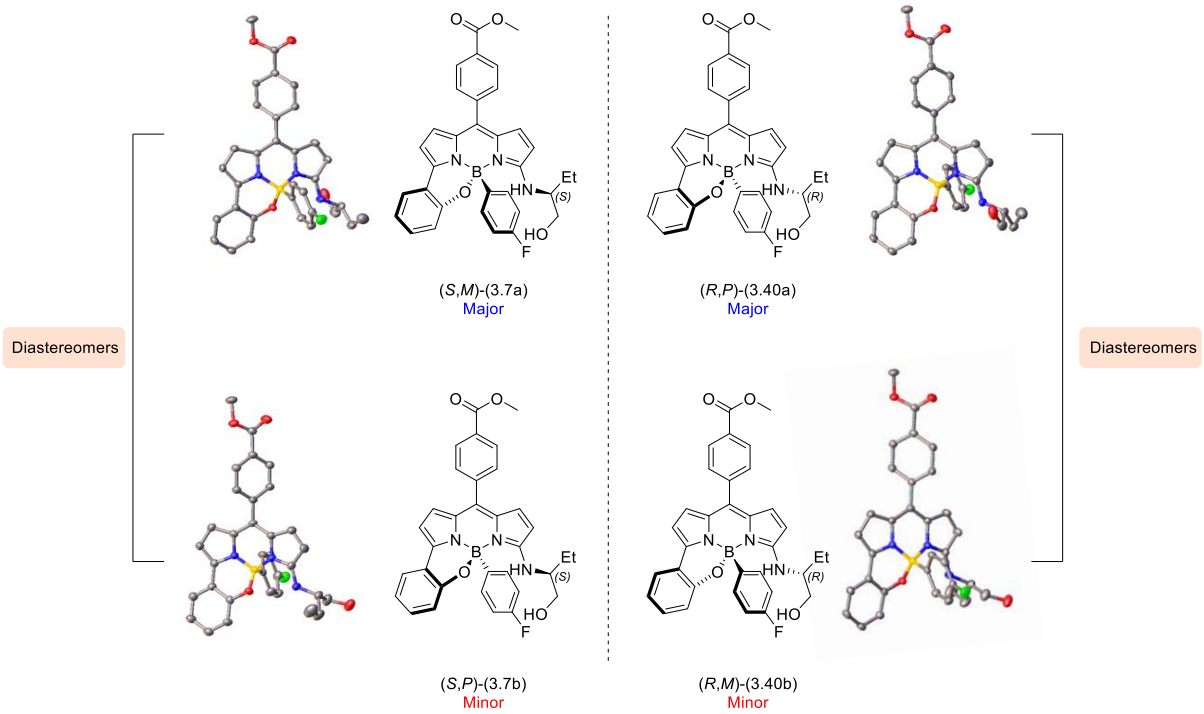

Figure 3.19: The first example of helically chiral BODIPYs through point-to-helical chirality transfer, this figure showed the four helically chiral (*S,M*)-*N,N,O,C*-3-((1-hydroxybutan-2-yl)amino) BODIPY (**3.7a**), (*S,P*)-*N,N,O,C*-3-((1-hydroxybutan-2-yl)amino) BODIPY (**3.7b**), (*R,P*)-*N,N,O,C*-3-((1-hydroxybutan-2-yl)amino) BODIPY (**3.40a**), and (*R,M*)-*N,N,O,C*-3-((1-hydroxybutan-2-yl)amino) BODIPY (**3.40b**).

Through this work we have demonstrated a novel point-to-helical control approach, which holds promise for future advances in chiral BODIPY design. Although our synthesized helically chiral BODIPYs displayed weak circularly polarized luminescence (CPL), future systems could be tailored to include CPL emission as a central aspect of their design. Concepts around improved CPL point-to-helical chiral BODIPYs will be further discussed in Chapter 6.

Chapter 4. Synthesis of Helically Chiral BODIPYs including 7-Membred Ring via Point-to-Helical Chirality Transfer

4.1 Introduction

In the previous chapter, we successfully demonstrated a synthesis of helically chiral *N,N,O,C*-BODIPYs, in which the helical chirality was controlled through a novel point-to-helical chirality approach. In this chapter we will look at alternative routes to accessing enantiopure helically chiral BODIPY systems using both point-to-helical control and resolution approaches.

Firstly, we aimed to utilise a similar point-to-helical chirality approach to access helically chiral BODIPYs, in which the helical chirality is formed simultaneously with a 7-membered ring formation with an enantiopure amino alcohol. Our aim is to explore the synthetic routes to these helically chiral BODIPYs, focusing on investigation the key mechanisms involved in their formation. Additionally, we will discuss the photophysical and chiroptical properties of these compounds (Scheme **4.1**).

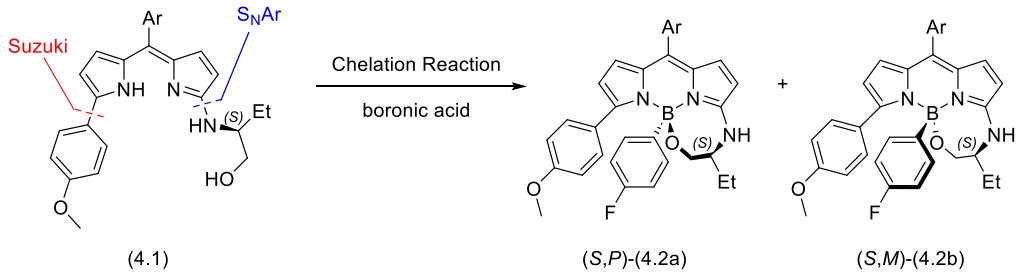

Scheme 4.1: Point-to-helical chirality control in helically chiral *N,N,O,O*-BODIPYs containing 7-membered ring system (Ar = *p*-($MeCO_2$)-C_6H_4-).

Secondly, we will explore the synthesis of symmetrical helically chiral BODIPYs, which include two 7-member rings. These will be synthesised through a double S_NAr reaction using enantiopure amino alcohols and boron chelation. We hope to control the chirality of the resulting BODIPY through the point-to-helical chirality approach as before (Scheme **4.2**).

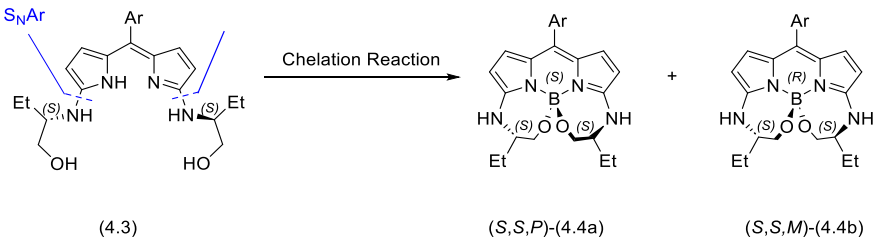

Scheme 4.2: Point-to-helical chirality control in helically chiral *N,N,O,O*-BODIPYs containing double 7-membered rings system (Ar = *p*-($MeCO_2$)-C_6H_4-).

Lastly, we will discuss methods to access enantiopure helically chiral *N,N,O,O*-BODIPYs through a chiral resolution type approach. Initially, we will synthesise a racemic mixture of a *meso*-ethyl-*N,N,O,O*-BODIPY system and then convert them into diastereomeric *N,N,O,O*-BODIPYs. This will be achieved using an enantioselective organocatalysed nucleophilic addition of the BODIPY to an MBH carbonate (formed via a Morita–Baylis–Hillman reaction), using quinine a chiral catalyst. Subsequently, we will measure the photophysical and chiroptical properties of these compounds (Scheme **4.3**).

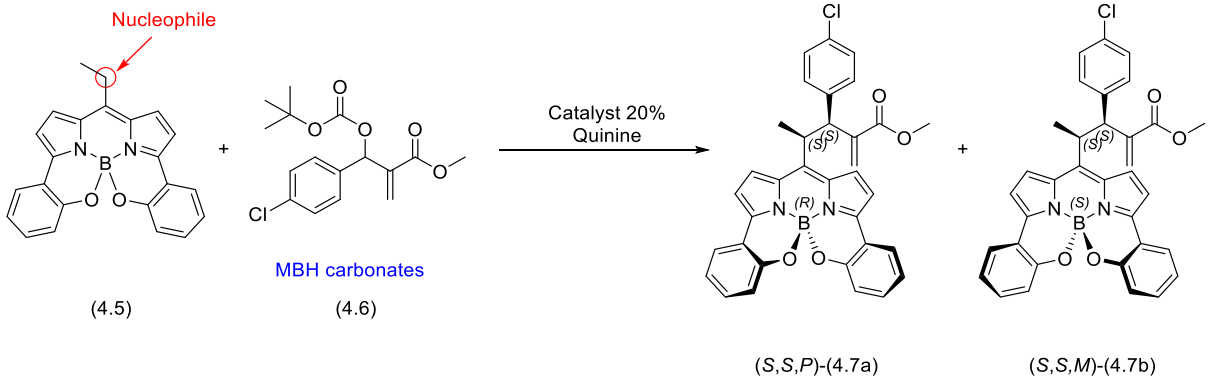

Scheme 4.3: Resolution of helically chiral *N,N,O,O*-BODIPYs via an enantioselective organocatalysed reaction

4.2 Synthetic Strategy Towards Helically Chiral BODIPY Containing 7-Membered Ring

For the first target system, our planned synthetic route to helically chiral BODIPY containing a 7-membered ring involves three new synthetic steps. We will start with (*S*)-3-(1-hydroxybutan-2-yl)amino)-5-iodo BODIPY (**3.2**), prepared as in chapter 3, which contains an enantiopure amino alcohol group at the 3-position of the BODIPY. Second, we will utilize a Suzuki Miyaura cross-coupling reaction to introduce a 4-methoxyphenyl group at the 5-position. Subsequently, a Lewis acid mediated de-chelation reaction will be used to remove the BF_2 group, followed by re-chelation reaction with (4-fluorophenyl)boronic acid to form diastereomeric helically chiral BODIPYs (**4.2a**) and (**4.2b**) containing a 7-membered ring involving the amino alcohol group chelating the boron (Scheme **4.4**).

4.2.1 Synthesis of Helically Chiral BODIPY Containing 7-Membered Ring

4.2.1.1 Suzuki Miyaura Cross-Coupling Reaction

Therefore, our first step was the Suzuki Miyaura cross-coupling reaction between (*S*)-3-(1-hydroxybutan-2-yl)amino)-5-iodo BODIPY (**3.2**) and (4-methoxyphenyl)boronic (**2.23**) acid.

In our first attempt, we carried out the reaction between one equivalent of (*S*)-3-(1-hydroxybutan-2-yl)amino)-5-iodo BODIPY (**3.2**) on 1.25 mmol scale and 2 equivalents of (4-methoxyphenyl)boronic acid (**2.23**) with 6 mol% XPhos Pd G3, in the presence of potassium phosphate in THF/Water in a

Schleck flask. Following degassing using three freeze-pump-thaw cycles, the reaction was heated to at 75 °C. Monitoring by TLC, showed the formation of new product after 1 h. It should be noted that the starting material (**3.2**) and the product formed had very similar retention factors on TLC, making accurate estimation of reaction completion difficult. Following an aqueous work-up and column chromatography, the desired product (*S*)-3-(1-hydroxybutan-2-yl)amino)-5-(4-methoxyphenyl) BODIPY (**4.8**) was obtained in moderate yield 52%, as a shiny red solid. We postulated that the moderate yield was due to incomplete reaction, thus further reactions would be carried out for longer.

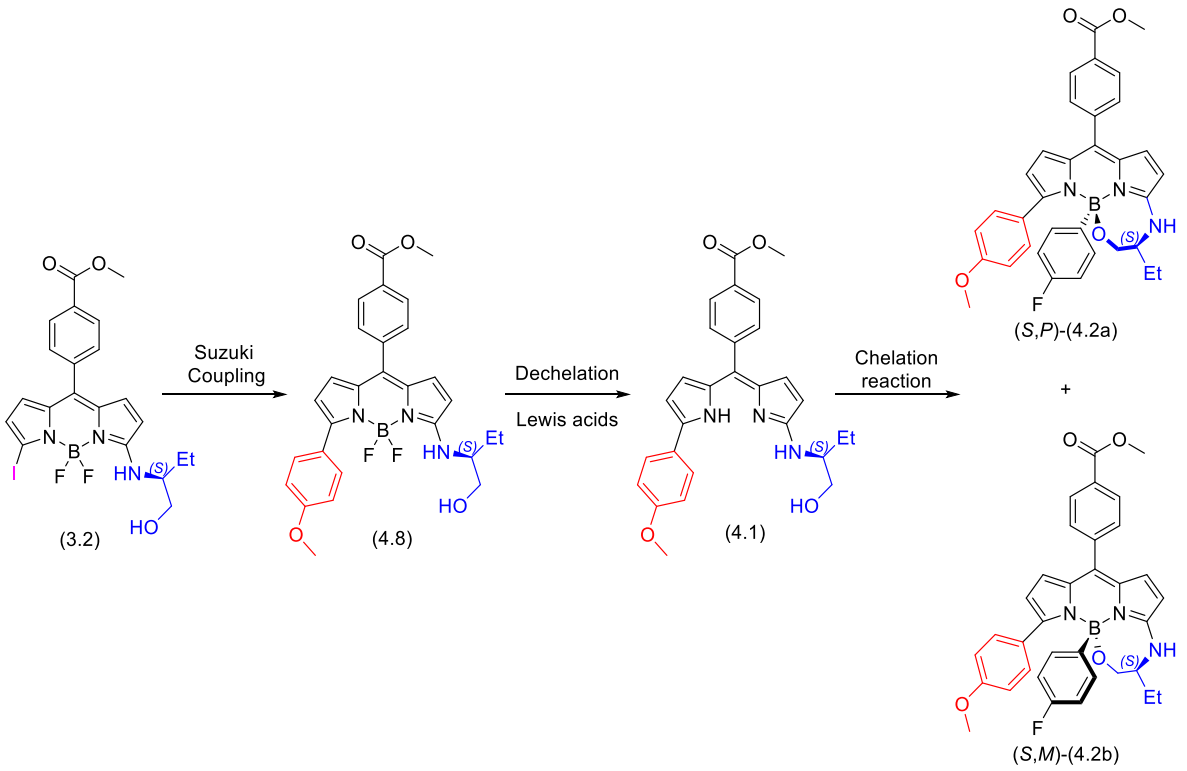

Scheme 4.4: Planned route to helically chiral BODIPYs containing a 7-membered ring, via point-to-helical chirality transfer.

Therefore, we repeated the Suzuki Miyaura reaction of (*S*)-3-(1-hydroxybutan-2-yl)amino)-5-iodo BODIPY (**3.2**) on a 0.80 mmol scale with 2 equivalents of (4-methoxyphenyl)boronic acid (**2.23**), following the previous procedure. The reaction was heated at 75 °C and monitored by TLC, which showed that the desired product had been formed and the starting material consumed after 3.5 h. After aqueous work-up and purification by column chromatography (*S*)-3-(1-hydroxybutan-2-yl)amino)-5-(4-methoxyphenyl) BODIPY (**4.8**) was isolated in an improved yield of 64% (Table **4.1**).

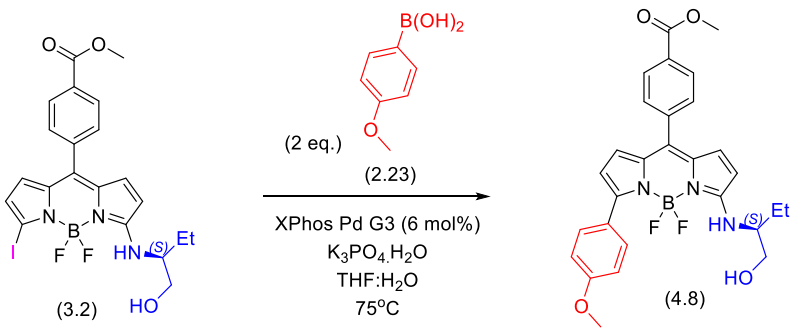

Entry	Scale/mmol	Reaction Time/ h	Yield/% [a]
1	1.25	1	52
2	0.80	3.5	64

Table 4.1: Synthesis of (*S*)-3-(1-hydroxybutan-2-yl)amino)-5-(4-methoxyphenyl) BODIPY (**4.8**), [a] Isolated yield.

The structure of (*S*)-3-(1-hydroxybutan-2-yl)amino)-5-(4-methoxyphenyl) BODIPY (**4.8**) was confirmed by the analysis of ^{1}H NMR spectra, which showed a singlet at 3.85 ppm and two new doublets at 7.76 ppm (d, *J* = 8.9 Hz, 2H) and 6.97 ppm (d, *J* = 9.0 Hz, 2H) corresponding to the newly added 4-methoxyphenyl group.

To further confirm the structure of (*S*)-3-(1-hydroxybutan-2-yl)amino)-5-(4-methoxyphenyl) BODIPY (**4.8**), crystals were grown via slow evaporation of a $CHCl_3$ solution. A suitable single crystal was analysed by single crystal X-ray diffraction (SCXRD), showing that (*S*)-3-(1-hydroxybutan-2-yl)amino)-5-(4-methoxyphenyl) BODIPY (**4.8**) had crystallised in the monoclinic C2 space group. Unfortunately, a Flack parameter of 0.14(13) was obtained for the crystal, preventing direct assignment of absolute stereochemistry (Figure **4.1**).

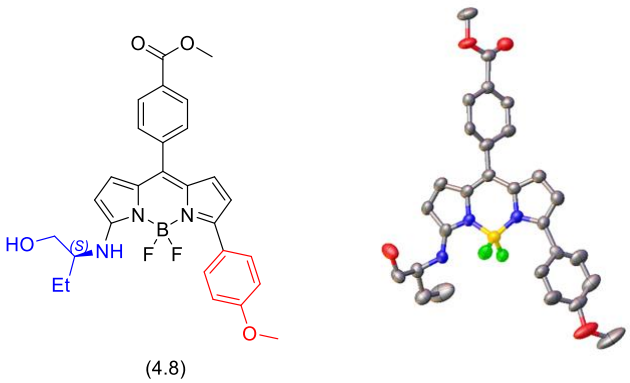

Figure 4.1: Single crystal X-ray structure of (*S*)-3-(1-hydroxybutan-2-yl)amino)-5-(4-methoxyphenyl) BODIPY (**4.8**).

After we had successfully synthesised (*S*)-3-(1-hydroxybutan-2-yl)amino)-5-(4-methoxyphenyl) BODIPY (**4.8**), next we planned to test the de-chelation reaction with $AlCl_3$, to remove the BF_2 group.

4.2.1.2 De-chelation Reaction of (*S*)-3-(1-hydroxybutan-2-yl)amino)-5-(4-methoxyphenyl) BODIPY (**4.8**)

The next step was the dechelation reaction of (*S*)-3-(1-hydroxybutan-2-yl)amino)-5-(4-methoxyphenyl) BODIPY (**4.8**). To do this, we followed the same procedure reported by Ravikanth and co-workers, that we used previously in chapter 3.[75]

Therefore, we reacted one equivalent of (*S*)-3-(1-hydroxybutan-2-yl)amino)-5-(4-methoxyphenyl) BODIPY (**4.8**) with five equivalents $AlCl_3$ in MeOH/MeCN at reflux. The reaction was monitored by TLC, which showed the presence of a new product and the disappearance of the starting material after 1.5 hours. Following aqueous work-up and column chromatography, the desired (*S*)-α-(1-hydroxybutan-2-yl)amino)-α'-(4-methoxyphenyl) dipyrromethene (**4.1**) was isolated in a good yield (70 %). In order to have enough (*S*)-α-(1-hydroxybutan-2-yl)amino)-α'-(4-methoxyphenyl) dipyrromethene (**4.1**) for further steps, the de-chelation reaction was repeated on a similar scale of 0.49 mmol. Following column chromatography, we obtained a 73 % isolated yield of the desired product. However, during purification we noticed that some of the desired product had remained on the column after the majority had been eluted. Since we had previously experienced solubility problems with similar molecules (Chapter 3, section 3.6.3), we decided to flush the column with methanol which resulted in more of the desired product being obtained, which was then purified by preparative TLC to give a further 7% of the desired product. Thus, the combined isolated yield of (*S*)-α-(1-hydroxybutan-2-yl)amino)-α'-(4-methoxyphenyl) dipyrromethene (**4.1**) was 80% (Table **4.2**).

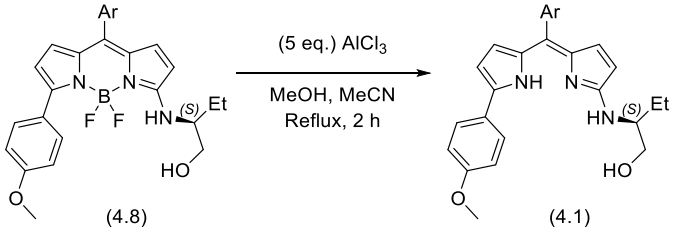

Entry	Scale/mmol	Yield/%
1	0.48	70[a]
2	0.49	80[b]

Table 4.2: Synthesis of (*S*)-α-(1-hydroxybutan-2-yl)amino)-α'-(4-methoxyphenyl) dipyrromethene (**4.1**), [a] Isolated yield following column chromatography; [b] Combined isolated yield following both column chromatography and additional preparative TLC.

The structure of (*S*)-α-(1-hydroxybutan-2-yl)amino)-α'-(4-methoxyphenyl) dipyrromethene (**4.1**) was validated by HRMS, which showed a molecular ion at *m/z* = 472.2229 $[M+H]^+$, which corresponded to a molecular formula of $C_{28}H_{30}N_3O_4$. The analysis of the ^{11}B and ^{19}F NMR spectra of (*S*)-α-(1-hydroxybutan-2-yl)amino)-α'-(4-methoxyphenyl) dipyrromethene (**4.1**) gave us confidence that the BF_2 group had been removed as there was no signal in either spectrum.

4.2.1.3 Chelation Reaction of (*S*)-α-(1-hydroxybutan-2-yl)amino)-α'-(4-methoxyphenyl) dipyrromethene (**4.1**)

The final step in our synthetic route was the chelation reaction between (*S*)-α-(1-hydroxybutan-2-yl)amino)-α'-(4-methoxyphenyl) dipyrromethene (**4.1**) and (4-fluorophenyl)boronic acid (**2.25**) to access the helically chiral (*S,M*)-*N,N,O,C*-3-(1-hydroxybutan-2-yl)amino)-5-(4-methoxyphenyl) BODIPY (**4.2b**) and (*S,P*)-*N,N,O,C*-3-(1-hydroxybutan-2-yl)amino)-5-(4-methoxyphenyl) BODIPY (**4.2a**) containing a 7-membered ring. We chose (4-fluorophenyl)boronic acid (**2.25**) for the re-chelation reaction as it has been shown an excellent NMR handle, allowing ^{19}F NMR to be used to estimate diastereomeric excess (%*de*) (Scheme **4.5**).

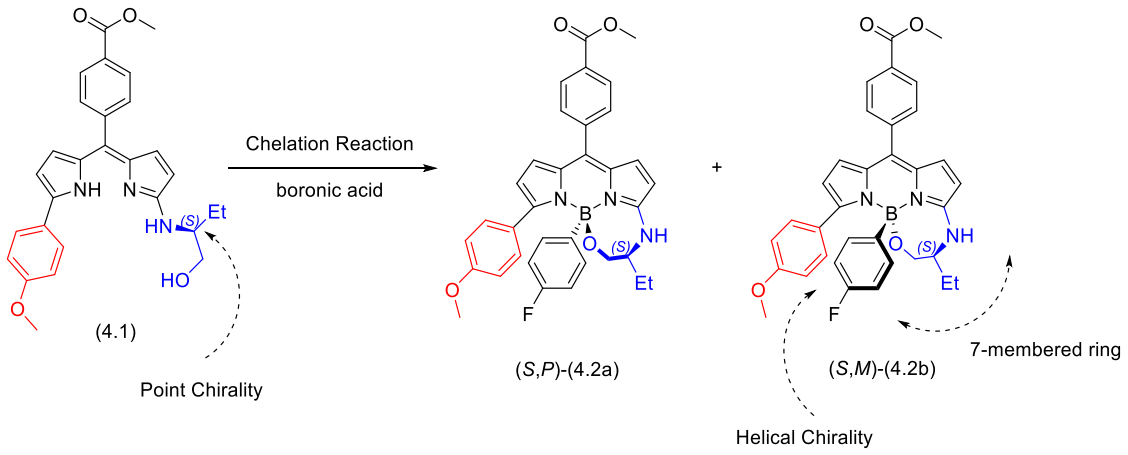

Scheme 4.5: Chelation reaction between (*S*)-α-(1-hydroxybutan-2-yl)amino)-α'-(4-methoxyphenyl) dipyrromethene (**4.1**) and (4-fluorophenyl)boronic acid (**2.25**)

In parallel work, another member in the Hall group performed the primary investigation of the conditions of the chelation reaction to form BODIPYs containing 7-membered rings. Initial work by J. Sample showed that chelation reactions to give 7-membered ring containing BODIPYs did not occur under our previous conditions ($CHCl_3$ at 35 °C) even after long periods of time (Scheme **4.6**).[83] Much higher reaction temperatures and longer times were needed for the chelation to take place.

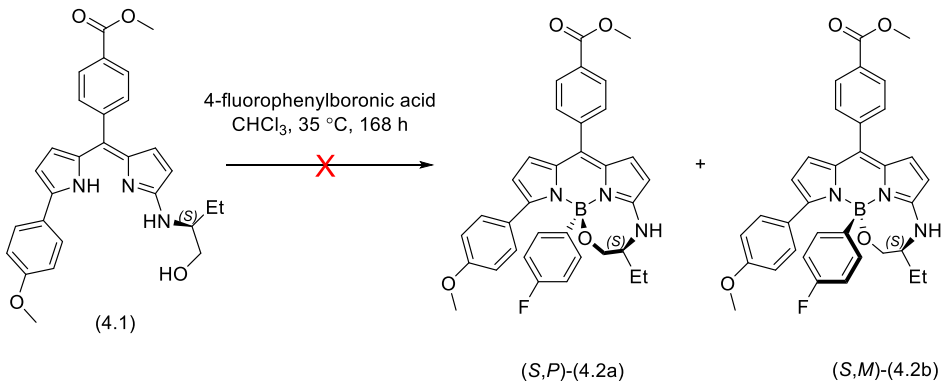

Scheme 4.6: Early attempt at the synthesis of helically chiral (*S,M*)-*N,N,O,C*-3-(1-hydroxybutan-2-yl)amino)-5-(4-methoxyphenyl) BODIPY (**4.2b**) and (*S,P*)-*N,N,O,C*-3-(1-hydroxybutan-2-yl)amino)-5-(4-methoxyphenyl) BODIPY (**4.2a**)

Therefore, we decided to examine the chelation reaction in this system with high boiling point solvents such as toluene and DMSO, allowing higher reaction temperatures and aiming to push the chelation reaction to completion. The reaction between (*S*)-α-(1-hydroxybutan-2-yl)amino)-α'-(4-methoxyphenyl) dipyrromethene (**4.1**) and 1.5 equivalents (4-fluorophenyl)boronic acid (**2.25**)was then carried out in toluene at 110 °C. The reaction was monitored by TLC which showed the formation of multiple new products after 30 hours. The crude reaction mixture was subjected to an aqueous work-up and analysed initially by ^{19}F NMR which showed presence of two signals at -117.8 ppm and -117.9 ppm corresponding to two fluorine environments, indicating that two diastereomers of (*S,P*)-*N,N,O,C*-3-(1-hydroxybutan-2-yl)amino)-5-(4-methoxyphenyl) BODIPY (**4.2a**) containing a 7-membered ring and (*S,M*)-*N,N,O,C*-3-(1-hydroxybutan-2-yl)amino)-5-(4-methoxyphenyl) BODIPY (**4.2b**) containing a 7-membered ring had been formed. Additionally, there were two weak signals at -109.4 ppm and -109.7 ppm, which maybe due to the presence of by-products from the reaction.

The diastereomeric excess (%*de*) was measured by integration of the ^{19}F NMR which showed moderate diastereoselectivity in the reaction (*%de* = 55). This NMR experiment was carried out using a long relaxation time of 30 seconds for more accurate integration of signals (Table **4.3**). The crude reaction mixture was purified by column chromatography to isolate each diastereomer to give 13% of the major diastereomer (**2.4a**) and 7% of minor diastereomer (**2.4b**) (minor) (Table **4.3**, Entry 1). Due to the similar R_f of both compounds, a mixed fraction was also obtained from the column, suggesting that the overall yield was higher than reported. In the second attempt, we reacted (*S*)-α-(1-hydroxybutan-2-yl)amino)-α'-(4-methoxyphenyl) dipyrromethene (**4.1**) and (4-fluorophenyl)boronic acid (**2.25**) in toluene at 110 °C. The reaction was stopped after 18 hours to minimise the formation of side products. Following an aqueous work-up, the diastereomeric excess was measured by the ^{19}F NMR of the crude mixture, which showed a low *de* of 22%. Purification by column chromatography to

isolate each diastereomer, gave 38% of (**4.2a**) (major) and 37% of (**4.2b**)(minor) (Table **4.3**, Entry 2), giving a *de* of 2% based on the isolated yield. We postulated that the differences in observed *de* are likely to arise due to losses during purification (Figure **4.2**).

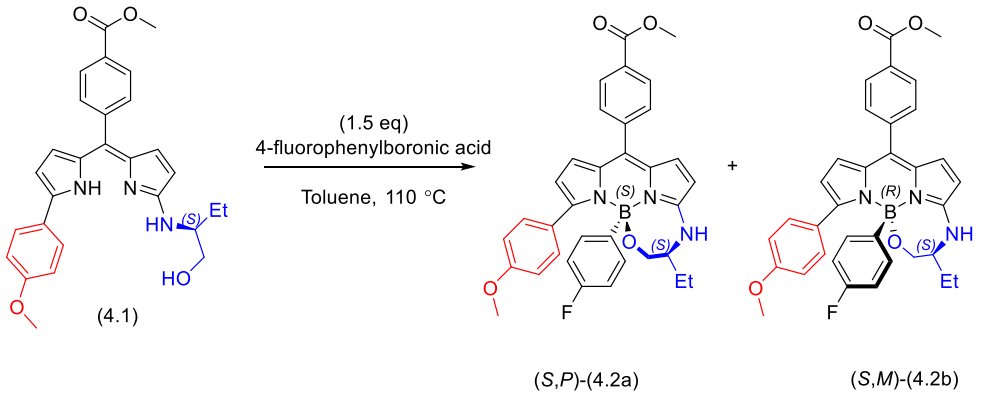

Entry	Reaction Time/h	*de* ^{19}F NMR/% [a]	*de* after purification/%[b]	Major Yield/%	Minor Yield/%	Yield/%[c]
1	30	55	30	13	7	20
2	18	22	2	38	37	75

Table 4.3: Synthesis of helically chiral (*S,P*)-*N,N,O,C*-3-(1-hydroxybutan-2-yl)amino)-5-(4-methoxyphenyl) BODIPY (**4.2a**) and (*S,M*)-*N,N,O,C*-3-(1-hydroxybutan-2-yl)amino)-5-(4-methoxyphenyl) BODIPY (**4.2b**); [a] *de* of the helically chiral (*S,P*),(*S,M*)-*N,N,O,C*-3-(1-hydroxybutan-2-yl)amino)-5-(4-methoxyphenyl) BODIPY before purification, measured by ^{19}F NMR; [b] *de* after purification measured by isolated yields, [c] Isolated combined yields following column chromatography.

The structures of the two diastereomers, (**4.2a**)(major) and (**4.2b**)(minor) were confirmed by ^{1}H NMR spectra. The major isomer showed two signals at 6.70 ppm (dd, J = 8.7, 8.7 Hz, 2H) and 6.64 ppm (dd, J = 8.7, 6.5 Hz, 2H) corresponding to the newly added 4-fluorophenyl ring including both H-H and H-F coupling, while the minor isomer showed corresponding signals at 6.66 ppm (dd, J = 8.8, 8.7 Hz, 2H), and 6.47 ppm (dd, J = 8.6, 6.3 Hz, 2H).

Furthermore, the structure of the major diastereomer (**4.2a**) was confirmed by the ^{13}C NMR spectrum, which showed three doublet signals with different coupling constant values corresponding to newly added 4-fluorophenyl ring (Figure **4.3**). Firstly, a doublet at 161.9 ppm with a large coupling constant ($^{1}J_{C\text{-}F}$ = 242.4 Hz) corresponding to C-28 indicated that fluorine is directly bonded to the carbon atom. Secondly, a doublet at 113.8 ppm ($^{2}J_{C\text{-}F}$ = 19.1 Hz) corresponding to C-27, indicating a two-bond separation. Lastly, a doublet at 132.5 ppm with a small coupling constant ($^{3}J_{C\text{-}F}$ = 6.8 Hz) was observed, suggesting a three-bond distance from the fluorine atom (C-26).

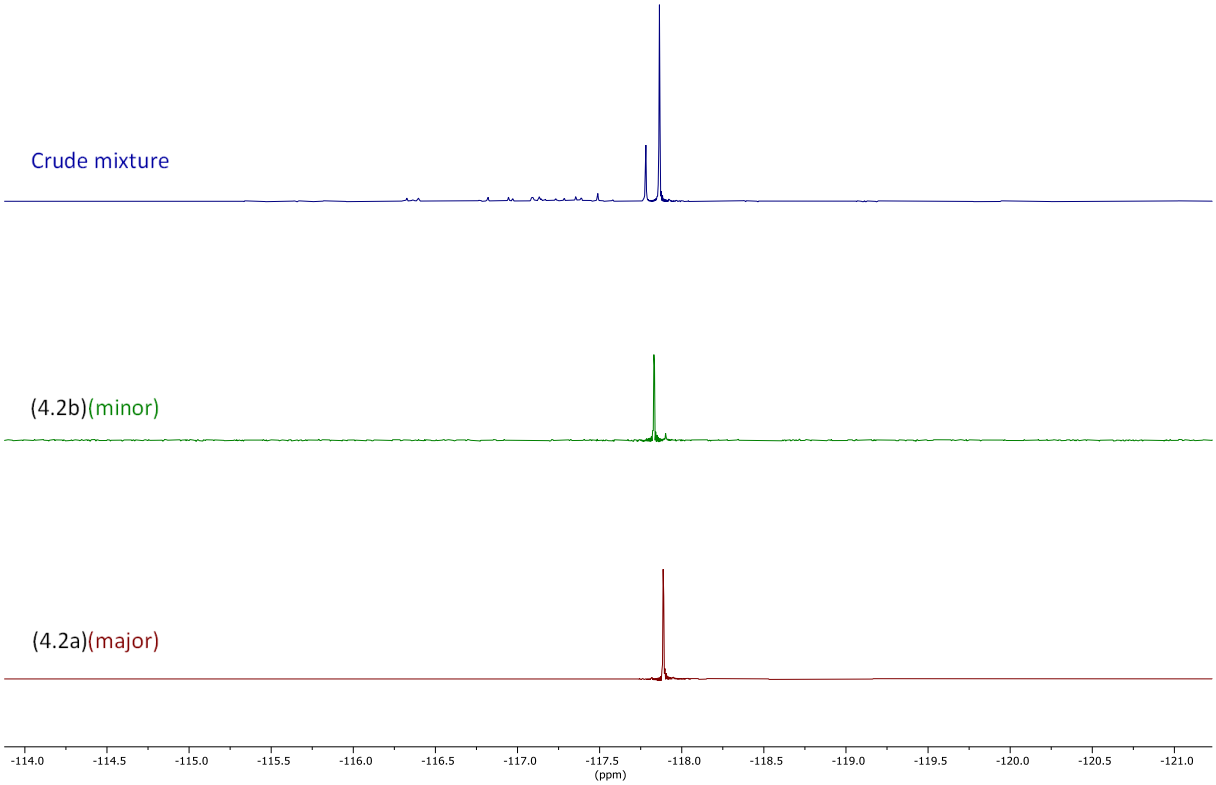

Figure 4.2: ^{19}F NMR spectrum (282 MHz, $CDCl_3$) of the (*S,P*)-*N,N,O,C*-3-(1-hydroxybutan-2-yl)amino)-5-(4-methoxyphenyl) BODIPY (**4.2a**) and (*S,M*)-*N,N,O,C*-3-(1-hydroxybutan-2-yl)amino)-5-(4-methoxyphenyl) BODIPY (**4.2b**). Top: ^{19}F NMR of the crude reaction mixture (*S,P*),(*S,M*)-*N,N,O,C*-3-(1-hydroxybutan-2-yl)amino)-5-(4-methoxyphenyl) BODIPY (blue), Middle: ^{19}F NMR of the minor isomer (green) following column chromatography , Bottom: ^{19}F NMR of the major isomer (red) following column chromatography

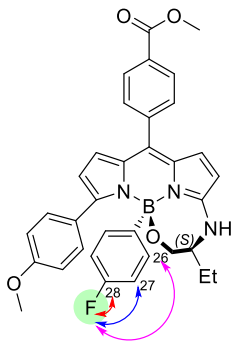

(S,P)-(4.2a)

C	δ_C/ppm	*J* value/ Hz
26	132.5	d, $^3J_{C\text{-}F}$ = 6.8
27	113.8	d, $^2J_{C\text{-}F}$ = 19.1
28	161.9	d, $^1J_{C\text{-}F}$ = 242.4

Figure 4.3: C-F Coupling constants in the ^{13}C NMR spectrum of (*S,P*)-*N,N,O,C*-3-(1-hydroxybutan-2-yl)amino)-5-(4-methoxyphenyl) BODIPY (**4.2a**) (major)

For further confirmation, the structures of diastereomers (**4.2a**) (major) and (**4.2b**) (minor) were validated by HRMS, showing 576.2477 and 576.2482 *m/z* values respectively, which are consistent with a formula of the $[M+H]^+$ ion for both, $C_{34}H_{32}{}^{11}BFN_3O_4$.

4.2.1.5 Absolute and Relative Stereochemistry of Helically Chiral (*S,P*)-*N,N,O,C*-3-(1-hydroxybutan-2-yl)amino)-5-(4-methoxyphenyl) BODIPY (**4.2a**) and (*S,M*)-*N,N,O,C*-3-(1-hydroxybutan-2-yl)amino)-5-(4-methoxyphenyl) BODIPY (**4.2b**)

To determine the absolute and relative stereochemistry of both diastereomers (**4.2a**) (major) and (**4.2b**)(minor), various crystallisation methods were attempted to grow crystals suitable for SCXRD. This included slow evaporation from a range of solvents (DCM, $CHCl_3$, methanol (note poor solubility), ethanol, toluene, MeCN, acetone, and DMF), layered liquid-liquid diffusion (DCM : hexane; DCM : diethyl ether; $CHCl_3$: petroleum ether; and acetone : petroleum ether), and vapour-vapour diffusion (DCM : hexane; and $CHCl_3$: petroleum ether). Unfortunately, all attempts at crystallisation through these methods were unsuccessful. Therefore, we used ECD, to assign of the absolute stereochemistry of the helical centre.

4.3 ECD Spectroscopy of Helically Chiral (*S,P*)-*N,N,O,C*-3-(1-hydroxybutan-2-yl)amino)-5-(4-methoxyphenyl) BODIPY (4.2a) and (*S,M*)-*N,N,O,C*-3-(1-hydroxybutan-2-yl)amino)-5-(4-methoxyphenyl) BODIPY (4.2b)

Next, we planned to measure the ECD spectra of the two diastereomeric (*S,P*)-*N,N,O,C*-3-(1-hydroxybutan-2-yl)amino)-5-(4-methoxyphenyl) BODIPY (**4.2a**) and (*S,M*)-*N,N,O,C*-3-(1-hydroxybutan-2-yl)amino)-5-(4-methoxyphenyl) BODIPY (**4.2b**) to examine the chirality at the boron centre and determine their absolute stereochemistry by comparison of experimental measurements with the calculated ECD spectra. The following ECD measurements were conducted using the compounds prepared by another member in the Hall group (M. Cracknell).[84]

Thus, ECD spectra for both diastereomers (*S,P*)-*N,N,O,C*-3-(1-hydroxybutan-2-yl)amino)-5-(4-methoxyphenyl) BODIPY (**4.2a**) and (*S,M*)-*N,N,O,C*-3-(1-hydroxybutan-2-yl)amino)-5-(4-methoxyphenyl) BODIPY (**4.2b**) were measured in DCM by Dr Jonathan Bogaerts. Interestingly, (*S,P*)-*N,N,O,C*-3-(1-hydroxybutan-2-yl)amino)-5-(4-methoxyphenyl) BODIPY (**4.2a**) and (*S,M*)-*N,N,O,C*-3-(1-hydroxybutan-2-yl)amino)-5-(4-methoxyphenyl) BODIPY (**4.2b**) showed almost mirror image spectra of each other. (*S,P*)-*N,N,O,C*-3-(1-Hydroxybutan-2-yl)amino)-5-(4-methoxyphenyl) BODIPY (**4.2a**) (major) showed a positive Cotton effect for the BODIPY S_0-S_1 transition at 531 nm, while (*S,M*)-*N,N,O,C*-3-(1-hydroxybutan-2-yl)amino)-5-(4-methoxyphenyl) BODIPY (**4.2b**) (minor) showed a negative Cotton effect at the same wavelength (**4.4**).

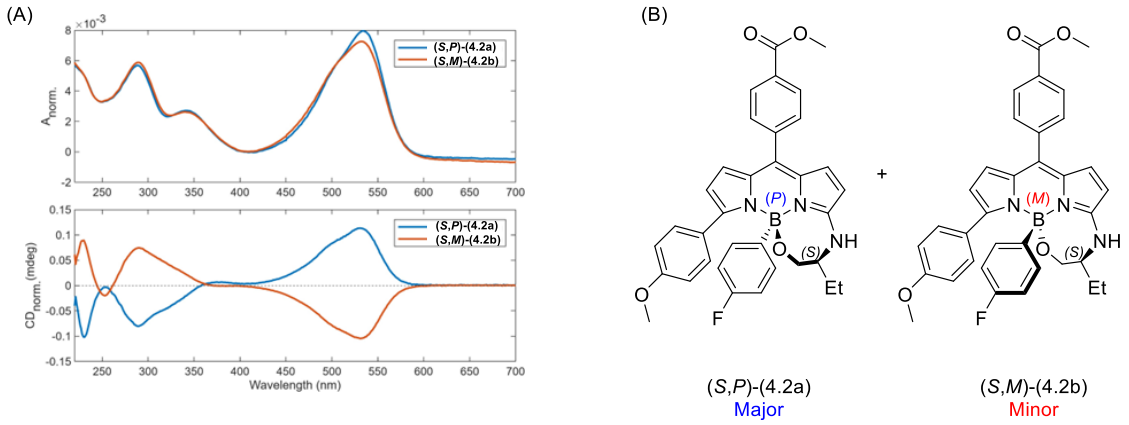

Figure 4.4: (A) Experimental ECD spectra in DCM; Top: UV-Vis (*S,P*)-*N,N,O,C*-3-(1-hydroxybutan-2-yl)amino)-5-(4-methoxyphenyl) BODIPY (**4.2a**) (blue) and (*S,M*)-*N,N,O,C*-3-(1-hydroxybutan-2-yl)amino)-5-(4-methoxyphenyl) BODIPY (**4.2b**) (red); Bottom: normalised ECD spectra of (*S,P*)-*N,N,O,C*-3-(1-hydroxybutan-2-yl)amino)-5-(4-methoxyphenyl) BODIPY (**4.2a**) (blue), and (*S,M*)-*N,N,O,C*-3-(1-hydroxybutan-2-yl)amino)-5-(4-methoxyphenyl) BODIPY (**4.2b**)(red); (B) The structure of (*S,P*)-*N,N,O,C*-3-(1-hydroxybutan-2-yl)amino)-5-(4-methoxyphenyl) BODIPY (**4.2a**) and (*S,M*)-*N,N,O,C*-3-(1-hydroxybutan-2-yl)amino)-5-(4-methoxyphenyl) BODIPY (**4.2b**) (Figure **4.4** was created by Dr Jonathan Bogaerts.

4.3.1 Calculated ECD Spectra of Helically Chiral (*S,P*)-*N,N,O,C*-3-(1-hydroxybutan-2-yl)amino)-5-(4-methoxyphenyl) BODIPY (**4.2a**) and (*S,M*)-*N,N,O,C*-3-(1-hydroxybutan-2-yl)amino)-5-(4-methoxyphenyl) BODIPY (**4.2b**)

ECD spectra were calculated for the two diastereomers, (*S,P*)-*N,N,O,C*-3-(1-hydroxybutan-2-yl)amino)-5-(4-methoxyphenyl) BODIPY (**4.2a**) and (*S,M*)-*N,N,O,C*-3-(1-hydroxybutan-2-yl)amino)-5-(4-methoxyphenyl) BODIPY (**4.2b**), by Dr Jonathan Bogaerts. Firstly, low-energy conformations were generated and optimised by DFT. Note that in this case molecular mechanics (MM) failed to provide a suitable set of low-energy conformations. Secondly, the computation of individual ECD spectra for each of these low-energy conformations was performed. It should be noted that the calculations were based on the 'R' configuration of the amino alcohol, and to align the results with the 'S' configuration used in experiment, the calculated ECD spectra was inverted. Additionally, to better match the calculated ECD spectra with the experimental data, a red shift of approximately 30 nm was applied to the calculated ECD when plotting the spectrum.

By comparison of the calculated ECD spectra and the experimental ECD spectra, we were able to assign the relative and absolute stereochemistry of each diastereomer as (*S,P*)-*N,N,O,C*-3-(1-hydroxybutan-

2-yl)amino)-5-(4-methoxyphenyl) BODIPY (**4.2a**) and (*S,M*)-*N,N,O,C*-3-(1-hydroxybutan-2-yl)amino)-5-(4-methoxyphenyl) BODIPY (**4.2b**)(Figure **4.5**).

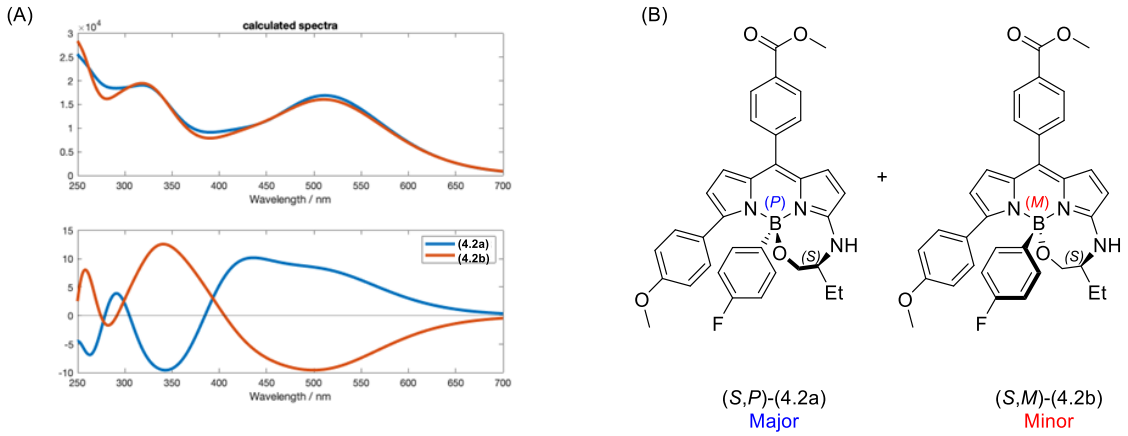

Figure 4.5: (A) Calculated Boltzmann-weighted ECD; Top: UV-Vis spectra of (*S,P*)-*N,N,O,C*-3-(1-hydroxybutan-2-yl)amino)-5-(4-methoxyphenyl) BODIPY (**4.2a**) (blue) and (*S,M*)-*N,N,O,C*-3-(1-hydroxybutan-2-yl)amino)-5-(4-methoxyphenyl) BODIPY (**4.2b**)(red); Bottom: (*S,P*)-*N,N,O,C*-3-(1-hydroxybutan-2-yl)amino)-5-(4-methoxyphenyl) BODIPY (**4.2a**) (blue), and (*S,M*)-*N,N,O,C*-3-(1-hydroxybutan-2-yl)amino)-5-(4-methoxyphenyl) BODIPY (**4.2b**)(red); (B) The structure of (*S,P*)-*N,N,O,C*-3-(1-hydroxybutan-2-yl)amino)-5-(4-methoxyphenyl) BODIPY (**4.2a**) and (*S,M*)-*N,N,O,C*-3-(1-hydroxybutan-2-yl)amino)-5-(4-methoxyphenyl) BODIPY (**4.2b**) (Figure **4.5** was created by Dr Jonathan Bogaerts).

From both the experimental and calculated ECD spectra, we observed that the "empirical rule" holds true for these two diastereomeric compounds. Helically chiral (*S,P*)-*N,N,O,C*-3-(1-hydroxybutan-2-yl)amino)-5-(4-methoxyphenyl) BODIPY (**4.2a**) showed a positive Cotton effect for the BODIPY S_0-S_1 transition, while helically chiral (*S,M*)-*N,N,O,C*-3-(1-hydroxybutan-2-yl)amino)-5-(4-methoxyphenyl) BODIPY (**4.2b**) showed a negative Cotton effect for the BODIPY S_0-S_1 transition at the same wavelength. Interestingly, this was consistent with the trends observed in the ECD spectra of our previous examples of helically chiral *N,N,O,C*-BODIPYs based on 6-membered ring systems.

Following the assignment of stereochemistry by ECD for the 7-membered ring systems, it should be noted that we have observed a reversal in stereoselectivity in the chelation reaction in comparision with the 6-membered ring systems. The 6-membered ring systems (in chapter 3) gave (*S,M*)- as the major diastereoisomer and (*S,P*)- as the minor, whilst in the in 7-membered ring systems (*S,P*)- is the major diastereomer formed and (*S,M*)- the minor.

4.4 Solvent Effects on the Diastereoselectivity of Formation of Helically Chiral (*S,P*)-*N,N,O,C*-3-(1-hydroxybutan-2-yl)amino)-5-(4-methoxyphenyl) BODIPY (4.2a) and (*S,M*)-*N,N,O,C*-3-(1-hydroxybutan-2-yl)amino)-5-(4-methoxyphenyl) BODIPY (4.2b)

We next planned to examine the chelation reactions in an alternative solvent, namely the high boiling aprotic polar solvent DMSO, to see if we could achieve a rate acceleration. Thus, under our previous chelation conditions, we reacted (*S*)-α-(1-hydroxybutan-2-yl)amino)-α'-(4-methoxyphenyl) dipyrromethene (**4.1**) with 1.5 equivalents of (4-fluorophenyl)boronic acid (**2.25**) in DMSO at 110 °C. The reaction was stopped after 30 hours, to allow us to compare it with the previous reactions in toluene (Table **4.4**). The reaction mixture was subjected to an aqueous work-up and analysed by ^{19}F NMR which showed the presence of two signals at -117.8 ppm and -117.9 ppm, confirming that the two diastereomers had been formed. Interestingly, in the ^{19}F NMR analysis we observed an inversion of preferred diastereomer, where now (*S,P*)-*N,N,O,C*-3-(1-hydroxybutan-2-yl)amino)-5-(4-methoxyphenyl) BODIPY (**4.2a**) appeared as the minor product and (*S,M*)-*N,N,O,C*-3-(1-hydroxybutan-2-yl)amino)-5-(4-methoxyphenyl) BODIPY (**4.2b**) as the major product. However, the chelation reaction in DMSO produced lower yields with very small quantities observed by ^{1}H NMR. This interesting effect of the polar solvent on the diastereocontrol at the boron centre will be the subject of follow-up studies (Figure **4.6**).

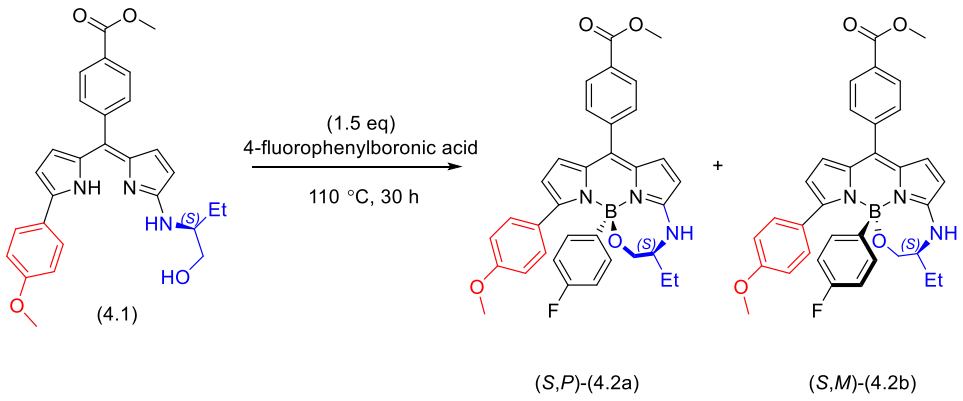

Entry	Solvent	*de* ^{19}F NMR/%	Major product
1[a]	Toluene	55	(4.2a)
2	DMSO	68[b]	(4.2b)

Table 4.4: Synthesis of helically chiral (*S,P*)-*N,N,O,C*-3-(1-hydroxybutan-2-yl)amino)-5-(4-methoxyphenyl) BODIPY (**4.2a**) and (*S,M*)-*N,N,O,C*-3-(1-hydroxybutan-2-yl)amino)-5-(4-methoxyphenyl) BODIPY (**4.2b**) in different solvents; [a] Previously discussed result, included for comparison; [b] Note that major/minor product ratios are inverted in comparison to experiment in toluene.

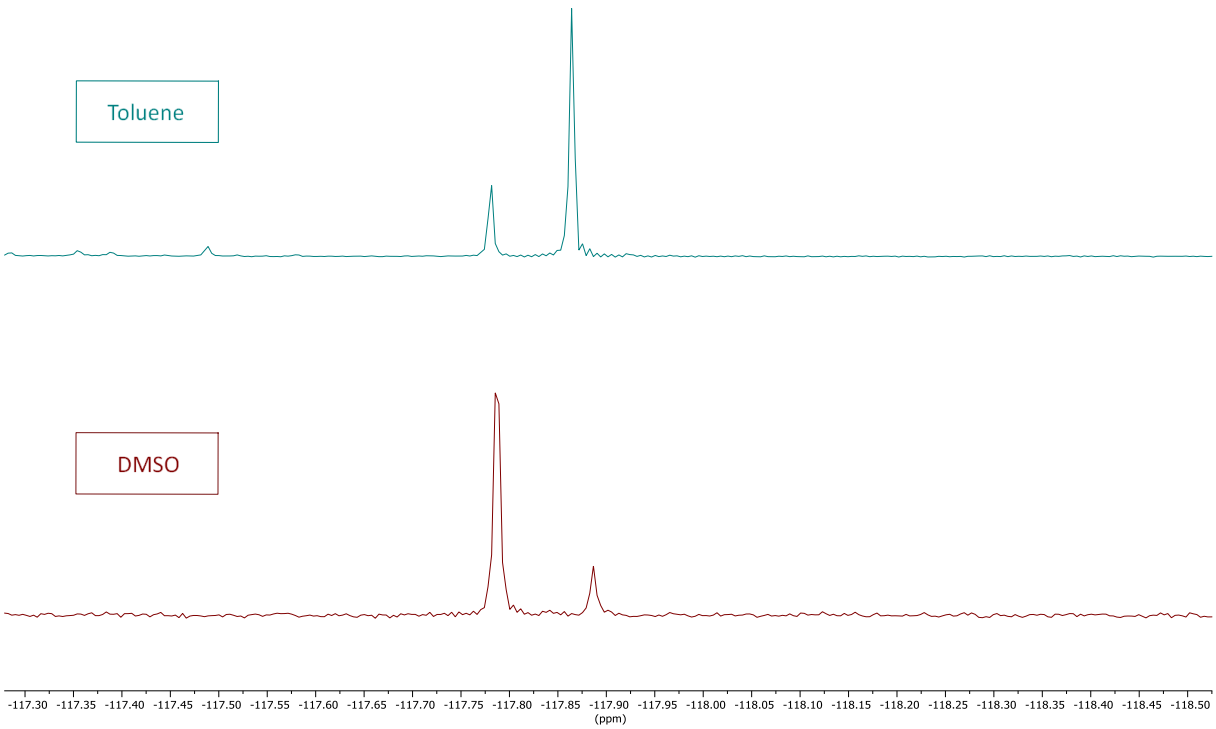

Figure 4.6: ^{19}F NMR spectrum (282 MHz, $CDCl_3$) of the (*S,P*),(*S,M*)-*N,N,O,C*-3-(1-hydroxybutan-2-yl)amino)-5-(4-methoxyphenyl) BODIPYs (**4.2a** and **4.2b**). Top: ^{19}F NMR of the crude reaction mixture (*S,P*),(*S,M*)-*N,N,O,C*-3-(1-hydroxybutan-2-yl)amino)-5-(4-methoxyphenyl) BODIPYs(**4.2a** and **4.2b**), the reaction undertaken in toluene (green); Bottom: ^{19}F NMR of the crude reaction mixture (*S,P*),(*S,M*)-*N,N,O,C*-3-(1-hydroxybutan-2-yl)amino)-5-(4-methoxyphenyl) BODIPYs (**4.2a** and **4.2b**), the reaction undertaken in DMSO (red)

4.5 Conclusions

We have successfully synthesized helically chiral (*S,P*)-*N,N,O,C*-3-(1-hydroxybutan-2-yl)amino)-5-(4-methoxyphenyl) BODIPY (**4.2a**) and (*S,M*)-*N,N,O,C*-3-(1-hydroxybutan-2-yl)amino)-5-(4-methoxyphenyl) BODIPY (**4.2b**) both containing a 7-membered ring, though a chelation reaction in both toluene and DMSO.

Unfortunately, we were unable to obtain single crystals of both diastereomeric helically chiral BODIPYs (**4.2a**) and (**4.2b**) to determine their relative and absolute stereochemistry, but we were able to assign relative and absolute stereochemistry be comparison of the experimental and calculated ECD spectra.

Interestingly, in this chelation reaction we observed that a different diastereomer was preferentially formed depending on the solvent, with helically chiral (*S,P*)-*N,N,O,C*-3-(1-hydroxybutan-2-yl)amino)-

5-(4-methoxyphenyl) BODIPY (**4.2a**) being the major product in toluene, whilst it was the minor product in DMSO.

In the future, we would wish to examine the boron chelation reaction with different solvents, to study the effect of solvent polarity on the diastereoselectivity of the reaction.

4.6 Synthesis of Helically Chiral BODIPY Containing Double 7-Membered Rings

The second aim of this chapter was the synthesis of helically chiral *N,N,O,C*-BODIPYs containing double 7-membered rings. We planned to synthesise these molecules from 3,5-dihalo-BODIPYs, via a double S_NAr chemistry to introduce two amino alcohol groups at both the 3- and 5-positions, followed by a de-chelation reaction to remove the BF_2 group, and finally a chelation reaction to induce the chirality in the boron centre (Scheme **4.7**).

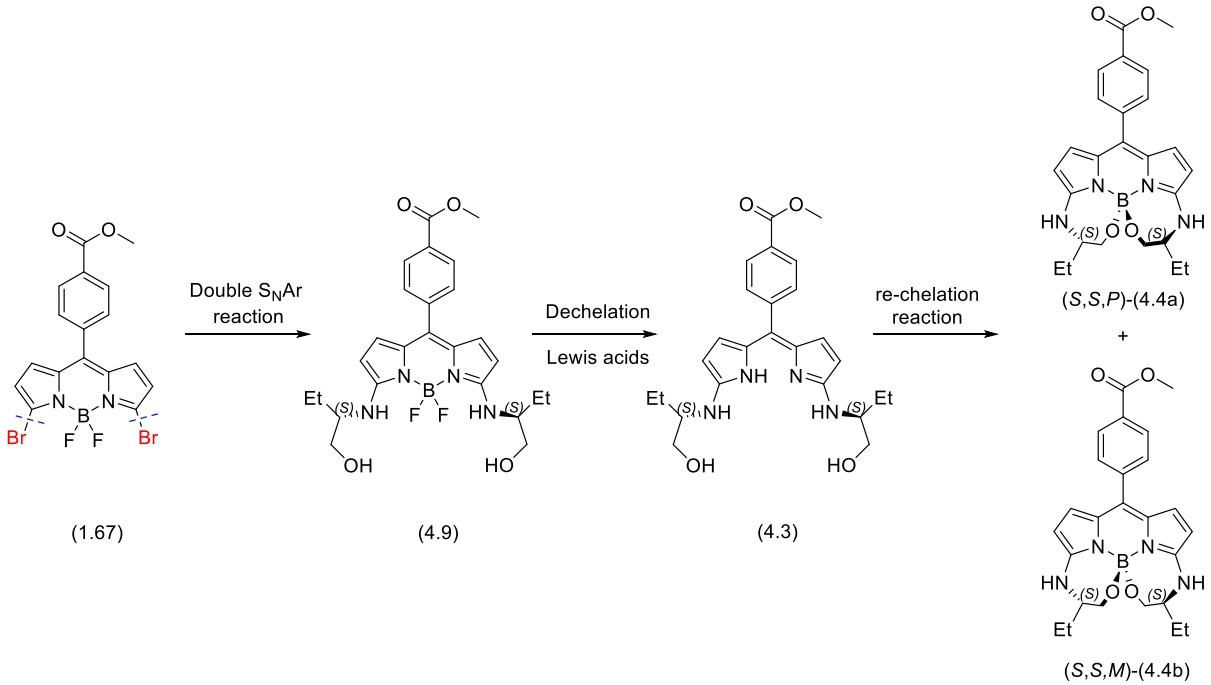

Scheme 4.7: Planned route to helically chiral *N,N,O,O*-BODIPYs containing double 7-membered rings, involving a point-to-helical chirality transfer.

4.6.1 Double S_NAr Reactions on 3,5-Dihalo BODIPYs from the Literature

Double S_NAr chemistry in the BODIPYs is known in the literature. Previous studies have highlighted S_NAr chemistry at the 3- and 5-positions of dichloro- and dibromo-BODIPYs. Among these, the 3,5-dichloro BODIPYs have proven to be good candidates for double S_NAr reactions with nitrogen nucleophiles, whilst the double S_NAr reactions with 3,5-dibromo BODIPYs is likely more challenging.[85] Next, we will explore selected examples of S_NAr chemistry with 3,5-dihalo-BODIPYs and different amine nucleophiles, including aromatics, aliphatics and chiral systems.

In 2005, the Dehaen group reported the synthesis of mono substituted BODIPYs via an S_NAr reaction. They reacted 3,5-dichloro BODIPY (**1.69**) with 2 equivalents of aniline as a nucleophile in MeCN, without an additional base, at room temperature for 30 minutes to form mono substituted BODIPY (**1.71**) in moderate yields. To synthesise disubstituted BODIPYs, they reacted 3,5-dichloro BODIPY (**1.69**) with an excess amount of aniline (4 eq.) in MeCN, increasing the temperature to reflux, and extending the reaction time to 8 hours (Scheme **4.8**). This demonstrates that double S_NAr reactions for 3,5-dichloro BODIPYs are possible, although more challenging in comparison to mono S_NAr reactions (example discussed in Chapter 1).

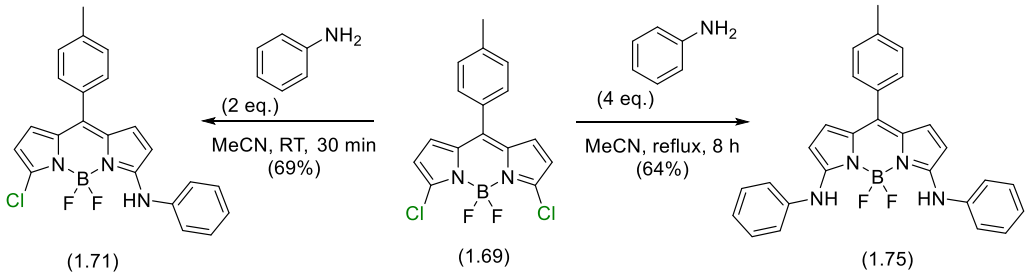

Scheme 4.8: Synthesis of mono and disubstituted BODIPYs from 3,5-dichloroBODIPY (**1.69**)

Tiwari's group reported conditions for synthesising disubstituted BODIPYs, containing aliphatic amine groups at the 3,5-positions, as fluorescent probes for protein surface-hydrophobicity.[86] Their procedure used the nucleophile 2-methoxyethylamine as the solvent in large excess, and the reaction carried out with 3,5-dichloro BODIPY (**4.10**) at reflux overnight. Even under these forcing conditions the yields for the double S_NAr reactions were approximately 50% (Scheme **4.9**).

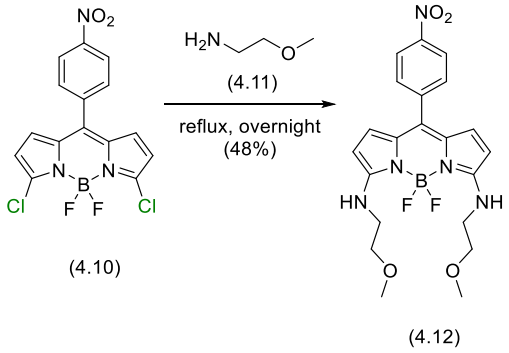

Scheme 4.9: S_NAr reaction of 3,5-dichloro BODIPY (**4.10**) with aliphatic amine nucleophile

In additional studies on double S_NAr reactions involving BODIPYs, Jiao's group have explored the potential for double S_NAr reactions on 2,3,5,6-tetrabromo-BODIPYs.[87] In their attempt, they reacted 2,3,5,6-tetrabromo-BODIPY (**4.13**) with 60 equivalents of aniline in 1,2-dichloroethane in presence of two equivalents of K_2CO_3, at 80 °C for 12 hours, to give good yields of the 3,5-disubsituted product.

Interestingly, the S_NAr reaction occurred preferentially at the 3,5-positions over the 2,6-positions (Scheme **4.10**).

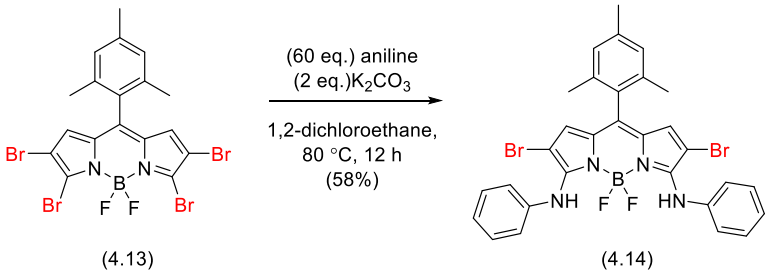

Scheme 4.10: S_NAr reaction of tetrabromo-BODIPY (**4.13**) with aniline

In 2020, Knight's group examined the S_NAr reactions of 3,5-dibromo BODIPYs. They showed that the reaction of 3,5-dibromo BODIPY (**4.15**) and 2 equivalents of (*S*)-1-phenylethan-1-amine (**4.16**) in MeCN at room temperature gave only the corresponding mono substituted-BODIPY (**4.17**), with no double S_NAr observed under these conditions. The strongly electron-donating amino substituent in mono substitution product deactivating the BODIPY to further nucleophilic attack. This highlights the complexity of achieving double substituted 3,5-BODIPYs via S_NAr chemistry and emphasises the need for innovative approaches for their synthesis (Scheme **4.11**).

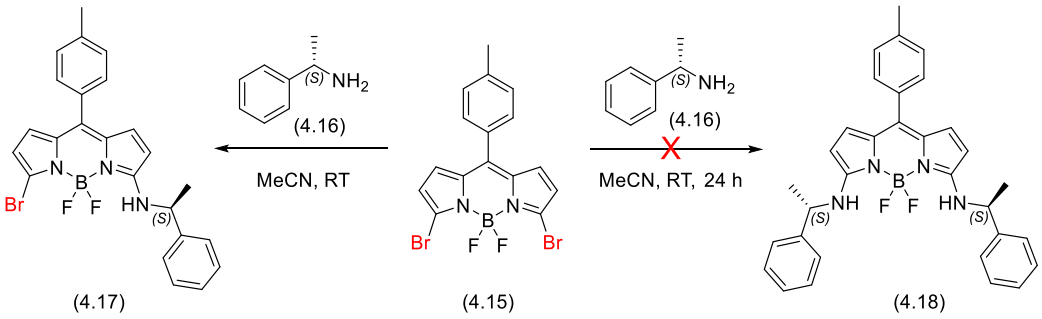

Scheme 4.11: S_NAr reaction of 3,5-dibromo BODIPY (**4.15**) with (*S*)-1-phenylethan-1-amine

4.6.2 Attempts to Synthesise Disubstituted Chiral BODIPY (**4.9**)

Next, we will examine our approach to double S_NAr chemistry of the BODIPYs, using the previously prepared 3,5-dibromo BODIPY (**1.67**) as a starting material and (*S*)-2-aminobutan-1-ol (**3.8**) as the nucleophile (see Chapter 2). Our aim was to discover possible optimal conditions for the synthesis of 3,5-disubstituted BODIPYs containing two chiral amino alcohols (Scheme **4.12**).

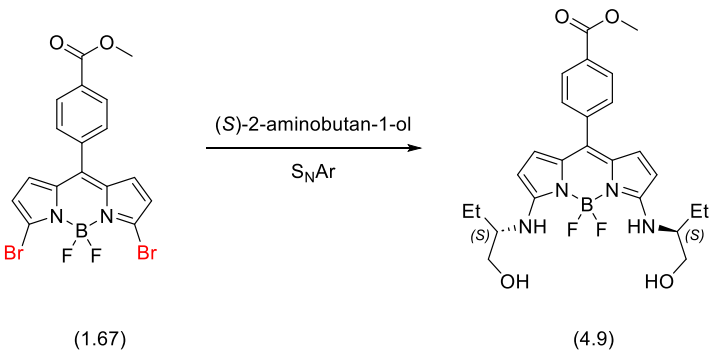

Scheme 4.12: Planned synthesis of (*S*)-3,5-di((1-hydroxybutan-2-yl)amino)-BODIPY (**4.9**)

In our initial attempts, we reacted one equivalent of 3,5-dibromo BODIPY (**1.67**), four equivalents of (*S*)-2-aminobutan-1-ol (**3.8**) and 2.2 equivalents of Et_3N in MeCN at room temperature for 24 hours. The reaction mixture was subjected to aqueous work-up and analysed by ^1H NMR spectrum which showed the formation of a mono-substituted BODIPY, with no sign of di-substitution occurring. The crude reaction mixture was purified by column chromatography to give (*S*)-3-(1-hydroxybutan-2-yl)amino)-5-bromo BODIPY (**3.1**) in quantitative yield, with spectral data matching that previously reported. In particular evidence for mono-substitution in the ^1H NMR included the appearance of a broad doublet for the NH group at 6.39 ppm (d, *J* = 9.6 Hz, 1H), and the desymmetrisation of the pyrrolic protons at 6.81 ppm (d, *J* = 5.1 Hz, 1H), 6.30 ppm (d, *J* = 5.5 Hz, 1H), 6.28 ppm (d, *J* = 3.9 Hz, 1H), and 6.23 ppm (d, *J* = 3.9 Hz, 1H)(Table **4.5**, Entry 2).

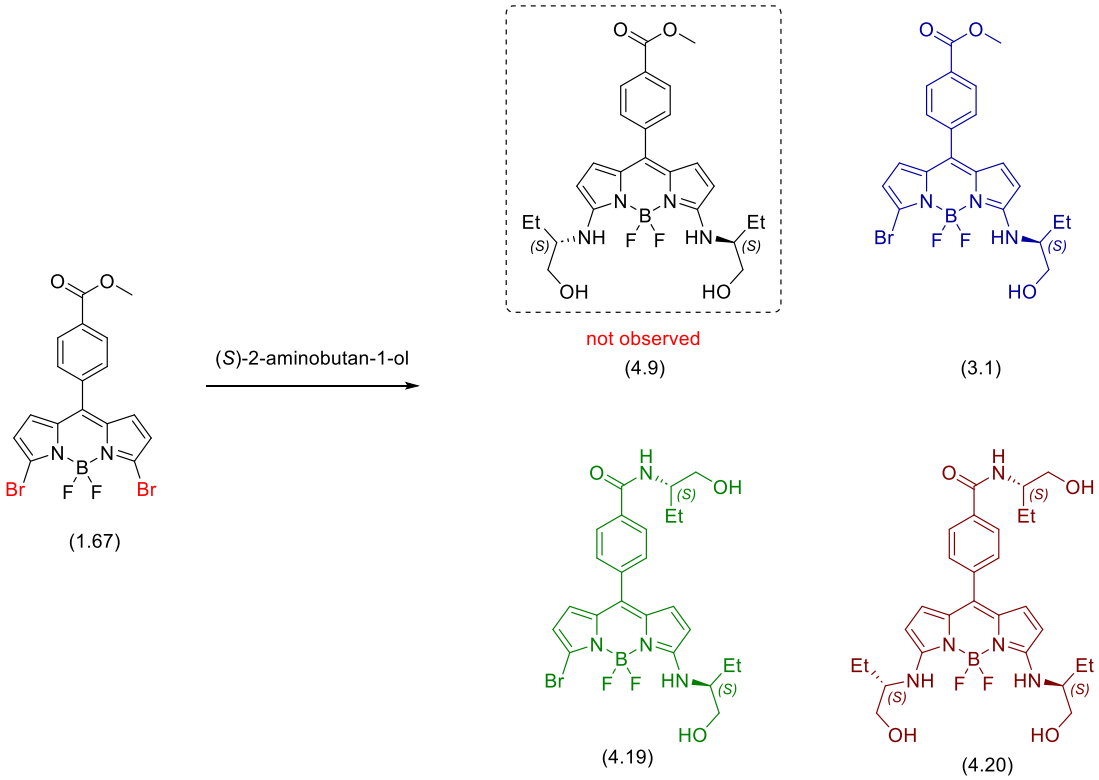

Entry	Solvent	Eq. of alcohol	Temp and time	Base	Yield[c]/%	Reaction Outcome
1[a]	MeCN	2	25 °C 4 h	Et_3N	Quant.	mono-BODIPY (**3.1**)
2	MeCN	4	25 °C 24 h	Et_3N	Quant.	mono-BODIPY (**3.1**)
3	MeCN	4	reflux 24 h	Et_3N	-	mono-BODIPY (**3.1**)[b]
4	Toluene	4	reflux 48 h	Et_3N	-	Major product mono-BODIPY (**3.1**)[b]
5	Toluene	60	reflux 15 d	Et_3N	-	Complex mixture[b]
6	1,2-dichloroethane	60	reflux 6 d	K_2CO_3	-	Major product mono-BODIPY (**3.1**)[b]
7	(*S*)-2-aminobutan-1-ol	-	RT for 48 h, then 140 °C for 30 min	-	Trace	BODIPY (**4.19**)
8	(*S*)-2-aminobutan-1-ol	-	140°C 5 h	-	9%	Triple BODIPY (**4.20**)

Table 4.5: Attempts to prepare (*S*)-3,5-di((1-hydroxybutan-2-yl)amino)-BODIPY (**4.9**), [a] Previously discussed result in Chapter 3, included for comparison, [b] Analysis by NMR only, [c] Isolated yield following column chromatography.

In the second attempt, the S_NAr reaction was repeated with the same equivalents in MeCN for 24 h, but with an increased the reaction temperature (reflux). The crude reaction mixture was subjected to aqueous work-up and inspection of the crude ^1H NMR spectrum showed the formation of only the mono substituted product, (*S*)-3-(1-hydroxybutan-2-yl)amino)-5-bromo BODIPY (**3.1**) (Table **4.5**, Entry 3).

Next, we decided to examine the double S_NAr reaction in high boiling point solvent, toluene, to attempt to push the reaction to form the desired (*S*)-3-(1-hydroxybutan-2-yl)amino)-5-bromo BODIPY (**3.1**). Thus, we reacted one equivalent of 3,5-dibromo BODIPY (**1.67**), four equivalents of (*S*)-2-aminobutan-1-ol (**3.8**) and 2.2 equivalents of Et_3N in toluene under reflux for 48 hours. The crude

reaction mixture was subjected to aqueous work-up and ^{1}H NMR showed the presence of two BODIPY compounds, the major product being (*S*)-3-(1-hydroxybutan-2-yl)amino)-5-bromo BODIPY (**3.1**), and a trace minor component that was not identified (Table **4.5**, Entry 4). We next repeated the S_NAr reaction between 3,5-dibromo BODIPY (**1.67**) and a large excess of (*S*)-2-aminobutan-1-ol (**3.8**) (60 equivalents), with 2.2 equivalents of Et_3N, in toluene under reflux for 15 days. An aqueous work-up was performed, but the ^{1}H NMR showed a highly complex mixture in which no specific products could be identified (Table **4.5**, Entry 5).

We also examined an alternative solvent, 1,2-dichloroethane, and an inorganic base, K_2CO_3 for the S_NAr reaction. We therefore reacted one equivalent of 3,5-dibromo BODIPY (**1.67**), with 60 equivalents of (*S*)-2-aminobutan-1-ol (**3.8**) and 2 equivalents of K_2CO_3 in 1,2-dichloroethane under reflux for 6 days. The crude reaction mixture was subjected to an aqueous work-up, and analysis by ^{1}H NMR showed the formation of only (*S*)-3-(1-hydroxybutan-2-yl)amino)-5-bromo BODIPY (**3.1**) (Table **4.5**, Entry 6). It should be noted that ^{1}H NMR of the crude showed small shift differences, mainly in the pyrrolic protons, however other analysis (*e.g.* ^{11}B NMR and ^{19}F NMR) matched the previously analysed material. We suspect that the observed differences were due to residual reaction solvent in the crude sample.

Finally, we decided to examine increasingly forcing conditions for the S_NAr reaction. Thus, we reacted 3,5-dibromo BODIPY (**1.67**) with (*S*)-2-aminobutan-1-ol (**3.8**) as the solvent at room temperature. The reaction progress was monitored by TLC which showed that the starting material had been consumed and (*S*)-3-(1-hydroxybutan-2-yl)amino)-5-bromo BODIPY (**3.1**) had been formed after 1 h. After a further 47 hours, TLC had not changed and (*S*)-3-(1-hydroxybutan-2-yl)amino)-5-bromo BODIPY (**3.1**) was still present. Therefore, the reaction temperature was increased to 140 °C, with monitoring by TLC which showed the formation of a new product after 30 min. The reaction mixture was then allowed to cool at room temperature and subjected to an aqueous work-up. Interestingly, the initial analysis of ^{1}H NMR showed that the presence of a new major product alongside trace (*S*)-3-(1-hydroxybutan-2-yl)amino)-5-bromo BODIPY (**3.1**) (Table **4.5**, Entry 7). Purification by column chromatography and ^{1}H NMR analysis of this unknown new product showed a loss of the expected singlet corresponding to the methyl ester, and the presence of two broad doublet signals at 6.54 ppm (d, *J* = 8.2 Hz, 1H) and 6.39 ppm (d, *J* = 9.6 Hz, 1H) corresponding to two different NH groups. In addition, the ^{1}H NMR showed four doublet signals at 6.73 ppm (d, *J* = 5.0 Hz, 1H), 6.28 ppm (d, *J* = 3.8 Hz, 1H), 6.27 ppm (t, *J* = 5.2 Hz, 1H), and 6.20 ppm (d, *J* = 3.8 Hz, 1H) corresponding to four chemically inequivalent pyrrolic protons, and two broad multiplets at 4.18 - 4.06 ppm (m, 1H) and 3.58 - 3.47 ppm (m, 1H) corresponding to two different aliphatic CH groups α to NH, from two chemically different (*S*)-1-hydroxybutan-2-yl)amino groups. Consequently, we believe that a di-substitution

reaction had occurred, with (*S*)-2-aminobutan-1-ol (**3.8**) reacting at both the 3-postion of the BODIPYand at the methyl ester of the *meso*-aromatic group, via a substitution at carbonyl reaction, to give the corresponding amide (*S*)-3-((1-hydroxybutan-2-yl)amino)-5-bromo-*N*-((*S*)-1-hydroxybutan-2-yl)benzamide-BODIPY (**4.19**) (Table **4.5**, Entry 7).

The substitution reaction was repeated once more, with 3,5-dibromo BODIPY (**1.67**) and (*S*)-2-aminobutan-1-ol (**3.8**) as the solvent, starting at 140 °C. The analysis of TLC indicated the formation of a new product, and the starting material was fully consumed after 5 h. The reaction mixture was then allowed to cool to room temperature, subjected to an aqueous work-up and purified by column chromatography using EtOAc, due to the high polarity of the product.

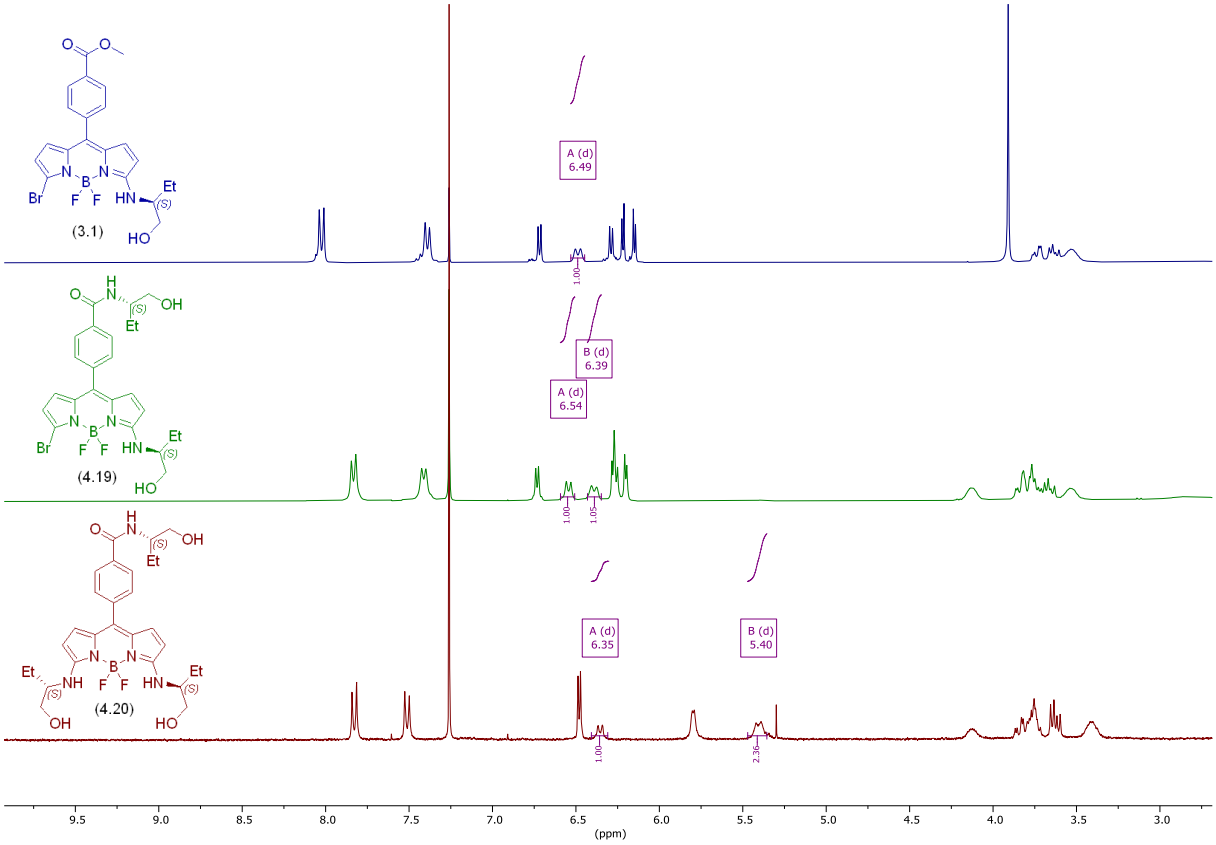

Figure 4.7: ^{1}H NMR spectra (300 MHz, $CDCl_3$). Top: ^{1}H NMR of the (*S*)-3-(1-hydroxybutan-2-yl)amino)-5-bromo BODIPY (**3.1**) (blue) following column chromatography; Middle: ^{1}H NMR of (*S*)-3-((1-hydroxybutan-2-yl)amino)-5-bromo-*N*-((*S*)-1-hydroxybutan-2-yl)benzamide-BODIPY (**4.19**)(green) following column chromatography ; Bottom: ^{1}H NMR of the (*S*)-3,5-di-(1-hydroxybutan-2-yl)amino)-*N*-((*S*)-1-hydroxybutan-2-yl)benzamide-BODIPY (**4.20**)(red), following column chromatography.

Interestingly, analysis of the ^{1}H NMR spectrum showed two broad doublets at 6.35 ppm (d, *J* = 7.9 Hz, 1H) and 5.40 ppm (d, *J* = 9.2 Hz, 2H), corresponding to three NH groups in two different chemical environments. In addition, two doublet signals at 6.48 ppm (d, *J* = 4.4 Hz, 2H) and 5.80 ppm (d, *J* = 3.8

Hz, 2H) were observed corresponding to the four pyrrolic protons, suggesting that the product obtained had C-2 symmetry, making the two pyrrolic rings chemically equivalent. Two complex multiplets at 4.19-4.03 ppm (m, 1H) and 3.47-3.33 ppm (m, 2H) were also observed, corresponding to three aliphatic CH groups α to NH, from two chemically inequivalent (*S*)-1-hydroxybutan-2-yl)amino groups. We propose that this product was a tri-substituted BODIPY, arising from a double S_NAr reaction and substitution at the carbonyl centre, to include three (*S*)-1-hydroxybutan-2-yl)amino groups. Thus (*S*)-3,5-di-(1-hydroxybutan-2-yl)amino)-*N*-((*S*)-1-hydroxybutan-2-yl)benzamide-BODIPY (**4.20**) was isolated in a 9 % yield (Table **3.5**, Entry 8)(Figure **3.7**).

4.7 Conclusion

In conclusion, in this section we have attempted to achieve a double S_NAr reaction on a 3,5-dihalo-BODIPY. Our initial attempts to synthesize (*S*)-3,5-di((1-hydroxybutan-2-yl)amino)-BODIPY (**4.9**) through a double S_NAr reaction with (*S*)-2-aminobutan-1-ol, we observed high yields of a mono substituted product (**3.1**) in keeping with the literature. However, further attempts to access (*S*)-3,5-di((1-hydroxybutan-2-yl)amino)-BODIPY (**4.9**) failed. Following initial mono-substitution by S_NAr on the BODIPY, we observed subsequent substitution at the methyl ester of the aryl group at the *meso*-position to form di-substituted BODIPY (**4.19**), containing a new amide group. This shows that the methyl ester group of (*S*)-3-(1-hydroxybutan-2-yl)amino)-5-bromo BODIPY (**3.1**) is more reactive than the aromatic bromo-substituent at the 5-position under our reaction conditions. Furthermore, it was possible to achieve a tri-substituted BODIPY (**4.20**), resulting from a S_NAr reaction at the 3-postition, a substitution at the methyl ester to form an amide, and finally a second S_NAr reaction at the 5-postition. Therefore, we have shown that it is not possible to form 3,5-disubstituted-BODIPYs by S_NAr reaction with amino alcohols, under thermal conditions.

In the future, a possible approach would be to attempt a double S_NAr reaction with 3,5-dichloro BODIPY (**1.66**), as we anticipate that 3,5-dichloro BODIPY (**1.66**) would be more reactive towards hard nucleophiles such as amines (Scheme **4.13**, A). An alternative method to synthesis (*S*)-3,5-di((1-hydroxybutan-2-yl)amino) BODIPY (**4.9**) could also be utilised, involving either a direct double Buchwald-Hartwig coupling or a two-step synthesis, involving an S_NAr reaction followed by a Buchwald-Hartwig coupling, which would allow access to non-symmetrical systems (Scheme **4.13**, B).[88,89] Furthermore, based on our previous observations, we could prepare (*S*)-3,5-di-(1-hydroxybutan-2-yl)amino)-*N*-((*S*)-1-hydroxybutan-2-yl)benzamide-BODIPY (**4.20**) via double S_NAr reaction on 3,5-dibromo BODIPY (**4.21**), which contained a less reaction *meso*-aryl group containing an amide (Scheme **4.13**, C).

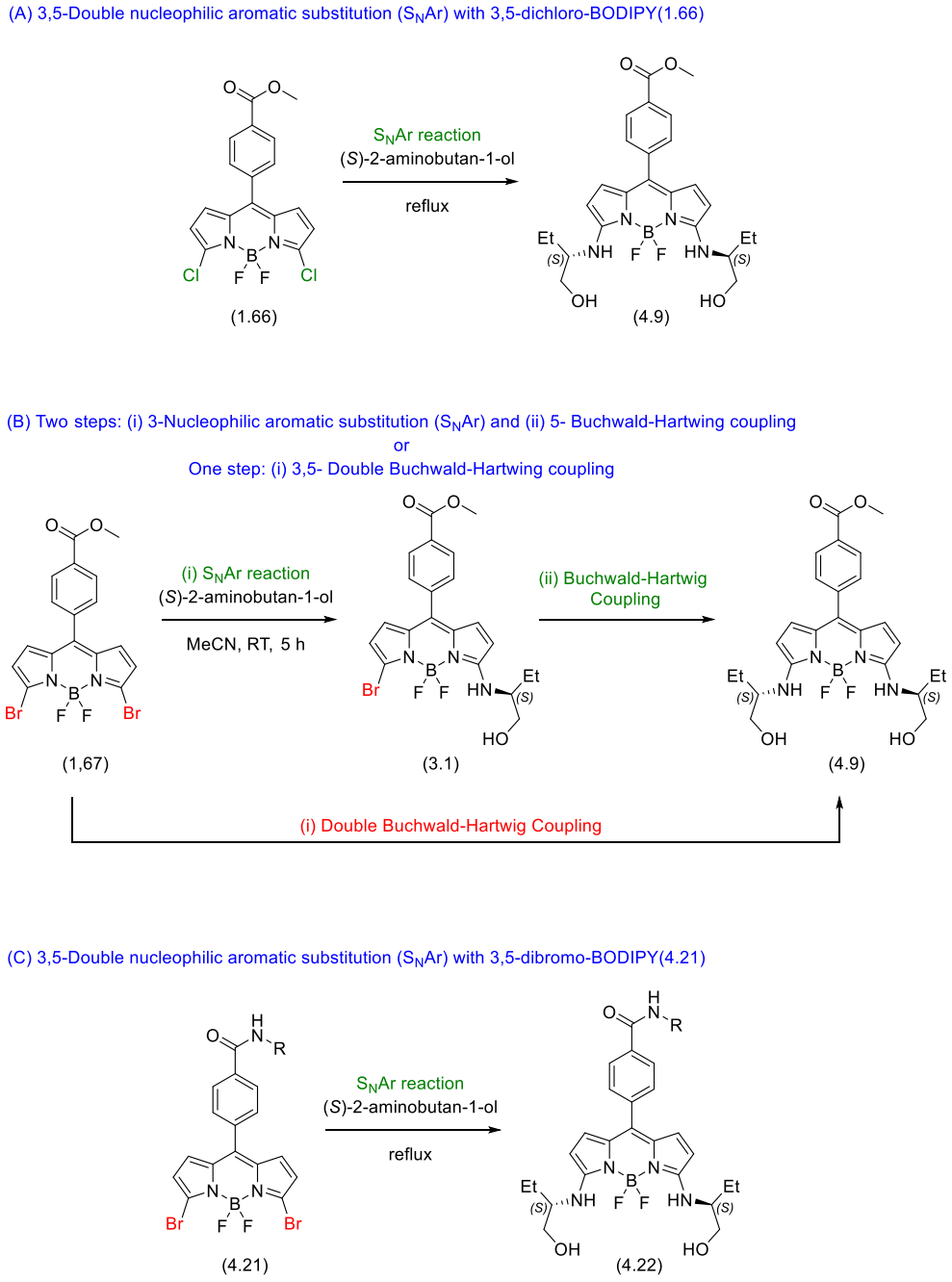

Scheme 4.13: Possible approaches to synthesize 3,5-disubstituted-BODIPYs

4.8 Synthesis of Diastereomeric Helically Chiral *N,N,O,O*-BODIPYs

In the third part of this chapter, we will discuss our attempts to access helically chiral *N,N,O,O*-BODIPYs through a chiral resolution type approach.

We planned to use an enantioselective organocatalysed nucleophilic addition of a *meso*-ethyl-*N,N,O,O*-BODIPY to an MBH carbonate, to create two diastereomers, which can be separated by chromatography to give two molecules with differing helical chirality.

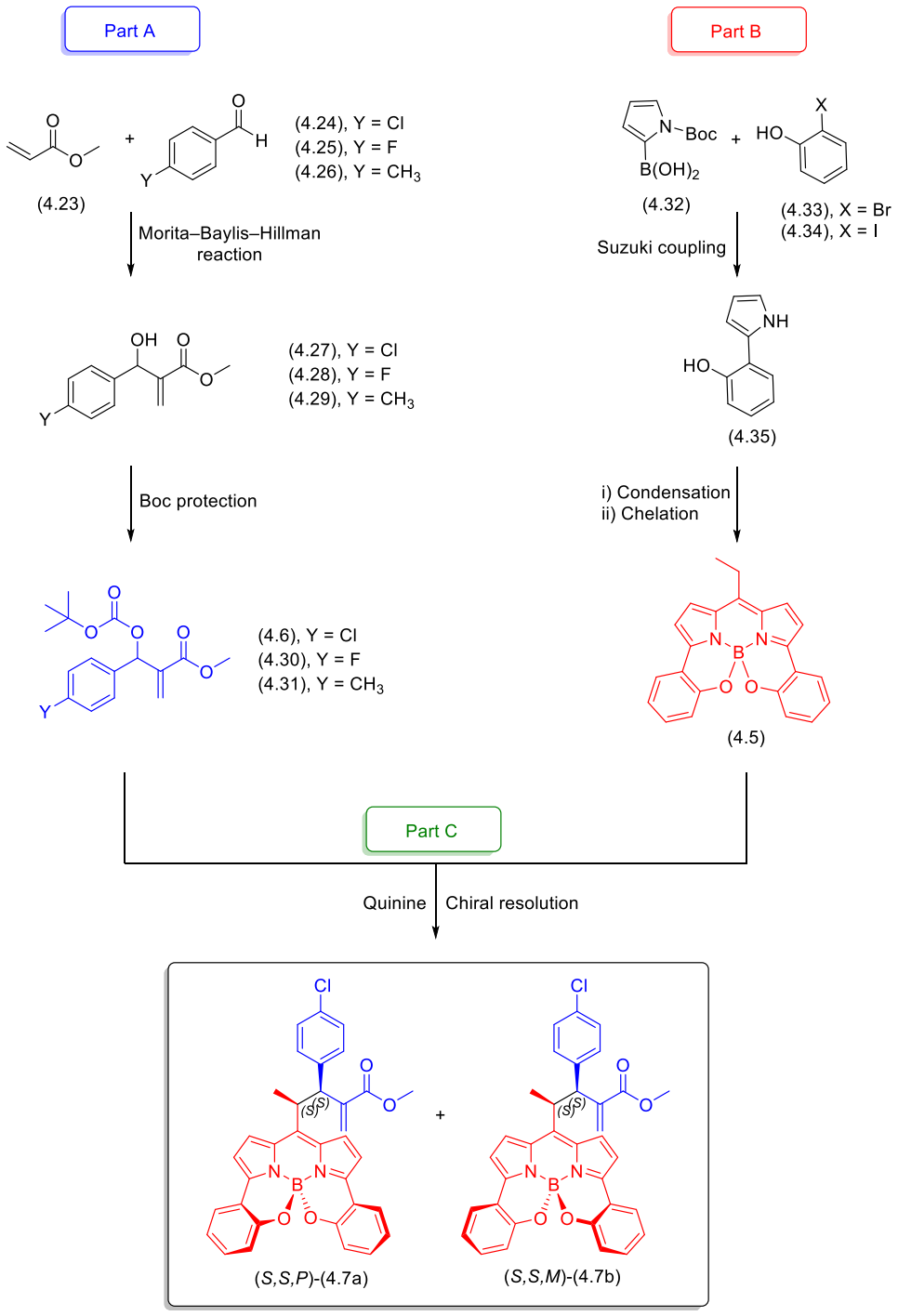

Scheme 4.14: Planned to synthesis and resolution of diastereomeric helically chiral *N,N,O,O*-BODIPYs via an enantioselective organocatalysed reaction

Our synthetic plan involves three parts: first, synthesising the electrophilic MBH carbonate (formed via a Morita–Baylis–Hillman reaction)(Scheme **4.14**, part A), and second, preparing the nucleophilic part the racemic helically chiral *meso*-ethyl-*N,N,O,O*-BODIPY (**4.5**)(Scheme **4.14**, part B). Finally in part three, we will examine an enantioselective organocatalysed nucleophilic addition of the racemic helically chiral *meso*-ethyl-*N,N,O,O*-BODIPY (**4.5**) to the MBH carbonate. The resulting two

diastereomeric helically chiral *N,N,O,O*-BODIPYs (**4.7a**) and (**4.7b**) will be separated by column chromatography. We aim to measure the photophysical and chiroptical properties of both diastereomeric helically chiral *N,N,O,O*-BODIPYs (**4.7a**) and (**4.7b**)(Scheme **4.14**).

4.8.1 Morita–Baylis–Hillman reaction (MBH) and Boc Protection (Part A)

The first building block in the proposed synthetic route to access diastereomeric helically chiral *N,N,O,O*-BODIPYs (**4.7**) will be prepared in two main steps: the Morita–Baylis–Hillman reaction (MBH) between methyl acrylate and a 4-substituted benzaldehyde to form the corresponding carbonate, followed by a subsequent Boc protection of the resulting carbonate product (Scheme **4.15**)

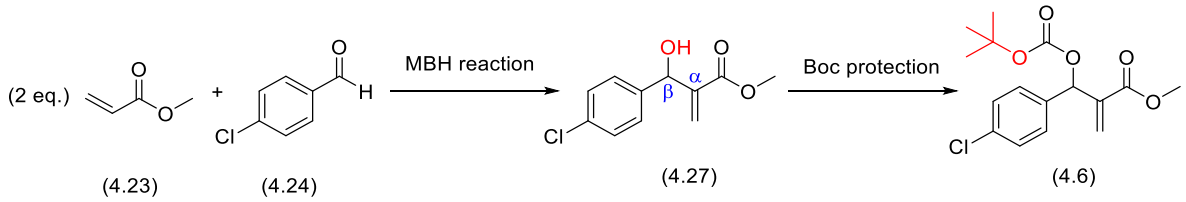

Scheme 4.15: Planned route to methyl 2-(((*tert*-butoxycarbonyl)oxy)(4-substituted phenyl)methyl)acrylate (**4.6**).

4.8.1.1 Morita–Baylis–Hillman reaction (MBH)

In order to prepare the MBH carbonates, we planned to examine the Morita–Baylis–Hillman reaction (MBH) between methyl acrylate and three different 4-substituted benzaldehydes under Lewis base catalysis, to form the corresponding β-hydroxy-α-methylene carbonyls (**4.27**). Our procedure was based on work of the Amarante group, in which examined the MBH reaction between activated alkenes and aldehydes or imines and with Lewis bases.[90]

Thus, we reacted 10 equivalents of methyl acrylate (**4.23**), with one equivalent of 4-chloro-benzaldehyde (**4.24**) and DABCO in MeOH at room temperature. The reaction was monitored by TLC which showed that a new product was formed, and the starting material was fully consumed after 6 days (Table **4.6**, Entry 1). Following an aqueous work-up and purification by column chromatography, the desired methyl 2-((4-chlorophenyl)(hydroxy)methyl)acrylate (**4.27**) was isolated in 66% yield.

We also tested MBH reaction with a two further 4-substituted benzaldehydes, one with an electron poor and one with an electron rich group. Therefore, we reacted 10 equivalents of methyl acrylate (**4.23**) with one equivalent of 4-fluoro-benzaldehyde (**4.25**) and DABCO in MeOH at room temperature for 6 days. The reaction mixture was subjected to an aqueous work-up, followed by purification by column chromatography to isolate methyl 2-((4-fluorophenyl)(hydroxy)methyl)acrylate (**4.28**) in a low yield 5% (Table **4.6**, Entry 2). In parallel, we reacted 4-methyl-benzaldehyde (**4.26**) and 10 equivalents

of methyl acrylate (**4.23**) under similar conditions for 6 days, following an aqueous work-up and column chromatography to obtain methyl 2-(hydroxy(*p*-tolyl)methyl)acrylate (**4.29**) in a good yield 56% (Table **4.6**, Entry 3).

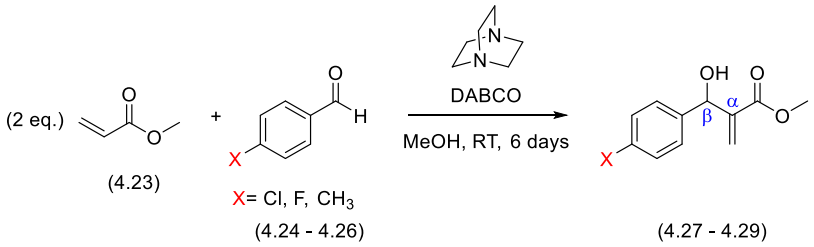

Entry	Starting material	Product	Yield /% [a]
1	(**4.24**), X = Cl	(**4.27**)	66
2	(**4.25**), X = F	(**4.28**)	5
3	(**4.26**), X = CH_3	(**4.29**)	56

Table 4.6: Synthesis of methyl 2-((4-substituted phenyl)(hydroxy)methyl)acrylate (**4.27** – **4.29**) through MBH reaction, [a] Isolated yield following column chromatography.

After successfully synthesising three different methyl 2-((4-substituted phenyl)(hydroxy)methyl)acrylates (**4.27**), (**4.28**) and (**4.29**) using a Morita–Baylis–Hillman reaction, next we planned to Boc protect OH group of these MBH products.

4.8.1.1 Boc Protection of MBH Carbonate compounds

Next, we planned to examine the Boc protection on MBH products to protect OH group. The reaction between 2-((4-chlorophenyl)(hydroxy)methyl)acrylate (**4.27**) and $(Boc)_2O$. Our procedure based on work of Coelho *et al.*, in which they examined *tert*-butoxycarbonyl (Boc) activation with MBH carbonate compounds in presence of DMAP in DCM.[91]

Thus, we reacted one equivalent of 2-((4-chlorophenyl)(hydroxy)methyl)acrylate (**4.27**), 1.1 equivalent of $(Boc)_2O$, and DMAP in dry DCM at room temperature for 90 min. The TLC analysis showed the formation of a new product and the starting material had been fully consumed. The reaction mixture was subjected to an aqueous work-up to form a colourless oil, which following purification by column chromatography gave 2-(((*tert*-butoxycarbonyl)oxy)(4-chloro phenyl)methyl)acrylate (**4.6**) as white crystal solid in 31 % yield (Scheme **4.16**).

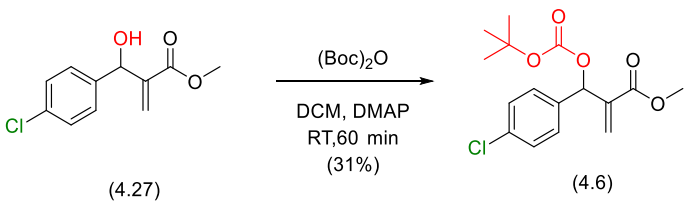

Scheme 4.16: Boc protection of MBH adduct to form 2-(((*tert*-butoxycarbonyl)oxy)(4-chloro phenyl)methyl)acrylate (**4.6**).

The structure of 2-(((*tert*-butoxycarbonyl)oxy)(4-chloro phenyl)methyl)acrylate (**4.6**) was confirmed by the analysis of ^{1}H NMR spectrum, which showed a 9H singlet in the aliphatic range at 1.46 ppm corresponding to newly added methyl groups of Boc. The structure of 2-(((*tert*-butoxycarbonyl)oxy)(4-chloro phenyl)methyl)acrylate (**4.6**) was further validated by HRMS, which showed a peak at 344.1268 *m/z* which is consistent with the predicted formula of $C_{16}H_{23}{}^{35}ClO_5N$ $[M+NH_4]^+$. For further confirmation, crystals were grown though liquid-liquid diffusion DCM with hexane (1:3). A suitable single crystal was analysed by single crystal X-ray diffraction, giving a triclinic crystal structure with the P-1 space group, with 2 molecules in the unit cell (Z = 2), one each in the (*R*) and (*S*) configurations (Figure **4.8**).

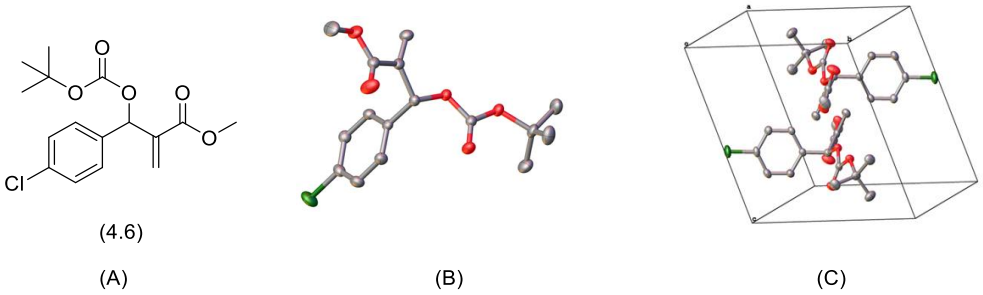

Figure 4.8: 2-(((*Tert*-butoxycarbonyl)oxy)(4-chloro phenyl)methyl)acrylate. (A) Molecular structure, (B) One molecule in the single crystal X-ray structure of 2-(((*tert*-butoxycarbonyl)oxy)(4-chloro phenyl)methyl)acrylate (**4.6**), (C) Packing of the molecules in the unit cell.

Once we successfully synthesised MBH carbonate, we next planned to examine the synthesis of a racemic helically chiral *meso*-ethyl-*N,N,O,O*-BODIPY (**4.5**) as the second part of our planned strategy.

4.8.2 Synthesis of Racemic Helically Chiral *meso*-Ethyl-*N,N,O,O*-BODIPY (Part B)

Our plan to synthesise a racemic helically chiral *meso*-ethyl-*N,N,O,O*-BODIPY (**4.5**) was based on previous work by the Hall group, and involves a Suzuki Miyaura cross-coupling reaction between (1-(*tert*-butoxycarbonyl)-1*H*-pyrrol-2-yl)boronic acid (**4.32**) and a suitable 2-halophenol, followed by an *in situ* deprotection.[55] Subsequently, we planned to attempt a condensation reaction between 2-(1*H*-pyrrol-2-yl)phenol (**4.35**) and trimethyl orthopropionate, followed by a boron chelation reaction

in one-pot procedure to directly form racemic helically chiral *meso*-ethyl-*N,N,O,O*-BODIPY (**4.5**) (Scheme **4.17**).

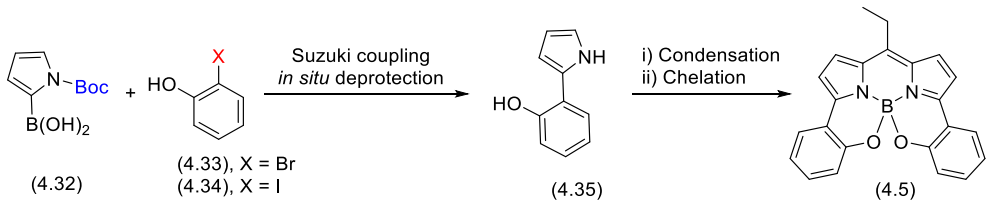

Scheme 4.17: Planned synthesis of racemic helically chiral *meso*-ethyl-*N,N,O,O*-BODIPY (**4.5**)

4.8.2.1 Suzuki Miyaura Cross-coupling Reaction between (1-(*tert*-butoxycarbonyl)-1*H*-pyrrol-2-yl)boronic acid (**4.32**) and 2-Iodophenol (**4.34**)

Thus, we performed a Suzuki Miyaura cross-coupling reaction between 1.5 equivalents of (1-(*tert*-butoxycarbonyl)-1*H*-pyrrol-2-yl)boronic acid (**4.32**) and one equivalent of 2-iodophenol (**4.34**) on a 1.2 mmol scale, catalysed by XPhos Pd G3 (3 mol%) in degassed THF/H_2O at 75 °C. The reaction was monitored by TLC which showed the disappearance of the starting material and the formation of multiple new products after 24 hours. Following an aqueous work-up and purification by column chromatography 2-(1*H*-pyrrol-2-yl)phenol (**4.35**) was isolated in a low yield 38% (Table **4.7**, Entry 1).

Since a number of compounds were identified by TLC, we hypothesised that the low yield might be due to the formation of by-products in the reaction. Therefore, we repeated the reaction under the similar conditions, but decreasing the reaction time, using 1.5 equivalents of (1-(*tert*-butoxycarbonyl)-1*H*-pyrrol-2-yl)boronic acid (**4.32**) and one equivalent of 2-iodophenol (**4.34**) on 2.5 mmol scale, catalysed by XPhos Pd G3 (3 mol%) in THF/H_2O at 75 °C. The reaction was stopped after 2 h, followed by an aqueous work-up and purification by column chromatography. The desired product 2-(1*H*-pyrrol-2-yl)phenol (**4.35**) was isolated in a low yield 7%. Starting material could be observed in the crude reaction mixture, suggesting the low yield was due to incomplete reaction (Table **4.7**, Entry 2).

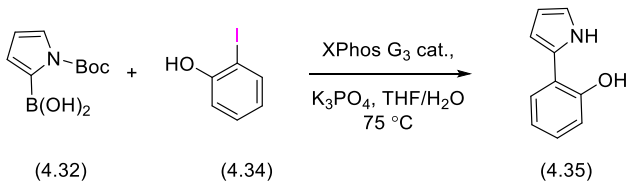

Entry	Scale/ mmol	Reaction Time/ h	Yield/%
1	1.2	24 h	38
2	2.5	2 h	7

Table 4.7: Synthesis of 2-(1*H*-pyrrol-2-yl)phenol (**4.35**) through Suzuki Miyaura cross-coupling reaction and *in situ* deprotection.

The structure of 2-(1*H*-pyrrol-2-yl)phenol (**4.35**) was confirmed by the analysis of ^{1}H NMR spectrum which showed a broad signal at 9.40 ppm corresponding to NH proton, indicating that *in situ* deprotection had occurred. For further confirmation, the analysis of the FT-IR spectrum showed a broad signal at 3422 cm^{-1} corresponding to OH group.

Once we had successfully analysed and confirmed the structure of the desired product 2-(1*H*-pyrrol-2-yl)phenol (**4.35**), we turned our attention to figuring out the structure of the two by-products identified, which we will call fraction 1 and fraction 2 based on retention time on column. Inspection of the ^{1}H NMR spectrum of fraction 1 showed one major compound, with the presence of two isopropyl groups identified through their characteristic heptet signals at 2.96 ppm, 2.60 ppm and doublet signals at 1.32 ppm, 1.08 ppm, each in a 1 to 6 ratio by integration. Therefore, we decided to attempt to grow single crystals to allow SCXRD analysis, which was achieved by slow evaporation from a chloroform solution. Subsequently, a suitable single crystal was submitted to X-ray analysis, and fraction 1 was identified as 2,4,6-triisopropyl-1,1'-biphenyl (**4.36**), which has come from the XPhos ligand following a cleavage of the P-C bond. Re-examination of the ^{1}H NMR spectrum for fraction 1, showed that 2,4,6-triisopropyl-1,1'-biphenyl (**4.36**) was indeed the major product (Scheme **4.18**).

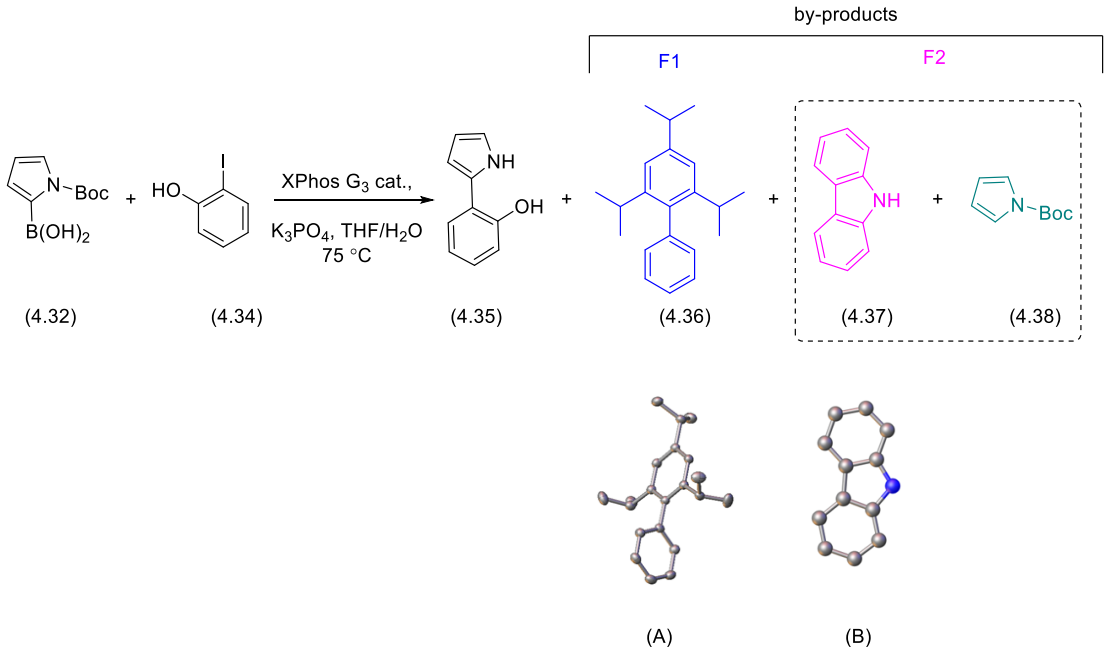

Scheme 4.18: By-products formed during the synthesis of 2-(1*H*-pyrrol-2-yl)phenol (**4.35**), (A) Single crystal X-ray structure of 2,4,6-triisopropyl-1,1'-biphenyl (**4.36**); (B) Single crystal X-ray structure of 9*H*-carbazole (**4.37**) (CCDC: CRBZOL)

The ^{1}H NMR for fraction 2, showed the presence of two double doublets at 7.25 ppm and 6.23 ppm, in a 1 to 1 ratio (Figure **4.9**). We then attempted to grow crystals of the fraction 2 by-product, which

were grown via a layered liquid-liquid diffusion experiment (DCM : hexane, 1:3), resulting in colourless crystals along with a quantity of light brown oily material. A suitable single crystal was submitted to X-ray, which resulted in a unit cell measurement which matched a known crystal structure (CCDC: CRBZOL), 9*H*-carbazole (**4.37**). The generation of 9*H*-carbazole is expected during the reaction, as it is formed via a base mediated reductive elimination from the XPhos Pd G3 pre-catalyst.[92]

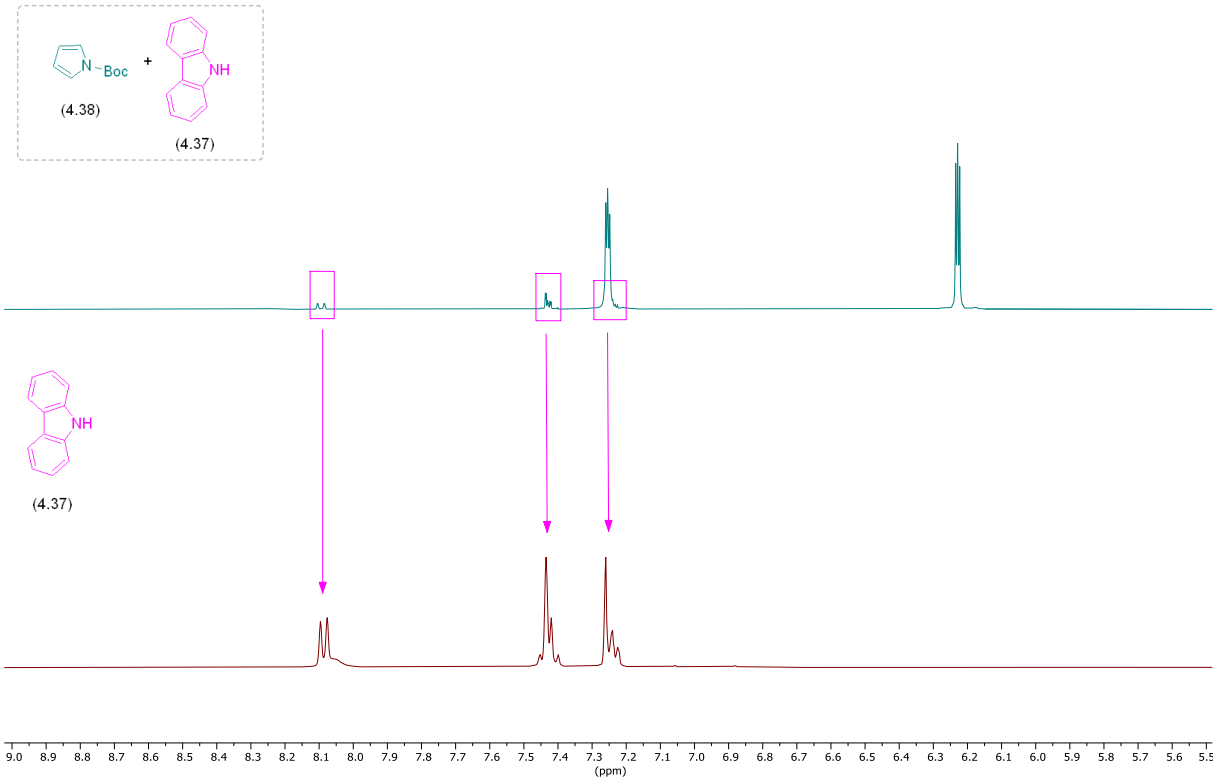

Figure 4.9: ^{1}H NMR spectrum (300 MHz, $CDCl_3$) of fraction 2; Top: ^{1}H NMR of the fraction 2 before crystallisation (green), Bottom: ^{1}H NMR of fraction 2 after crystallisation, colourless crystal (red)

Interestingly, the structure of 9*H*-carbazole (**4.37**) did not agree with the ^{1}H NMR spectra for fraction 2. Examination of the ^{1}H NMR of the crystalline material showed that 9*H*-carbazole was a minor component of the fraction 2 sample, with the NMR suggesting that the major component of fraction 2 was *tert*-butyl 1*H*-pyrrole-1-carboxylate (**4.38**), arising from a protodeboronation of (1-(*tert*-butoxycarbonyl)-1*H*-pyrrol-2-yl)boronic acid (**4.32**) (Figure **4.10**).[93]

Next, we planned to examine an alternative starting material 2-bromophenol (**4.33**) in the Suzuki Miyaura cross-coupling reaction to synthesis 2-(1*H*-pyrrol-2-yl)phenol (**4.35**).

4.8.2.2 Suzuki Miyaura cross-coupling Reaction Between (1-(*Tert*-butoxycarbonyl)-1*H*-pyrrol-2-yl)boronic acid (**4.32**) and 2-Bromophenol (**4.33**)

We performed a Suzuki Miyaura cross-coupling reaction between 1.5 equivalents of (1-(*tert*-butoxycarbonyl)-1*H*-pyrrol-2-yl)boronic acid (**4.32**) and one equivalent of 2-bromophenol (**4.33**) on 1.2 mmol scale, catalysed by XPhos Pd G3 (3 mol%) in THF/H_2O at 75 °C. The reaction was monitored by TLC which showed that the starting material had been fully consumed and a new product formed after 28 hours. Following an aqueous work-up and purification by column chromatography 2-(1*H*-pyrrol-2-yl)phenol (**4.35**) was isolated in an excellent yield 71%, a significant improvement on the yields previously obtained with 2-iodophenol (**4.34**) (Table **4.8**, Entry 1).

In order to obtain sufficient amounts of 2-(1*H*-pyrrol-2-yl)phenol (**4.35**) for subsequent steps, we carried out the Suzuki Miyaura cross-coupling reaction between 1.5 equivalents of (1-(*tert*-butoxycarbonyl)-1*H*-pyrrol-2-yl)boronic acid (**4.32**) and one equivalent of 2-bromophenol (**4.33**) under our standard Suzuki Miyaura cross-coupling conditions. After 28 hours, reaction mixture was subjected to an aqueous work-up and purification by column chromatography 2-(1*H*-pyrrol-2-yl)phenol (**4.35**) was isolated in 57% yield when performed on a 2.5 mmol scale (Table **4.8**, Entry 2). We repeated Suzuki Miyaura cross-coupling reaction again under the previous conditions on a 5 mmol scale, which following an aqueous work-up and purification by column chromatography, gave 2-(1*H*-pyrrol-2-yl)phenol (**4.35**) in a decreased yield of 28 % (Table **4.8**, Entry 3).

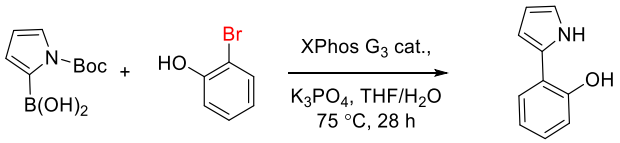

(4.32) (4.33) (4.35)

Entry	Scale/ mmol	Yield/%
1	1.2	71
2	2.5	57
3	5.0	28

Table 4.8: Synthesis of 2-(1*H*-pyrrol-2-yl)phenol (**4.35**) through Suzuki Miyaura cross-coupling reaction and *in situ* deprotection.

The structure of 2-(1*H*-pyrrol-2-yl)phenol (**4.35**) was confirmed by SCXRD, crystals were grown though liquid-liquid diffusion DCM with hexane (1:3). A suitable single crystal was analysed by single crystal X-ray diffraction, giving a monoclinic crystal structure with the $P2_1/c$ space group, with 4 molecules in the unit cell (Z = 4) (Figure **4.10**).

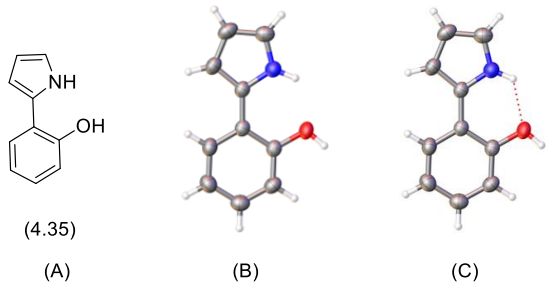

Figure 4.10: 2-(1*H*-pyrrol-2-yl)phenol (**4.35**), (A) Molecular structure, (B) Single crystal X-ray structure; (C) The crystal structure including intramolecular H-bond

We have therefore successfully synthesised 2-(1*H*-pyrrol-2-yl)phenol (**4.35**) with an excellent yield of 71%, albeit on small scale, through the Suzuki Miyaura cross-coupling reaction and *in situ* deprotection. It should be noted that the reaction yields decreased significantly on scale-up, and this would need to be address in future work. However, we successfully synthesised sufficient material for the next steps in which we will synthesise a racemic helically chiral *meso*-ethyl-*N,N,O,O*-BODIPY (**4.5**) as part B in our synthetic strategy.

4.8.2.3 Synthesis of Racemic Helically chiral *meso*-Ethyl-*N,N,O,O*-BODIPY (**4.5**)

The final step in part B of our synthetic route involved the condensation and boron chelation, in a one-pot procedure, followed by *in situ* B-O bond formation to produce a racemic helically chiral *meso*-ethyl-*N,N,O,O*-BODIPY (**4.5**).

We followed an adapted procedure reported by Hall *et al.*, in which one equivalent of 2-(1*H*-pyrrol-2-yl)phenol (**4.35**), 7.4 equivalents of trimethyl orthopropionate (**4.39**) and 3 equivalents of TFA were reacted in DCM at room temperature for 45 minutes. The solvent and excess trimethyl orthopropionate (**4.39**) was then removed under reduced pressure. The resulting residue was re-dissolved in DCM and treated with $BF_3.OEt_2$ in the presence of Hünig's base at room temperature. The reaction mixture was monitored by TLC which showed that the starting material had disappeared, and multiple new products had been formed after one hour. The reaction mixture was then quenched with saturated $NaHCO_3$ solution, followed by an aqueous work-up and purification by column chromatography in DCM, and the racemic helically chiral *meso*-ethyl-*N,N,O,O*-BODIPY (**4.5**) was isolated with a low yield of 5% over two steps. We repeated the reaction multiple times under similar reaction conditions but on different reaction scales, resulting in low to moderate yields (5-32%). Yields for the reaction were improved with the use of EtOAc/petroleum ether as the column solvent, to improve separation, and the use of large volume columns, due to the poor solubility of the product (Table **4.9**).

The structure of the racemic helically chiral *meso*-ethyl-*N,N,O,O*-BODIPY (**4.5**) was confirmed by the analysis of the ^{1}H NMR spectrum, which showed a 2H multiplet at 3.07-2.86 ppm corresponding to diastereoisomeric protons of CH_2 groups at the *meso*-position, indicating the presence of chirality in the molecule. In addition, the ^{1}H NMR spectrum showed two doublet signals at 7.38 ppm (d, *J* = 4.4 Hz, 2H) and 6.88 ppm (d, *J* = 4.4 Hz, 2H). These signals arise from the C-2 symmetry of the molecule and correspond to the four pyrrolic protons.

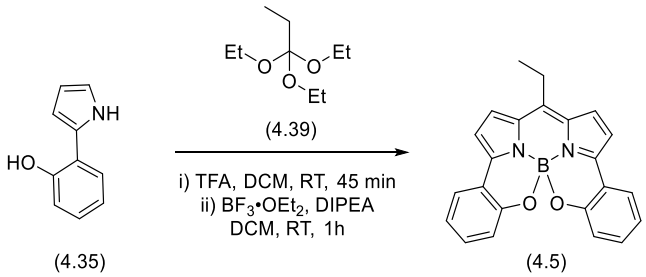

(4.35) (4.5)

Entry	Scale/mmol	Yield/%
1	0.62	5
2	0.70	8
3	0.62	10
4	0.62	32[a]

Table 4.9: Synthesis of a racemic helically chiral *meso*-ethyl-*N,N,O,O*-BODIPY (**4.5**); [a] Product contained minor impurities following column chromatography.

The racemic helically chiral *meso*-ethyl-*N,N,O,O*-BODIPY (**4.5**) was successfully crystallised through a layered liquid-liquid diffusion experiment with $CHCl_3$ (solvent) and Et_2O (anti-solvent) (1:3). A suitable single crystal was analysed by single crystal X-ray diffraction, giving a monoclinic crystal structure with the $P2_1/c$ space group, with the crystal containing a 1:1 mixture of the two enantiomers (Figure **4.11**).

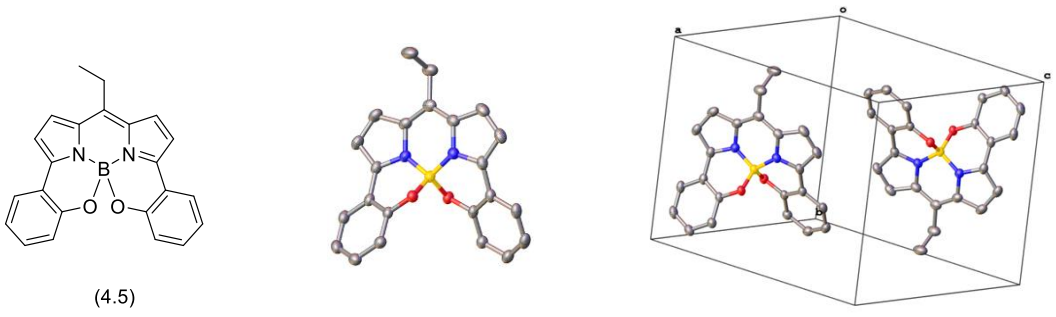

(4.5)

(A) (B) (C)

Figure 4.11: Racemic helically chiral *meso*-ethyl-*N,N,O,O*-BODIPY (**4.5**); (A) Molecular structure, (B) One molecule in the single crystal X-ray structure of racemic helically chiral *N,N,O,O*-BODIPY (**4.5**), (C) Packing of the molecules in the unit cell.

Due to the low yield of racemic helically chiral *meso*-ethyl-*N,N,O,O*-BODIPY (**4.5**) obtained in a one-pot procedure involving condensation and boron chelation reactions, we decided to isolate the product after the condensation reaction and carry out the boron chelation in a separate step as we hoped this would enhance the overall yield (Scheme **4.19**).

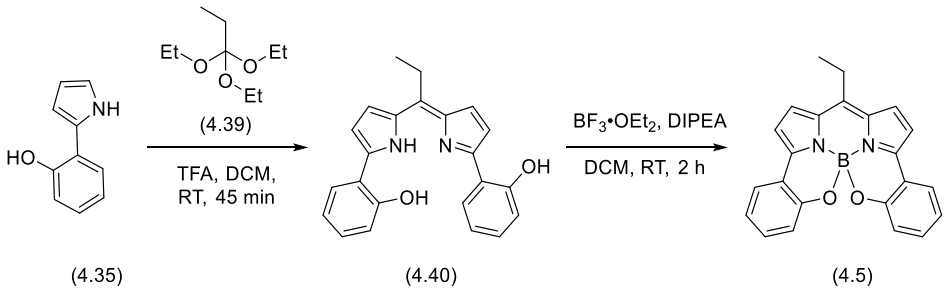

Scheme 4.19: Synthesis of racemic helically chiral *meso*-ethyl-*N,N,O,O*-BODIPY (**4.5**) over two steps

We therefore performed a condensation reaction between one equivalent of 2-(1*H*-pyrrol-2-yl)phenol (**4.35**) and 7.4 equivalents of trimethyl orthopropionate (**4.39**) with 3 equivalents of TFA in DCM at room temperature for 45 minutes. The solvent and excess trimethyl orthopropionate were removed under reduced pressure followed by purification by column chromatography to isolated *α,α'*-di(2-hydroxyphenyl) dipyrromethene (**4.40**) in low yield of 13%. Purification by column proved challenging as the product "streaked" in the column, likely due to poor solubility and possible interaction of the chelating groups with the silica. Post-purification, the ^{1}H NMR spectrum showed the presence of the desired product with trace impurities. Therefore, due to low yields and difficult purifications in the first step, we did not continue with our two-step synthetic approach. Instead we continued to use our previous one-pot procedure for synthesising racemic helically chiral *meso*-ethyl-*N,N,O,O*-BODIPY (**4.5**). Next, we will examine the final step in our synthetic route to access diastereomeric helically chiral *N,N,O,O*-BODIPYs.

4.8.3 Synthesis of diastereomeric helically chiral *N,N,O,O*-BODIPYs (Part C)

The final step in our synthetic route was synthesis of diastereomeric helically chiral *N,N,O,O*-BODIPYs. To do this, we will examine an enantioselective organocatalysed nucleophilic addition of the racemic helically chiral *meso*-ethyl-*N,N,O,O*-BODIPY (**4.5**)(part A) to the MBH carbonate (part B). Our procedure was based on work of Rios and co-workers, with preliminary work on this step carried out by another member in the Hall group (Dr R.T. Aldeen).[94]

We reacted one equivalent of racemic helically chiral *meso*-ethyl-*N,N,O,O*-BODIPY (**4.5**), two equivalents of methyl 2-(((*tert*-butoxycarbonyl)oxy)(4-chlorophenyl)methyl)acrylate (**4.6**), and quinine in $CHCl_3$ at room temperature. The reaction was monitored by TLC which showed that the

starting material had been consumed and new products had been formed after 5 days, at which point the solvent was removed directly under reduced pressure. Upon the inspection of ^{1}H NMR spectrum of the crude reaction mixture, two diastereomeric BODIPY products could be observed, along with the remaining methyl 2-(((*tert*-butoxycarbonyl)oxy)(4-chlorophenyl)methyl) acrylate (**4.6**). The crude reaction mixture was purified by column chromatography to give two diastereomeric helically chiral *N,N,O,O*-BODIPYs (**4.7a**) and (**4.7b**) in an excellent combined yield of 94%, in an approximate 1:1.1 ratio based on ^{1}H NMR analysis, however separation of the two diastereomers would prove challenging due to their similar R_f values (Scheme **4.20**).

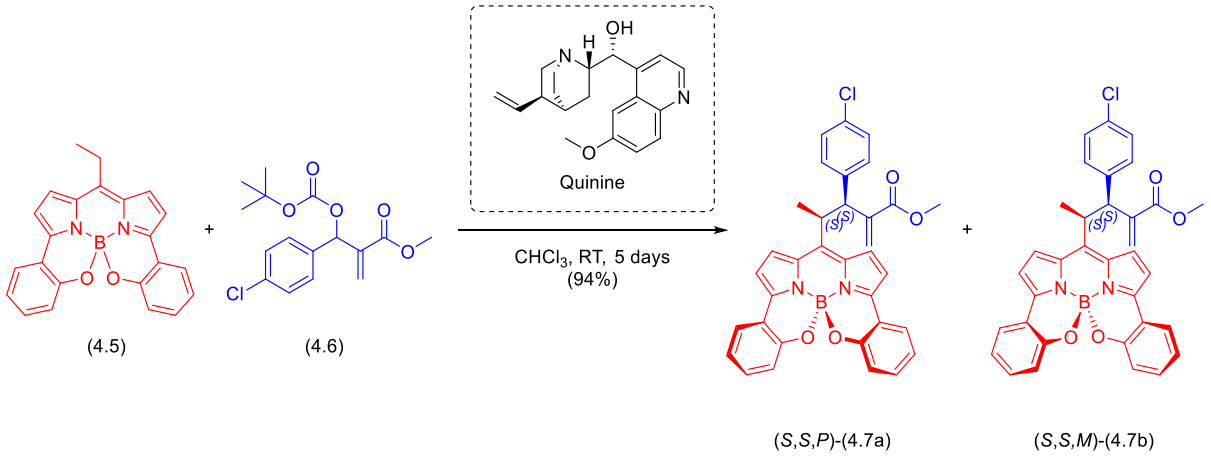

Scheme 4.20: Synthesis of diastereomeric helically chiral *N,N,O,O*-BODIPYs (**4.7a**) and (**4.7b**)

First, we attempted to separate the two diastereomeric helically chiral *N,N,O,O*-BODIPYs (**4.7a**) and (**4.7a**) using normal phase HPLC, with the help of Dr A. Charlton. The sample was dissolved in DCM or toluene, filtered, and injected into an analytical normal phase HPLC column (Luna 5μm Silica(2)100 Å (100 x 4.6 mm), 3 mL/min) fitted with a diode array detector. Elution with hexane gave only a single peak, with the solvent front (rt = 1.28 min, 3 mL/min), suggesting that the sample had been carried through in the injected DCM and may have been poorly soluble in hexane. Therefore, we changed the eluent to a mixture of toluene: hexane using a solvent gradient of 50:50 to 80:20. This resulted in an improved retention time (rt = 13.3 min, 2.5 mL/min), however no separation of the diastereomers was achieved. Finally, we examined DCM as an isocratic solvent system, resulting in much greater retention on the column (rt ~ 31 and 34 min, 2 mL/min), and showing two distinct if overlapping peaks. Unfortunately, due to the extent of overlap, separation was not possible with this method. It was a challenge to separate the diastereomers by preparative normal phase column.

Next, we attempted to separate the two diastereomeric helically chiral *N,N,O,O*-BODIPYs (**4.7a**) and (**4.7b**) by standard silica column chromatography, using a long column (40 cm x 2.5 cm) and DCM as the eluent. This allowed us to isolated a pure sample of one of the diastereomeric helically chiral

N,N,O,O-BODIPY, the first to elute from the column, as well as mixed fractions containing both helically chiral *N,N,O,O*-BODIPYs (**4.7a**) and (**4.7b**).

The structure of the isolated helically chiral *N,N,O,O*-BODIPY was confirmed by the analysis of ^{1}H NMR spectrum which showed a 3H doublet at 1.60 ppm corresponding to methyl group and a 3H singlet at 3.78 ppm corresponding to methyl ester group (Figure **4.12**). The structure of the isolated helically chiral *N,N,O,O*-BODIPYs was further validated by HRMS, which showed a peak at 573.1762 *m/z* which is consistent with a the predicted formula of $C_{34}H_{27}{}^{11}B^{35}ClN_2O_4$ $[M+H]^+$.

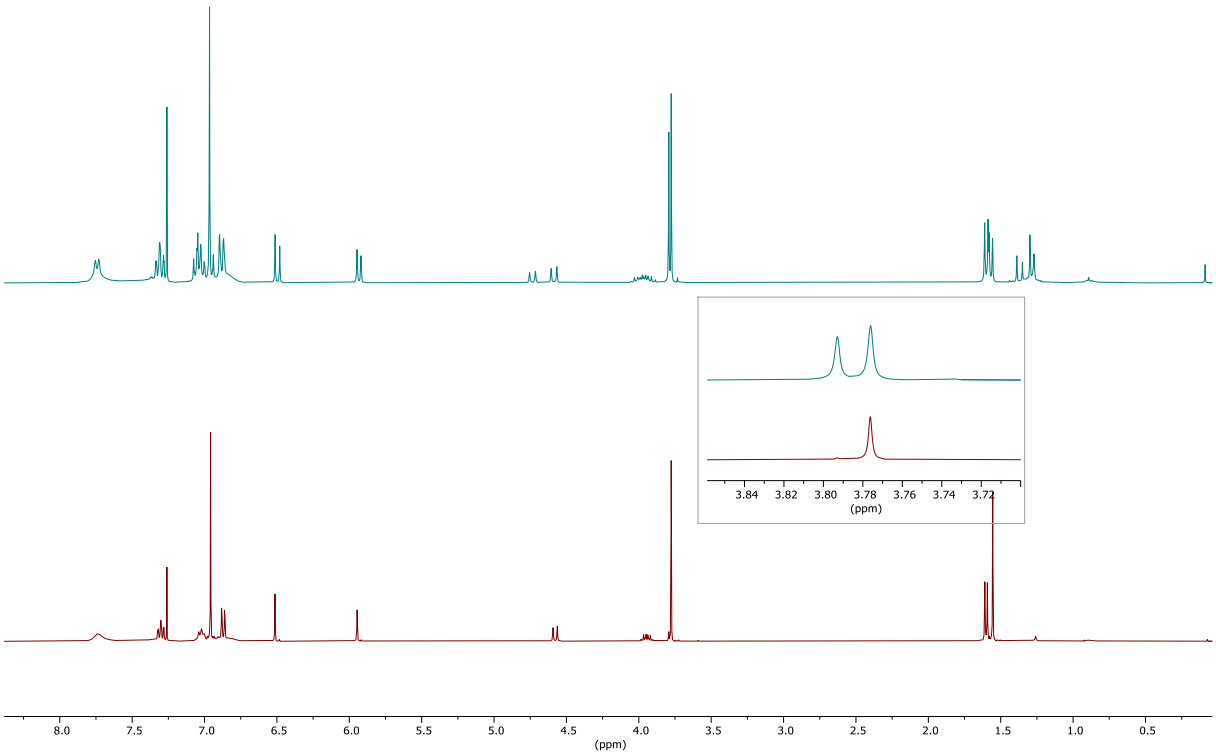

Figure 4.12: ^{1}H NMR spectrum (300 MHz, $CDCl_3$). Top: mixture of two diastereomeric helically chiral *N,N,O,O*-BODIPYs (**4.7a**) and (**4.7b**) (green) from the reaction. Bottom: isolated diastereomeric helically chiral *N,N,O,O*-BODIPY (red)

Once we successfully synthesised helically chiral *N,N,O,O*-BODIPY (**4.7**), we turned our attention to measure the photophysical properties including UV-Vis absorption and emission spectra, molar extinction coefficient (ε), the fluorescence quantum yield (ϕ_F).

Hence, we measured the absorption and emission spectra for helically chiral *N,N,O,O*-BODIPY (**4.7**) in DCM at room temperature, which exhibited absorption maxima at 623 nm and emission maxima at 637 nm (Figure **4.13**). The fluorescence quantum yields (ϕ_F) of helically chiral *N,N,O,O*-BODIPY (**4.7**) was also measured, using cresyl violet as a standard. These systems showed acceptable quantum

yields of around 0.13. Comparison of the photophysical properties of helically chiral *N,N,O,O*-BODIPY (**4.7**) to the parent racemic helically chiral *meso*-methyl-*N,N,O,O*-BODIPY (**4.41**), as reported by Dr. Hall's group, showed that the introduction of a new chiral group in the *meso*-position did not overly impact on the photophysical properties (Table **4.10**).

BODIPY	Solvent	λ_{abs}/nm	ε / mol^{-1} cm^{-1}	λ_{em}/nm	ϕ_F[a]
4.7	DCM	623	79 829	637	0.13
4.41	$CHCl_3$	615	49 020	635	0.74

Table 4.10: Photophysical properties of helically chiral *N,N,O,O*-BODIPY (**4.7** and **4.41**). [a] Measured with respect to cresyl violet standard in ethanol (ϕ_F = 0.56), excitation wavelength = 586 nm.[82]

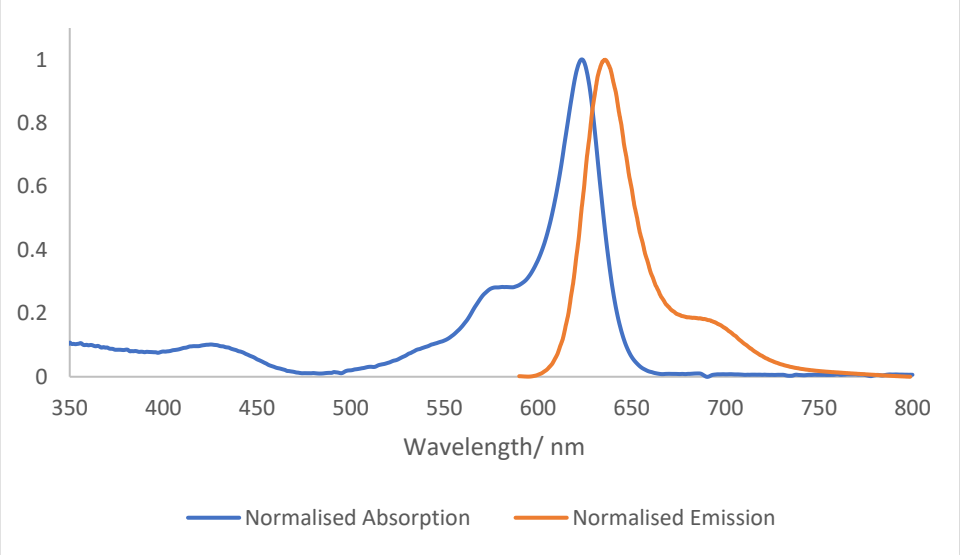

Figure 4.13: UV-Vis and fluorescence spectra of helically chiral *N,N,O,O*-BODIPY (**4.7**) in DCM, normalised spectra.

As we mentioned previously, following the separation of the two diastereomeric helically chiral *N,N,O,O*-BODIPYs (**4.7a**) and (**4.7b**) by column chromatography, we were able to isolated one diastereomer and a mixed fraction containing both diastereomeric helically chiral *N,N,O,O*-BODIPYs (**4.7a**) and (**4.7b**).

We decided to use chiral HPLC to further examine the separation of the mixed fraction. In our initial attempts, with the help of Dr X. Wen, a sample containing both diastereomeric helically chiral *N,N,O,O*-BODIPYs (**4.7a**) and (**4.7b**) was dissolved in isopropanol, filtered, and injected into an analytical chiral HPLC column (OD-H (250 x 4.6 mm)) fitted with a diode array detector. Elution with a mixture of isopropanol and hexane (flow rate: 0.5 mL/min, injection volume: 10 µL/min) using a solvent gradient of 5:95 to 80:10 over 31 min, resulted in a major peak at 11.22 min, likely accounting for a mixture of the two diastereomers, and a very minor peak at 14.02 min, potential from an

enantiomer of one of the diastereomeric helically chiral *N,N,O,O*-BODIPYs (**4.7**). Unfortunately, no separation of the diastereomers was achieved under these conditions, so in the second attempt, we utilized a different analytical chiral HPLC column (IA (250 x 4.6 mm)) using a mobile phase of isopropanol and hexane using a solvent gradient ranging from 5:95 to 80:10 over 41 min, with a flow rate of 0.5 mL/min and injection volume of 10 µL/min. This resulted in an improved separation of the diastereomers, with two main peaks (rt = 19.63 and 21.48 min) observed, along with a minor peak at 26.29 min.

Due to the appearance of minor peaks in the HPLC traces, following test chiral HPLC analysis, we decided to re-analyse the HPLC sample stored in isopropanol, containing both diastereomeric helically chiral *N,N,O,O*-BODIPYs (**4.7a**) and (**4.7b**). The ^{1}H NMR showed the presence of both of the diastereomeric helically chiral *N,N,O,O*-BODIPYs (**4.7a**) and (**4.7b**), alongside a new compound (**4.42**), as observed by the presence of a new 3H singlet at 3.77 ppm for the methyl ester and two new 1H singlets at 5.99 and 6.50 ppm for the terminal alkene protons.

Therefore, we purified the mixture by column chromatography to isolate the two diastereomeric helically chiral *N,N,O,O*-BODIPYs (**4.7a**) and (**4.7b**) and unknown compound (**4.42**). The analysis of the ^{11}B NMR of compound (**4.42**) showed no signals present, indicating the loss of boron centre. Therefore, we postulated that the compound (**4.42**) was a dipyrromethene arising from a spontaneous de-chelation reaction. To confirm this, we planned to examine a boron re-chelation reaction with dipyrromethene (**4.42**).

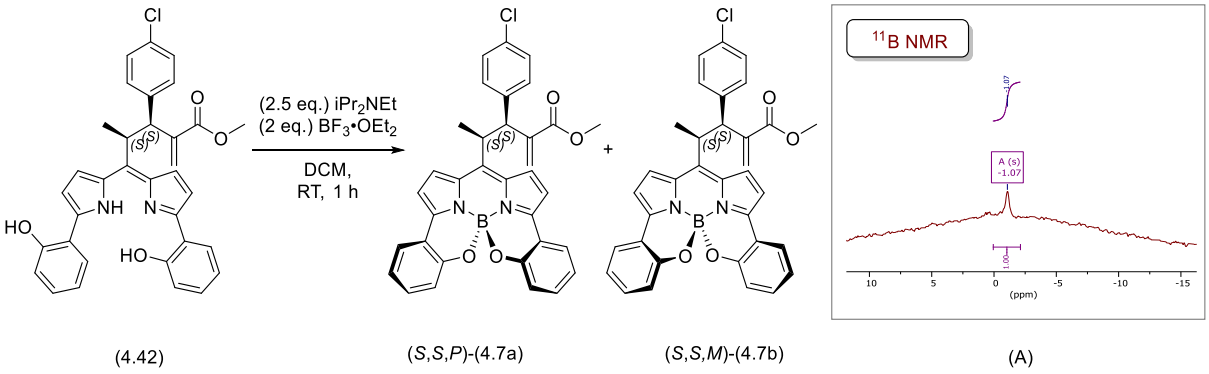

(4.42) (*S,S,P*)-(4.7a) (*S,S,M*)-(4.7b) (A)

Scheme 4.21: Reaction of unknown compound with BF_3.OEt and DIPEA to give the two diastereomeric helically chiral *N,N,O,O*-BODIPYs (**4.7a**) and (**4.7b**); (A) ^{11}B NMR spectrum (300 MHz, $CDCl_3$) of the crude diastereomeric helically chiral *N,N,O,O*-BODIPYs (**4.7a**) and (**4.7b**).

4.9 Conclusions

In this section, we have achieved the successful synthesis of diastereomeric helically chiral *N,N,O,O*-BODIPY (**4.7a**) and (**4.7b**) in five steps and 4% overall yield. We have then examined the resolution of

racemic helically chiral *N,N,O,O*-BODIPY (**4.5**) through an enantioselective reactiond with methyl 2-(((*tert*-butoxycarbonyl)oxy)(4-chlorophenyl)methyl)acrylate (**4.6**) in the presence of quinine a chiral organocatalyst. This resulted in the formation of two helically chiral *N,N,O,O*-BODIPYs (**4.7a**) and (**4.7b**) with an excellent combined yield of 94%. We successfully showed that isolation of one of diastereomers of the helically chiral *N,N,O,O*-BODIPYs was possible through column chromatography, suggesting that in the future work both diastereomers would be separable using standard lab techniques, completing a resolution approach to enantiopure helically chiral *N,N,O,O*-BODIPYs. In the future we would also examine alternative chiral organocatalysts in an attempt to explore potential kinetic resolution approaches.

4.10 Chapter Conclusions

The aims of this chapter were to develop routes for the synthesis of helically chiral *N,N,O,C*-3-((*S,P*)-2-aminobutan-1-ol)-5-(4-methoxyphenyl)-BODIPY and *N,N,O,C*-3-((*S,M*)-2-aminobutan-1-ol)-5-(4-methoxyphenyl)-BODIPY both containing a 7-membered ring through a point-to-helical chirality approach. The chapter also explores our attempts to synthesis of symmetrical helically chiral BODIPYs containing two 7-member rings through a point-to-helical chirality transfer. The final aim of this chapter was investigate a novel method for accessing enantiopure helically chiral *N,N,O,O*-BODIPYs through a chiral resolution type approach.

Thus, we have successfully synthesised helically chiral (*S,P*)-*N,N,O,C*-3-(1-hydroxybutan-2-yl)amino)-5-(4-methoxyphenyl) BODIPY (**4.2a**) and (*S,M*)-*N,N,O,C*-3-(1-hydroxybutan-2-yl)amino)-5-(4-methoxyphenyl) BODIPY (**4.2b**) through point-to-helical chirality transfer approach over a nine steps, achieving a high yields of up to 75 % and *de* up to 22%. In this approach, enantiopure amino alcohols were chosen as chiral axillaries as previously demonstrated to be excellent chiral directing group for controlling chirality in the formation of helically chiral BODIPYs in chapter 3. It is interesting that these systems show an inversion of diasteroselectivity depending on solvent polarity, which would be an area to explore in the future.

Unfortunately, we were unable to synthesize (*S*)-3,5-di((1-hydroxybutan-2-yl)amino)-BODIPY (**4.9**) through double S_NAr chemistry under thermal conditions. However, during our attempts to access (*S*)-3,5-di((1-hydroxybutan-2-yl)amino)-BODIPY (**4.9**), we observed that 3,5-dibromo BODIPY (**1.67**) could undergo an S_NAr reaction at the 3-position to form (*S*)-3-(1-hydroxybutan-2-yl)amino)-5-bromo BODIPY (**3.1**), followed by a substitution rection at the methyl ester of the aryl group at the *meso*-position to form di-substituted BODIPY (**4.19**), containing a new amide group. Furthermore, increasing the reaction time caused the formation of tri-substituted BODIPY (**4.20**). For future work to access

these substrates, we have suggested several possible approaches, including S_NAr reactions in which the *meso*-aryl group does not contain a methyl ester or the use of Buchwald-Hartwig coupling.

Finally, we have synthesized helically chiral *N,N,O,O*-BODIPYs through a chiral resolution approach, achieving high combined yield of 94%. We were able to show separation of the two diastereomers (**4.7a**) and (**4.7b**), suggesting that this approach could be used in the future for the resolution of helically chiral *N,N,O,O*-BODIPYs.

Chapter 5: Synthesis of Helically Chiral Di-BODIPYs via Point -to- Helical Chirality Transfer

5.1 Introduction

In the final chapter, we will discuss the synthesis strategies to access dimeric and trimeric helically chiral BODIPY arrays through point-to-helical chirality transfer, whilst in the second part of this chapter we will also explore the synthesis of stacked helically chiral bis BODIPYs.

Firstly, we will discuss the development of a synthetic route to access dimeric helically chiral BODIPY arrays through a point-to-helical chirality approach. Our aim is to link two helically chiral *N,N,O,C*-BODIPY units to each other through their boron centres. To achieve this, we planned to use commercially available di-boronic acids as a linker to react with two previously prepared dipyrromethenes. We will also extend our idea to make trimeric helically chiral *N,N,O,C*-BODIPY arrays. To do this, we planned to build a tri-boronic acid linker through amide coupling reactions, followed by chelation reaction with three dipyrromethenes. Such dimeric and trimeric systems are interesting synthetically, in particular we were interested in if such a construction would be possible, as there are only a few known boron linked BODIPY systems, and no chiral systems.[95] In addition, we were interested as to explore the potential for stereocontrol in these systems, the proposed dimeric structure having a possible three diastereomers with the potential for the stereochemistry of one BODIPY to influence the formation of the second. Furthermore, chiral BODIPY dimers and trimers have the potential for increased CPL due to their increased size and large chiral fields, as seen from CPL in polymers and liquid crystals.[96] Finally, simple assemble of large BODIPY arrays may also be interesting in light harvesting applications (Scheme **5.1**).[97]

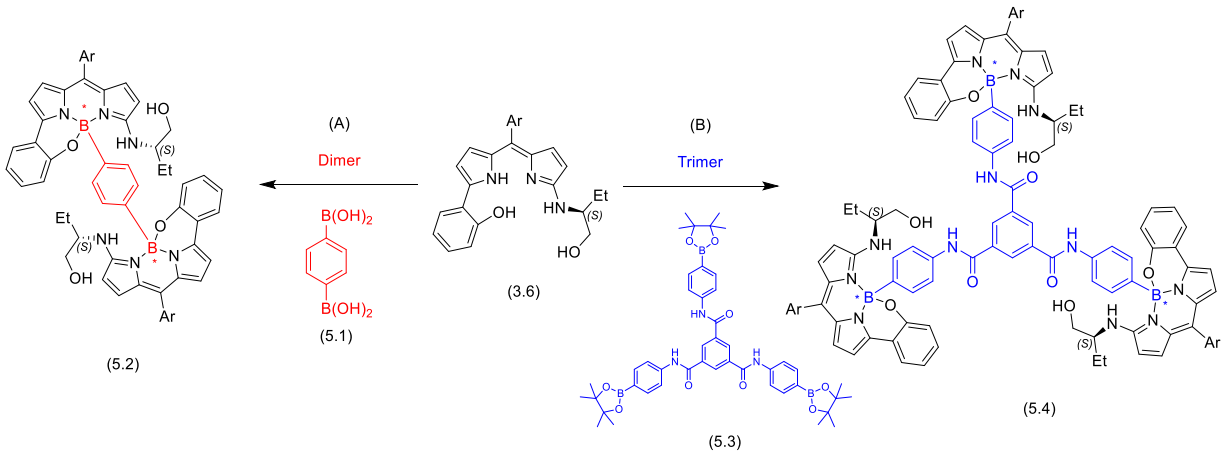

Scheme 5.1: Point-to-helical chirality control in dimeric and trimeric helically chiral BODIPYs.

Secondly, we will develop synthetic routes for stacked helically chiral bis BODIPYs, aiming to make architectures for visible spectrum solution-phase CPL. As above we anticipate that larger chiral arrays of multiple BODIPYs may have the potential for increased CPL emission (Scheme **5.2**). A similar synthesis route for this system (**5.6**) was previously reported by Harvey and co-workers.[98] However, neither chirality nor CPL studies were reported on this system.

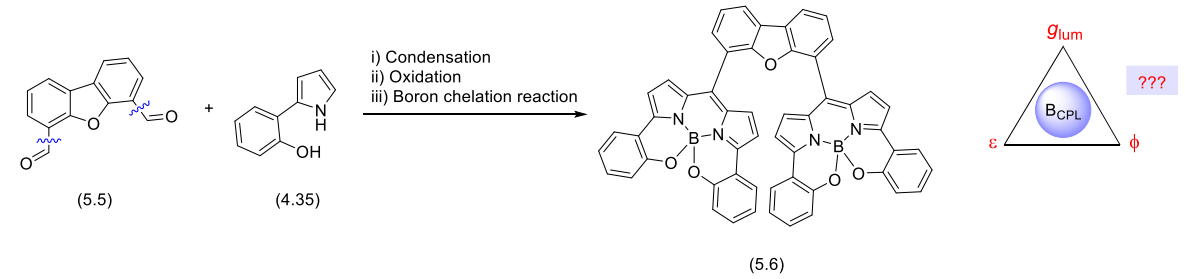

Scheme 5.2: Planned route to stacked helically chiral bis BODIPYs.

5.2 Synthetic Routes Toward Dimeric Helically Chiral BODIPY Arrays

Our planned synthetic route to form dimeric helically chiral *N*,*N*,*O*,*C*-BODIPY arrays, through point-to-helical chirality transfer, involves multiple steps. Firstly, we will synthesize (*S*)-α-(1-hydroxybutan-2-yl)amino)-α'-(2-hydroxyphenyl) dipyrromethene (**3.6**) following a described procedure in Chapter 3. Secondly, we will examine chelation reaction between (*S*)-α-(1-hydroxybutan-2-yl)amino)-α'-(2-hydroxyphenyl) dipyrromethene (**3.6**) and 1,4-phenylenediboronic acid (**5.1**). Subsequently, we will assign the absolute stereochemistry of the diastereomeric dimeric helically chiral *N*,*N*,*O*,*C*-BODIPY (**5.2a**), (**5.2b**) and (**5.2c**), and measure their photophysical and chiroptical properties (Scheme **5.3**).

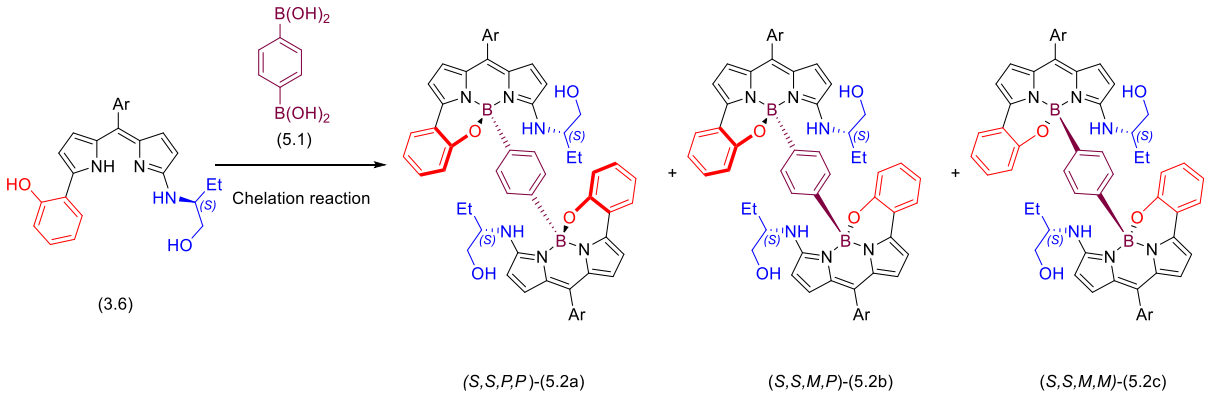

Scheme 5.3: Chelation reaction to synthesis dimeric helically chiral *N*,*N*,*O*,*C*-BODIPY arrays (Ar = *p*-($MeCO_2$)-C_6H_4-)

Therefore, following the synthesis of (*S*)-α-(1-hydroxybutan-2-yl)amino)-α'-(2-hydroxyphenyl) dipyrromethene (**3.6**) as described previously. We reacted two equivalents of (*S*)-α-(1-hydroxybutan-2-yl)amino)-α'-(2-hydroxyphenyl) dipyrromethene (**3.6**) with 1,4-phenylenediboronic acid (**5.1**) in

$CHCl_3$ at 35 °C, on a 0.1 mmol scale. The reaction was monitored by TLC which showed the starting material had been consumed and three new coloured products had been formed after 96 hours, along with trace starting material. The reaction mixture was subjected to an aqueous work-up and purified by column chromatography to separate the three new products, fraction one being well separated, whilst fractions two and three were much more close running. This resulted in the isolation of three diastereomeric helically chiral BODIPYs (**5.2a**), (**5.2b**), and (**5.2c**) in an overall yield of 64%, with the diastereomers isolated in an approximate 1:2:2 ratio (Table **5.1**).

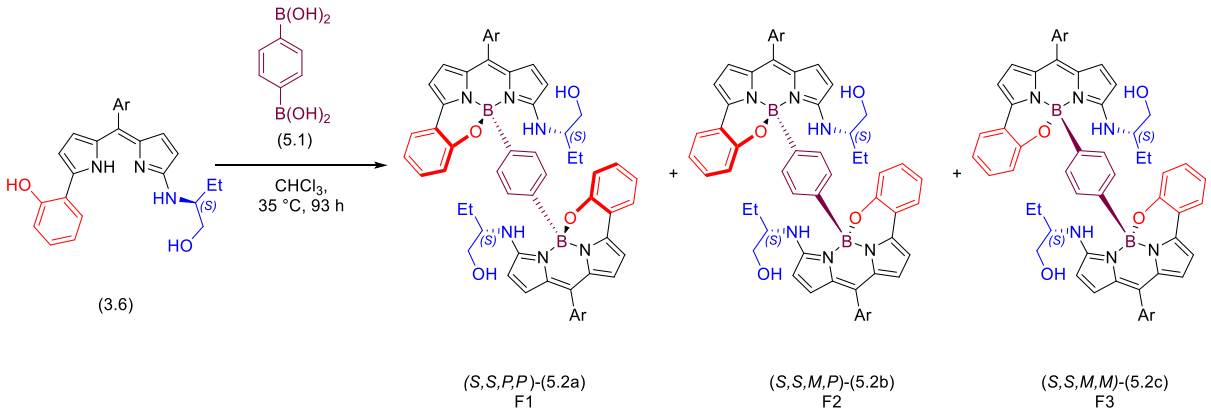

Entry	Yield (5.2a)/% F1	Yield (5.2b)/% F2	Yield (5.2c)/% F3	Yield/%[a]
1	12	27	25	64
2	33	40	24	97

Table 5.1: Synthesis of dimeric helically chiral BODIPYs (Ar = *p*-($MeCO_2$)-C_6H_4-), [a] Isolated yield following column chromatography.

To provide more material for analysis, the chelation reaction was repeated on the scale of 0.1 mmol as previously, to give an improved overall yield of 97%, this time with the diastereomers isolated in an approximate 1.5:2:1 ratio (Table 5.1).

The initial inspection of ^{1}H NMR spectra of each diastereomer showed that fraction 1 (**5.2a**) and fraction 3 (**5.2c**) showed two fold symmetry, with only a single set of ^{1}H NMR signals for the two BODIPY units. However, fraction 2 appeared to be an unsymmetrical structure as it showed two sets of signals, one for each of the two BODIPY units, for example there are two triplet signals at 0.99 ppm and 0.59 ppm corresponding to two methyl group environments for the amino alcohol substituents (Figure **5.1**).

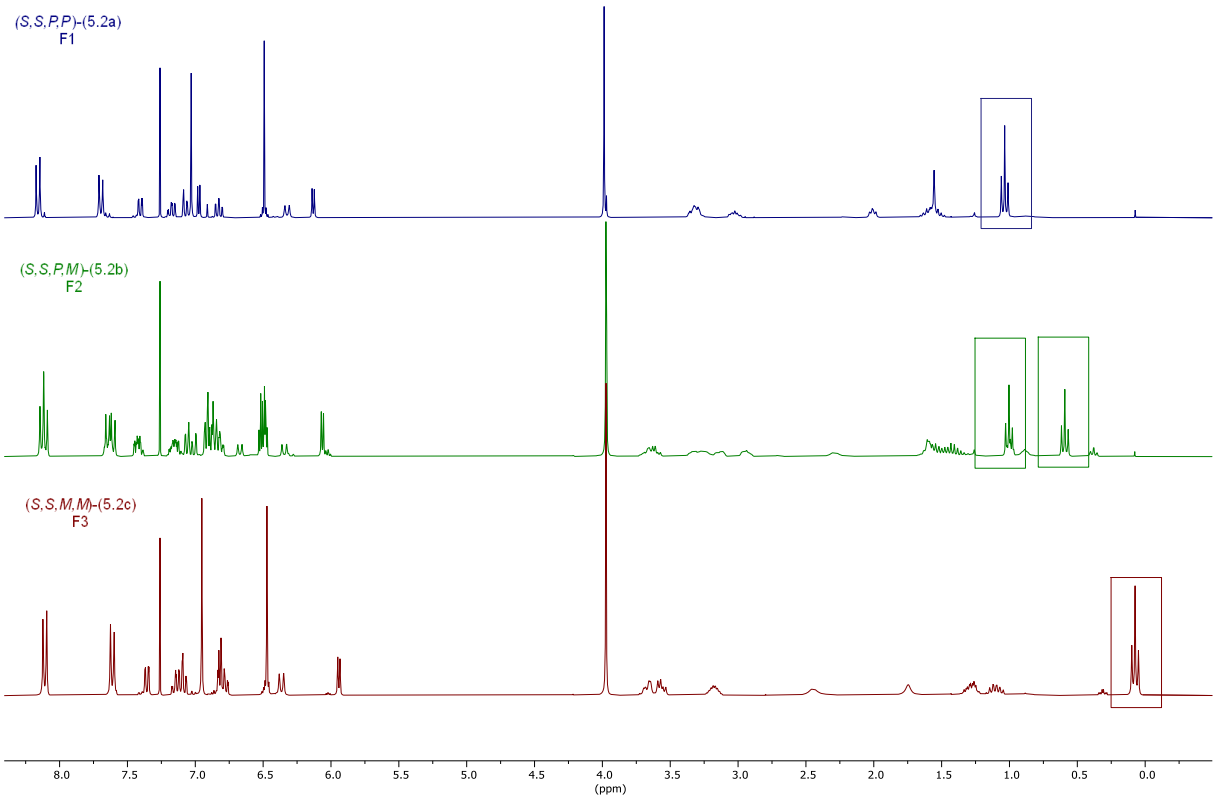

Figure 5.1: ^{1}H NMR spectrum (300 MHz, $CDCl_3$) of the three diastereomeric helically chiral BODIPYs (**5.2a**), (**5.2b**), and (**5.2c**) following column chromatography. Top: ^{1}H NMR of the fraction one (**5.2a**)(blue), Middle: ^{1}H NMR of the fraction two (**5.2b**)(green), Bottom: ^{1}H NMR of the fraction three(**5.2c)**(red).

To confirm that we had formed a set of diastereomeric dimeric BODIPYs we measured their mass spectra. The three diastereomers fraction one (**5.2a**), fraction two (**5.2b**) and fraction three (**5.2c**) gave HRMS of 1009.4313, 1009.4273 and 1009.4264 *m/z* values respectively, which are consistent with a formula of the $[M+H]^+$ ion for each diastereomer, $C_{60}H_{55}{}^{11}B_2N_6O_8$.

After successfully synthesizing our target dimeric helically chiral BODIPYs via a point-to-helical stereo controlled reaction, our next step is to further explore the structure and stereochemistry of the diastereomeric dimeric helically chiral BODIPYs formed (**5.2a**), (**5.2b**), and (**5.2a**).

5.2.1 Absolute Stereochemistry of Dimeric Helically Chiral BODIPYs

To gain a better understanding of the structure and absolute stereochemistry of the three diastereomeric dimeric BODIPYs, we decided to grow single crystals suitable for SCXRD. From crystal structure, we will then be able to assign the structure, relative and absolute stereochemistry. Thus, following attempted crystallisation of all three fractions, we successfully crystallised fraction one and

fraction three through slow evaporation of solutions in DCM, and crystals were submitted to SCXRD analysis (Table **5.2**).

Interestingly, fraction one crystallised as triclinic crystal system with a P1 space group, allowing assignment of the structure as one of the desired dimeric chiral BODIPY species. A Flack parameter of 0.022(11) was obtained allowed direct measurement of the relative and absolute stereochemistry, allowing assignment of the molecule as (*S,S,P,P*)-*N,N,O,C*-3-(2-aminobutan-1-ol) BODIPY (**5.2a**) (Figure **5.2**). Fraction three had crystallised in the tetragonal I422 space group, showing that this fraction also contained a diastereomeric dimeric BODIPYs. A Flack parameter of 0.26(8) was obtained, that unfortunately was not sufficient for direct assignment of absolute stereochemistry, however relative stereochemistry of the product could be determined. Assuming that the amino alcohol substituents have retained their (*S*)-stereochemistry, we can therefore assign fraction 3 as of dimeric helically chiral (*S,S,M,M*)-*N,N,O,C*-3-(2-aminobutan-1-ol) BODIPY (**5.2c**). Unfortunately attempts to grow crystals for fraction two failed, and thus we were unable to further examine this structure by SCXRD.

Comp.	Crystal Ref.	Crystal system	Space group	Flack	Direct Absolute	Absolute stereochem.
F1 (**5.2a**)	mjh220063_fa	triclinic	P1	0.022(11)	Y	(*S,S,P,P*)
F3 (**5.2c**)	mjh220062_fa	Tetragonal	I422	0.26(8)	N	(*S,S,M,M*)[a]

Table 5.2: Crystal data of dimeric helically chiral BODIPYs, [a] absolute stereochemistry determined by relative stereochemistry vs existing amino alcohol stereocentre.

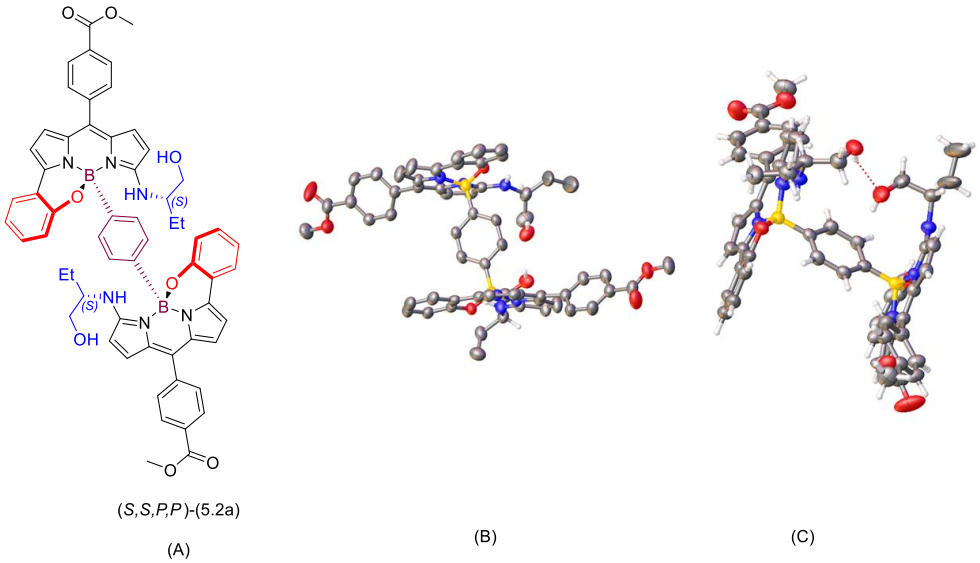

Figure 5.2: Dimeric helically chiral (*S,S,P,P*)-*N,N,O,C*-3-(2-aminobutan-1-ol) BODIPY (**5.2a**); (A) Molecular structure; (B) Single crystal X-ray structure; (C) The crystal structure including Intramolecular H-bond.

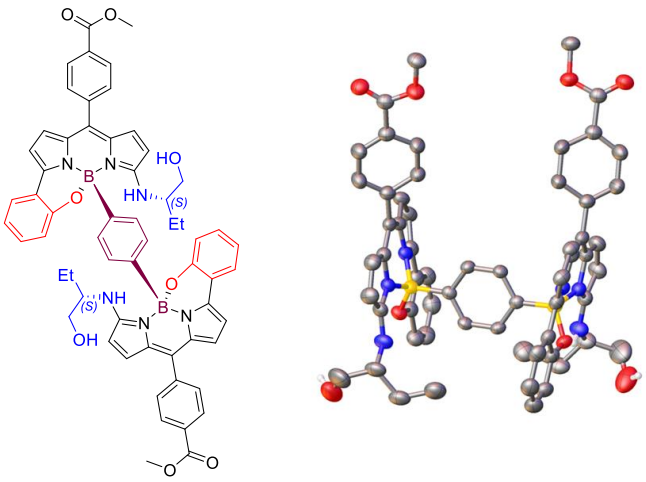

Figure 5.3: Single crystal X-ray structure of dimeric helically chiral (*S,S,M,M*) *N,N,O,C*-3-(2-aminobutan-1-ol)-BODIPY (**5.2c**)

The SCXRD data for both fraction one (*S,S,P,P*)-*N,N,O,C*-3-(2-aminobutan-1-ol) BODIPY (**5.2a**) and fraction three (*S,S,M,M*)-*N,N,O,C*-3-(2-aminobutan-1-ol) BODIPY (**5.2c**) were consistent with NMR data. The analysis of ^{1}H NMR of (*S,S,P,P*)-*N,N,O,C*-3-(2-aminobutan-1-ol) BODIPY (**5.2a**) showed a 6 H triplet at 1.04 ppm corresponding to two methyl groups for the amino alcohol substituents and 6 H singlet at 3.99 ppm corresponding to methoxy groups on the phenyl groups and (*S,S,M,M*)-*N,N,O,C*-3-(2-aminobutan-1-ol) BODIPY (**5.2c**) showed 6 H triplet at 0.07 ppm corresponding to two methyl groups and 6 H singlet at 3.97 ppm corresponding to methoxy groups. NMR analysis of fraction 2 still however proved complex, comparison of similar fraction 2 material from different reactions suggested that more than one species might be present, or that the product might be interconverting with on of the other diastereomers observed, thus this product will require further investigation in the future.

Once we have successfully determined the absolute stereo chemistry of both dimeric helically chiral (*S,S,P,P*)-*N,N,O,C*-3-(2-aminobutan-1-ol) BODIPY (**5.2a**) and (*S,S,M,M*)-*N,N,O,C*-3-(2-aminobutan-1-ol) BODIPY (**5.2c**), we turned our attention to measure their photophysical and chiroptical properties.

5.2.2 Photophysical Properties of Dimeric Helically Chiral (*S,S,P,P*)-*N,N,O,C*-3-(2-aminobutan-1-ol) BODIPY (**5.2a**), Fraction 2 (**5.2b**), and (*S,S,M,M*)-*N,N,O,C*-3-(2-aminobutan-1-ol) BODIPY (**5.2c**)

After we have successfully isolated the three diastereomeric dimeric helically chiral BODIPYs (**5.2a**), (**5.2b**), and (**5.2c**). We planned to measure UV-vis absorption and emission spectra, molar extinction coefficient (ε), the fluorescence quantum yield (ϕ_F) for each of the reaction products.

Hence, we measured the absorption and emission spectra for each diastereomeric dimeric helically chiral BODIPYs in DCM at room temperature, including for fraction 2. All three reaction products exhibited absorption maxima at around 574 nm and emission maxima at around 633 nm, with very similar peak shapes. The fluorescence quantum yields (ϕ_F) of each dimeric helically chiral (*S,S,P,P*)-*N,N,O,C*-3-(2-aminobutan-1-ol) BODIPY (**5.2a**), fraction 2 (**5.2b**), and (*S,S,M,M*)-*N,N,O,C*-3-(2-aminobutan-1-ol) BODIPY (**5.2c**) was also measured, using cresyl violet as a standard. These systems showed relatively low quantum yields of around 0.003, compared to standard BODIPYs (Table **5.3**). Interestingly, dimeric helically chiral BODIPYs exhibited a high molar extinction coefficient ($\varepsilon > 77\,000$ $mol^{-1}.cm^{-1}$) in comparison to the mono-helically chiral BODIPYs in Chapter 3.

BODIPY	Solvent	λ_{max} (abs)/nm	ε / $mol^{-1}\,cm^{-1}$	λ_{max} (em)/nm	ϕ_F[a]
(**5.2a**)	DCM	574	77 787	631	0.003
(**5.2b**)	DCM	575	51 369	633	0.003
(**5.2c**)	DCM	573	72 134	633	0.003

Table 5.3: Photophysical properties of (**5.2a**), (**5.2b**), and (**5.2c**). [a] Measured with respect to cresyl violet standard in ethanol (ϕ_F = 0.56), excitation wavelength = 547 nm.[82]

5.2.3 ECD Spectroscopy of Dimeric Helically Chiral (*S,S,P,P*)-*N,N,O,C*-3-(2-aminobutan-1-ol) BODIPY (**5.2a**), Fraction 2 (**5.2b**), and (*S,S,M,M*)-*N,N,O,C*-3-(2-aminobutan-1-ol) BODIPY (**5.2c**)

Next, we planned to measure the ECD spectra of the three diastereomeric dimeric helically chiral (*S,S,P,P*)-*N,N,O,C*-3-(2-aminobutan-1-ol) BODIPY (**5.2a**), fraction 2 and (*S,S,M,M*)-*N,N,O,C*-3-(2-aminobutan-1-ol) BODIPY (**5.2c**) to help to examine their chirality and to help to confirm their absolute stereochemistry by comparison of experimental measurements with the calculated ECD spectra.

Therefore, ECD spectra for the three diastereomeric dimeric helically chiral (*S,S,P,P*)-*N,N,O,C*-3-(2-aminobutan-1-ol) BODIPY (**5.2a**), fraction 2 (**5.2b**), and (*S,S,M,M*)-*N,N,O,C*-3-(2-aminobutan-1-ol) BODIPY (**5.2c**) were measured in DCM by Dr Jonathan Bogaerts. Interestingly, dimeric helically chiral (*S,S,P,P*)-*N,N,O,C*-3-(2-aminobutan-1-ol) BODIPY (**5.2a**) showed a strong Cotton effect ($\Delta\varepsilon_{max} \approx +85.6$ L mol^{-1} cm^{-1}) for the S_0-S_1 transition (λ_{max} = 593 nm), while, both diastereomeric dimeric helically chiral (*S,S,M,M*)-*N,N,O,C*-3-(2-aminobutan-1-ol) BODIPY (**5.2c**) and fraction 2 (**5.2b**) showed weak Cotton effects ($\Delta\varepsilon_{max} \approx -19.0$ L mol^{-1} cm^{-1}) and ($\Delta\varepsilon_{max} \approx +9.6$ L mol^{-1} cm^{-1}), respectively, for the S_0-S_1 transitions (λ_{max} = 599 nm and 577 nm) (Figure **5.4**). These results align with the crystal data and empirical rules in which *P* configuration showed positive Cotton effect, while *M* configuration exhibited negative Cotton effects as discussed in Chapter 3 with mono-helically chiral BODIPYs.

For further confirmation, we are awaiting the calculated ECD spectra from the team of Prof Hereabout for each diastereomer. This will allow us to compare them to the experimental data and help to assign their absolute stereochemistry.

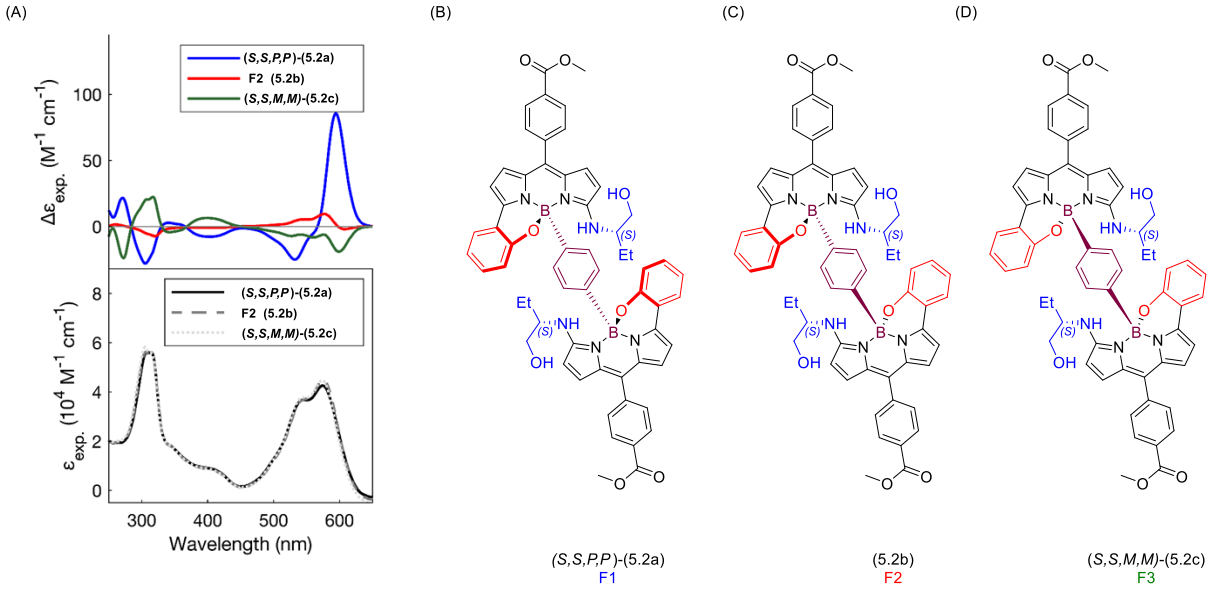

Figure 5.4: Experimental ECD spectra in DCM, (A) Top left: Helically chiral (*S,S,P,P*)-*N,N,O,C*-3-(2-aminobutan-1-ol) BODIPY (**5.2a**)(blue), fraction 2 (**5.2b**)(red) and (*S,S,M,M*)-*N,N,O,C*-3-(2-aminobutan-1-ol) BODIPY (**5.2c**)(green); (A) Bottom left: UV-vis spectrum of (*S,S,P,P*)-*N,N,O,C*-3-(2-aminobutan-1-ol) BODIPY (**5.2a**), fraction 2 (**5.2b**), and (*S,S,M,M*)-*N,N,O,C*-3-(2-aminobutan-1-ol) BODIPY (**5.2c**); (B) Molecular structure of (*S,S,P,P*)-*N,N,O,C*-3-(2-aminobutan-1-ol) BODIPY (**5.2a**); (C) Molecular structure of fraction 2 (**5.2b**); (D) Molecular structure of (*S,S,M,M*)-*N,N,O,C*-3-(2-aminobutan-1-ol) BODIPY (**5.2c**); (Figure **5.4** was created by Dr Jonathan Bogaerts).

5.2.4 CPL Spectroscopy of Dimeric Helically Chiral (*S,S,P,P*)-*N,N,O,C*-3-(2-aminobutan-1-ol) BODIPY (**5.2a**), Fraction 2 (**5.2b**), and (*S,S,M,M*)-*N,N,O,C*-3-(2-aminobutan-1-ol) BODIPY (**5.2c**)

To further understand the chiroptical properties of the three diastereomeric *S,S,P,P*)-*N,N,O,C*-3-(2-aminobutan-1-ol) BODIPY (**5.2a**), fraction 2 (**5.2b**), and (*S,S,M,M*)-*N,N,O,C*-3-(2-aminobutan-1-ol) BODIPY (**5.2c**), CPL spectra measurements were undertaken.

Thus, CPL spectra for all three dimeric diastereomeric (*S,S,P,P*)-*N,N,O,C*-3-(2-aminobutan-1-ol) BODIPY (**5.2a**), fraction 2 (**5.2b**), and (*S,S,M,M*)-*N,N,O,C*-3-(2-aminobutan-1-ol) BODIPY (**5.2c**), were measured (by Dr Dominic Black at Durham University). Unfortunately, all the three dimeric helically chiral BODIPYs showed very weak CPL spectra and as a result, we were not able to calculate g_{lum} for these systems. (Figure **5.5**).

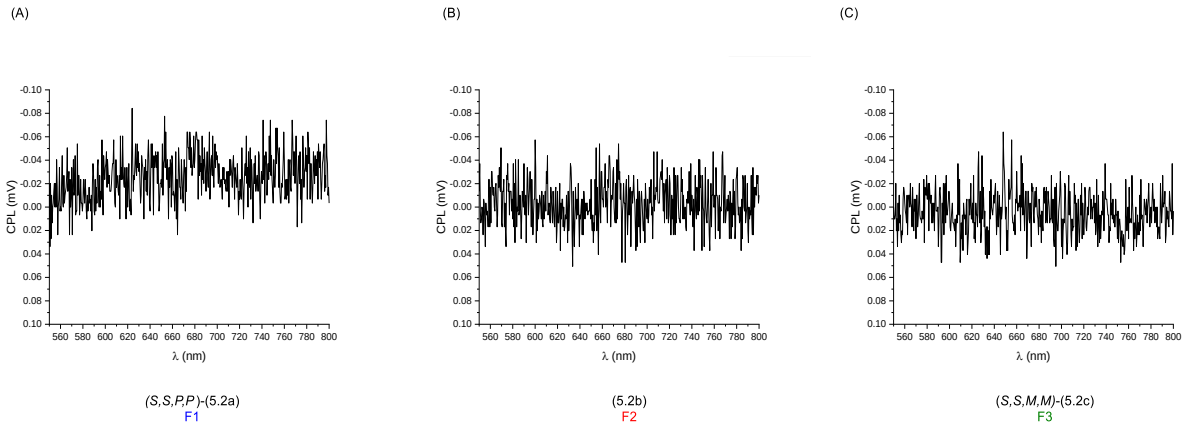

Figure 5.5: Experimental CPL spectra in DCM, excitation wavelength = 547. (A) CPL spectra of (*S,S,P,P*)-*N,N,O,C*-3-(2-aminobutan-1-ol) BODIPY (**5.2a**); (B) CPL spectra of fraction 2 (**5.2b**); and (C) CPL spectra of (*S,S,M,M*)-*N,N,O,C*-3-(2-aminobutan-1-ol) BODIPY (**5.2c**).

After reporting the first examples of dimeric helically chiral BODIPYs and characterized their photophysical and chiroptical properties, we planned to examine the chelation reaction with further phenyl di-boronic acid linkers.

5.3 Expansion of the Dimeric Helically Chiral BODIPY Series

Next, we planned to test the chelation reaction with three different commercially available aryl diboronic acids. We wished to explore both length and angle in the diboronic acid linkers, so we chose including [1,1'-biphenyl]-4,4'-diyldiboronic (**5.7**) acid, [2,2'-bithiophene]-5,5'-diyldiboronic acid (**5.8**) and dibenzo[*b,d*]furan-4,6-diyldiboronic acid (**5.9**).

Therefore, under our previous conditions, we reacted 2 equivalents of (*S*)-α-(1-hydroxybutan-2-yl)amino)-α'-(2-hydroxyphenyl) dipyrromethene (**3.6**) with [1,1'-biphenyl]-4,4'-diyldiboronic (**5.7**) in $CHCl_3$ at 35 °C for 91 hours. Following an aqueous work-up and purification by column chromatography to isolated three fractions, likely corresponding to two diastereomeric biphenyl-linked helically chiral BODIPYs (**5.10a**), (**5.10b**) in fractions 1 and 2, and fraction 3 (**5.10c**) potentially containing two different diastereomeric biphenyl-linked dimeric helically chiral BODIPYs (**5.10**), in a combined yield of 62% (Table **5.4**, Entry **1**).

In parallel, we reacted [2,2'-bithiophene]-5,5'-diyldiboronic acid (**5.8**) and two equivalents of (*S*)-α-(1-hydroxybutan-2-yl)amino)-α'-(2-hydroxyphenyl) dipyrromethene (**3.6**) in $CHCl_3$ at 35 °C for 40 hours, following an aqueous work-up and column chromatography to obtain three fractions containing diastereomeric bithiophene-linked helically chiral BODIPYs (**5.11a**), (**5.11b**), and (**5.11c**). Although further purification of the fractions is likely needed (Table **5.4**, Entry **2**).

In the final experiment, we reacted dibenzo[*b*,*d*]furan-4,6-diyldiboronic acid (**5.9**) and two equivalents of (*S*)-α-(1-hydroxybutan-2-yl)amino)-α'-(2-hydroxyphenyl) dipyrromethene (**3.6**) in $CHCl_3$ at 35 °C for 18 hours, at which time the TLC showed more than five products present. The reaction was therefore continued for a total of 63 hours, at which the TLC still showed four different products. Following work up the crude NMR showed a complex mixture of products present. Although this reaction was promising, further work on reaction optimisation, purification and product identification will be required in the future.

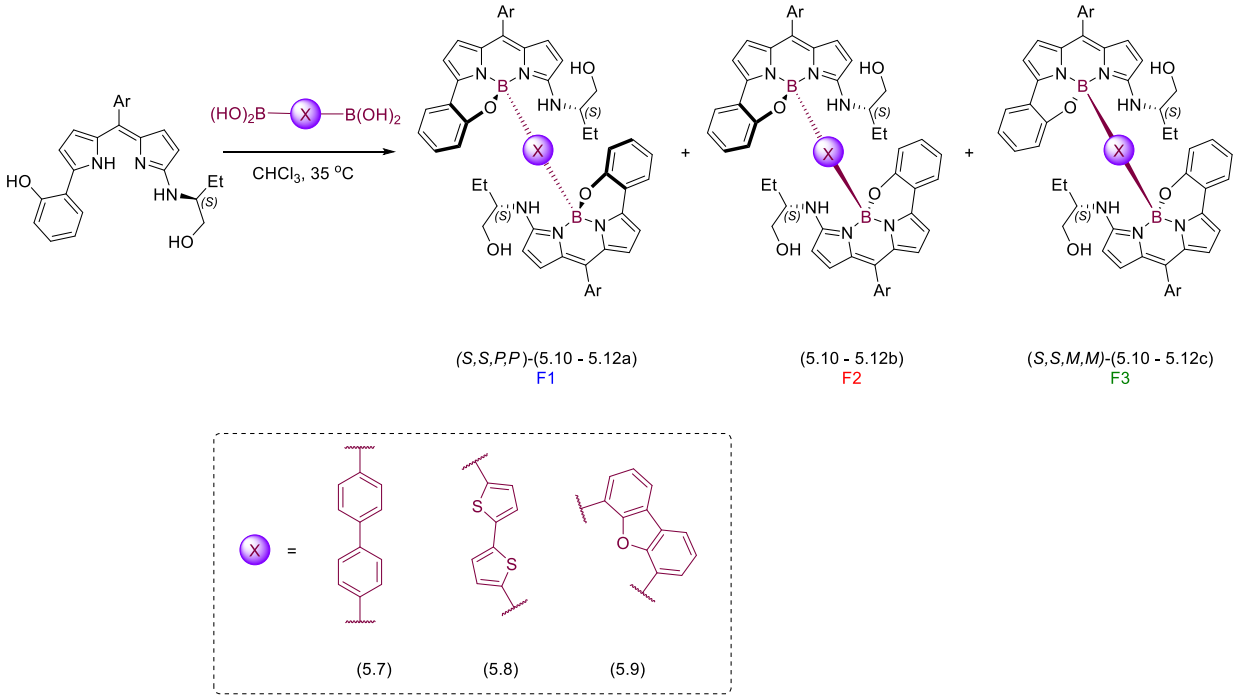

Entry	Boronic acid	Products	Yield/% F1	Yield/% F2	Yield/% F3	Yield /%
1	[1,1'-biphenyl]-4,4'-diyldiboronic acid (**5.7**)	(**5.10**)	10	28	24	62[a]
2	[2,2'-bithiophene]-5,5'-diyldiboronic acid (**5.8**)	(**5.11**)	-	11	17	28[b]
3	dibenzo[*b,d*]furan-4,6-diyldiboronic acid (**5.9**)	(**5.12**)	-	-	-	complex mixture

Table 5.4: Synthesis of dimeric helically chiral BODIPYs, [a] Isolated combined yield following column chromatography; [b] Isolated combined yield of fraction 2 and 3 only following column chromatography (Ar = *p*-($MeCO_2$)-C_6H_4-).

The ^{1}H NMR spectra of dimeric diastereomeric biphenyl-linked (*S,S,P,P*)-*N,N,O,C*-3-(2-aminobutan-1-ol) BODIPY (**5.10a**) from fraction 1, (*S,S,M,M*)-*N,N,O,C*-3-(2-aminobutan-1-ol) BODIPY (**5.10c**) from

fraction 3, showed that these molecules were symmetric dimers. In each case a 6H triplet in the aliphatic range, at 1.06 ppm (fraction 1) and 0.52 ppm (fraction 3), was observed corresponding to two chemically identical environments for the methyl groups of amino alcohol substituent. This was also supported by HRMS which gave 1085.4581 *m/z* for fraction 1, which matches with the formula $C_{66}H_{59}{}^{11}B_2N_6O_8$.

However, in the case of fraction 2 (**5.10b**), the ^{1}H NMR showed what appeared to be two triplet signals at 0.58 ppm (t, *J* = 7.4 Hz, 3H) and 1.06 ppm (t, *J* = 7.4 Hz, 3H) corresponding to methyl groups of the amino alcohol substituent, indicating the likely presence of two unsymmetrical BODIPY dimers. Interestingly, the HRMS did give 1085.4587 m/z, which matches the expected formula for a dimeric BODIPY system. Therefore, additional investigation will be needed in the future to confirm the structures of these molecules.

To gain further information about the structure of these products, we examined the ^{11}B NMR spectrum of biphenyl-linked (*S,S,P,P*)-*N,N,O,C*-3-(2-aminobutan-1-ol) BODIPY (**5.10a**)(fraction 1), to understand how many boron environments would be present. Unexpectedly, no signal was observed in the ^{11}B NMR spectra in $CDCl_3$ by 300 MHz NMR. Repeating the ^{11}B NMR spectra in $CDCl_3$ using a 500 MHz NMR showed a broad signal at ~2 ppm, which spanned from around 60 to -40 ppm, which was assigned as the borosilicate glass peak. However, a small additional overlapping peak could be observed, which we postulated was related to our sample (Figure **5.6**, Top). Borosilicate glass is known in the literature to give a broad peak with a shift of around 30 and -30 ppm, and this was confirmed through by running a ^{11}B NMR experiment using an empty NMR tube (Figure **5.6**, Middle). It was then possible to subtract the borosilicate glass peak from the original ^{11}B NMR spectra, allowing a single ^{11}B peak at 2.10 ppm to be observed for biphenyl-linked (*S,S,P,P*)-*N,N,O,C*-3-(2-aminobutan-1-ol) BODIPY (**5.10a**), again suggesting a symmetrical product had been formed (Figure **5.6**, Bottom). Note that the NMR experiments were done by Dr C. Wills and Dr C. Dixon.

With a successfully demonstration of the formation of dimeric helically chiral BODIPYs through point-to-helical chirality approach. Next, we planned to simplify our previous dimeric chiral system by removing the chiral axillaries to reduce the number of products formed, and to better understand if the chirality of the first forming boron centre will influence the formation of the second boron centre.

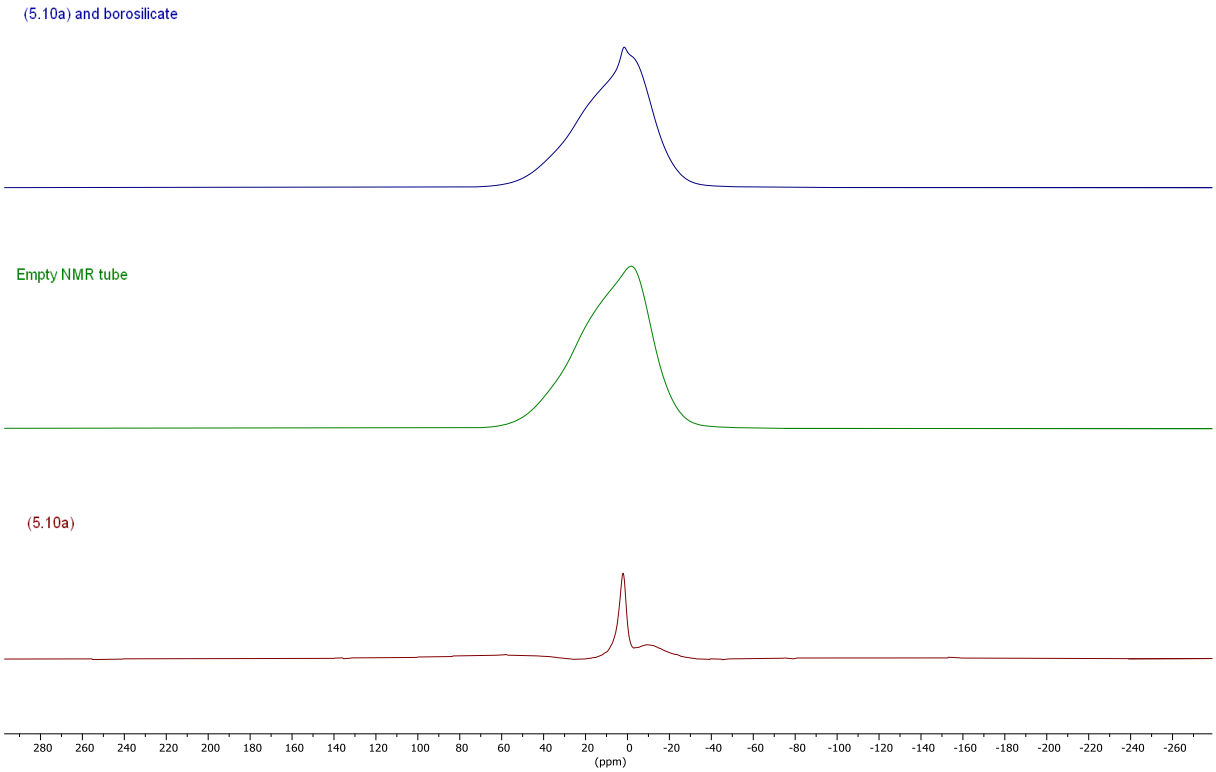

Figure 5.6: ^{11}B NMR spectra (700 MHz, $CDCl_3$). Top: ^{11}B NMR of *S,S,P,P*)-*N,N,O,C*-3-(2-aminobutan-1-ol) BODIPY (**5.10a**)(blue); Middle: ^{11}B NMR of empty NMR tube (green); Bottom: ^{11}B NMR of *S,S,P,P*)-*N,N,O,C*-3-(2-aminobutan-1-ol) BODIPY (**5.10a**) after removing the borosilicate peak (red).

5.4 Synthesis of Dimeric Helically Chiral BODIPYs without Chiral axillaries

Next we planned to synthesize dimeric helically chiral BODIPYs without chiral amino alcohols groups to simplify the system and study the number of dimeric BODIPYs that will form. To do this, we planned to use a pyrrole group instead of chiral amino alcohols at the 3-position of the dipyrromethene starting materials, followed by chelation with a dimeric boronic acid.

Our synthetic route therefore involves four steps: an S_NAr reaction to introduce a 1*H*-pyrrole group at the 3-position of a 3,5-dihalo-BODIPYs, followed by a Suzuki Miyaura cross-coupling between 3-(1*H*-pyrrol-2-yl)-5-halo BODIPY (**5.13** or **5.14**) and (2-hydroxyphenyl)boronic acid (**3.19**). Subsequently, a de-chelation reaction will be used to remove BF_2 group using $AlCl_3$. Finally, chelation step will be performed to form dimeric helically chiral BODIPYs (**5.16**) (Scheme **5.4**).

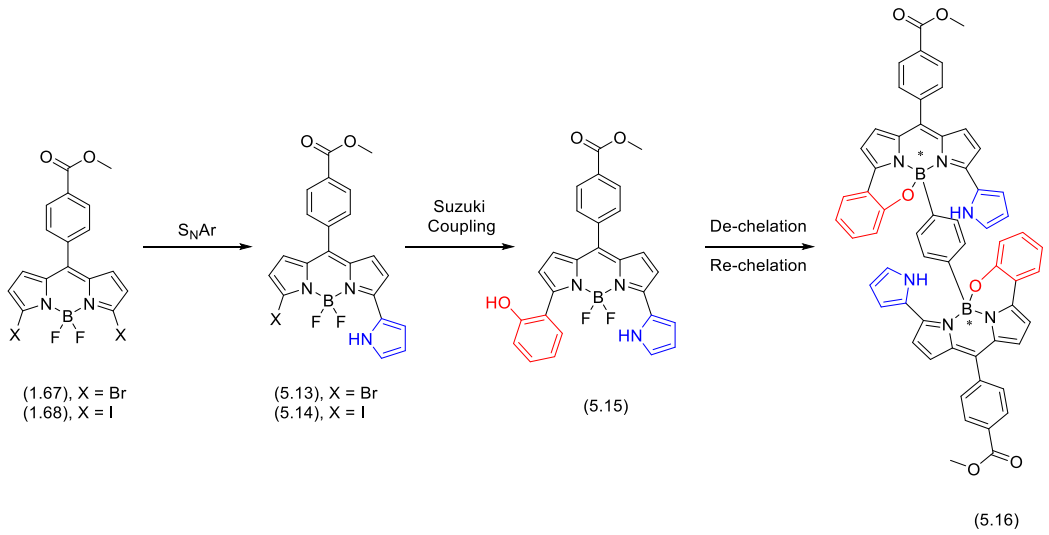

Scheme 5.4: Planned route to dimeric helically chiral BODIPYs.

5.4.1 Synthesis of 3-(1*H*-pyrrol-2-yl)-5-bromo BODIPY (**5.13**) and 3-(1*H*-pyrrol-2-yl)-5-iodo BODIPY (**5.14**) via S_NAr reaction

The first step of our synthetic route was synthesis of 3-(1*H*-pyrrol-2-yl)-5-bromo BODIPY (**5.13**) and 3-(1*H*-pyrrol-2-yl)-5-iodo BODIPY (**5.14**), via an S_NAr reaction between 3,5-dihalo-BODIPYs and 1*H*-pyrrole. Our procedure was based on the work of Jiao *et al*., in which they showed S_NAr reactions between 3,5-dibromo BODIPYs and neat 1*H*-pyrrole or substituted pyrroles in toluene under reflux.[99]

Therefore, we reacted 3,5-dibromo BODIPY (**1.67**) and excess of 1*H*-pyrrole in toluene at 80 °C. The reaction was monitored by TLC which showed the formation of a new purple product after 1 hour, alongside remaining starting material. After a further 8 hours of reaction, TLC showed an increasing presence of the new purple product, however the starting material was still present. Therefore, we increased the temperature of the reaction to reflux for a further 1 hour, after which TLC showed the presence of a new purple product, starting material, and a new blue product. As a result of this the reaction was stopped by cooling to room temperature, to minimise the formation by-products such as di-substituted-BODIPYs. The reaction mixture was diluted with DCM, and following aqueous work-up and purification by column chromatography the desired 3-(1*H*-pyrrol-2-yl)-5-bromo-BODIPY (**5.13**) was isolated in a 37% yield (Table **5.5**, Entry 1).

Next, we examined S_NAr reaction between 3,5-diiodo BODIPY (**1.68**) and 1*H*-pyrrole (**1.32**), used as a solvent, at 80 °C. The reaction was monitored by TLC which showed that the starting material was consumed, and a new purple product had been formed after 24 hours. The excess amount of 1*H*-pyrrole was removed under reduced pressure and the crude reaction mixture was purified by column

chromatography to obtain 3-(1*H*-pyrrol-2-yl)-5-iodo-BODIPY (**5.14**) in a yield of 78% (Table **5.5**, Entry 2).

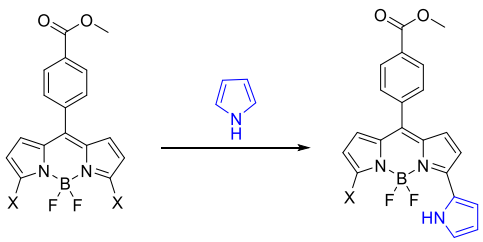

(1.67), X = Br
(1.68), X = I

(5.13), X = Br
(5.14), X = I

Entry	Starting material	Solvent	Reaction Temp. and Time	Product	Yield/%
1	(**1.67**), X = Br	Toluene	80 °C, 8 h then reflux for 1 h	(**5.13**)	37
2	(**1.68**), X = I	Pyrrole	80 °C, 24 h	(**5.14**)	78

Table 5.5: Synthesis of 3-(1*H*-pyrrol-2-yl)-5-bromo BODIPY (**5.13**) and 3-(1*H*-pyrrol-2-yl)-5-iodo-BODIPY (**5.14**) via S_NAr reaction.

The structure of both 3-(1*H*-pyrrol-2-yl)-5-bromo BODIPY (**5.13**) and 3-(1*H*-pyrrol-2-yl)-5-iodo BODIPY (**5.14**) were confirmed by NMR spectra. The analysis of ^{1}H NMR of 3-(1*H*-pyrrol-2-yl)-5-bromo-BODIPY (**5.13**) showed signals corresponding to four chemically inequivalent pyrrolic protons at 6.95 ppm (d, *J* = 4.8 Hz, 1H), 6.85 ppm (d, *J* = 4.8 Hz, 1H), 6.47 ppm (d, *J* = 4.1 Hz, 1H), and 6.43 ppm (d, *J* = 4.1 Hz, 1H) indicating that a single substitution had occurred to desymmetrise the BODIPY. In addition, there was a broad signal at 10.55 ppm corresponding to NH group of the newly added pyrrole ring (Figure **5.7**).

The analysis of ^{1}H NMR of 3-(1*H*-pyrrol-2-yl)-5-iodo BODIPY (**5.14**) was similar and showed four doublets at 6.95 ppm (d, *J* = 4.8 Hz, 1H), 6.84 ppm (d, *J* = 4.8 Hz, 1H), 6.63 ppm (d, *J* = 4.0 Hz, 1H), and 6.39 ppm (d, *J* = 4.0 Hz, 1H) corresponding to pyrrolic ring of the core of BODIPY. Additionally, a broad signal at 10.56 ppm corresponding to NH group of the newly added pyrrole ring (Figure **5.7**). For further confirmation, the structure of 3-(1*H*-pyrrol-2-yl)-5-iodo BODIPY (**5.14**) was validated by HRMS, which showed a molecular ion at *m/z* = 518.0342 $[M+H]^+$, which corresponded to a molecular formula of $C_{21}H_{16}{}^{11}BF_2IN_3O_2$.

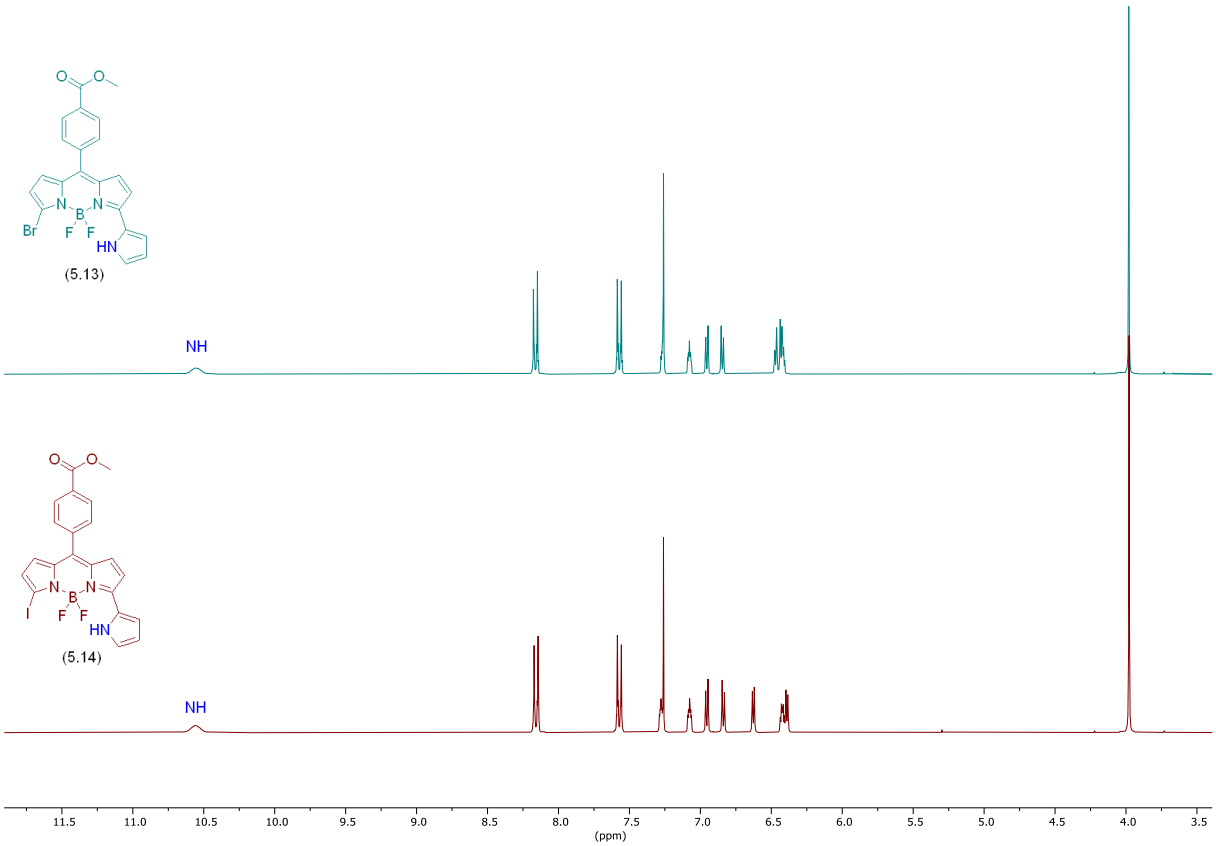

Figure 5.7: ^{1}H NMR spectra (300 MHz, $CDCl_3$). Top: ^{1}H NMR of the 3-(1*H*-pyrrol-2-yl)-5-bromo BODIPY (**5.13**) (blue) following column chromatography; Bottom: ^{1}H NMR 3-(1*H*-pyrrol-2-yl)-5-iodo BODIPY (**5.14**) (red), following column chromatography

For further support to confirm the structure of each 3-(1*H*-pyrrol-2-yl)-5-bromo BODIPY (**5.13**) and 3-(1*H*-pyrrol-2-yl)-5-iodo BODIPY (**5.14**) as a mono-substituted BODIPY, SCXRD was employed. Crystals were grown through a layered liquid-liquid diffusion experiment (DCM : hexane, 1:3) for both samples. A suitable single crystal of both 3-(1*H*-pyrrol-2-yl)-5-bromo BODIPY (**5.13**) and 3-(1*H*-pyrrol-2-yl)-5-iodo BODIPY (**5.14**) were analysed by single crystal X-ray diffraction. Interestingly, the two compounds have isomorphous crystal structures, both monoclinic with the $P2_1$ space group, with 4 molecules in the unit cell (Z = 4), and showing an intramolecular H-bond, from NH to F (Figure **5.8**).

In conclusion, we have successfully demonstrated that both 3,5-dibromo BODIPY (**1.67**) and 3,5-diiodo BODIPY (**1.68**) can be undergo S_NAr reaction to form 3-(1*H*-pyrrol-2-yl)-5-bromo BODIPY (**5.13**) and 3-(1*H*-pyrrol-2-yl)-5-iodo BODIPY (**5.14**). The structures were confirmed by NMR and SCXRD analysis. In future, we plan to complete our proposed synthetic route to produce helically dimeric BODIPYs, building upon our methodologies outlined in Chapter 3 and 4 of our previous work.

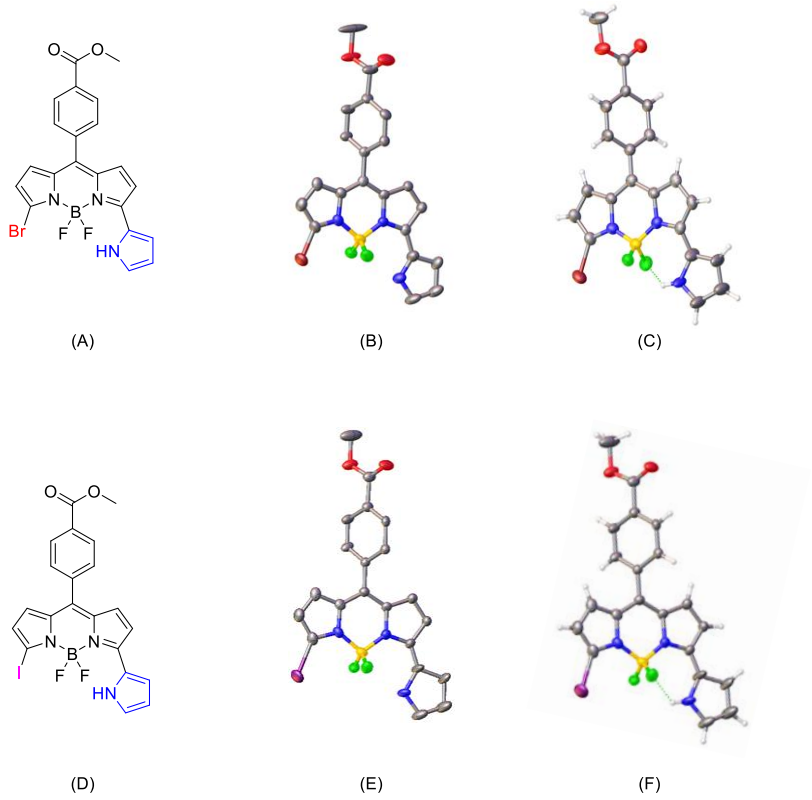

Figure 5.8: (A) Molecular structure of 3-(1*H*-pyrrol-2-yl)-5-bromo BODIPY (**5.13**), (B) Single crystal X-ray structure of 3-(1*H*-pyrrol-2-yl)-5-bromo BODIPY (**5.13**); (C) Intramolecular H-bond; (D) Molecular structure of 3-(1*H*-pyrrol-2-yl)-5-iodo BODIPY (**5.14**), (E) Single crystal X-ray structure of 3-(1*H*-pyrrol-2-yl)-5-iodo BODIPY (**5.14**); (F) Intramolecular H-bond

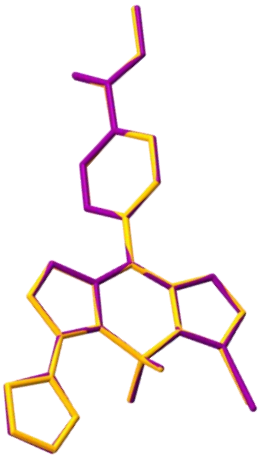

Figure 5.9: Overlay diagram for both 3-(1*H*-pyrrol-2-yl)-5-bromo BODIPY (**5.13**) (orange) and 3-(1*H*-pyrrol-2-yl)-5-iodo BODIPY (**5.14**) (purple), (Figure **5.9** created by Dr P. Waddell).

5.5 Synthetic Routes Toward Trimeric Helically Chiral BODIPY Arrays

Next, we planned to return to the use of point-to-helical chirality transfer approaches, but to synthesize larger chiral BODIPY arrays, namely a trimeric helically chiral *N,N,O,C*-BODIPY. To achieve this, we need to build a tri-boronic acid linker which can be used to chelate three units of amino alcohol substituted dipyrromethenes (**3.6**) (Scheme **5.5**).

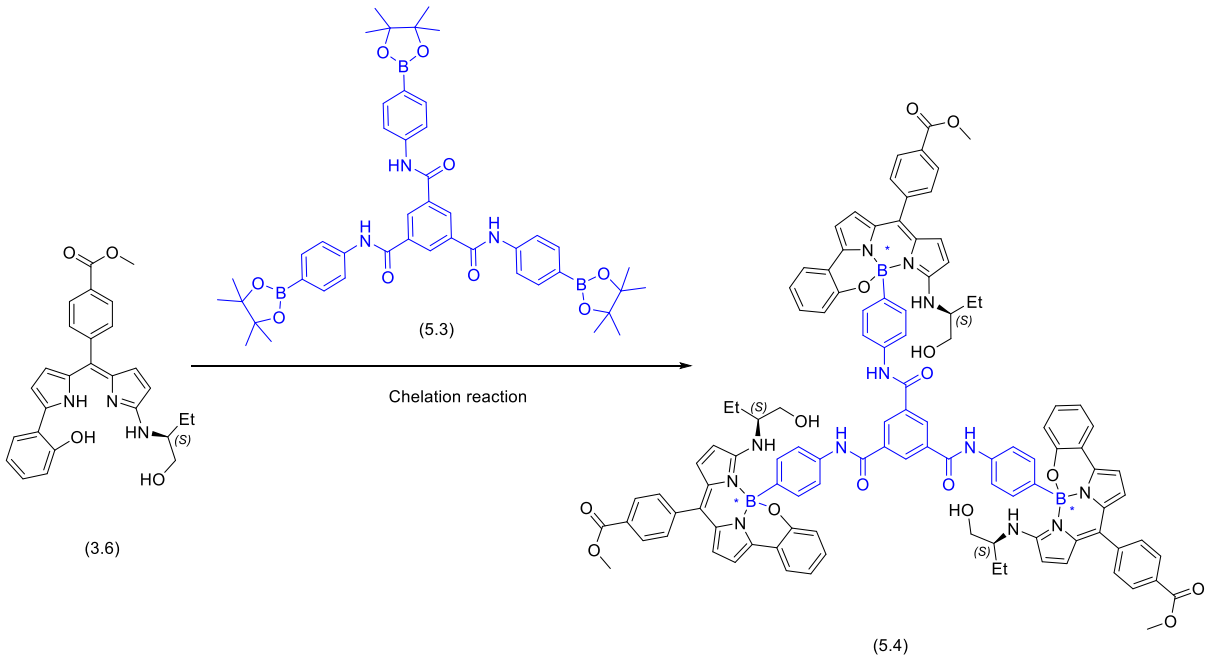

Scheme 5.5: Planned route to trimeric helically chiral BODIPY arrays via a tri-boronic acid linker

5.5.1 Synthesis of Tri-boronic Acid Linker

To achieve our planned trimeric helically chiral BODIPY arrays, first we need to synthesize a suitable tri-boronic acid linker. We planned to make this linker via an amide coupling approach, using benzene-1,3,5-tricarboxylic acid (**5.18**) as the central core, to which we could couple commercially available aryl boronic acids (Scheme **5.6**).

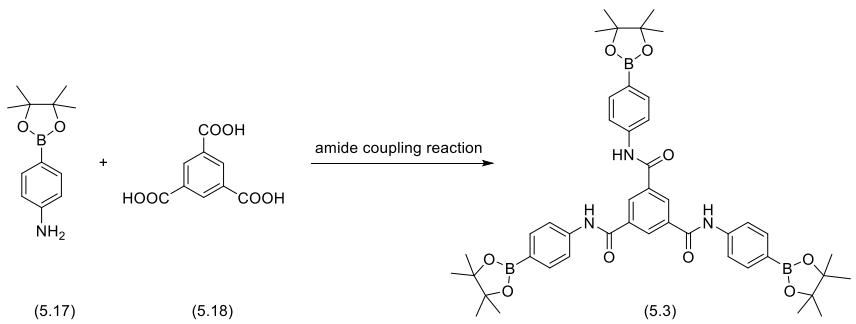

Scheme 5.6: Synthesis of N^1,N^3,N^5-tris(4-(4,4,5,5-tetramethyl-1,3,2-dioxaborolan-2-yl)phenyl)benzene-1,3,5-tricarboxamide (**5.3**)

5.5.2 Amide Coupling between Amine and Benzoic Acid (**5.19**)

As a test reaction of the proposed amide coupling, we decided to first make a mono-boronic acid including an amide linker.[100] Therefore, we activated 1 eq. of benzoic acid (**5.19**) with HATU in dry DMF at room temperature, followed by the addition of 1 eq. of 4-(4,4,5,5-tetramethyl-1,3,2-dioxaborolan-2-yl)aniline (**5.17**) and 2.5 equivalents of DIPEA. The reaction mixture was stirred for 18 hours then quenched with water, extracted with ethyl acetate, and washed with aqueous 0.2 M NaOH, 0.4 M HCl, brine, dried over Na_2SO_4 and the solvent removed under reduced pressure. The crude reaction mixture was then purified by column chromatography to obtain the desired *N*-(4-(4,4,5,5-tetramethyl-1,3,2-dioxaborolan-2-yl)phenyl)benzamide (**5.20**), in an excellent yield 71% (Scheme **5.7**), along with a second fraction containing an expected by-product from the HATU coupling in a 8% yield, 3*H*-[1,2,3]triazolo[4,5-*b*]pyridin-3-yl benzoate (**5.21**) as determined by ^{1}H NMR (Figure **5.12**). This test coupling was repeated with 1.1 eq. of benzoic acid, resulting in a quantitative yield of *N*-(4-(4,4,5,5-tetramethyl-1,3,2-dioxaborolan-2-yl)phenyl)benzamide (**5.20**) following chromatography.

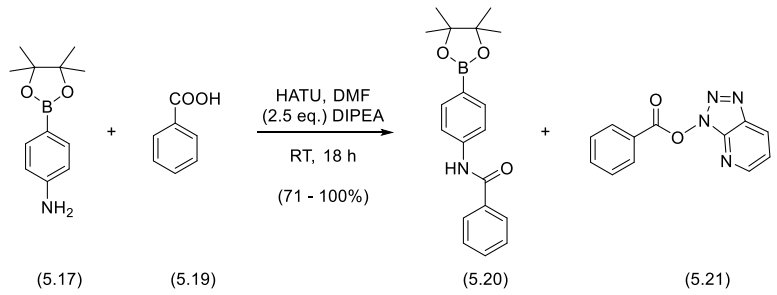

Scheme 5.7: HATU coupling to synthesize *N*-(4-(4,4,5,5-tetramethyl-1,3,2-dioxaborolan-2-yl)phenyl)benzamide (**5.20**).

The structure of *N*-(4-(4,4,5,5-tetramethyl-1,3,2-dioxaborolan-2-yl)phenyl)benzamide (**5.20**) was confirmed by the analysis of ^{1}H NMR spectrum which showed 12 H singlet in aliphatic range at 1.34 ppm corresponding to four methyl groups and broad signal at 8.02 ppm corresponding to NH group. In addition, two doublets at 7.81 ppm (d, *J* = 8.6 Hz, 2H) and 7.68 ppm (d, *J* = 8.6 Hz, 2H) corresponding to 1,4-subistituted phenyl and 5H multiples at 7.87-7.83 ppm (m, 2H),7.56-7.49 ppm (m, 1H), and 7.49-7.41 ppm (m, 2H) corresponding to phenyl ring.

For further supported for the structure of *N*-(4-(4,4,5,5-tetramethyl-1,3,2-dioxaborolan-2-yl)phenyl)benzamide (**5.20**), crystals were grown via slow evaporation of methanol solution. A suitable single crystal was analysed by SCXRD, showing that *N*-(4-(4,4,5,5-tetramethyl-1,3,2-dioxaborolan-2-yl)phenyl)benzamide (**5.20**) had crystallised in the monoclinic $P2_1/c$ space group with 4 molecules in the unit cell (Z = 4) (Figure **5.10**).

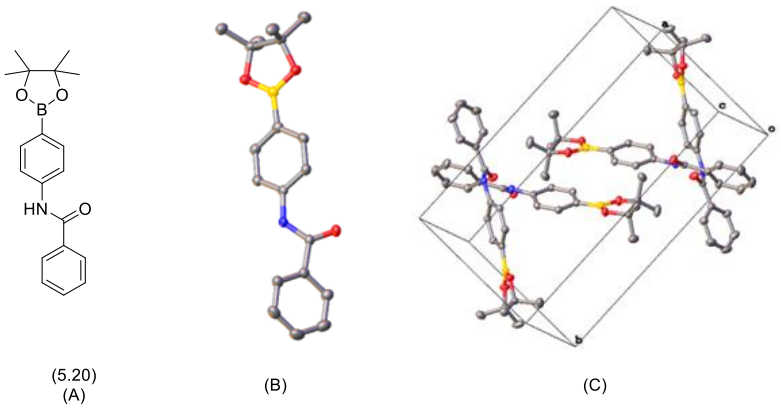

Figure 5.10: *N*-(4-(4,4,5,5-tetramethyl-1,3,2-dioxaborolan-2-yl)phenyl)benzamide (**5.20**); (A) Molecular structure, (B) One molecule in the single crystal X-ray structure, (C) Packing of the molecules in the unit cell.

The structure of the by-product 3*H*-[1,2,3]triazolo[4,5-*b*]pyridin-3-yl benzoate (**5.21**) was confirmed by ^{1}H NMR spectrum which showed the presence of three double doublets at 8.74 ppm (dd, *J* = 4.5, 1.4 Hz, 1H), 8.47 ppm (dd, *J* = 8.4, 1.4 Hz, 1H), and 7.47 ppm (dd, *J* = 8.4, 4.5 Hz, 1H) corresponding to pyridinic protons, and three multiples at 8.34-8.28 ppm (m, 2H), 7.81-7.73 ppm (m, 1H), and 7.64-7.57 ppm (m, 2H) corresponding to the phenyl group (Figure **5.12**).

For further confirmation, we attempted to grow crystal of the by-product 3*H*-[1,2,3]triazolo[4,5-*b*]pyridin-3-yl benzoate (**5.21**), through slow evaporation of methanol solution. Interestingly, although crystals were obtained, analysis by SCXRD showed that instead of the expected molecule, we got a crystal of a new molecule, 3*H*-[1,2,3]triazolo[4,5-*b*]pyridin-3-ol (**5.22**), which matched the known crystal structure in the (CCDC: BELBUP) (Figure **5.11**).

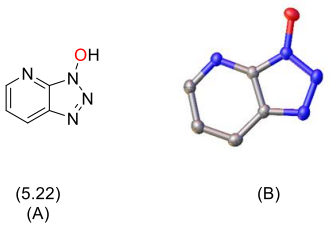

Figure 5.11: 3*H*-[1,2,3]triazolo[4,5-*b*]pyridin-3-ol (**5.22**); (A) Molecular structure, (B) Single crystal X-ray structure of 3*H*-[1,2,3]triazolo[4,5-*b*]pyridin-3-ol (**5.22**) (CCDC: BELBUP).

The observation of a crystal of 3*H*-[1,2,3]triazolo[4,5-*b*]pyridin-3-ol (**5.22**) was surprising as it does not match the ^{1}H NMR of the by-product from the reaction, which we had assigned as 3*H*-[1,2,3]triazolo[4,5-*b*]pyridin-3-yl benzoate (**5.21**). Examination of the ^{1}H NMR of the crystalline material, obtained from the recrystallization experiment, showed that the presence of only three

double doublets at 8.65 ppm (dd, *J* = 4.5, 1.3 Hz, 1H), 8.46 ppm (dd, *J* = 8.4, 1.3 Hz, 1H) and 7.43 ppm (dd, *J* = 8.4, 4.7 Hz, 1H) corresponding to pyridinic protons, suggesting that the bulk crystalline material was 3*H*-[1,2,3]triazolo[4,5-*b*]pyridin-3-ol (**5.22**) (Figure **5.12**).

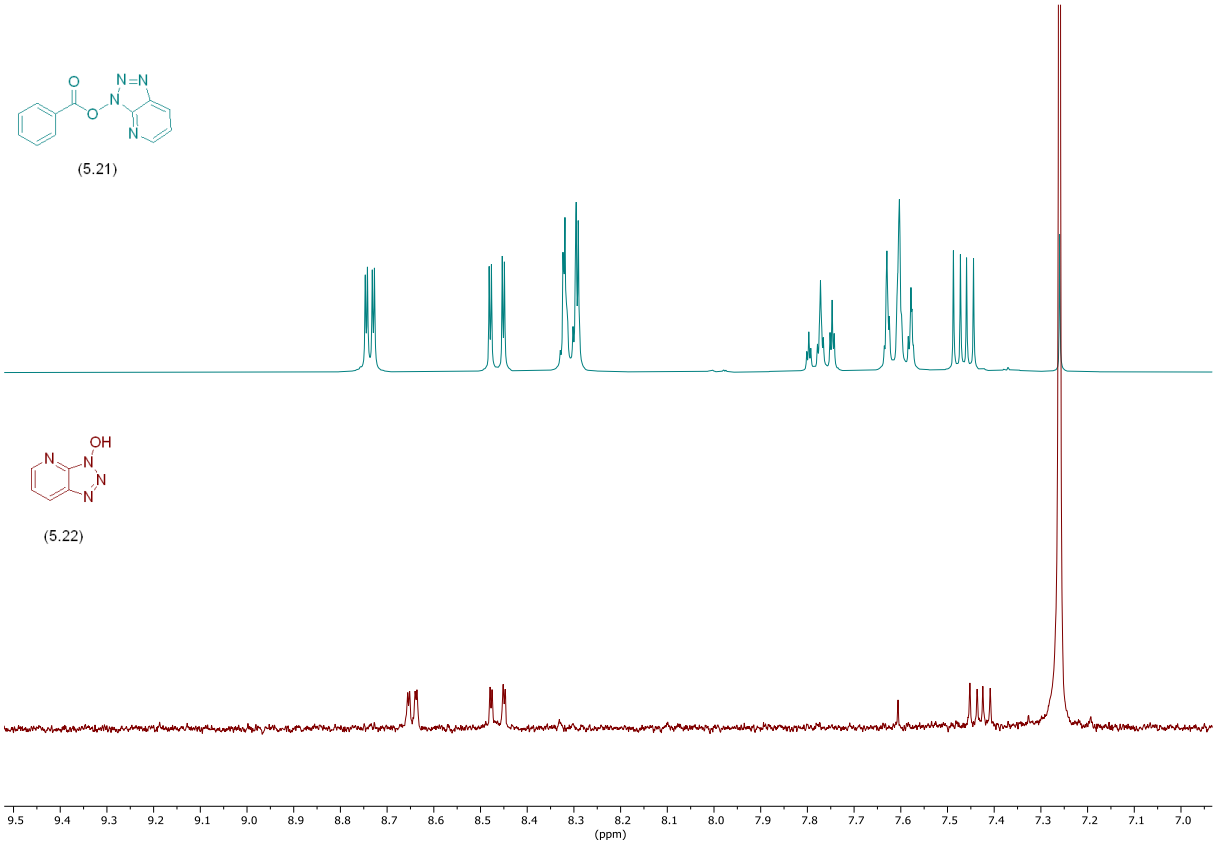

Figure 5.12: Comparison of the ^{1}H NMR spectra (300 MHz, $CDCl_3$) for 3*H*-[1,2,3]triazolo[4,5-*b*]pyridin-3-yl benzoate (**5.21**) before crystallisation (Top, green) and 3*H*-[1,2,3]triazolo[4,5-*b*]pyridin-3-ol (**5.22**) after crystallisation (Bottom, red).

We propose that 3*H*-[1,2,3]triazolo[4,5-*b*]pyridin-3-ol (**5.22**) had been formed in the crystallisation experiment, by the reaction between 3*H*-[1,2,3]triazolo[4,5-*b*]pyridin-3-yl benzoate (**5.21**) and either the methanol crystallisation solvent, or water.

In conclusion, we successfully have synthesised a mono-boronic acid including an amide linker through a test amide coupling reaction between benzoic acid (**5.19**) and 4-(4,4,5,5-tetramethyl-1,3,2-dioxaborolan-2-yl)aniline (**5.17**). Next, we planned to use the similar conditions to synthesis a tri-boronic acid linker.

5.5.3 Synthesis of Tri-boronic Acid Linker (**5.3**)

We planned to synthesise a tri-boronic acid linker (**5.3**) which will be used to chelate three units of (*S*)-α-(1-hydroxybutan-2-yl)amino)-α'-(2-hydroxyphenyl) dipyrromethene (**3.6**) to make novel trimeric-

helically chiral BODIPYs. We planned to use two different methods for the synthesis of N^1,N^3,N^5-tris(4-(4,4,5,5-tetramethyl-1,3,2-dioxaborolan-2-yl)phenyl)benzene-1,3,5-tricarboxamide (**5.3**) (Scheme **5.8**).

Method A will be based on our previous amide coupling conditions, using the HATU reagent. The reaction will involve benzene-1,3,5-tricarboxylic acid (**5.18**) and 4-(4,4,5,5-tetramethyl-1,3,2-dioxaborolan-2-yl)aniline (**5.17**). Similarly, Method B will involve the reaction between benzene-1,3,5-tricarbonyl trichloride (**5.23**) and 4-(4,4,5,5-tetramethyl-1,3,2-dioxaborolan-2-yl)aniline (**5.17**) (Scheme **5.8**).

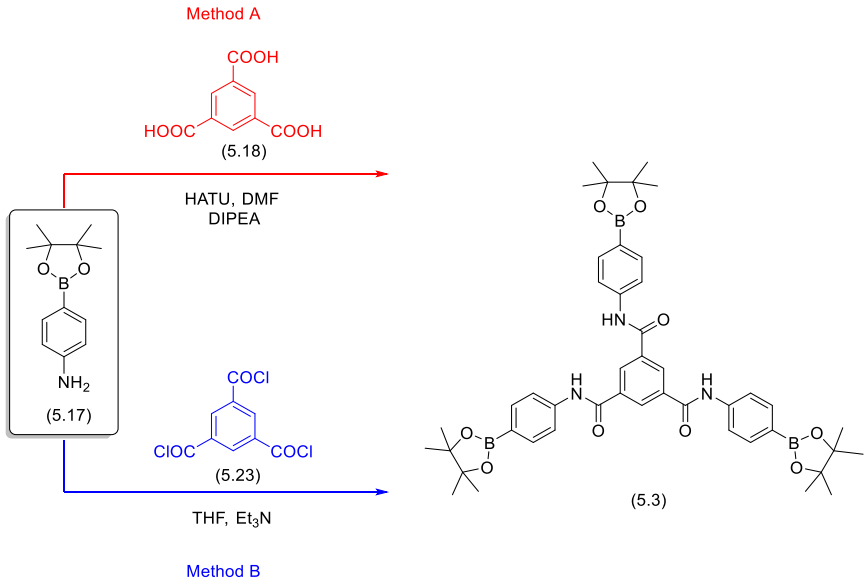

Scheme 5.8: Plan to synthesis of N^1,N^3,N^5-tris(4-(4,4,5,5-tetramethyl-1,3,2-dioxaborolan-2-yl)phenyl)benzene-1,3,5-tricarboxamide (**5.3**)

We started with method A, following preliminary experiments, we activated 1 eq. of benzene-1,3,5-tricarboxylic acid (**5.18**) with 3.5 equivalents of HATU in dry DMF at room temperature, followed by the dropwise addition of 3.5 eq. of 4-(4,4,5,5-tetramethyl-1,3,2-dioxaborolan-2-yl)aniline (**5.17**) in dry DMF, and finally 10 equivalents of DIPEA. The reaction mixture was stirred for 48 hours then quenched with water, at which point a white precipitate was formed, which was dissolved in ethyl acetate. The mixture was extracted with further ethyl acetate, and the solvent removed under reduced pressure. Methanol was then added to the crude product, resulting to form a white precipitate. This was collected by filtration, washed with water and methanol, and left to dry in air, to give a white solid in a yield of 67% (Scheme **5.9**).

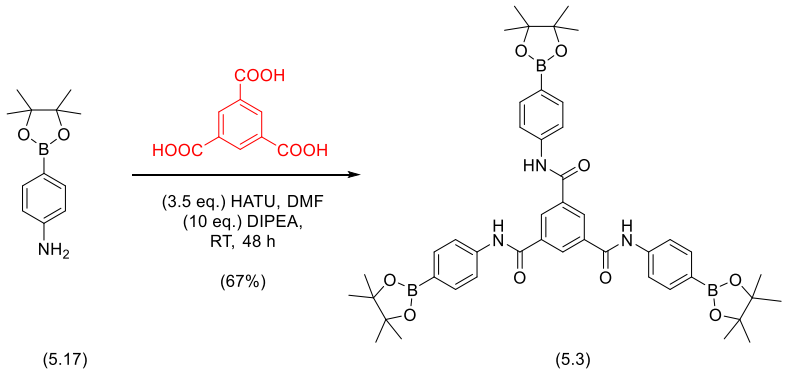

Scheme 5.9: Synthesis of N^1,N^3,N^5-tris(4-(4,4,5,5-tetramethyl-1,3,2-dioxaborolan-2-yl)phenyl)benzene-1,3,5-tricarboxamide (**5.3**)

The structure of N^1,N^3,N^5-tris(4-(4,4,5,5-tetramethyl-1,3,2-dioxaborolan-2-yl)phenyl)benzene-1,3,5-tricarboxamide (**5.3**) was confirmed by ^{1}H NMR spectrum in d_6-DMSO which showed a 36H singlet in aliphatic range at 1.30 ppm corresponding to the 12 methyl groups of the boron esters, two doublets at 7.86 ppm (d, J = 8.7 Hz, 6H) and 7.70 ppm (d, J = 8.4 Hz, 6H) corresponding to the *para*-substituted aromatic rings. In addition, a broad peak at 10.67 ppm was observed corresponding to the three NH amide groups. The structure of N^1,N^3,N^5-tris(4-(4,4,5,5-tetramethyl-1,3,2-dioxaborolan-2-yl)phenyl)benzene-1,3,5-tricarboxamide (**5.3**) was further validated by HRMS, which showed a peak at 811.4332 *m/z* which is consistent with the mass of 811.4326 *m/z* as calculated for the $[M+H]^+$ ion, $C_{45}H_{55}{}^{10}B_3N_3O_9$.

We attempted to grow crystals of N^1,N^3,N^5-tris(4-(4,4,5,5-tetramethyl-1,3,2-dioxaborolan-2-yl)phenyl)benzene-1,3,5-tricarboxamide (**5.3**) by slow evaporation from different solvents including DCM, chloroform, methanol (poor solubility), DMSO, and DMF. We successfully obtained crystals of N^1,N^3,N^5-tris(4-(4,4,5,5-tetramethyl-1,3,2-dioxaborolan-2-yl)phenyl)benzene-1,3,5-tricarboxamide (**5.3**) from DMF solution. A single crystal then was analysed by SCXRD showing that N^1,N^3,N^5-tris(4-(4,4,5,5-tetramethyl-1,3,2-dioxaborolan-2-yl)phenyl)benzene-1,3,5-tricarboxamide (**5.3**) had crystallised in the monoclinic $P2_1/c$ space group as a tetra-DMF solvate. Interestingly the crystal structure contained four molecules in the unit cell, showing H--O H-bond between N^1,N^3,N^5-tris(4-(4,4,5,5-tetramethyl-1,3,2-dioxaborolan-2-yl)phenyl)benzene-1,3,5-tricarboxamide (**5.3**) and DMF (Figure **5.13**).

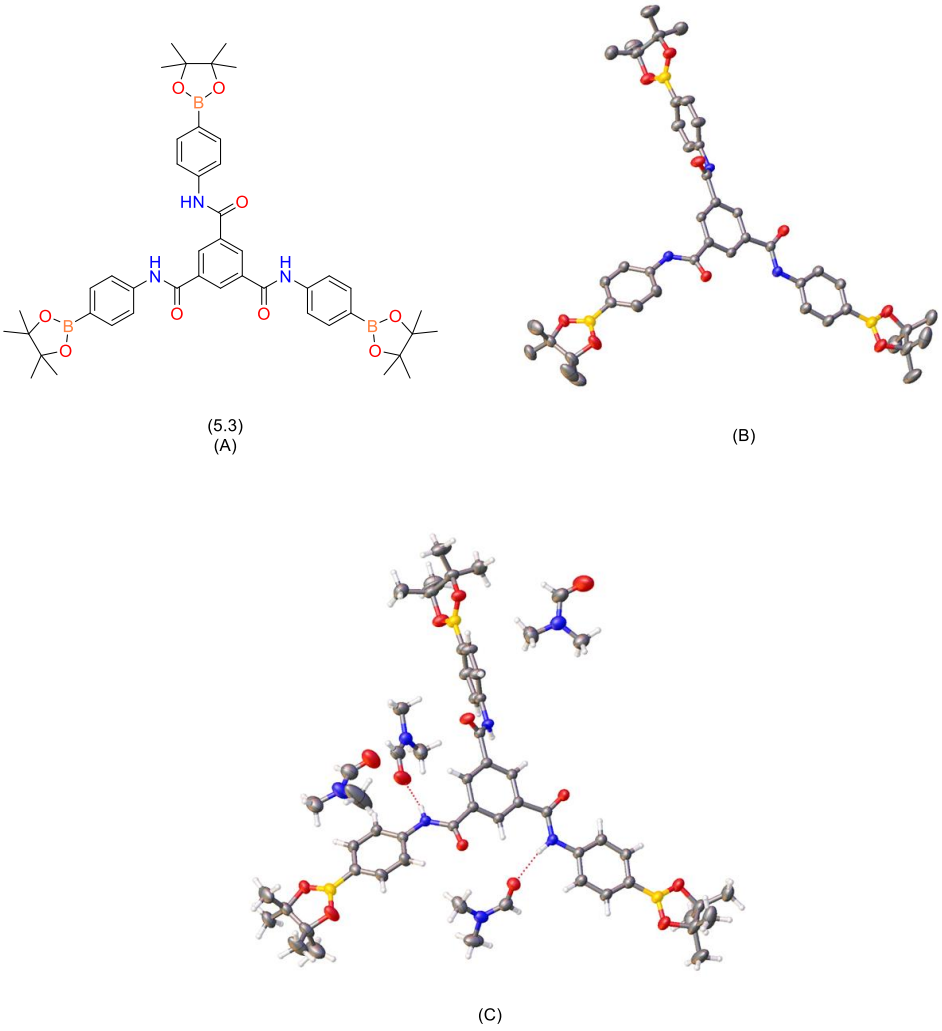

Figure 5.13: (A) N^1,N^3,N^5-tris(4-(4,4,5,5-tetramethyl-1,3,2-dioxaborolan-2-yl)phenyl)benzene-1,3,5-tricarboxamide (**5.3**), (B) Single crystal X-ray structure; (C) Showing H-bonding with DMF.

In parallel work, via method B we examined the amide coupling reaction between benzene-1,3,5-tricarbonyl trichloride (**5.23**) and 4-(4,4,5,5-tetramethyl-1,3,2-dioxaborolan-2-yl)aniline (**5.17**). Following the procedure reported literature, we dissolved one equivalent of benzene-1,3,5-tricarbonyl trichloride (**5.23**) in dry THF at 0 °C for 10 min, and then added 4-(4,4,5,5-tetramethyl-1,3,2-dioxaborolan-2-yl)aniline (**5.17**) in a small portions to form a suspension. The reaction mixture was then stirred at room temperature for 96 h, after which the solvent was removed under reduced pressure. The resulting solid product was then suspended in methanol, filtered, and the collected solid was washed with water and methanol to obtain the desired N^1,N^3,N^5-tris(4-(4,4,5,5-tetramethyl-1,3,2-dioxaborolan-2-yl)phenyl)benzene-1,3,5-tricarboxamide (**5.3**) in a yield of 34% (Scheme **5.10**).

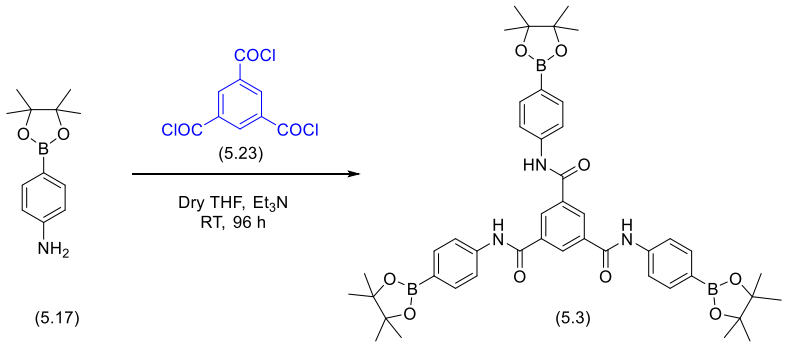

Scheme 5.10: Synthesis of N^1,N^3,N^5-tris(4-(4,4,5,5-tetramethyl-1,3,2-dioxaborolan-2-yl)phenyl)benzene-1,3,5-tricarboxamide (**5.3**)

The ^{1}H NMR spectrum of N^1,N^3,N^5-tris(4-(4,4,5,5-tetramethyl-1,3,2-dioxaborolan-2-yl)phenyl)benzene-1,3,5-tricarboxamide (**5.3**) match with our previous results, helping to confirm the structure. Interestingly, ^{11}B NMR spectrum in d_6-DMSO showed a broad signal spanned from 61 to -41 ppm which assigned a borosilicate glass peak, as we have discussed previously. Even with the use of a quartz NMR tube, the broad signal remained, due to the presence of borosilicate glass in the NMR probe. Therefore, we measured a ^{11}B NMR spectra using a quartz NMR tube containing only d_6-DMSO, and used this spectra to subtract the borosilicate glass peak from a ^{11}B NMR spectra of our sample, allowing a single ^{11}B peak at 30.44 ppm to be observed for N^1,N^3,N^5-tris(4-(4,4,5,5-tetramethyl-1,3,2-dioxaborolan-2-yl)phenyl)benzene-1,3,5-tricarboxamide (**5.3**).

We have therefore successfully synthesized N^1,N^3,N^5-tris(4-(4,4,5,5-tetramethyl-1,3,2-dioxaborolan-2-yl)phenyl)benzene-1,3,5-tricarboxamide (**5.3**) through two different conditions. With a tri-boronic acid linker (**5.3**) in hand, next we planned to examine boron chelation rection between the prepared linker and three units of (*S*)-α-(1-hydroxybutan-2-yl)amino)-α'-(2-hydroxyphenyl) dipyrromethene (**3.6**).

5.5.4 Synthesis of Trimeric Helically Chiral BODIPY Arrays

Next, we planned to synthesize our target trimeric helically chiral BODIPY (**5.4**), through a chelation reaction, based on our previous conditions. The reaction was performed between the prepared N^1,N^3,N^5-tris(4-(4,4,5,5-tetramethyl-1,3,2-dioxaborolan-2-yl)phenyl)benzene-1,3,5-tricarboxamide (**5.3**) and 3 eq. of (*S*)-α-(1-hydroxybutan-2-yl)amino)-α'-(2-hydroxyphenyl) dipyrromethene (**3.6**) at 45 °C in $CHCl_3$. The reaction was monitored by TLC which showed that the starting material had been consumed and six new products had been formed after 120 hours. The reaction mixture was diluted in DCM and subjected to an aqueous work-up. Following column chromatography, we were able to isolate a fraction that contained the desired trimeric helically chiral BODIPY arrays (**5.4**) and a by-product (**5.24**)(Scheme **5.11**).

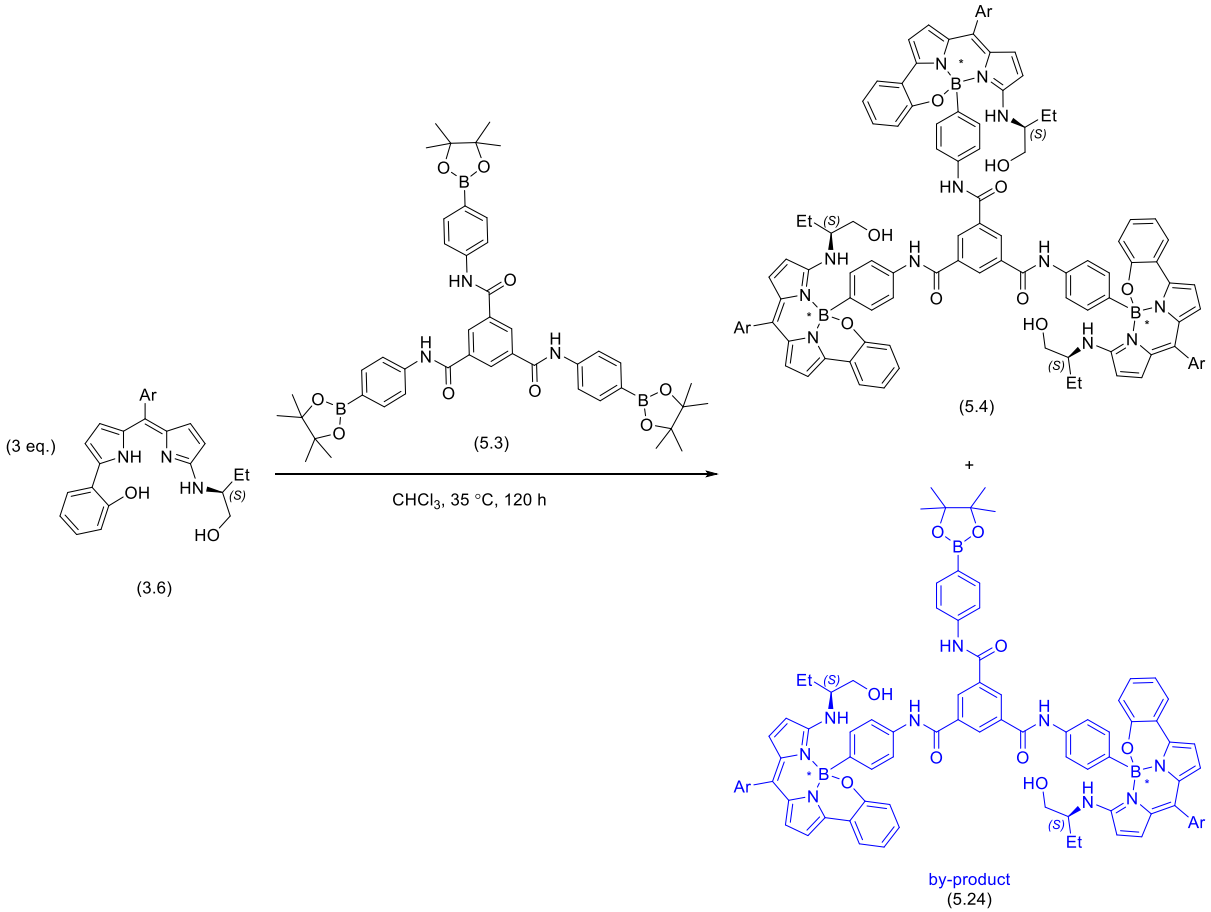

Scheme 5.11: Synthesis of trimeric helically chiral BODIPY arrays (**5.4**)(Ar = *p*-(MeCO$_2$)-C$_6$H$_4$-).

The structure of trimeric helically chiral BODIPY arrays (**5.4**) was validated by HRMS, which showed a doubly charged molecular ion at *m/z* = 916.8680 $[M+2H]^{2+}$, which corresponded to a molecular formula of $C_{108}H_{95}{}^{11}B_3N_{12}O_{15}$. It is however likely that this fraction contains more than one diastereomer of trimeric helically chiral BODIPY array (**5.4**).

In addition, the structure of by-product (**5.24**) was validated by HRMS, which showed peak at *m/z* = 1492.6252, which corresponded to a molecular formula of $C_{87}H_{81}{}^{11}B_3N_9O_{13}$ $[M]^+$, suggesting that two chelation reactions have occurred.

5.6 Conclusions

In conclusion, in this section we have successfully synthesized dimeric helically chiral BODIPY arrays through a point-to-helical chirality approach. We have also reported several examples of dimeric helically chiral BODIPYs with different di-boronic acid linkers. In addition, we designed and synthesized a tri-boronic acid linker (**5.3**), and used it to chelate three units of (*S*)-α-(1-hydroxybutan-2-yl)amino)-α'-(2-hydroxyphenyl) dipyrromethene (**3.6**) to make a trimeric-helically chiral BODIPY (**5.4**). However,

the separation of trimeric-helically chiral BODIPY isomers proved challenging. In the future, we aim to find a suitable method to separate trimeric-helically chiral BODIPY isomers.

5.7 Synthesis of Stacked Helically Chiral Bis BODIPYs

In the second part of this chapter, we will discuss our work towards the synthesis of stacked helically chiral bis BODIPYs.

Our synthetic plan involves three parts: firstly, synthesis of dibenzo[*b,d*]furan-4,6-dicarbaldehyde (**5.5**) from dibenzofuran (**5.25**) via an organolithium mediated formylation (Scheme **5.12**, Part A), secondly, preparation of 2-(1*H*-pyrrol-2-yl)phenol (**4.35**) via a Suzuki Miyaura cross-coupling reaction between 2-bromophenol (**4.33**) and (1-(*tert*-butoxycarbonyl)-1*H*-pyrrol-2-yl)boronic acid (**4.32**), followed by *in situ* deprotection (Scheme **5.**12, Part B, Route 1) and thirdly, synthesis of stacked helically chiral bis BODIPY (**5.6**) by a condensation between dibenzo[*b,d*]furan-4,6-dicarbaldehyde (**5.5**) and 2-(1*H*-pyrrol-2-yl)phenol (**4.35**), followed by oxidation, and boron chelation (Scheme **5.12**, Part C).

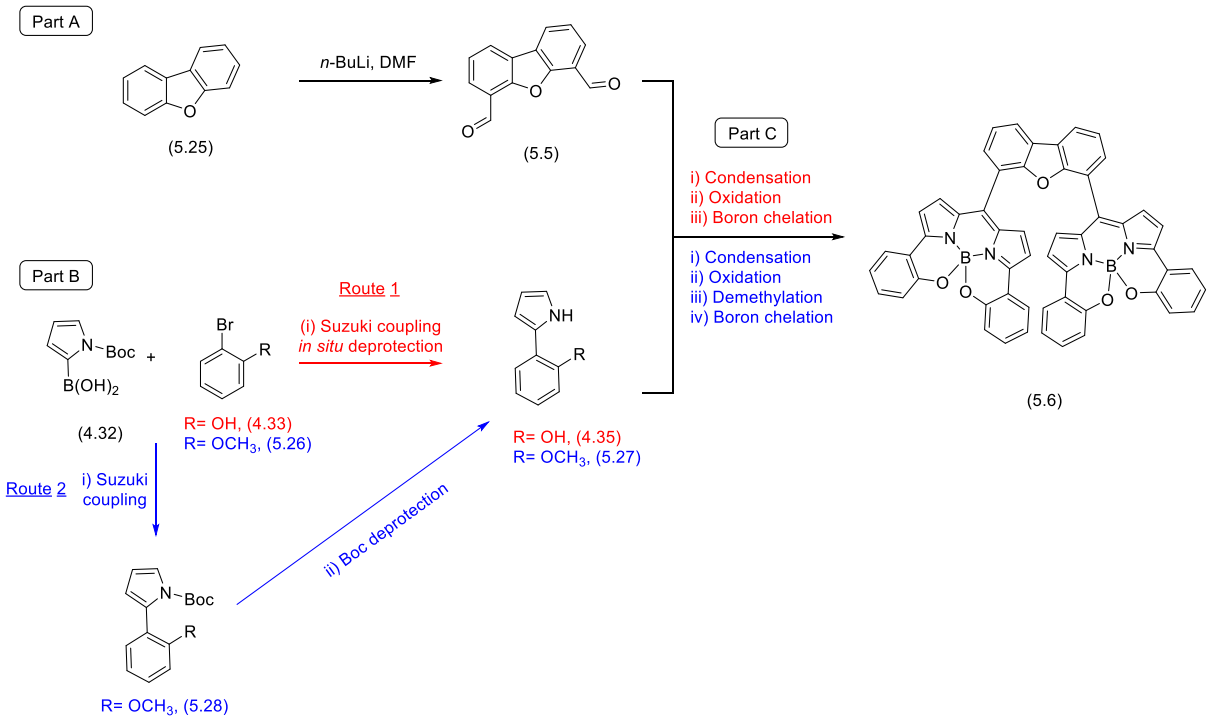

Scheme 5.12: Planned synthesis of stacked helically chiral bis BODIPYs (**5.6**)

We planned also to examine another synthetic pathway to access 2-(2-methoxyphenyl)-1H-pyrrole (**5.27**) through two synthetic steps; first step is a Suzuki Miyaura cross-coupling reaction between 1-bromo-2-methoxybenzene (**5.26**) and (1-(*tert*-butoxycarbonyl)-1*H*-pyrrol-2-yl)boronic acid (**4.32**); second step is removing the Boc protecting group via a thermolytic deprotection process (Scheme **5.12**, Part B, Route 2). Finally, to access synthesis of stacked helically chiral bis BODIPY (**5.6**) by a

condensation between dibenzo[*b,d*]furan-4,6-dicarbaldehyde (**5.5**) and 2-(2-methoxyphenyl)-1H-pyrrole (**5.27**), followed by oxidation, demethylation and boron chelation (Scheme **5.12**, part C).

Therefore, we mixed one equivalent of dibenzofuran (**5.25**) with three equivalents of TMEDA in dry Et_2O, followed by the then dropwise addition of three equivalents of *n*-BuLi solution (1.6 M) at room temperature. The reaction mixture was then refluxed for 16 hours, then cooled to 0 °C, after which dry DMF was added over a period of 10 min. The reaction mixture was stirred at room temperature for 24 hours, before quenching into cold water, followed by the addition of HCl solution (1 M) resulting in precipitation of the product. DCM was added to dissolve the product, the reaction underwent an aqueous work up, and the solvent was removed under reduced pressure. The crude rection mixture was purified by column chromatography to isolated the desired dibenzo[*b,d*]furan-4,6-dicarbaldehyde (**5.5**) as a colourless crystalline solid, in moderate yield of 55 % (Scheme **5.13**).

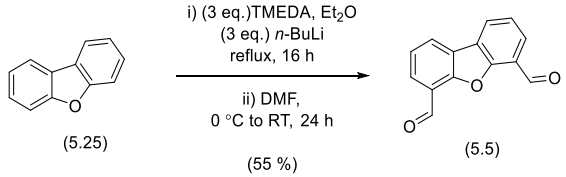

Scheme 5.13: Synthesis of dibenzo[*b,d*]furan-4,6-dicarbaldehyde (**5.5**)

5.7.2 Synthesis of 2-(1*H*-pyrrol-2-yl)phenol (**4.35**) (Part B)

Part B of our synthetic route, requires access to 2-(1*H*-pyrrol-2-yl)phenol (**4.35**). We have previously described the synthesis of 2-(1*H*-pyrrol-2-yl)phenol (**4.35**) via a Suzuki Miyaura cross-coupling reaction in (Chapter 4, section 4.8.2.2) (Scheme **5.14**). Therefore, we used material prepared previously for the rest of this synthesis.

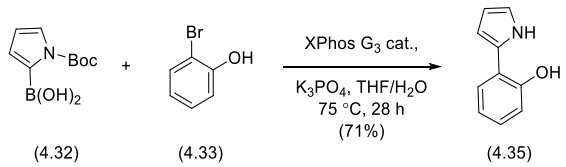

Scheme 5.14: Synthesis of 2-(1*H*-pyrrol-2-yl)phenol (**4.35**), as described in Chapter 4

5.7.3 Synthesis of 2-(2-methoxyphenyl)-1*H*-pyrrole (**5.27**)(Part B)

We examined a Suzuki Miyaura cross-coupling between 1-bromo-2-methoxybenzene (**5.26**) and (1-(*tert*-butoxycarbonyl)-1*H*-pyrrol-2-yl)boronic acid (**4.32**), followed by Boc deprotection to synthesis 2-(2-methoxyphenyl)-1*H*-pyrrole (**5.27**).

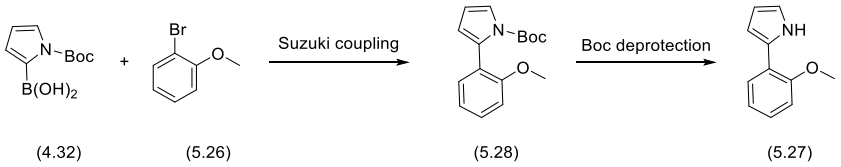

(4.32) (5.26) (5.28) (5.27)

Scheme 5.15: Synthesis of 2-(2-methoxyphenyl)-1*H*-pyrrole (**5.27**)

Therefore we reacted 1.5 equivalents of (1-(*tert*-butoxycarbonyl)-1*H*-pyrrol-2-yl)boronic acid (**4.32**) and one equivalent 1-bromo-2-methoxybenzene (**5.26**) on a 2.5 mmol scale, catalysed by XPhos Pd G3 (3 mol%) in degassed THF/H_2O at 75 °C. The reaction was monitored by TLC which showed the disappearance of the starting material and the formation of a new product after 28 hours. Following an aqueous work-up and purification by column chromatography *tert*-butyl 2-(2-methoxyphenyl)-1*H*-pyrrole-1-carboxylate (**5.28**) was isolated in an excellent yield of 86% as a colourless oil (Scheme **5.16**). The structure of *tert*-butyl 2-(2-hydroxyphenyl)-1*H*-pyrrole-1-carboxylate (**5.28**) was confirmed by the analysis of ^{1}H NMR spectrum which showed 9H singlet at 1.37 ppm corresponding to three methyl in the Boc group and 3H singlet at 3.79 ppm corresponding to methoxy group.

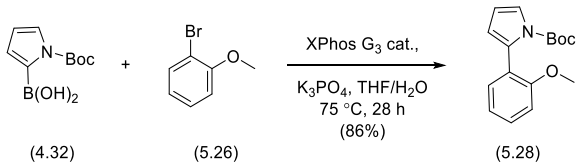

(4.32) (5.26) (5.28)

Scheme 5.16: Synthesis of *tert*-butyl 2-(2-hydroxyphenyl)-1*H*-pyrrole-1-carboxylate (**5.28**) via a Suzuki-coupling reaction

The next step in our planned approach was the thermal Boc deprotection of *tert*-butyl 2-(2-hydroxyphenyl)-1*H*-pyrrole-1-carboxylate (**5.28**). Therefore, we heated a Schleck flask containing *tert*-butyl 2-(2-hydroxyphenyl)-1*H*-pyrrole-1-carboxylate (**5.28**) to 200 °C using a metal heating block under nitrogen atmosphere for 30 minutes, resulting in the evolution of gas (CO_2 and isobutene). The inspection of the ^{1}H NMR spectra of the crude product showed that 2-(2-methoxyphenyl)-1*H*-pyrrole (**5.27**) had been formed. The crude product was purified by column chromatography to isolate the desired 2-(2-methoxyphenyl)-1*H*-pyrrole (**5.27**) in yield of 81%. To have sufficient material of 2-(2-methoxyphenyl)-1*H*-pyrrole (**5.27**) for the next step, the Boc deprotection was repeated under similar reaction conditions, with a slightly longer reaction time of 40 minutes. Analysis of the crude product by ^{1}H NMR showed a very high degree of purity, however purification by column chromatography was still carried out to obtain 2-(2-methoxyphenyl)-1*H*-pyrrole (**5.27**) in an improved yield of 88 % (Scheme **5.17**).

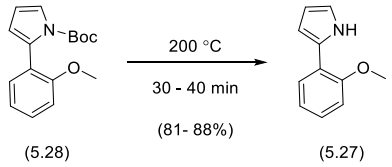

Scheme 5.17: Synthesis of 2-(2-methoxyphenyl)-1*H*-pyrrole (**5.27**)

5.7.4 Synthesis of Stacked Helically Chiral Bis BODIPYs from 2-(1*H*-pyrrol-2-yl)phenol (**4.35**)(Prat C)

The final step in our synthetic route to access stacked helically chiral bis BODIPY (**5.6**) was the reaction between dibenzo[*b,d*]furan-4,6-dicarbaldehyde (**5.6**) and 2-(1*H*-pyrrol-2-yl)phenol (**4.35**) in a one-pot condensation, oxidation and boron chelation reaction.

Therefore, we reacted one equivalent of dibenzo[*b,d*]furan-4,6-dicarbaldehyde (**5.5**) and four equivalents of 2-(1*H*-pyrrol-2-yl)phenol (**4.35**), in the presence of 20 equivalents of TFA in dry DCM at room temperature. The reaction was monitored by TLC which showed that the starting materials had disappeared and a new product had formed after 3 hours. After the disappearance of the dibenzo[*b,d*]furan-4,6-dicarbaldehyde (**5.5**) by TLC, we added two equivalents of DDQ and the reaction mixture was stirred at room temperature for 1 hour. Following this, 11.8 equivalents of DIPEA were added to the reaction mixture, followed by the addition of 13.6 equivalents of $BF_3.Et_2O$ and the reaction mixture stirred for 18 hours at room temperature. After an aqueous work-up and purification by column chromatography, two main fractions were isolated which gave blue/green solids on removal of the solvent.

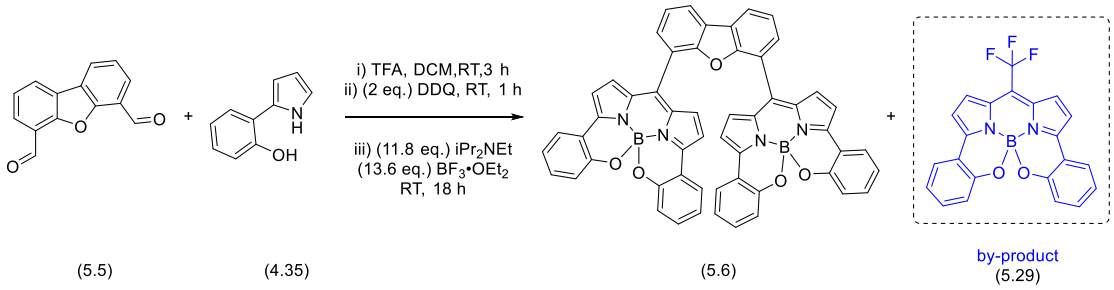

Scheme 5.18: Synthesis of stacked helically chiral bis BODIPY (**5.6**).

Initial inspection of the ^{1}H NMR spectrum for fraction 2 showed the presence of complex BODIPY type signals, including pyrrolic doublets. However, more than one molecule could be observed in the spectra, and further analysis of this fraction will require additional separation of the close running components.

Analysis of the ^{1}H NMR of fraction 1 showed for formation of a symmetrical BODIPY system with two sets of signals in the aromatic range, one for two 1,2-disubsituted benzene rings at 7.81 ppm (dd, *J* = 7.8, 1.7 Hz, 2H), 7.38 ppm (ddd, *J* = 8.6, 7.3, 1.7 Hz, 2H), 7.08 ppm (ddd, *J* = 8.1, 7.2, 1.1 Hz, 2H), and 6.95 (dd, *J* = 8.3, 1.1 Hz, 2H), and one for a two pyrrolic rings at 7.50 ppm (dq, *J* = 4.3, 2.1 Hz, 2H) and 7.01 ppm (d, *J* = 4.5 Hz, 2H). Interestingly, the $^{19}F\{^{1}H\}$ NMR showed the presence of singlet signal at -55.93 ppm, whilst one of the pyrrolic protons (7.50 ppm (dq, *J* = 4.3, 2.1 Hz, 2H)) showed an unusual additional quartet coupling, all of which suggested incorporation of fluorine atoms into the structure. We therefore decided to grow a crystal to unambiguously determine the structure of the newly formed BODIPY. We grew crystals through slow evaporation of a $CDCl_3$ solution in an NMR tube, and a single crystal was submitted to SCXRD, giving a monoclinic crystal system with the $P2_1/n$ space group. The SCXRD confirmed that the by-product formed was helically chiral *meso*-(trifluoromethyl)-*N*,*N*,*O*,*O*-BODIPY (**5.29**) (Figure **5.14**).

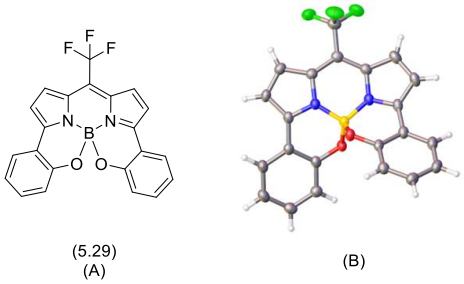

Figure 5.14: Helically chiral *meso*-(trifluoromethyl)-*N*,*N*,*O*,*O*-BODIPY (**5.29**); (A) Molecular structure; (B) Single crystal X-ray structure.

We postulated that the helically chiral *meso*-(trifluoromethyl)-*N*,*N*,*O*,*O*-BODIPY (**5.29**) had been formed through a condensation reaction between 2-(1*H*-pyrrol-2-yl)phenol (**4.35**) and the trifluoroacetic acid present in the reaction, followed by boron chelation.

To test our postulate, we reacted two equivalents of 2-(1*H*-pyrrol-2-yl)phenol (**4.35**) and one equivalent of TFA in dry DCM at room temperature. After 13 hours the disappearance of 2-(1*H*-pyrrol-2-yl)phenol (**4.35**) was observed by TLC, therefore, three equivalents of DIPEA was added, followed by the addition of four equivalents of $BF_3.OEt_2$, and the reaction mixture was stirred at room temperature for 24 hours. Following an aqueous work-up and purification by column chromatography, we isolated helically chiral *meso*-(trifluoromethyl)-*N*,*N*,*O*,*O*-BODIPY (**5.29**) in low yield of 10 %.

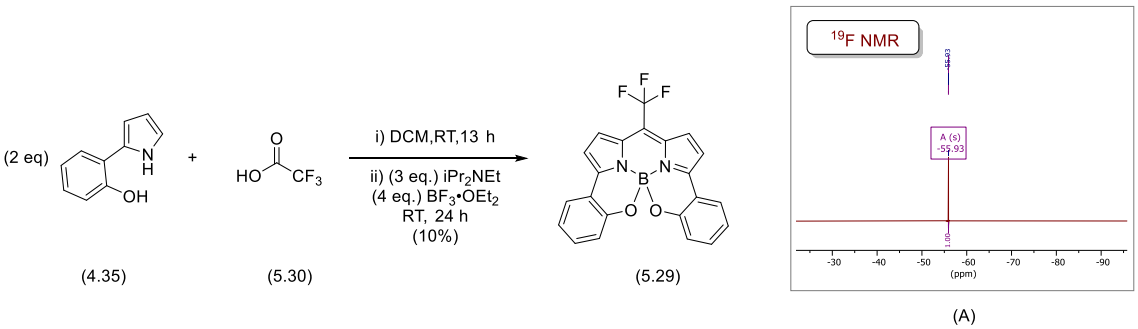

Scheme 5.19: Synthesis of helically chiral *meso*-(trifluoromethyl)-*N*,*N*,*O*,*O*-BODIPY (**5.29**); (A) $^{19}F\{^{1}H\}$ NMR spectrum (282 MHz, $CDCl_3$) of the helically chiral *meso*-(trifluoromethyl)-*N*,*N*,*O*,*O*-BODIPY (**5.29**) following column chromatography.

5.7.5 Synthesis of Stacked Helically Chiral Bis BODIPYs from 2-(2-methoxyphenyl)-1*H*-pyrrole (**5.27**) (Prat C)

Next, we planned to examine an alternative synthetic pathway to access stacked helically chiral bis BODIPY (**5.6**), in which the hydroxyl group of the 2-aryl-subsituted pyrrole unit would be protected as the methyl ether. Although this approach would add an additional synthetic step, we anticipated improved yields and the potential for isolation of intermediates. Therefore our plan involved through four key synthetic steps: condensation reaction of two units of 2-(2-methoxyphenyl)-1H-pyrrole (**5.27**) with dibenzo[*b,d*]furan-4,6-dicarbaldehyde (**5.5**), oxidation to the dipyrromethenes, demethylation by BBr_3 and finally boron chelation. Our procedure was based on the work of Harvey and co-workers (Scheme **5.20**).[98]

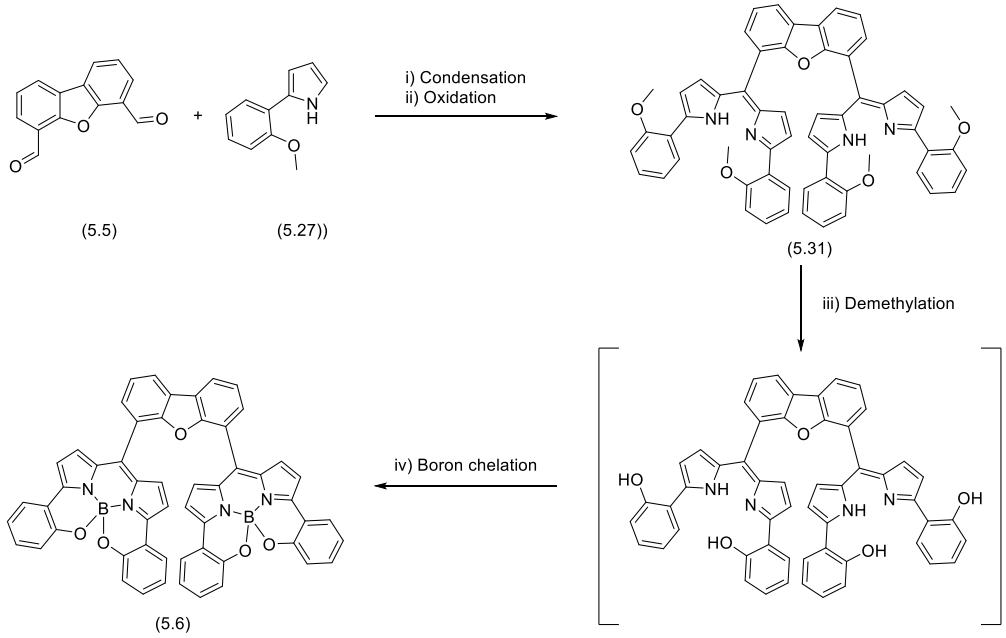

Scheme 5.20: Second generation planned synthesis of stacked helically chiral bis BODIPY (**5.6**).

The first step in our synthetic route was the condensation of 3.7 equivalents of 2-(2-methoxyphenyl)-1*H*-pyrrole (**5.27**), as prepared earlier, with one equivalent of dibenzo[*b,d*]furan-4,6-dicarbaldehyde (**5.5**) in dry DCM, in presence of 1.2 equivalents of TFA at room temperature in the dark under nitrogen. After 5 hours the disappearance of dibenzo[*b,d*]furan-4,6-dicarbaldehyde (**5.5**) was observed by TLC analysis, therefore, 1.6 equivalents of DDQ was added and the reaction mixture was stirred at room temperature for 4 hours. Following an aqueous work-up, purification by column chromatography allowed isolation of stacked bis dipyrromethene (**5.31**) in a yield of 15% (Scheme **5.21**)

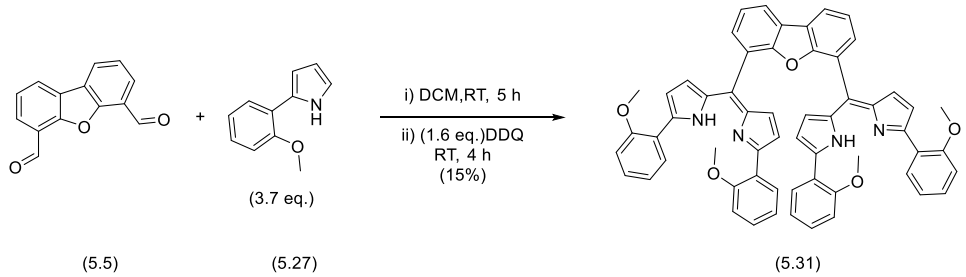

Scheme 5.21: Condensation/oxidation reaction to give stacked bis dipyrromethene (**5.31**).

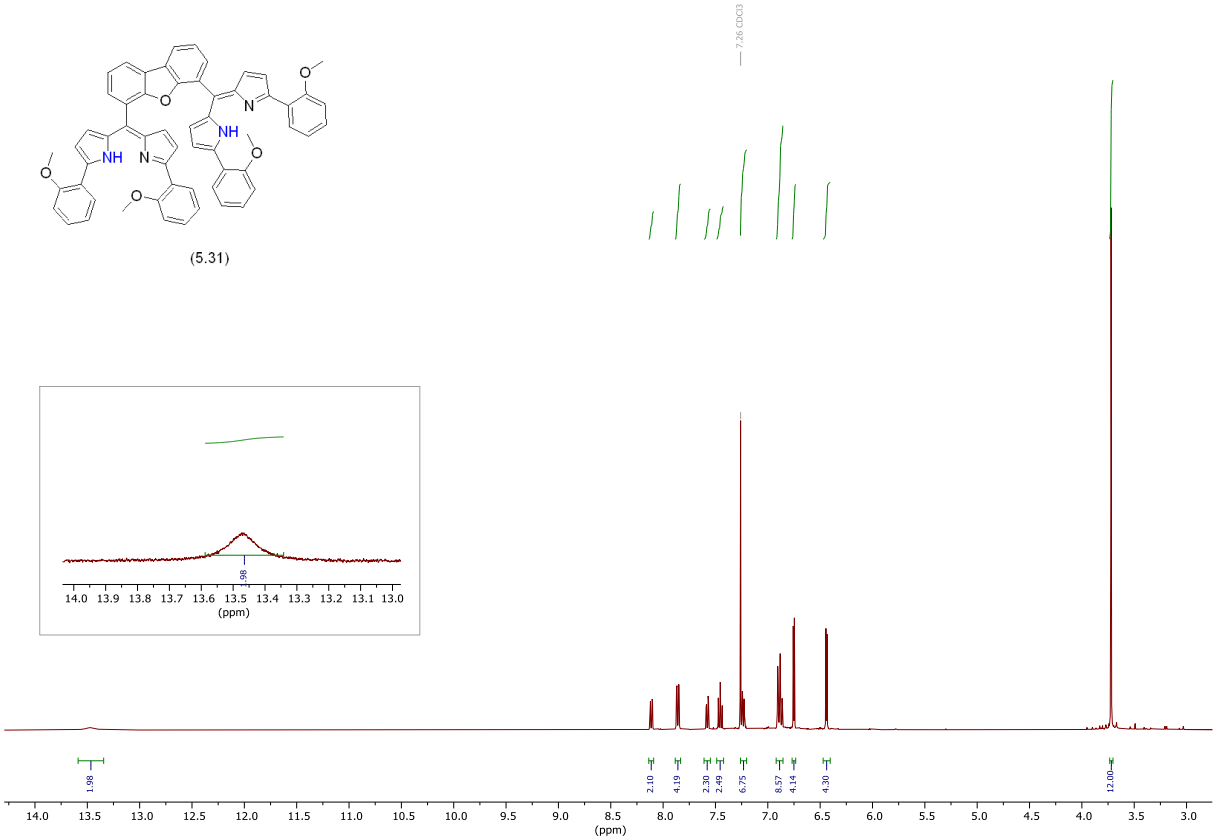

Figure 5.15: ^{1}H NMR spectra (400 MHz, $CDCl_3$) of stacked bis dipyrromethene (**5.31**), following column chromatography.

The structure of stacked bis dipyrromethene (**5.31**) was confirmed by the analysis of ^{1}H NMR spectrum which showed a molecule with a high degree of symmetry, including nine aromatic proton environments (*e.g*. two doublets at 6.75 ppm (d, *J* = 4.3 Hz, 4H) and 6.44 ppm (d, *J* = 4.3 Hz, 4H) each corresponding to four pyrrolic protons), a 12H singlet at 3.72 ppm corresponding to the four methoxy groups and a broad peak at 13.47 ppm corresponding to two NH groups (Figure **5.15**).

The next steps in our synthetic route were the demethylation of methoxy groups, followed by boron chelation. Thus, in the first attempt at a quadruple demethylation of stacked bis dipyrromethene (**5.31**), we added 37 equivalents of boron tribromide to a solution of bis dipyrromethene (**5.31**) in dry DCM at 78 °C. The reaction mixture was stirred for 3 days at room temperature and quenched with methanol. The mixture was evaporated, redissolved in methanol and conc. HCl was added. The reaction mixture was refluxed for 3 hours then allowed to cool to room temperature. The acidic mixture was neutralized with saturated solution of $NaHCO_3$ and extracted with ethyl acetate. The organic layer was dried over Na_2SO_4 and solvent removed under reduced pressure. Subsequently, the crude product was dissolved in dry $CHCl_3$ and reacted with 16 equivalents of $B(OMe)_3$ under reflux for 3 hours. Following removal of the solvent under reduced pressure and purification by column chromatography, resulting in isolation of two diastereomers. The first fraction containing a pure sample of the first diastereomer to elute gave an isolated yield of 2.1%, with a second fraction containing a purified diastereomer in a 0.9% yield. Due to the similar R_f of both diastereomers, a mixed fraction was also obtained from the column in a 1.2% yield, giving an overall isolated yield of around 4.2%. We anticipated that this reaction should give two diastereomers, a racemic (*R*,*R*)/(*S*,*S*)-diastereomer and a (*R*,*S*)-*meso*-diastereomer (Scheme **5.22**).

Both diastereomeric stacked helically chiral bis BODIPYs (**5.6a**) and (**5.6b**) were examined by ^{1}H NMR spectra, although we cannot at this this stage assign stereochemistry to the molecules. The stacked helically chiral bis BODIPYs (**5.6a**)(fraction 1) in acetone-d_6 showed four set of signals at 7.58 ppm (d, *J* = 4.3 Hz, 2H), 7.22 ppm (d, *J* = 4.4 Hz, 2H), 7.04 ppm (d, *J* = 4.4 Hz, 2H), and 6.99 ppm (d, *J* = 4.4 Hz, 2H) corresponding to four pyrrolic proton environments. For further confirmation, the ^{11}B NMR showed singlet at -0.95 ppm which gave us confidence a new boron centre had been formed.

The analysis of ^{1}H NMR spectrum of stacked helically chiral bis BODIPY (**5.6b**)(fraction 2) in acetone-d_6 also showed four signals of pyrrolic protons 7.20 (d, *J* = 4.3 Hz, 2H), 7.16 (d, *J* = 4.3 Hz, 2H), 7.10 (d, *J* = 4.4 Hz, 2H), and 6.74 (d, *J* = 4.4 Hz, 2H). The structure further confirmed by ^{11}B NMR spectrum which showed the presence of singlet at -0.89 ppm. It should be noted that the fraction 2 also contained a small amount of the diastereomer from fraction 1. Therefore, further purification was attempted by preparative TLC (toluene: DCM, 1:1). This aided in separation, however over time it was

observed that fraction 2 showed an increasing trace quantity of the diastereomer from fraction 1, suggesting that an epimerisation of one of the stereocenters was occurring.

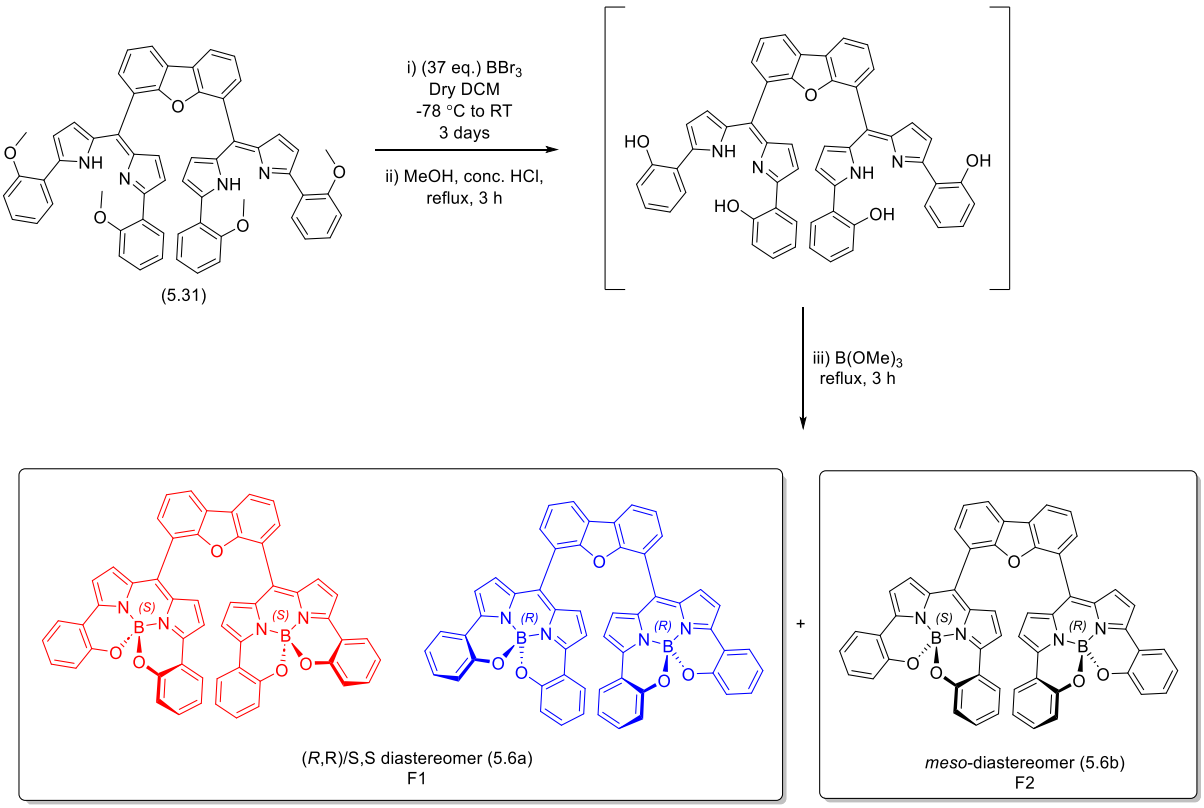

Scheme 5.22: Demethylation and boron chelation reaction to give stacked helically chiral bis BODIPYs.

Once we had pure samples of the two diastereomeric stacked helically chiral bis BODIPY (**5.6**) in hand, we measured the absorption and emission spectra for stacked helically chiral *N,N,O,O*-BODIPY (**5.6a**) and (**5.6b**) in DCM at room temperature. The absorption maxima were observed at 624 and 625 nm, while the emission maxima were obsereved at 660 and 667 nm, respectively.

The fluorescence quantum yields (ϕ_F) of both stacked helically chiral *N,N,O,O*-BODIPY (**5.6a**) and (**5.6b**) were also measured, using cresyl violet as a standard. These systems showed good quantum yields in the range of 0.39 to 0.55 (Table 5.4).

BODIPY	Solvent	λ_{abs}/nm	λ_{em}/nm	ϕ_F[a]
(5.6a)	DCM	624	660	0.39
(5.6b)	DCM	625	667	0.55

Table 5.6: Photophysical properties of stacked helically chiral *N,N,O,O*-BODIPY (**5.6a**) and (**5.6b**). [a] Measured with respect to cresyl violet standard in methanol (ϕ_F = 0.56), excitation wavelength = 580 nm.

5.8 Conclusion

In the section, we have successfully synthesized stacked helically chiral bis BODIPYs and isolated two diastereomers through column chromatography. In the future we would need to prepare more of both diastereoisomers, and assign relative stereochemistry likely by SCXRD. In the case of the (*R*,*R*)/(*S*,*S*)-diastereomer the two enantiomers would need to be separated by chiral HPLC and their chiroptical properties measured, and absolute stereochemistry assigned.

5.9 Chapter Conclusion

In conclusion we have successfully demonstrated the synthesis of dimeric and trimeric helically chiral BODIPY arrays through point-to-helical chirality transfer. The photophysical and chiroptical were measured for dimeric helically chiral BODIPY arrays. Interestingly, we were able to assign the absolute stereochemistry for (*S,S,P,P*)-*N,N,O,C*-3-(2-aminobutan-1-ol)-BODIPY (**5.2a**) and (*S,S,M,M*)-*N,N,O,C*-3-(2-aminobutan-1-ol)-BODIPY (**5.2c**) via SCXRD.

In the second part of this chapter, we have successfully prepared stacked helically chiral bis BODIPYs, albeit with a low yield obtained. We separated the two diastereomers (**5.6a**) and (**5.6b**) by column chromatography. The formation of two diastereomers suggests that the chiral boron centre formed first can control the chirality of another boron chiral centre, which may be interesting in the future design of stacked helically chiral bis BODIPYs.

Chapter 6 Conclusions and Future Work

During the course of this project, we have optimised routes for the synthesis of 3,5-dibromo BODIPY (**1.67**) through 4 main steps, demonstrating improvements in yields up to 86%. Additionally, we have explored the conversion of 3,5-dibromo BODIPY (**1.67**) to 3,5-diodo BODIPY (**1.68**), following the previously published methodology by Hall *et al.*, via an aromatic Finkelstein reaction. Both 3,5-dibromo BODIPY (**1.67**) and 3,5-diodo BODIPY (**1.68**) have been shown to be suitable intermediate for S_NAr reaction and Suzuki Miyaura cross-coupling. The prepared 3,5-dibromo BODIPY (**1.67**) and 3,5-diodo BODIPY (**1.68**) have been utilized to produce novel chiral 3-bromo-substituted BODIPY (**2.18**) and chiral 3-iodo-substituted BODIPY (**2.19**). Furthermore, we have explored two different synthetic approaches to access chiral bis (3-bromo-substituted BODIPY) (**2.3**) and chiral bis (3-iodo-substituted-BODIPY) (**2.4**). The first approach was a one-pot double S_NAr reaction between 3,5-halo-BODIPY (**1.67** or **1.68**) and (1*S*,2*S*)-1,2-diphenylethane-1,2-diamine (**2.15**). The second approach was a stepwise sequential S_NAr approach. We found that the first approach was more convenient for synthesizing chiral bis(3-halo-substituted BODIPY), as it required fewer synthetic steps and provided a moderate yield.

We have also developed a new synthetic route to produce helically chiral BODIPYs. This route involved: i) introducing a chiral auxiliary in the form of enantiopure amino alcohol via S_NAr chemistry, ii) introduction of a 2-hydroxyphenyl boronic acid through Suzuki cross-coupling, iii) de-chelation of BF_2 moiety, and iv) re-chelation of the boron centre, leading to an *in-situ* ring closure between the boron and the oxygen on the 2-hydroxyphenyl group. This results in the formation of two diastereomeric helically chiral *N,N,O,C*-BODIPYs, (*S,M*)-*N,N,O,C*-3-((1-hydroxybutan-2-yl)amino) BODIPY (**3.7a**) and (*S,P*)-*N,N,O,C*-3-((1-hydroxybutan-2-yl)amino) BODIPY (**3.7b**). This route represents the first instance of point-to-helical chirality control in BODIPY structures, with a high diastereomeric excess (*de* = 74%). Following the successful implementation of the point-to-helical chirality approach in BODIPY structures, a variety of amino alcohols have been investigated to further enhance the observed diastereomeric excess (*de*) of the resulting helically chiral BODIPYs. Moreover, we have applied this point-to-helical chirality approach to synthesized a range of helically chiral BODIPYs including, *N,N,O,C*-BODIPYs containing 7-membered rings as well as novel dimeric, trimeric helically chiral *N,N,O,C*-BODIPY arrays (Scheme **6.1**).

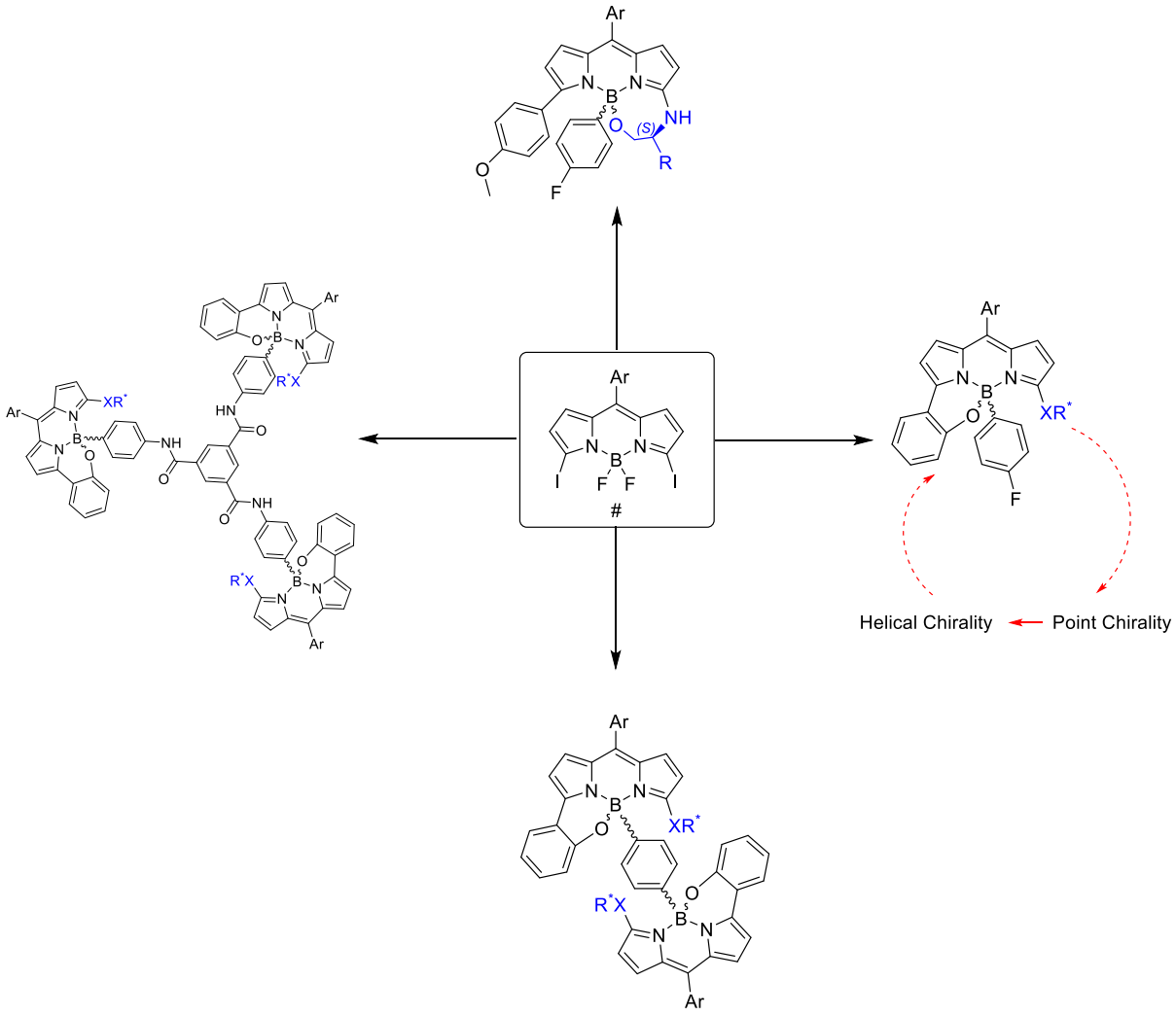

Scheme 6.1: Helically chiral BODIPYs demonstrating point-to-helical chirality transfer approach (Ar = *p*-($MeCO_2$)-C_6H_4-), XR* = enantiopure chiral auxiliary.

In addition, we have developed a synthetic route to produce novel helically chiral *N,N,O,O*-BODIPYs (**4.7a** and **4.7b**) in high yield 94%, through a chiral resolution approach, aiming to measure their chiroptical properties in the future. As well as developing alternative routes to other chiral stacked bis BODIPY systems.

This thesis opens the door to several potential future projects, one of which involves synthesizing helically chiral *N,N,O,O*-BODIPYs containing double-7-membered rings using our successful point-to-helical chirality approach. The aim is to make rigid structures with double-7-membered rings, connecting at the boron centre. We hypothesize that the increasing molecular rigidity could enhance fluorescence quantum yield (ϕ_F) by reducing the vibration relaxation processes, thereby improving and circularly polarized luminescence (CPL) efficiency. Synthesizing helically chiral BODIPYs containing double-7-membered rings would involve a double S_NAr reaction, based on chemistry developed in Chapter 4, followed by dechelation and rechelation of the boron centre (Scheme **6.2**).

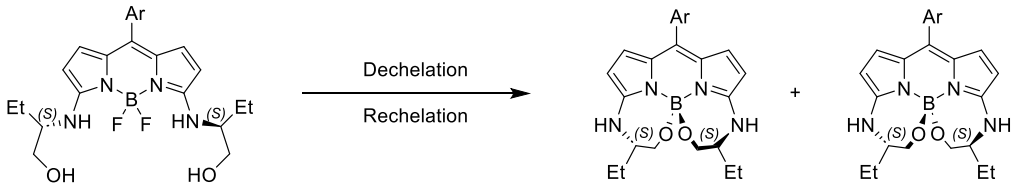

(6.1) (6.2a) (6.2b)

Scheme 6.2: Proposed synthesis of helically chiral *N,N,O,O*-BODIPYs containing double-7-membered rings.

As an additional future plan, we also aim to produce *N*-bridged *meso*-annulated *N,N,O,O*-BODIPYs with a focus on synthesizing CPL-SOMs with improved chiroptical properties. Our objective is to achieve both high fluorescence quantum yield (ϕ_F) and high luminescence dissymmetric factors (g_{lum}) in the same molecule. This will involve designing molecules that both extend the twisted conjugated π system within the chiral BODIPYs, whilst also increasing rigidity through ring-fused structures. The ultimate goal is to shift the emission towards the red or near-infrared (NIR) region, whilst also maximising g_{lum} (Figure **6.1**).

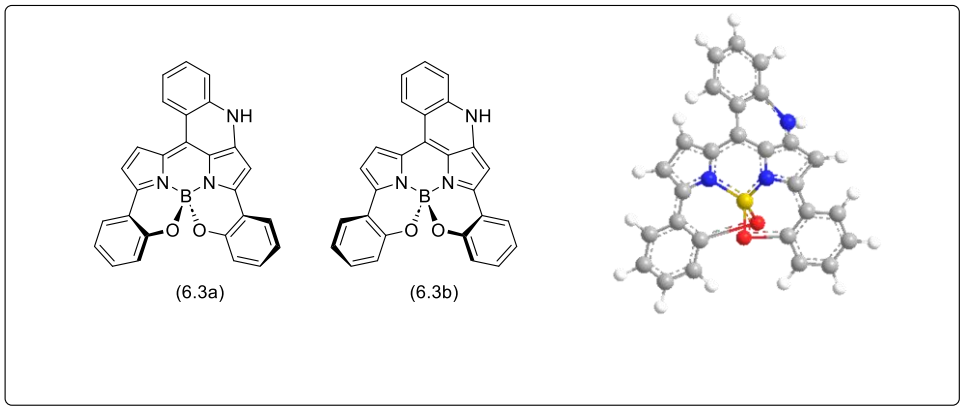

(6.3a) (6.3b)

Figure 6.1: Proposed *N*-bridged *meso*-annulated *N,N,O,O*-BODIPYs (**6.3a**) and (**6.3b**).

The synthesis of such *N*-bridged *meso*-annulated *N,N,O,O*-BODIPYs (**6.3a** and **6.3b**) could be achieved through a series of steps: condensation reaction between 2-nitrobenzaldehyde (**6.4**) and 2-(1*H*-pyrrol-2-yl)phenol (**4.35**) followed by oxidation and boron chelation reaction. Subsequently, *N,N,O,O* BODIPY (**6.5**) would be reduced by PPh_3 in 1,2-dichlorobenzene. In this process, the *ortho*-nitro group on the *meso* phenyl substituent will be utilized to form a C-N bond via an intramolecular reductive cyclization approach, known as the Cadogan reaction (Scheme **6.3**).[102]

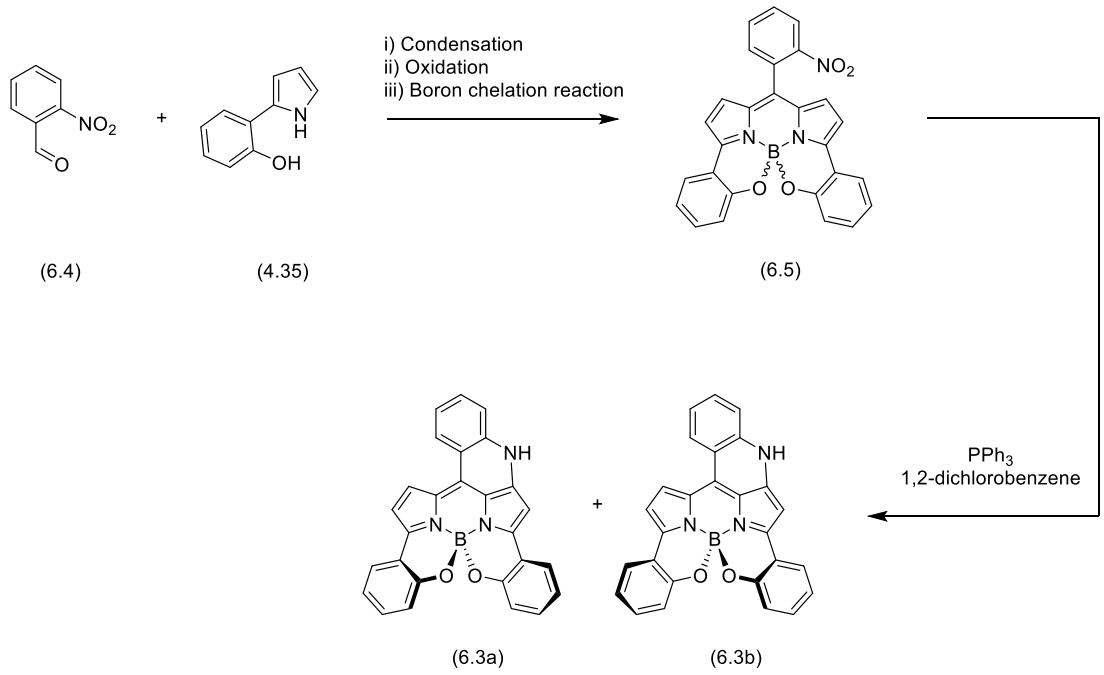

Scheme 6.3: Proposed synthetic routes to *N*-bridged *meso*-annulated *N,N,O,O*-BODIPYs (**6.3a**) and (**6.3b**).

Chapter 7. Experimental Methods and Characterisation

7.1 General Experimental Information

7.1.1 Analysis

The NMR spectra of ^{1}H, ^{13}C, ^{11}B, and ^{19}F were directly recorded using either a Bruker Advance III HD 700 MHz, Jeol Lambda 500 MHz, Jeol ECS-400 MHz, or Brucker Avance 300 MHz instrument. Infrared (IR) spectra were obtained by scanning neat samples using a Varian 800 FT-IR Scimitar Series spectrometer over the range of 4000-600 cm^{-1}. High resolution mass spectra (HRMS) data were provided by the EPSRC National Mass Spectrometry Service at the University of Swansea. UV-Vis spectra were obtained using a UV-1800 Shimadzu UV spectrophotometer by scanning from 300 to 800 nm. Fluorescence quantum yield spectra were acquired using a Shimadzu RF-6000 spectrofluorophotometer. The fluorescence quantum yield data was compared to a standard reference of either Cresyl violet or Rhodamine 6G, 99% pure, laser grade. The measurement of specific optical rotation ($[\alpha]_D$) was measured using an automatic polarimeter Optical Activity PolAAR 2001.

7.1.2 Procedures

Standard Schlenk techniques were used for all experiments involving air-sensitive reagents, under an atmosphere of nitrogen. Solvents were dried over activated molecular sieves and used directly. Manual column chromatography was performed using Geduran silicagel 60 (40-63 µm).

7.2 Experimental Procedures and Characterisation Data

7.2.1 Chapter 2

7.2.1.1 Methyl 4-(di(1*H*-pyrrol-2-yl)methyl)benzoate (**2.2**)

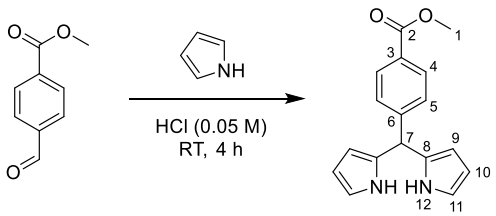

To a 250 mL round bottom flask was added pyrrole (2.28 ml, 33 mmol) to an aqueous solution of HCl (0.05 M, 100 ml), followed by the gradual addition of crushed methyl 4-formylbenoate (1.81 g, 11 mmol) in small portions. The reaction mixture was stirred at room temperature for 4 hours. The light pink precipitate was filtered off and the solid was washed with water (100 ml) and petroleum ether (100 ml). The crude product was air-dried overnight to give methyl 4-(di(1*H*-pyrrol-2-yl)methyl)benzoate (2.64 g, 9.41 mmol, 86%) as a pale pink solid.

R_f: 0.33 (petrol : ethyl acetate, 3:1; UV light). **Mp:** 160 - 161 °C [lit. 162.1 - 162.7 °C]. **^{1}H NMR** (300 MHz, Chloroform-*d*) δ 7.98 (m*, *J* = 8.3 Hz, 4H, $H^{4,12}$), 7.29 (d, *J* = 8.3 Hz, 2H, H^5), 6.75-6.68(m, 2H, H^{11}), 6.17 (dd, *J* = 2.8,2.8, 2H, H^{10}), 5.89-5.86 (m, 2H, H^9), 5.53 (s, 1H, H^7), 3.91 (s, 3H, H^1). **^{13}C NMR** (75 MHz, Chloroform-*d*) δ 167.0 (C^2), 147.5 (C^6), 131.7 (C^8), 130.1 (C^4), 129.3 (C^3), 128.5 (C^5), 117.7 (C^{11}), 108.7 (C^{10}), 107.7 (C^9), 52.3 (C^1), 44.1 (C^7). **IR (neat):** υ_{max}/cm^{-1} 3334 (N-H, m), 1702 (C=O, m), 1607 (w), 1568 (w). **HRMS** (TOF MS ES$^+$) calcd for $C_{17}H_{17}N_2O_2$ $[M+H]^+$: 281.1285, found 281.1286.

*Doublet corresponding to H^4 with multiplet underneath corresponding to H^{12}

Observed data (^{1}H, ^{13}C, IR) are consistent with those previously reported by Hall *et al*.[12]

7.2.1.2 Methyl (*Z*)-4-((5-bromo-1*H*-pyrrol-2-yl)(5-bromo-2*H*-pyrrol-2-ylidene)methyl)benzoate (**2.14**)

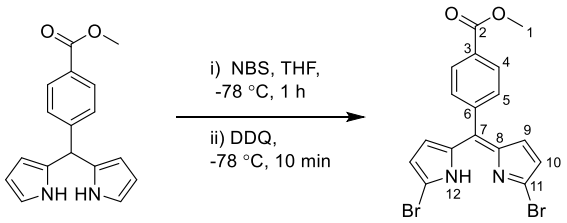

To a 250 mL round bottom flask was added methyl 4-(di(1*H*-pyrrol-2-yl)methyl)benzoate (1.50 g, 5.35 mmol) dissolved in THF (80 mL). The reaction mixture was left to cool to -78 °C over 1 hour. Recrystallized NBS (1.90 g, 10.7 mmol) was then added in two portions over 10 min. The reaction mixture was stirred at -78 °C for 1 hour then added DDQ (1.21 g, 5.35 mmol) in small portions over 10 minutes. The reaction mixture was wormed to room temperature and quenched with saturated solution of sodium sulfite (100 mL) and diluted with DCM (100 mL). The organic layer was washed with water (100 mL x 3), dried over $MgSO_4$, filtered and the solvent was removed under reduced pressure. The crude product was purified through silica gel column chromatography (DCM) to give methyl (*Z*)-4-((5-bromo-1*H*-pyrrol-2-yl)(5-bromo-2*H*-pyrrol-2-ylidene)methyl)benzoate (1.58 g, 3.46 mmol, 65 %).

R_f: 0.43 (petrol : DCM, 1:1). **Mp:** 128 - 130 °C .**^{1}H NMR** (300 MHz, Chloroform-*d*) δ 12.29 (br, 1H, H^{12}), 8.11 (d, *J* = 8.5 Hz, 2H, H^4), 7.51 (d, *J* = 8.5 Hz, 2H, H^5), 6.41 (d, *J* = 4.3 Hz, 2H, H^9), 6.34 (d, *J* = 4.3 Hz, 2H, H^{10}), 3.97 (s, 3H, H^1). **^{13}C NMR** (75 MHz, Chloroform-*d*) δ 166.3 (C^2), 139.9 (C^6), 139.8 (C^8), 137.7 (C^9), 130.9 (C^7), 130.7 (C^4), 130.1 (C^5), 129.8 (C^3), 129.0 (C^{11}), 120.8 (C^{10}), 52.4 (C^1). **IR (neat):** υ_{max}/cm^{-1} 3329 (N-H, w), 3139 (w), 1714 (C=O, m). **HRMS** (TOF MS ES$^+$) calcd for $C_{17}H_{13}N_2O_2{}^{79}Br^{81}Br$ $[M+H]^+$: 438.9323, found 438.9339.

Observed data (^{1}H, ^{13}C, IR) are consistent with those previously reported by Hall *et al*.[12]

7.2.1.3 Methyl 4-(3,7-dibromo-5,5-difluoro-5*H*-4λ^4,5λ^4-dipyrrolo[1,2-*c*:2',1'-*f*][1,3,2]diazaborinin-10-yl)benzoate (**1.67**)

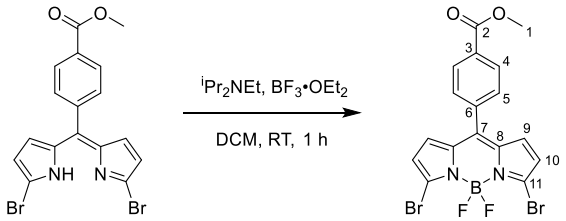

To a 250 mL round bottomed flask, under an atmosphere of nitrogen, was added methyl (*Z*)-4-((5-bromo-1*H*-pyrrol-2-yl)(5-bromo-2*H*-pyrrol-2-ylidene)methyl)benzoate (2.00 g, 4.58 mmol) was DCM (20 mL), ^{i}Pr$_2$NEt (1.99 mL, 11.45 mmol) and $BF_3.OEt_2$ (1.12 mL, 9.16 mmol). The reaction mixture was stirred at room temperature for 1 hour, then diluted with DCM (100 mL), washed with NaOH solution (0.1 M, 100 ml), HCl solution (0.1 M, 100 mL), water (100 mL x 2), and brine (100 mL). The organic was dried over $MgSO_4$, filtered and the solvent was removed under reduced pressure. The crude product was purified through silica gel column chromatography (DCM) to give methyl 4-(3,7-dibromo-5,5-difluoro-5*H*-4λ^4,5λ^4-dipyrrolo[1,2-*c*:2',1'-*f*][1,3,2]diazaborinin-10-yl)benzoate as red solid (2.23 g , 4.60 mmol, 100 %) as a red solid.

R_f: 0.45 (petrol : ethyl acetate, 3:1). **Mp:** 249 - 250 °C [lit. 249 - 250 °C]. **^{1}H NMR** (300 MHz, Chloroform-*d*) δ 8.18 (d, *J* = 8.6 Hz, 2H, H^4), 7.57 (d, *J* = 8.6 Hz, 2H, H^5), 6.74 (d, *J* = 4.2 Hz, 2H, H^9), 6.55 (d, *J* = 4.2 Hz, 2H, H^{10}), 3.98 (s, 3H, H^1). **^{13}C NMR** (75 MHz, Chloroform-*d*) δ 166.2 (C^2), 141.6 (C^6), 136.8 (C^7), 135.4 (C^4), 133.7 (C^3), 132.5 (C^5), 131.6 (C^8), 130.6 (C^9), 129.8 (C^{11}), 123.3 (C^{10}), 52.7 (C^1). **^{11}B NMR** (96 MHz, $CDCl_3$) δ 0.33 (t, $J_{B\text{-}F}$ = 28.2 Hz).**^{19}F NMR** (282 MHz, $CDCl_3$) δ -146.8 (q, $J_{B\text{-}F}$= 28.1 Hz). **IR (neat):** υ_{max}/ cm^{-1} 3092(C-H, w), 1711 (C=O, m). **HRMS** (TOF MS ES$^+$) calcd for $C_{17}H_{12}N_2O_2{}^{79}Br^{81}Br\ ^{10}BF_2$ $[M+H]^+$: 484.9310, found 484.9313. **UV-Vis: λ_{max}** (abs) = 526 nm. **Molar extinction coefficient** (ε) = 84,000 M^{-1} cm^{-1} (DCM).

X-Ray code: mjh190038_fa

Observed data (^{1}H, ^{13}C, ^{11}B, ^{19}F, IR) are consistent with those previously reported by Hall *et al*.[12]

7.2.1.4 Methyl 4-(5,5-difluoro-3,7-diiodo-5*H*-4λ^4,5λ^4-dipyrrolo[1,2-*c*:2',1'-*f*][1,3,2]diazaborinin-10 yl)benzoate (**1.68**)

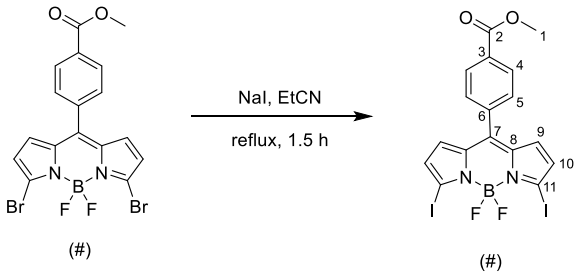

To a round bottom flask was added methyl 4-(3,7-dibromo-5,5-difluoro-5*H*-4λ^4,5λ^4-dipyrrolo[1,2-*c*:2',1'-*f*][1,3,2]diazaborinin-10-yl)benzoate (2.86 g, 5.91 mmol) dissolved in saturated solution of NaI in propionitrile (60 mL). The reaction mixture was refluxed for 1.5 hours then left to cool to room temperature. The reaction mixture was diluted with DCM (100 mL) and washed with water (3 x 100 mL). The organic layer was dried over $MgSO_4$, filtered, the solvent removed under reduced pressure. The crude product was purified through silica gel column chromatography (DCM) to give methyl 4-(5,5-difluoro-3,7-diiodo-5*H*-4λ^4,5λ^4-dipyrrolo[1,2-*c*:2',1'-*f*][1,3,2]diazaborinin-10 yl)benzoate (3.10 g, 5.37 mmol, 91 %) as a purple solid.

R_f: 0.82 (DCM). **Mp:** 156-158 °C [lit. 156 - 157 °C]. **^{1}H NMR** (300 MHz, Chloroform-*d*) δ 8.17 (d, *J* = 8.3 Hz, 2H, H^4), 7.57 (d, *J* = 8.3 Hz, 2H, H^5), 6.72 (d, *J* = 4.2 Hz, 2H, H^9), 6.61 (d, *J* = 4.2 Hz, 2H, H^{10}), 3.98 (s, 3H, H^1). **^{13}C NMR** (75 MHz, Chloroform-*d*) δ 166.2 (C^2), 139.7 (C^7), 137.7 (C^8), 136.8 (C^3), 132.3 (C^6), 131.6 (C^{10}), 130.6 – 130.4 (*m,* C^9), 130.4 (C^5), 129.8 (C^4), 104.0 (C^{11}), 52.7 (C^1). **^{11}B NMR** (96 MHz, Chloroform-*d*) δ 0.72 (t, $J_{B\text{-}F}$ = 29.4 Hz). **^{19}F NMR** (282 MHz, Chloroform-*d*) δ -144.8 (q, $J_{B\text{-}F}$= 29.4 Hz). **IR** (neat): υ_{max}/cm^{-1} 3107 (C-H, w), 1711 (C=O, m). **HRMS** (ASAP+) calcd for $C_{17}H_{11}BI_2F_2N_2O_2$ $[M\text{-}F]^+$: 558.8990, found 558.8995. **UV-Vis: λ_{max}** (abs) = 545 nm. **Molar extinction coefficient** (ε) = 63,000 M^{-1} cm^{-1} (DCM).

X-Ray code: mjh220039

Observed data (^{1}H, ^{13}C, ^{11}B, ^{19}F, IR) are consistent with those previously reported by Hall *et al*.[45]

7.2.1.5 Methyl 4-(3-(((1*S*,2*S*)-2-amino-1,2-diphenylethyl)amino)-7-bromo-5,5-difluoro-5*H*-5λ^4,6λ^4-dipyrrolo[1,2-*c*:2',1'-*f*][1,3,2]diazaborinin-10-yl)benzoate (**2.18**)

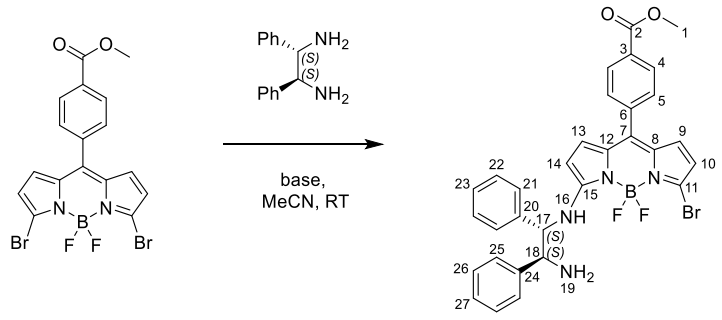

Method A:

To a round bottom flask, under an atmosphere of nitrogen, was added methyl 4-(3,7-dibromo-5,5-difluoro-5*H*-4λ^4,5λ^4-dipyrrolo[1,2-*c*:2',1'-*f*][1,3,2]diazaborinin-10-yl)benzoate (200 mg, 0.41 mmol), (1*S*,2*S*)-1,2-diphenylethane-1,2-diamine (87.6 mg, 0.41 mmol), K_2CO_3 (171 mg, 1.24 mmol), and MeCN (50 mL). The reaction mixture was stirred at room temperature for 18 hours, diluted with DCM (50 mL) and washed with water (3 x 50 mL). The organic layer was dried over $MgSO_4$, filtered, and removed solvent under reduced pressure. The crude product was purified through silica gel column chromatography (DCM → DCM: methanol, 100:0.5) to give methyl 4-(3-(((1*S*,2*S*)-2-amino-1,2-diphenylethyl)amino)-7-bromo-5,5-difluoro-5*H*-5λ^4,6λ^4-dipyrrolo[1,2-*c*:2',1' *f*][1,3,2]diazaborinin-10-yl)benzoate (247 mg, 0.40 mmol, 97 %) as an orange solid.

Method B:

To a 50 mL round bottom flask, under an atmosphere of nitrogen, was added methyl 4-(3,7-dibromo-5,5-difluoro-5*H*-4λ^4,5λ^4-dipyrrolo[1,2-*c*:2',1'-*f*][1,3,2]diazaborinin-10-yl)benzoate (48.4 mg, 0.10 mmol), (1*S*,2*S*)-1,2-diphenylethane-1,2-diamine (42.5 mg, 0.20 mmol), Et_3N (30 µL , 0.22 mmol), and MeCN (20 mL). The reaction mixture was stirred at room temperature for 20 hours, and the solvent was removed under reduced pressure. The crude product was purified through silica gel column chromatography (petrol : ethyl acetate, 2:1) to give methyl 4-(3-(((1*S*,2*S*)-2-amino-1,2-diphenylethyl)amino)-7-bromo-5,5-difluoro-5*H*-5λ^4,6λ^4-dipyrrolo[1,2-*c*:2',1' *f*][1,3,2]diazaborinin-10-yl)benzoate (55.3 mg, 0.09 mmol, 90%) as an orange solid.

R_f: 0.4 (DCM : methanol, 100:1). **Mp:** 132 - 134 °C. **^{1}H NMR** (300 MHz, Chloroform-*d*) δ 8.39 (d, *J* = 7.8 Hz, 1H, H^{16}), 8.03 (d, *J* = 8.4 Hz, 2H, H^4), 7.52 (d, *J* = 7.1 Hz, 2H, Ar), 7.46-7.25 (m, 10H, H^5, Ar), 6.53 (d, *J* = 5.0 Hz, 1H, H^{14}), 6.28 (d, *J* = 3.9 Hz, 1H, H^{10}), 6.21 (d, *J* = 3.9 Hz, 1H, H^9), 5.70 (d, *J* = 5.0 Hz, 1H, H^{13}), 4.66 (dd, *J* = 7.8, 2.6 Hz, 1H, H^{17}), 4.46 (d, *J* = 2.6 Hz, 1H, H^{18}), 3.92 (s, 3H, H^1). **^{13}C NMR** (75 MHz, Chloroform-*d*) δ 166.5 (C^2), 161.7 (C^{11}), 141.6, 140.2, 138.5 (C^3), 135.3 (C^{14}), 133.5 (C^6), 133.2

(C^{7}),130.7, 130.3 (C^{12}), 129.4 (C^{5}), 129.2 (C^{4}), 128.8 (C^{15}), 128.2, 128.2, 126.8, 126.3, 120.0 (C^{9}), 116.7 (C^{10}), 115.3 (C^{8}), 112.9 (C^{13}), 77.4, 63.5 (C^{17}), 60.5 (C^{18}), 52.4 (C^{1}). **^{11}B NMR** (96 MHz, Chloroform-*d*) δ 1.13 (t, J_{B-F} = 32.5 Hz). **^{19}F NMR** (282 MHz, Chloroform-*d*) δ -146.5 (dq, J_{F-F}= 97.5, J_{B-F} = 30.5 Hz), -147.7 (dq, J_{F-F}= 100.6, J_{B-F}= 30.6 Hz). **IR** (neat): υ_{max}/cm^{-1} 3317 (C-H, w), 1716 (C=O, m), 1594 (s). **HRMS** (pNSI) calcd for $C_{31}H_{27}{}^{11}B^{81}BrF_2N_4O_2$ $[M+H]^+$: 617.1363, found 617.1363. **$[\alpha]^{25}_D$** -194, (c 0.1, DCM). **UV-Vis: λ_{max}** (abs) = 505 nm. **Molar extinction coefficient** (ε) = 46,128 M^{-1} cm^{-1}. **ϕ_F** = 0.20 (DCM).

X-Ray code: mjh220057_fa

7.2.1.6 Methyl 4-(3-(((1*S*,2*S*)-2-amino-1,2-diphenylethyl)amino)-5,5-difluoro-7-iodo-5*H*-5λ^4,6λ^4-dipyrrolo[1,2-*c*:2',1'-*f*][1,3,2]diazaborinin-10-yl)benzoate (**2.19**)

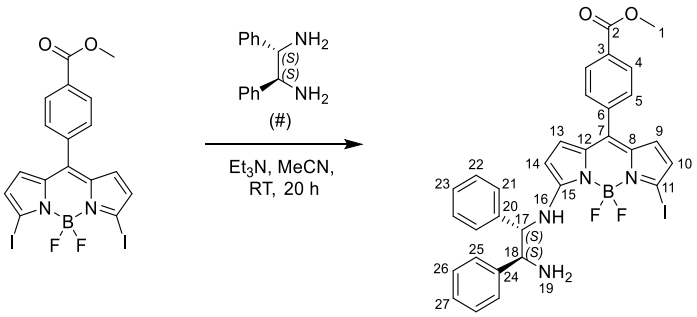

To a 50 mL round bottom flask, under an atmosphere of nitrogen, was added methyl 4-(5,5-difluoro-3,7-diiodo-5*H*-4λ^4,5λ^4-dipyrrolo[1,2-*c*:2',1'-*f*][1,3,2]diazaborinin-10 yl)benzoate (115 mg, 0.20 mmol), (1*S*,2*S*)-1,2-diphenylethane-1,2-diamine (42.5 mg, 0.20 mmol), Et_3N (55 µL, 0.40 mmol), and MeCN (20 mL). The reaction mixture was stirred at room temperature for 20 hours, diluted with DCM (50 mL) and washed with water (3 x 50 mL). The organic layer was dried over $MgSO_4$, filtered, and removed solvent under reduced pressure. The crude product was purified through silica gel column chromatography (DCM → DCM: ethyl acetate, 1:1) to give methyl 4-(3-(((1*S*,2*S*)-2-amino-1,2-diphenylethyl)amino)-5,5-difluoro-7-iodo-5*H*-5λ^4,6λ^4-dipyrrolo[1,2-*c*:2',1'-*f*][1,3,2]diazaborinin-10-yl)benzoate (113 mg, 0.17 mmol, 85 %) as an orange solid.

R_f: 0.1 (DCM). **Mp:** 152 - 154 °C **^{1}H NMR** (300 MHz, Chloroform-*d*) δ 8.35 (br, 1H, H^{16}), 8.05 (d, *J* = 8.5 Hz, 2H, H^4), 7.57-7.28 (m, 12 H, H^5, Ar), 6.56 (d, *J* = 5.0 Hz, 1H, H^{14}), 6.51 (d, *J* = 3.8 Hz, 1H, H^{10}), 6.17 (d, *J* = 3.8 Hz, 1H, H^9), 5.75 (d, *J* = 5.1 Hz, 1H, H^{13}), 4.66 (br, 1H, H^{17}), 4.46 (d, *J* = 3.1 Hz, 1H, H^{18}), 3.93 (s, 3H, H^1). **^{13}C NMR** (75 MHz, Chloroform-*d*) δ 166.6 (C^2), 161.9, 141.6, 140.2, 138.7, 135.9, 135.3, 133.7, 130.8, 130.4, 129.5, 129.3, 129.0, 128.9, 128.3, 128.2, 126.8, 126.4, 124.6, 120.9, 112.9, 81.8, 76.7, 64.6, 52.4 (C^1). **^{11}B NMR** (96 MHz, $CDCl_3$) δ 1.12 (t, $J_{B\text{-}F}$ = 33.1 Hz). **^{19}F NMR** (282 MHz, Chloroform-*d*) δ -145.6 (dq, $J_{F\text{-}F}$= 98.8, $J_{B\text{-}F}$ = 32.1 Hz), -146.7 (dq, $J_{F\text{-}F}$= 101.1, $J_{B\text{-}F}$= 32.3 Hz). **IR** (neat): υ_{max}/cm^{-1} 1720 (C=O, m), 1599 (C=C, s). **HRMS** (pNSI) calcd for $C_{31}H_{27}{}^{11}BIF_2N_4O_2$ $[M+H]^+$: 663.1242, found 663.1238. **UV-Vis:** λ_{max} (abs) = 511 nm. **Molar extinction coefficient** (ε) = 65,688 M^{-1} cm^{-1}. **ϕ_F** = 0.35 (DCM).

X-Ray code: mjh220053_fa

7.2.1.7 Methyl 4-(3-bromo-7-(((1*S*,2*S*)-2-((7-bromo-5,5-difluoro-10-(4-(methoxycarbonyl)phenyl)-5*H*-5λ^4,6λ^4-dipyrrolo[1,2-*c*:2',1'-*f*][1,3,2]diazaborinin-3-yl)amino)-1,2-diphenylethyl)amino)-5,5-difluoro-5*H*-4λ^4,5λ^4-dipyrrolo[1,2-*c*:2',1'-*f*][1,3,2]diazaborinin-10-yl)benzoate (**2.3**)

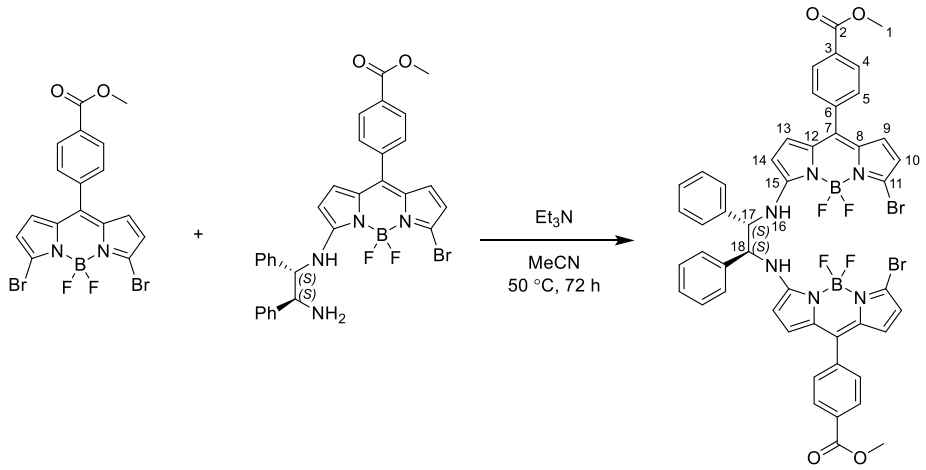

To a 50 mL round bottom flask, under an atmosphere of nitrogen, was added methyl 4-(3,7-dibromo-5,5-difluoro-5*H*-4λ^4,5λ^4-dipyrrolo[1,2-*c*:2',1'-*f*][1,3,2]diazaborinin-10-yl)benzoate (58.9 mg, 0.12 mmol), methyl 4-(3-(((1*S*,2*S*)-2-amino-1,2-diphenylethyl)amino)-7-bromo-5,5-difluoro-5*H*-5λ^4,6λ^4-dipyrrolo[1,2-*c*:2',1'-*f*][1,3,2]diazaborinin-10-yl)benzoate (75 mg, 0.12 mmol),Et_3N (29 µL, 0.21 mmol), and MeCN (15 mL). The reaction mixture was heated to 50 °C for 72 hours, the solvent was removed under reduced pressure. The crude product was purified through silica gel column chromatography (DCM) to give (76 mg, 0.07 mmol, 62%) as an orange solid.

R_f: 0.6 (DCM). **Mp:** 300 °C (decomposed). **^{1}H NMR** (300 MHz, Chloroform-*d*) δ 8.08 (d, *J* = 8.5 Hz, 4H, H^4), 7.46 (d, *J* = 7.8 Hz, 4H, H^5), 7.37 – 7.29 (m, 6H, Ar), 7.10 – 7.00 (m, 6H, Ar), 6.75 (d, *J* = 5.0 Hz, 2H, H^9), 6.33 (d, *J* = 3.9 Hz, 2H, H^{13}), 6.30 (d, *J* = 4.0 Hz, 2H, H^{14}), 6.09 (d, *J* = 5.0 Hz, 2H, H^{10}), 5.03 (d, *J* = 6.6 Hz, 2H, $H^{17,18}$), 3.95 (s, 6H, H^1). **^{11}B NMR** (96 MHz, Chloroform-*d*) δ 0.93 (t, *J* = 33.0 Hz). **^{19}F NMR** (282 MHz, Chloroform-*d*) δ -146.5 – -146.6 (m), -147.2 – -148.3 (m).

^{1}H NMR (700 MHz, DMSO-d_6) δ 8.83 (br, 2H, H^{16}), 8.05 (d, *J* = 8.1 Hz, 4H, H^4), 7.60 (br, 4H, H^5), 7.37 (d, *J* = 7.2 Hz, 4H, Ar), 7.19 (t, *J* = 7.5 Hz, 4H, Ar), 7.15 – 7.11 (m, 2H, A), 7.02 (d, *J* = 5.2 Hz, 2H, $H^{9/10}$), 6.93 (d, *J* = 5.3 Hz, 2H, $H^{9/10}$), 6.33 (d, *J* = 3.8 Hz, 2H, $H^{13/14}$), 6.18 (d, *J* = 3.8 Hz, 2H, $H^{13/14}$), 5.87 (dd, *J* = 6.4, 2.7 Hz, 2H, $H^{17,18}$), 3.89 (s, 6H, H^1). **^{13}C NMR** (176 MHz, DMSO-d_6) δ 165.8 (C^2), 162.2, 139.0, 138.0, 135.5 ($C^{9/10}$), 133.5, 132.3, 130.6 (C^5), 130.1, 129.2 (C^4), 128.3, 127.9, 127.7, 127.4, 118.4 ($C^{13/14}$), 116.12 ($C^{13/14}$), 116.0 ($C^{9/10}$), 112.7, 79.2, 62.6 ($C^{17,18}$), 52.4 (C^1). **^{19}F NMR** (659 MHz, DMSO-d_6) δ -143.08 – -143.65 (m). **IR** (neat): υ_{max}/cm^{-1} 3393 (C-H, w), 1736 (C=O, m), 1583 (C=C, m). **HRMS** (pNSI) calcd for

$C_{48}H_{36}{}^{10}B_2{}^{81}Br_2F_3N_6O_4$ $[M-F]^+$: 999.1263, found 999.1293. **UV-Vis:** λ_{max} (abs) = 525 nm. **Molar extinction coefficient** (ε) = 85,850 M^{-1} cm^{-1}. $\boldsymbol{\phi_F}$ = 0.02 (DCM).

7.2.1.8 Methyl 4-(3-(((1S,2S)-2-((5,5-difluoro-7-iodo-10-(4-(methoxycarbonyl)phenyl)-5*H*-5λ^4,6λ^4-dipyrrolo[1,2-*c*:2',1'-*f*][1,3,2]diazaborinin-3-yl)amino)-1,2-diphenylethyl)amino)-5,5-difluoro-7-iodo-5*H*-5λ^4,6λ^4-dipyrrolo[1,2-*c*:2',1'-*f*][1,3,2]diazaborinin-10-yl)benzoate (**2.4**)

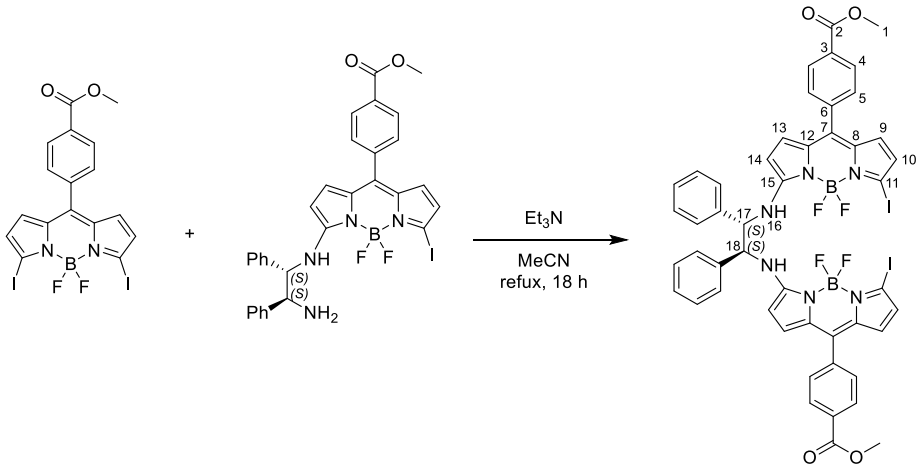

To a round bottom flask, under an atmosphere of nitrogen, was added methyl 4-(5,5-difluoro-3,7-diiodo-5*H*-4λ^4,5λ^4-dipyrrolo[1,2-*c*:2',1'-*f*][1,3,2]diazaborinin-10 yl)benzoate (29 mg, 0.05 mmol), methyl 4-(3-(((1*S*,2*S*)-2-amino-1,2-diphenylethyl)amino)-5,5-difluoro-7-iodo-5*H*-5λ^4,6λ^4-dipyrrolo[1,2-*c*:2',1'-*f*][1,3,2]diazaborinin-10-yl)benzoate (33 mg, 0.05 mmol), Et_3N (13.8 µL, 0.10 mmol), and MeCN (2 mL). The reaction mixture was heated to reflux and stirred for 18 hours, diluted with DCM (50 mL) and washed with water (3 x 50 mL). The organic layer was dried over $MgSO_4$, and the solvent removed under reduced pressure. The crude product was purified through silica gel column chromatography (DCM) to give methyl 4-(3-(((1*S*,2*S*)-2-((5,5-difluoro-7-iodo-10-(4-(methoxycarbonyl)phenyl)-5*H*-5λ^4,6λ^4-dipyrrolo[1,2-*c*:2',1'-*f*][1,3,2]diazaborinin-3-yl)amino)-1,2-diphenylethyl)amino)-5,5-difluoro-7-iodo-5*H*-5λ^4,6λ^4-dipyrrolo[1,2-*c*:2',1'-*f*][1,3,2]diazaborinin-10-yl)benzoate (17.2 mg, 0.02 mmol, 31%) as an orange solid.

R_f: 0.4 (DCM). **Mp:** 118 - 120 °C. **^{1}H NMR** (300 MHz, Chloroform-*d*) δ 8.08 (d, *J* = 7.9 Hz, 4H, H^4), 7.46 (d, *J* = 7.8 Hz, 4H, H^5), 7.37 – 7.29 (m, 6H, Ar), 7.12 – 6.98 (m*, 6H, Ar, H^{16}), 6.74 (d, *J* = 5.0 Hz, 2H, $H^{10/11}$), 6.53 (d, *J* = 3.9 Hz, 2H, $H^{13/14}$), 6.24 (d, *J* = 3.9 Hz, 2H, $H^{10/11}$), 6.09 (d, *J* = 5.0 Hz, 2H, $H^{13/14}$), 5.04 (d, *J* = 6.8 Hz, 2H, $H^{17.18}$), 3.95 (s, 6H, H^1). **^{13}C NMR** (176 MHz, Chloroform-d) δ 166.6 (C^2), 161.1, 138.3, 136.0, 135.8 ($C^{9/10}$), 135.2, 133.3, 131.5, 131.2, 130.4, 129.6, 129.5, 129.3, 127.7, 125.4 ($C^{13/14}$), 122.7 ($C^{13/14}$), 111.8 ($C^{9/10}$), 84.2, 63.0 ($C^{17,18}$), 52.5 (C^1). **^{11}B NMR** (96 MHz, Chloroform-*d*) δ 0.96 (t, *J* = 34.2 Hz). **^{19}F NMR** (282 MHz, Chloroform-*d*) δ -145.31 – -145.38 (m), -146.29 – -146.35 (m). **IR** (neat): υ_{max}/cm^{-1} 3317 (C-H, w), 1716 (C=O, m), 1594 (C=C, s). **HRMS** (pNSI) calcd for $C_{48}H_{36}{}^{11}B_2F_4I_2N_6O_4Na$ $[M+Na]^+$: 1135.0917, found 1135.0922. **UV-Vis:** λ_{max} (abs) = 531 nm. **Molar extinction coefficient** (ε) = 42,276 M^{-1} cm^{-1}. **ϕ_F** = 0.03 (DCM).

7.2.1.9 Methyl 4-(3-bromo-7-((4-((7-bromo-5,5-difluoro-10-(4-(methoxycarbonyl)phenyl)-5*H*-4λ^4,5λ^4-dipyrrolo[1,2-c:2',1'-*f*][1,3,2]diazaborinin-3-yl)amino)butyl)amino)-5,5-difluoro-5*H*-4λ^4,5λ^4-dipyrrolo[1,2-*c*:2',1'-*f*][1,3,2]diazaborinin-10-yl)benzoate (**2.28**)

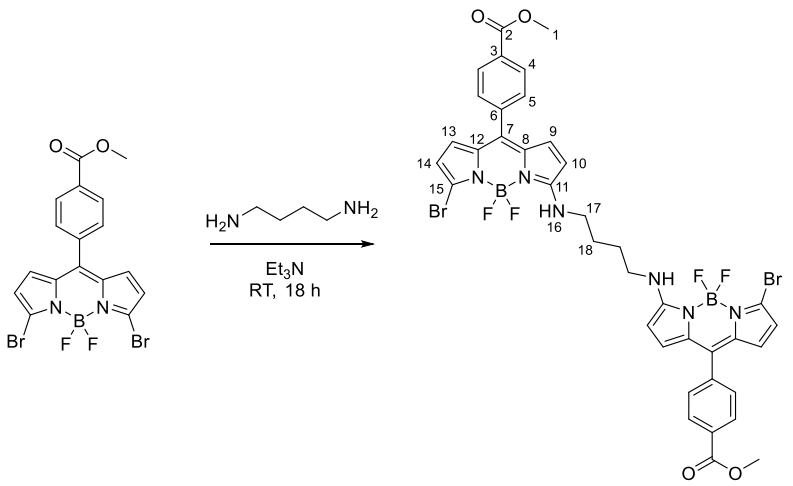

To a 25 mL round bottom flask, under an atmosphere of nitrogen, was added methyl 4-(3,7-dibromo-5,5-difluoro-5*H*-4λ^4,5λ^4-dipyrrolo[1,2-*c*:2',1'-*f*][1,3,2]diazaborinin-10-yl)benzoate (48.3 mg, 0.10 mmol), butane-1,4-diamine (4.41 mg, 0.05 mmol), Et_3N (30 µL, 0.22 mmol), and MeCN (5 mL). The reaction mixture was stirred at room temperature for 18 hours, diluted with DCM (50 mL) and washed with water (3 x 50 mL). The organic layer was dried over Na_2SO_4, filtered, and removed solvent under reduced pressure. The crude product was purified through silica gel column chromatography (DCM → DCM: ethyl acetate, 3:1) to give methyl 4-(3-bromo-7-((4-((7-bromo-5,5-difluoro-10-(4-(methoxycarbonyl)phenyl)-5*H*-4λ^4,5λ^4-dipyrrolo[1,2-c:2',1'-*f*][1,3,2]diazaborinin-3-yl)amino)butyl)amino)-5,5-difluoro-5*H*-4λ^4,5λ^4-dipyrrolo[1,2-*c*:2',1'-*f*][1,3,2]diazaborinin-10-yl)benzoate (40.6 mg, 0.05 mmol, 91%) as an orange solid.

R_f: 0.25 (DCM). **Mp:** 160 °C (decomposed). **^{1}H NMR** (300 MHz, Chloroform-*d*) δ 8.10 (d, *J* = 8.5 Hz, 4H, H^4), 7.48 (d, *J* = 8.6 Hz, 4H, H^5), 6.84 (d, *J* = 5.0 Hz, 2H, H^{10}), 6.30 (d, *J* = 3.9 Hz, 2H $H^{13/14}$), 6.45 (br, 2H), 6.26 (d, *J* = 3.9 Hz, 2H, $H^{13/14}$), 6.25 (d, *J* = 5.0 Hz, 2H, H^9), 3.96 (s, 6H, H^1), 3.54 – 3.42 (m, 4H, H^{17}), 1.88 – 1.77 (m, 4H, H^{18}). **^{13}C NMR** (75 MHz, Chloroform-d) δ 166.6 (C^2), 162.1, 138.4, 136.0 (C^{10}), 133.4, 133.3, 131.1, 130.5, 130.3 (C^5), 129.6 (C^4), 120.7 ($C^{13/14}$), 117.1 ($C^{13/14}$), 115.8, 111.6 (C^9), 52.5 (C^1), 44.5 (C^{17}), 27.2 (C^{18}). **^{11}B NMR** (96 MHz, Chloroform-*d*) δ 0.95 (t, *J* = 34.4 Hz). **^{19}F NMR** (282 MHz, Chloroform-*d*) δ -147.11 (q, $J_{B\text{-}F}$ = 31.1 Hz). **IR** (neat): υ_{max}/cm^{-1} 3325 (N-H, w), 1722 (C=O, m), 1603 (C=C, m). **LRMS** calcd for $C_{38}H_{33}{}^{11}B_2{}^{79}Br_2F_4N_6O_4$ $[M+H]^+$: 893.1047, found 890.0000.

X-Ray code: mjh230021_fa

7.2.1.10 Methyl 4-(3-(((1*S*,2*S*)-2-amino-1,2-diphenylethyl)amino)-5,5-difluoro-7-(4-methoxyphenyl)-5*H*-5λ^4,6λ^4-dipyrrolo[1,2-*c*:2',1'-*f*][1,3,2]diazaborinin-10-yl)benzoate (**2.24**)

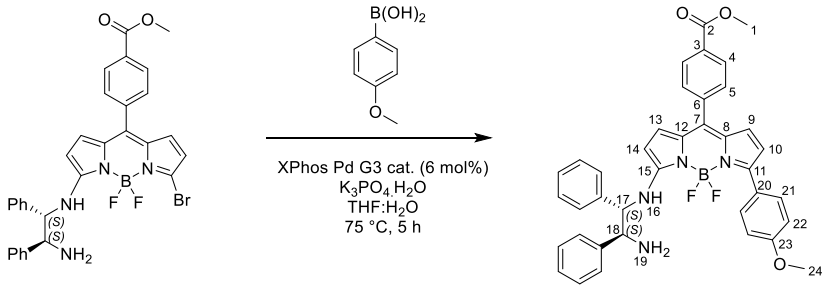

To a Schlenk flask, under nitrogen atmosphere, was added methyl 4-(3-(((1*S*,2*S*)-2-amino-1,2-diphenylethyl)amino)-7-bromo-5,5-difluoro-5*H*-5λ^4,6λ^4-dipyrrolo[1,2-*c*:2',1'-*f*][1,3,2]diazaborinin-10-yl)benzoate (63 mg, 0.10 mmol), (4-methoxyphenyl)boronic acid (31 mg, 0.20 mmol), XPhos Pd G3 (5.18 mg, 6 mol %, 0.006 mmol), $K_3PO_4.H_2O$ (46.9 g, 0.20 mmol), dry THF (8 mL), water (1.2 mL) and was degassed using freeze-pump-thaw method (x3). The reaction mixture was heated, using an oil bath, to 75 °C, stirred for 5 hours then diluted with DCM (50 mL). The organic layer was washed with water (3 x 50 mL), dried over $MgSO_4$, filtered and solvent removed under reduced pressure. The crude product was purified through silica gel column chromatography (DCM : ethyl acetate 100:2 → 100:20) to give methyl 4-(3-(((1*S*,2*S*)-2-amino-1,2-diphenylethyl)amino)-5,5-difluoro-7-(4-methoxyphenyl)-5*H*-5λ^4,6λ^4-dipyrrolo[1,2-*c*:2',1'-*f*][1,3,2]diazaborinin-10-yl)benzoate (26 mg, 0.04 mmol, 41 %) as dark pink/red solid.

R_f: 0.76 (DCM : ethyl acetate 10:1). **^{1}H NMR** (700 MHz, Chloroform-*d*) δ 8.07 (d, *J* = 8.0 Hz, 2H, H^4), 8.03 (d, *J* = 7.7 Hz, 1H, H^{16}), 7.89 (d, *J* = 8.8 Hz, 2H, H$^{21/22}$), 7.51 (d, *J* = 8.0 Hz, 2H, H^5), 7.43 (d, *J* = 7.4 Hz, 2H, Ar), 7.41 – 7.31 (m, 6H, Ar), 7.31 – 7.26 (m, 2H, Ar), 7.02 (d, *J* = 8.9 Hz, 2H, H$^{21/22}$), 6.57 (d, *J* = 4.9 Hz, 1H, H$^{13/14}$), 6.40 (d, *J* = 3.9 Hz, 1H, H$^{9/10}$), 6.39 (d, *J* = 3.9 Hz, 1H, H$^{9/10}$), 5.69 (d, *J* = 4.9 Hz, 1H, H$^{13/14}$), 4.63 (dd, *J* = 7.7, 3.5 Hz, 1H, H^{17}), 4.40 (d, *J* = 3.4 Hz, 1H, H^{18}), 3.94 (s, 3H, H^1), 3.89 (s, 3H, H^{24}). **^{13}C NMR** (176 MHz, Chloroform-*d*) δ 166.8, 161.1, 159.6, 148.6, 141.9, 140.4, 139.7, 134.1, 132.6, 131.2, 130.7, 130.6, 130.5, 129.4, 129.2, 128.9, 128.2, 128.2, 127.1, 127.0, 126.5, 121.7, 115.7, 113.7, 111.3, 64.2, 60.8, 55.4, 53.6, 52.4. **^{11}B NMR** (96 MHz, Chloroform-*d*) δ 1.64 (t, *J* = 34.1 Hz). **^{19}F NMR** (282 MHz, Chloroform-*d*) δ -139.90 – -141.52 (m), -141.93 – -143.12 (m). **IR** (neat): υ_{max}/cm^{-1} 3344 (N-H, w), 2926 (C-H, w), 1719 (C=O, m), 1595 (C=C, s). **HRMS** (pNSI) calcd for $C_{38}H_{34}{}^{11}BF_2N_4O_3$ $[M+H]^+$: 643.2693, found 643.2675.

7.2.1.11 Methyl 4-(3-(((1*S*,2*S*)-2-amino-1,2-diphenylethyl)amino)-5,5-difluoro-7-(4-fluorophenyl)-5*H*-5λ^4,6λ^4-dipyrrolo[1,2-*c*:2',1'-*f*][1,3,2]diazaborinin-10-yl)benzoate (**2.26**)

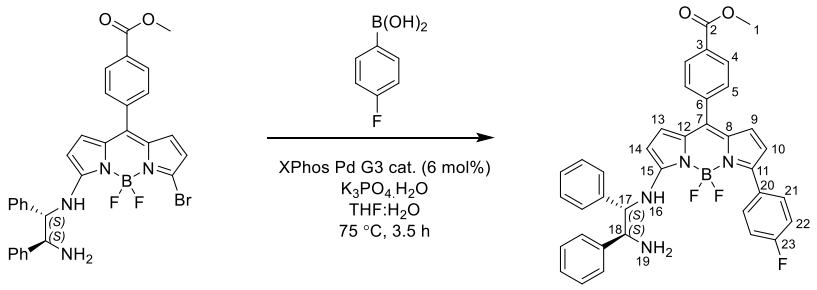

To a Schlenk flask, under nitrogen atmosphere, was added methyl 4-(3-(((1*S*,2*S*)-2-amino-1,2-diphenylethyl)amino)-7-bromo-5,5-difluoro-5*H*-5λ^4,6λ^4-dipyrrolo[1,2-*c*:2',1'-*f*][1,3,2]diazaborinin-10-yl)benzoate (50 mg, 0.08 mmol), (4-fluorophenyl)boronic acid (22.7 mg, 0.16 mmol), XPhos Pd G3 (4.12 mg, 6 mol %, 0.005 mmol), $K_3PO_4.H_2O$ (37.4 mg, 0.16 mmol), dry THF (10 mL), water (1.5 mL) and was degassed (x3). The reaction mixture was heated, using an oil bath, to 75 °C, stirred for 3.5 hours then diluted with DCM (50 mL). The organic layer was washed with water (3 x 50 mL), dried over $MgSO_4$, filtered and solvent removed under reduced pressure. The crude product was purified through silica gel column chromatography (petrol: ethyl acetate 3:1) to give methyl 4-(3-(((1*S*,2*S*)-2-amino-1,2-diphenylethyl)amino)-5,5-difluoro-7-(4-fluorophenyl)-5H-5λ^4,6λ^4-dipyrrolo[1,2-*c*:2',1'-*f*][1,3,2]diazaborinin-10-yl)benzoate (2 mg, 0.003 mmol, 4 %) as a red solid.

R_f: 0.76 (DCM : ethyl acetate 10:1). **^{11}B NMR** (96 MHz, Chloroform-*d*) δ 1.56 (t, *J* = 35.4 Hz). **^{19}F NMR** (282 MHz, Chloroform-*d*) δ-114.6 (s), -140.8 – -141.7 (m), -141.8 – -143.1 (m). **HRMS** (pNSI) calcd for $C_{37}H_{31}{}^{11}BF_3N_4O_2$ $[M+H]^+$: 631.2493, found 631.2471.

7.2.2 Chapter 3

7.2.2.1 Methyl (*S*)-4-(3-bromo-5,5-difluoro-7-((1-hydroxybutan-2-yl)amino)-5*H*-5λ^4,6λ^4-dipyrrolo[1,2-*c*:2',1'-*f*][1,3,2]diazaborinin-10-yl)benzoate (**3.1**)

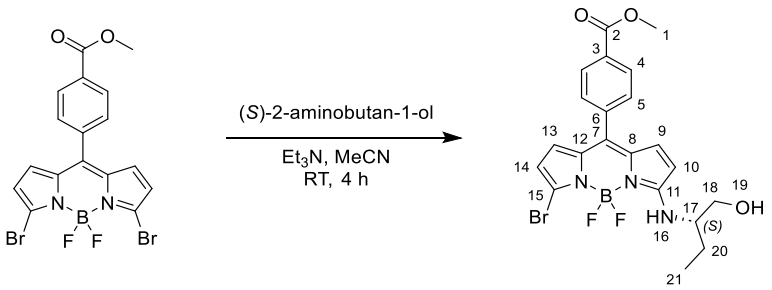

To a round bottom flask under an inert atmosphere was added methyl 4-(3,7-dibromo-5,5- difluoro-5*H*-4λ^4,5λ^4-dipyrrolo[1,2-*c*:2',1'-*f*] [1,3,2]diazaborinin10-yl)benzoate (922 mg, 1.91 mmol), (*S*)-2-aminobutan-1-ol (360 µL, 3.81 mmol), Et_3N (584 µL, 4.19 mmol) and MeCN (100 ml). The reaction mixture was stirred at room temperature for 4 hours, diluted with DCM (100 mL) and washed with water (3 x 100 mL). The aqueous layer was extracted with DCM (2 x 50 ml). The organic layers were combined and dried over Na_2SO_4, filtered and the solvent was removed under reduced pressure. The crude product was purified through silica gel column chromatography (petrol : ethyl acetate 2:1→1:1) to give methyl (*S*)-4-(3-bromo-5,5-difluoro-7-((1-hydroxybutan-2-yl)amino)-5*H*-5λ^4,6λ^4-dipyrrolo[1,2-*c*:2',1'-*f*][1,3,2]diazaborinin-10-yl)benzoate (865 mg, 1.76 mmol, 92 %) as an orange solid.

R_f: 0.20 (petrol : ethyl acetate, 2:1). **Mp:** 158-159 °C. **^{1}H NMR** (300 MHz, Chloroform-*d*) δ 8.02 (d, *J* = 8.2 Hz, 2H, H^4), 7.39 (d, *J* = 8.2 Hz, 2H, H^5), 6.72 (d, *J* = 5.1 Hz, 1H, H^9), 6.49 (d, *J* = 9.1 Hz, 1H, H^{16}), 6.29 (d, *J* = 5.1 Hz, 1H, H^{10}), 6.22 (d, *J* = 3.9 Hz, 1H, H^{14}), 6.15 (d, *J* = 3.9 Hz, 1H, H^{13}), 3.74 (s, 3H, H^1), 3.74 (dd, *J* = 11.3, 3.9 Hz, 1H, H^{18}), 3.63 (dd, *J* = 11.3, 6.1 Hz, 1H, $H^{18'}$), 3.57 – 3.47 (m, 1H, H^{17}), 1.78 – 1.47 (m, 2H, $H^{20,20'}$), 0.96 (t, *J* = 7.4 Hz, 3H, H^{21}). **^{13}C NMR** (75 MHz, Chloroform-*d*) δ 166.5 (C^2), 162.5 (C^{15}), 138.3 (C^3), 135.5 (C^7), 133.3 (C^{14}), 133.0 (C^{12}), 130.6 (C^6), 130.2 (C^5), 129.4 (C^4), 128.8 (C^{11}), 119.6 (C^{10}), 116.5 (C^9), 114.4 (C^{13}), 113.1 (C^8), 64.4 (C^{18}), 59.2 (C^{17}), 52.4 (C^1), 24.7 (C^{20}), 10.3 (C^{21}). **^{11}B NMR** (96 MHz, Chloroform-*d*) δ 1.00 (t, *J* = 34.6 Hz). **^{19}F NMR** (282 MHz, Chloroform-*d*) δ -145.4 (dq, $J_{F\text{-}F}$= 94.4 Hz, $J_{B\text{-}F}$= 25.8 Hz), -147.1 (dq, $J_{F\text{-}F}$= 97.4 Hz, $J_{B\text{-}F}$= 24.4 Hz). **IR** (neat): υ_{max}/cm^{-1} 3378 (C-H, w), 1716 (C=O, m). **HRMS** (TOF MS ES+) calcd for $C_{21}H_{22}{}^{11}B^{81}BrF_2N_3O_3$ $[M+H]^+$: 494.0891, found 494.0698.

X-Ray code: mjh220013_fa

7.2.2.2 Methyl (*S*)-4-(3-bromo-5,5-difluoro-7-((2-hydroxy-1-phenylethyl)amino)-5*H*-5λ^4,6λ^4-dipyrrolo[1,2-*c*:2',1'-*f*][1,3,2]diazaborinin-10-yl)benzoate (**3.10**)

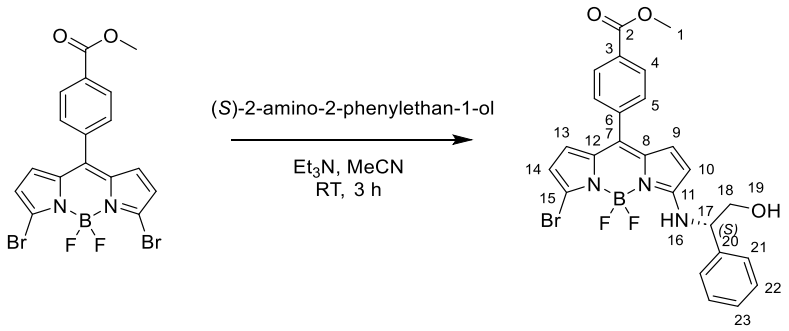

To a round bottom flask, under an atmosphere of nitrogen, was added methyl 4-(3,7-dibromo-5,5-difluoro-5*H*-4λ^4,5λ^4-dipyrrolo[1,2-*c:*2',1'-*f*] [1,3,2]diazaborinin10-yl)benzoate (100 mg, 0.21 mmol), (*S*)-2-amino-2-phenylethan-1-ol (56.7 mg, 0.41 mmol), Et_3N (63 µL, 0.45 mmol) and MeCN (40 mL). The reaction mixture was stirred at room temperature for 3 hours. The solvent was removed under reduced pressure, diluted with DCM (50 mL) and washed with water (2 x 50 mL). The organic layer was dried over $MgSO_4$, filtered, and solvent removed under reduced pressure. The crude product was purified through silica gel column chromatography (DCM→ DCM: Ethyl acetate 2:1) to give methyl (*S*)-4-(3-bromo-5,5-difluoro-7-((2-hydroxy-1-phenylethyl)amino)-5*H*-5λ^4,6λ^4-dipyrrolo[1,2-*c*:2',1'-*f*][1,3,2]diazaborinin-10-yl)benzoate (110 mg, 0.19 mmol, 91%) as an orange solid.

R_f: 0.60 (petrol : ethyl acetate, 1:1). **Mp:** 90 - 91 °C. **^{1}H NMR** (300 MHz, Chloroform-*d*) δ 8.06 (d, *J* = 8.3 Hz, 2H, H^4), 7.43 (d, *J* = 8.3 Hz, 2H, H^5), 7.38 – 7.27 (m, 5H, Ar), 7.21 (d, *J* = 6.6 Hz, 1H, H^{16}), 6.65 (d, *J* = 5.0 Hz, 1H, H^{14}), 6.29 (d, *J* = 3.9 Hz, 1H, H^9), 6.24 (d, *J* = 3.9 Hz, 1H, H^{10}), 5.99 (d, *J* = 5.0 Hz, 1H, H^{13}), 4.83 – 4.74 (m, 1H, H^{17}), 4.05 (dd, *J* = 11.4, 4.1 Hz, 1H, H^{18}), 3.94 (s, 3H, H^1), 3.89 (dd, *J* = 11.4, 6.9 Hz, 1H, $H^{18'}$), 2.77 (s, 1H, H^{19}). **^{13}C NMR** (75 MHz, Chloroform-*d*) δ 166.6 (C^2), 162.2 (C^{11}), 138.3, 138.3 (C^{20}), 135.5 (C^9), 133.3 (C^8), 130.9 (C^7), 130.4 (C^5), 129.5 (C^4), 129.3 (Ar), 128.5 (Ar), 126.6 (Ar), 120.7 (C^{14}), 117.1 (C^{13}), 115.9 (C^{15}), 112.9 (C^{10}), 66.2 (C^{18}), 60.6 (C^{17}), 52.5 (C^1). **^{11}B NMR** (96 MHz, Chloroform-*d*) δ 1.06 (t, $J_{B\text{-}F}$ = 34.0 Hz). **^{19}F NMR** (282 MHz, Chloroform-*d*) δ -146.2 (dq, $J_{F\text{-}F}$= 99.1 Hz, $J_{B\text{-}F}$= 32.1 Hz), (dq, $J_{F\text{-}F}$= 100.2 Hz, $J_{B\text{-}F}$= 32.2 Hz). **IR** (neat): υ_{max}/cm^{-1} 3378 (NH, w), 1716 (CO, s). **HRMS** (TOF MS ES+) calcd for $C_{25}H_{22}{}^{11}B^{81}BrF_2N_3O_3$ $[M+H]^+$: 542.0893, found 542.0894. **$[\alpha]^{25}_D$** -2898, (c 0.1, DCM).

Note: Two carbon signals were not identified in the analysis of the ^{13}C NMR spectrum.

7.2.2.3 Methyl (*S*)-4-(5,5-difluoro-3-((1-hydroxybutan-2-yl)amino)-7-iodo-5*H*-4λ^4,5λ^4-dipyrrolo[1,2-*c*:2',1'-*f*][1,3,2]diazaborinin-10-yl)benzoate (**3.2**)

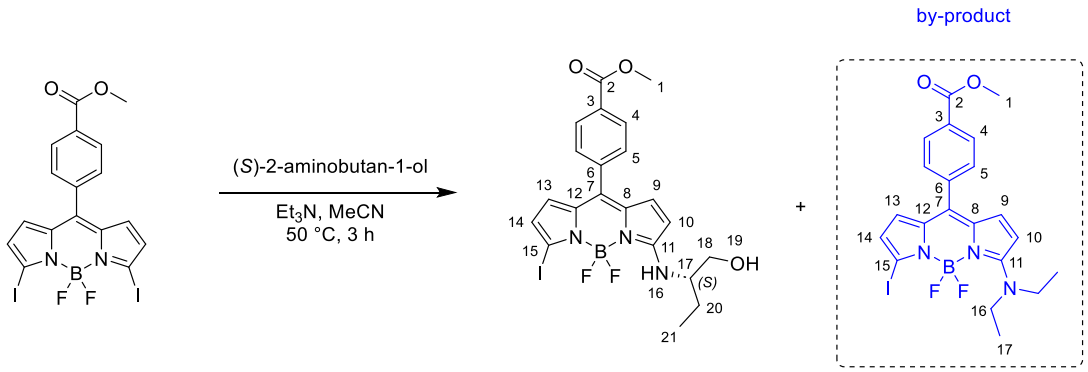

To a round bottom flask was added methyl 4-(5,5-difluoro-3,7-diiodo-5*H*-4λ^4,5λ^4-dipyrrolo[1,2-*c*:2',1'-*f*][1,3,2]diazaborinin-10-yl)benzoate (1.87 g, 3.24 mmol), (*S*)-2-aminobutan-1-ol (0.61 mL, 6.48 mmol), Et_3N (0.99 mL, 7.12 mmol) and MeCN (230 mL). The reaction mixture was stirred at 50 °C for 3 hours, then allowed to cool to room temperature. The reaction mixture was diluted with DCM (200 mL) and washed with water (3 x 200 mL), dried over $MgSO_4$, filtered and the solvent was removed under reduced pressure. The crude product was purified through silica gel column chromatography (DCM → DCM : ethyl acetate, 1:1) to give methyl (*S*)-4-(5,5-difluoro-3-((1-hydroxybutan-2-yl)amino)-7-iodo-5*H*-4λ^4,5λ^4-dipyrrolo[1,2-*c*:2',1'-*f*][1,3,2]diazaborinin-10-yl)benzoate (1.75 g, 3.24 mmol, 100%) as an orange solid.

R_f: 0.37 (petrol: ethyl acetate, 1:1). **Mp:** 119 -120 °C. **^{1}H NMR** (300 MHz, Chloroform-*d*) δ 8.08 (d, *J* = 7.9 Hz, 2H, H^4), 7.46 (d, *J* = 7.9 Hz, 2H, H^5), 6.78 (d, *J* = 5.1 Hz, 1H, H^9), 6.48 (d, *J* = 3.8 Hz, 1H, H^{14}), 6.40 (d, *J* = 9.1 Hz, 1H, H^{16}), 6.30 (d, *J* = 5.1 Hz, 1H, H^{10}), 6.16 (d, *J* = 3.8 Hz, 1H, H^{13}), 3.95 (s, 3H, H^1), 3.79 (dd, *J* = 11.3, 4.0 Hz, 1H, H^{18}), 3.67 (dd, *J* = 11.3, 6.4 Hz, 1H, $H^{18'}$), 3.61 – 3.49 (m, 1H, H^{17}), 2.72 (s, 1H, H^{19}), 1.84 – 1.50 (m, 2H, $H^{20,20'}$), 1.01 (t, *J* = 7.4 Hz, 3H, H^{21}). **^{13}C NMR** (75 MHz, Chloroform-*d*) δ 166.6 (C^2), 162.7 (C^{11}), 138.6 (C^6), 135.7 (C^{12}), 135.6 (C^9), 133.6 (C^8), 130.9 (C^3), 130.4 (C^5), 129.6 (C^4), 128.8 (C^7), 124.6 (C^{14}), 120.8 (C^{13}), 113.0 (C^{10}), 81.2 (C^{15}), 64.9 (C^{18}), 59.4 (C^{17}), 52.5 (C^1), 24.9 (C^{20}), 10.5 (C^{21}). **^{11}B NMR** (96 MHz, Chloroform-*d*) δ 1.02 (t, *J* = 33.0 Hz). **^{19}F NMR** (282 MHz, Chloroform-*d*) δ -144.8 (dq, J_{F-F}= 99.0, J_{B-F}= 31.5 Hz), -145.9 (dq, J_{F-F}= 99.6, J_{B-F}= 30.7 Hz). **IR** (neat): υ_{max}/cm^{-1} 3378 (N-H, w), 1716 (C=O, m), 1602 (C=C, s), 1275 (C-O, m). **HRMS** (pNSI) calcd for $C_{21}H_{22}{}^{11}B^{81}BrF_2N_3O_3$ $[M+H]^+$: 540.0761, found 540.0760. **$[\alpha]^{25}_D$** +30 (c 0.1, DCM), taken as an average over 3 measurements.

X-Ray code: mjh220049_fa

by product:

Methyl 4-(3-(diethylamino)-5,5-difluoro-7-iodo-5*H*-4λ^4,5λ^4-dipyrrolo[1,2-*c*:2',1'-*f*][1,3,2]diazaborinin-10-yl)benzoate (**2.20**)

Yield: Trace amount. **R_f:** 0.7 (petrol: ethyl acetate, 1:1). **^{1}H NMR** (300 MHz, Chloroform-*d*) δ 8.10 (d, *J* = 8.6 Hz, 2H, H^4), 7.50 (d, *J* = 8.1 Hz, 2H, H^5), 6.77 (d, *J* = 5.3 Hz, 1H), 6.51 (d, *J* = 3.8 Hz, 1H), 6.28 (d, *J* = 5.3 Hz, 1H), 6.09 (d, *J* = 3.8 Hz, 1H), 3.96 (s, 3H, H^1), 3.87 (q, *J* = 7.0 Hz, 4H, H^{16}), 1.38 (t, *J* = 7.0 Hz, 6H, H^{17}). **^{11}B NMR** (96 MHz, Chloroform-*d*) δ 1.19 (t, *J* = 34.7 Hz). **^{19}F NMR** (282 MHz, Chloroform-*d*) δ -132.1 (q, *J* = 33.5 Hz).

7.2.2.4 Methyl (*R*)-4-(5,5-difluoro-3-((1-hydroxybutan-2-yl)amino)-7-iodo-5*H*-4λ^4,5λ^4-dipyrrolo[1,2-*c*:2',1'-*f*][1,3,2]diazaborinin-10-yl)benzoate (**3.14**)

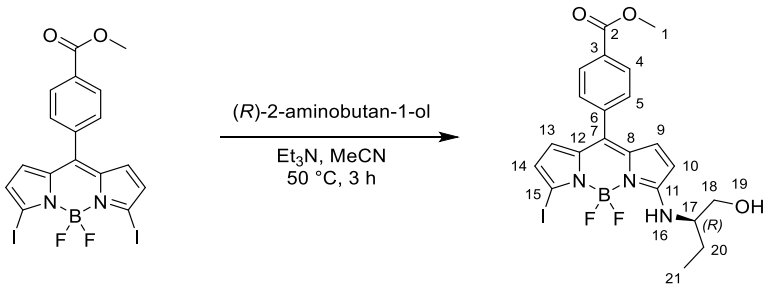

To a round bottom flask was added methyl 4-(5,5-difluoro-3,7-diiodo-5*H*-4λ^4,5λ^4-dipyrrolo[1,2-*c*:2',1'-*f*][1,3,2]diazaborinin-10-yl)benzoate (500 g, 0.87 mmol), (*R*)-2-aminobutan-1-ol (163 µL, 1.73 mmol), Et_3N (265 µL, 1.89 mmol) and MeCN (70 mL). The reaction mixture was stirred at 50 °C for 3 hours, then allowed to cool to room temperature. The reaction mixture was diluted with DCM (100 mL) and washed with water (3 x 100 mL), dried over $MgSO_4$, filtered and the solvent was removed under reduced pressure. The crude product was purified through silica gel column chromatography (DCM → DCM : Ethyl acetate, 1:1) to give methyl (*R*)-4-(5,5-difluoro-3-((1-hydroxybutan-2-yl)amino)-7-iodo-5*H*-4λ^4,5λ^4-dipyrrolo[1,2-*c*:2',1'-*f*][1,3,2]diazaborinin-10-yl)benzoate (466 mg, 0.86 mmol, 100%) as an orange solid.

R_f: 0.35 (petrol: ethyl acetate, 1:1). **Mp:** 119-120 °C. **^{1}H NMR** (300 MHz, Chloroform-*d*) δ 8.09 (d, *J* = 8.5 Hz, 2H, H^4), 7.47 (d, *J* = 8.2 Hz, 2H, H^5), 6.79 (d, *J* = 5.0 Hz, 1H, H^9), 6.49 (d, *J* = 3.8 Hz, 1H, H^{14}), 6.38 (d, *J* = 9.6 Hz, 1H, H^{16}), 6.30 (d, *J* = 5.1 Hz, 1H, H^{10}), 6.17 (d, *J* = 3.8 Hz, 1H, H^{13}), 3.95 (s, 3H, H^1), 3.79 (ddd, *J* = 10.6, 6.2, 4.1 Hz, 1H, H^{18}), 3.67 (ddd, *J* = 11.2, 6.4, 4.6 Hz, 1H, $H^{18'}$), 3.62 – 3.49 (m, 1H, H^{17}), 2.51 (t, *J* = 5.6 Hz, 1H, H^{19}), 1.77 (dqd, *J* = 15.0, 7.5, 5.2 Hz, 1H, H^{20}), 1.61 (dqd, *J* = 14.6, 7.4, 7.4 Hz, 1H, $H^{20'}$), 1.02 (t, *J* = 7.4 Hz, 3H, H^{21}). **^{13}C NMR** (75 MHz, Chloroform-*d*) δ 166.7 (C^2), 162.7 (C^{11}), 138.6 (C^6), 135.8 (C^{12}), 135.6 (C^9), 133.7 (C^8), 130.9 (C^3), 130.4 (C^5), 129.6 (C^4), 129.0 (C^7), 124.7 (C^{14}), 121.0 (C^{13}), 112.9 (C^{10}), 81.4 (C^{15}), 65.0 (C^{18}), 59.5 (C^{17}), 52.5 (C^1), 24.9 (C^{20}), 10.6 (C^{21}). **^{11}B NMR** (96 MHz, Chloroform-*d*) δ 1.03 (t, *J* = 33.2 Hz). **^{19}F NMR** (282 MHz, Chloroform-*d*) δ -145.0 (dq, $J_{F\text{-}F}$= 100.0, $J_{B\text{-}F}$= 32.0 Hz), -146.0 (dq, $J_{F\text{-}F}$= 100.1, $J_{B\text{-}F}$= 32.1 Hz). **IR** (neat): υ_{max}/cm^{-1} 3378 (N-H, w), 1716 (C=O, m), 1602 (C=C, s), 1275 (C-O, m). **HRMS** (pNSI) calcd for $C_{21}H_{21}{}^{11}B^{81}BrF_2N_3O_3Na$ $[M+Na]^+$: 562.0582, found 562.0585. **$[\alpha]^{25}_D$** -19 (c 0.1, DCM), taken as an average over 3 measurements.

X-Ray code: mjh230079_2_fa

7.2.2.5 Methyl (*S*)-4-(5,5-difluoro-3-((1-hydroxypropan-2-yl)amino)-7-iodo-5*H*-4λ^4,5λ^4-dipyrrolo[1,2-*c*:2',1'-*f*][1,3,2]diazaborinin-10-yl)benzoate (**3.15**)

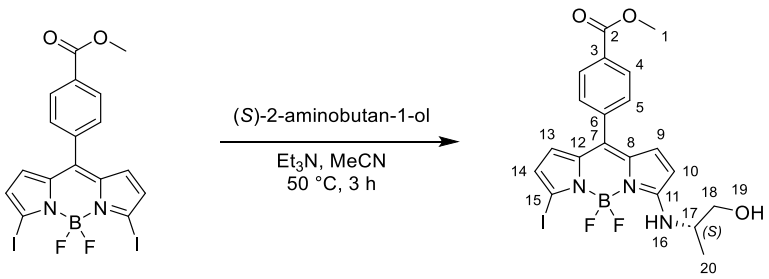

To a round bottom flask was added methyl 4-(5,5-difluoro-3,7-diiodo-5*H*-4λ^4,5λ^4-dipyrrolo[1,2-*c*:2',1'-*f*][1,3,2]diazaborinin-10-yl)benzoate (300 mg, 0.52 mmol), (*S*)-2-aminopropan-1-ol (78.0 mg, 1.04 mmol), Et_3N (158 µL, 1.14 mmol) and MeCN (50 mL). The reaction mixture was stirred at 50 °C for 3 hours, then allowed to cool to room temperature. The reaction mixture was diluted with DCM (50 mL) and washed with water (3 x 50 mL), dried over $MgSO_4$, filtered and the solvent was removed under reduced pressure. The crude product was purified through silica gel column chromatography (DCM → DCM : Ethyl acetate, 1:1) to give methyl (*S*)-4-(5,5-difluoro-3-((1-hydroxypropan-2-yl)amino)-7-iodo-5*H*-4λ^4,5λ^4-dipyrrolo[1,2-*c*:2',1'-*f*][1,3,2]diazaborinin-10-yl)benzoate (307 mg, 0.59 mmol, quant.) as an orange solid.

R_f: 0.27 (DCM: ethyl acetate, 6:1). **^{1}H NMR** (300 MHz, Chloroform-*d*) δ 8.02 (d, *J* = 8.3 Hz, 2H, H^4), 7.38 (d, *J* = 7.8 Hz, 2H, H^5), 6.51 (d, *J* = 5.1 Hz, 1H, H^9), 6.51 (d, *J* = 8.6 Hz, 1H, H^{16}), 6.43 (d, *J* = 3.8 Hz, 1H, H^{13}), 6.29 (d, *J* = 5.1 Hz, 1H, H^{10}), 6.11 (d, *J* = 3.8 Hz, 1H, H^{14}), 3.92 (s, 3H, H^1), 3.82 –3.70 (m, 2H, $H^{17,18}$), 3.61 (dd, *J* = 11.2, 6.3 Hz, 1H, H^{18}), 3.31 (br, 1H, H^{19}), 1.31 (d, *J* = 6.5 Hz, 3H, H^{20}). **^{13}C NMR** (75 MHz, Chloroform-*d*) δ 166.6 (C^2), 162.1 (C^{11}), 138.4 (C^3), 135.5 (C^7), 133.5 (C^8), 130.6 (C^{12}), 130.2 (C^5), 129.4 (C^4), 128.5 (C^9), 124.4 (C^{13}), 120.6 (C^{14}), 113.1 (C^{10}), 80.9 (C^{15}), 77.4 (C^6), 66.0 (C^{18}), 53.0 (C^{17}), 52.4 (C^1), 17.7 (C^{20}). **^{11}B NMR** (96 MHz, Chloroform-*d*) δ 1.00 (t, *J* = 34.8 Hz). **^{19}F NMR** (282 MHz, Chloroform-*d*) δ -145.4, -146.2 (m). **LRMS** (ASAP-) calcd for $C_{20}H_{18}{}^{11}BF_2IN_3O_3$ $[M-H]^-$: 524.0454, found 524.0000.

7.2.2.6 Methyl (*S*)-4-(5,5-difluoro-3-((2-hydroxy-1-phenylethyl)amino)-7-iodo-5*H*-4λ^4,5λ^4-dipyrrolo[1,2-*c*:2',1'-*f*][1,3,2]diazaborinin-10-yl)benzoate (**3.16**)

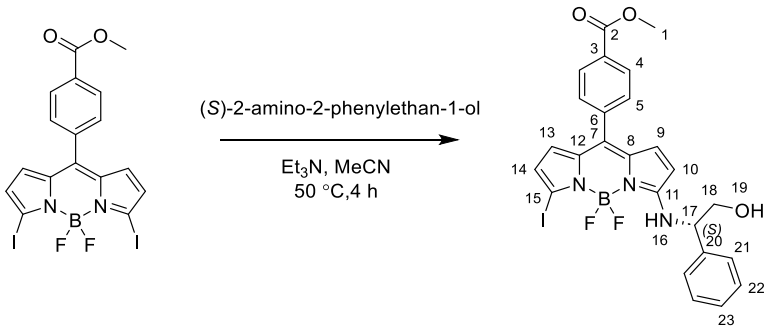

To a round bottom flask, under an atmosphere of nitrogen, was added methyl 4-(5,5-difluoro-3,7-diiodo-5*H*-4λ^4,5λ^4-dipyrrolo[1,2-*c*:2',1'-*f*][1,3,2]diazaborinin-10 yl)benzoate (300 mg, 0.52 mmol), (*S*)-2-amino-2-phenylethan-1-ol (142 mg, 1.03 mmol), Et_3N (159 µL, 1.14 mmol) and MeCN (50 ml). The reaction was stirred at 50 °C for 4 hours, then allowed to cool to room temperature. The reaction mixture was diluted with DCM (100 mL) and washed with water (100 mL). The organic layer was dried over $MgSO_4$, filtered and solvent removed under reduced pressure. The crude product was purified through silica gel column chromatography (DCM → DCM : ethyl acetate, 1:1) to give methyl (*S*)-4-(5,5-difluoro-3-((2-hydroxy-1-phenylethyl)amino)-7-iodo-5*H*-4λ^4,5λ^4-dipyrrolo[1,2-*c*:2',1'-*f*][1,3,2]diazaborinin-10-yl)benzoate (300 mg, 0.51 mmol, 99%) as an orange solid.

R_f: 0.30 (petrol : ethyl acetate, 2:1). **Mp:** 120-121 °C. **^{1}H NMR** (300 MHz, Chloroform-*d*) δ 8.06 (d, *J* = 8.5 Hz, 2H, H^4), 7.44 (d, *J* = 8.5 Hz, 2H, H^5), 7.39 – 7.27 (m, 5H, Ar), 7.19 (d, *J* = 6.8 Hz, 1H, H^{16}), 6.66 (d, *J* = 5.0 Hz, 1H, H^9), 6.50 (d, *J* = 3.8 Hz, 1H, H^{14}), 6.19 (d, *J* = 3.8 Hz, 1H, H^{13}), 6.00 (d, *J* = 5.0 Hz, 1H, H^{10}), 4.84 – 4.72 (m, 1H, H^{17}), 4.06 (dd, *J* = 11.5, 4.1 Hz, 1H, H^{18}), 3.94 (s, 3H, H^1), 3.92 – 3.87 (dd, 1H, , *J* = 11.5, 4.1 Hz, $H^{18'}$), 2.74 (s, 1H, H^{19}). **^{13}C NMR** (75 MHz, Chloroform-*d*) δ 166.6 (C^2), 162.3 (C^{11}), 138.5 (C^6), 138.2 (C^{20}), 135.8 (C^{15}), 135.5 (C^9), 133.5 (C^8), 131.0 (C^3), 130.4 (C^5), 130.0 (Ar), 129.6 (C^4), 129.3 (C^7), 128.6 (Ar), 126.6 (Ar), 124.9 (C^{14}), 121.6 (C^{13}), 113.0 (C^{10}), 82.5 (C^{12}), 66.3 (C^{18}), 60.8 (C^{17}), 52.5 (C^1). **^{11}B NMR** (96 MHz, Chloroform-*d*) δ 1.07(t, $J_{B\text{-}F}$ = 33.0 Hz). **^{19}F NMR** (282 MHz, Chloroform-*d*) δ -144.9 (dq, $J_{F\text{-}F}$= 99.3 Hz, $J_{B\text{-}F}$= 31.8 Hz) -146.3 (dq, $J_{F\text{-}F}$= 99.0 Hz, $J_{B\text{-}F}$= 31.3 Hz). **IR** (neat): υ_{max}/cm^{-1} 3379 (N-H, w), 1716 (C=O, m), 1598 (C=C, s), 1276 (C-O, m). **HRMS** (TOF MS ES+) calcd for $C_{25}H_{21}{}^{11}BF_2IN_3O_3Na$ $[M+Na]^+$: 610.0586, found 610.0620. **Molar extinction coefficient** (ε) = 28,000 M^{-1} cm^{-1} (MeCN).

7.2.2.7 Methyl (*S*)-4-(5,5-difluoro-3-((1-hydroxy-3,3-dimethylbutan-2-yl)amino)-7-iodo-5*H*-4λ^4,5λ^4-dipyrrolo[1,2-*c*:2',1'-*f*][1,3,2]diazaborinin-10-yl)benzoate (**3.17**)

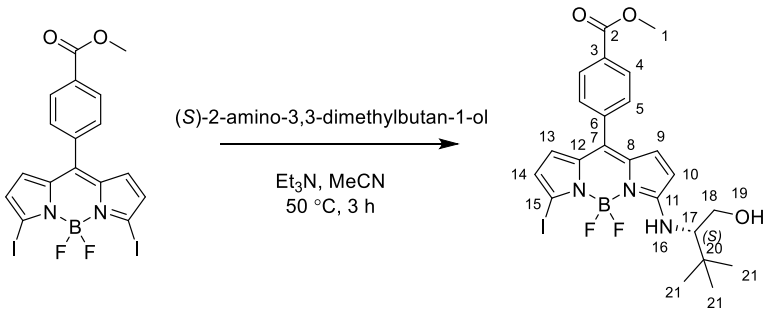

To a round bottom flask was added methyl 4-(5,5-difluoro-3,7-diiodo-5*H*-4λ^4,5λ^4-dipyrrolo[1,2-*c*:2',1'-*f*][1,3,2]diazaborinin-10-yl)benzoate (136 mg, 0.24 mmol), (*S*)-2-amino-3,3-dimethylbutan-1-ol (55.2 mg, 0.47 mmol), Et_3N (72 µL, 0.52 mmol) and MeCN (20 ml). The reaction mixture was stirred at 50 °C for 3 hours, then allowed to cool to room temperature. The reaction mixture was diluted with DCM (50 mL). The organic layer was washed with water (3 x 50 mL), dried over $MgSO_4$, filtered and solvent removed under reduced pressure. The crude product was purified through silica gel column chromatography (DCM → DCM : Ethyl acetate, 1:1) to give methyl (*S*)-4-(5,5-difluoro-3-((1-hydroxy-3,3-dimethylbutan-2-yl)amino)-7-iodo-5*H*-4λ^4,5λ^4-dipyrrolo[1,2-*c*:2',1'-*f*][1,3,2]diazaborinin-10-yl)benzoate (209 g, 0.37 mmol, quant.) as an orange solid.

R_f: 0.3 (petrol : ethyl acetate, 2:1). **^{1}H NMR** (300 MHz, Chloroform-*d*) δ 8.03 (d, *J* = 8.6 Hz, 2H, H^4), 7.40 (d, *J* = 7.7 Hz, 2H, H^5), 6.70 (d, *J* = 5.0 Hz, 1H, H^9), 6.46 (br, 1H, H^{16}), 6.44 (d, *J* = 3.8 Hz, 1H, H^{13}), 6.29 (d, *J* = 5.2 Hz, 1H, H^{10}), 6.10 (d, *J* = 3.8 Hz, 1H, H^{14}), 3.92 (s, 3H, H^1), 3.94 – 3.86 (m, 1H, H^{18}), 3.65 (dd, *J* = 11.4, 8.7 Hz, 1H, $H^{18'}$), 3.34 (ddd, *J* = 11.9, 8.8, 3.3 Hz, 1H, H^{17}), 2.94 (s, 1H, H^{19}), 1.00 (s, 9H, H^{21}). **^{13}C NMR** (75 MHz, Chloroform-*d*) δ 166.6 (C^2), 163.4 (C^{11}), 138.5 (C^6), 135.6 (C^7), 135.4 (C^9), 133.5 (C^8), 130.7 (C^3), 130.3 (C^5), 129.5 (C^4), 128.4 (C^{12}), 124.4 (C^{13}), 120.5 (C^{14}), 113.4 (C^{10}), 80.8 (C^{15}), 66.8 (C^{17}), 62.0 (C^{18}), 52.4 (C^1), 34.3 (C^{20}), 26.7 (C^{21}). **^{11}B NMR** (96 MHz, Chloroform-*d*) δ 1.06 (t, J_{B-F} = 34.6 Hz). **^{19}F NMR** (282 MHz, Chloroform-*d*) δ -143.5 – -144.5 (m), -145.6 – -146.8 (m).

7.2.2.8 Methyl (*S*)-4-(5,5-difluoro-3-((1-hydroxybutan-2-yl)amino)-7-(2-hydroxyphenyl)-5*H*-4λ^4,5λ^4-dipyrrolo[1,2-*c*:2',1'-*f*][1,3,2]diazaborinin-10-yl)benzoate (**3.5**)

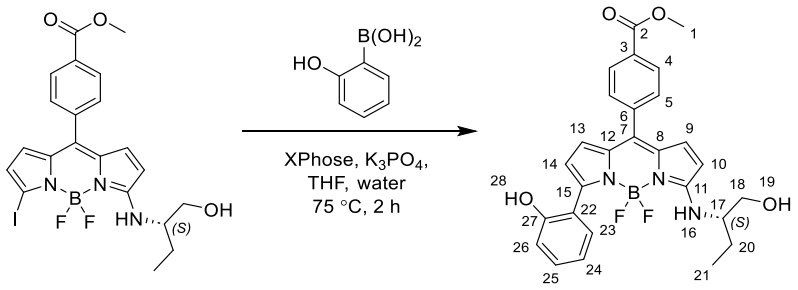

To a Schlenk flask, under nitrogen atmosphere, was added methyl (*S*)-4-(5,5-difluoro-3-((1-hydroxybutan-2-yl)amino)-7-iodo-5*H*-4λ^4,5λ^4-dipyrrolo[1,2-*c*:2',1'-*f*][1,3,2]diazaborinin-10-yl)benzoate (1.15 g, 2.12 mmol), (2-hydroxyphenyl)boronic acid (0.59 g, 4.25 mmol), XPhos Pd G3 (0.11 g, 6 mol %, 0.13 mmol), $K_3PO_4.H_2O$ (0.98 g, 4.25 mmol), dry THF (60 mL), water (10 mL) and was degassed using freeze-pump-thaw method (x3). The reaction mixture was heated, using an oil bath, to 75 °C, stirred for 2 hours then diluted with DCM (200 mL). The organic layer was washed with water (3 x 200 mL), dried over $MgSO_4$, filtered and solvent removed under reduced pressure. The crude product was purified through silica gel column chromatography (DCM : ethyl acetate 3:1) to give methyl (*S*)-4-(5,5-difluoro-3-((1-hydroxybutan-2-yl)amino)-7-(2-hydroxyphenyl)-5*H*-4λ^4,5λ^4-dipyrrolo[1,2-*c*:2',1'-*f*][1,3,2]diazaborinin-10-yl)benzoate (0.87 g, 1.72 mmol, 81 %).

R_f: 0.54 (DCM: Ethyl acetate, 3:1). **Mp:** 113-115 °C. **^{1}H NMR** (300 MHz, Chloroform-*d*) δ 8.14 (d, *J* = 8.4 Hz, 2H, H^4), 7.57 (d, *J* = 8.4 Hz, 2H, H^5), 7.49 (dd, J = 7.7, 1.5 Hz, 1H, H^{23}), 7.32 (ddd, *J* = 8.3, 7.3, 1.7 Hz, 1H, H^{25}), 7.05 – 6.96 (m, 2H, $H^{24,26}$), 6.86 (d, *J* = 5.0 Hz, 1H, H^9), 6.44 (d, *J* = 3.7 Hz, 1H, H^{13}), 6.35 (d, *J* = 3.7 Hz, 1H, H^{14}), 6.28 (d, *J* = 5.1 Hz, 1H, H^{10}), 6.23 (d, *J* = 9.5 Hz, 1H, H^{16}), 5.77 (t, *J* = 3.2 Hz, 1H, H^{28}), 3.97 (s, 3H, H^1), 3.71 (dd, *J* = 11.1, 3.8 Hz, 1H, H^{18}), 3.50 (dd, *J* = 11.1, 6.6 Hz, 1H, $H^{18'}$), 3.52 – 3.42 (m, 1H, H^{17}), 2.20 (t, *J* = 5.6 Hz, 1H, H^{19}), 1.77 – 1.41 (m, 2H, $H^{20,20'}$), 0.96 (t, *J* = 7.4 Hz, 3H, H^{21}). **^{13}C NMR** (75 MHz, Chloroform-*d*) δ 166.7 (C^2), 162.5 (C^{11}), 154.0 (C^{22}), 140.4 (C^{15}), 139.2 (C^6), 135.6 (C^{10}), 133.9 (C^{12}), 133.6 (C^8), 131.6 (C^{23}), 130.9 (C^3), 130.7 (C^7), 130.5 (C^5), 130.3 (C^{25}), 129.6 (C^4), 121.5 (C^{27}), 120.3 (C^{14}), 120.0 (C^{24}), 116.0 (C^{26}), 115.9 (C^{13}), 112.6 (C^9), 65.0 (C^{18}), 59.5 (C^{17}), 52.5 (C^1), 24.9 (C^{20}), 10.6 (C^{21}). **^{11}B NMR** (96 MHz, Chloroform-*d*) δ 1.25 (t, 34.6 Hz). **^{19}F NMR** (282 MHz, Chloroform-*d*) δ -142.9 – -144.1 (m), -144.2 – -145.2 (m). **IR** (neat): υ_{max}/cm^{-1} 3381 (NH, w), 2965 (C-H, w), 1716 (C=O, m), 1602 (NH, s), 1277 (C-O). **HRMS:** (pNSI) calcd for $C_{27}H_{25}BF_2N_3O_4$ $[M-H]^-$: 504.1916, found 504.1916.

7.2.2.9 Methyl (*R*)-4-(5,5-difluoro-3-((1-hydroxybutan-2-yl)amino)-7-(2-hydroxyphenyl)-5*H*-4λ^4,5λ^4-dipyrrolo[1,2-*c*:2',1'-*f*][1,3,2]diazaborinin-10-yl)benzoate (**3.29**)

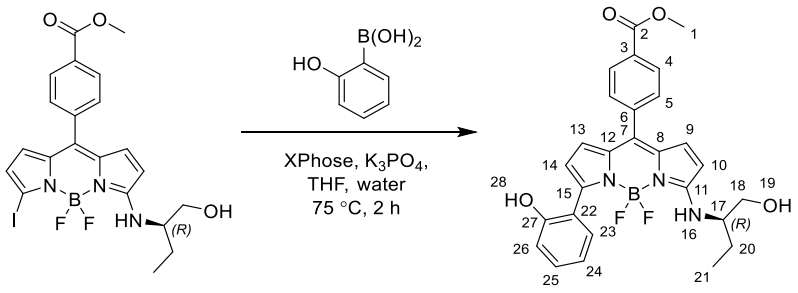

To a Schlenk flask, under nitrogen atmosphere, was added methyl (*R*)-4-(5,5-difluoro-3-((1-hydroxybutan-2-yl)amino)-7-iodo-5*H*-4λ^4,5λ^4-dipyrrolo[1,2-*c*:2',1'-*f*][1,3,2]diazaborinin-10-yl)benzoate (409 mg, 0.76 mmol), (2-hydroxyphenyl)boronic acid (209 mg, 1.51 mmol), XPhos Pd G3 (38 mg, 6 mol %, 0.05 mmol), $K_3PO_4.H_2O$ (350 mg, 1.52 mmol), dry THF (20 mL), water (3.3 mL) and was degassed using freeze-pump-thaw method (x3). The reaction mixture was heated, using an oil bath, to 75 °C, stirred for 2 hours then diluted with DCM (100 mL). The organic layer was washed with water (3 x 100 mL), dried over $MgSO_4$, filtered and solvent removed under reduced pressure. The crude product was purified through silica gel column chromatography (DCM : ethyl acetate 6:1) to give methyl (*R*)-4-(5,5-difluoro-3-((1-hydroxybutan-2-yl)amino)-7-(2-hydroxyphenyl)-5*H*-4λ^4,5λ^4-dipyrrolo[1,2-*c*:2',1'-*f*][1,3,2]diazaborinin-10-yl)benzoate (334 mg, 0.66 mmol, 87 %).

R_f: 0.42 (DCM : ethyl acetate, 6:1). **Mp:** 113-115 °C. **^{1}H NMR** (300 MHz, Chloroform-*d*) δ 8.12 (d, *J* = 8.2 Hz, 2H, H^4), 7.54 (d, *J* = 8.1 Hz, 2H, H^5), 7.49 (dd, *J* = 7.6, 1.7 Hz, 1H, H^{23}), 7.34 – 7.27 (m, 1H, H^{25}), 7.03 – 6.95 (m, 2H, $H^{24,26}$), 6.82 (d, *J* = 5.1 Hz, 1H, H^9), 6.41 (d, *J* = 3.7 Hz, 1H, H^{13}), 6.34 (d, *J* = 3.7 Hz, 1H, H^{14}), 6.25 (m*, *J* = 5.1 Hz, 2H, H^{10}, H^{16}), 5.89 (s, 1H, H^{28}), 3.96 (s, 3H, H^1), 3.64 (dd, *J* = 11.0, 3.9 Hz, 1H, H^{18}), 3.57 – 3.48 (m, 1H, $H^{18'}$), 3.48 – 3.39 (m, 1H, H^{17}), 1.65 (dqd, *J* = 14.8, 7.5, 4.9 Hz, 1H, H^{20}), 1.56 – 1.40 (m, 1H, $H^{20'}$), 0.94 (t, *J* = 7.4 Hz, 3H, H^{21}). **^{13}C NMR** (75 MHz, Chloroform-*d*) δ 166.7 (C^2), 162.5 (C^{11}), 154.0 (C^{22}), 140.3 (C^{15}), 139.1 (C^6), 135.5 (C^{10}), 133.8 (C^{12}), 133.5 (C^8), 131.6 (C^{23}), 130.8 (C^3), 130.5 (C^7), 130.4 (C^5), 130.1 (C^{25}), 129.6 (C^4), 121.5 (C^{27}), 120.1 (C^{14}), 119.9 (C^{24}), 115.94 (C^{26}), 115.986 (C^{13}), 112.7 (C^9), 64.8 (C^{18}), 59.4 (C^{17}), 52.5 (C^1), 24.8 (C^{20}), 10.5 (C^{21}). **^{11}B NMR** (96 MHz, Chloroform-*d*) δ 1.27 (t, 35.9 Hz). **^{19}F NMR** (282 MHz, Chloroform-*d*) δ -142.4 – -143.6 (m), -143.8 – -145.1 (m). **IR** (neat): υ_{max}/cm^{-1} 3381 (NH, w), 2965 (C-H, w), 1716 (C=O, m), 1602 (NH, s), 1277 (C-O). **HRMS:** (TOF MS ASAP+) calcd for $C_{27}H_{26}BFN_3O_4$ $[M-F]^-$: 466.1943, found 466.1952.

*Doublet corresponding to H^{10} with broad signal underneath corresponding to H^{16}

7.2.2.10 Methyl (*S*)-4-(5,5-difluoro-3-(2-hydroxyphenyl)-7-((1-hydroxypropan-2-yl)amino)-5*H*-5λ^4,6λ^4-dipyrrolo[1,2-*c*:2',1'-*f*][1,3,2]diazaborinin-10-yl)benzoate (**3.30**)

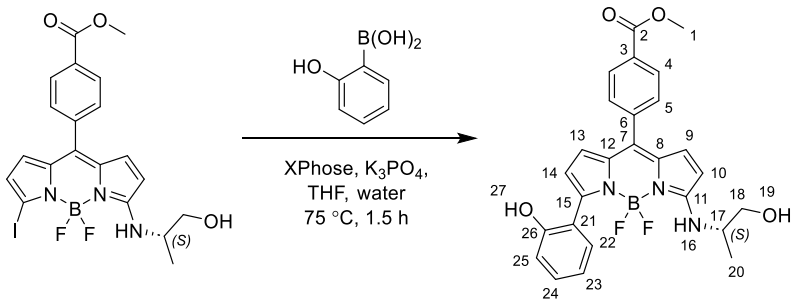

To a Schlenk flask, under nitrogen atmosphere, was added methyl (*S*)-4-(5,5-difluoro-3-((1-hydroxypropan-2-yl)amino)-7-iodo-5*H*-4λ^4,5λ^4-dipyrrolo[1,2-*c*:2',1'-*f*][1,3,2]diazaborinin-10-yl)benzoate (109 mg, 0.21 mmol), (2-hydroxyphenyl)boronic acid (57.2 mg, 0.42 mmol), XPhos Pd G3 (10.2 mg, 6 mol %, 0.01 mmol), $K_3PO_4.H_2O$ (95.6 mg, 0.42 mmol), dry THF (10 mL), water (1.5 mL) and was degassed using freeze-pump-thaw method (x3). The reaction mixture was heated, using an oil bath, to 75 °C, stirred for 1.5 hours then diluted with DCM (50 mL). The organic layer was washed with water (3 x 50 mL), dried over $MgSO_4$, filtered and solvent removed under reduced pressure. The crude product was purified through silica gel column chromatography (DCM : ethyl acetate 6:1) to give methyl (*S*)-4-(5,5-difluoro-3-(2-hydroxyphenyl)-7-((1-hydroxypropan-2-yl)amino)-5*H*-5λ^4,6λ^4-dipyrrolo[1,2-*c*:2',1'-*f*][1,3,2]diazaborinin-10-yl)benzoate (75.5 mg, 0.15 mmol, 74 %).

R_f: 0.35 (DCM: ethyl acetate, 6:1). **^{1}H NMR** (300 MHz, Chloroform-*d*) δ 8.12 (d, *J* = 8.0 Hz, 2H, H^4), 7.54 (d, *J* = 8.0 Hz, 2H, H^5), 7.48 (dd, J = 7.5, 1.6 Hz, 1H, H^{22}), 7.30 (td, *J* = 7.9, 1.8 Hz, 1H, H^{24}), 7.05 – 6.95 (m, 2H, H^{23,26}), 6.82 (d, *J* = 5.0 Hz, 1H, H^9), 6.42 (d, *J* = 3.7 Hz, 1H, H^{13}), 6.34 (d, *J* = 3.7 Hz, 1H, H^{14}), 6.30 (sb, 1H, H^{16}) 6.26 (d, *J* = 5.0 Hz, 1H, H^{10}), 5.86 (s, 1H, H^{27}), 3.97 (s, 3H, H^1), 3.76 – 3.57 (m, 2H, H^{17,18}), 3.48 (dd, *J* = 11.1, 6.6 Hz, 1H, H$^{18'}$), 2.73 (s, 1H, H^{19}), 1.23 (d, *J* = 6.5 Hz, 3H, H^{20}). **^{13}C NMR** (75 MHz, Chloroform-*d*) δ 166.7 (C^2), 161.9 (C^{11}), 154.0 (C^{21}), 140.4 (C^{15}), 139.1 (C^6), 135.5 (C^{10}), 133.8 (C^{12}), 133.5 (C^8), 131.6 (C^{22}), 130.8 (C^7), 130.6 (C^3), 130.5 (C^5), 130.2 (C^{24}), 129.6 (C^4), 121.5 (C^{26}), 120.2 (C^{14}), 120.0 (C^{23}), 115.9 (C^{25}), 115.9 (C^{13}), 112.6 (C^9), 66.2 (C^{18}), 53.1 (C^{17}), 52.5 (C^1), 17.6 (C^{20}). **^{11}B NMR** (96 MHz, Chloroform-*d*) δ 1.23 (t, 35.8 Hz). **^{19}F NMR** (282 MHz, Chloroform-*d*) δ -142.6 – -143.8 (m), -143.8 – -144.9 (m). **HRMS:** (TOF MS ES+) calcd for $C_{26}H_{25}BF_2N_3O_4$ $[M+H]^+$: 492.1911, found 492.1888.

7.2.2.11 Methyl (S)-4-(5,5-difluoro-3-((2-hydroxy-1-phenylethyl)amino)-7-(2-hydroxyphenyl)-5*H*-4λ^4,5λ^4-dipyrrolo[1,2-*c*:2',1'-*f*][1,3,2]diazaborinin-10-yl)benzoate (**3.31**)

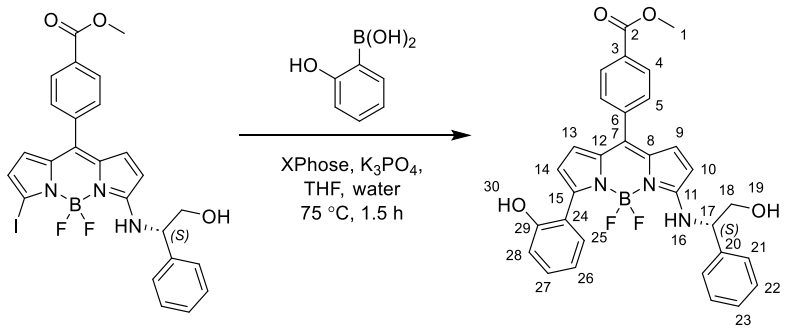

To a Schlenk flask, under nitrogen atmosphere, was added methyl (*S*)-4-(5,5-difluoro-3-((2-hydroxy-1-phenylethyl)amino)-7-iodo-5*H*-4λ^4,5λ^4-dipyrrolo[1,2-*c*:2',1'-*f*][1,3,2]diazaborinin-10-yl)benzoate (201 mg, 0.34 mmol), (2-hydroxyphenyl)boronic acid (94 mg, 0.68 mmol), XPhos Pd G3 (16.9 mg, 6 mol %, 0.02 mmol), $K_3PO_4.H_2O$ (157 mg, 0.68 mmol), dry THF (15 mL), water (2.2 mL) and was degassed (x3). The reaction mixture was heated, using an oil bath, to 75 °C, stirred for 1.5 hours then diluted with DCM (100 mL). The organic layer was washed with water (3 x 100 mL), dried over $MgSO_4$, filtered and solvent removed under reduced pressure. The crude product was purified through silica gel column chromatography (DCM : ethyl acetate 6:1) to give methyl (S)-4-(5,5-difluoro-3-((2-hydroxy-1-phenylethyl)amino)-7-(2-hydroxyphenyl)-5*H*-4λ^4,5λ^4-dipyrrolo[1,2-*c*:2',1'-*f*][1,3,2]diazaborinin-10-yl)benzoate (157 mg, 0.28 mmol, 84%).

R_f: 0.45 (DCM: ethyl acetate, 6:1). **^{1}H NMR** (700 MHz, Chloroform-*d*) δ 8.08 (d, *J* = 8.5 Hz, 2H, H^4), 7.54 (dd, *J* = 7.6, 1.6 Hz, 1H, H^{25}), 7.47 (d, *J* = 8.2 Hz, 2H, H^5), 7.32 (dd, *J* = 8.1, 6.7 Hz, 2H, H^{22}), 7.30 – 7.26 (m, 3H, Ar), 7.06 (d, *J* = 6.7 Hz, 1H, H^{16}), 7.01 – 6.96 (m, 2H, Ar), 6.65 (d, *J* = 5.1 Hz, 1H, H^9), 6.42 (d, *J* = 3.7 Hz, 1H, H^{13}), 6.36 (d, *J* = 3.7 Hz, 1H, H^{14}), 6.00 (s, 1H, H^{30}), 5.93 (d, *J* = 5.1 Hz, 1H, H^{10}), 4.64 (td, *J* = 7.0, 4.2 Hz, 1H, H^{17}), 3.95 (s, 3H, H^1), 3.82 (dt, *J* = 11.4, 4.1 Hz, 1H, H^{18}), 3.67 (ddd, *J* = 11.0, 7.2, 2.7 Hz, 1H, $H^{18'}$), 2.91 (s, 1H, H^{19}). **^{13}C NMR** (176 MHz, Chloroform-*d*) δ 166.7 (C^2), 162.0 (C^{11}), 154.0 (C^{24}), 141.0 (C^{15}), 138.9 (C^6), 138.3 (C^{20}), 135.2 (C^9), 133.7 (C^{12}), 133.3 (C^8), 131.7 (C^{25}), 131.2, 130.8 , 130.4 (C^5), 130.1 (Ar), 129.5 (C^4), 129.1 (C^{22}), 128.4 (C^{27}), 126.5 (C^{21}), 121.4 (Ar), 120.7 (C^{13}), 119.9 (Ar), 116.1 (Ar), 116.0 (C^{14}), 112.9 (C^{10}), 65.8 ($C^{18,18'}$), 60.6 (C^{17}), 52.5 (C^1). **^{11}B NMR** (96 MHz, Chloroform-*d*) δ 1.19 (t, 37.6 Hz). **^{19}F NMR** (659 MHz, Chloroform-*d*) δ -142.3 – -142.9 (m), -143.9 – -144.4 (m).

7.2.2.12 Methyl (*S*)-4-(5,5-difluoro-3-((1-hydroxy-3,3-dimethylbutan-2-yl)amino)-7-(2-hydroxyphenyl)-5*H*-4λ^4,5λ^4-dipyrrolo[1,2-*c*:2',1'-*f*][1,3,2]diazaborinin-10-yl)benzoate (**3.32**)

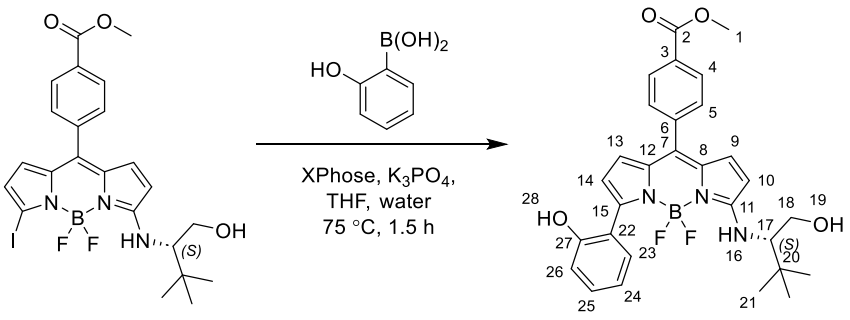

To a Schlenk flask, under nitrogen atmosphere, was added methyl (*S*)-4-(5,5-difluoro-3-((1-hydroxy-3,3-dimethylbutan-2-yl)amino)-7-iodo-5*H*-4λ^4,5λ^4-dipyrrolo[1,2-*c*:2',1'-*f*][1,3,2]diazaborinin-10-yl)benzoate (188 mg, 0.33 mmol), (2-hydroxyphenyl)boronic acid (91.6 mg, 0.67 mmol), XPhos Pd G3 (16.9 mg, 6 mol %, 0.02 mmol), $K_3PO_4.H_2O$ (155 mg, 0.67 mmol), dry THF (12 mL), water (2 mL) and was degassed (x3). The reaction mixture was heated, using an oil bath, to 75 °C, stirred for 1.5 hours then diluted with DCM (50 mL). The organic layer was washed with water (3 x 50 mL), dried over $MgSO_4$, filtered and solvent removed under reduced pressure. The crude product was purified through silica gel column chromatography (DCM : ethyl acetate 6:1) to give methyl (*S*)-4-(5,5-difluoro-3-((1-hydroxy-3,3-dimethylbutan-2-yl)amino)-7-(2-hydroxyphenyl)-5*H*-4λ^4,5λ^4-dipyrrolo[1,2-*c*:2',1'-*f*][1,3,2]diazaborinin-10-yl)benzoate (130 mg, 0.24 mmol, 74%).

R_f: 0.47 (DCM : ethyl acetate, 6:1). **Mp:** 152-153 °C. **^{1}H NMR** (700 MHz, Chloroform-*d*) δ 8.15 (d, *J* = 8.5 Hz, 2H, H^4), 7.59 (d, *J* = 8.5 Hz, 2H, H^5), 7.49 (dd, *J* = 7.6, 1.8 Hz, 1H, H^{23}), 7.32 (ddd, *J* = 8.2, 7.4, 1.7 Hz, 1H, H^{25}), 7.04 (dd, *J* = 8.3, 1.2 Hz, 1H, H^{26}), 7.01 (td, *J* = 7.5, 1.2 Hz, 1H, H^{24}), 6.88 (d, *J* = 5.1 Hz, 1H, H^9), 6.45 (d, *J* = 3.8 Hz, 1H, H^{13}), 6.35 (d, *J* = 3.7 Hz, 1H, H^{14}), 6.31 (d, *J* = 5.2 Hz, 1H, H^{10}), 6.27 (d, *J* = 11.5 Hz, 1H, H^{16}), 5.77 (s, 1H, H^{28}), 3.98 (s, 3H, H^1), 3.91 (dd, *J* = 11.4, 3.4 Hz, 1H, H^{18}), 3.60 (dd, *J* = 11.6, 9.1 Hz, 1H, $H^{18'}$), 3.35 – 3.31 (m, 1H, H^{17}), 1.92 (s, 1H, H^{19}), 0.98 (s, 9H, H^{21}). **^{13}C NMR** (176 MHz, Chloroform-*d*) δ 166.7 (C^2), 163.4 (C^{11}), 154.0 (C^{22}), 140.6 (C^{15}), 139.2 (C^6), 135.5 (C^9), 134.0 (C^{12}), 133.5 (C^8), 131.6 (C^{23}), 131.0 (C^3), 130.8 (C^7), 130.6 (C^5), 130.2 (C^{25}), 129.7 (C^4), 121.6 (C^{27}), 120.4 (C^{13}), 120.2 (C^{24}), 116.1 (C^{26}), 116.0 (C^{14}), 112.9 (C^{10}), 67.2 (C^{17}), 62.3 (C^{18}), 52.5 (C^1), 34.3 (C^{20}), 26.9 (C^{21}). **^{11}B NMR** (96 MHz, Chloroform-*d*) δ 1.31 (t, 34.9 Hz). **^{19}F NMR** (282 MHz, Chloroform-*d*) δ -142.4 – -143.6 (m), -144.0 – -145.1 (m). **HRMS:** (pNSI) calcd for $C_{29}H_{30}BF_2N_3O_4Na$ $[M+Na]^+$: 556.2195, found 556.2179.

7.2.2.13 Methyl (*S*,*Z*)-4-((5-((1-hydroxybutan-2-yl)amino)-2*H*-pyrrol-2-ylidene)(5-(2-hydroxyphenyl)-1*H*-pyrrol-2-yl)methyl)benzoate (**3.6**)

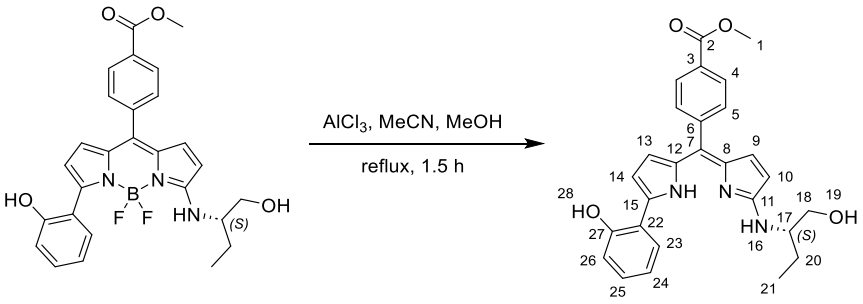

To a 500 mL round bottom flask was added methyl (*S*)-4-(5,5-difluoro-3-((1-hydroxybutan-2-yl)amino)-7-(2-hydroxyphenyl)-5*H*-4λ^4,5λ^4-dipyrrolo[1,2-*c*:2',1'-*f*][1,3,2]diazaborinin-10-yl)benzoate (873 mg, 1.73 mmol), MeCN (150 mL), and $AlCl_3$ (1.15 g, 8.64 mmol) dissolved in MeOH (25 mL). The reaction mixture was heated, using an oil bath, to reflux, stirred for 1.5 hours then diluted with DCM (200 mL) and washed with water (3 x 200 mL). The organic layer was dried over $MgSO_4$, filtered and solvent was removed under reduced pressure. The crude product was purified through silica gel column chromatography (DCM : methanol, 100:4 → 100:8) to give methyl (*S*,*Z*)-4-((5-((1-hydroxybutan-2-yl)amino)-2*H*-pyrrol-2-ylidene)(5-(2-hydroxyphenyl)-1*H*-pyrrol-2-yl)methyl)benzoate (595 mg, 1.30 mmol, 75%) as a red/shiny black solid.

R_f: 0.70 (ethyl acetate). **Mp:** 141-142 °C. **^{1}H NMR** (300 MHz, Methanol-d_4) δ 8.04 (d, *J* = 8.5 Hz, 2H, H^4), 7.60 (dd, *J* = 7.9, 1.6 Hz, 1H, H^{26}), 7.50 (d, *J* = 8.4 Hz, 2H, H^5), 7.10 – 6.99 (m, 1H, H^{24}), 6.92 – 6.80 (m, 2H, $H^{23,25}$), 6.57 (d, *J* = 4.7 Hz, 2H, $H^{9,14}$), 6.24 (d, *J* = 4.7 Hz, 1H, H^{10}), 5.93 (d, *J* = 3.9 Hz, 1H, H^{13}), 4.28 – 4.13 (m, 1H, H^{17}), 3.84 (dd, *J* = 10.4, 4.5 Hz, 1H, H^{18}), 3.65 (dd, *J* = 10.4, 6.9 Hz, 1H, $H^{18'}$), 1.94 (ddt, *J* = 14.6, 11.6, 7.4 Hz, 1H, H^{20}), 1.54 (ddt, *J* = 14.3, 8.9, 7.1 Hz, 1H, $H^{20'}$), 1.05 (t, *J* = 7.4 Hz, 3H, H^{21}). **^{13}C NMR** (75 MHz, Methanol-d_4) δ 169.3 (C^2), 168.4 (C^{11}), 154.4 (C^{27}), 149.0 (C^8), 145.3 (C^6), 137.6 (C^9), 135.6 (C^{15}), 133.6 (C^7), 132.4 (C^5), 130.4 (C^3), 129.8 (C^4), 128.4 (C^{24}), 127.7 (C^{26}), 126.2 (C^{12}), 121.1 (C^{25}), 120.8 (C^{22}), 120.4 (C^{10}), 117.4 (C^{23}), 116.6 (C^{13}), 108.8 (C^{14}), 65.3 (C^{18}), 56.7 (C^{17}), 52.7 (C^1), 25.6 (C^{20}), 11.0 (C^{21}). **IR** (neat): υ_{max}/cm^{-1} 2960 (NH, w), 1701 (C=O, m), 1589 (C=C, S), 1272 (C-O, m). **HRMS:** (pNSI) calcd for $C_{27}H_{26}N_3O_4$ $[M-H]^-$: 456.1929, found 456.1932.

7.2.2.14 Methyl (*R*,*Z*)-4-((5-((1-hydroxybutan-2-yl)amino)-2*H*-pyrrol-2-ylidene)(5-(2-hydroxyphenyl)-1*H*-pyrrol-2-yl)methyl)benzoate (**3.36**)

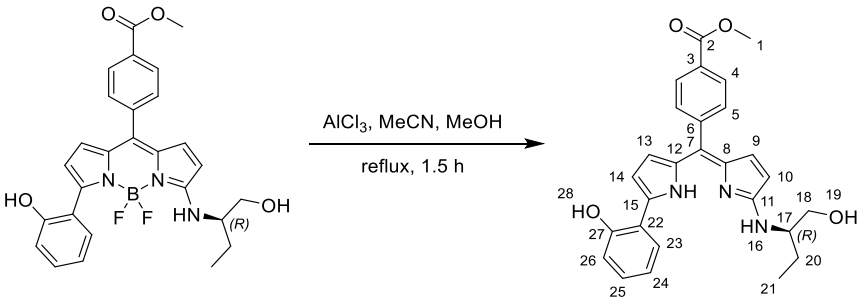

To a 250 mL round bottom flask was added methyl (*R*)-4-(5,5-difluoro-3-((1-hydroxybutan-2-yl)amino)-7-(2-hydroxyphenyl)-5*H*-4λ^4,5λ^4-dipyrrolo[1,2-*c*:2',1'-*f*][1,3,2]diazaborinin-10-yl)benzoate (232 mg, 0.46 mmol), MeCN (50 mL), and $AlCl_3$ (306 mg, 2.30 mmol) dissolved in MeOH (10 mL). The reaction mixture was heated, using an oil bath, to reflux, stirred for 1.5 hours then diluted with DCM (100 mL) and washed with water (3 x 100 mL). The organic layer was dried over $MgSO_4$, filtered and solvent was removed under reduced pressure. The crude product was purified through silica gel column chromatography (DCM : methanol, 100:4 → 100:8) to give methyl (*R*,*Z*)-4-((5-((1-hydroxybutan-2-yl)amino)-2*H*-pyrrol-2-ylidene)(5-(2-hydroxyphenyl)-1*H*-pyrrol-2-yl)methyl)benzoate (141 mg, 0.31 mmol, 67%) as a red/shiny black solid.

R_f: 0.70 (ethyl acetate). **Mp:** 143-145 °C. **^{1}H NMR** (700 MHz, Methanol-d_4) δ 8.03 (d, *J* = 8.5 Hz, 2H, H^4), 7.60 (dd, *J* = 7.9, 1.6 Hz, 1H, H^{26}), 7.50 (d, *J* = 8.5 Hz, 2H, H^5), 7.03 (ddd, *J* = 8.5, 7.2, 1.6 Hz, 1H, H^{24}), 6.87 (dd, *J* = 8.1, 1.2 Hz, 1H, H^{23}), 6.85 – 6.82 (m, 1H, H^{25}), 6.58 – 6.55 (m, 2H, $H^{9,14}$), 6.24 (d, *J* = 4.6 Hz, 1H, H^{10}), 5.93 (d, *J* = 3.8 Hz, 1H, H^{13}), 4.26 – 4.16 (m, 1H, H^{17}), 3.90 (s, 3H, H^1), 3.83 (dd, *J* = 10.8, 4.6 Hz, 1H, H^{18}), 3.65 (dd, *J* = 10.7, 7.0 Hz, 1H, $H^{18'}$), 1.97 – 1.88 (m, 1H, H^{20}), 1.55 (ddq, *J* = 14.6, 9.2, 7.4 Hz, 1H, $H^{20'}$), 1.04 (t, *J* = 7.4 Hz, 3H, H^{21}). **^{13}C NMR** (176 MHz, Methanol-d_4) δ 169.2 (C^2), 168.4 (C^{11}), 154.4 (C^{27}), 148.9 (C^8), 145.3 (C^6), 137.6 (C^9), 135.7 (C^{15}), 133.5 (C^7), 132.4 (C^5), 130.4 (C^3), 129.8 (C^4), 128.4 (C^{24}), 127.7 (C^{26}), 126.2 (C^{12}), 121.1 (C^{25}), 120.8 (C^{22}), 120.4 (C^{10}), 117.4 (C^{23}), 116.7 (C^{13}), 108.8 (C^{14}), 65.3 (C^{18}), 56.7 (C^{17}), 52.7 (C^1), 25.5 (C^{20}), 10.9 (C^{21}). **IR** (neat): υ_{max}/cm^{-1} 2960 (NH, w), 1701 (C=O, m), 1589 (C=C, s), 1272 (C-O, m). **HRMS:** (pNSI) calcd for $C_{27}H_{26}N_3O_4$ $[M-H]^-$: 456.1929, found 456.1935.

7.2.2.15 Methyl (*S*,*Z*)-4-((5-(2-hydroxyphenyl)-1*H*-pyrrol-2-yl)(5-((1-hydroxypropan-2-yl)amino)-2*H*-pyrrol-2-ylidene)methyl)benzoate (**3.37**)

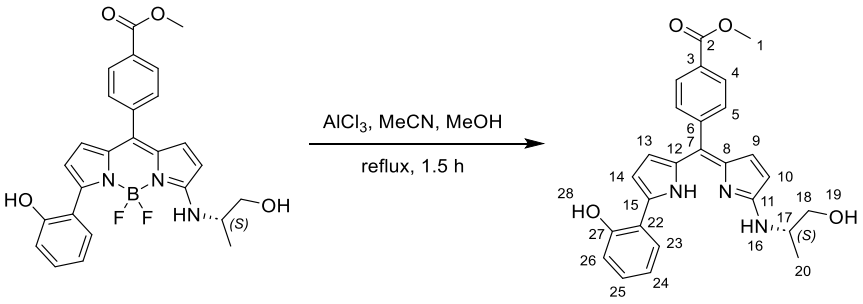

To a 50 mL round bottom flask was added methyl (*S*)-4-(5,5-difluoro-3-(2-hydroxyphenyl)-7-((1-hydroxypropan-2-yl)amino)-5*H*-5λ^4,6λ^4-dipyrrolo[1,2-*c*:2',1'-*f*][1,3,2]diazaborinin-10-yl)benzoate (97.3 mg, 0.19 mmol), MeCN (30 mL), and $AlCl_3$ (132 mg, 0.99 mmol) dissolved in MeOH (5 mL). The reaction mixture was heated, using an oil bath, to reflux, stirred for 1.5 hours then diluted with DCM (50 mL) and washed with water (3 x 50 mL). The organic layer was dried over $MgSO_4$, filtered and solvent removed under reduced pressure. The crude product was purified through silica gel column chromatography (DCM : methanol, 100:4 → 100:8) to give methyl (*S*,*Z*)-4-((5-(2-hydroxyphenyl)-1*H*-pyrrol-2-yl)(5-((1-hydroxypropan-2-yl)amino)-2*H*-pyrrol-2-ylidene)methyl)benzoate (40 mg, 0.09 mmol, 46%) as a red/shiny black solid.

R_f: 0.70 (ethyl acetate). **Mp:** 153-154 °C. **^{1}H NMR** (700 MHz, Methanol-d_4) δ 8.04 (d, *J* = 8.3 Hz, 2H, H^4), 7.61 (dd, *J* = 7.8, 1.5 Hz, 1H, H^{25}), 7.50 (d, *J* = 8.3 Hz, 2H, H^5), 7.04 (ddd, *J* = 8.6, 7.2, 1.5 Hz, 1H, H^{23}), 6.88 (dd, *J* = 8.1, 1.2 Hz, 1H, H^{22}), 6.86 – 6.82 (m, 1H, H^{24}), 6.58 (d, *J* = 3.9 Hz, 1H, H^{14}), 6.57 (d, *J* = 4.6 Hz, 1H, H^9), 6.22 (d, *J* = 4.7 Hz, 1H, H^{10}), 5.94 (d, *J* = 3.8 Hz, 1H, H^{13}), 4.40 – 4.32 (m, 1H, H^{17}), 3.92 (s, 3H, H^1), 3.83 (dd, *J* = 10.5, 4.7 Hz, 1H, H^{18}), 3.62 (dd, *J* = 10.6, 6.8 Hz, 1H, $H^{18'}$), 1.35 (d, *J* = 6.7 Hz, 3H, H^{20}).**^{13}C NMR** (176 MHz, Methanol-d_4) δ 168.6 (C^2), 168.4 (C^{11}), 154.4 (C^{26}), 148.8 (C^8), 145.3 (C^6), 137.6 (C^9), 135.7 (C^{15}), 133.5 (C^7), 132.4 (C^5), 130.5 (C^3), 129.8 (C^4), 128.4 (C^{23}), 127.7 (C^{25}), 126.4 (C^{12}), 121.1 (C^{24}), 120.8 (C^{21}), 120.3 (C^{10}), 117.4 (C^{22}), 116.7 (C^{13}), 108.7 (C^{14}), 66.8 (C^{18}), 52.7 (C^{17}), 50.8 (C^1), 17.8 (C^{20}). **IR** (neat): υ_{max}/cm^{-1} 2960 (NH, w), 1701 (C=O, m), 1589 (C=C, S), 1272 (C-O, m). **HRMS:** (pNSI) calcd for $C_{26}H_{24}N_3O_4$ $[M-H]^-$: 442.1772, found 442.1779.

7.2.2.16 Methyl (*S*,*Z*)-4-((5-((2-hydroxy-1-phenylethyl)amino)-2*H*-pyrrol-2-ylidene)(5-(2-hydroxyphenyl)-1*H*-pyrrol-2-yl)methyl)benzoate (**3.38**)

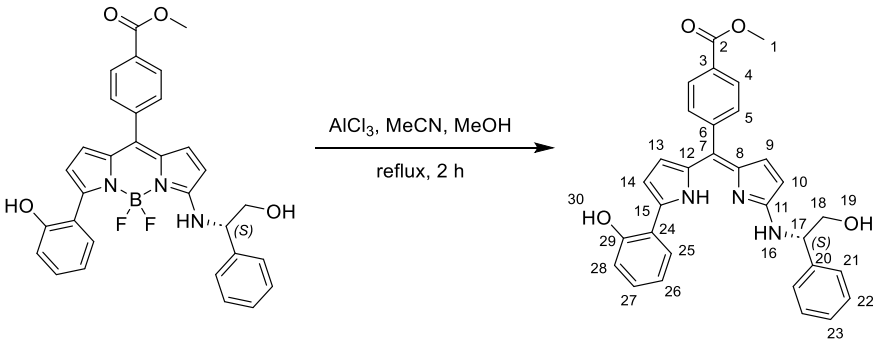

To a round bottom flask was added methyl (S)-4-(5,5-difluoro-3-((2-hydroxy-1-phenylethyl)amino)-7-(2-hydroxyphenyl)-5*H*-4λ^4,5λ^4-dipyrrolo[1,2-*c*:2',1'-*f*][1,3,2]diazaborinin-10-yl)benzoate (123 mg, 0.22 mmol), MeCN (30 mL), and $AlCl_3$ (148 mg, 1.11 mmol) dissolved in MeOH (5 mL). The reaction mixture was heated, using an oil bath, to reflux, stirred for 2 hours then diluted with DCM (50 mL) and washed with water (3 x 50 mL). The organic layer was dried over $MgSO_4$, filtered and solvent removed under reduced pressure. The crude product was purified through silica gel column chromatography (DCM : methanol, 50:5) to give methyl (*S*,*Z*)-4-((5-((2-hydroxy-1-phenylethyl)amino)-2*H*-pyrrol-2-ylidene)(5-(2-hydroxyphenyl)-1*H*-pyrrol-2-yl)methyl)benzoate (107 mg, 0.21 mmol, 95%) as a red/shiny black solid.

R_f: 0.77 (ethyl acetate). **^{1}H NMR** (700 MHz, Methanol-*d*$_4$) δ 8.03 (d, *J* = 8.5 Hz, 2H, H^4), 7.60 (dd, *J* = 7.8, 1.5 Hz, 1H, H^{28}), 7.50 (d, *J* = 7.9 Hz, 2H, H^{21}), 7.48 (d, *J* = 8.1 Hz, 2H, H^5), 7.27 (t, *J* = 7.6 Hz, 2H, H^{22}), 7.22 – 7.18 (m, 1H, H^{23}), 7.10 – 7.06 (m, 1H, H^{26}), 6.92 (d, *J* = 8.1 Hz, 1H, H^{23}), 6.89 (td, *J* = 7.5, 1.2 Hz, 1H, H^{27}), 6.57 (d, *J* = 3.9 Hz, 1H, H^9), 6.55 (d, *J* = 4.5 Hz, 1H, H^{14}), 6.25 (d, *J* = 4.6 Hz, 1H, H^{10}), 5.94 (d, *J* = 3.8 Hz, 1H, H^{13}), 5.45 – 5.37 (m, 1H, H^{17}), 4.06 – 4.00 (m, 1H, H^{18}), 3.98 (dd, *J* = 10.9, 6.8 Hz, 1H, H$^{18'}$), 3.91 (s, 3H, H^1). **^{13}C NMR** (176 MHz, Methanol-*d*$_4$) δ 168.43(C^2), 168.39 (C^{11}), 154.6 (C^{29}), 148.5 (C^8), 145.2 (C^6), 142.0 (C^{20}), 137.6 (C^9), 135.8 (C^{15}), 133.5 (C^7), 132.4 (C^5), 130.5 (C^3), 129.8 (C^4), 129.5 (C^{22}), 128.6 (C^{21}), 128.4 (C^{23}), 128.0 (C^{28}), 126.9 (C^{12}), 121.2 (C^{24}), 120.6 (C^{27}), 120.5 (C^{10}), 117.4 (C^{25}), 116.9 (C^{13}), 109.1 (C^{14}), 66.2 (C^{18}), 59.4 (C^{17}), 52.7 (C^1). **IR** (neat): υ_{max}/cm^{-1} 2960 (NH, w), 1701 (C=O, m), 1589 (C=C, s), 1272 (C-O, m). **HRMS:** (pNSI) calcd for $C_{31}H_{26}N_3O_4$ [M-H]$^-$: 504.1929, found 504.1939.

7.2.2.17 Methyl (*S*,*Z*)-4-((5-((1-hydroxy-3,3-dimethylbutan-2-yl)amino)-2*H*-pyrrol-2-ylidene)(5-(2-hydroxyphenyl)-1*H*-pyrrol-2-yl)methyl)benzoate (3.39)

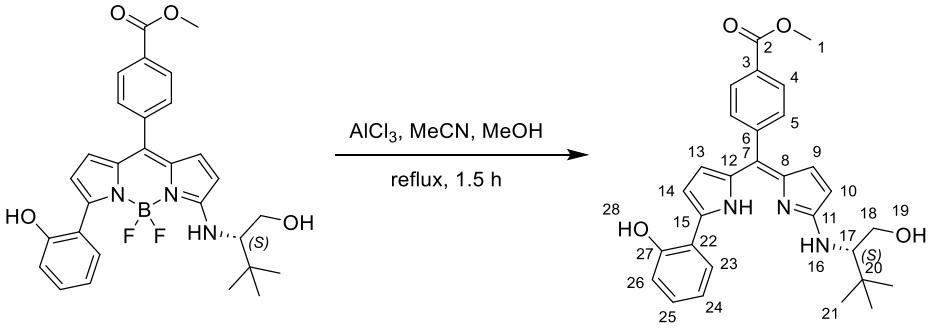

To a round bottom flask was added methyl (*S*)-4-(5,5-difluoro-3-((1-hydroxy-3,3-dimethylbutan-2-yl)amino)-7-(2-hydroxyphenyl)-5*H*-4λ^4,5λ^4-dipyrrolo[1,2-*c*:2',1'-*f*][1,3,2]diazaborinin-10-yl)benzoate (100 mg, 0.19 mmol), MeCN (25 mL), and $AlCl_3$ (125 mg, 0.95 mmol) dissolved in MeOH (4 mL). The reaction mixture was heated, using an oil bath, to reflux, stirred for 1.5 hours then diluted with DCM (50 mL) and washed with water (3 x 50 mL). The organic layer was dried over $MgSO_4$, filtered and solvent removed under reduced pressure. The crude product was purified preparative TLC (DCM : methanol, 50:5) to give methyl (*S*,*Z*)-4-((5-((1-hydroxy-3,3-dimethylbutan-2-yl)amino)-2*H*-pyrrol-2-ylidene)(5-(2-hydroxyphenyl)-1*H*-pyrrol-2-yl)methyl)benzoate (58.1 mg, 0.12 mmol, 64%) as a red/shiny black solid.

R_f: 0.70 (ethyl acetate). **Mp:** 141-142 °C. **^{1}H NMR** (700 MHz, Methanol-d_4) δ 8.05 (d, *J* = 8.4 Hz, 2H, H^4), 7.61 (dd, *J* = 7.8, 1.7 Hz, 1H, H^{26}), 7.52 (d, *J* = 8.3 Hz, 2H, H^5), 7.05 (t, *J* = 7.1 Hz, 1H, H^{24}), 6.91 – 6.84 (m, 1H, $H^{23,25}$), 6.63 – 6.57 (m, 2H, $H^{9,14}$), 6.33 (d, 1H, H^{10}), 5.96 (d, 1H, H^{13}), 4.28 – 4.18 (m, 1H, H^{17}), 4.01 – 3.97 (m, 1H, H^{18}), 3.93 (s, 3H, H^1), 3.70 (dd, *J* = 11.3, 7.2 Hz, 1H, $H^{18'}$), 1.07 (s, 9H, H^{21}). **^{13}C NMR** (176 MHz, Methanol-d_4) δ 170.2, 168.5, 155.0, 149.1, 145.4, 137.5, 135.4, 133.8, 132.4, 130.5, 129.8, 128.4, 127.6, 125.8, 121.0, 117.8, 116.4, 109.6, 63.7, 52.6, 49.9, 35.6, 30.7, 27.6, 25.7. **HRMS:** (pNSI) calcd for $C_{29}H_{32}N_3O_4$ $[M+H]^+$: 486.2387, found 486.2377.

7.2.2.18 Methyl (*S*)-4-(10b-(4-fluorophenyl)-10-((1-hydroxybutan-2-yl)amino)-10b*H*-11-oxa-4b^{1},10aλ^{4}-diaza-10bλ^{4}-boracyclopenta[*e*]aceanthrylen-7-yl)benzoate (**3.7a**) and (**3.7b**)

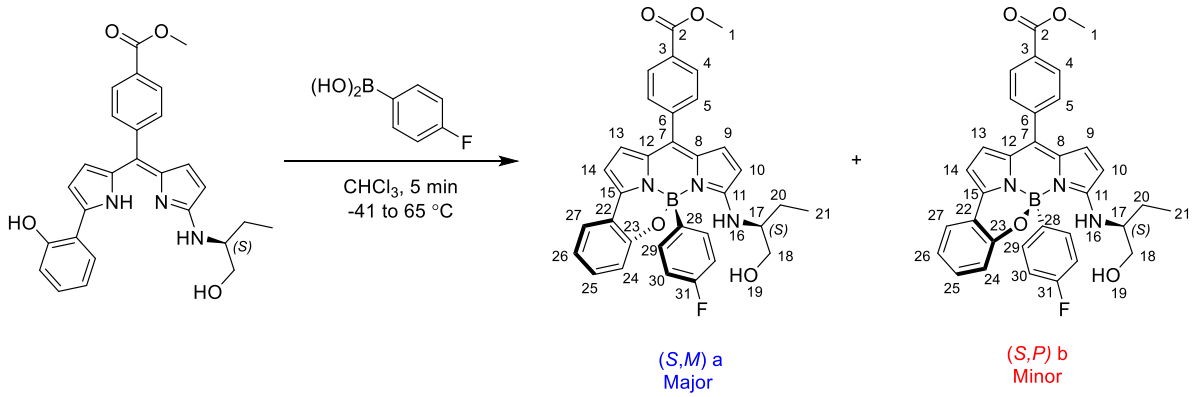

To a 50 mL round bottom flask, under an atmosphere of nitrogen, was added methyl (*S*,*Z*)-4-((5-((1-hydroxybutan-2-yl)amino)-2*H*-pyrrol-2-ylidene)(5-(2-hydroxyphenyl)-1*H*-pyrrol-2-yl)methyl)benzoate (45.7 mg , 0.10 mmol) and $CHCl_3$ (15 mL). The reaction mixture was equilibrated at the desired reaction temperature, stirred for 30 mins (see table **7.1**), and 4-fluorphenyl boronic acid (20.9 mg, 0.15 mmol) dissolved in $CHCl_3$ (5 mL), under an atmosphere of nitrogen, was added dropwise to the reaction mixture over 5 mins. The reaction mixture was quenched with water then diluted with DCM (50 mL), washed with water (3 x 50 mL), dried over $MgSO_4$, filtered and the solvent was removed under reduced pressure to give a purple product. The crude product was purified through silica gel column chromatography (DCM: methanol, 100 : 0.05→ 100 : 0.2) to give:

Major (*S*,*M*)-(3.7a):

R_f: 0.62 (DCM: ethyl acetate, 4:1). **Mp:** 143-145 °C.**^{1}H NMR** (700 MHz, Chloroform-*d*) δ 8.16 (d, *J* = 8.5 Hz, 2H, H^{4}), 7.69 (d, *J* = 8.1 Hz, 2H, H^{5}), 7.49 (dd, *J* = 7.6, 1.7 Hz, 1H, H^{24}), 7.25 – 7.20 (m, 1H, H^{26}), 7.17 – 7.13 (m, 3H, $H^{27,29}$), 6.99 (d, *J* = 4.8 Hz, 1H, H^{10}), 6.89 (td, *J* = 7.4, 1.2 Hz, 1H, H^{25}), 6.77 – 6.73 (m, 2H, H^{30}), 6.69 (d, *J* = 9.8 Hz, 1H, H^{16}), 6.60 (d, *J* = 3.9 Hz, 1H, H^{14}), 6.58 (d, *J* = 3.9 Hz, 1H, H^{13}), 6.15 (d, *J* = 4.9 Hz, 1H, H^{9}), 3.98 (s, 3H, H^{1}), 3.82 (dd, *J* = 12.4, 2.9 Hz, 1H, H^{18}), 3.73 (dd, *J* = 11.2, 5.8 Hz, 1H, $H^{18'}$), 3.43 (tt, *J* = 9.4, 4.8 Hz, 1H, H^{17}), 2.17 (s, 1H, H^{19}), 1.63 – 1.59 (m, 1H, H^{20}), 1.50 – 1.42 (m, 1H, $H^{20'}$), 0.67 (t, *J* = 7.4 Hz, 3H, H^{21}). **^{13}C NMR** (176 MHz, Chloroform-*d*) δ 166.8 (C^{2}), 162.3 (d, *J* = 243.3 Hz, C^{31}), 161.1 (C^{8}), 154.1 (C^{23}),142.2 (C^{28}), 140.1 (C^{15}), 139.6 (C^{6}), 134.0 (C^{10}), 133.3(C^{11}), 132.9 (d, *J* = 7.0 Hz, C^{29}), 132.2 (C^{7}), 130.9 (C^{3}), 130.5 (C^{5}), 129.8 (C^{26}), 129.7 (C^{4}), 129.6 (C^{12}), 125.0 (C^{24}), 121.4 (C^{13}), 120.2 (C^{22}), 120.1 (C^{25}), 119.3 (C^{27}), 114.2 (d, *J* = 19.4 Hz, C^{30}), 109.8 (C^{14}), 109.7 (C^{9}), 65.2 (C^{18}), 58.6 (C^{17}), 52.5 (C^{1}), 25.5 (C^{20}), 10.1 (C^{21}). **^{11}B NMR** (96 MHz, Chloroform-*d*) δ 2.05. **^{19}F NMR** (282 MHz, Chloroform-*d*) δ -116.8. **IR** (neat): υ_{max}/cm^{-1} 3351 (C-H, w), 1710 (C=O, m), 1589 (C=C, s). **HRMS:** (pNSI) calcd for $C_{33}H_{29}BF_1N_3O_4Na$ $[M+Na]^+$: 584.2133, found 584.2132; $C_{33}H_{30}BF_1N_3O_4$ $[M+H]^+$: 562.2314, found

562.2315. **UV-Vis:** λ_{max} (abs) = 577 nm (DCM). **Molar extinction coefficient** (ε) = 43,212 M^{-1} cm^{-1} (DCM). ϕ_F = 0.04 (DCM).

X-Ray code: mjh220014_1_fa

Minor (*S,P*)-(3.7b):

R_f: 0.77 (DCM: ethyl acetate, 4:1). **Mp:** 143-145 °C. **^{1}H NMR** (700 MHz, Chloroform-*d*) δ 8.18 (d, *J* = 8.5 Hz, 2H, H^4), 7.71 (d, *J* = 8.1 Hz, 2H, H^5), 7.51 (dd, *J* = 7.6, 1.7 Hz, 1H, H^{24}), 7.26 – 7.22 (m, 1H, H^{26}), 7.20 – 7.14 (m, 3H, $H^{27,29}$), 7.03 (d, *J* = 4.8 Hz, 1H, H^{10}), 6.90 (td, *J* = 7.4, 1.2 Hz, 1H, H^{25}), 6.79 (t, *J* = 9.0 Hz, 2H, H^{30}), 6.65 (d, *J* = 9.7 Hz, 1H, H^{16}), 6.61 (d, *J* = 3.9 Hz, 1H, H^{14}), 6.60 (d, *J* = 3.9 Hz, 1H, H^{13}), 6.17 (d, *J* = 4.8 Hz, 1H, H^9), 3.99 (s, 3H, H^1), 3.52 (ddd, *J* = 11.1, 7.3, 3.5 Hz, 1H, H^{18}), 3.47 – 3.42 (m, 1H, H^{17}), 3.40 (dt, *J* = 11.2, 5.5 Hz, 1H, $H^{18'}$), 1.77 (dtd, *J* = 15.1, 7.4, 5.5 Hz, 1H, H^{20}), 1.73 – 1.65 (m, 1H, $H^{20'}$), 1.09 (t, *J* = 7.4 Hz, 3H, H^{21}). **^{13}C NMR** (176 MHz, Chloroform-*d*) δ 166.8 (C^2), 162.3 (d, *J* = 244.4 Hz, C^{31}), 161.4 (C^8), 154.3 (C^{23}),142.9 (C^{28}), 140.2 (C^{15}), 139.6 (C^6), 134.1 (C^{10}), 133.2(C^{11}), 132.8 (d, *J* = 7.0 Hz, C^{29}), 132.3 (C^7), 131.0 (C^3), 130.5 (C^5), 129.9 (C^{26}), 129.8 (C^4), 129.6 (C^{12}), 125.0 (C^{24}), 121.7 (C^{13}), 120.2 (C^{22}), 120.0 (C^{25}), 119.3 (C^{27}), 114.5 (d, *J* = 19.4 Hz, C^{30}), 110.0 (C^{14}), 109.8 (C^9), 65.4 (C^{18}), 58.7 (C^{17}), 52.5 (C^1), 24.9 (C^{20}), 10.5 (C^{21}). **^{11}B NMR** (96 MHz, Chloroform-*d*) δ 1.71. **^{19}F NMR** (282 MHz, Chloroform-*d*) δ -115.8. **IR** (neat):): υ_{max}/cm^{-1} 3352 (C-H, w), 1720 (C=O, m), 1600 (C=C, s). **HRMS:** (pNSI) calcd for $C_{33}H_{29}BF_1N_3O_4Na$ $[M+Na]^+$: 584.2128, found 584.2127. **UV-Vis:** λ_{max} (abs) = 578 nm (DCM). **Molar extinction coefficient** (ε) = 39,637 M^{-1} cm^{-1} (DCM). ϕ_F = 0.05 (DCM).

X-Ray code: mjh220005_fa

Entry	Reaction Temp./°C	*de* before purification[a]/%	*de* after purification[b]/%	Minor/%	Major/%	Yield[c]/%
1	-41	47	44	19	46	65 [d]
2	0	62	41	25	61	86
3	RT (25)	70	62	18	80	98
4	35	74	64	19.9	90.6	100
5	45	65	50	24	72	96
6	55	64	61	17	70	87
7	Reflux (65)	61	61	17	69	86

Table 7.1: [a] *de* of final helically chiral (*S,M*)/(*S,P*)-*N,N,O,C*-3-((1-hydroxybutan-2-yl)amino) BODIPYs before purification, measured by ^{19}F NMR.[b] *de* after purification by column chromatography. [c] Isolated combined yield following column chromatography. [d] Isolated yield following re-column chromatography.

7.2.2.19 Methyl (*R*)-4-(10b-(4-fluorophenyl)-10-((1-hydroxybutan-2-yl)amino)-10b*H*-11-oxa-4b^{1},10aλ^{4}-diaza-10bλ^{4}-boracyclopenta[*e*]aceanthrylen-7-yl)benzoate (**3.40a**) and (**3.40b**)

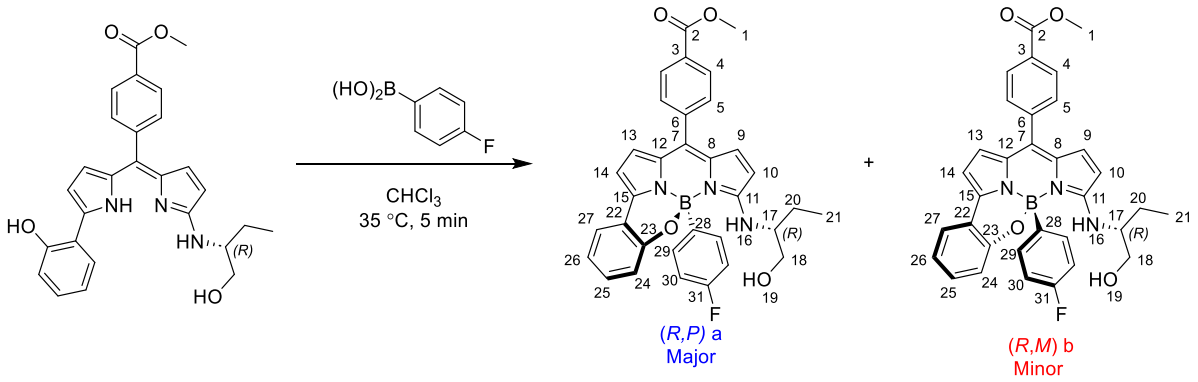

To a 50 mL round bottom flask, under an atmosphere of nitrogen, was added methyl (*R*,*Z*)-4-((5-((1-hydroxybutan-2-yl)amino)-2*H*-pyrrol-2-ylidene)(5-(2-hydroxyphenyl)-1*H*-pyrrol-2-yl)methyl)benzoate (45.7 mg , 0.10 mmol) and $CHCl_3$ (15 mL). The reaction mixture was equilibrated at 35 °C, stirred for 30 mins, and 4-fluorphenyl boronic acid (20.9 mg, 0.15 mmol) dissolved in $CHCl_3$ (5 mL), under an atmosphere of nitrogen, was added dropwise to the reaction mixture over 5 mins. The reaction mixture was quenched with water then diluted with DCM (50 mL), washed with water (3 x 50 mL), dried over $MgSO_4$, filtered and the solvent was removed under reduced pressure to give a purple product. The crude product was purified through silica gel column chromatography (DCM: methanol, 100 : 0.05 → 100 : 0.2) to give:

Major (*R*,*P*)-(3.40a):

R_f: 0.62 (DCM: ethyl acetate, 4:1). **Mp:** 143 -145 °C.**^{1}H NMR** (700 MHz, Chloroform-*d*) δ 8.16 (d, *J* = 8.5 Hz, 2H, H^{4}), 7.69 (d, *J* = 8.1 Hz, 2H, H^{5}), 7.49 (dd, *J* = 7.6, 1.6 Hz, 1H, H^{24}), 7.22 (dd, *J* = 8.5, 1.4 Hz, 1H, H^{26}), 7.17 – 7.13 (m, 3H, $H^{27,29}$), 6.99 (d, *J* = 4.8 Hz, 1H, H^{10}), 6.89 (td, *J* = 7.3, 1.4 Hz, 1H, H^{25}), 6.77 – 6.73 (m, 2H, H^{30}), 6.68 (d, *J* = 9.8 Hz, 1H, H^{16}), 6.60 (d, *J* = 3.9 Hz, 1H, H^{14}), 6.58 (d, *J* = 3.9 Hz, 1H, H^{13}), 6.15 (d, *J* = 4.8 Hz, 1H, H^{9}), 3.98 (s, 3H, H^{1}), 3.83 (dd, *J* = 11.2, 5.2 Hz, 1H, H^{18}), 3.75 – 3.70 (m, 1H, $H^{18'}$), 3.46 – 3.39 (m, 1H, H^{17}), 2.21 (s, 1H, H^{19}), 1.63 – 1.59 (m, 1H, H^{20}), 1.49 – 1.42 (m, 1H, $H^{20'}$), 0.66 (t, *J* = 7.4 Hz, 3H, H^{21}). **^{13}C NMR** (176 MHz, Chloroform-*d*) δ 166.8 (C^{2}), 162.3 (d, *J* = 243.3 Hz, C^{31}), 161.1 (C^{8}), 154.1 (C^{23}), 142.5 (C^{28}), 140.1 (C^{15}), 139.6 (C^{6}), 134.1 (C^{10}), 133.3(C^{11}), 132.9 (d, *J* = 7.0 Hz, C^{29}), 132.1 (C^{7}), 130.9 (C^{3}), 130.5 (C^{5}), 129.8 (C^{26}), 129.7 (C^{4}), 129.6 (C^{12}), 125.0 (C^{24}), 121.4 (C^{13}), 120.1 (C^{22}), 120.1 (C^{25}), 119.3 (C^{27}), 114.2 (d, *J* = 19.4 Hz, C^{30}), 109.8 (C^{14}), 109.7 (C^{9}), 65.2 (C^{18}), 58.6 (C^{17}), 52.5 (C^{1}), 25.5 (C^{20}), 10.1 (C^{21}).**^{11}B NMR** (96 MHz, Chloroform-*d*) δ 1.86. **^{19}F NMR** (282 MHz, Chloroform-*d*) δ -116.8. **IR** (neat): υ_{max}/cm^{-1} 3358 (CH, w), 1713 (C=O, w), 1689 (C=C, m).

X-Ray code: mjh220026_1_fa

Minor (*R*,*M*)-(3.40b)

R_f: 0.77 (DCM: ethyl acetate, 4:1). **Mp:** 143-145 °C. **^{1}H NMR** (700 MHz, Chloroform-*d*) δ 8.18 (d, *J* = 8.5 Hz, 2H, H^4), 7.71 (d, *J* = 8.1 Hz, 2H, H^5), 7.51 (dd, *J* = 7.6, 1.7 Hz, 1H, H^{24}), 7.26 – 7.21 (m, 1H, H^{26}), 7.20 – 7.14 (m, 3H, $H^{27,29}$), 7.03 (d, *J* = 4.8 Hz, 1H, H^{10}), 6.90 (td, *J* = 7.4, 1.2 Hz, 1H, H^{25}), 6.79 (t, *J* = 9.0 Hz, 2H, H^{30}), 6.65 (d, *J* = 9.7 Hz, 1H, H^{16}), 6.61 (d, *J* = 3.9 Hz, 1H, H^{14}), 6.60 (d, *J* = 3.9 Hz, 1H, H^{13}), 6.17 (d, *J* = 4.8 Hz, 1H, H^9), 3.99 (s, 3H, H^1), 3.52 (ddd, *J* = 10.9, 7.0, 3.6 Hz, 1H, H^{18}), 3.44 (ddt, *J* = 7.9, 6.1, 4.7 Hz, 1H, H^{17}), 3.40 (dt, *J* = 10.9, 5.1 Hz, 1H, $H^{18'}$), 1.77 (dqd, *J* = 14.9, 7.5, 5.3 Hz, 1H, H^{20}), 1.72 – 1.65 (m, 1H, $H^{20'}$), 1.09 (t, *J* = 7.5 Hz, 3H, H^{21}), 1.00 (t, *J* = 6.5 Hz, 1H, H^{19}). **^{13}C NMR** (176 MHz, Chloroform-*d*) δ 166.8 (C^2), 162.3 (d, *J* = 244.6 Hz, C^{31}), 161.3 (C^8), 154.3 (C^{23}),142.8 (C^{28}), 140.2 (C^{15}), 139.6 (C^6), 134.1 (C^{10}), 133.2(C^{11}), 132.8 (d, *J* = 7.0 Hz, C^{29}), 132.3 (C^7), 131.0 (C^3), 130.5 (C^5), 129.9 (C^{26}), 129.8 (C^4), 129.6 (C^{12}), 125.0 (C^{24}), 121.7 (C^{13}), 120.2 (C^{22}), 120.0 (C^{25}), 119.3 (C^{27}), 114.5 (d, *J* = 19.4 Hz, C^{30}), 109.9 (C^{14}), 109.8 (C^9), 65.3 (C^{18}), 58.7 (C^{17}), 52.5 (C^1), 24.9 (C^{20}), 10.5 (C^{21}). **^{11}B NMR** (96 MHz, Chloroform-*d*) δ 1.56. **^{19}F NMR** (282 MHz, Chloroform-*d*) δ -115.8. **IR** (neat): υ_{max}/cm^{-1} 3361 (C-H, w), 1709 (C=O, m), 1600 (C=C, m).

X-Ray code: mjh220038_1_fa

7.2.2.20 Methyl (*S*)-4-(10b-(4-fluorophenyl)-10-((1-hydroxypropan-2-yl)amino)-10b*H*-11-oxa-4b^{1}, 10aλ^{4}-diaza-10bλ^{4}-boracyclopenta[*e*]aceanthrylen-7-yl)benzoate (**3.51a**) and (**3.51b**)

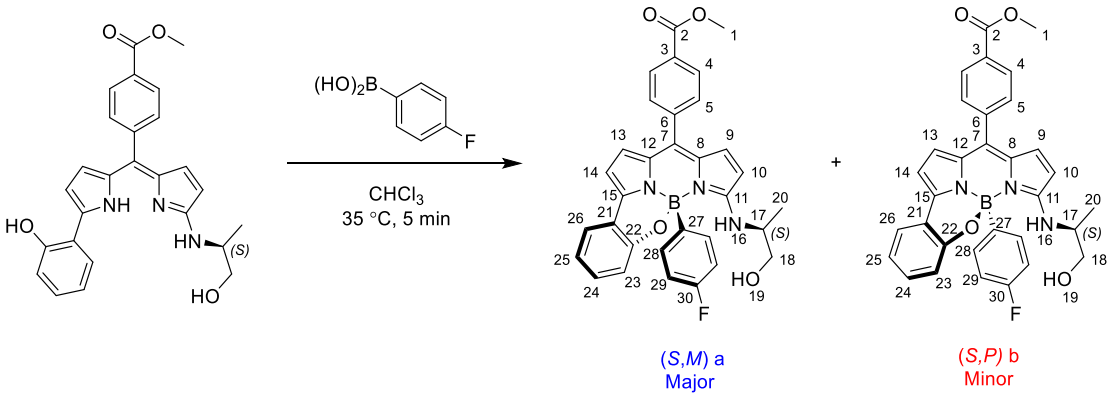

To a 25 mL round bottom flask, under an atmosphere of nitrogen, was added methyl (*S*,*Z*)-4-((5-(2-hydroxyphenyl)-1*H*-pyrrol-2-yl)(5-((1-hydroxypropan-2-yl)amino)-2*H*-pyrrol-2-ylidene)methyl)benzoate (30.0 mg , 0.07 mmol) and $CHCl_3$ (10 mL). The reaction mixture was equilibrated at 35 °C, stirred for 30 mins, and 4-fluorphenyl boronic acid (14.2 mg, 0.10 mmol) dissolved in $CHCl_3$ (5 mL), under an atmosphere of nitrogen, was added dropwise to the reaction mixture over 5 mins. The reaction mixture was quenched with water then diluted with DCM (50 mL), washed with water (3 x 50 mL), dried over $MgSO_4$, filtered and the solvent was removed under reduced pressure to give a purple product. The crude product was purified through silica gel column chromatography (DCM: methanol, 100 : 0.05 → 100 : 1) to give:

Major (*S*,*M*)-(3.51a):

Yield = (24.3 mg, 0.04 mmol, 66%). **R_f:** 0.6 (DCM: ethyl acetate, 4:1). **Mp:** 245 °C (decomposed). **^{1}H NMR** (300 MHz, Chloroform-*d*) δ 8.16 (d, *J* = 8.3 Hz, 2H, H^{4}), 7.67 (d, *J* = 8.2 Hz, 2H, H^{5}), 7.49 (dd, *J* = 7.6, 1.5 Hz, 1H, Ar), 7.21 (d, *J* = 7.5 Hz, 1H, Ar), 7.14 (dd, *J* = 8.3, 6.5 Hz, 3H, H^{28}, Ar), 6.97 (d, *J* = 4.7 Hz, 1H, $H^{9/10}$), 6.88 (td, *J* = 7.4, 1.4 Hz, 1H, Ar), 6.81 – 6.70 (m, 3H, H^{29}, H^{16}), 6.61 (d, *J* = 3.9 Hz, 1H, $H^{13/14}$), 6.59 (d, *J* = 3.8 Hz, 1H, $H^{13/14}$), 6.14 (d, *J* = 4.8 Hz, 1H, $H^{9/10}$), 3.98 (s, 3H, H^{1}), 3.87 – 3.74 (m, 1H, H^{18}), 3.73 – 3.59 (m, 2H, $H^{17, 18'}$), 2.31 (br, 1H, H^{19}), 1.16 (d, *J* = 6.1 Hz, 3H, H^{20}). **^{13}C NMR** (75 MHz, Chloroform-*d*) δ 166.8 (C^{2}), 162.2 (d, *J* = 243.4 Hz, C^{30}), 160.7 (C^{8}), 154.1, 142.5 (C^{28}), 139.6, 134.1 ($C^{9/10}$), 132.8 (d, *J* = 7.0 Hz, C^{28}), 130.9, 130.5 (C^{5}), 129.8, 129.7 (C^{4}), 125.0, 121.5 ($C^{13/14}$), 120.2, 120.1, 119.4, 114.1 (d, *J* = 19.3 Hz, C^{29}), 109.8 ($C^{13/14}$), 109.6 ($C^{9/10}$), 66.6 (C^{18}), 52.5 ($C^{1,17}$), 18.1 (C^{20}).**^{11}B NMR** (96 MHz, Chloroform-*d*) δ 1.80. **^{19}F NMR** (282 MHz, Chloroform-*d*) δ -116.7. **IR** (neat): υ_{max}/cm^{-1} 3363 (C-H, w), 1710 (C=O, m). **HRMS:** (TOF MS ASAP+) calcd for $C_{32}H_{28}{}^{11}BFN_3O_4$ $[M+H]^+$: 548.2162, found 548.2162.

X-Ray code: mjh220052_fa.

Note: Four carbon signals were not identified in the analysis of the ^{13}C NMR spectrum.

Minor (*S*,*P*)-(3.51b):

Yield = (10.8 mg, 0.02 mmol, 29%). **R_f:** 0.75 (DCM: ethyl acetate, 4:1). **Mp:** 245 °C (decomposed). **^{1}H NMR** (300 MHz, Chloroform-*d*) δ 8.18 (d, *J* = 8.4 Hz, 2H, H^{4}), 7.71 (d, *J* = 8.3 Hz, 2H, H^{5}), 7.50 (dd, *J* = 7.7, 1.3 Hz, 1H, Ar), 7.25 – 7.13 (m, 4H, H^{28}, Ar), 7.03 (d, *J* = 4.8 Hz, 1H, $H^{9/10}$), 6.90 (td, J = 7.4, 1.4 Hz, 1H, Ar), 6.82 – 6.74 (m, 2H, H^{29}, Ar), 6.65 (d, *J* = 9.4 Hz, 1H, H^{16}), 6.61 (d, *J* = 4.7 Hz, 2H, $H^{13,14}$), 6.18 (d, *J* = 4.8 Hz, 1H, $H^{9/10}$), 3.99 (s, 3H, H^{1}), 3.76 – 3.62 (m, 1H, H^{17}), 3.58 – 3.47 (m, 1H, H^{18}), 3.41 – 3.29 (m, 1H, $H^{18'}$), 1.38 (d, *J* = 6.7 Hz, 3H, H^{20}), 1.06 (s, 1H, H^{19}). **^{13}C NMR** (75 MHz, Chloroform-*d*) δ 166.8 (C^{2}), 162.3 (d, *J* = 244.5 Hz, C^{30}), 160.9 (C^{8}), 154.3, 143.3 (C^{28}), 140.3, 139.6, 134.1 ($C^{9/10}$), 133.2, 132.8 (d, *J* = 7.0 Hz, C^{28}), 132.5, 131.0, 130.5 (C^{5}), 129.9, 129.8 (C^{4}), 129.6, 125.0, 121.7 ($C^{13/14}$), 120.2, 119.9, 119.3, 114.4 (d, *J* = 19.2 Hz, C^{29}), 110.0 ($C^{13/14}$), 109.6 ($C^{9/10}$), 66.9 (C^{18}), 52.6 (C^{1}), 52.5 (C^{17}), 17.7 (C^{20}). **^{11}B NMR** (96 MHz, Chloroform-*d*) δ 1.50. **^{19}F NMR** (282 MHz, Chloroform-*d*) δ -115.8. **HRMS:** (TOF MS ASAP+) calcd for $C_{32}H_{28}{}^{11}BFN_3O_4$ $[M+H]^+$: 548.2162, found 548.2167.

X-Ray code: mjh220050_fa

7.2.2.21 Methyl (*S*)-4-(10b-(4-fluorophenyl)-10-((1-hydroxy-3,3-dimethylbutan-2-yl)amino)-10b*H*-11-oxa-4b^{1},10aλ^{4}-diaza-10bλ^{4}-boracyclopenta[*e*]aceanthrylen-7-yl)benzoate (**3.53a**) and (**3.53b**)

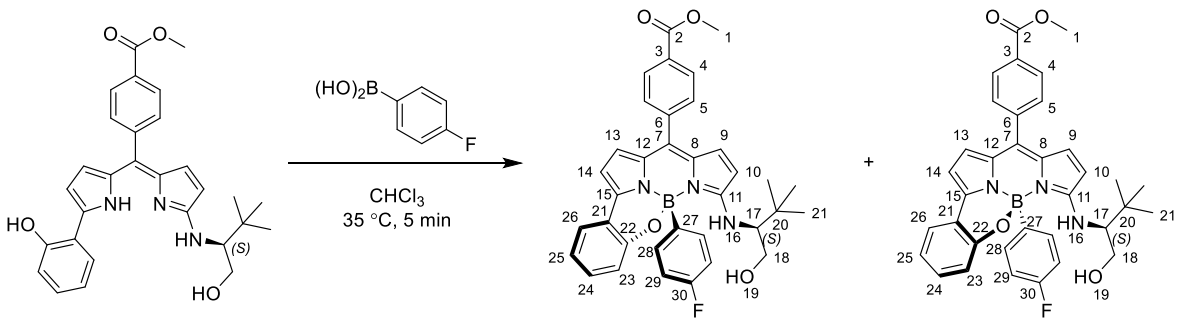

To a 50 mL round bottom flask, under an atmosphere of nitrogen, was added methyl (*S*,*Z*)-4-((5-((1-hydroxy-3,3-dimethylbutan-2-yl)amino)-2*H*-pyrrol-2-ylidene)(5-(2-hydroxyphenyl)-1*H*-pyrrol-2-yl)methyl)benzoate (34.7 mg , 0.07 mmol) and $CHCl_3$ (15 mL). The reaction mixture was equilibrated at 35 °C, stirred for 30 mins, and 4-fluorphenyl boronic acid (14.7 mg, 0.10 mmol) dissolved in $CHCl_3$ (5 mL), under an atmosphere of nitrogen, was added dropwise to the reaction mixture over 5 mins. The reaction mixture was quenched with water then diluted with DCM (50 mL), washed with water (3 x 50 mL), dried over $MgSO_4$, filtered and the solvent was removed under reduced pressure to give a purple product. The crude product was purified through silica gel column chromatography (DCM: methanol, 100 : 0.1 → 100 : 0.2) to give:

Major (*S*,*M*)-(3.53a):

Yield = (22.8 mg, 0.04 mmol, 55%). **R_f:** 0.75 (DCM: ethyl acetate, 4:1). **^{1}H NMR** (400 MHz, Chloroform-*d*) δ 8.16 (d, *J* = 7.9 Hz, 2H, H^{4}), 7.69 (d, *J* = 7.9 Hz, 2H, H^{5}), 7.50 (dd, *J* = 7.7, 1.7 Hz, 1H, Ar), 7.25 – 7.21 (m, 1H, Ar), 7.20 – 7.11 (m, 3H, H^{28}, Ar), 7.00 (d, *J* = 4.9 Hz, 1H, $H^{9/10}$), 6.95 – 6.87 (m,1H, Ar), 6.77 – 6.69 (m, 3H, H^{29}, H^{16}), 6.58 (d, *J* = 4.1 Hz, 1H, $H^{13/14}$), 6.56 (d, *J* = 4.0 Hz, 1H, $H^{13/14}$), 6.20 (d, *J* = 4.9 Hz, 1H, $H^{9/10}$), 3.98 (s, 3H, H^{1}), 3.96 – 3.90 (m, 1H, H^{18}), 3.72 (dd, *J* = 11.5, 8.4 Hz, 1H, $H^{18'}$), 3.21 (ddd, *J* = 11.4, 8.3, 3.4 Hz, 1H, H^{17}), 2.28 (s, 1H, H^{19}), 0.67 (s, 9H, H^{21}). **^{13}C NMR** (101 MHz, Chloroform-*d*) δ 166.7 (C^{2}), 162.2 (d, *J* = 243.3 Hz, C^{30}), 161.9, 154.0, 142.3, 139.53, 139.50 , 133.8 ($C^{9/10}$), 133.4, 132.9 (d, *J* = 7.1 Hz, C^{28}), 131.8 , 130.8 , 130.3 (C^{5}), 129.6 (C^{4}), 129.2 , 124.9, 121.2 ($C^{13/14}$), 120.2 , 120.0, 119.0, 114.2 (d, *J* = 19.2 Hz, C^{29}), 110.1 ($C^{9/10}$), 109.6 ($C^{13/14}$), 66.1 (C^{17}), 62.6 (C^{18}), 52.4 (C^{1}), 33.9 (C^{20}), 26.3 (C^{21}). **^{11}B NMR** (128 MHz, Chloroform-*d*) δ 1.98. **^{19}F NMR** (376 MHz, Chloroform-*d*) δ -116.7.

Note: one carbon signal was not identified in the analysis of the ^{13}C NMR spectrum.

Minor (*S*,*P*)-(3.53b):

Yield = (14.3 mg, 0.02 mmol, 35%). **R_f:** 0.87 (DCM: ethyl acetate, 4:1). **^{1}H NMR** (400 MHz, Chloroform-*d*) δ 8.18 (d, *J* = 7.5 Hz, 2H, H^4), 7.72 (d, *J* = 7.9 Hz, 2H, H^5), 7.51 (dd, *J* = 7.7, 1.7 Hz, 1H, Ar), 7.25 – 7.17 (m, 3H, Ar), 7.12 (d, *J* = 8.1 Hz, 1H, Ar), 7.05 (d, *J* = 4.9 Hz, 1H, $H^{9/10}$), 6.95 – 6.88 (m,1H, Ar), 6.84 – 6.77 (m, 3H, H^{29}, H^{16}), 6.62 – 6.58 (m*, 2H, $H^{13,14}$), 6.20 (d, *J* = 4.9 Hz, 1H, $H^{9/10}$), 3.99 (s, 3H, H^1), 3.72 (dd, *J* = 11.8, 3.3 Hz, 1H, H^{18}), 3.35 (dd, *J* = 11.7, 8.9 Hz, 1H, $H^{18'}$), 3.22 (td, *J* = 9.9, 3.2 Hz, 1H, H^{17}), 1.11 (s, 9H, H^{21}). **^{13}C NMR** (101 MHz, Chloroform-*d*) δ 166.8 (C^2), 162.3 (d, *J* = 244.9 Hz, C^{30}), 162.1, 154.2, 142.4, 139.9, 139.6 , 134.1 ($C^{9/10}$), 133.2, 132.7 (d, *J* = 6.9 Hz, C^{28}), 132.0, 131.0 , 130.5 (C^5), 129.8 (C^4), 129.7 , 125.1, 121.6 ($C^{13/14}$), 120.0 , 120.0, 119.1, 114.6 (d, *J* = 19.3 Hz, C^{29}), 110.1 ($C^{9/10}$), 109.9 ($C^{13/14}$), 66.4 (C^{17}), 62.9 (C^{18}), 52.5 (C^1), 34.1 (C^{20}), 26.8 (C^{21}). **^{11}B NMR** (128 MHz, Chloroform-*d*) δ 1.43. **^{19}F NMR** (376 MHz, Chloroform-*d*) δ -115.4.

X-Ray code: mjh230082_fa.

*Two doublets overlapping corresponding to H^{13} and H^{14}

Note: one carbon signal was not identified in the analysis of the ^{13}C NMR spectrum.

7.2.2.22 methyl (*S*)-4-(10b-(4-fluorophenyl)-10-((2-hydroxy-1-phenylethyl)amino)-10b*H*-11-oxa-4b^1, 10aλ^4-diaza-10bλ^4-boracyclopenta[*e*]aceanthrylen-7-yl)benzoate (**3.52a**) and (**3.52b**)

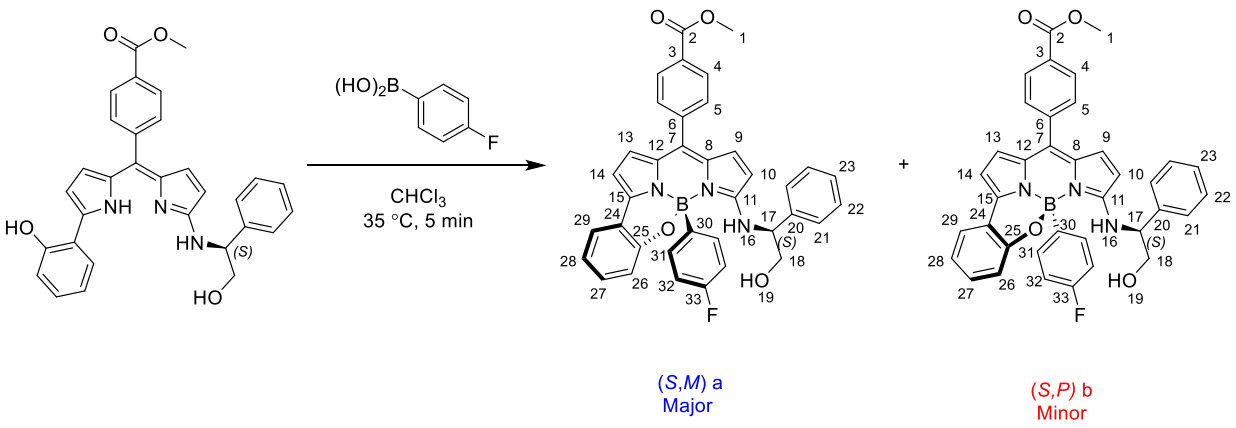

To a 50 mL round bottom flask, under an atmosphere of nitrogen, was added methyl (*S*,*Z*)-4-((5-((2-hydroxy-1-phenylethyl)amino)-2*H*-pyrrol-2-ylidene)(5-(2-hydroxyphenyl)-1*H*-pyrrol-2-yl)methyl)benzoate (50.5 mg , 0.10 mmol) and $CHCl_3$ (15 mL). The reaction mixture was equilibrated at 35 °C, stirred for 30 mins, and 4-fluorphenyl boronic acid (20.9 mg, 0.15 mmol) dissolved in $CHCl_3$ (5 mL), under an atmosphere of nitrogen, was added dropwise to the reaction mixture over 5 mins. The reaction mixture was quenched with water then diluted with DCM (50 mL), washed with water (3 x 50 mL), dried over $MgSO_4$, filtered and the solvent was removed under reduced pressure to give a purple product. The crude product was purified through silica gel column chromatography (DCM: Methanol, 100:0.05 → 100:1) to give:

Major (*S*,*M*)-(3.52a):

Yield = (43.5 mg, 0.07 mmol, 71%). **R_f:** 0.13 (DCM: methanol, 100 : 0.1). **Mp:** 153-155 °C. **^{1}H NMR** (300 MHz, Chloroform-*d*) δ 8.10 (d, *J* = 8.5 Hz, 2H, H^4), 7.61 (d, *J* = 8.2 Hz, 2H, H^5), 7.56 – 7.51 (m, 1H, Ar), 7.41 (d, *J* = 6.4 Hz, 1H, H^{16}), 7.30 – 7.27 (m, 2H, Ar), 7.25 – 7.08 (m, 5H, Ar), 6.97 – 6.90 (m, 1H, Ar), 6.85 – 6.80 (m,2H, Ar), 6.77 (d, *J* = 5.1 Hz, 1H, $H^{9/10}$), 6.70 – 6.65 (m, 2H), 6.63 (d, *J* = 4.0 Hz, 1H, $H^{9/10}$), 6.60 (d, *J* = 4.0 Hz, 1H, $H^{9/10}$), 5.70 (d, *J* = 4.8 Hz, 1H, $H^{13/14}$), 4.63 (td, *J* = 6.3, 4.0 Hz, 1H, H^{17}), 4.05 (ddd, *J* = 11.1, 6.4, 3.9 Hz, 1H, H^{18}), 3.96 (s, 3H, H^1), 3.82 (ddd, *J* = 11.3, 5.6, 5.6 Hz, 1H, $H^{18'}$), 2.50 (br, 1H, H^{19}). **^{13}C NMR** (75 MHz, Chloroform-*d*) δ 166.7 (C^2), 162.4 (d, *J* = 243.6 Hz, C^{33}), 160.5, 154.3, 142.3, 140.5, 139.4, 138.3 , 133.6, 133.4 (d, *J* = 7.0 Hz, C^{31}), 133.2 , 132.7 , 130.9, 130.4, 130.1 , 129.7, 129.6, 129.0, 128.2, 126.4, 125.1, 121.9, 120.3, 120.1, 119.5, 114.3 (d, *J* = 19.3 Hz, C^{32}), 110.2, 110.1, 66.8 (C^{17}), 60.0 (C^{18}), 52.5 (C^1). **^{11}B NMR** (96 MHz, Chloroform-*d*) δ 1.92. **^{19}F NMR** (282 MHz, Chloroform-*d*)

δ -116.6. **IR** (neat): υ_{max}/cm^{-1} 3353 (C-H, w), 2981 (C-H, w), 1719 (C=O, m). **HRMS:** (TOF MS ASAP+) calcd for $C_{37}H_{30}{}^{11}BFN_3O_4$ $[M+H]^+$: 610.2320, found 610.2319.

Minor (*S*,*P*)-(3.52b):

Yield = (22.5 mg, 0.04 mmol, 36%). **R_f:** 0.28 (DCM: methanol, 100 : 0.1). **Mp:** 153 - 154 °C. **^{1}H NMR** (300 MHz, Chloroform-*d*) δ 8.07 (d, *J* = 8.5 Hz, 2H, H^4), 7.59 (d, *J* = 8.3 Hz, 2H, H^5), 7.48 – 7.39 (m, 2H, Ar, ,H^{16}), 7.35 – 7.28 (m, 5H, Ar), 7.20 – 7.09 (m, 5H, Ar), 6.82 (m^*, *J* = 4.6 Hz, 2H, $H^{9/10}$, Ar), 6.78 – 6.65 (m, 2H, Ar), 6.56 – 6.51 (m, 2H, $H^{13,14}$), 5.82 (d, *J* = 4.8 Hz, 1H, $H^{9/10}$), 4.55 (ddd, *J* = 8.2, 5.5, 3.9 Hz, 1H, H^{17}), 3.86 (s, 3H, H^1), 3.83 (dd, *J* = 7.8, 3.9 Hz, 1H, H^{18}), 3.73 (ddd, *J* = 11.0, 5.0, 5.0 Hz, 1H, $H^{18'}$). **^{13}C NMR** (75 MHz, Chloroform-*d*) δ 166.8 (C^2), 162.3 (d, *J* = 243.8 Hz, C^{33}), 160.6, 154.4, 142.5, 140.8, 139.5, 138.6 , 133.7, 133.1, 133.0 (d, *J* = 7.0 Hz, C^{31}), 132.9, 131.0 , 130.5, 130.1, 129.74 , 129.72, 129.3, 128.5, 126.5, 125.1, 122.1, 120.1, 119.9, 119.5, 114.3 (d, *J* = 19.2 Hz, C^{32}), 110.2, 109.6, 66.9 (C^{17}), 60.1 (C^{18}), 52.5 (C^1). **^{11}B NMR** (96 MHz, Chloroform-*d*) δ 1.87. **^{19}F NMR** (282 MHz, Chloroform-*d*) δ -116.3. **IR** (neat): υ_{max}/cm^{-1} 3363 (C-H, w), 2981 (C-H, w), 1704 (C=O, m), 1596 (C=C, s). **HRMS:** (TOF MS ASAP+) calcd for $C_{37}H_{30}{}^{11}BFN_3O_4$ $[M+H]^+$: 610.2320, found 610.2324.

X-Ray code: mjh220046_fa

7.2.2.23 Methyl (*S*)-4-(10-((1-hydroxybutan-2-yl)amino)-10b-(*p*-tolyl)-10b*H*-11-oxa-4b^{1}, 10aλ^{4}-diaza-10bλ^{4}-boracyclopenta[*e*]aceanthrylen-7-yl)benzoate (**3.49a**) and (**3.49b**)

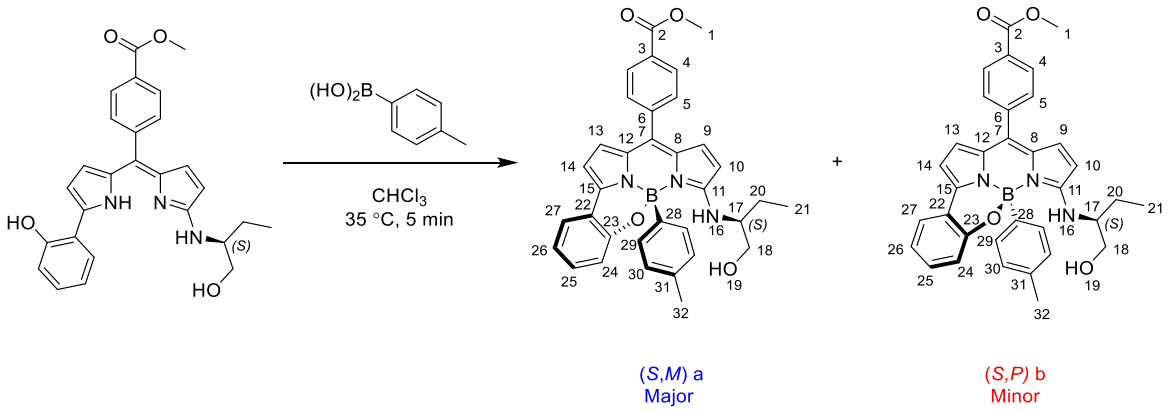

To a round bottom flask, under an atmosphere of nitrogen, was added methyl (*S*,*Z*)-4-((5-((1-hydroxybutan-2-yl)amino)-2*H*-pyrrol-2-ylidene)(5-(2-hydroxyphenyl)-1*H*-pyrrol-2-yl)methyl)benzoate (45.7 mg , 0.10 mmol) and $CHCl_3$ (15 mL). The reaction mixture was equilibrated at 35 °C, stirred for 30 mins, and 4-methylphenyl boronic acid (20.4 mg, 0.15 mmol) dissolved in $CHCl_3$ (5 mL), under an atmosphere of nitrogen, was added dropwise to the reaction mixture over 5 mins. The reaction mixture was quenched with water then diluted with DCM (50 mL), washed with water (3 x 50 mL), dried over $MgSO_4$, filtered and the solvent was removed under reduced pressure to give a purple product. The crude product was purified through silica gel column chromatography (DCM: methanol, 100:0.05 → 100:0.2) to give:

Major (*S*,*M*)-(3.49a):

Yield = (28.6 mg, 0.05 mmol, 51%). **R_f:** 0.68 (DCM: ethyl acetate, 4:1). **^{1}H NMR** (300 MHz, Chloroform-*d*) δ 8.15 (d, *J* = 8.5 Hz, 2H, H^{4}), 7.67 (d, *J* = 8.3 Hz, 2H, H^{5}), 7.47 (dd, *J* = 7.7, 1.4 Hz, 1H, Ar), 7.24 – 7.12 (m, 2H, Ar), 7.12 – 7.07 (m, 2H, Ar), 6.92 (d, *J* = 4.9 Hz, 1H, $H^{9/10}$), 6.91 – 6.83 (m, 3H, Ar), 6.65 (d, *J* = 9.8 Hz, 1H, H^{16}), 6.59 (d, *J* = 4.0 Hz, 1H, $H^{13/14}$), 6.56 (d, *J* = 4.0 Hz, 1H, $H^{13/14}$), 6.07 (d, *J* = 4.8 Hz, 1H, $H^{9/10}$), 3.99 (s, 3H, H^{1}), 3.82 – 3.73 (m, 1H, H^{18}), 3.72 – 3.62 (m, 1H, $H^{18'}$), 3.37 (ddd, *J* = 10.7, 7.0, 2.8 Hz, 1H, H^{17}), 2.73 (br, 1H, H^{19}), 2.17 (s, 3H, H^{32}), 1.61 (ddd, *J* = 14.1, 7.4, 5.2 Hz, 1H, H^{20}), 1.44 (ddd, *J* = 15.6, 14.4, 7.5 Hz, 1H, $H^{20'}$), 0.67 (t, *J* = 7.4 Hz, 3H, H^{21}). **^{13}C NMR** (75 MHz, Chloroform-*d*) δ 166.8 (C^{2}), 161.1, 154.1, 140.0, 139.7, 135.9, 133.9, 133.3 ($C^{9/10}$), 132.0, 131.4, 130.8, 130.4 (C^{5}), 129.7 (C^{4}), 129.6, 129.6, 128.2 ($C^{29/30}$) , 125.0, 121.1 ($C^{13/14}$), 120.3, 120.1, 119.3, 109.7 ($C^{9/10}$), 109.6 ($C^{13/14}$), 65.2 (C^{18}), 58.7 (C^{17}), 52.5 (C^{1}), 25.3 (C^{20}), 21.3 (C^{32}), 10.1 (C^{21}). **^{11}B NMR** (96 MHz, Chloroform-*d*) δ 2.16. **HRMS:** (TOF MS ASAP+) calcd for $C_{34}H_{33}{}^{11}BN_3O_4$ $[M+H]^+$: 558.2570, found 558.2571. **UV-Vis:** λ_{max} (abs) = 578 nm (DCM). **Molar extinction coefficient** (ε) = 51 074 M^{-1} cm^{-1} (DCM). **ϕ_F** = 0.01 (DCM).

X-Ray code: mjh220077_fa

Minor (*S*,*P*)-(3.49b):

Yield = (16.7 mg, 0.03 mmol, 30%). **R_f:** 0.85 (DCM: ethyl acetate, 4:1). **^{1}H NMR** (300 MHz, Chloroform-*d*) δ 8.18 (d, *J* = 8.5 Hz, 2H, H^4), 7.72 (d, *J* = 8.4 Hz, 2H, H^5), 7.49 (dd, *J* = 7.7, 1.4 Hz, 1H, Ar), 7.25 – 7.15 (m, 2H, Ar), 7.15 – 7.10 (m, 2H, Ar), 7.02 (d, *J* = 4.8 Hz, 1H, $H^{9/10}$), 6.96 – 6.84 (m, 3H, Ar), 6.59 (d, *J* = 4.0 Hz, 1H, $H^{13/14}$), 6.58 (d, *J* = 4.0 Hz, 1H, $H^{13/14}$), 6.54 (br, 1H, H^{16}), 6.15 (d, *J* = 4.8 Hz, 1H, $H^{9/10}$), 3.99 (s, 3H, H^1), 3.53 – 3.26 (m, 3H, $H^{17,18,18'}$), 2.18 (s, 3H, H^{32}), 1.80 – 1.59 (m, 2H, H^{20}), 1.09 (t, *J* = 7.4 Hz, 3H, H^{21}), 0.85 (dd, *J* = 7.9, 5.7 Hz, 1H, H^{19}).**^{13}C NMR** (75 MHz, Chloroform-*d*) δ 166.8 (C^2), 161.5, 154.6, 140.4, 139.8, 136.5, 133.9, 133.3 ($C^{9/10}$), 132.3, 131.3, 130.9, 130.5 (C^5), 129.8 (C^4), 129.77, 129.72, 128.5 ($C^{29/30}$) , 125.0, 121.6 ($C^{13/14}$), 120.1, 120.0, 119.3, 109.9 ($C^{9/10}$), 109.8 ($C^{13/14}$), 65.5 (C^{18}), 59.0 (C^{17}), 52.5 (C^1), 24.8 (C^{20}), 21.3 (C^{32}), 10.6 (C^{21}). **^{11}B NMR** (96 MHz, Chloroform-*d*) δ 1.94. **HRMS:** (TOF MS ASAP+) calcd for $C_{34}H_{33}{}^{11}BN_3O_4$ $[M+H]^+$: 558.2570, found 558.2578. **UV-Vis:** λ_{max} (abs) = 578 nm (DCM). **Molar extinction coefficient** (ε) = 42 592 M^{-1} cm^{-1} (DCM). **ϕ_F** = 0.01 (DCM).

7.2.2.24 Methyl (*S*)-4-(10-((1-hydroxybutan-2-yl)amino)-10b-(4-methoxyphenyl)-10b*H*-11-oxa-4b^{1}, 10aλ^{4}-diaza-10bλ^{4}-boracyclopenta[*e*]aceanthrylen-7-yl)benzoate (**3.50a**) and (**3.50b**)

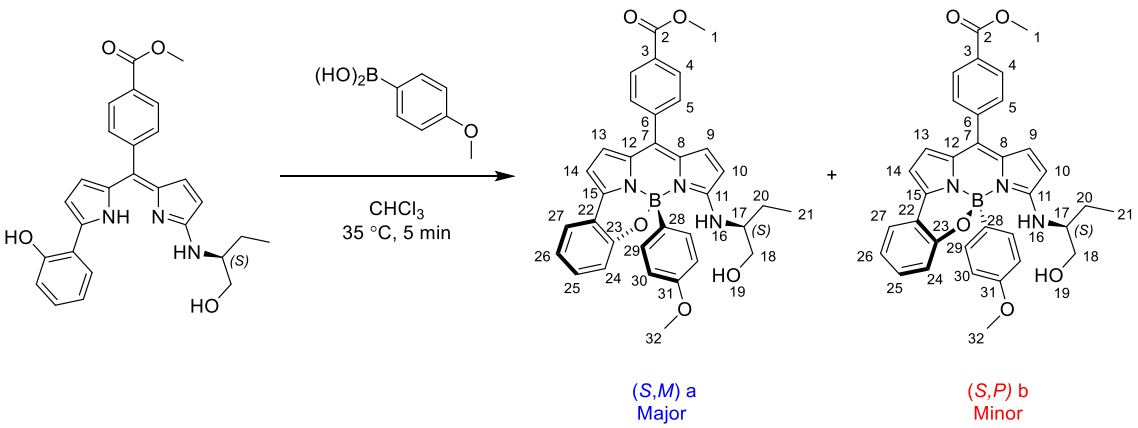

To a round bottom flask, under an atmosphere of nitrogen, was added methyl (*S*,*Z*)-4-((5-((1-hydroxybutan-2-yl)amino)-2*H*-pyrrol-2-ylidene)(5-(2-hydroxyphenyl)-1*H*-pyrrol-2-yl)methyl)benzoate (45.7 mg , 0.10 mmol) and $CHCl_3$ (15 mL). The reaction mixture was equilibrated at 35 °C, stirred for 30 mins, and 4-methoxyphenyl boronic acid (22.8 mg, 0.15 mmol) dissolved in $CHCl_3$ (5 mL), under an atmosphere of nitrogen, was added dropwise to the reaction mixture over 5 mins. The reaction mixture was quenched with water then diluted with DCM (50 mL), washed with water (3 x 50 mL), dried over Na_2SO_4, filtered and the solvent was removed under reduced pressure to give a purple product. The crude product was purified through silica gel column chromatography (DCM : methanol, 100:0.02→ 100:0.2) to give:

Major (*S*,*M*)-(3.50a):

Yield = (29 mg, 0.05 mmol, 51%). **Mp:** 156-158 °C. **R_f:** 0.63 (DCM: ethyl acetate, 4:1). **^{1}H NMR** (300 MHz, Chloroform-*d*) δ 8.15 (d, *J* = 8.5 Hz, 2H, H^{4}), 7.67 (d, *J* = 8.4 Hz, 2H, H^{5}), 7.47 (dd, *J* = 7.7, 1.5 Hz, 1H, Ar), 7.24 – 7.08 (m, 4H, Ar), 6.94 (d, *J* = 4.8 Hz, 1H, $H^{9/10}$), 6.87 (ddd, *J* = 7.7, 7.0, 1.5 Hz, 1H, Ar), 6.69 – 6.61 (m, 3H, Ar, H^{16}), 6.59 (d, *J* = 3.9 Hz, 1H, $H^{13/14}$), 6.56 (d, *J* = 3.9 Hz, 1H, $H^{13/14}$), 6.09 (d, *J* = 4.9 Hz, 1H, $H^{9/10}$), 3.99 (s, 3H, H^{1}), 3.74 (dd, *J* = 25.8, 8.7 Hz, 2H, $H^{18,18'}$), 3.66 (s, 3H, H^{32}), 3.45 – 3.31 (m, 1H, H^{17}), 2.54 (br, 1H, H^{19}), 1.60 (ddd, *J* = 14.2, 7.4, 5.2 Hz, 1H, H^{20}), 1.44 (ddd, *J* = 14.0, 8.1, 7.1 Hz, 1H, $H^{20'}$), 0.66 (t, *J* = 7.4 Hz, 3H, H^{21}). **^{13}C NMR** (75 MHz, Chloroform-*d*) δ 166.8 (C^{2}), 161.1, 158.6, 154.2, 140.0, 139.7, 133.9 ($C^{9/10}$), 133.3, 132.5, 132.0, 130.8, 130.5 (C^{5}), 129.7 (C^{4}), 129.63, 129.59, 125.0 ($C^{29/30}$), 121.2 ($C^{13/14}$), 120.2, 120.1, 119.3, 113.0, 109.72 ($C^{9/10}$), 109.67 ($C^{13/14}$), 65.2 (C^{18}), 58.6 (C^{17}), 55.0 (C^{32}), 52.5 (C^{1}), 25.4 (C^{20}), 10.1 (C^{21}). **^{11}B NMR** (96 MHz, Chloroform-*d*) δ 2.19. **HRMS:** (TOF MS ASAP+) calcd for $C_{34}H_{33}{}^{11}BN_3O_5$ $[M+H]^+$: 574.2520, found 574.2520.

X-Ray code: mjh220064_fa

Minor (*S*,*P*)-(3.50b):

Yield = (15 mg, 0.03 mmol, 26%). **R_f:** 0.73 (DCM: ethyl acetate, 4:1). **^{1}H NMR** (300 MHz, Chloroform-*d*) δ 8.18 (d, *J* = 8.5 Hz, 2H, H^4), 7.72 (d, *J* = 8.4 Hz, 2H, H^5), 7.50 (dd, *J* = 7.7, 1.5 Hz, 1H, Ar), 7.24 – 7.11 (m, 4H, Ar), 7.03 (d, *J* = 4.8 Hz, 1H, $H^{9/10}$), 6.89 (ddd, *J* = 7.6, 7.6, 1.4 Hz, 1H, Ar), 6.70 – 6.63 (m, 2H, Ar), 6.60 (d, *J* = 4.0 Hz, 1H, $H^{13/14}$), 6.58 (d, *J* = 4.0 Hz, 1H, $H^{13/14}$), 6.56 (s, 1H, H^{16}), 6.16 (d, *J* = 4.8 Hz, 1H, $H^{9/10}$), 3.99 (s, 3H, H^1), 3.66 (s, 3H, H^{32}), 3.54 – 3.37 (m, 2H, $H^{17,18}$), 3.37 – 3.26 (m, 1H, $H^{18'}$), 1.79 – 1.60 (m, 2H, $H^{20,20'}$), 1.09 (t, *J* = 7.4 Hz, 3H, H^{21}), 0.88 (t, *J* = 6.6 Hz, 1H, H^{19}). **^{13}C NMR** (75 MHz, Chloroform-*d*) δ 166.8 (C^2), 161.5, 158.8 ($C^{29/30}$), 154.6, 140.3, 139.7, 133.9 ($C^{9/10}$), 133.3, 132.5, 132.3, 130.9, 130.5 (C^5), 129.8, 129.7, 129.6 (C^4), 125.0, 121.6, 120.1 ($C^{13/14}$), 120.0, 119.3, 113.3, 109.9 ($C^{9/10}$), 109.8 ($C^{13/14}$), 65.5 (C^{18}), 58.9 (C^{17}), 55.1 (C^{32}), 52.5 (C^1), 24.8 (C^{20}), 10.6 (C^{21}). **^{11}B NMR** (96 MHz, Chloroform-*d*) δ 1.66. **HRMS:** (TOF MS ASAP+) calcd for $C_{34}H_{33}{}^{11}BN_3O_5$ $[M+H]^+$: 574.2520, found 574.2523.

X-Ray code: mjh220061_fa

7.2.2.25 Methyl (*S*)-4-(10-((1-hydroxybutan-2-yl)amino)-10b-(4-(trifluoromethyl)phenyl)-10b*H*-11-oxa-4b^1, 10aλ^4-diaza-10bλ^4-boracyclopenta[*e*]aceanthrylen-7-yl)benzoate (**3.46a**) and (**3.46b**)

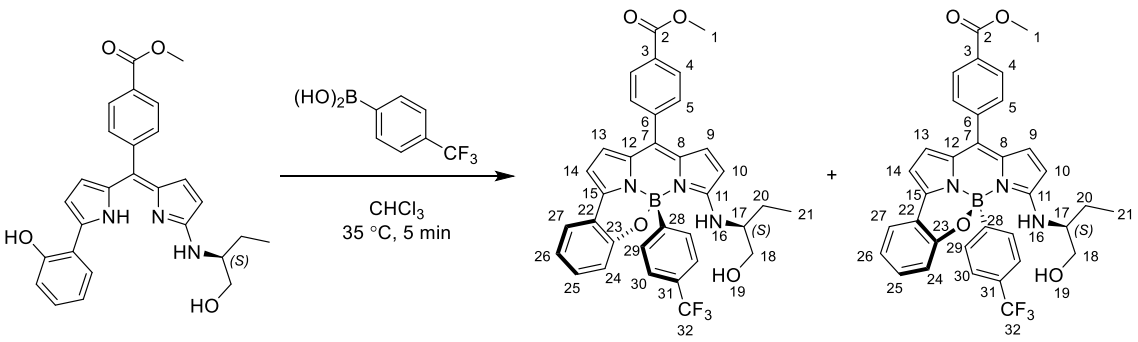

To a round bottom flask, under an atmosphere of nitrogen, was added methyl (*S,Z*)-4-((5-((1-hydroxybutan-2-yl)amino)-2*H*-pyrrol-2-ylidene)(5-(2-hydroxyphenyl)-1*H*-pyrrol-2-yl)methyl)benzoate (45.7 mg , 0.10 mmol) and $CHCl_3$ (15 mL). The reaction mixture was equilibrated at 35 °C, stirred for 30 mins, and (4-(trifluoromethyl)phenyl)boronic acid (28.5 mg, 0.15 mmol) dissolved in $CHCl_3$ (5 mL), under an atmosphere of nitrogen, was added dropwise to the reaction mixture over 5 mins. The reaction mixture was quenched with water then diluted with DCM (50 mL), washed with water (3 x 50 mL), dried over $MgSO_4$, filtered and the solvent was removed under reduced pressure to give a purple product. The crude product was purified through silica gel column chromatography (DCM: Methanol, 100:0.2→ 100:0.2) to give:

Major (*S,M*)-(3.46a):

Yield = (31.9 mg, 0.05 mmol, 52%). **R_f:** 0.63 (DCM: ethyl acetate, 4:1). **^{1}H NMR** (700 MHz, Chloroform-*d*) δ 8.16 (d, *J* = 7.2 Hz, 2H, H^4), 7.67 (d, *J* = 8.0 Hz, 2H, H^5), 7.49 (dd, *J* = 7.6, 1.6 Hz, 1H, Ar), 7.32 – 7.29 (m, 4H, Ar), 7.23 (ddd, *J* = 8.6, 7.2, 1.6 Hz, 1H, Ar), 7.18 (dd, *J* = 8.2, 1.2 Hz, 1H, Ar), 6.97 (d, *J* = 4.6 Hz, 1H, $H^{9/10}$), 6.90 (td, J = 7.4, 1.3 Hz, 1H, Ar), 6.69 (d, *J* = 9.9 Hz, 1H, H^{16}), 6.61 (d, *J* = 3.9 Hz, 1H, $H^{13/14}$), 6.60 (d, *J* = 4.0 Hz, 1H, $H^{13/14}$), 6.11 (d, *J* = 4.9 Hz, 1H, $H^{9/10}$), 3.99 (s, 3H, H^1), 3.84 – 3.78 (m, 1H, H^{18}), 3.73 – 3.67 (m, 1H, $H^{18'}$), 3.42 – 3.35 (m, 1H, $H^{17'}$), 1.62 – 1.54 (m, 1H, H^{20}), 1.46 – 1.39 (m, 1H, $H^{20'}$), 0.59 (t, *J* = 7.5 Hz, 3H, H^{21}). **^{13}C NMR** (176 MHz, Chloroform-*d*) δ 166.8, 161.2, 153.8, 151.7, 139.8, 139.4, 134.3, 133.2, 132.0, 131.5, 131.0, 130.4, 129.8, 129.8, 129.5, 128.6 (q, $^2J_{C\text{-}F}$ = 31.8 Hz, H^{30}), 125.0, 124.7 (q, $^1J_{C\text{-}F}$ = 271.7 Hz, H^{32}), 124.1 (q, $^3J_{C\text{-}F}$ = 3.8 Hz, H^{29}), 121.4, 120.5, 120.1, 119.3, 109.9, 109.8, 65.1, 58.6, 52.5, 25.4, 9.9. **^{11}B NMR** (96 MHz, Chloroform-*d*) δ 1.65. **^{19}F NMR** (282 MHz, Chloroform-*d*) δ -62.5. **HRMS:** (TOF MS ASAP+) calcd for $C_{34}H_{30}{}^{11}BF_3N_3O_4$ $[M+H]^+$: 612.2288, found 612.2288. **UV-Vis:** **λ_{max}** (abs) = 578 nm (DCM). **Molar extinction coefficient** (ε) = 40,285 M^{-1} cm^{-1} (DCM). **ϕ_F** = 0.07 (DCM).

Minor (*S*,*P*)-(3.46b):

Yield = (17.5 mg, 0.03 mmol, 29%). **R_f:** 0.83 (DCM: ethyl acetate, 4:1). **^{1}H NMR** (700 MHz, Chloroform-*d*) δ 8.18 (d, *J* = 8.5 Hz, 2H, H^4), 7.71 (d, *J* = 8.3 Hz, 2H, H^5), 7.51 (dd, *J* = 7.6, 1.7 Hz, 1H, Ar), 7.35 – 7.31 (m, 4H, Ar), 7.26 – 7.23 (m, 1H, Ar), 7.17 (dd, *J* = 8.2, 1.2 Hz, 1H, Ar), 7.03 (d, *J* = 4.8 Hz, 1H, $H^{9/10}$), 6.91 (td, *J* = 7.4, 1.2 Hz, 1H, Ar), 6.78 (d, *J* = 9.4 Hz, 1H, H^{16}), 6.63 (d, *J* = 4.0 Hz, 1H, $H^{13/14}$), 6.62 (d, *J* = 4.0 Hz, 1H, $H^{13/14}$), 6.18 (d, *J* = 4.8 Hz, 1H, $H^{9/10}$), 3.99 (s, 3H, H^1), 3.58 – 3.54 (m, 1H, H^{18}), 3.51 – 3.43 (m, 2H, $H^{17,18'}$), 1.84 – 1.76 (m, 1H, H^{20}), 1.76 – 1.67 (m, 1H, $H^{20'}$), 1.09 (t, *J* = 7.5 Hz, 3H, H^{21}). **^{13}C NMR** (176 MHz, Chloroform-*d*) δ 166.8, 161.3, 154.1, 152.3, 140.1, 139.5, 134.2, 133.2, 132.3, 131.4, 131.0, 130.5, 129.9, 129.8, 129.6, 128.6 (q, $^2J_{c\text{-}F}$ = 31.8 Hz, H^{30}), 125.4, 124.7 (q, $^1J_{c\text{-}F}$ = 271.7 Hz, H^{32}), 124.2 (q, $^3J_{c\text{-}F}$ = 3.7 Hz, H^{29}), 121.7, 120.3, 119.9, 119.4, 110.0, 109.8, 65.1, 58.4, 52.5, 25.0, 10.5. **^{11}B NMR** (96 MHz, Chloroform-*d*) δ 1.47. **^{19}F NMR** (282 MHz, Chloroform-*d*) δ -62.3. **HRMS:** (TOF MS ASAP+) calcd for $C_{34}H_{30}{}^{11}BF_3N_3O_4$ $[M+H]^+$: 612.2288, found 612.2294. **UV-Vis:** λ_{max} (abs) = 578 nm (DCM). **Molar extinction coefficient** (ε) = 42,591 M^{-1} cm^{-1} (DCM). **ϕ_F** = 0.06 (DCM).

7.2.2.26 Methyl (*S*)-4-(10-((1-hydroxybutan-2-yl)amino)-10b-(4-nitrophenyl)-10b*H*-11-oxa-4b^{1}, 10aλ^{4}-diaza-10bλ^{4}-boracyclopenta[*e*]aceanthrylen-7-yl)benzoate (**3.47a**) and (**3.47b**)

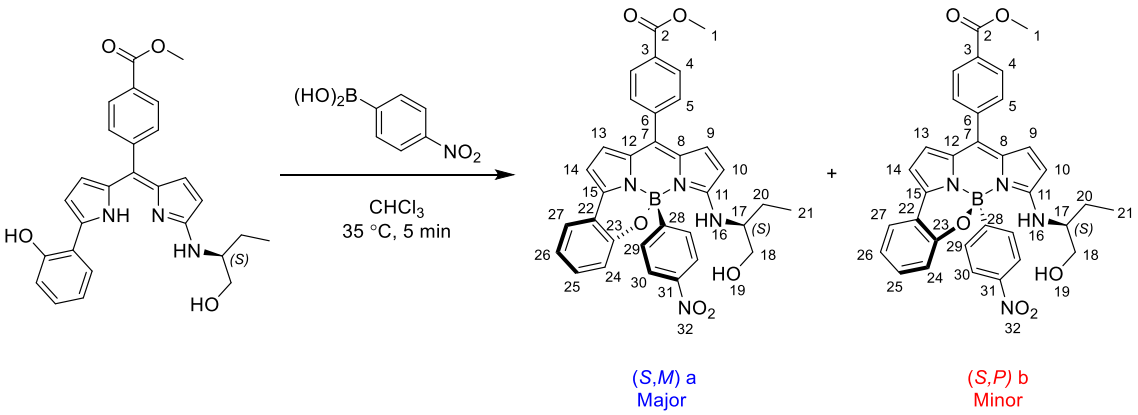

To a round bottom flask, under an atmosphere of nitrogen, was added methyl (*S,Z*)-4-((5-((1-hydroxybutan-2-yl)amino)-2*H*-pyrrol-2-ylidene)(5-(2-hydroxyphenyl)-1*H*-pyrrol-2-yl)methyl)benzoate (45.7 mg , 0.10 mmol) and $CHCl_3$ (15 mL). The reaction mixture was equilibrated at 35 °C, stirred for 30 mins, and (4-nitrophenyl)boronic acid (25 mg, 0.15 mmol) dissolved in $CHCl_3$ (5 mL), under an atmosphere of nitrogen, was added dropwise to the reaction mixture over 5 mins. The reaction mixture was quenched with water then diluted with DCM (50 mL), washed with water (3 x 50 mL), dried over $MgSO_4$, filtered and the solvent was removed under reduced pressure to give a purple product. The crude product was purified through silica gel column chromatography (DCM: Methanol, 100:0.2→ 100:0.2) to give:

Major (*S,M*)-(3.47a):

Yield = (31.9 mg, 0.05 mmol, 54%). **R_f:** 0.63 (DCM: ethyl acetate, 4:1). **Mp:** 211 °C (decomposed). **^{1}H NMR** (300 MHz, Chloroform-*d*) δ 8.17 (d, *J* = 8.4 Hz, 2H, H^{4}), 7.88 (d, *J* = 8.6 Hz, 2H, $H^{29/30}$), 7.66 (d, *J* = 8.2 Hz, 2H, H^{5}) 7.47 (dd, *J* = 7.7, 1.4 Hz, 1H, Ar), 7.32 (d, *J* = 8.6 Hz, 2H, $H^{29/30}$), 7.24 – 7.14 (m, 1H, Ar), 7.00 (d, *J* = 4.8 Hz, 1H, $H^{9/10}$), 6.93 – 6.86 (m, 1H, Ar), 6.79 (d, *J* = 9.7 Hz, 1H, H^{16}), 6.62 – 6.59 (m*, *J* = 4.0, 4.0 Hz, 2H, $H^{13,14}$), 6.15 (d, *J* = 4.9 Hz, 1H, $H^{9/10}$), 3.99 (s, 3H, H^{1}), 3.90 – 3.79 (m, 1H, H^{18}), 3.74 (dd, *J* = 11.1, 5.4 Hz, 1H, $H^{18'}$), 3.51 – 3.35 (m, 1H, H^{17}), 2.46 (br, 1H, H^{19}), 1.63 (ddd, *J* = 14.2, 7.4, 5.4 Hz, 1H, H^{20}), 1.53 – 1.38 (m, 1H, $H^{20'}$), 0.66 (t, *J* = 7.4 Hz, 3H, H^{21}). **^{1}H NMR** (700 MHz, Chloroform-*d*) δ 8.16 (d, *J* = 7.2 Hz, 2H, H^{4}), 7.88 (dd, *J* = 8.7, 1.7 Hz, 2 H, $H^{29/30}$), 7.66 (d, *J* = 6.3 Hz, 2H, H^{5}), 7.48 (d, *J* = 7.5 Hz, 1H, Ar), 7.32 (dd, *J* = 8.8, 1.3 Hz, 2H, $H^{29/30}$), 7.23 (ddd, *J* = 8.6, 7.1, 1.5 Hz, 1H, Ar), 7.17 (dd, *J* = 8.2, 1.2 Hz, , 1H, Ar), 6.99 (dd, *J* = 4.9, 2.1 Hz, 1H, $H^{9/10}$), 6.90 (tt, *J* = 7.3, 1.2 Hz, 1H, Ar), 6.78 (d, *J* = 9.9 Hz, 1H, H^{16}), 6.60 (d, *J* = 1.5 Hz, 2H, $H^{13,14}$), 6.15 (dd, *J* = 5.0, 2.1 Hz, 1H, $H^{9/10}$), 3.99 (s, 3H, H^{1}), 3.86 – 3.80 (m,

1H, H^{18}), 3.78 – 3.69 (m, 1H, $H^{18'}$), 3.47 – 3.37 (m, 1H, H^{17}), 2.54 (d, *J* = 34.7 Hz, 1H, H^{19}), 1.62 (dddd, *J* = 15.0, 7.8, 5.3, 2.5 Hz, 1H, H^{20}), 1.51 – 1.40 (m, 1H, $H^{20'}$), 0.66 (td, *J* = 7.4, 2.7 Hz, 3H, H^{21}). **^{13}C NMR** (176 MHz, Chloroform-*d*) δ 166.7 (C^{2}), 161.2, 156.4, 153.5, 147.0, 139.8, 139.3, 134.4 ($C^{9/10}$), 133.1, 132.1, 132.0, 131.0, 130.4 (C^{5}), 129.9, 129.8 (C^{4}), 129.4, 125.0, 122.3 ($C^{29/30}$), 121.6 ($C^{13/14}$), 120.6, 119.9, 119.3, 110.0 ($C^{13/14}$), 109.9 ($C^{9/10}$), 64.9 (C^{18}), 58.4 (C^{17}), 52.5 (C^{1}), 25.4 (C^{20}), 10.2 (C^{21}). **^{11}B NMR** (96 MHz, Chloroform-*d*) δ 1.26. **HRMS:** (TOF MS ASAP+) calcd for $C_{33}H_{30}{}^{11}BN_4O_6$ $[M+H]^+$: 589.2264, found 589.2262.

X-Ray code: mjh220078_fa

Minor (*S*,*P*)-(3.47b):

Yield = (17.8 mg, 0.03 mmol, 30%). **R_f:** 0.78 (DCM: ethyl acetate, 4:1). **^{1}H NMR** (300 MHz, Chloroform-*d*) δ 8.18 (d, *J* = 8.5 Hz, 2H, H^{4}), 7.92 (d, *J* = 8.7 Hz, 2H, $H^{29/30}$), 7.70 (d, *J* = 8.1 Hz, 2H, H^{5}) 7.51 (dd, *J* = 7.6, 1.6 Hz, 1H, Ar), 7.36 (d, *J* = 8.7 Hz, 2H, $H^{29/30}$), 7.24 (ddd, *J* = 8.2, 7.3, 1.7 Hz, 1H, Ar), 7.17 (dd, *J* = 8.2, 1.2 Hz, 1H, Ar), 7.04 (d, *J* = 4.4 Hz, 1H, $H^{9/10}$), 6.93 – 6.88 (m, 2H, Ar), 6.65 – 6.63 (m*, *J* = 4.0, 4.0 Hz, 2H, $H^{13,14}$), 6.19 (d, *J* = 4.8 Hz, 1H, $H^{9/10}$), 3.99 (s, 3H, H^{1}), 3.63 – 3.54 (m, 2H, $H^{18,18'}$) , 3.51 – 3.45 (m, 1H, H^{17}), 1.89 – 1.80 (m, 1H, H^{20}), 1.79 – 1.70 (m, 1H, $H^{20'}$), 1.34 (br, 1H, H^{19}), 1.09 (t, *J* = 7.5 Hz, 3H, H^{21}). **^{13}C NMR** (176 MHz, Chloroform-*d*) δ 166.7 (C^{2}), 161.2, 156.6, 153.8, 147.1, 140.1, 139.3, 134.4 ($C^{9/10}$), 133.0, 132.3, 131.9, 131.1, 130.4 (C^{5}), 130.0, 129.8 (C^{4}), 129.5, 125.0, 122.4 ($C^{29/30}$), 121.8 ($C^{13/14}$), 120.5, 119.8, 119.4, 110.0 ($C^{13/14}$), 109.8 ($C^{9/10}$), 64.9 (C^{18}), 58.2 (C^{17}), 52.6 (C^{1}), 25.1 (C^{20}), 10.5 (C^{21}). **^{11}B NMR** (96 MHz, Chloroform-*d*) δ 1.43. **HRMS:** (TOF MS ASAP+) calcd for $C_{33}H_{30}{}^{11}BN_4O_6$ $[M+H]^+$: 589.2264, found 589.2267.

*Two doublet signals overlapping corresponding to pyrrolic protons H^{13} and H^{14}.

7.2.2.27 Methyl (*S*)-4-(10b-(2,4-difluorophenyl)-10-((1-hydroxybutan-2-yl)amino)-10b*H*-11-oxa-4b^{1}, 10aλ^{4}-diaza-10bλ^{4}-boracyclopenta[*e*]aceanthrylen-7-yl)benzoate (**3.48a**) and (**3.48b**)

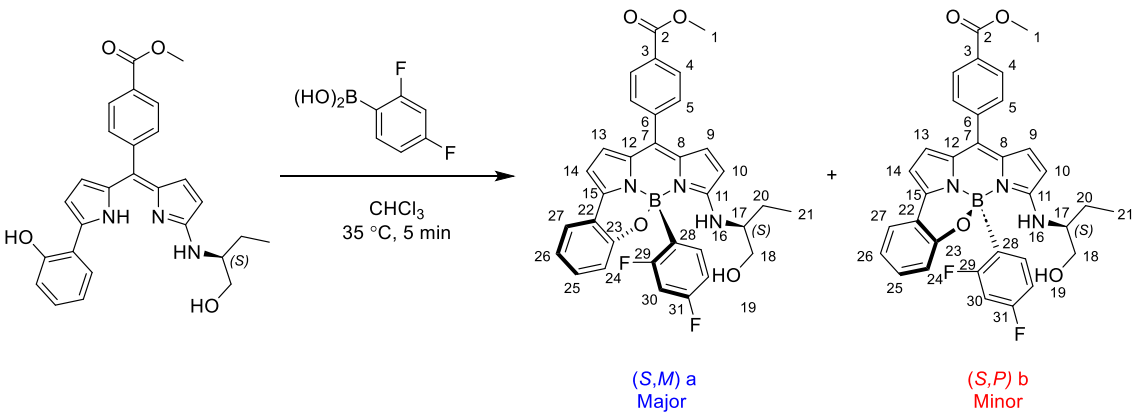

To a round bottom flask, under an atmosphere of nitrogen, was added methyl (*S,Z*)-4-((5-((1-hydroxybutan-2-yl)amino)-2*H*-pyrrol-2-ylidene)(5-(2-hydroxyphenyl)-1*H*-pyrrol-2-yl)methyl)benzoate (40.6 mg , 0.09 mmol) and $CHCl_3$ (15 mL). The reaction mixture was equilibrated at 35 °C, stirred for 30 mins, and (2,4-difluorophenyl)boronic acid (20.8 mg, 0.13 mmol) dissolved in $CHCl_3$ (5 mL), under an atmosphere of nitrogen, was added dropwise to the reaction mixture over 5 mins. The reaction mixture was quenched with water then diluted with DCM (50 mL), washed with water (3 x 50 mL), dried over $MgSO_4$, filtered and the solvent was removed under reduced pressure to give a purple product. The crude product was purified through silica gel column chromatography (DCM: Methanol, 100:0.1→ 100:0.2) to give:

Major (*S,M*)-(3.48a):

Yield = (16 mg, 0.03 mmol, 31%). **R_f:** 0.12 (DCM). **^{1}H NMR** (300 MHz, Chloroform-*d*) δ 8.06 (d, *J* = 8.0 Hz, 2H, H^{4}), 7.57 (d, *J* = 8.2 Hz, 2H, H^{5}), 7.39 (dd, *J* = 7.6, 1.5 Hz, 1H, Ar), 7.18 – 7.01 (m, 2H, Ar), 6.92 (q, *J* = 7.7 Hz, 1H, Ar), 6.83 (d, *J* = 4.8 Hz, 1H, $H^{9/10}$), 6.81 – 6.72 (m, 2H, Ar), 6.52 (d, *J* = 3.9 Hz, 1H, $H^{13/14}$), 6.50 (d, *J* = 3.8 Hz, 1H, $H^{13/14}$), 6.41 (td, *J* = 9.7, 2.4 Hz, 1H, Ar), 6.02 (d, *J* = 4.9 Hz, 1H, $H^{9/10}$), 3.90 (s, 3H, H^{1}), 3.80 – 3.70 (m, 1H, H^{18}), 3.68 – 3.62 (m, 1H, $H^{18'}$), 3.39 – 3.33 (m, 1H, H^{17}), 2.52 (br, 1H, H^{19}), 1.65 – 1.32 (m, 2H, $H^{20,20'}$), 0.65 (t, *J* = 7.3 Hz, 3H, H^{21}).**^{13}C NMR** (75 MHz, Chloroform-*d*) δ 166.8, 161.2, 153.5, 139.8, 139.6, 135.4, 135.3, 135.1, 134.4, 133.4, 132.0, 130.8, 130.4, 130.1, 129.7, 129.6, 124.7, 120.7, 120.5, 120.4, 119.4, 110.4, 110.2, 109.7, 109.5, 103.4, 103.0, 102.9, 102.6, 65.2, 58.9, 52.5, 25.2, 10.2. **^{11}B NMR** (96 MHz, Chloroform-*d*) δ 1.02. **^{19}F NMR** (282 MHz, Chloroform-*d*) δ -102.6 (d, *J* = 8.4 Hz), -113.6 (d, *J* = 7.7 Hz). **HRMS:** (TOF MS ASAP+) calcd for $C_{33}H_{29}{}^{11}BF_2N_3O_4$ $[M+H]^+$: 580.2225, found 580.2227.

X-Ray code: mjh220067_fa

Minor (*S*,*P*)-(3.48b):

Yield = (9.02 mg, 0.02 mmol, 18%). **R_f:** 0.12 (DCM). **^{1}H NMR** (300 MHz, Chloroform-*d*) δ 8.16 (d, *J* = 8.2 Hz, 2H, H^4), 7.67 (d, *J* = 8.2 Hz, 2H, H^5), 7.49 (d, *J* = 7.6 Hz, 1H, Ar), 7.19 (d, *J* = 7.5 Hz, 1H, Ar), 7.11 (d, *J* = 7.8 Hz, 1H, Ar), 6.96 (d, *J* = 4.7 Hz, 1H, $H^{9/10}$), 6.93 – 6.84 (m, 3H, Ar), 6.65 – 6.45 (m, 4H, $H^{13,14}$, Ar), 6.20 – 6.13 (br, 1H, $H^{9/10}$), 3.98 (s, 3H, H^1), 3.76 – 3.45 (m, 3H, $H^{17,18,18'}$), 1.90 – 1.63 (m, 2H, $H^{20,20'}$), 1.50 (br, 1H, H^{19}), 1.10 (t, *J* = 7.4 Hz, 3H, H^{21}). **^{13}C NMR** (75 MHz, Chloroform-*d*) δ 166.8, 161.2, 153.6, 139.6, 135.3, 135.0, 134.4, 130.8, 130.4, 129.7, 129.6, 124.7, 120.8, 120.3, 120.1, 119.4, 110.4, 109.5, 103.4, 103.1, 77.6, 77.2, 76.7, 65.2, 58.7, 52.5, 25.0, 10.4. **^{11}B NMR** (96 MHz, Chloroform-*d*) δ 0.99. **^{19}F NMR** (282 MHz, Chloroform-*d*) δ -103.0(d, *J* = 8.2 Hz), -113.1 (d, *J* = 7.9 Hz). **HRMS:** (TOF MS ASAP+) calcd for $C_{33}H_{29}{}^{11}BF_2N_3O_4$ $[M+H]^+$: 580.2225, found 580.2226.

X-Ray code: mjh220070_fa

7.2.2.28 XPhos G3 Precatalyst (**3.24**)

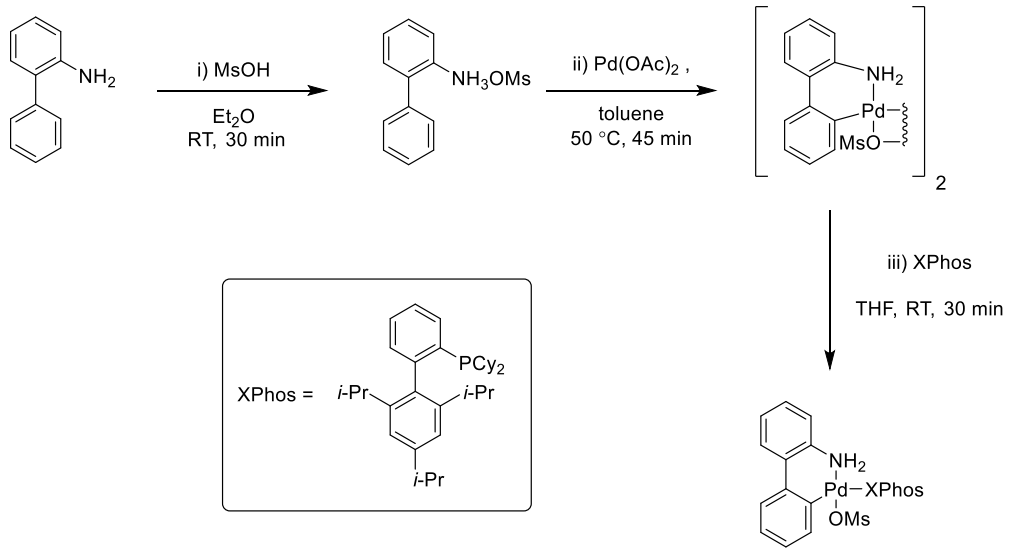

To a round bottom flask, was added 2-aminobiphenyl (5 g, 29.5 mmol) and diethyl ether (100 mL). Methanesulfonic acid (1.92 mL, 29.5 mmol) dissolved in diethyl ether (15 mL) was added slowly to the reaction mixture. The reaction mixture was stirred at room temperature for 30 min then the precipitate was filtered and washed with diethyl ether (3 x 15 mL). The precipitate was dried under vacuum overnight to give [1,1'-biphenyl]-2-yl- λ^5-azaneyl methanesulfonate (7.30 g, 27.5 mmol, 93%) as a white solid, without the need for further purification.

^{1}H NMR (300 MHz, Methanol-*d*$_4$) δ 7.60 – 7.42 (m, 9H), 4.91 (br, 2H), 2.67 (s, 3H). **^{13}C NMR** (75 MHz, Methanol-*d*$_4$) δ 137.1, 136.3, 131.6, 129.4, 129.2, 128.9, 128.8, 128.5, 127.7, 123.6, 38.1.

To a round bottom flask, under a nitrogen atmosphere, was added [1,1'-biphenyl]-2-yl- λ^5-azaneyl methanesulfonate (1.06 g, 4 mmol), palladium acetate (0.898, 4 mmol) and dry toluene (20 mL). The reaction mixture was heated to 50 °C, stirred for 45 min and cooled to room temperature. The suspension was filtered, and the precipitate was washed with toluene (25 mL) and diethyl ether (3 x 25 mL) and then dried under vacuum overnight to afford the organopalladium intermediate as a creamy to tan solid.

To a 50 mL round bottom flask was added the organopalladium intermediate (370 mg, 0.50 mmol), XPhos (476 mg, 1 mmol) and THF (10 mL). The reaction mixture was stirred at room temperature for 30 mins. About 90% of the solvent was removed under reduced pressure and then the product was triturated from pentane (x3) to afford XPhos Pd G3 (341 mg, 0.40 mmol, 81%) as beige/brown solid.

^{31}P NMR (121 MHz, Methanol-*d*$_4$) δ 36.53.

Observed data (^{1}H, ^{13}C) are consistent with that previously reported by Buchwald *et al*.[77]

7.2.3 Chapter 4

7.2.3.1 Methyl (*S*)-4-(5,5-difluoro-3-((1-hydroxybutan-2-yl)amino)-7-(4-methoxyphenyl)-5*H*-4λ⁴,5λ⁴-dipyrrolo[1,2-*c*:2',1'-*f*][1,3,2]diazaborinin-10-yl)benzoate (**4.8**)

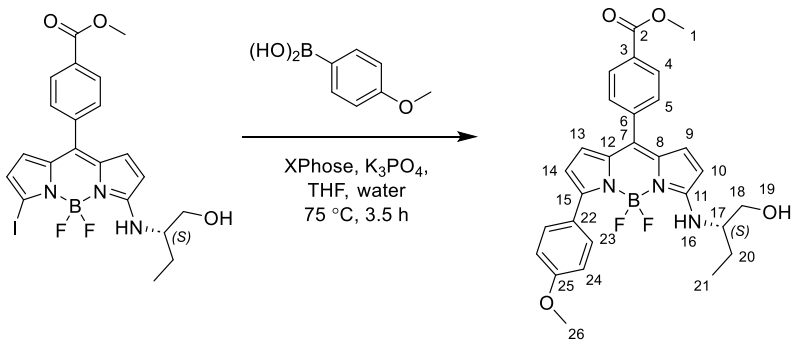

To a Schlenk flask, under nitrogen atmosphere, was added methyl (*S*)-4-(5,5-difluoro-3-((1-hydroxybutan-2-yl)amino)-7-iodo-5*H*-4λ⁴,5λ⁴-dipyrrolo[1,2-*c*:2',1'-*f*][1,3,2]diazaborinin-10-yl)benzoate (431 mg, 0.80 mmol), (4-methoxyphenyl)boronic acid (243 mg, 1.60 mmol), XPhos Pd G3 (40.6 mg, 6 mol %, 0.048 mmol), $K_3PO_4.H_2O$ (368 mg, 1.60 mmol), dry THF (23 mL) and water (4 mL) and was degassed (x3). The reaction mixture was heated to 75 °C, stirred for 3.5 hours then diluted with DCM (100 mL) and washed with water (3 x 100 mL). The organic layer was dried over $MgSO_4$, filtered, and the solvent was removed under reduced pressure. The crude product was purified through silica gel column chromatography (DCM : ethyl acetate, 6:1) to give methyl (*S*)-4-(5,5-difluoro-3-((1-hydroxybutan-2-yl)amino)-7-(4-methoxyphenyl)-5*H*-4λ⁴,5λ⁴-dipyrrolo[1,2-*c*:2',1'-*f*][1,3,2]diazaborinin-10-yl)benzoate (266 mg, 0.51 mmol, 64 %) as a red solid.

R_f: 0.4 (DCM: ethyl acetate 6:1). **Mp:** 110-112 °C. **^{1}H NMR** (300 MHz, Chloroform-*d*) δ 8.13 (d, *J* = 8.2 Hz, 2H, H^4), 7.76 (d, *J* = 8.8 Hz, 2H, $H^{23/24}$), 7.57 (d, *J* = 8.2 Hz, 2H, H^5), 6.97 (d, *J* = 8.8 Hz, 2H, $H^{23/24}$), 6.81 (d, *J* = 5.0 Hz, 1H, $H^{9/10}$), 6.40 (d, *J* = 3.9 Hz, 1H, $H^{13/14}$), 6.37 (d, *J* = 3.9 Hz, 1H, $H^{13/14}$), 6.20 (d, *J* = 5.0 Hz, 1H, $H^{9/10}$), 6.17 (br, 1H, H^{14}), 3.97 (s, 3H, H^1), 3.85 (s, 3H, H^{26}), 3.75 (dd, *J* = 11.0, 4.7 Hz, 1H, H^{18}), 3.60 (dd, *J* = 11.0, 3.8 Hz, 1H, $H^{18'}$), 3.56 – 3.43 (m, 1H, H^{17}), 1.80 – 1.62 (m, 1H, H^{20}), 1.61 – 1.47 (m, 1H, $H^{20'}$), 0.99 (t, *J* = 7.4 Hz, 3H, H^{21}). **^{13}C NMR** (75 MHz, Chloroform-*d*) δ 166.8 (C^2), 161.9, 159.6, 148.4, 139.5, 134.5, 133.8, 132.5, 131.3, 130.8, 130.6, 130.4, 129.5, 127.0, 121.7, 115.6, 113.6, 111.0, 65.2 (C^{18}), 59.3 (C^{17}), 55.3 (C^{26}), 52.5 (C^1), 25.0 (C^{20}), 10.6 (C^{21}). **^{11}B NMR** (96 MHz, Chloroform-*d*) δ 1.53 (t, *J* = 35.8 Hz). **^{19}F NMR** (282 MHz, Chloroform-*d*) δ -140.11 – -141.44 (m), -141.77 – -143.15 (m). **HRMS:** (TOF MS ASAP+) calcd for $C_{28}H_{29}{}^{11}BF_2N_3O_4$ $[M+H]^+$: 520.2224, found 520.2227.

X-Ray code: mjh220041_fa

7.2.3.2 Methyl (*S*,*Z*)-4-((5-((1-hydroxybutan-2-yl)amino)-2*H*-pyrrol-2-ylidene)(5-(4-methoxyphenyl)-1*H*-pyrrol-2-yl)methyl)benzoate (**4.1**)

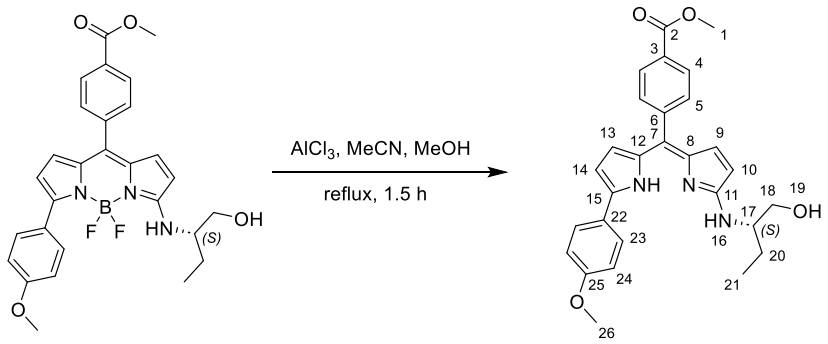

To a round bottom flask, was added methyl (*S*)-4-(5,5-difluoro-3-((1-hydroxybutan-2-yl)amino)-7-(4-methoxyphenyl)-5*H*-4λ^4,5λ^4-dipyrrolo[1,2-*c*:2',1'-*f*][1,3,2]diazaborinin-10-yl)benzoate (253 mg, 0.49 mmol), MeCN (60 mL), and $AlCl_3$ (325 mg, 2.44 mmol) dissolved in MeOH (10 mL). The reaction mixture was heated to reflux, stirred for 1.5 hours then diluted with DCM (100 mL). The organic layer was washed with H_2O (3 x 100 mL), dried over $MgSO_4$, filtered and the solvent was removed under reduced pressure to give dark brown solid. The crude product was purified through silica gel column chromatography (DCM : methanol 100:2) to give methyl (*S*,*Z*)-4-((5-((1-hydroxybutan-2-yl)amino)-2*H*-pyrrol-2-ylidene)(5-(4-methoxyphenyl)-1*H*-pyrrol-2-yl)methyl)benzoate (161 mg, 0.34 mmol, 70%).

R_f: 0.13 (DCM: methanol 5:0.1). **Mp:** 97-99 °C. **^{1}H NMR** (300 MHz, Methanol-d_4) δ 8.06 (d, *J* = 8.2 Hz, 2H, H^4), 7.57 (d, *J* = 8.8 Hz, 2H, $H^{23/24}$), 7.52 (d, *J* = 8.3 Hz, 2H, H^5), 6.96 (d, *J* = 8.8 Hz, 2H, $H^{23/24}$), 6.63 (d, *J* = 4.7 Hz, 1H, $H^{9/10}$), 6.40 (d, *J* = 3.8 Hz, 1H, $H^{13/14}$), 6.29 (d, *J* = 4.7 Hz, 1H, $H^{9/10}$), 5.95 (d, *J* = 3.8 Hz, 1H, $H^{13/14}$), 4.15 – 4.02 (m, 1H, H^{17}), 3.94 (s, 3H, H^1), 3.82 (s, 3H, H^{26}), 3.81 – 3.77 (m, 2H, $H^{18.18'}$), 1.92 (ddd, *J* = 13.6, 7.7, 5.9 Hz, 1H, H^{20}), 1.8 – 1.6 (m, 1H,$H^{20'}$), 1.08 (t, *J* = 7.4 Hz, 3H, H^{21}). **^{13}C NMR** (75 MHz, Methanol-d_4) δ 169.0, 168.4, 160.2, 149.2, 144.8, 137.4, 136.9, 134.6, 132.3, 130.6, 129.9, 126.6, 126.2, 125.7, 120.9, 116.9, 115.5, 107.3, 64.7, 57.8, 55.8, 52.7, 25.4, 11.1. **HRMS:** (pNSI) calcd for $C_{28}H_{27}N_3O_4$ $[M+H]^+$: 472.2231, found 472.2229.

7.2.3.3 Methyl (*S*)-4-(3-ethyl-10b-(4-fluorophenyl)-10-(4-methoxyphenyl)-2,3,4,10b-tetrahydro-1-oxa-4, 4a^{1}λ^4,10a-triaza-10bλ^4-boracyclohepta[*cd*]-*s*-indacen-7-yl)benzoate (**4.2a**) and (**4.2b**)

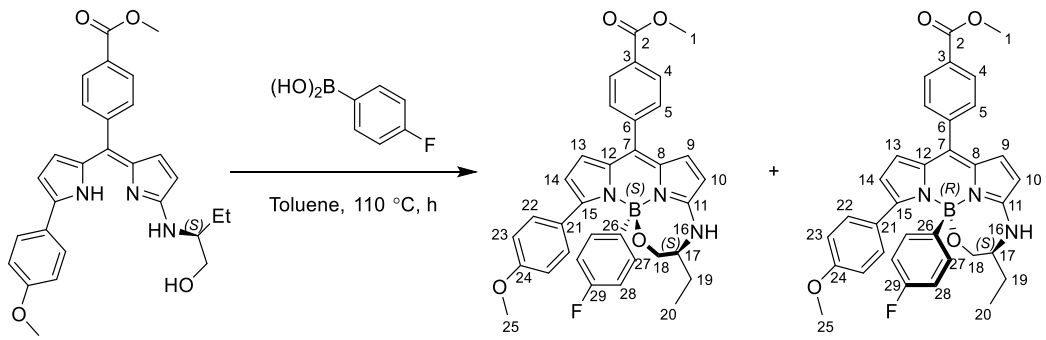

To a round bottom flask, under an atmosphere of nitrogen, was added methyl (*S,Z*)-4-((5-((1-hydroxybutan-2-yl)amino)-2*H*-pyrrol-2-ylidene)(5-(4-methoxyphenyl)-1*H*-pyrrol-2-yl)methyl)benzoate (47.2 mg, 0.10 mmol), (4-fluorophenyl)boronic acid (20.9 mg, 0.15 mmol), and toluene (10 mL). The reaction mixture was heated to reflux, stirred for 30 hours then diluted with DCM (50 mL). The crude mixture was washed with water (3 x 50 mL). The organic layer was dried over $MgSO_4$, filtered and removed solvent under reduced pressure to give a pink/red product. The crude product was purified through silica gel column chromatography (DCM : ethyl acetate 100:1) to give :

Major (*S,P*)-(4.2a):

Yield = (21.9 mg, 0.04 mmol, 38%). **R_f:** 0.67 (DCM : methanol, 100:1). **^{1}H NMR** (700 MHz, Chloroform-*d*) δ 8.11 (d, *J* = 8.5 Hz, 2H,H^4), 7.70 (d, *J* = 8.9 Hz, 2H, H$^{22/23}$), 7.55 (d, *J* = 8.4 Hz, 2H, H^5), 6.93 (d, *J* = 8.9 Hz, 2H, H$^{22/23}$), 6.84 (d, *J* = 4.7 Hz, 1H, H$^{9/10}$), 6.66 (dd, *J* = 9.5, 8.7 Hz, 2H, Ar), 6.47 (dd, *J* = 8.6, 6.3 Hz, 2H, Ar), 6.39 (d, *J* = 3.9 Hz, 1H, H$^{13/14}$), 6.24 (d, *J* = 3.9 Hz, 1H, H$^{13/14}$), 6.15 (d, *J* = 4.7 Hz, 1H, H$^{9/10}$), 4.98 (br, 1H, H^{16}), 3.96 (s, 3H, H^1), 3.90 (s, 3H, H^{25}), 3.74 (dd, *J* = 12.1, 1.8 Hz, 1H, H^{18}), 3.54 – 3.48 (m, 1H, H^{17}), 3.30 (dd, *J* = 12.1, 9.0 Hz, 1H, H$^{18'}$), 1.58 – 1.52 (m, 1H, H^{19}), 1.49 – 1.42 (m, 1H, H$^{19'}$), 1.00 (t, *J* = 7.5 Hz, 3H, H^{20}). **^{13}C NMR** (176 MHz, Chloroform-*d*) δ 166.9 (C^2), 161.9 (d, *J* = 242.6 Hz, C^{29}), 161.7, 159.3, 151.0, 143.8, 140.2, 134.4, 134.3, 133.5, 133.2 (d, *J* = 6.7 Hz, C^{27}), 132.5, 132.0, 130.6, 129.3, 128.3, 122.3, 117.5, 114.0, 113.8 (d, *J* = 19.0 Hz, C^{28}), 112.2, 65.4, 62.6, 55.4, 52.4, 25.3, 10.6.**^{11}B NMR** (96 MHz, Chloroform-*d*) δ 4.06. **^{19}F NMR** (282 MHz, Chloroform-*d*) δ -117.8. **HRMS:** (TOF MS ASAP+) calcd for $C_{34}H_{32}{}^{11}BFN_3O_4$ $[M+H]^+$: 576.2476, found 576.2482.

Note: one carbon signal was not identified in the analysis of the ^{13}C NMR spectrum. We believe it is located around 130 ppm, as it appears to be a broad signal.

Minor (*S*,*M*)-(4.2b)

Yield = (21.8 mg, 0.04 mmol, 38%). **R_f:** 0.62 (DCM : methanol, 100:1). **^{1}H NMR** (700 MHz, Chloroform-*d*) δ 8.10 (d, *J* = 8.5 Hz, 2H,H^4), 7.60 (d, *J* = 8.9 Hz, 2H, $H^{22/23}$), 7.55 (d, *J* = 8.4 Hz, 2H, H^5), 6.86 (d, *J* = 8.9 Hz, 2H, $H^{22/23}$), 6.80 (d, *J* = 4.7 Hz, 1H, $H^{9/10}$), 6.70 (dd, *J* = 9.5, 8.7 Hz, 2H, Ar), 6.64 (dd, *J* = 8.7, 6.5 Hz, 2H, Ar), 6.39 (d, *J* = 3.9 Hz, 1H, $H^{13/14}$), 6.25 (d, *J* = 3.9 Hz, 1H, $H^{13/14}$), 6.06 (d, *J* = 4.7 Hz, 1H, $H^{9/10}$), 5.30 (d, *J* = 3.6 Hz, 1H, H^{16}), 3.96 (s, 3H, H^1), 3.93 (dd, *J* = 12.3, 5.9 Hz, 1H, H^{18}), 3.87 (s, 3H, H^{25}), 3.61 (dd, *J* = 12.4, 2.1 Hz, 1H, H^{18}), 3.48 – 3.44 (m, 1H, H^{17}), 1.82 – 1.75 (m, 1H, H^{19}), 1.73 – 1.67 (m, 1H, $H^{19'}$), 0.98 (t, *J* = 7.5 Hz, 3H, H^{20}). **^{13}C NMR** (176 MHz, Chloroform-*d*) δ 166.9 (C^2), 161.9 (d, *J* = 242.4 Hz, C^{29}), 160.5, 159.2, 150.3, 145.7 140.3, 134.6, 133.7, 133.4, 132.7, 132.5(d, *J* = 6.8 Hz, C^{27}), 132.1, 130.6, 130.5, 129.4, 128.3, 121.4, 115.6, 114.2, 113.8 (d, *J* = 19.1 Hz, C^{28}), 112.3, 64.2, 61.6, 55.4, 52.4, 25.6, 10.7.**^{11}B NMR** (96 MHz, Chloroform-*d*) δ 4.11. **^{19}F NMR** (282 MHz, Chloroform-*d*) δ -117.9. **HRMS:** (TOF MS ASAP+) calcd for $C_{34}H_{32}{}^{11}BFN_3O_4$ $[M+H]^+$: 576.2476, found 576.2477.

7.2.3.4 Methyl 2-((4-chlorophenyl)(hydroxy)methyl)acrylate (**4.27**)

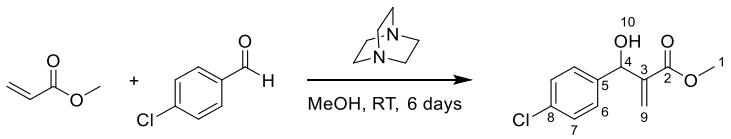

To a 25 mL round bottom flask, under an atmosphere of nitrogen, was added 4-chlorobenzaldehyde (0.70 g, 5 mmol), methyl acrylate (4.5 mL, 50 mmol), 1,4-diazabicyclo[2.2.2]octane (DABCO) (0.56 g, 5 mmol) and methanol (15 mL). The reaction mixture was stirred at room temperature for 6 days then diluted with ethyl acetate (50 mL) and washed with water (3 x 50 mL). The organic layer was dried over $MgSO_4$, filtered and removed solvent under reduced pressure. The crude product was purified through silica gel column chromatography (petrol : ethyl acetate, 7:3) to give methyl 2-((4-chlorophenyl)(hydroxy)methyl)acrylate (0.74 g, 3.26 mmol, 66%) as a colourless oil.

R_f: 0.5 (petrol : ethyl acetate, 7:3). **^{1}H NMR** (300 MHz, Chloroform-*d*) δ 7.31 (s, 4H, $H^{6,7}$), 6.34 (t, *J* = 0.8 Hz, 1H, H^9), 5.83 (t, *J* = 1.1 Hz, 1H, $H^{9'}$), 5.52 (ddd, *J* = 5.7, 1.3, 0.7 Hz, 1H, H^4), 3.72 (s, 3H, H^1), 3.12 (d, *J* = 5.7 Hz, 1H, H^{10}). **^{13}C NMR** (75 MHz, Chloroform-*d*) δ 166.6 (C^2), 141.7 (C^5), 139.8 (C^8), 133.6 (C^3), 128.6 ($C^{6/7}$), 128.0 ($C^{6/7}$), 126.4 (C^9), 72.6 (C^4), 52.1(C^1). **HRMS:** (pNSI) calcd for $C_{11}H_{11}ClO_3Na$ $[M+Na]^+$: 249.0289, found 249.0294.

Observed data (^{1}H, ^{13}C) are consistent with those previously reported by Amarante *et al*.[90]

7.2.3.5 Methyl 2-((4-fluorophenyl)(hydroxy)methyl)acrylate (**4.28**)

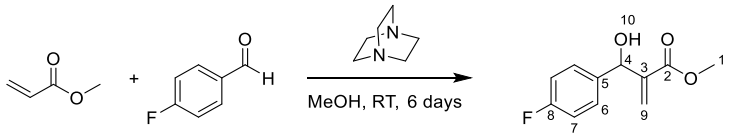

To a 25 mL round bottom flask, under an atmosphere of nitrogen, was added 4-fluorobenzaldehyde (0.62 g, 5 mmol), methyl acrylate (4.5 mL, 10 mmol), 1,4-diazabicyclo[2.2.2]octane (DABCO) (0.56 g, 5 mmol) and methanol (15 mL). The reaction mixture was stirred at room temperature for 6 days then diluted with ethyl acetate (50 mL), washed with water (3 x 50 mL) and washed with brine (50 mL). The organic layer was dried over Na_2SO_4, filtered and removed solvent under reduced pressure. The crude product was purified through silica gel column chromatography (petrol : ethyl acetate, 7:3) to give methyl 2-((4-fluorophenyl)(hydroxy)methyl)acrylate (54.4 mg, 0.26 mmol, 5%) as a colourless oil.

R_f: 0.5 (petrol : ethyl acetate, 7:3). **^{1}H NMR** (300 MHz, Chloroform-*d*) δ 7.37 – 7.29 (m, 2H, H^6), 7.06 – 6.97 (m, 2H, H^7), 6.32 (t, *J* = 1.0 Hz, 1H, H^9), 5.83 (t, *J* = 1.2 Hz, 1H, $H^{9'}$), 5.53 (d, *J* = 5.0 Hz, 1H, H^4), 3.71 (s, 3H, H^1), 3.16 (d, *J* = 5.4 Hz, 1H, H^{10}). **^{13}C NMR** (75 MHz, Chloroform-*d*) δ 166.8 (C^2), 162.4 (d, $^1J_{c\text{-}F}$ = 246.0 Hz, C^8), 142.0 (C^3), 137.17 (d, $^4J_{c\text{-}F}$ = 3.1 Hz, C^5), 128.5 (d, $^3J_{c\text{-}F}$ = 8.1 Hz, C^6), 126.2 (C^9), 115.4 (d, $^2J_{c\text{-}F}$ = 21.5 Hz, C^7), 72.7 (C^4), 52.1 (C^1). **^{19}F NMR** (282 MHz, Chloroform-*d*) δ -114.7. **HRMS:** (pNSI) calcd for $C_{11}H_{11}FO_3Na$ $[M+Na]^+$: 233.0584, found 233.0586.

Observed data (^{1}H, ^{13}C) are consistent with those previously reported by Amarante *et al*.[90]

7.2.3.6 Methyl 2-(hydroxy(*p*-tolyl)methyl)acrylate (**4.29**)

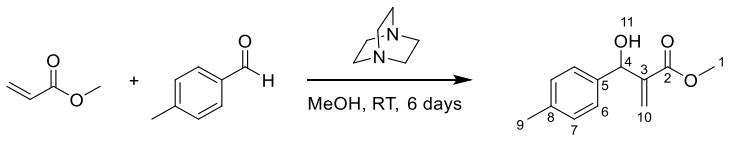

To a 25 mL round bottom flask, under an atmosphere of nitrogen, was added 4-methylbenzaldehyde (0.60 g, 5 mmol), methyl acrylate (4.5 mL, 50 mmol), 1,4-diazabicyclo[2.2.2]octane (DABCO) (0.56 g, 5 mmol) and methanol (15 mL). The reaction mixture was stirred at room temperature for 6 days then diluted with ethyl acetate (50 mL), washed with water (3 x 50 mL) and washed with brine (50 mL). The organic layer was dried over Na_2SO_4, filtered and removed solvent under reduced pressure. The crude product was purified through silica gel column chromatography (petrol : ethyl acetate, 7:3) to give methyl 2-(hydroxy(*p*-tolyl)methyl)acrylate (0.58 g, 2.78 mmol, 56%) as a colourless oil.

R_f: 0.62 (petrol : ethyl acetate, 7:3). **^{1}H NMR** (400 MHz, Chloroform-*d*) δ 7.26 (d, *J* = 8.3 Hz, 2H, $H^{6/7}$), 7.15 (d, *J* = 7.8 Hz, 2H, $H^{6/7}$), 6.33 (t, *J* = 1.0 Hz, 1H, H^{10}), 5.85 (t, *J* = 1.3 Hz, 1H, $H^{10'}$), 5.53 (d, *J* = 4.8 Hz, 1H, H^4), 3.72 (s, 3H, H^1), 2.96 (d, *J* = 5.4 Hz, 1H, H^{11}), 2.34 (s, 3H, H^9). **^{13}C NMR** (75 MHz, Chloroform-*d*) δ 166.7 (C^2), 142.2 (C^5), 138.5 (C^8), 137.4 (C^3), 129.1 ($C^{6/7}$), 126.6 ($C^{6/7}$), 125.6 (C^{10}), 72.8 (C^4), 51.9(C^1), 21.1 (C^9). **HRMS:** (pNSI) calcd for $C_{12}H_{14}O_3Na$ $[M+Na]^+$: 229.0835, found 229.0838.

X-Ray code: mjh230083_fa

Observed data (^{1}H, ^{13}C) are consistent with those previously reported by Amarante *et al*.[90]

7.2.3.7 Methyl 2-(((*tert*-butoxycarbonyl)oxy)(4-chlorophenyl)methyl)acrylate (**4.6**)

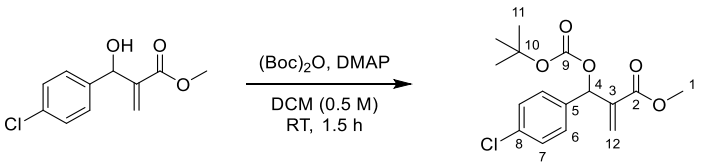

To a 25 mL round bottom flask, under an atmosphere of nitrogen, was added methyl 2-((4-chlorophenyl)(hydroxy)methyl)acrylate (226 mg, 1 mmol), di-*tert*-butyl decarbonate ($(Boc)_2O$) (240 g, 1.10 mmol), dry DCM (3 mL) and 4-(dimethylamino)pyridine (DMAP)(24.4 mg, 0.20 mmol). The reaction mixture was stirred at room temperature for 2 hours then diluted with DCM (20 mL) and washed with water (2 x 20 mL). The aqueous layer was extracted with DCM (2 x 20 mL). The organic layers were combined and dried over Na_2SO_4, filtered and removed solvent under reduced pressure to give colourless oil product. The crude product was purified through silica gel column chromatography (petrol : ethyl acetate, 4:1) to give methyl 2-(((*tert*-butoxycarbonyl)oxy)(4-chlorophenyl)methyl)acrylate (108 mg, 0.33 mmol, 33%) as a white crystal solid.

R_f: 0.65 (DCM). **^{1}H NMR** (300 MHz, Chloroform-*d*) δ 7.30 – 7.19 (m, 4H, $H^{6/7}$), 6.37 (t, *J* = 1.3 Hz, 1H, H^{12}), 6.34 (t, *J* = 0.8 Hz, 1H, H^{12}), 5.87 (dd, *J* = 1.5, 0.7 Hz, 1H, H^4), 3.64 (s, 3H, H^1), 1.39 (s, 9H, H^{11}). **^{13}C NMR** (75 MHz, Chloroform-*d*) δ 165.3, 152.3, 139.4, 136.3, 134.4, 129.2, 128.7, 126.0, 82.9, 75.1, 52.1, 27.8.

X-Ray code: mjh230010_fa

Observed data (^{1}H, ^{13}C) are consistent with those previously reported by Coelho *et al*.[91]

7.2.3.8 2-(1*H*-pyrrol-2-yl)phenol (**4.35**)

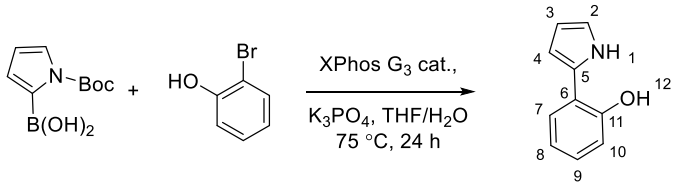

Method A:

To a Schlenk flask, under nitrogen atmosphere, was added (1-(*tert*-butoxycarbonyl)-1*H*-pyrrol-2-yl)boronic acid (379 mg, 1.80 mmol), 2-bromophenol (207 mg, 1.20 mmol), XPhos Pd G3 (30.5 mg, 3 mol %, 0.036 mmol), $K_3PO_4.H_2O$ (552 mg, 2.40 mmol), dry THF (3 mL), water (1 mL) and was degassed using freeze-pump-thaw method (x3). The reaction mixture was heated, using an oil bath, to 75 °C, stirred for 24 hours then diluted with DCM (50 mL) and washed with water (3 x 50 mL). The organic layer was dried over Na_2SO_4, filtered and the solvent was removed under reduced pressure. The crude product was purified through silica gel column chromatography (DCM) to give 2-(1*H*-pyrrol-2-yl)phenol (136 mg, 0.512 mmol, 71 %) as a white crystal solid.

R_f: 0.37 (DCM). **Mp:** 90-92 °C . **^{1}H NMR** (300 MHz, Chloroform-*d*) δ 9.40 (br, 1H, H^1), 7.55 (dd, *J* = 7.7, 1.7 Hz, 1H, Ar), 7.10 (ddd, *J* = 8.1, 7.4, 1.7 Hz, 1H, Ar), 6.98 (td, *J* = 7.5, 1.3 Hz, 1H, Ar), 6.91 (td, *J* = 2.7, 1.5 Hz, 1H, $H^{2/3/4}$), 6.83 (dd, *J* = 8.0, 1.3 Hz, 1H), 6.59 (ddd, *J* = 3.9, 2.5, 1.5 Hz, 1H, $H^{2/3/4}$), 6.34 (dt, *J* = 3.5, 2.7 Hz, 1H, $H^{2/3/4}$), 5.39 (s, 1H, H^{12}). **^{13}C NMR** (75 MHz, Chloroform-*d*) δ 151.1 (C^6), 128.8 (C^5), 127.3 (C^7), 127.2, 121.6, 119.8, 118.7 ($C^{2/3/4}$), 116.4, 109.4 ($C^{2/3/4}$), 106.4 ($C^{2/3/4}$). **IR (neat):** υ_{max}/cm^{-1} 3422 (O-H, br), 2981 (C-H, w).

X-Ray code: mjh230001_fa

Observed data (^{1}H, ^{13}C) are consistent with those previously reported by Knölker *et al*.[103]

Method B:

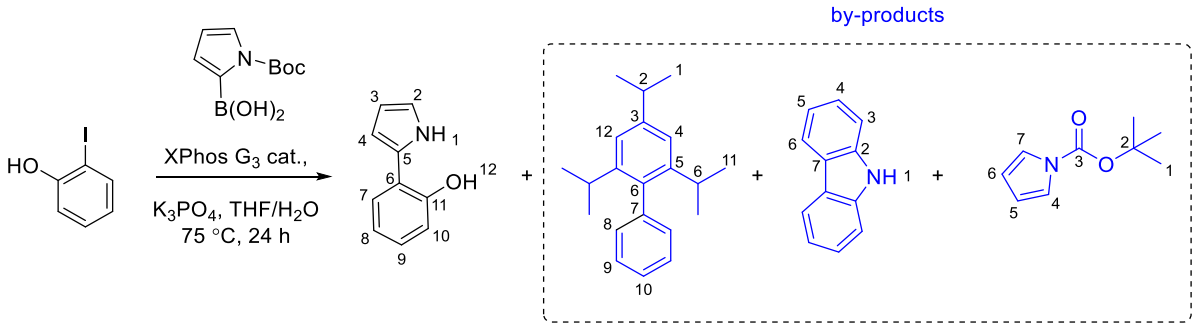

To a Schlenk flask, under nitrogen atmosphere, was added (1-(*tert*-butoxycarbonyl)-1*H*-pyrrol-2-yl)boronic acid (379 mg, 1.80 mmol), 2-iodophenol (264 mg, 1.20 mmol), XPhos Pd G3 (30.5 mg, 3 mol %, 0.036 mmol), $K_3PO_4.H_2O$ (552 mg, 2.40 mmol), dry THF (3 mL), water (1 mL) and was degassed using freeze-pump-thaw method (x3). The reaction mixture was heated, using an oil bath, to 75 °C, stirred for 24 hours then diluted with DCM (50 mL) and washed with water (3 x 50 mL). The organic layer was dried over $MgSO_4$, filtered and the solvent was removed under reduced pressure. The crude product was purified through silica gel column chromatography (DCM) to give 2-(1*H*-pyrrol-2-yl)phenol (72.7 mg, 0.45 mmol, 38 %) as a white crystal solid.

R_f: 0.37 (DCM). **Mp:** 90-92 °C . **^{1}H NMR** (400 MHz, Chloroform-*d*) δ 9.40 (s, 1H), 7.54 (dd, *J* = 7.7, 1.7 Hz, 1H), 7.10 (ddd, *J* = 8.1, 7.4, 1.7 Hz, 1H), 6.97 (td, *J* = 7.5, 1.2 Hz, 1H), 6.90 (td, *J* = 2.7, 1.5 Hz, 1H), 6.84 (dd, *J* = 8.0, 1.2 Hz, 1H), 6.58 (ddd, *J* = 3.9, 2.6, 1.5 Hz, 1H), 6.33 (dt, *J* = 3.6, 2.6 Hz, 1H).

By products:

2,4,6-triisopropyl-1,1'-biphenyl (**4.36**) **Yield:** (18.4 mg, 0.05 mmol, 5%). **R_f:** 0.8 (DCM). **^{1}H NMR** (400 MHz, Chloroform-*d*) δ 7.49 – 7.31 (m, 3H, Ar), 7.22 – 7.15 (m, 2H, Ar), 7.06 (s, 2H, Ar), 2.96 (h, *J* = 6.9 Hz, 1H, H^2), 2.60 (hept, *J* = 6.8 Hz, 2H, H^6), 1.32 (d, *J* = 6.9 Hz, 6H, H^1), 1.08 (d, *J* = 6.9 Hz, 12H, H^{11}).

X-Ray code: mjh230012_fa

9*H*-carbazole (**4.37**): **R_f:** 0.75 (DCM). **^{1}H NMR** (400 MHz, Chloroform-*d*) δ 8.09 (d, *J* = 7.8 Hz, 3H, Ar, H^1), 7.49 – 7.36 (m, 3H, Ar), 7.29 – 7.17 (m, 3H, Ar)

tert-butyl 1*H*-pyrrole-1-carboxylate (**4.38**): **R_f:** 0.62 (DCM). **^{1}H NMR** (400 MHz, Chloroform-*d*) δ δ 7.28 – 7.24 (m, 2H), 6.23 (dd, *J* = 2.6, 2.1 Hz, 2H), 1.62 (s, 9H, H^1).

7.2.3.9 Racemic Helically chiral *meso*-ethyl- *N*,*N*,*O*,*O*-BODIPY (**4.5**)

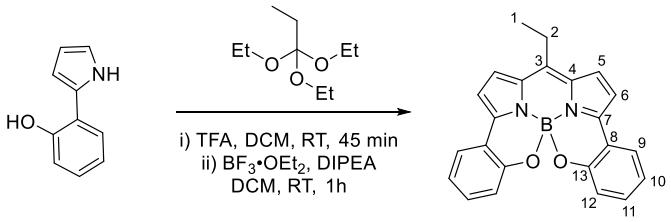

To a pear shape flask was added 2-(1*H*-pyrrol-2-yl)phenol (100 mg, 0.63 mmol), dry DCM (6.5 mL), and triethyl orthopropionate (0.93 mL, 4.65 mmol). A TFA (0.14 mL, 1.88 mmol) was added slowly to the reaction mixture, the reaction mixture was stirred for 45 min at room temperature. The solvent was removed under reduced pressure. The obtained dark green residue was dissolved in dry DCM (11 mL) then DIPEA (0.32 mL, 1.88 mmol) was added, and the reaction mixture left to stir at room temperature for 10 min. Following reaction time, BF_3OEt_2 (0.36 g, 2.51 mmol) was added in dropwise to the reaction mixture, stirred at room temperature for 2 hours and quenched with saturated solution of $NaHCO_3$ (100 mL). The reaction mixture was diluted with DCM (100 mL) and washed with water (3 x 100 mL). The organic layer was dried over $MgSO_4$, filtered and the solvent removed under reduced pressure. The crude product was purified through silica gel column chromatography (petrol : ethyl acetate, 20:3) to give the desired product (74.1 mg, 0.20 mmol, 32%).

R_f: 0.63 (petrol : ethyl acetate, 20:3). **^{1}H NMR** (300 MHz, Chloroform-*d*) δ 7.77 (dd, *J* = 7.7, 1.7 Hz, 2H, Ar), 7.38 (d, *J* = 4.4 Hz, 2H, $H^{5,6}$), 7.32 (ddd, *J* = 8.2, 7.3, 1.7 Hz, 2H, Ar), 7.04 (td, *J* = 7.5, 1.2 Hz, 2H, Ar), 6.93 (dd, *J* = 8.3, 1.1 Hz, 2H, Ar), 6.88 (d, *J* = 4.4 Hz, 2H, $H^{5,6}$), 3.08 – 2.86 (m, 2H, H^2), 1.45 (t, *J* = 7.7 Hz, 3H, H^1). **^{13}C NMR** (75 MHz, Chloroform-*d*) δ 154.0, 149.8, 142.9, 134.6, 132.2, 126.3 ($C^{5/6}$), 125.9, 120.5, 119.9, 115.5 ($C^{5/6}$), 23.3 (C^2), 18.0 (C^1). **^{11}B NMR** (96 MHz, Chloroform-*d*) δ -0.88.

X-Ray code: mjh230006_fa

Note: one carbon signal was not identified in the analysis of the ^{13}C NMR spectrum.

7.2.3.10 Helically chiral methyl (4-chlorophenyl)-2-methylenepentanoate substituted *N,N,O,O*-BODIPY (**4.7a**) and (**4.7b**)

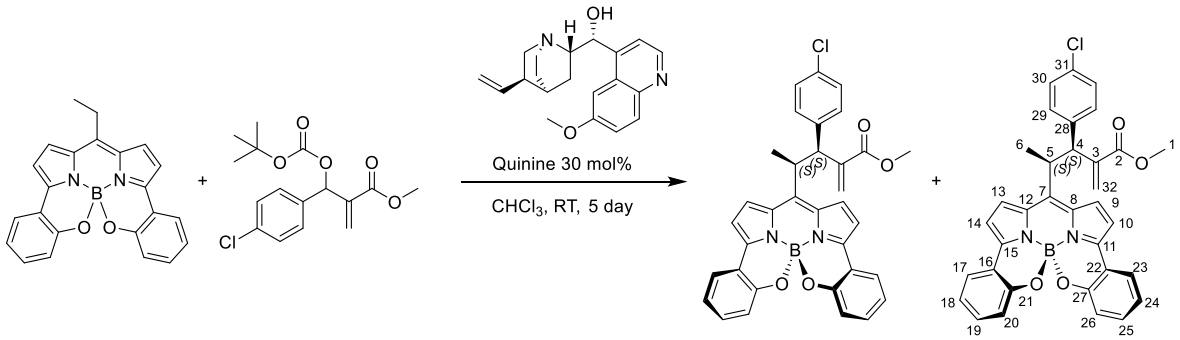

To a 10 mL round bottom flask, under an atmosphere of nitrogen, was added 8-Et-*N,N,O,O*-BODIPY (22.8 mg, 0.06 mmol), 2-(((*tert*-butoxycarbonyl)oxy)(4-chlorophenyl)methyl)acrylate (41.1 mg, 0.13 mmol), quinine (6.1 mg , 30 mol%, 0.02 mmol), and $CHCl_3$ (2 mL). The reaction mixture was stirred at room temperature for 5 days and the solvent was removed under reduced pressure. The crude product was purified through silica gel column chromatography (hexane : ethyl acetate, 7:3) to give the desired products as two diastereomers (33.9 mg, 0.20 mmol, 32%) as a blue solid. Following the separation of the two diastereomers through silica gel column chromatography (DCM) to give:

Diastereomer 1

R_f: 0.67 (petrol : ethyl acetate, 7:3). **^{1}H NMR** (700 MHz, Chloroform-*d*) δ 7.71 (dd, J = 5.7, 3.3 Hz, 3H), 7.30 (ddd, *J* = 8.7, 7.2, 1.7 Hz, 2H), 7.08 – 6.76 (m, 11H), 6.51 (s, 1H, H^{32}), 5.95 (s, 1H, $H^{32'}$), 4.58 (d, *J* = 11.2 Hz, 1H, H^4), 3.94 (dq, *J* = 11.7, 6.9 Hz, 1H, H^5), 3.78 (s, 3H, H^1), 1.60 (d, *J* = 6.9 Hz, 3H, H^6).**^{13}C NMR** (176 MHz, Chloroform-*d*) δ 167.3, 154.1, 143.7, 141.8, 138.7, 135.9, 132.9, 129.4, 128.6, 127.2, 126.1, 125.9, 120.4, 119.8, 119.6, 116.1, 115.1, 53.7, 52.5, 40.1, 21.3. **^{11}B NMR** (96 MHz, Chloroform-*d*) δ -1.08. **HRMS** (TOF MS ASAP+) calcd for $C_{34}H_{27}{}^{11}B^{35}ClF_3N_2O_4$ $[M+H]^+$: 573.1758, found 573.1762. **UV-Vis:** λ_{max} (abs) = 623 nm. **Molar extinction coefficient** (ε) = 79,829 M^{-1} cm^{-1}. **ϕ_F** = 0.13 (DCM).

7.2.4 Chapter 5

7.2.4.1 Dimethyl 4,4'-(1,4-phenylenebis(10-(((*S*)-1-hydroxybutan-2-yl)amino)-10b*H*-11-oxa-4b^{1},10aλ^{4}-diaza-10bλ^{4}-boracyclopenta[*e*]aceanthrylene-10b,7-diyl))dibenzoate (**5.2a**), (**5.2b**), and (**5.2c**)

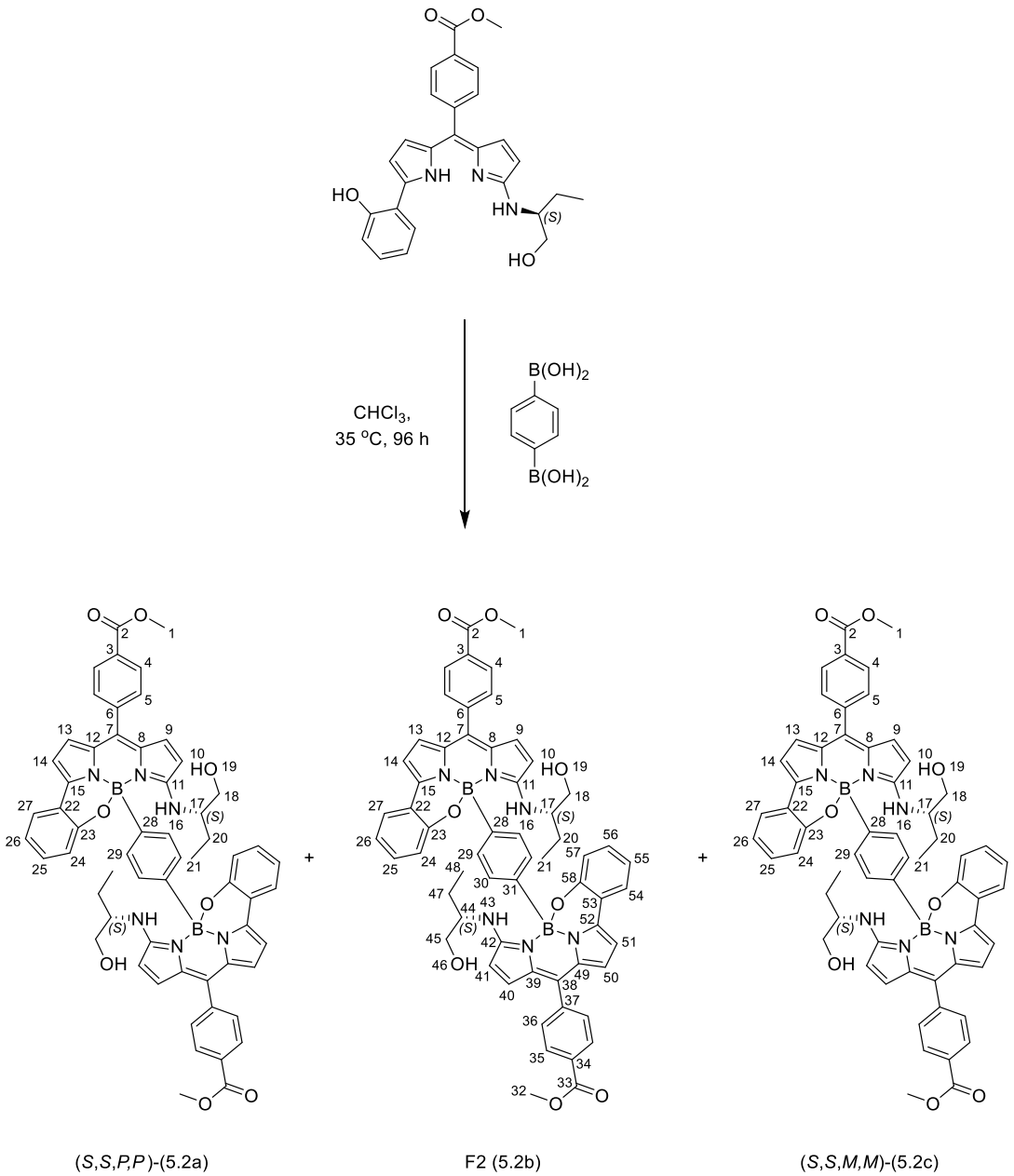

(*S*,*S*,*P*,*P*)-(5.2a) + F2 (5.2b) + (*S*,*S*,*M*,*M*)-(5.2c)

To a 25 mL round bottom flask, under an atmosphere of nitrogen, was added methyl (*S*,*Z*)-4-((5-((1-hydroxybutan-2-yl)amino)-2*H*-pyrrol-2-ylidene)(5-(2-hydroxyphenyl)-1*H*-pyrrol-2-yl)methyl)benzoate (45.7 mg , 0.10 mmol), 1,4-phenylenediboronic acid (8.28 mg, 0.05 mmol) and $CHCl_3$ (4 mL). The reaction mixture was stirred at 35 °C for 96 hours and quenched with water then diluted with DCM (50 mL), washed with water (3 x 50 mL). The organic layer was dried over $MgSO_4$, filtered and the

solvent was removed under reduced pressure to give a purple product. The crude product was purified through silica gel column chromatography (DCM: methanol, 100 : 0.05 → 100 : 0.5) to give:

(*S*,*S*,*P*,*P*)-(5.2a):

Yield: (16.6 mg, 0.02 mmol, 33%). **R_f:** 0.75 (DCM: methanol, 100:5). **^{1}H NMR** (300 MHz, Chloroform-*d*) δ 8.16 (d, *J* = 8.5 Hz, 4H, H^4), 7.70 (d, *J* = 8.6 Hz, 4H, H^5), 7.41 (dd, *J* = 7.7, 1.6 Hz, 2H, Ar), 7.23 – 7.13 (m, 2H, Ar), 7.07 (dd, *J* = 8.2, 1.2 Hz, 6H, Ar), 6.97 (d, *J* = 4.5 Hz, 2H, $H^{9/10}$), 6.83 (td, *J* = 7.2, 1.3 Hz, 2H, Ar), 6.32 (d, *J* = 9.7 Hz, 2H, H^{16}), 6.51 (d, *J* = 3.9 Hz, 2H, $H^{13/14}$), 6.49 (d, *J* = 3.9 Hz, 2H, $H^{13/14}$), 6.13 (d, *J* = 4.9 Hz, 2H, $H^{9/10}$), 3.99 (s, 6H, H^1), 3.38 – 3.25 (m, 4H, $H^{17,18}$), 3.09 – 2.93 (m, 2H, $H^{18'}$), 2.05 – 1.96 (m, 2H, H^{19}), 1.67 – 1.45 (m, 4H, $H^{20,20'}$), 1.04 (t, *J* = 7.4 Hz, 6H, H^{21}). **^{1}H NMR** (700 MHz, Chloroform-*d*) δ 8.16 (d, *J* = 8.5 Hz, 4H), 7.70 (d, *J* = 7.7 Hz, 4H), 7.40 (dd, *J* = 7.5, 1.6 Hz, 2H), 7.20 – 7.15 (m, 2H), 7.07 (d, *J* = 8.1 Hz, 2H), 7.03 (s, 4H), 6.97 (d, *J* = 4.8 Hz, 2H), 6.83 (t, *J* = 7.4 Hz, 2H), 6.50 (d, *J* = 4.0 Hz, 2H), 6.49 (d, *J* = 4.0 Hz, 2H), 6.32 (d, *J* = 9.7 Hz, 2H), 6.13 (d, *J* = 4.8 Hz, 2H), 3.99 (s, 6H), 3.36 – 3.27 (m, 4H), 3.02 (ddd, *J* = 13.2, 8.0, 5.4 Hz, 2H), 2.01 (dd, *J* = 8.4, 5.6 Hz, 2H), 1.60 (dqd, *J* = 14.7, 7.5, 4.8 Hz, 2H), 1.55 – 1.49 (m, 2H), 1.03 (t, *J* = 7.4 Hz, 6H). **^{13}C NMR** (176 MHz, Chloroform-*d*) δ 166.8 (C^2), 161.6, 154.4, 145.6 (C^{28}), 139.9, 139.8, 133.5, 133.2 ($C^{9/10}$), 131.8, 130.82, 130.76, 130.6, 130.5, 129.7, 129.59, 129.55, 124.9, 121.4 ($C^{13/14}$), 120.1, 119.9, 119.1 ($C^{13/14}$), 110.2 ($C^{9/10}$), 109.8, 65.8 (C^{18}), 59.5 (C^{17}), 52.5 (C^1), 24.8 (C^{20}), 10.5 (C^{21}). **^{11}B NMR** (96 MHz, Chloroform-*d*) δ 1.40. **IR** (neat): υ_{max}/cm^{-1} 3344 (C-H, w), 2981 (C-H, w), 1719 (C=O, m). **HRMS:** (pNSI) calcd for $C_{60}H_{55}{}^{11}B_2N_6O_8$ $[M+H]^+$: 1009.4269, found 1009.4313. **UV-Vis:** λ_{max} (abs) = 574 nm (DCM). **Molar extinction coefficient** (ε) = 77,787 M^{-1} cm^{-1} (DCM). **ϕ_F** = 0.003 (DCM).

X-Ray code: mjh220063_fa

F2-(5.2b):

Yield: (20.4 mg, 0.02 mmol, 40%). **R_f:** 0.28 (DCM: methanol, 100:5). **^{1}H NMR** (300 MHz, Chloroform-*d*) δ 8.12 (t, *J* = 8.1 Hz, 4H, $H^{4,35}$), 7.65 (d, *J* = 7.9 Hz, 2H, $H^{5/36}$), 7.60 (d, *J* = 8.0 Hz, 2H, $H^{5/36}$), 7.47 – 7.37 (m, 2H, Ar), 7.16 (td, *J* = 7.7, 4.5 Hz, 2H), 7.06 (d, *J* = 7.3 Hz, 2H), 7.01 (d, *J* = 8.4 Hz, 1H), 6.96 – 6.77 (m, 7H), 6.67 (d, *J* = 9.2 Hz, 1H, $H^{16/43}$), 6.55 – 6.45 (m, 4H), 6.34 (d, *J* = 10.2 Hz, 1H, $H^{16/43}$), 6.06 (d, *J* = 4.9 Hz, 2H), 3.97 (d, *J* = 1.4 Hz, 6H, $H^{1,32}$), 3.62 (dd, *J* = 15.8, 10.1 Hz, 2H), 3.40 – 3.19 (m, 2H), 3.13 (d, *J* = 11.7 Hz, 1H), 3.00 – 2.87 (m, 1H), 2.29 (br, 1H, $H^{19/46}$), 1.45 (dtt, *J* = 29.3, 14.7, 7.4 Hz, 4H), 1.00 (t, *J* = 7.4 Hz, 3H, $H^{21,48}$), 0.89 (br, 1H, $H^{19/46}$), 0.59 (t, *J* = 7.4 Hz, 3H, $H^{21,48}$). **^{13}C NMR** (75 MHz, Chloroform-*d*) δ 166.7, 161.6, 160.8, 154.5, 154.2, 139.9, 139.84, 139.76, 139.6, 133.32, 133.28, 131.9, 131.6, 130.64, 130.60, 130.5, 130.4, 129.51, 129.47, 129.4, 124.69, 124.66, 121.1, 120.0, 119.9, 119.7, 119.6, 119.2, 119.1, 110.0, 109.7, 109.6, 109.5, 65.4, 64.5, 58.9, 58.4, 52.3, 24.9, 24.5, 10.4, 10.1.**^{11}B NMR** (96 MHz,

Chloroform-*d*) δ 2.02. **IR** (neat): υ_{max}/cm^{-1} 3343 (C-H, w), 2981 (C-H, w), 1707 (C=O, m). **HRMS:** (pNSI) calcd for $C_{60}H_{55}{}^{11}B_2N_6O_8$ $[M+H]^+$: 1009.4269, found 1009.4273. **UV-Vis:** λ_{max} (abs) = 575 nm (DCM). **Molar extinction coefficient** (ε) = 51,369 M^{-1} cm^{-1} (DCM). $\boldsymbol{\phi_F}$ = 0.003 (DCM).

Note: 14 carbon signals were not identified in the analysis of the ^{13}C NMR spectrum due to the low concentration of the sample and poor solubility in $CDCl_3$.

(*S*,*S*,*M*,*M*)-(5.2c):

Yield: (12.3 mg, 0.01 mmol, 24%). **R_f:** 0.20 (DCM: methanol, 100:5). **^{1}H NMR** (700 MHz, Chloroform-*d*) δ 8.12 (d, *J* = 8.3 Hz, 4H, H^4), 7.62 (d, *J* = 7.6 Hz, 4H, H^5), 7.36 (d, *J* = 7.2 Hz, 2H, Ar), 7.15 (t, *J* = 7.7 Hz, 2H, Ar), 7.09 (d, *J* = 8.0 Hz, 2H, Ar), 6.96 (s, 4H, Ar), 6.84 (d, *J* = 4.8 Hz, 2H, H$^{9/10}$), 6.81 – 6.77 (m, 2H,), 6.48 (m*, 4H, H$^{13/14}$), 6.38 (d, *J* = 9.3 Hz, 2H, H^{16}), 5.98 (d, *J* = 4.8 Hz, 2H, H$^{9/10}$), 3.97 (s, 6H, H^1), 3.71 – 3.66 (m, 2H, H^{18}), 3.62 – 3.54 (m, 2H, H$^{18'}$), 3.24 – 3.17 (m, 2H, H^{17}), 2.38 (br, 2H, H^{19}), 1.33 – 1.07 (m, 4H, H$^{20,20'}$), 0.09 (t, *J* = 7.2 Hz, 6H, H^{21}). **^{13}C NMR** (176 MHz, Chloroform-*d*) δ 166.8 (C^2), 161.1, 154.4, 143.8 (C^{28}), 139.9, 139.8, 133.7, 133.3 (C$^{9/10}$), 131.8, 130.8, 130.7, 130.5, 130.4, 129.65, 129.62, 129.4, 124.7, 120.8 (C$^{13/14}$), 120.5, 119.8, 119.4 (C$^{13/14}$), 109.8 (C$^{9/10}$), 109.4, 65.5 (C^{18}), 59.0 (C^{17}), 52.5 (C^1), 25.3 (C^{20}), 9.7 (C^{21}). **^{11}B NMR** (96 MHz, Chloroform-*d*) δ 0.97. **IR** (neat): υ_{max}/cm^{-1} 2981 (C-H, w), 1721 (C=O, m). **HRMS:** (pNSI) calcd for $C_{60}H_{55}{}^{11}B_2N_6O_8$ $[M+H]^+$: 1009.4269, found 1009.4281. **UV-Vis:** λ_{max} (abs) = 573 nm (DCM). **Molar extinction coefficient** (ε) = 72,134 M^{-1} cm^{-1} (DCM). $\boldsymbol{\phi_F}$ = 0.003 (DCM).

X-Ray code: mjh220062_fa

*Two doublet signals overlapping corresponding to pyrrolic four protons H^{13} and H^{14}

7.2.4.2 Dimethyl 4,4'-([1,1'-biphenyl]-4,4'-diylbis(10-(((*S*)-1-hydroxybutan-2-yl)amino)-10b*H*-11-oxa-4b^{1},10aλ^{4}-diaza-10bλ^{4}-boracyclopenta[*e*]aceanthrylene-10b,7-diyl))dibenzoate (**5.10a**), (**5.10b**), and (**5.10c**)

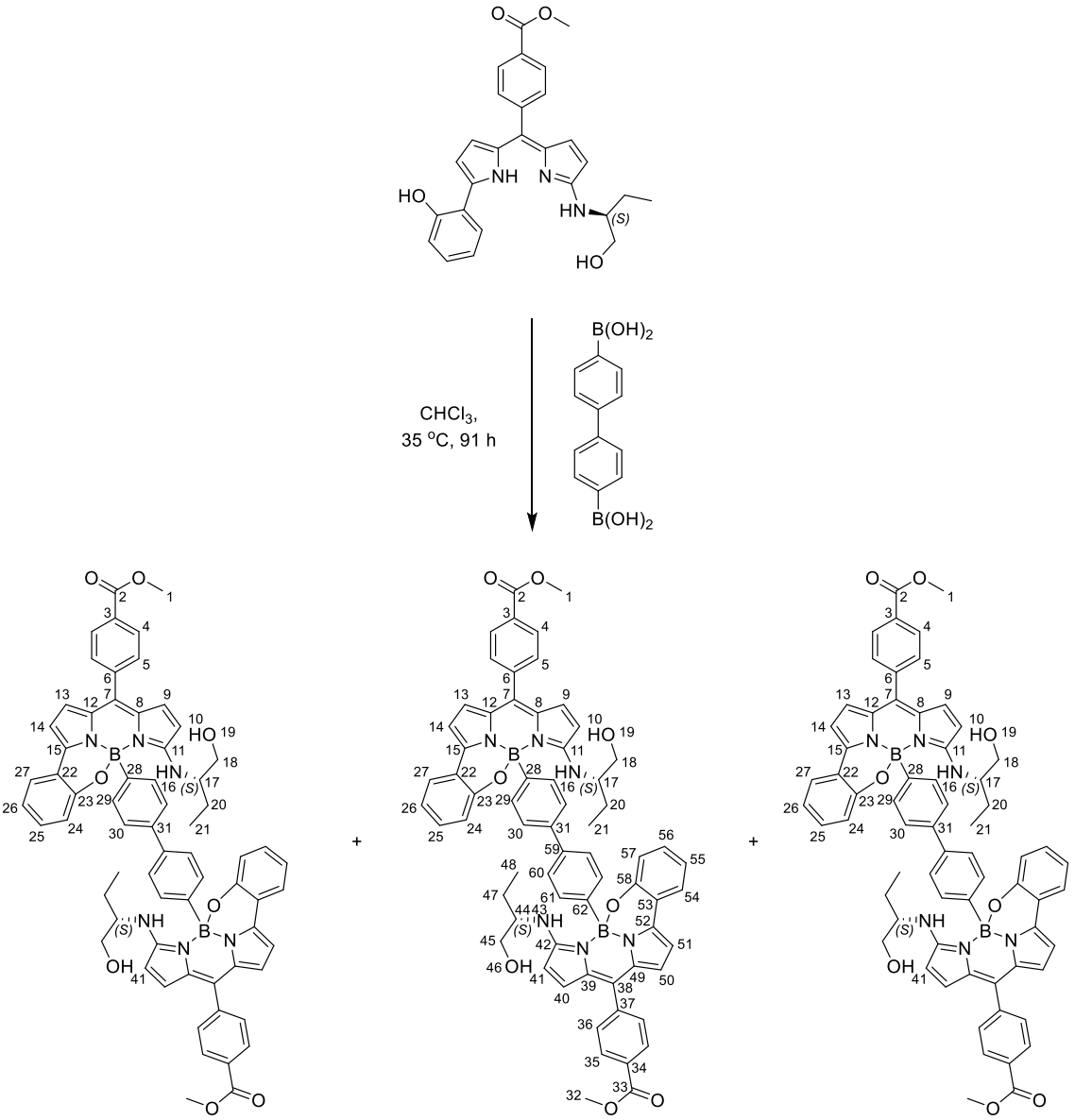

To a 25 mL round bottom flask, under an atmosphere of nitrogen, was added methyl (*S*,*Z*)-4-((5-((1-hydroxybutan-2-yl)amino)-2*H*-pyrrol-2-ylidene)(5-(2-hydroxyphenyl)-1*H*-pyrrol-2-yl)methyl)benzoate (45.7 mg , 0.10 mmol), [1,1'-biphenyl]-4,4'-diyldiboronic acid (12.1 mg, 0.05 mmol) and $CHCl_3$ (4 mL). The reaction mixture was stirred at 35 °C for 91 hours and quenched with water then diluted with

DCM (50 mL), washed with water (3 x 50 mL). The organic layer was dried over $MgSO_4$, filtered and the solvent was removed under reduced pressure to give a purple product. The crude product was purified through silica gel column chromatography (DCM: methanol, 100 : 1) to give:

(*S*,*S*,*P*,*P*)-(5.10a)

Yield: (5.5 mg, 0.005 mmol, 10%). **R_f:** 0.3 (DCM: methanol, 100:1). **^{1}H NMR** (500 MHz, Chloroform-*d*) δ 8.17 (d, *J* = 8.5 Hz, 4H, H^4), 7.71 (d, *J* = 8.3 Hz, 4H, H^5), 7.49 (dd, *J* = 7.6, 1.6 Hz, 2H, Ar), 7.25 – 7.15 (m, 12H, Ar), 7.01 (d, *J* = 5.5 Hz, 2H, $H^{9/10}$), 6.88 (td, *J* = 7.4, 1.3 Hz, 2H, Ar), 6.59 (d, *J* = 3.9 Hz, 2H, $H^{13/14}$), 6.57 (d, *J* = 3.9 Hz, 2H, $H^{13/14}$), 6.53 (d, *J* = 9.8 Hz, 2H, H^{16}), 6.13 (d, *J* = 4.8 Hz, 2H, $H^{9/10}$), 3.98 (s, 6H, H^1), 3.39 – 3.32 (m, 4H, $H^{18,18'}$), 3.26 – 3.18 (m, 2H, H^{17}), 1.75 – 1.58 (m, 4H, $H^{20,20'}$), 1.06 (t, *J* = 7.4 Hz, 6H, H^{21}). **^{13}C NMR** (126 MHz, Chloroform-*d*) δ 166.8, 161.5, 154.5, 146.1, 140.3, 139.7, 139.7, 134.0, 133.3, 132.2, 131.7, 130.9, 130.5, 129.8, 129.7, 129.6, 126.2, 126.1, 125.0, 121.6, 120.1, 120.0, 119.3, 109.9, 65.4, 58.9, 52.5, 24.7, 10.5. **^{11}B NMR** (160 MHz, Chloroform-*d*) δ 2.10. **IR** (neat): υ_{max}/cm^{-1} 3351 (C-H, w), 2971 (C-H, w), 1720 (C=O, m). **HRMS:** (pNSI) calcd for $C_{66}H_{59}{}^{11}B_2N_6O_8$ $[M+H]^+$: 1085.4595, found 1085.4581.

F2 (5.10b):

Yield: (15.1 mg, 0.01 mmol, 28%). **R_f:** 0.18 (DCM: methanol, 100:1). **^{1}H NMR** (300 MHz, Chloroform-*d*) δ 8.16 (dd, *J* = 8.4, 2.7 Hz, 4H), 7.70 (dd, *J* = 8.1, 6.5 Hz, 4H), 7.48 (t, *J* = 6.8 Hz, 2H), 7.25 – 7.10 (m, 12H), 7.02 (d, *J* = 4.8 Hz, 1H), 6.98 (d, *J* = 4.9 Hz, 1H), 6.87 (q, *J* = 7.4 Hz, 2H), 6.65 (d, *J* = 9.9 Hz, 1H), 6.60 – 6.55 (m, 4H), 6.53 (d, *J* = 9.9 Hz, 1H), 6.14 (d, *J* = 4.7 Hz, 2H), 3.98 (d, *J* = 0.8 Hz, 6H), 3.85 – 3.75 (m, 1H), 3.70 (dd, J = 11.3, 5.9 Hz, 1H), 3.46 – 3.14 (m, 4H), 2.37 – 2.06 (m, 4H), 1.06 (t, *J* = 7.4 Hz, 3H), 0.88 (t, *J* = 6.4 Hz, 3H), 0.62 – 0.53 (m, 2H). **IR** (neat): υ_{max}/cm^{-1} 2981 (C-H, m), 1717 (C=O, m). **HRMS:** (pNSI) calcd for $C_{66}H_{59}{}^{11}B_2N_6O_8$ $[M+H]^+$: 1085.4595, found 1085.4587.

(*S*,*S*,*M*,*M*)-(5.10c):

Yield: (12.9 mg, 0.01 mmol, 24%). **R_f:** 0.13 (DCM: methanol, 100:1). **^{1}H NMR** (300 MHz, Chloroform-*d*) δ 8.14 (d, *J* = 8.6 Hz, 4H, H^4), 7.67 (d, *J* = 8.5 Hz, 4H, H^5), 7.46 (dd, *J* = 7.6, 1.5 Hz, 2H, Ar), 7.25 – 7.09 (m, 12H, Ar), 6.94 (d, *J* = 4.9 Hz, 2H, $H^{9/10}$), 6.86 (ddd, *J* = 7.7, 6.8, 1.6 Hz, 2H, Ar), 6.60 (br, 2H, H^{16}), 6.57 (d, *J* = 4.0 Hz, 2H, $H^{13/14}$), 6.55 (d, *J* = 4.0 Hz, 2H, $H^{13/14}$), 6.08 (d, *J* = 4.9 Hz, 2H, $H^{9/10}$), 3.98 (s, 6H, H^1), 3.76 (dd, *J* = 11.4, 4.0 Hz, 2H, H^{18}), 3.65 (dd, *J* = 11.3, 6.0 Hz, 2H, $H^{18'}$), 3.34 (dddd, *J* = 9.8, 5.0, 4.9, 4.9 Hz, 2H, H^{17}), 1.51 (ddd, *J* = 14.1, 7.3, 4.9 Hz, 2H, H^{20}), 1.42 – 1.21 (m, 2H, H^{20}), 0.50 (t, *J* = 7.4 Hz, 6H, H^{21}). **^{1}H NMR** (500 MHz, Chloroform-*d*, at 298 K) δ 8.15 (d, *J* = 8.5 Hz, 4H, H^4), 7.68 (d, *J* = 8.2 Hz, 4H, H^5), 7.47 (d, *J* = 7.7 Hz, 2H, Ar), 7.23 – 7.11 (m, 12H, Ar), 6.96 (d, *J* = 4.8 Hz, 2H, $H^{9/10}$), 6.86 (td, *J* = 7.5, 1.3 Hz, 2H, Ar), 6.62 (d, *J* = 10.2 Hz, 2H, H^{16}), 6.57 (m*, *J* = 4.0 Hz, 4H, $H^{13/14}$), 6.11 (br, 2H, $H^{9/10}$), 3.98

(s, 6H, H^{1}), 3.82 – 3.74 (m, 2H, H^{18}), 3.68 (dd, *J* = 11.3, 6.0 Hz, 2H, $H^{18'}$), 3.42 – 3.32 (m, 2H, H^{17}), 1.53 (ddd, *J* = 14.2, 7.4, 5.0 Hz, 2H, H^{20}), 1.42 – 1.33 (m, 2H, $H^{20'}$), 0.52 (t, *J* = 7.4 Hz, 6H, H^{21}). **^{13}C NMR** (75 MHz, Chloroform-*d*) δ 166.8, 161.2, 154.2, 146.1, 140.0, 139.9, 139.7, 134.0, 133.3, 132.0, 131.7, 130.8, 130.5, 129.7, 129.6, 126.0, 125.0, 121.2, 120.2, 120.1, 119.3, 109.8, 109.7, 65.3, 58.8, 52.5, 25.4, 9.9. **HRMS:** (TOF MS ES+) calcd for $C_{66}H_{59}{}^{11}B_2N_6O_8$ $[M+H]^+$: 1085.4595, found 1085.4521, $C_{66}H_{59}{}^{10}B\,{}^{11}BN_6O_8$ $[M+H]^+$: 1084.4623, found 1084.4482.

*Two doublet signals overlapping corresponding to pyrrolic four protons H^{13} and H^{14}

Note: one carbon signal was not identified in the analysis of the ^{13}C NMR spectrum.

7.2.4.3 Dimethyl 4,4'-([2,2'-bithiophene]-5,5'-diylbis(10-(((*S*)-1-hydroxybutan-2-yl)amino)-10b*H*-11-oxa-4b^{1},10aλ^{4}-diaza-10bλ^{4}-boracyclopenta[*e*]aceanthrylene-10b,7-diyl))dibenzoate (**5.11a**), (**5.11b**), and (**5.11c**)

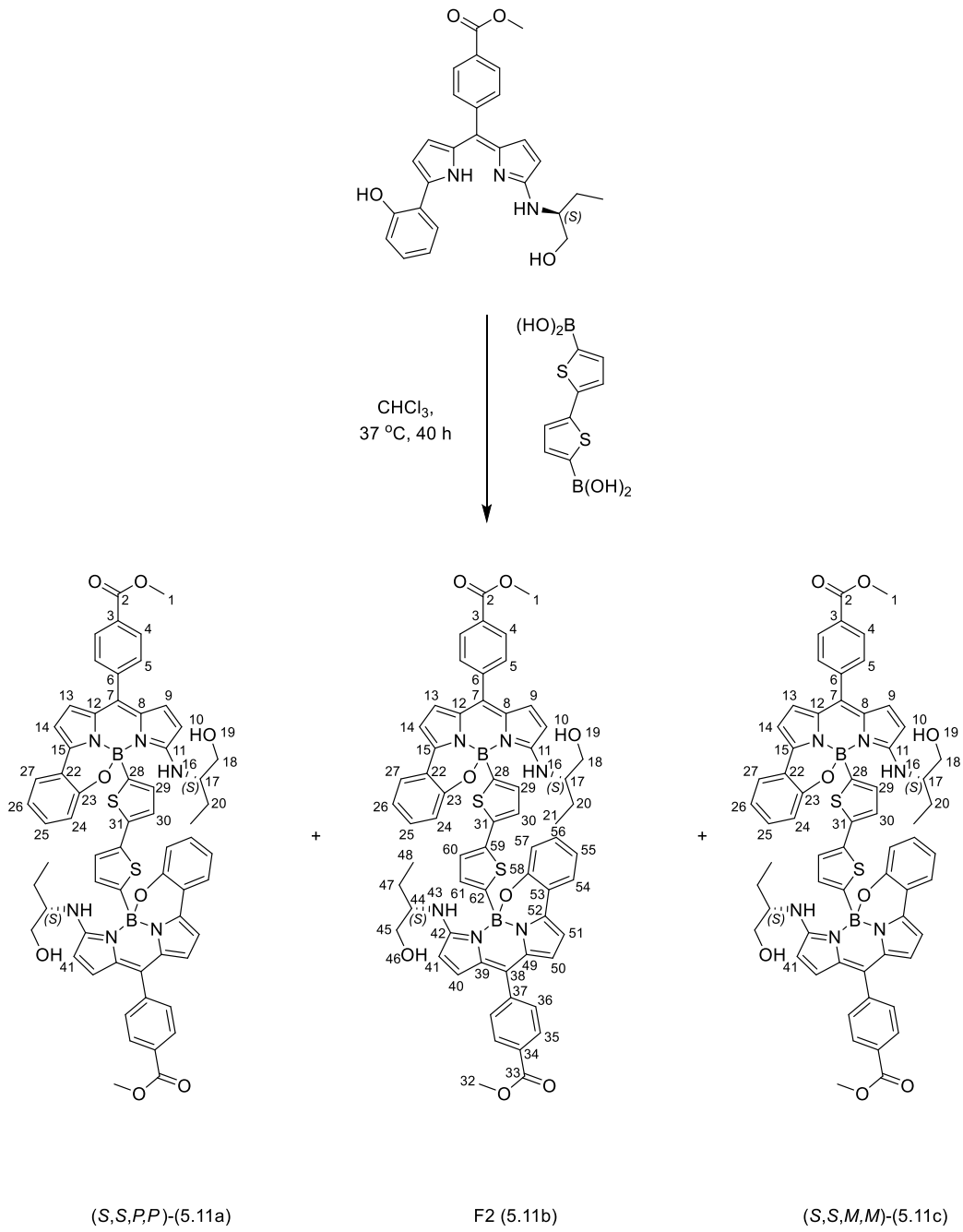

(*S*,*S*,*P*,*P*)-(5.11a) + F2 (5.11b) + (*S*,*S*,*M*,*M*)-(5.11c)

To a 25 mL round bottom flask, under an atmosphere of nitrogen, was added methyl (*S*,*Z*)-4-((5-((1-hydroxybutan-2-yl)amino)-2*H*-pyrrol-2-ylidene)(5-(2-hydroxyphenyl)-1*H*-pyrrol-2-yl)methyl)benzoate (45.7 mg , 0.10 mmol), [2,2'-bithiophene]-5,5'-diyldiboronic acid (12.7 mg, 0.05 mmol) and $CHCl_3$ (4 mL). The reaction mixture was stirred at 37 °C for 40 hours and quenched with water then diluted

with DCM (50 mL), washed with water (3 x 50 mL). The organic layer was dried over $MgSO_4$, filtered and the solvent was removed under reduced pressure to give a purple product. The crude product was purified through silica gel column chromatography (DCM: methanol, 100 : 0.1→ 100 : 1) to give:

F1: (This Fraction contained more than one compound, making data analysis difficult).

F2 (5.11b):

Yield: (6.3 mg, 0.005 mmol, 11%). **R_f:** 0.53 (DCM: methanol, 10:1). **^{1}H NMR** (400 MHz, Chloroform-*d*) δ 8.15 (d, *J* = 2.4 Hz, 2H, $H^{4/35}$), 8.12 (d, *J* = 2.4 Hz, 2H, $H^{4/35}$), 7.66 (d, *J* = 3.4 Hz, 2H, $H^{5/36}$), 7.64 (d, *J* = 1.7 Hz, 2H, $H^{5/36}$), 7.50 (td, *J* = 7.6, 1.7 Hz, 2H, Ar), 7.23 – 7.15 (m, 2H, Ar), 7.08 (dt, *J* = 8.3, 1.6 Hz, 2H, Ar), 6.99 (d, *J* = 4.8 Hz, 1H, $H^{9/10}$), 6.96 (d, *J* = 4.8 Hz, 1H, $H^{40/41}$), 6.89 (tdd, *J* = 7.1, 5.6, 1.2 Hz, 2H, Ar), 6.75 (d, *J* = 9.7 Hz, 1H, $H^{16/43}$), 6.67 (m*, 3H, $H^{13/14,50/51,16}$), 6.60 (d, *J* = 3.9 Hz, 1H, H^{29}), 6.58 (d, *J* = 3.9 Hz, 1H, H^{30}), 6.55 (d, *J* = 3.9 Hz, 1H, H^{60}), 6.53 (d, *J* = 3.9 Hz, 1H, H^{61}), 6.45 (d, *J* = 3.3 Hz, 2H, $H^{13/14,\ 50/51}$), 6.19 – 6.12 (m, 2H, $H^{9/10,\ 40/41}$), 3.98 (s, 6H, $H^{1,32}$), 3.80 (dd, *J* = 11.5, 4.0 Hz, 1H, H^{18}), 3.71 (dd, *J* = 11.3, 5.8 Hz, 1H, $H^{18'}$), 3.60 – 3.41 (m, 4H, $H^{17,45,45'}$), 1.76 – 1.48 (m, 4H, $H^{20,20',47,47'}$), 1.06 (t, *J* = 7.5 Hz, 3H, $H^{21,48}$), 0.77 (t, *J* = 7.4 Hz, 3H, $H^{21,48}$).

(*S*,*S*,*M*,*M*)-(5.11c):

Yield: (9.2 mg, 0.008 mmol, 17%). **R_f:** 0.50 (DCM: methanol, 10:1). **^{1}H NMR** (400 MHz, Chloroform-*d*) δ 8.04 (d, *J* = 8.3 Hz, 4H, H^4), 7.55 (d, *J* = 8.2 Hz, 4H, H^5), 7.41 (dd, *J* = 7.7, 1.6 Hz, 2H, Ar), 7.10 (td, *J* = 7.7, 1.6 Hz, , 2H, Ar), 7.01 (d, *J* = 8.0 Hz, 2H, Ar), 6.86 (d, *J* = 4.8 Hz, 2H, $H^{9/10}$), 6.80 (td, *J* = 7.4, 1.1 Hz, 2H, Ar), 6.63 (d, *J* = 9.4 Hz, 2H, H^{14}), 6.58 (d, *J* = 3.4 Hz, 2H, $H^{29/30}$), 6.50 (d, *J* = 3.9 Hz, 2H, $H^{13/14}$), 6.45 (d, *J* = 3.9 Hz, 2H, $H^{13/14}$), 6.37 (t, *J* = 3.8 Hz, 2H, $H^{29/30}$), 6.05 (d, *J* = 4.9 Hz, 2H, $H^{9/10}$), 3.90 (s, 6H, H^1), 3.75 – 3.66 (m, 2H, H^{18}), 3.65 – 3.54 (m, 2H, $H^{18'}$), 3.40 – 3.28 (m, 2H, H^{17}), 2.13 (br, 2H, H^{19}), 1.54 (dt, *J* = 13.3, 6.7 Hz, 2H, H^{20}), 1.43 (dt, *J* = 14.4, 7.4 Hz, 2H, $H^{20'}$), 0.67 (t, *J* = 7.4 Hz, 6H, H^{21}).

7.2.4.4 Methyl 4-(3-bromo-5,5-difluoro-7-(1*H*-pyrrol-2-yl)-5*H*-5λ^4,6λ^4-dipyrrolo[1,2-*c*:2',1'-*f*][1,3,2]diazaborinin-10-yl)benzoate (**5.13**)

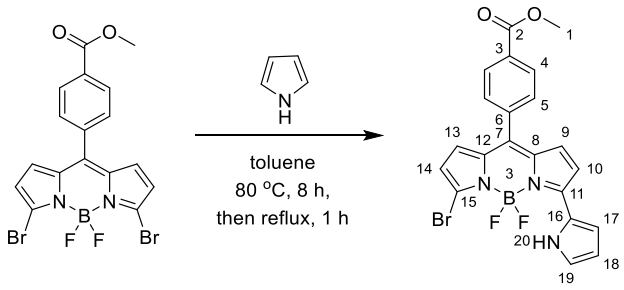

To a 25 mL round bottom flask, under an atmosphere of nitrogen, was added methyl 4-(3,7-dibromo-5,5-difluoro-5*H*-4λ^4,5λ^4-dipyrrolo[1,2-*c*:2',1'-*f*][1,3,2]diazaborinin-10-yl)benzoate (96.7 mg, 0.20 mmol), 1*H*-pyrrole (0.5 mL, 7.4 mmol), and toluene (4 mL). The reaction mixture was heated to 80 °C, stirred for 8 hours then the temperature was increased to reflux and stirred for 1 hour. The reaction mixture was left to cool to room temperature and diluted with DCM. The crude mixture was washed with water (x2). The organic layer was dried over Na_2SO_4, filtered and removed solvent under reduced pressure. The crude product was purified through silica gel column chromatography (DCM : petrol, 7:3) to give methyl 4-(3-bromo-5,5-difluoro-7-(1*H*-pyrrol-2-yl)-5*H*-5λ^4,6λ^4-dipyrrolo[1,2-*c*:2',1'-*f*][1,3,2]diazaborinin-10-yl)benzoate (35 mg, 0.07 mmol, 37%) as a purple solid.

R_f: 0.65 (DCM). **^{1}H NMR** (300 MHz, Chloroform-*d*) δ 10.55 (br, 1H, H^{20}), 8.16 (d, *J* = 8.5 Hz, 2H, H^4), 7.57 (d, *J* = 8.6 Hz, 2H, H^5), 7.27 (dd, *J* = 2.9, 1.4 Hz, 1H), 7.08 (ddd, *J* = 3.9, 2.5, 1.4 Hz, 1H), 6.95 (d, *J* = 4.8 Hz, 1H, $H^{9/10}$), 6.85 (d, *J* = 4.8 Hz, 1H, $H^{9/10}$), 6.47 (d, *J* = 4.1 Hz, 1H, $H^{13/14}$), 6.43 (d, *J* = 3.6 Hz, 1H, $H^{13/14}$), 6.42 – 6.40 (m, 1H), 3.98 (s, 3H, H^1). **^{13}C NMR** (75 MHz, Chloroform-*d*) δ 166.5 (C^2), 152.5, 138.4, 137.7, 135.8, 134.0, 132.7 ($C^{9/10}$), 131.6, 130.6 (C^5), 129.7 (C^4), 127.9, 124.9 ($C^{13/14}$), 123.6, 122.6, 122.4 ($C^{9/10}$), 120.1, 119.6 ($C^{13/14}$), 112.3, 52.6 (C^1).**^{11}B NMR** (96 MHz, Chloroform-*d*) δ 1.30 (t, *J* = 34.1 Hz). **^{19}F NMR** (282 MHz, Chloroform-*d*) δ -141.6 (q, *J* = 34.0 Hz).

X-Ray code: mjh230011_fa

7.2.4.5 Methyl 4-(5,5-difluoro-3-iodo-7-(1*H*-pyrrol-2-yl)-5*H*-5λ^4,6λ^4-dipyrrolo[1,2-*c*:2',1'-*f*][1,3,2]diazaborinin-10-yl)benzoate (**5.14**)

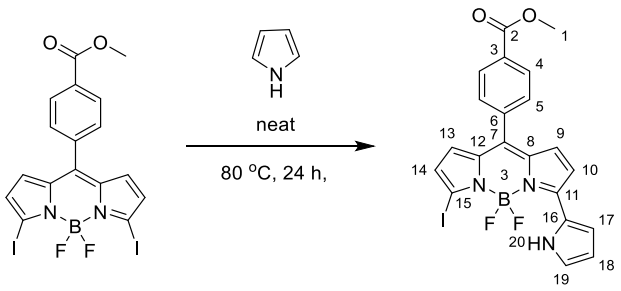

To a 25 mL round bottom flask, under an atmosphere of nitrogen, was added methyl 4-(5,5-difluoro-3,7-diiodo-5*H*-4λ^4,5λ^4-dipyrrolo[1,2-*c*:2',1'-*f*][1,3,2]diazaborinin-10 yl)benzoate (20 mg, 0.03 mmol) and 1*H*-pyrrole (1 mL). The reaction mixture was heated to 80 °C, stirred for 24 hours and diluted with DCM. The solvent and excess amount of pyrrole were removed under reduced pressure. The crude product was purified through silica gel column chromatography (DCM : petrol, 1:1) to give methyl 4-(5,5-difluoro-3-iodo-7-(1*H*-pyrrol-2-yl)-5*H*-5λ^4,6λ^4-dipyrrolo[1,2-*c*:2',1'-*f*][1,3,2]diazaborinin-10-yl)benzoate (13.8 mg, 0.03 mmol, 78%) as a purple solid.

R_f: 0.42 (DCM : petrol, 1:1). **^{1}H NMR** (300 MHz, Chloroform-*d*) δ 10.56 (br, 1H, H^{20}), 8.16 (d, *J* = 8.6 Hz, 2H, H^4), 7.57 (d, *J* = 8.6 Hz, 2H, H^5), 7.28 (ddd, *J* = 2.8, 1.3, 1.3 Hz, 1H), 7.08 (ddd, *J* = 4.0, 2.5, 1.4 Hz, 1H), 6.95 (d, *J* = 4.9 Hz, 1H), 6.84 (d, *J* = 4.9 Hz, 1H), 6.63 (d, *J* = 4.0 Hz, 1H), 6.42 (ddd, *J* = 4.2, 2.3, 2.3 Hz, 1H), 6.39 (d, *J* = 4.0 Hz, 1H), 3.98 (s, 3H, H^1). **^{13}C NMR** (75 MHz, Chloroform-*d*) δ 166.5 (C^2), 152.7, 138.5, 137.9, 136.5, 135.0, 132.7, 131.5, 130.5 (C^5), 129.7 (C^4), 128.0, 127.2, 125.4, 123.6, 122.7, 122.3, 120.1, 112.3, 52.6 (C^1). **^{11}B NMR** (96 MHz, Chloroform-*d*) δ 1.32 (t, *J* = 34.6 Hz). **^{19}F NMR** (282 MHz, Chloroform-*d*) δ -140.4 (q, *J* = 34.5 Hz). **HRMS:** (pNSI) calcd for $C_{21}H_{16}{}^{11}BF_2IN_3O_2$ $[M+H]^+$: 518.0347, found 518.0342.

X-Ray code: mjh230084_fa

7.2.4.6 *N*-(4-(4,4,5,5-tetramethyl-1,3,2-dioxaborolan-2-yl)phenyl)benzamide (**5.20**)

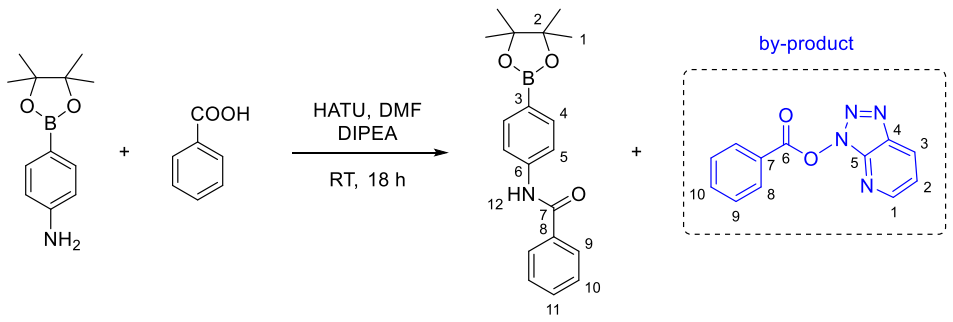

To a 25 mL round bottom flask, under an atmosphere of nitrogen, was added benzoic acid (55.6 mg, 0.46 mmol) and dry DMF (5 mL), then HATU (173 mg, 0.46). 4-(4,4,5,5-Tetramethyl-1,3,2-dioxaborolan-2-yl)aniline (100 mg, 0.46 mmol) dissolved in dry DMF (4 mL) was added into the reaction mixture, then DIPEA (0.19 mL, 1.14 mmol) was added and stirred at room temperature for 18 hours. The reaction mixture was quenched with water then diluted with ethyl acetate (20 mL) washed with NaOH solution (0.2 M)(3 x 20 mL), HCl solution (0.4 M)(3 x 20 mL), and brine. The organic layer was dried over Na_2SO_4, filtered, and the solvent removed under reduced pressure. The crude product was purified through silica gel column chromatography (petrol : ethyl acetate, 2:1) to give *N*-(4-(4,4,5,5-tetramethyl-1,3,2-dioxaborolan-2-yl)phenyl)benzamide (63.6 mg, 0.32 mmol, 71 %) as a white solid.

R_f: 0.67 (petrol : ethyl acetate, 2:1). **^{1}H NMR** (300 MHz, Chloroform-*d*) δ 8.02 (br, 1H, H^{12}), 7.87 – 7.83 (m, 2H), 7.81 (d, *J* = 8.6 Hz, 2H, H^5), 7.68 (d, *J* = 8.6 Hz, 2H, H^4), 7.56 – 7.49 (m, 1H), 7.49 – 7.41 (m, 2H), 1.34 (s, 12H, H^1). **^{13}C NMR** (75 MHz, Chloroform-*d*) δ 165.9 (C^7), 140.8, 136.0, 135.0 (C^5), 132.0, 128.9, 127.2, 124.8 (C^3), 119.1 (C^4), 83.9 (C^2), 25.0 (C^1). **^{11}B NMR** (96 MHz, Chloroform-*d*) δ 30.67.

X-Ray code: mjh230004_2_fa

Note: C^3 was identified via HMBC.

by-product:

3*H*-[1,2,3]triazolo[4,5-b]pyridin-3-yl benzoate (**5.20**)

Yield: (8.3 mg, 0.03 mmol, 8%). **R_f:** 0.40 (petrol : ethyl acetate, 2:1; UV light). **^{1}H NMR** (300 MHz, Chloroform-*d*) δ 8.74 (dd, *J* = 4.5, 1.4 Hz, 1H, $H^{1/2/3}$), 8.46 (dd, *J* = 8.4, 1.4 Hz, 1H, $H^{1/2/3}$), 8.35 – 8.26 (m, 2H, $H^{8/9/10}$), 7.81 – 7.73 (m, 1H, $H^{8/9/10}$), 7.65 – 7.55 (m, 2H, $H^{8/9/10}$), 7.46 (dd, *J* = 8.4, 4.5 Hz, 1H, $H^{1/2/3}$). **^{13}C NMR** (75 MHz, Chloroform-*d*) δ 162.7 (C^6), 151.9 ($C^{1/2/3}$), 140.9 ($C^{4/5}$), 135.6 ($C^{8/9/10}$), 135.2 ($C^{4/5}$), 131.0 ($C^{8/9/10}$), 129.7 ($C^{1/2/3}$), 129.3 ($C^{8/9/10}$), 124.8 (C^7), 121.1 ($C^{1/2/3}$).

7.2.4.7 N^1,N^3,N^5-tris(4-(4,4,5,5-tetramethyl-1,3,2-dioxaborolan-2-yl)phenyl)benzene-1,3,5-tricarboxamide (**5.3**)

Method A:

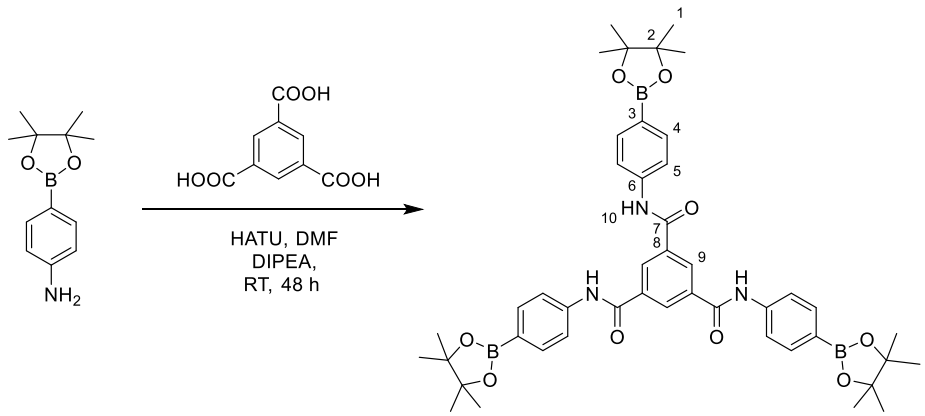

To a round bottom flask, under an atmosphere of nitrogen, was added benzene-1,3,5-tricarboxylic acid (105 mg, 0.50 mmol), HATU (665 mg, 1.75 mmol) and dry DMF (5 mL). 4-(4,4,5,5-Tetramethyl-1,3,2-dioxaborolan-2-yl)aniline (383 mg, 1.75 mmol) dissolved in dry DMF (5 mL) was added into the reaction mixture, then DIPEA (0.48 mL, 5 mmol) was added and stirred at room temperature for 48 hours. The reaction mixture was quenched with water, then diluted with ethyl acetate. The mixture was extracted with further ethyl acetate and the solvent removed under reduced pressure. Methanol was then added to the crude product, filtered, the white solid was washed with water then methanol to give N^1,N^3,N^5-tris(4-(4,4,5,5-tetramethyl-1,3,2-dioxaborolan-2-yl)phenyl)benzene-1,3,5-tricarboxamide (272 mg, 0.33 mmol, 67 %) as a white solid.

Method B:

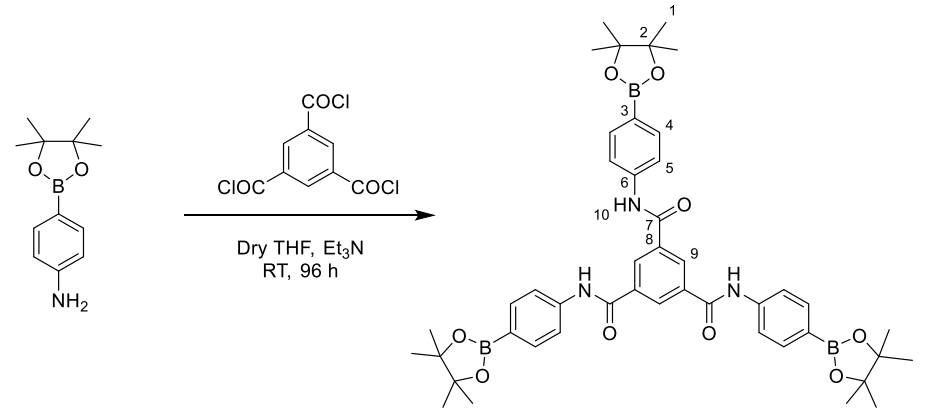

To a round bottom flask, under an atmosphere of nitrogen, was added benzene-1,3,5-tricarbonyl trichloride (133 mg, 0.50 mmol) and dry THF (5 mL) then stirred at 0 °C for 10 min. 4-(4,4,5,5-Tetramethyl-1,3,2-dioxaborolan-2-yl)aniline (438 mg, 2 mmol) was added in small portions then Et_3N

(0.55 mL, 4 mmol) was added to the reaction mixture and stirred at room temperature for 48 hours. The reaction mixture was filtered to collect the solid product. The white solid was washed with water (20 mL) then methanol (20 mL). The product was air-dried overnight to *N*^{1},*N*^{3},*N*^{5}-tris(4-(4,4,5,5-tetramethyl-1,3,2-dioxaborolan-2-yl)phenyl)benzene-1,3,5-tricarboxamide (137 mg, 1.35 mmol, 34 %) as a white solid.

R_f: 0.5 (petrol : ethyl acetate, 7:3; UV light). **^{1}H NMR** (400 MHz, DMSO-d_6) δ 10.67 (s, 3H, H^{10}), 8.71 (s, 3H, H^{9}), 7.86 (d, *J* = 8.6 Hz, 6H, H^{5}), 7.70 (d, *J* = 8.4 Hz, 6H, H^{4}), 1.30 (s, 36H, H^{1}).**^{13}C NMR** (126 MHz, DMSO-d_6) δ 164.6 (C^{7}), 141.8 (C^{6}), 135.34 (C^{8}), 135.26 (C^{4}), 130.0 (C^{9}), 123.7 (C^{3}), 119.4 (C^{5}), 83.5 (C^{2}), 24.7 (C^{1}). **^{11}B NMR** (160 MHz, DMSO-d_6) δ 30.46. **HRMS:** (TOF MS ASAP+) calcd for $C_{45}H_{55}{}^{11}B_3N_3O_9$ $[M+H]^+$: 814.4239, found 814.4247.

X-Ray code: mjh230072_fa

Note: C^{3} was identified via the analysis of HMBC NMR

7.2.4.8 Dibenzo[*b*,*d*]furan-4,6-dicarbaldehyde (**5.5**)

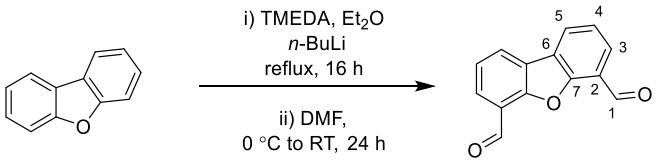

To a Schlenk flask, under nitrogen atmosphere, was added dibenzo[*b,d*]furan (1.92 g, 11.4 mmol), TMEDA (5.1 mL, 34.3 mmol), and dry diethyl ether (67 mL). A (1.6 M) solution of n-butyllithium (21.3 mL, 34.3 mmol) was added dropwise and the mixture refluxed for 16 hours. Dry DMF (2.6 mL, 34.3 mmol) was added over a period of 10 min at 0 °C, then the mixture was stirred at room temperature for 24 hours. The reaction mixture was poured into cold HCl (1 M) (50 mL) and the aqueous layer was extracted with DCM (x 3). The combined organic extracts were washed with water and brine. The organic layer was dried over $MgSO_4$, filtered, and the solvent removed under reduced pressure. The crude product was purified through silica gel column chromatography (DCM) to give dibenzo[*b*,*d*]furan-4,6-dicarbaldehyde (1.41 g, 6.27 mmol, 55%) as a white crystalline solid.

R_f: 0.37 (DCM; UV light). **^{1}H NMR** (700 MHz, Chloroform-*d*) δ 10.70 (s, 2H, H^1), 8.22 (dd, *J* = 7.6, 1.3 Hz, 2H), 8.03 (dd, *J* = 7.6, 1.3 Hz, 2H), 7.54 (t, *J* = 7.6 Hz, 2H). **^{13}C NMR** (176 MHz, Chloroform-*d*) δ 187.4 (C^1), 156.7 (C^6), 127.9 (C^2), 126.8, 124.9, 124.0, 121.9 (C^7). **HRMS:** (pNSI) calcd for $C_{14}H_{12}NO_3$ $[M+NH_4]^+$: 242.0812, found 242.0815.

X-Ray code: mjh230013_fa

Observed data (^{1}H, ^{13}C) are consistent with those previously reported by Lehn *et al*.[101]

7.2.4.9 *Tert*-butyl 2-(2-methoxyphenyl)-1*H*-pyrrole-1-carboxylate (**5.28**)

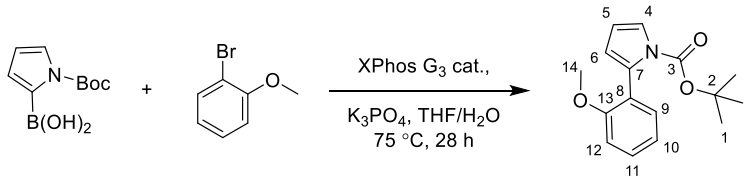

To a Schlenk flask, under nitrogen atmosphere, was added (1-(*tert*-butoxycarbonyl)-1*H*-pyrrol-2-yl)boronic acid (791 mg, 3.75 mmol), 1-bromo-2-methoxybenzene (0.31 mL, 2.5 mmol), XPhos Pd G3 (70 mg, 3 mol %, 0.075 mmol), $K_3PO_4.H_2O$ (1.15 mg, 5 mmol), dry THF (7.5 mL), water (2.5 mL) and was degassed (x3). The reaction mixture was heated, using an oil bath, to 75 °C, stirred for 28 hours then diluted with DCM (50 mL) and washed with water (3 x 50 mL). The organic layer was dried over Na_2SO_4, filtered and the solvent removed under reduced pressure. The crude product was purified through silica gel column chromatography (petrol: ethyl acetate, 15:1) to give *tert*-butyl 2-(2-methoxyphenyl)-1H-pyrrole-1-carboxylate (590 mg, 2.15 mmol, 86 %) as a colourless oil.

R_f: 0.37 (petrol: ethyl acetate, 15:1; UV light). **^{1}H NMR** (400 MHz, Chloroform-*d*) δ 7.40 (dd, *J* = 3.3, 1.8 Hz, 1H), 7.37 – 7.34 (m, 1H), 7.33 – 7.29 (m, 1H), 7.00 (td, *J* = 7.4, 1.0 Hz, 1H), 6.90 (dd, *J* = 8.2, 1.0 Hz, 1H), 6.29 (t, *J* = 3.3 Hz, 1H), 6.19 (dd, *J* = 3.2, 1.8 Hz, 1H), 3.79 (s, 3H, H^{14}), 1.37 (s, 9H, H^1). **^{13}C NMR** (75 MHz, Chloroform-*d*) δ 157.3 (C^3), 149.4, 131.1, 130.2, 128.9, 124.2, 121.7, 120.1, 113.7, 110.3, 109.8, 82.6, 55.1 (C^{14}), 27.4 (C^1).

7.2.4.10 2-(2-Methoxyphenyl)-1*H*-pyrrole (**5.27**)

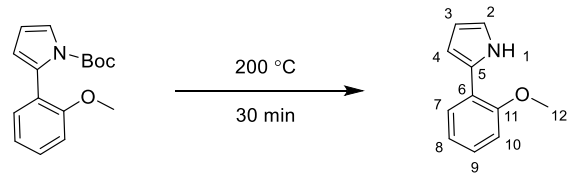

Tert-butyl 2-(2-methoxyphenyl)-1*H*-pyrrole-1-carboxylate (409 mg, 1.49 mmol) was placed in a Schlenk flask under nitrogen atmosphere. Subsequently the flask was heated to 200 °C resulting in the evolution of gas (CO_2, isobutene), and rapid colour change of the oil. After 30 minutes the flask was allowed to cool to room temperature. The dark brown oil was purified through silica gel column chromatography (DCM: hexane, 1:1) to give 2-(2-methoxyphenyl)-1*H*-pyrrole (210 mg, 1.21 mmol, 81%) as a white crystalline solid.

R_f: 0.4 (DCM: hexane, 1:1 ; UV light). **^{1}H NMR** (400 MHz, Chloroform-*d*) δ 9.83 (br, 1H, H^1), 7.68 (dd, *J* = 7.7, 1.7 Hz, 1H), 7.17 (ddd, *J* = 8.2, 7.3, 1.7 Hz, 1H), 7.06 – 6.95 (m, 2H), 6.88 (td, *J* = 2.7, 1.5 Hz, 1H), 6.64 (ddd, *J* = 3.6, 2.5, 1.5 Hz, 1H), 6.30 (dt, *J* = 3.6, 2.6 Hz, 1H), 3.97 (s, 3H, H^{12}). **^{13}C NMR** (75 MHz, Chloroform-*d*) δ 154.8 (C^2), 129.9, 126.8, 126.7, 121.5, 121.2, 117.9, 111.7, 108.9, 106.2, 55.7 (C^1).

X-Ray code: mjh230017_fa

Observed data (^{1}H, ^{13}C) are consistent with those previously reported by Andrioletti *et al*.[104]

7.2.4.11 4,6-Bis((*Z*)-(5-(2-methoxyphenyl)-1*H*-pyrrol-2-yl)(5-(2-methoxyphenyl)-2*H*-pyrrol-2-ylidene)methyl)dibenzo[*b*,*d*]furan (**5.31**)

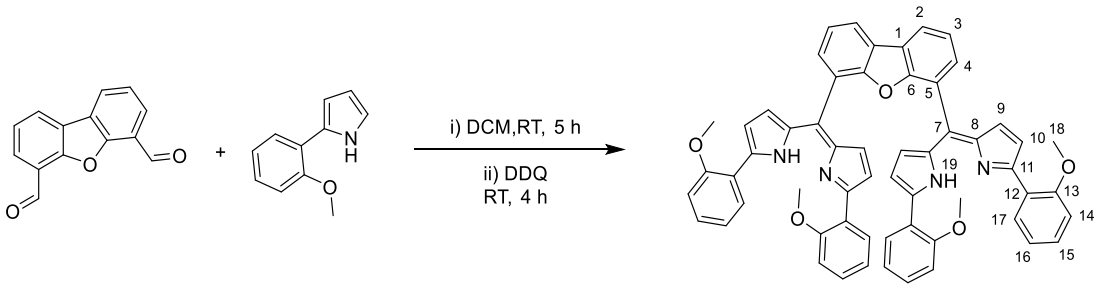

To a Schlenk flask, under nitrogen atmosphere, was added dibenzo[*b*,*d*]furan-4,6-dicarbaldehyde (86.5 mg, 0.39 mmol), 2-(2-methoxyphenyl)-1*H*-pyrrole (250 mg, 1.45 mmol), and dry DCM (40 mL). TFA (37.5 µL, 0.49 mmol) was added into the reaction mixture and stirred for 5 hours at room temperature in the dark (until TLC indicated complete consumption of the aldehyde). DDQ (150 mg, 0.65 mmol) was added, and the reaction was further stirred at room temperature for 4 hours. The reaction mixture was washed with water (x2) and brine. The organic layer was dried over $MgSO_4$, filtered and the solvent removed under reduced pressure. The crude product was purified through silica gel column chromatography (DCM: ethyl acetate, 4:1) to give 4,6-bis((*Z*)-(5-(2-methoxyphenyl)-1*H*-pyrrol-2-yl)(5-(2-methoxyphenyl)-2*H*-pyrrol-2-ylidene)methyl)dibenzo[*b*,*d*]furan (52 mg, 0.06 mmol, 15%).

R_f: 0.4 (DCM: ethyl acetate, 4:1). **^{1}H NMR** (400 MHz, Chloroform-*d*) δ 13.47 (br, 2H, H^{19}), 8.11 (dd, *J* = 7.7, 1.3 Hz, 2H), 7.86 (dd, *J* = 7.6, 1.7 Hz, 4H), 7.58 (dd, *J* = 7.4, 1.3 Hz, 2H), 7.45 (t, *J* = 7.6 Hz, 2H), 7.26 – 7.20 (m, 4H), 6.92 – 6.84 (m, 8H), 6.75 (d, *J* = 4.3 Hz, 4H, $H^{9/10}$), 6.44 (d, *J* = 4.3 Hz, 4H, $H^{9/10}$), 3.72 (s, 12H, H^{18}). **^{13}C NMR** (126 MHz, Chloroform-*d*) δ 157.4, 154.7, 152.4, 140.9, 133.0, 130.7, 129.4, 129.2, 128.4 ($C^{9/10}$), 124.4, 122.9, 122.8, 122.3, 121.0, 120.9, 118.6 ($C^{9/10}$), 111.6, 56.0 (C^{18}).

Observed data (^{1}H, ^{13}C) are consistent with those previously reported by *Harvey et al*.[98]

7.2.4.12 Stacked Helically Chiral bis BODIPYs (**5.6a**) and (**5.6b**)

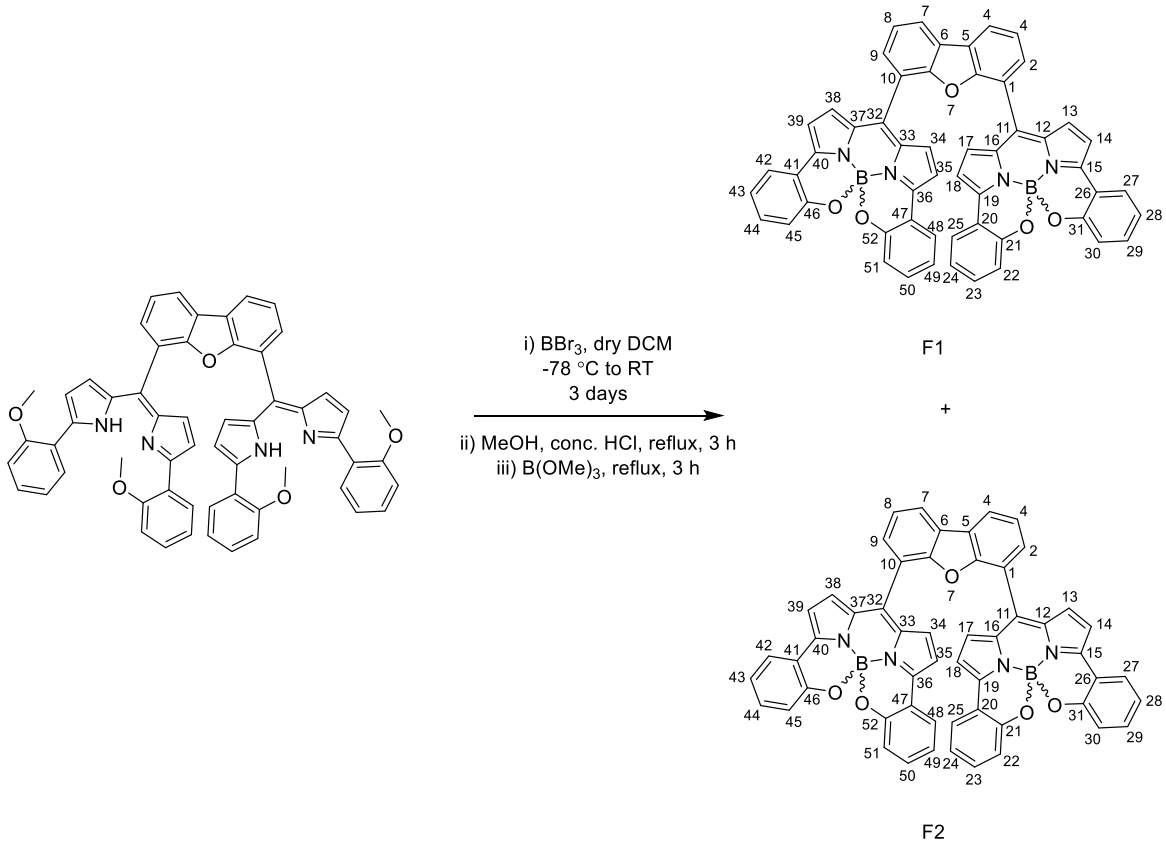

To a 25 mL round bottom flask, under an atmosphere of nitrogen, was added 4,6-bis((*Z*)-(5-(2-methoxyphenyl)-1*H*-pyrrol-2-yl)(5-(2-methoxyphenyl)-2*H*-pyrrol-2-ylidene)methyl)dibenzo[*b*,*d*]furan (35.7 mg, 0.04 mmol) and Dry DCM (3.5 mL). BBr_3 (0.14 mL, 1.48 mmol) was added to the reaction mixture at -78 °C. The reaction mixture was stirred for 3 days allowed to warm up to room temperature and quenched with methanol. The mixture was evaporated and dissolved again with methanol. Conc. HCl (0.35 mL) was added to reaction mixture and heated to reflux for 3 hours. The reaction mixture was left to cool to room temperature and neutralized with saturated solution of $NaHCO_3$ then extracted with ethyl acetate. The organic layer was dried over Na_2SO_4, filtered, and the solvent removed under reduced pressure. The crude product was dissolved in dry $CHCl_3$ (7 mL) under an atmosphere of nitrogen. $B(OMe)_3$ (72 µL) was added, and the mixture was heated to reflux for 3 h. The reaction mixture was left to cool to room temperature and the solvent removed under reduced pressure. The crude product was purified through silica gel column chromatography (DCM : toluene, 1:1) to give stacked helically chiral bis BODIPYs as a two diastereomers with combined yields (1.4 mg, 0.001 mmol, 4%) as a green solid.

F1 (5.6a)

Yield: (0.7 mg, 0.0008 mmol, 2.1%). **R_f:** 0.6 (DCM: toluene, 1:1). **^{1}H NMR** (700 MHz, Acetone-*d_4*) δ 8.53 (dd, *J* = 7.9, 1.2 Hz, 2H), 8.02 (dd, *J* = 7.7, 1.7 Hz, 2H), 7.97 (dd, *J* = 7.5, 1.3 Hz, 2H), 7.82 (dd, *J* = 7.6, 1.6 Hz, 2H), 7.74 (t, *J* = 7.6 Hz, 2H), 7.60 (d, *J* = 4.4 Hz, 2H), 7.38 (ddd, *J* = 8.3, 7.3, 1.7 Hz, 2H), 7.28 (ddd, *J* = 8.6, 7.2, 1.7 Hz, 2H), 7.24 (d, *J* = 4.4 Hz, 2H), 7.12 (td, *J* = 7.5, 1.1 Hz, 2H), 7.05 (d, *J* = 4.4 Hz, 2H), 7.00 (d, *J* = 4.4 Hz, 2H), 6.98 (dd, *J* = 7.5, 1.2 Hz, 1H), 6.86 (dd, *J* = 8.4, 1.1 Hz, 2H), 6.76 (dd, *J* = 8.5, 1.2 Hz, 2H). **^{11}B NMR** (96 MHz, Acetone-*d_4*) δ -0.95. **HRMS:** (pNSI) calcd for $C_{54}H_{31}{}^{11}B_2N_4O_5$ $[M+H]^+$: 837.2492, found 837.2498. **UV-Vis:** λ_{max} (abs) = 624 nm. $\boldsymbol{\phi_F}$ = 0.39 (DCM).

F2 (5.6b)

Yield: (0.3 mg, 0.0004 mmol, 0.9%). **R_f:** 0.5 (DCM: toluene, 1:1). **^{1}H NMR** (700 MHz, Acetone-*d_4*) δ 8.50 (dd, *J* = 7.9, 1.2 Hz, 2H), 7.96 (dd, *J* = 7.7, 1.7 Hz, 2H), 7.89 (dd, *J* = 7.4, 1.2 Hz, 2H), 7.71 (t, *J* = 7.6 Hz, 2H), 7.61 (dd, *J* = 7.8, 1.7 Hz, 2H), 7.36 (ddd, *J* = 8.5, 7.2, 1.7 Hz, 2H), 7.34 – 7.29 (m, 2H), 7.20 (d, *J* = 4.3 Hz, 2H), 7.16 (d, *J* = 4.3 Hz, 2H), 7.12 – 7.08 (m*, 4H), 7.00 (td, *J* = 7.5, 1.1 Hz, 2H), 6.81 (dd, *J* = 8.3, 1.1 Hz, 2H), 6.78 (dd, *J* = 8.3, 1.1 Hz, 2H), 6.74 (d, *J* = 4.4 Hz, 2H). **^{11}B NMR** (96 MHz, Acetone-*d_4*) δ -0.89. **HRMS:** (pNSI) calcd for $C_{54}H_{31}{}^{11}B_2N_4O_5$ $[M+H]^+$: 837.2492, found 837.2492. **UV-Vis:** λ_{max} (abs) = 625 nm. $\boldsymbol{\phi_F}$ = 0.55 (DCM).

*Doublet corresponding to two pyrrolic protons with multiplet underneath corresponding to two aromatic protons.

Note: The NMR data analysis for F2(**5.6b**) was based on the mix fractions NMR of (**5.6a** ana **5.6b**) after the first column chromatography.

7.2.4.13 Chiral *meso*-(trifluoromethyl)-*N*,*N*,*O*,*O*-BODIPY (**5.29**)

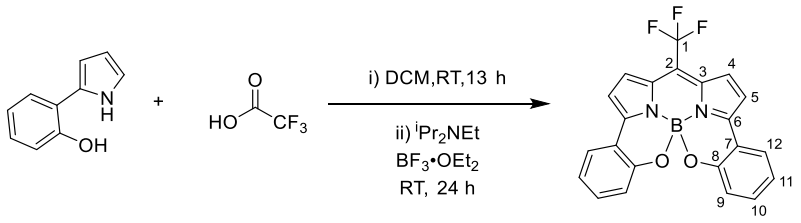

To a 25 mL round bottom flask, under an atmosphere of nitrogen, was added 2-(1*H*-pyrrol-2-yl)phenol (34.9 mg, 0.25 mmol), dry DCM (3 mL), and TFA (10 µL, 0.13 mmol). The reaction mixture was stirred at room temperature for 13 hours. Following reaction time, $^{i}Pr_2NEt$ (60 µL, 0.38 mmol) and $BF_3.OEt_2$ was added to the reaction mixture and stirred for 24 hours at room temperature. The reaction mixture was diluted with DCM, quenched with saturated solution of $NaHCO_3$, and washed with water and brine. The organic layer was dried over $MgSO_4$, filtered, and the solvent removed under reduced pressure. The crude product was purified through silica gel column chromatography (toluene) to give chiral *meso*-(trifluoromethyl)-*N*,*N*,*O*,*O*-BODIPY (5 mg, 0.01 mmol, 10%) as a green solid.

R_f: 0.75 (DCM: toluene, 1:1). **^{1}H NMR** (700 MHz, Chloroform-*d*) δ 7.80 (dd, *J* = 7.5, 1.9 Hz, 2H, Ar), 7.50 (dq, *J* = 4.3, 2.1 Hz, 2H, H^4), 7.38 (ddd, *J* = 8.3, 7.2, 1.7 Hz, 2H, Ar), 7.08 (ddd, *J* = 7.8, 7.2, 1.1 Hz, 2H, Ar), 7.01 (d, *J* = 4.6 Hz, 2H, H^5), 6.95 (dd, *J* = 8.2, 1.1 Hz, 2H, Ar). **^{13}C NMR** (176 MHz, Chloroform-*d*) δ 154.7, 152.8, 133.5, 132.3, 128.9 (C^4), 127.33 (q, $^{1}J_{C\text{-}F}$ = 244.9 Hz, H^1), 126.3, 121.51 (q, $^{2}J_{C\text{-}F}$ = 34.4 Hz, H^2), 120.9, 119.9, 118.8, 117.9 (C^5). **^{11}B NMR** (96 MHz, Chloroform-*d*) δ -0.93. **^{19}F NMR** (282 MHz, Chloroform-*d*) δ -55.9.

X-Ray code: mjh230036_fa

7.3 Photophysical and Chiroptical Measurements

7.3.1 UV/Vis Absorption and Emission spectra.

7.3.1.1 Methyl 4-(3-(((1*S*,2*S*)-2-amino-1,2-diphenylethyl)amino)-7-bromo-5,5-difluoro-5*H*-5λ^4,6λ^4-dipyrrolo[1,2-*c*:2',1'-*f*][1,3,2]diazaborinin-10-yl)benzoate (**2.18**)

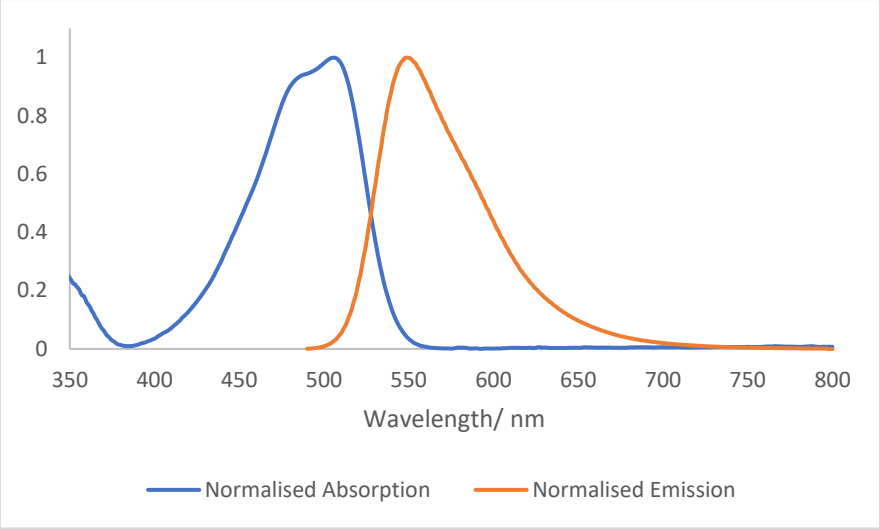

Figure 7.1: Normalised absorption and emission spectra of BODIPY (**2.18**), measured in DCM. Excitation wavelength for emission: 480 nm (DCM).

7.3.1.2 Methyl 4-(3-(((1*S*,2*S*)-2-amino-1,2-diphenylethyl)amino)-5,5-difluoro-7-iodo-5*H*-5λ^4,6λ^4-dipyrrolo[1,2-*c*:2',1'-*f*][1,3,2]diazaborinin-10-yl)benzoate (**2.19**)

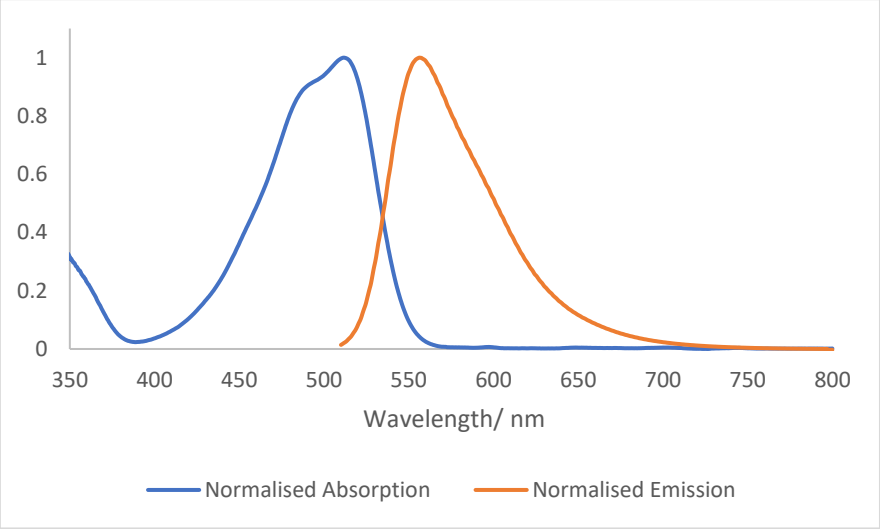

Figure 7.2: Normalised absorption and emission spectra of BODIPY (**2.19**), measured in DCM. Excitation wavelength for emission: 500 nm (DCM).

7.3.1.3 Methyl 4-(3-(((1S,2S)-2-((5,5-difluoro-7-iodo-10-(4-(methoxycarbonyl)phenyl)-5*H*-5λ^4,6λ^4-dipyrrolo[1,2-*c*:2',1'-*f*][1,3,2]diazaborinin-3-yl)amino)-1,2-diphenylethyl)amino)-5,5-difluoro-7-iodo-5*H*-5λ^4,6λ^4-dipyrrolo[1,2-*c*:2',1'-*f*][1,3,2]diazaborinin-10-yl)benzoate (**2.4**)

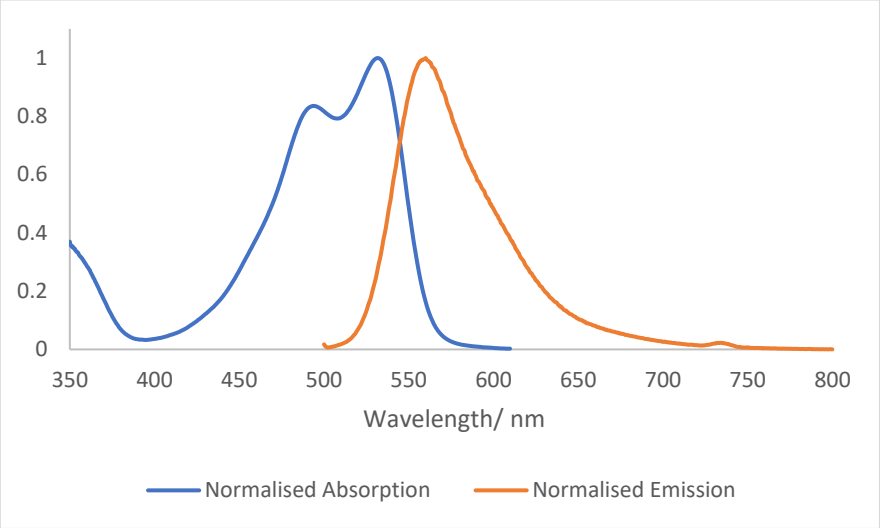

Figure 7.3: Normalised absorption and emission spectra of BODIPY (**2.4**), measured in DCM. Excitation wavelength for emission: 490 nm (DCM).

7.3.1.4 Methyl (*S*)-4-(10b-(4-fluorophenyl)-10-((1-hydroxybutan-2-yl)amino)-10b*H*-11-oxa-4b^1,10aλ^4-diaza-10bλ^4-boracyclopenta[*e*]aceanthrylen-7-yl)benzoate (**3.7a**)

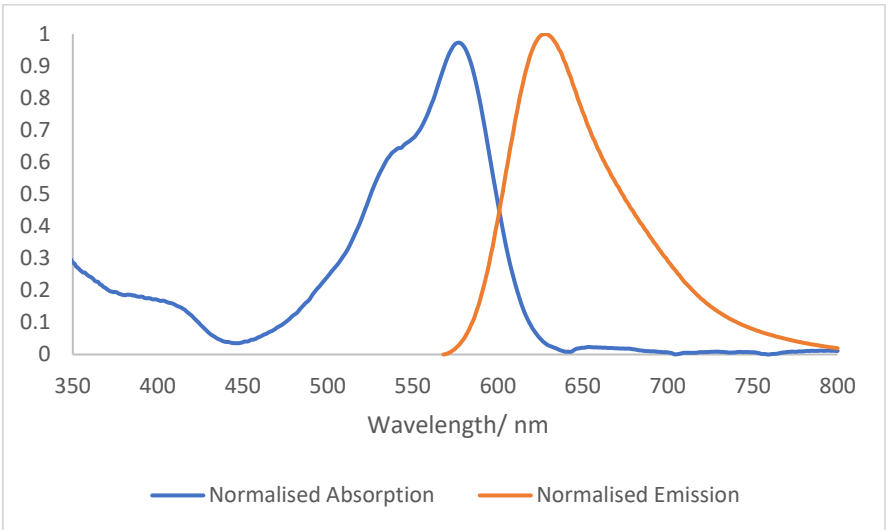

Figure 7.4: Normalised absorption and emission spectra of BODIPY (**3.7a**), measured in DCM. Excitation wavelength for emission: 554 nm (DCM).

7.3.1.5 Methyl (*S*)-4-(10b-(4-fluorophenyl)-10-((1-hydroxybutan-2-yl)amino)-10b*H*-11-oxa-4b^{1},10aλ^{4}-diaza-10bλ^{4}-boracyclopenta[*e*]aceanthrylen-7-yl)benzoate (**3.7b**)

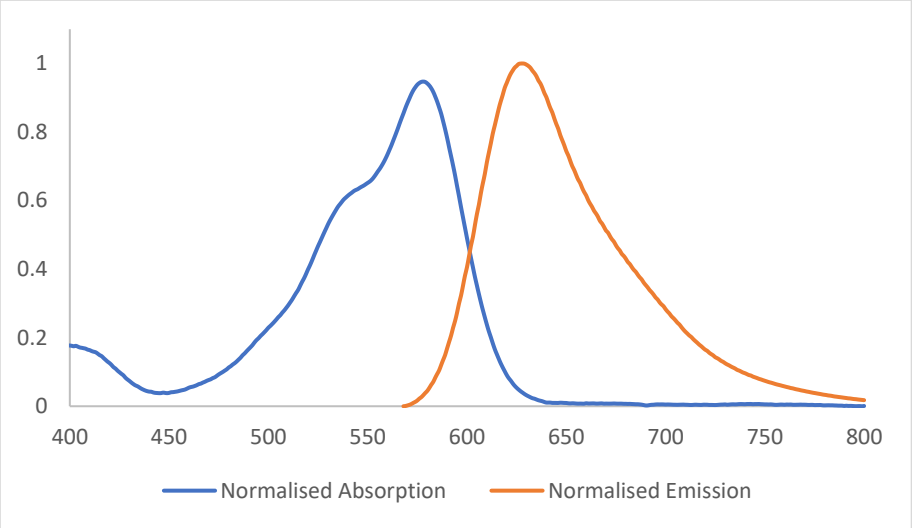

Figure 7.5: Normalised absorption and emission spectra of BODIPY (**3.7b)**, measured in DCM. Excitation wavelength for emission: 554 nm (DCM).

7.3.1.6 Methyl (*S*)-4-(10-((1-hydroxybutan-2-yl)amino)-10b-(4-(trifluoromethyl)phenyl)-10b*H*-11-oxa-4b^{1}, 10aλ^{4}-diaza-10bλ^{4}-boracyclopenta[*e*]aceanthrylen-7-yl)benzoate (**3.46a**)

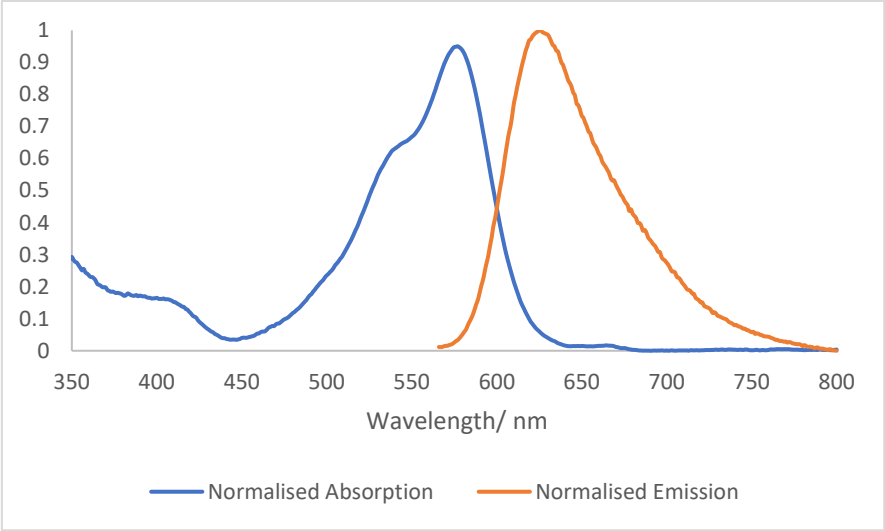

Figure 7.6: Normalised absorption and emission spectra of BODIPY (**3.46a**), measured in DCM. Excitation wavelength for emission: 570 nm (DCM).

7.3.1.7 Methyl (*S*)-4-(10-((1-hydroxybutan-2-yl)amino)-10b-(4-(trifluoromethyl)phenyl)-10b*H*-11-oxa-4b^{1}, 10aλ^{4}-diaza-10bλ^{4}-boracyclopenta[*e*]aceanthrylen-7-yl)benzoate (**3.46b**)

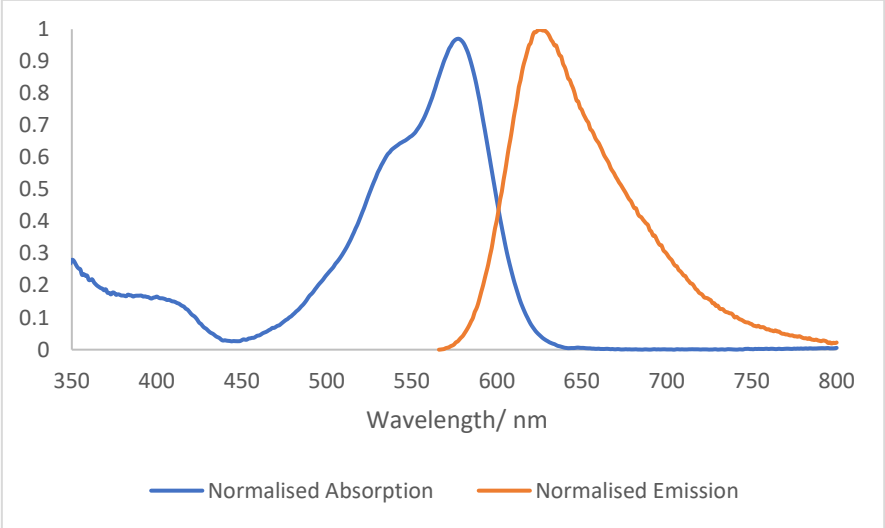

Figure 7.7: Normalised absorption and emission spectra of BODIPY (**3.46b**), measured in DCM. Excitation wavelength for emission: 630 nm (DCM).

7.3.1.8 Methyl (*S*)-4-(10-((1-hydroxybutan-2-yl)amino)-10b-(*p*-tolyl)-10b*H*-11-oxa-4b^{1}, 10aλ^{4}-diaza-10bλ^{4}-boracyclopenta[*e*]aceanthrylen-7-yl)benzoate (**3.49a**)

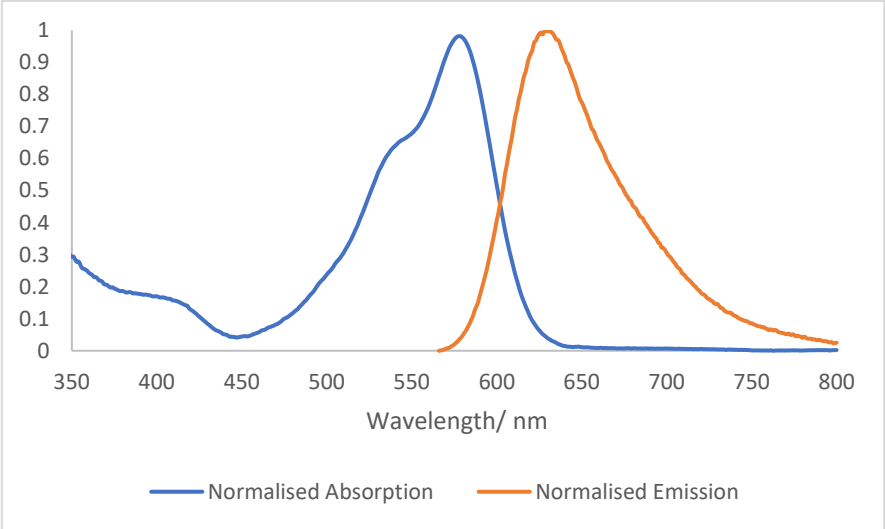

Figure 7.8: Normalised absorption and emission spectra of BODIPY (**3.49a**), measured in DCM. Excitation wavelength for emission: 542 nm (DCM).

7.3.1.9 Methyl (*S*)-4-(10-((1-hydroxybutan-2-yl)amino)-10b-(*p*-tolyl)-10b*H*-11-oxa-4b^{1}, 10aλ^{4}-diaza-10bλ^{4}-boracyclopenta[*e*]aceanthrylen-7-yl)benzoate (**3.49b**)

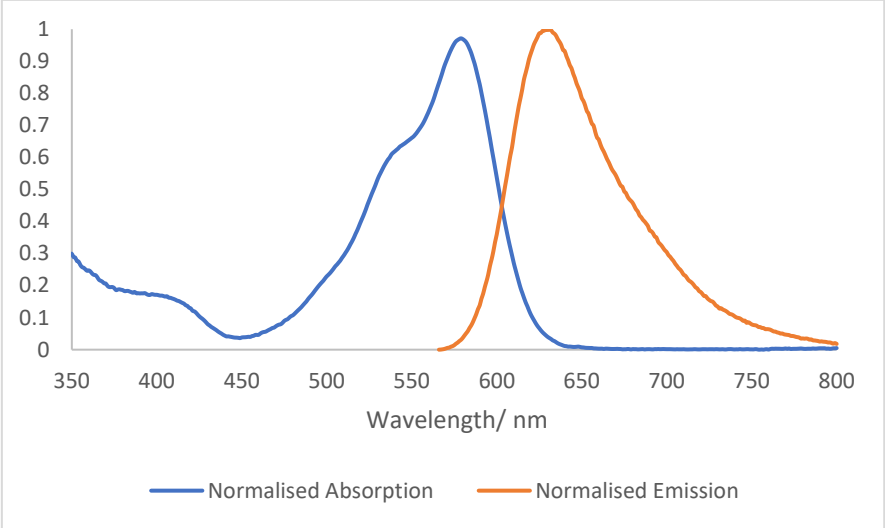

Figure 7.9: Normalised absorption and emission spectra of BODIPY (**3.49b**), measured in DCM. Excitation wavelength for emission: 542 nm (DCM).

7.3.1.10 Dimethyl 4,4'-(1,4-phenylenebis(10-(((*S*)-1-hydroxybutan-2-yl)amino)-10b*H*-11-oxa-4b^{1},10aλ^{4}-diaza-10bλ^{4}-boracyclopenta[*e*]aceanthrylene-10b,7-diyl))dibenzoate (**5.2a**)

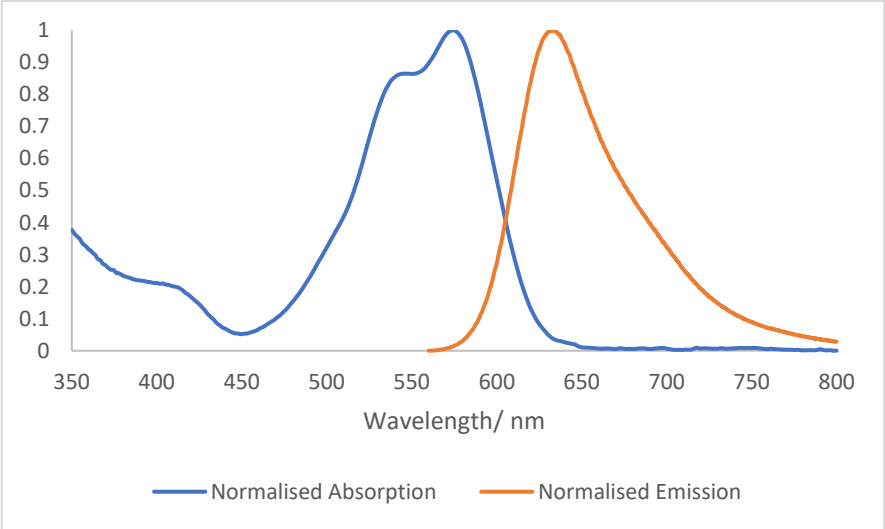

Figure 7.10: Normalised absorption and emission spectra of BODIPY (**5.2a**), measured in DCM. Excitation wavelength for emission: 550 nm (DCM).

7.3.1.11 Dimethyl 4,4'-(1,4-phenylenebis(10-(((*S*)-1-hydroxybutan-2-yl)amino)-10b*H*-11-oxa-4b^{1},10aλ^{4}-diaza-10bλ^{4}-boracyclopenta[*e*]aceanthrylene-10b,7-diyl))dibenzoate (**5.2b**)

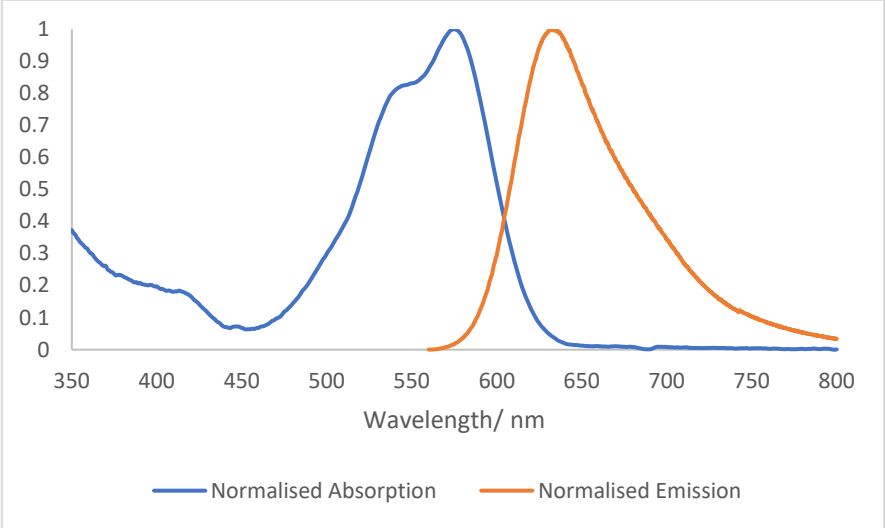

Figure 7.11: Normalised absorption and emission spectra of BODIPY (**5.2b**), measured in DCM. Excitation wavelength for emission: 550 nm (DCM).

7.3.1.12 Dimethyl 4,4'-(1,4-phenylenebis(10-(((*S*)-1-hydroxybutan-2-yl)amino)-10b*H*-11-oxa-4b^{1},10aλ^{4}-diaza-10bλ^{4}-boracyclopenta[*e*]aceanthrylene-10b,7-diyl))dibenzoate (**5.2c**)

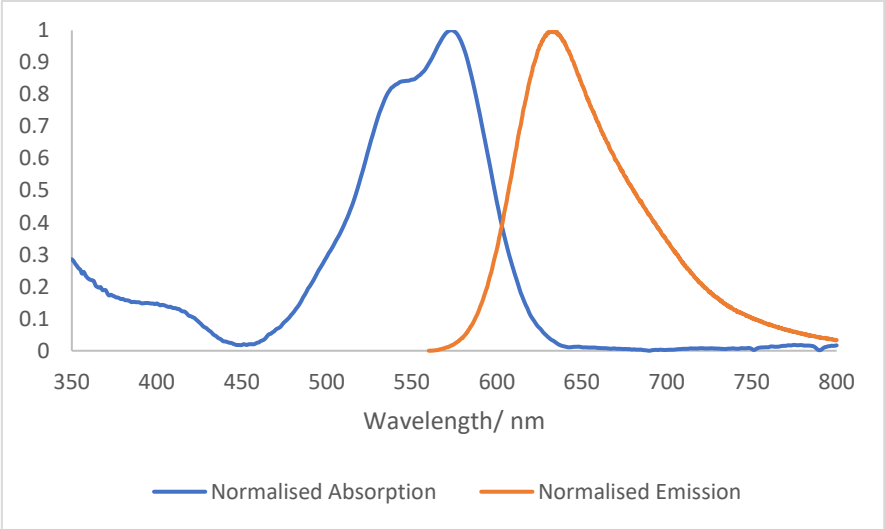

Figure 7.12: Normalised absorption and emission spectra of BODIPY (**5.2c**), measured in DCM. Excitation wavelength for emission: 550 nm (DCM).

7.3.1.13 Helically chiral methyl (4-chlorophenyl)-2-methylenepentanoate substituted *N*,*N*,*O*,*O*-BODIPY (**4.7**)

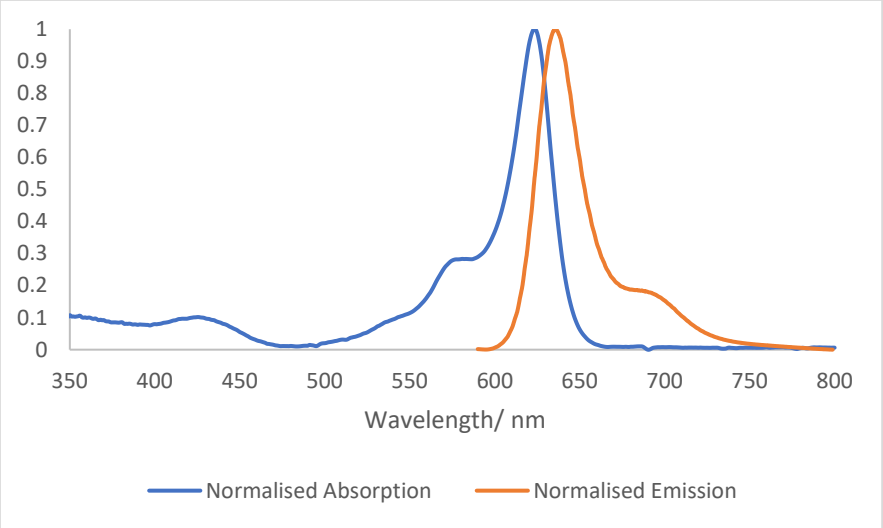

Figure 7.13: Normalised absorption and emission spectra of BODIPY (**4.7**), measured in DCM. Excitation wavelength for emission: 590 nm (DCM).

7.3.1.14 Stacked Helically Chiral bis BODIPYs (**5.6a**)

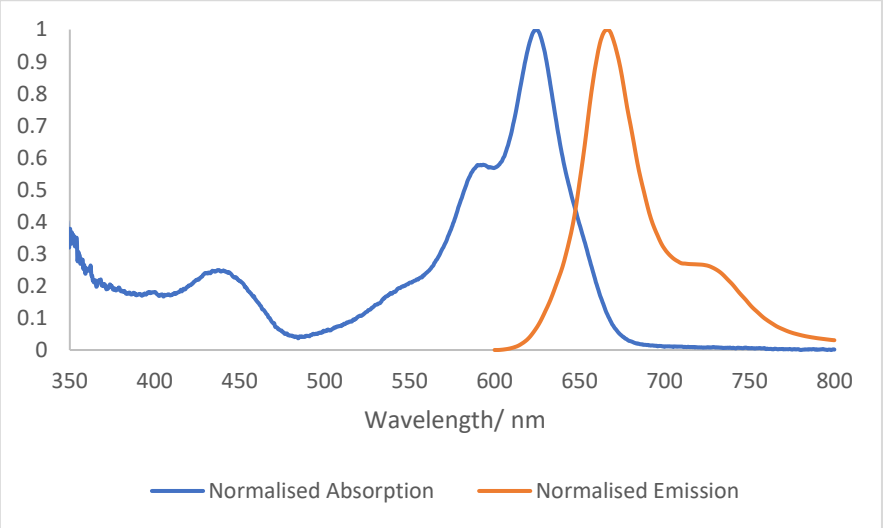

Figure 7.14: Normalised absorption and emission spectra of BODIPY (**5.6a**), measured in DCM. Excitation wavelength for emission: 592 nm (DCM).

7.3.1.15 Stacked Helically Chiral bis BODIPYs (**5.6b**)

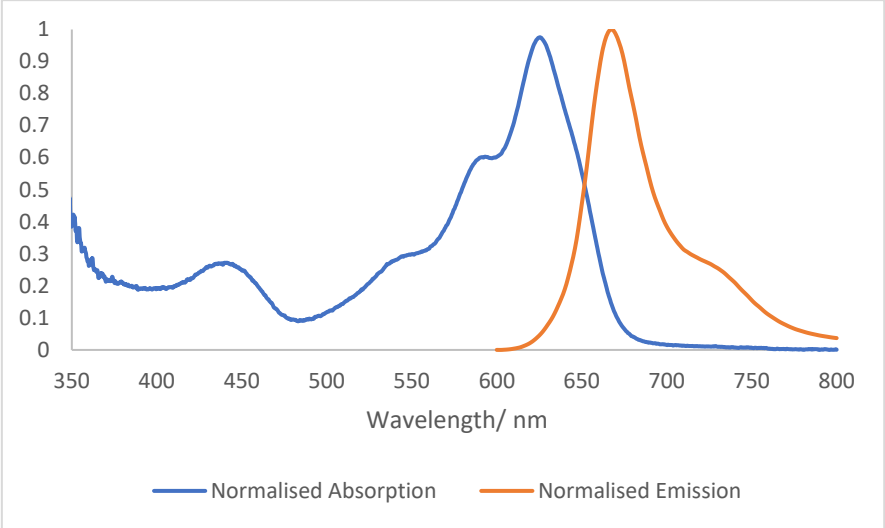

Figure 7.15: Normalised absorption and emission spectra of BODIPY (**5.6b)**, measured in DCM. Excitation wavelength for emission: 592 nm (DCM).

7.3.2 Molar Extinction Coefficient Measurements and UV/Vis absorption Spectra

Molar extinction coefficients were determined by measuring the absorbance at the wavelength of maximum absorption (λ_{max}) across a 5 to 8 points dilution series. Subsequently, the absorbance values for each point in the series were plotted against their respective molar concentrations. This allowed for the calculation of the molar extinction coefficient (ε) using the following equation:

$$A = \varepsilon c l$$

Where A = absorption, ε = molar extinction coefficient ($M^{-1}cm^{-1}$), c = concentration (M), and l = path length (cm).

7.3.2.1 Methyl 4-(3-(((1*S*,2*S*)-2-amino-1,2-diphenylethyl)amino)-5,5-difluoro-7-iodo-5*H*-5λ^4,6λ^4-dipyrrolo[1,2-*c*:2',1'-*f*][1,3,2]diazaborinin-10-yl)benzoate (**2.19**)

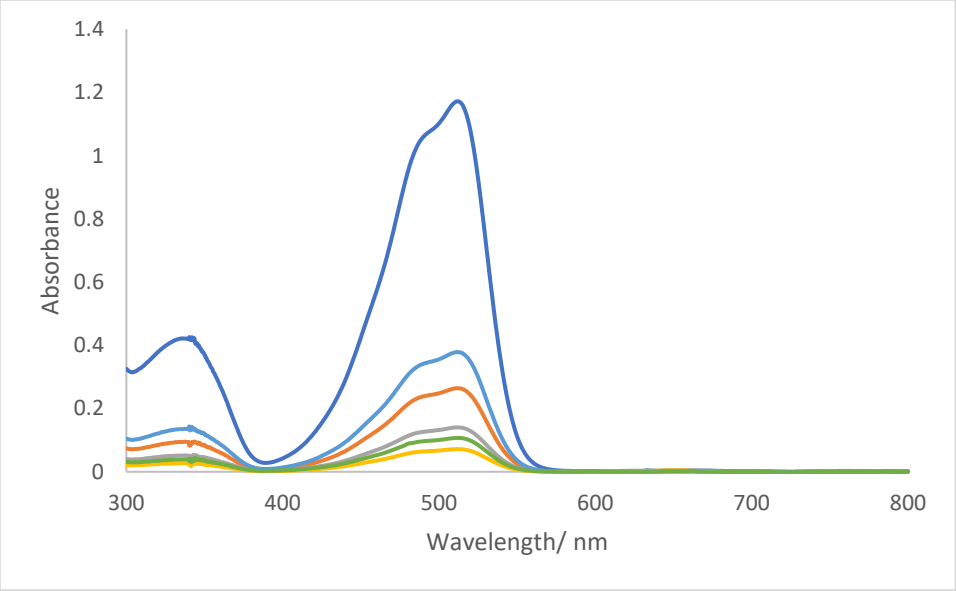

Figure 7.16: UV-vis spectrum of BODIPY (**2.19**) in DCM, concentrations (M): 1.75 x10^{-5}, 3.50 x10^{-6}, 1.75 x10^{-6}, 8.75 x10^{-7}, 5.25 x10^{-6}, 1.31 x10^{-6}, respectively.

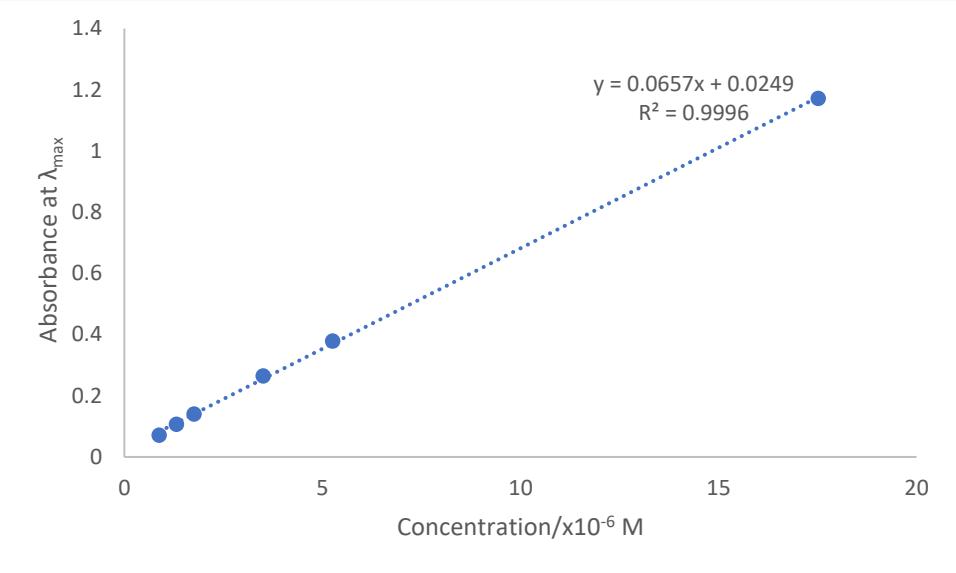

Figure 7.17: Absorbance of BODIPY (**2.19**) at λ_{max} with respect to concentration, molar extinction coefficient (ε) = 65,688 M^{-1} cm^{-1}

7.3.2.2 Methyl 4-(3-(((1S,2S)-2-((5,5-difluoro-7-iodo-10-(4-(methoxycarbonyl)phenyl)-5*H*-5λ^4,6λ^4-dipyrrolo[1,2-*c*:2',1'-*f*][1,3,2]diazaborinin-3-yl)amino)-1,2-diphenylethyl)amino)-5,5-difluoro-7-iodo-5*H*-5λ^4,6λ^4-dipyrrolo[1,2-*c*:2',1'-*f*][1,3,2]diazaborinin-10-yl)benzoate (**2.4**)

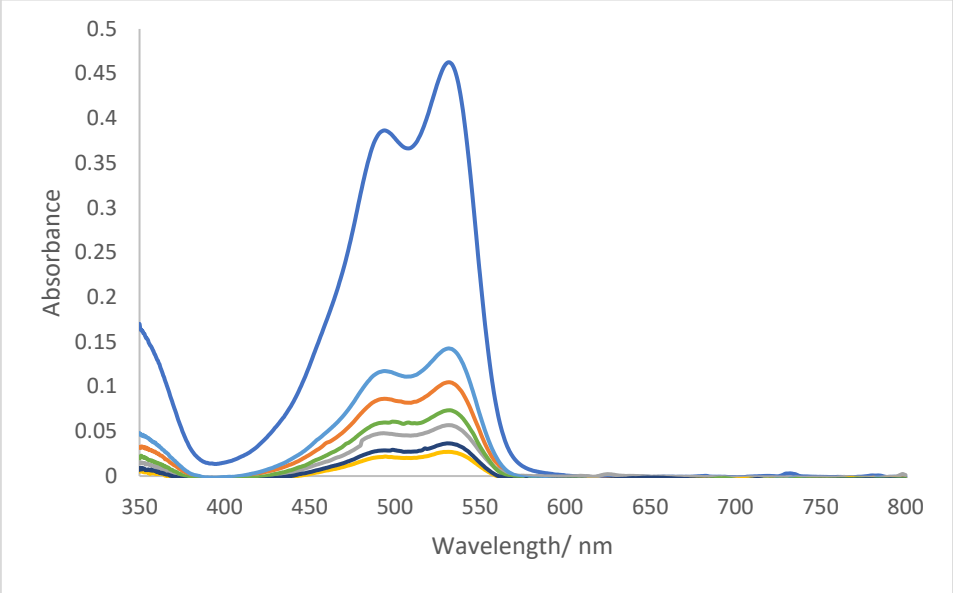

Figure 7.18: UV-vis spectrum of BODIPY (**2.4**) in DCM, concentrations (M): 1.08 x10^{-5}, 2.16 x10^{-6}, 1.08 x10^{-6}, 5.39 x10^{-7}, 3.24 x10^{-6}, 1.62 x10^{-6}, 8.09 x10^{-7} respectively.

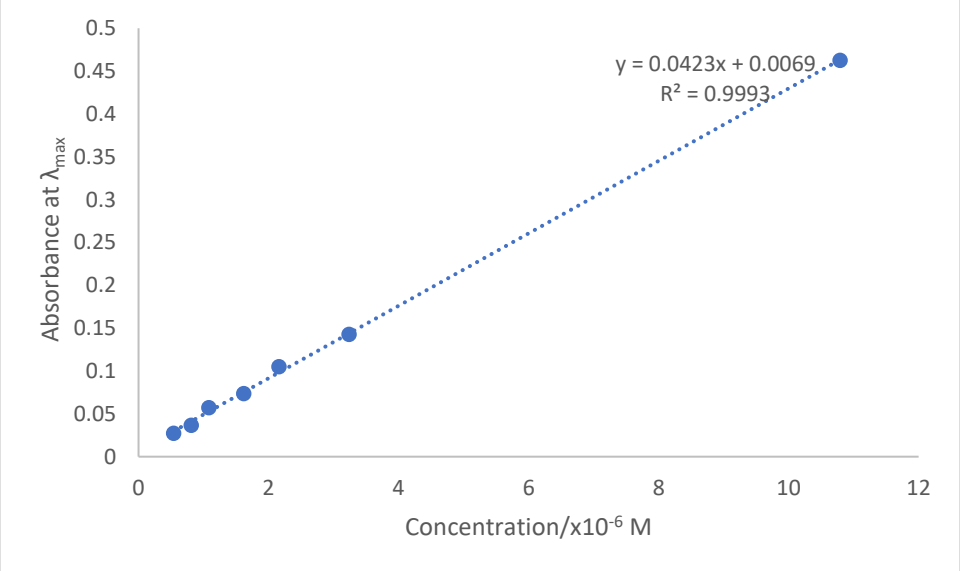

Figure 7.19: Absorbance of BODIPY (**2.4**) at λ_{max} with respect to concentration, molar extinction coefficient (ε) = 42,276 M^{-1} cm^{-1}

7.3.2.3 Methyl (*S*)-4-(10b-(4-fluorophenyl)-10-((1-hydroxybutan-2-yl)amino)-10b*H*-11-oxa-4b^{1},10aλ^{4}-diaza-10bλ^{4}-boracyclopenta[*e*]aceanthrylen-7-yl)benzoate (**3.7a**)

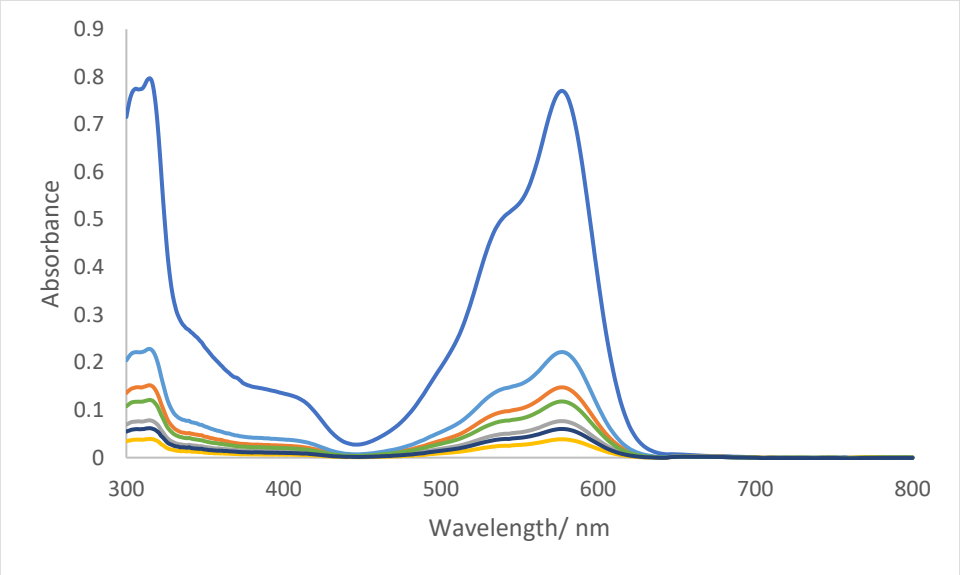

Figure 7.20: UV-vis spectrum of BODIPY (**3.7a**) in DCM, concentrations (M): 1.78 x10^{-5}, 3.56 x10^{-6}, 1.78 x10^{-6}, 8.91 x10^{-7}, 5.34 x10^{-6}, 2.67 x10^{-6}, 1.34 x10^{-6} respectively.

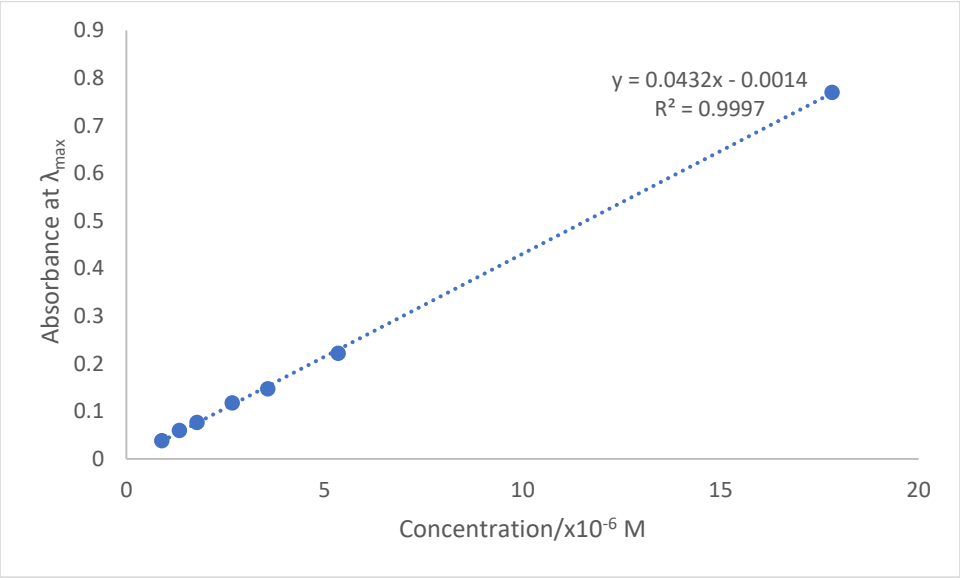

Figure 7.21: Absorbance of BODIPY (**3.7a**) at λ_{max} with respect to concentration, molar extinction coefficient (ε) = 43,212 M^{-1} cm^{-1}

7.3.2.4 Methyl (*S*)-4-(10b-(4-fluorophenyl)-10-((1-hydroxybutan-2-yl)amino)-10b*H*-11-oxa-4b^{1},10aλ^{4}-diaza-10bλ^{4}-boracyclopenta[*e*]aceanthrylen-7-yl)benzoate (**3.7b**)

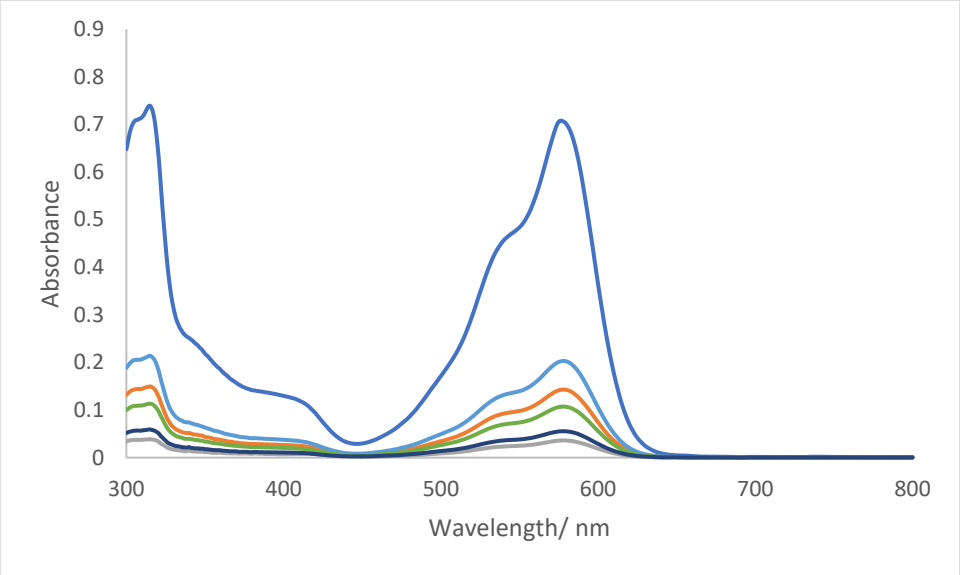

Figure 7.22: UV-vis spectrum of BODIPY (**3.7b**) in DCM, concentrations (M): 1.78 x10^{-5}, 3.56 x10^{-6}, 8.91 x10^{-7}, 5.34 x10^{-6}, 2.67 x10^{-6}, 1.34 x10^{-6} respectively.

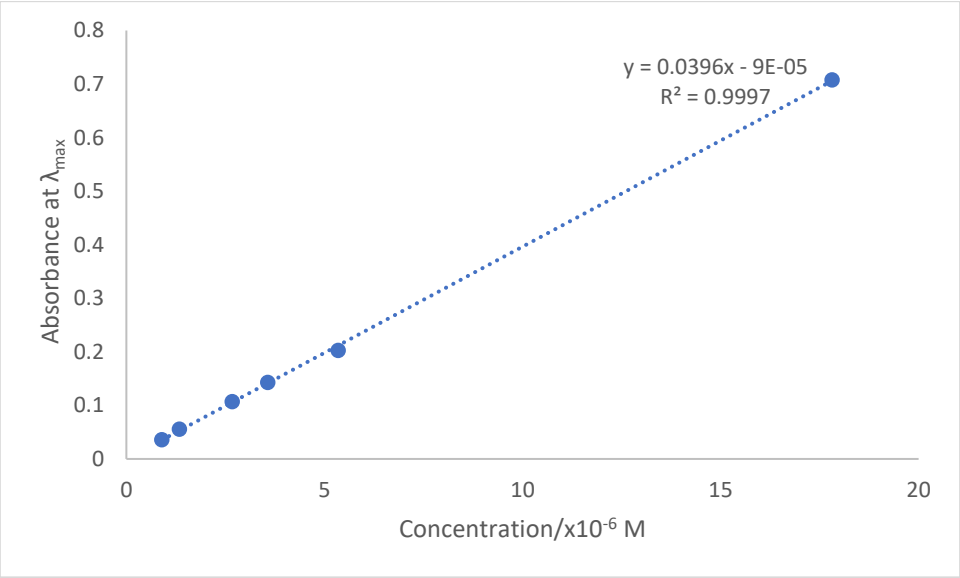

Figure 7.23: Absorbance of BODIPY (**3.7b**) at λ_{max} with respect to concentration, molar extinction coefficient (ε) = 39,637 M^{-1} cm^{-1}

7.3.2.5 Methyl (*S*)-4-(10-((1-hydroxybutan-2-yl)amino)-10b-(4-(trifluoromethyl)phenyl)-10b*H*-11-oxa-4b^{1}, 10aλ^{4}-diaza-10bλ^{4}-boracyclopenta[*e*]aceanthrylen-7-yl)benzoate (**3.46a**)

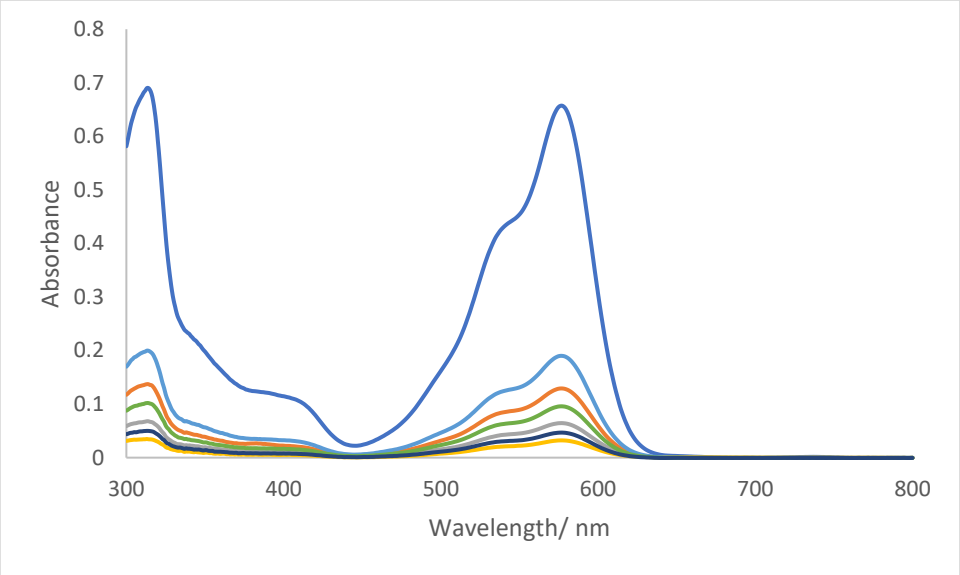

Figure 7.24: UV-vis spectrum of BODIPY (**3.46a**) in DCM, concentrations (M): 1.64 x10^{-5}, 3.27 x10^{-6}, 1.64 x10^{-6} 8.18 x10^{-7}, 4.91 x10^{-6}, 2.45 x10^{-6}, 1.23 x10^{-6} respectively.

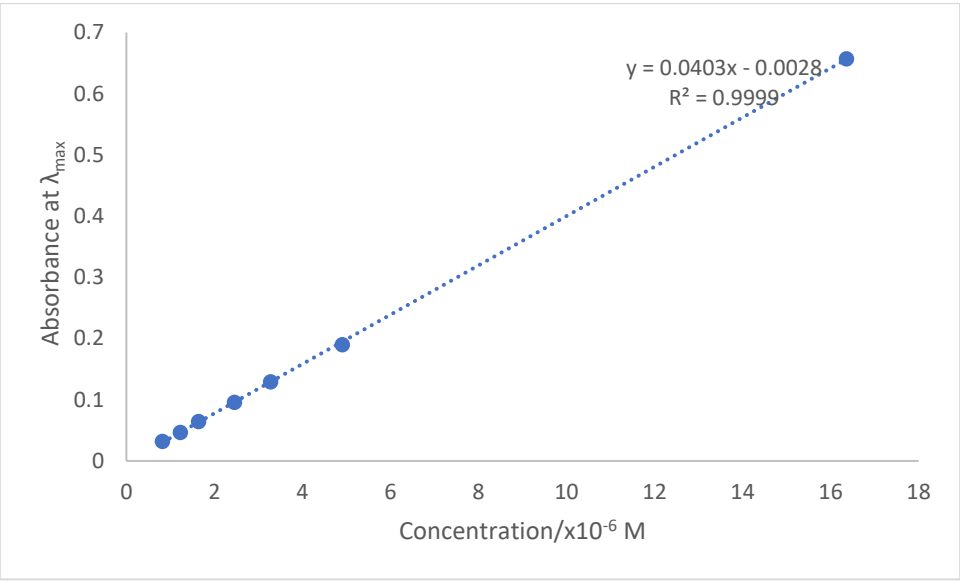

Figure 7.25: Absorbance of BODIPY (**3.46a**) at λ_{max} with respect to concentration, molar extinction coefficient (ε) = 40,285 M^{-1} cm^{-1}

7.3.2.6 Methyl (*S*)-4-(10-((1-hydroxybutan-2-yl)amino)-10b-(4-(trifluoromethyl)phenyl)-10b*H*-11-oxa-4b^{1}, 10aλ^{4}-diaza-10bλ^{4}-boracyclopenta[*e*]aceanthrylen-7-yl)benzoate (**3.46b**)

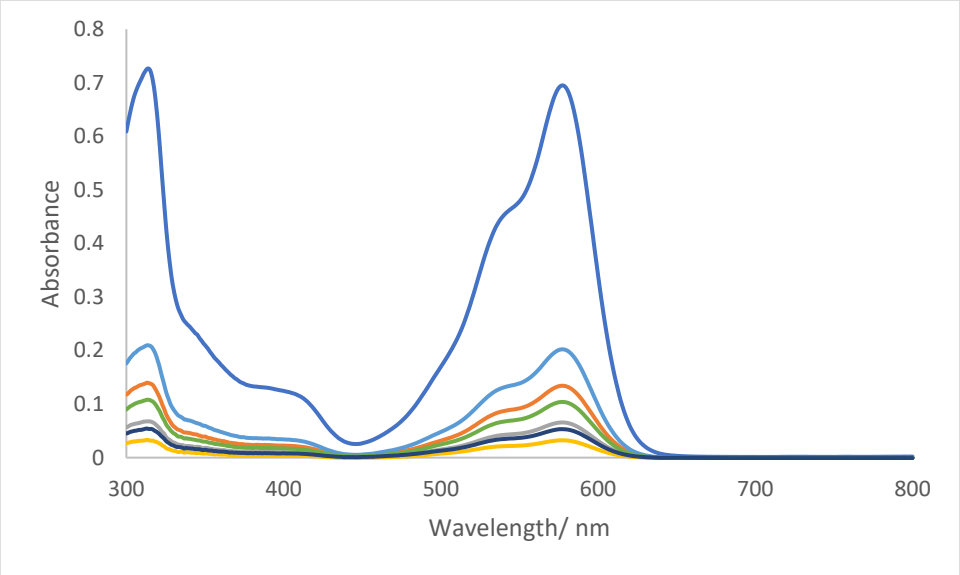

Figure 7.26: UV-vis spectrum of BODIPY (**3.46b**) in DCM, concentrations (M): 1.64 x10^{-5}, 3.27 x10^{-6}, 1.64 x10^{-6}, 8.18 x10^{-7}, 4.91 x10^{-6}, 2.45 x10^{-6}, 1.23 x10^{-6} respectively.

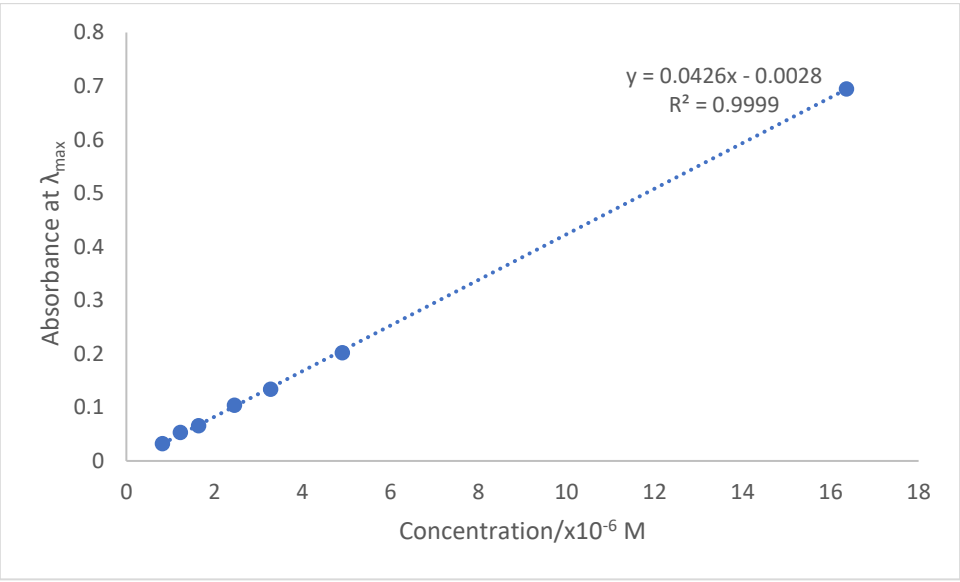

Figure 7.27: Absorbance of BODIPY (**3.46b**) at λ_{max} with respect to concentration, molar extinction coefficient (ε) = 42,592 M^{-1} cm^{-1}

7.3.2.7 Methyl (*S*)-4-(10-((1-hydroxybutan-2-yl)amino)-10b-(*p*-tolyl)-10b*H*-11-oxa-4b^{1}, 10aλ^{4}-diaza-10bλ^{4}-boracyclopenta[*e*]aceanthrylen-7-yl)benzoate (**3.49a**)

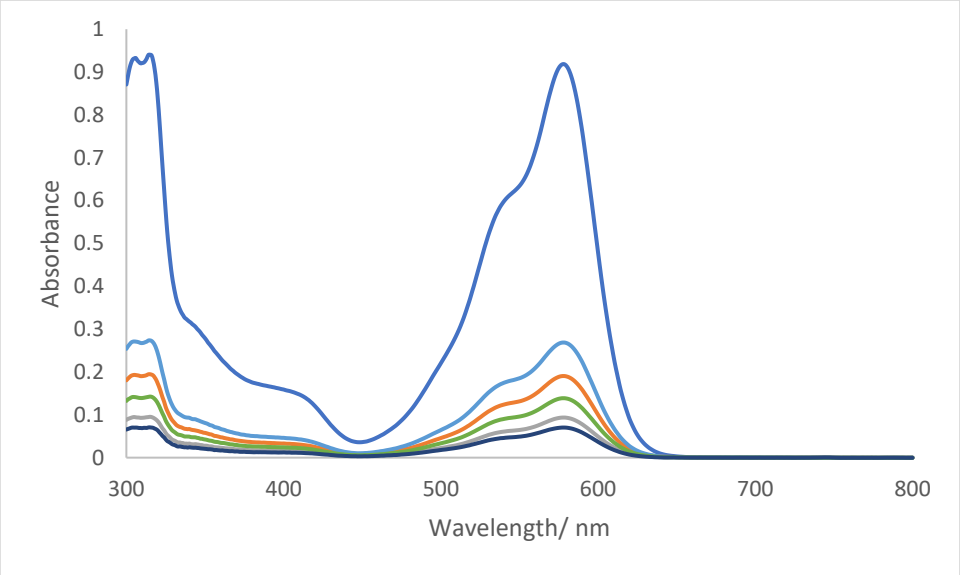

Figure 7.28: UV-vis spectrum of BODIPY (**3.49a**) in DCM, concentrations (M): 1.79 x10^{-5}, 3.59 x10^{-6}, 1.79 x10^{-6}, 8.97 x10^{-7}, 5.38 x10^{-6}, 2.69 x10^{-6}, 1.35 x10^{-6} respectively.

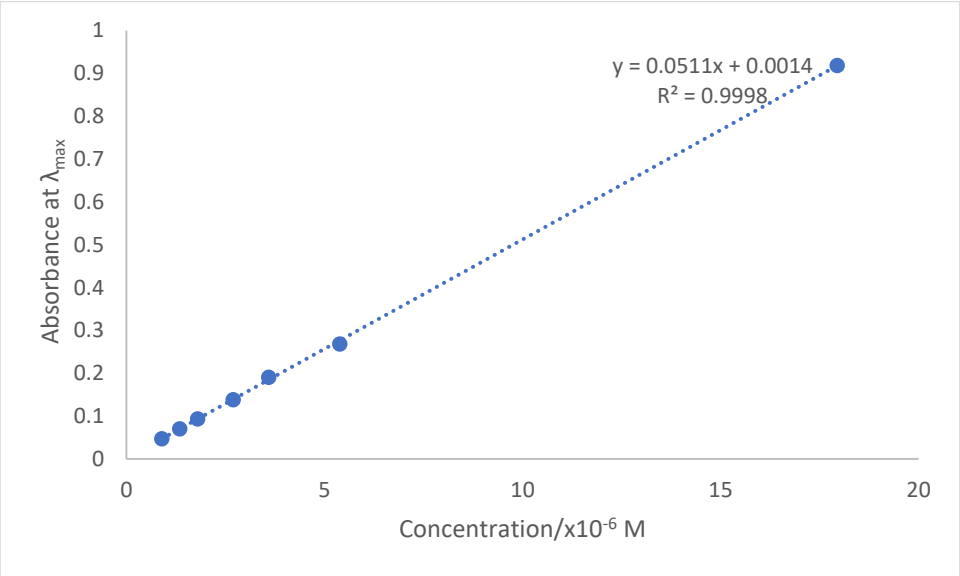

Figure 7.29: Absorbance of BODIPY (**3.49a**) at λ_{max} with respect to concentration, molar extinction coefficient (ε) = 51,074 M^{-1} cm^{-1}

7.3.2.8 Methyl (*S*)-4-(10-((1-hydroxybutan-2-yl)amino)-10b-(*p*-tolyl)-10b*H*-11-oxa-4b^{1}, 10aλ^{4}-diaza-10bλ^{4}-boracyclopenta[*e*]aceanthrylen-7-yl)benzoate (**3.49b**)

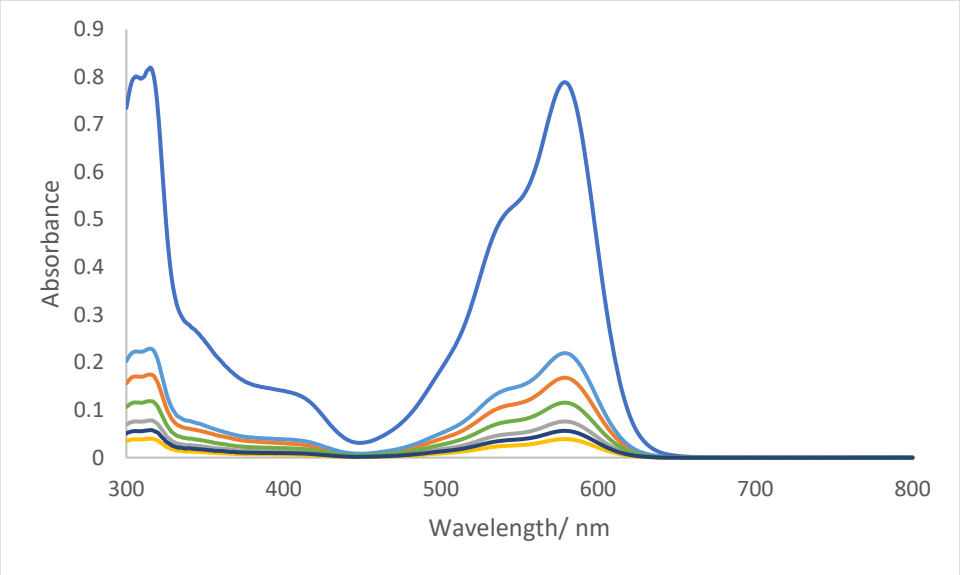

Figure 7.30: UV-vis spectrum of BODIPY (**3.49b**) in DCM, concentrations (M): 1.79 x10^{-5}, 3.59 x10^{-6}, 1.79 x10^{-6},8.97 x10^{-7}, 5.38 x10^{-6}, 2.69 x10^{-6}, 1.35 x10^{-6} respectively.

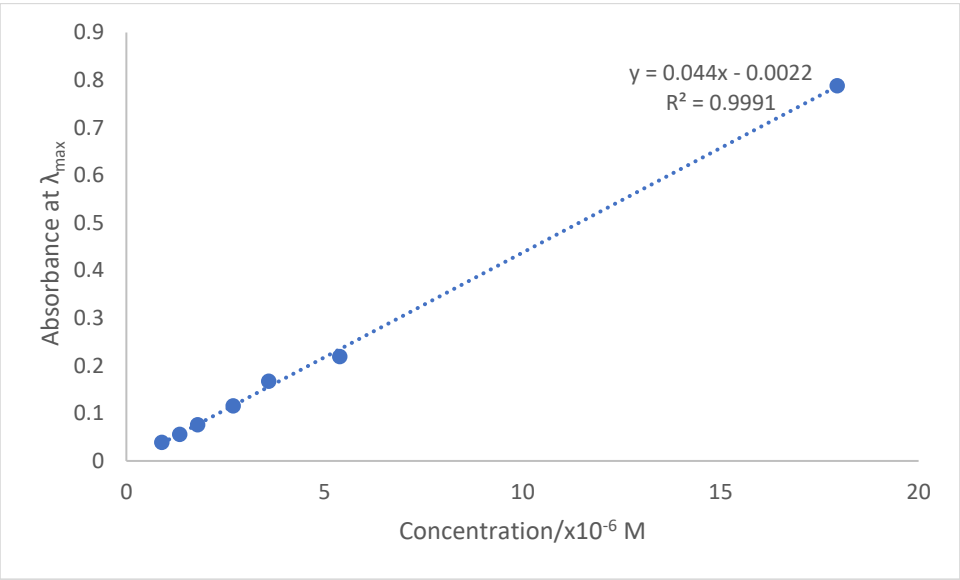

Figure 7.31: Absorbance of BODIPY (**3.49b**) at λ_{max} with respect to concentration, molar extinction coefficient (ε) = 43,973 M^{-1} cm^{-1}

7.3.2.9 Dimethyl 4,4'-(1,4-phenylenebis(10-(((*S*)-1-hydroxybutan-2-yl)amino)-10b*H*-11-oxa-4b^{1},10aλ^{4}-diaza-10bλ^{4}-boracyclopenta[*e*]aceanthrylene-10b,7-diyl))dibenzoate (**5.2a**)

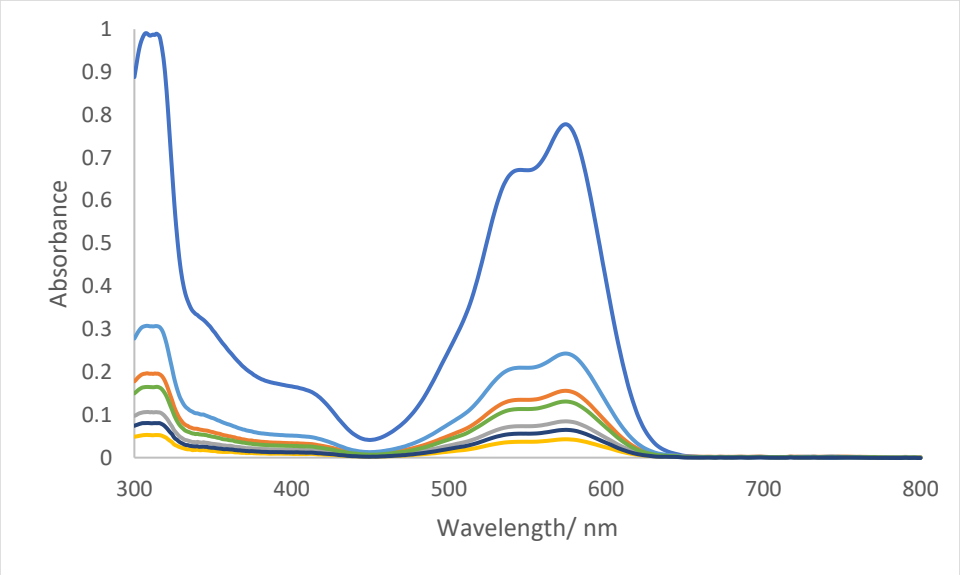

Figure 7.32: UV-vis spectrum of BODIPY (**5.2a**) in DCM, concentrations (M): 9.91 x10^{-6}, 1.98 x10^{-6}, 9.91 x10^{-7}, 4.96 x10^{-7}, 2.97 x10^{-6}, 1.49 x10^{-6}, 7.43 x10^{-7} respectively.

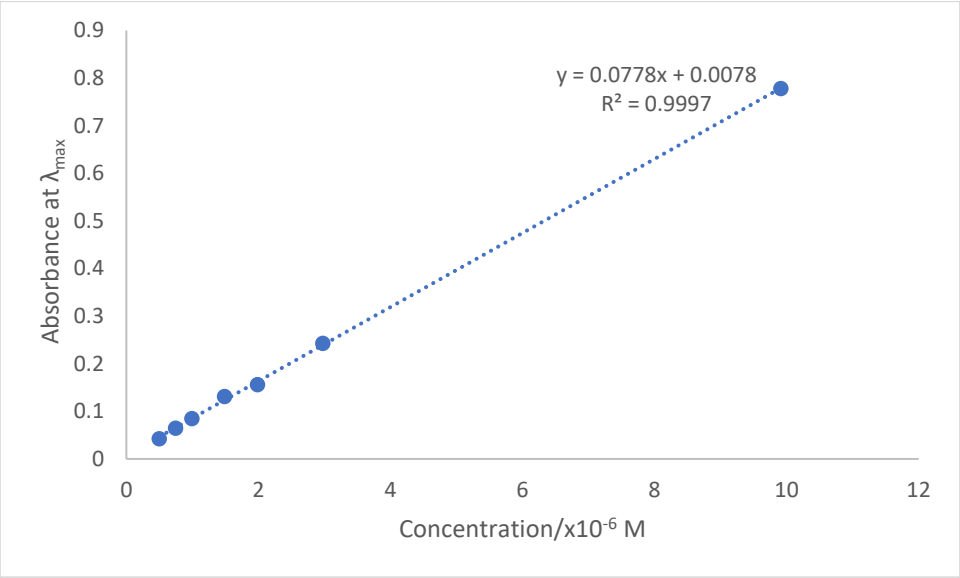

Figure 7.33: Absorbance of BODIPY (**5.2a**) at λ_{max} with respect to concentration, molar extinction coefficient (ε) = 77,787 M^{-1} cm^{-1}

7.3.2.10 Dimethyl 4,4'-(1,4-phenylenebis(10-(((*S*)-1-hydroxybutan-2-yl)amino)-10b*H*-11-oxa-4b^{1},10aλ^{4}-diaza-10bλ^{4}-boracyclopenta[*e*]aceanthrylene-10b,7-diyl))dibenzoate (**5.2b**)

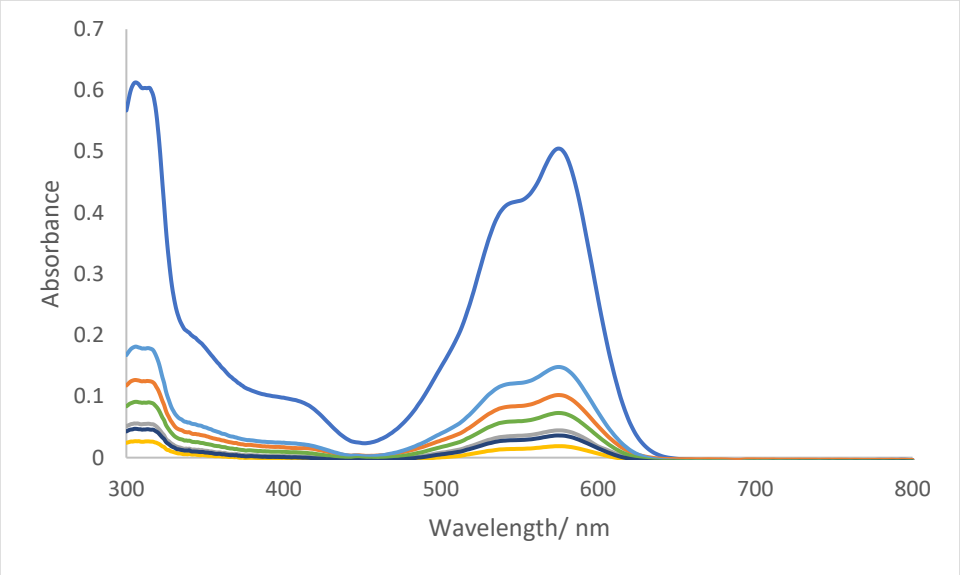

Figure 7.34: UV-vis spectrum of BODIPY (**5.2b**) in DCM, concentrations (M): 9.91 x10^{-6}, 1.98 x10^{-6}, 9.91 x10^{-7}, 4.96 x10^{-7}, 2.97 x10^{-6}, 1.49 x10^{-6}, 7.43 x10^{-7} respectively.

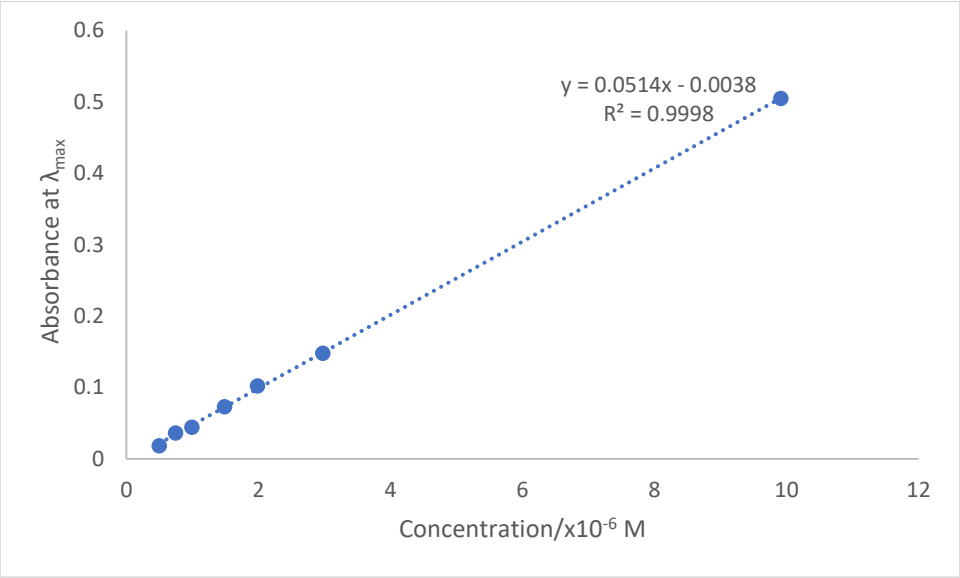

Figure 7.35: Absorbance of BODIPY (**5.2b**) at λ_{max} with respect to concentration, molar extinction coefficient (ε) = 51,369 M^{-1} cm^{-1}

7.3.2.11 Dimethyl 4,4'-(1,4-phenylenebis(10-(((*S*)-1-hydroxybutan-2-yl)amino)-10b*H*-11-oxa-4b^{1},10aλ^{4}-diaza-10bλ^{4}-boracyclopenta[*e*]aceanthrylene-10b,7-diyl))dibenzoate (**5.2c**)

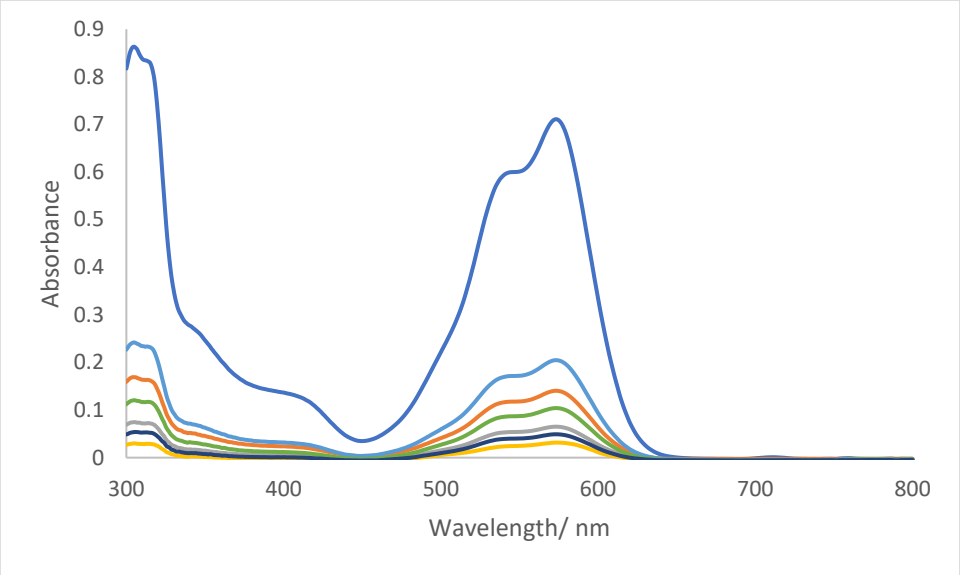

Figure 7.36: UV-vis spectrum of BODIPY (**5.2c**) in DCM, concentrations (M): 9.91 x10^{-6}, 1.98 x10^{-6}, 9.91 x10^{-7}, 4.96 x10^{-7}, 2.97 x10^{-6}, 1.49 x10^{-6}, 7.43 x10^{-7} respectively.

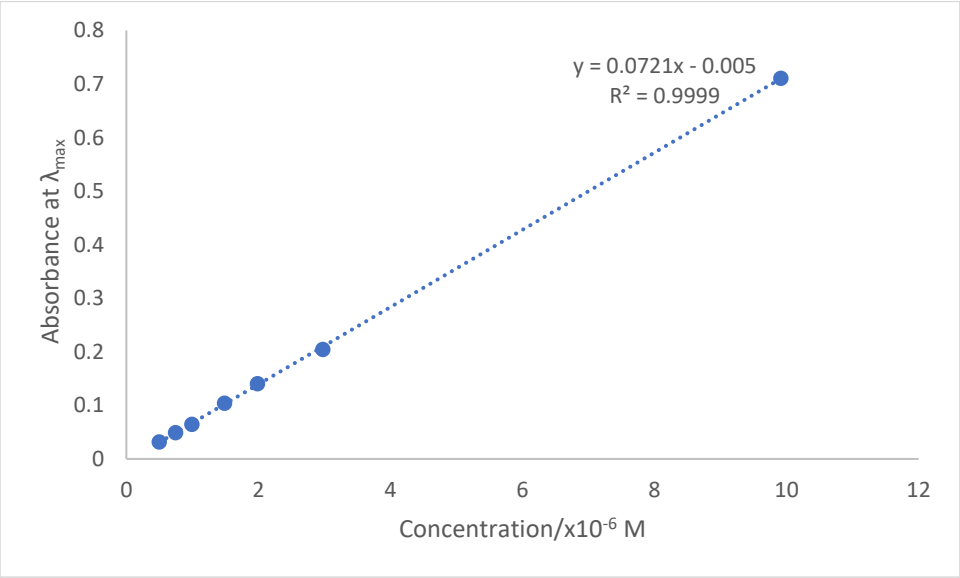

Figure 7.37: Absorbance of BODIPY (**5.2c**) at λ_{max} with respect to concentration, molar extinction coefficient (ε) = 72,134 M^{-1} cm^{-1}

7.3.2.12 Helically chiral methyl (4-chlorophenyl)-2-methylenepentanoate substituted *N*,*N*,*O*,*O*-BODIPY (**4.7**)

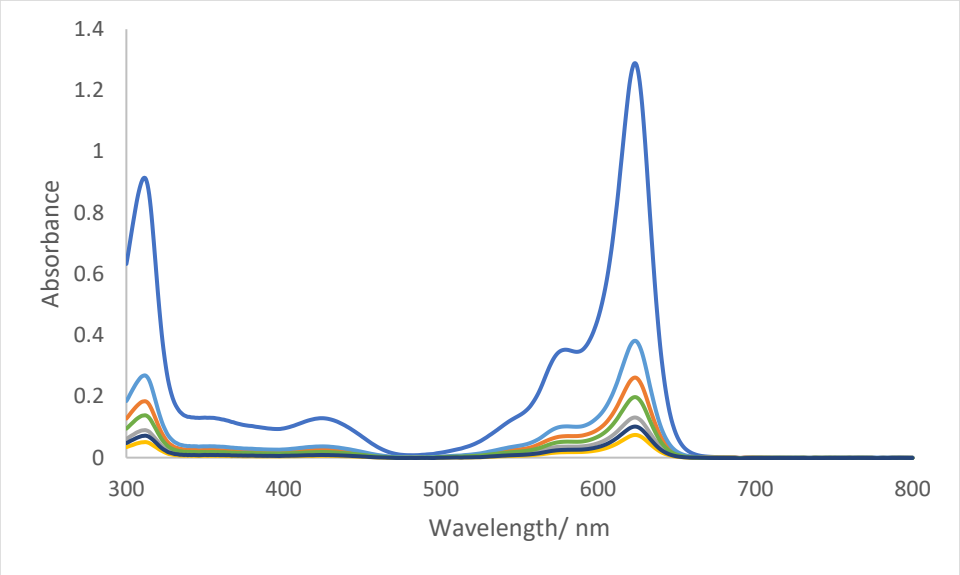

Figure 7.38: UV-vis spectrum of BODIPY (4.7) in DCM, concentrations (M): 1.61 x10^{-5}, 3.21 x10^{-6}, 1.61 x10^{-6}, 8.03 x10^{-7}, 4.81 x10^{-6}, 2.41 x10^{-6}, 1.20 x10^{-6} respectively.

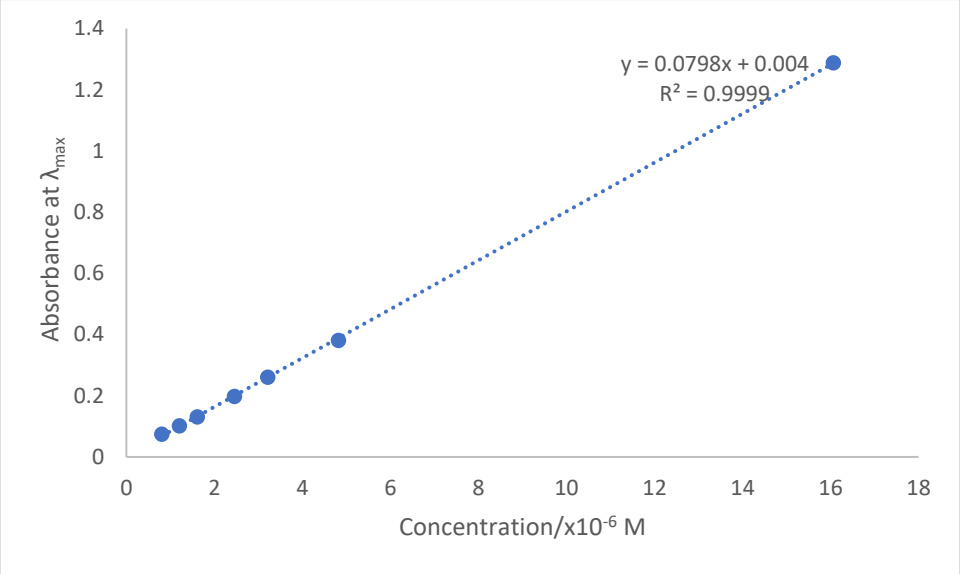

Figure 7.39: Absorbance of BODIPY (**4.7**) at λ_{max} with respect to concentration, molar extinction coefficient (ε) = 79,829 M^{-1} cm^{-1}.

7.3.3 Fluorescence quantum yields measurements

Fluorescence quantum yields (ϕ_F) were determined by recording emission spectra of a suitable reference compound alongside those of the BODIPY. It is important that the emission peak of the reference compound overlaps with the emission peak of the BODIPY to ensure accurate measurement of ϕ_F. Additionally, the absorbance at the excitation wavelength of the reference sample should be almost similar to that of the BODIPY sample, and both measurements should employ the same excitation wavelength.

The fluorescence quantum yield was then calculated using the following equation:

$$QY = QY_{ref}\frac{\eta^2}{\eta_{ref}^2}\frac{I}{A}\frac{A_{ref}}{I_{ref}}$$

In which QY = quantum yield, η = refractive index of solvent, I = peak area (area under emission spectra) and A = absorbance at excitation wavelength

7.3.3.1 Methyl (*S*)-4-(10b-(4-fluorophenyl)-10-((1-hydroxybutan-2-yl)amino)-10b*H*-11-oxa-4b^1,10aλ^4-diaza-10bλ^4-boracyclopenta[*e*]aceanthrylen-7-yl)benzoate (**3.7a**)

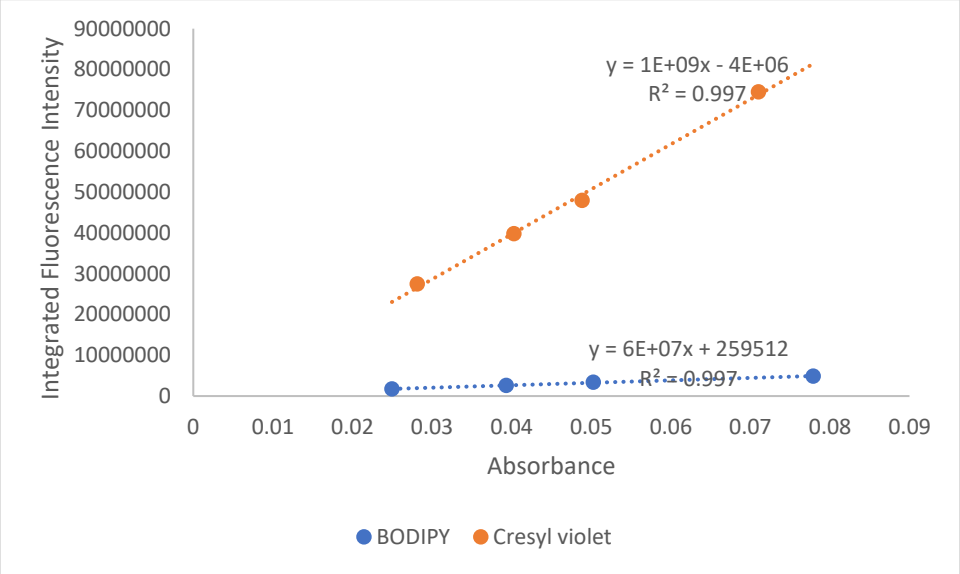

Figure 7.40: Fluorescence quantum yields of BODIPY (**3.7a**) (ϕ_F = 0.04, DCM), measured with respect to cresyl violet standard in ethanol (ϕ_F = 0.56), excitation wavelength = 542 nm.

7.3.3.2 Methyl (*S*)-4-(10b-(4-fluorophenyl)-10-((1-hydroxybutan-2-yl)amino)-10b*H*-11-oxa-4b^{1},10aλ^{4}-diaza-10bλ^{4}-boracyclopenta[*e*]aceanthrylen-7-yl)benzoate (**3.7b**)

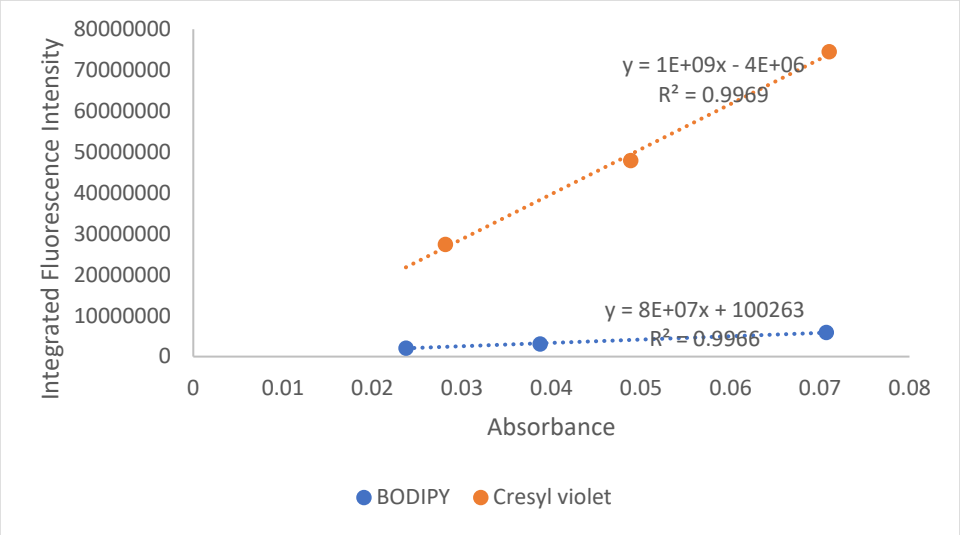

Figure 7.41: Fluorescence quantum yields of BODIPY (**3.7b**) (ϕ_F = 0.05, DCM), measured with respect to cresyl violet standard in ethanol (ϕ_F = 0.56), excitation wavelength = 542 nm.

7.3.3.3 Methyl (*S*)-4-(10-((1-hydroxybutan-2-yl)amino)-10b-(4-(trifluoromethyl)phenyl)-10b*H*-11-oxa-4b^{1}, 10aλ^{4}-diaza-10bλ^{4}-boracyclopenta[*e*]aceanthrylen-7-yl)benzoate (**3.46a**)

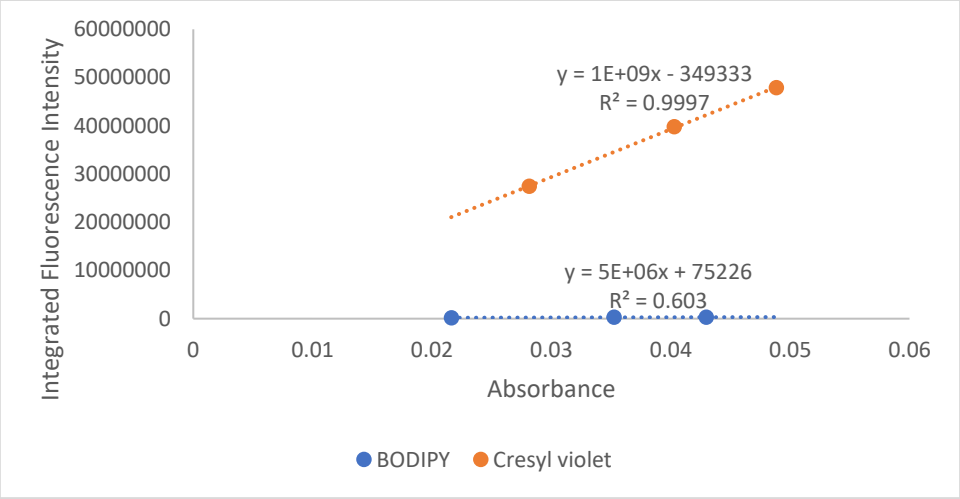

Figure 7.42: Fluorescence quantum yields of BODIPY (**3.46a**)(ϕ_F = 0.003, DCM), measured with respect to cresyl violet standard in ethanol (ϕ_F = 0.56), excitation wavelength = 542 nm.

7.3.3.4 Methyl (*S*)-4-(10-((1-hydroxybutan-2-yl)amino)-10b-(4-(trifluoromethyl)phenyl)-10b*H*-11-oxa-4b^{1}, 10aλ^{4}-diaza-10bλ^{4}-boracyclopenta[*e*]aceanthrylen-7-yl)benzoate (**3.46b**)

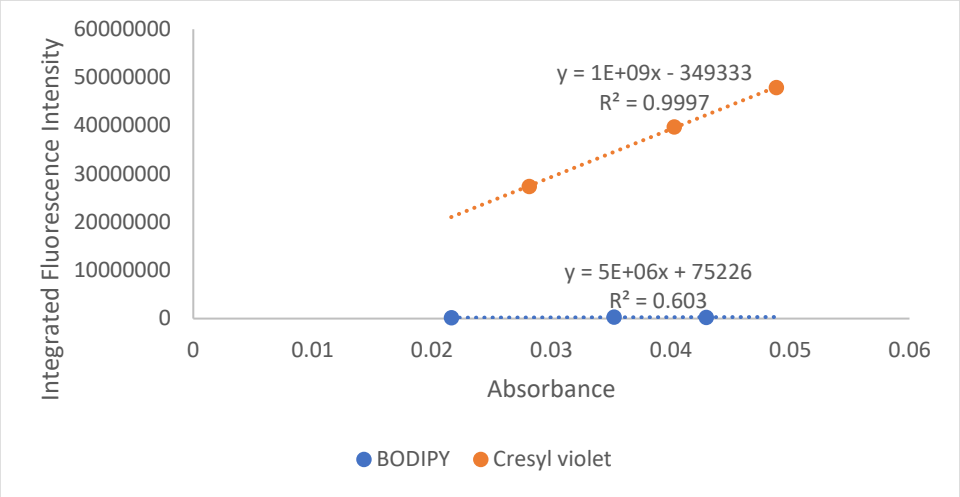

Figure 7.43: Fluorescence quantum yields of BODIPY (**3.46b**) (ϕ_F = 0.004, DCM), measured with respect to cresyl violet standard in ethanol (ϕ_F = 0.56), excitation wavelength = 542 nm.

7.3.3.5 Methyl (*S*)-4-(10-((1-hydroxybutan-2-yl)amino)-10b-(*p*-tolyl)-10b*H*-11-oxa-4b^{1}, 10aλ^{4}-diaza-10bλ^{4}-boracyclopenta[*e*]aceanthrylen-7-yl)benzoate (**3.49a**)

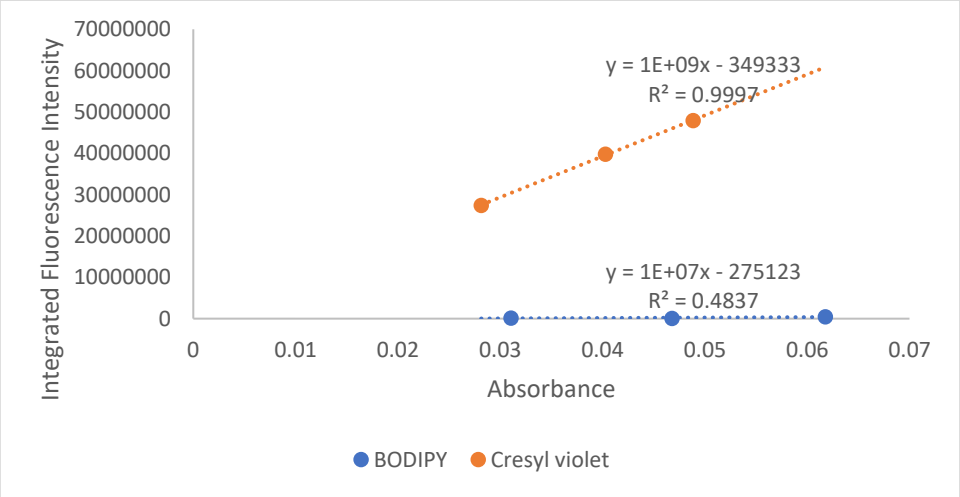

Figure 7.44: Fluorescence quantum yields of BODIPY (**3.49a**)(ϕ_F = 0.01, DCM), measured with respect to cresyl violet standard in ethanol (ϕ_F = 0.56), excitation wavelength = 542 nm.

7.3.3.6 Methyl (*S*)-4-(10-((1-hydroxybutan-2-yl)amino)-10b-(*p*-tolyl)-10b*H*-11-oxa-4b^{1}, 10aλ^{4}-diaza-10bλ^{4}-boracyclopenta[*e*]aceanthrylen-7-yl)benzoate (**3.49b**)

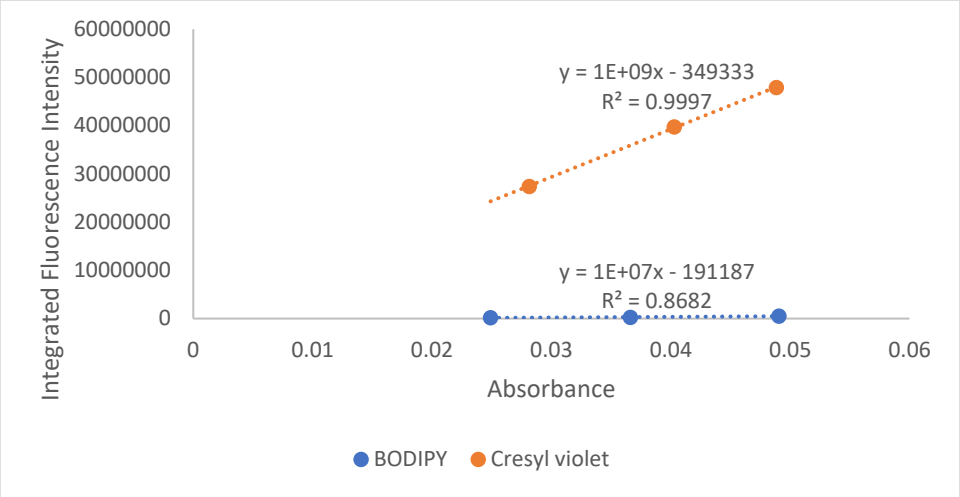

Figure 7.45: Fluorescence quantum yields of BODIPY (**3.49b**) (ϕ_F = 0.01, DCM), measured with respect to cresyl violet standard in ethanol (ϕ_F = 0.56), excitation wavelength = 542 nm.

7.3.3.7 Helically chiral methyl (4-chlorophenyl)-2-methylenepentanoate substituted *N*,*N*,*O*,*O*-BODIPY (4.7)

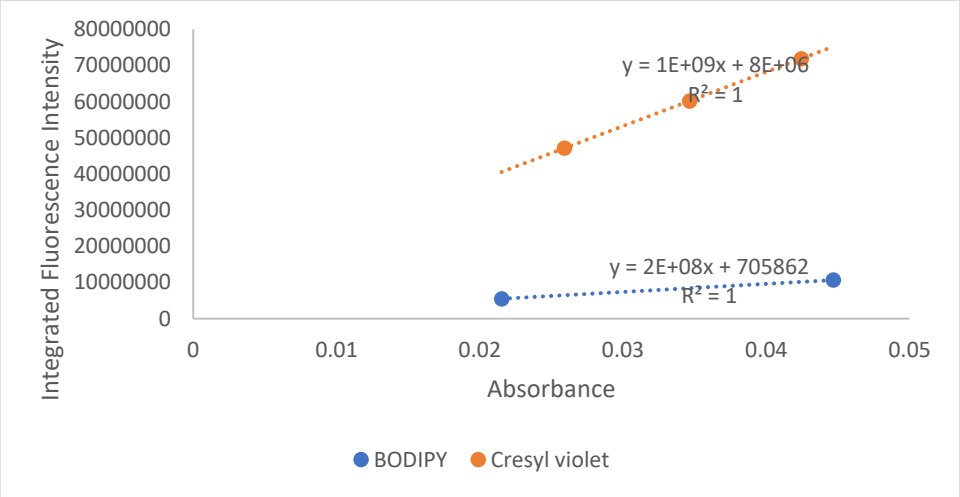

Figure 7.46: Fluorescence quantum yields of BODIPY (**4.7**) (ϕ_F = 0.13, DCM), measured with respect to cresyl violet standard in methanol (ϕ_F = 0.54), excitation wavelength = 580 nm.

Compound	Quantum yield $_{ref}$	$\phi_{F\ ref}$	Solvent reference	η_{ref}	Solvent sample	η	λ_{ex} / nm	A	A_{ref}	I	I_{ref}	ϕ_F
(**2.18**)	Rhodamine 6G	0.95	Water	1.33	DCM	1.4125	480	0.05544	0.04741	2541665	11829136	0.20
(**2.19**)	Rhodamine 6G	0.95	Water	1.33	DCM	1.4125	500	0.06445	0.05765	4086223	11337275	0.35
(**2.3**)	Rhodamine 6G	0.95	Water	1.33	DCM	1.4125	488	0.04254	0.04204	147569	8623206	0.02
(**2.4**)	Rhodamine 6G	0.95	Water	1.33	DCM	1.4125	490	0.02144	0.02225	112455	3943482	0.03
(**3.7a**)	Cresyl violet	0.56	EtOH	1.3614	DCM	1.4125	542	0.039291	0.040283	2572552	39756245	0.04
(**3.7b**)	Cresyl violet	0.56	EtOH	1.3614	DCM	1.4125	542	0.023743	0.0281137	2116155	27434705	0.05
(**3.7b**)	Cresyl violet	0.56	EtOH	1.3614	EtOH	1.3614	540	0.035217	0.017715	2206651	15879813	0.04
(**3.46a**)	Cresyl violet	0.56	EtOH	1.3614	DCM	1.4125	590	0.030884	0.034866	343150	2743705	0.07
(**3.46b**)	Cresyl violet	0.56	EtOH	1.3614	DCM	1.4125	590	0.035248	0.034866	304222	2743705	0.06
(**3.49a**)	Cresyl violet	0.56	EtOH	1.3614	DCM	1.4125	554	0.031052	0.028137	1446418	27434705	0.01
(**3.49b**)	Cresyl violet	0.56	EtOH	1.3614	DCM	1.4125	554	0.024902	0.028137	191436	27434705	0.01
(**5.2a**)	Cresyl violet	0.56	EtOH	1.3614	DCM	1.4125	550	0.037094	0.034866	153994	2743705	0.003
(**5.2b**)	Cresyl violet	0.56	EtOH	1.3614	DCM	1.4125	550	0.035812	0.034866	132191	2743705	0.003
(**5.2c**)	Cresyl violet	0.56	EtOH	1.3614	DCM	1.4125	550	0.040024	0.034866	182419	2743705	0.003
(**4.7a**)	Cresyl violet	0.54	MeOH	1.3284	DCM	1.4125	590	0.035919	0.034637	7048269	60132351	0.13
(**5.6a**)	Cresyl violet	0.54	MeOH	1.3284	DCM	1.4125	582	0.022598	0.02373	1863371	2260828	0.39
(**5.6b**)	Cresyl violet	0.54	MeOH	1.3284	DCM	1.4125	582	0.025528	0.02373	2109987	2260828	0.55

Table 7.2: Data used to calculate the fluorescence quantum yields of final BODIPY products.

7.4 Chiral HPLC Spectra

7.4.1 Methyl (*S*)-4-(10b-(4-fluorophenyl)-10-((1-hydroxybutan-2-yl)amino)-10b*H*-11-oxa-4b^{1},10aλ^{4}-diaza-10bλ^{4}-boracyclopenta[*e*]aceanthrylen-7-yl)benzoate (**3.7a**) and methyl (*R*)-4-(10b-(4-fluorophenyl)-10-((1-hydroxybutan-2-yl)amino)-10b*H*-11-oxa-4b^{1},10aλ^{4}-diaza-10bλ^{4}-boracyclopenta[*e*]aceanthrylen-7-yl)benzoate (**3.40a**)

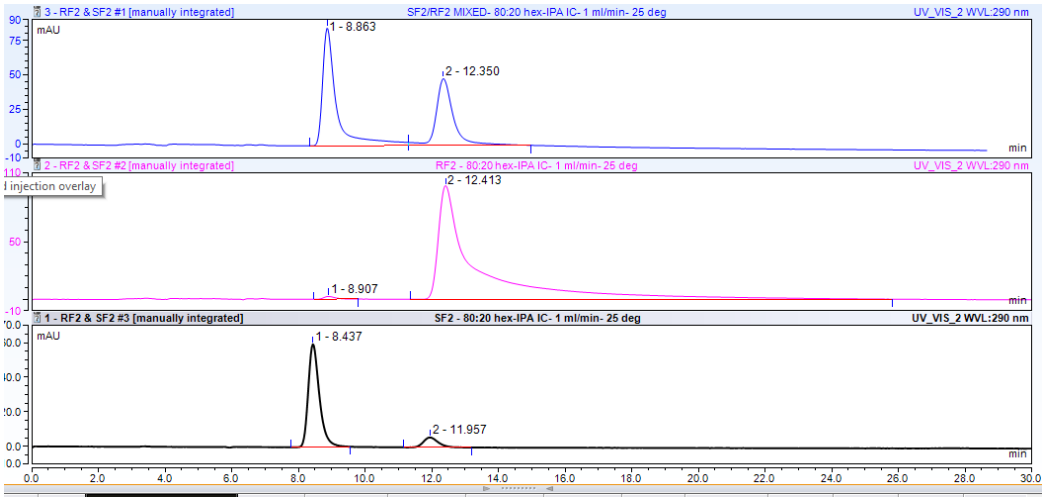

Figure 7.47: Chiral HPLC spectra of BODIPY (**3.7a**) and BODIPY (**3.40a**) using chiral column (CHIRALPAK®IC), Eluent gradient: (hexane: isopropanol 80:20).

7.4.2 Methyl (*S*)-4-(10b-(4-fluorophenyl)-10-((1-hydroxybutan-2-yl)amino)-10b*H*-11-oxa-4b^{1},10aλ^{4}-diaza-10bλ^{4}-boracyclopenta[*e*]aceanthrylen-7-yl)benzoate (**3.7b**) and methyl (*R*)-4-(10b-(4-fluorophenyl)-10-((1-hydroxybutan-2-yl)amino)-10b*H*-11-oxa-4b^{1},10aλ^{4}-diaza-10bλ^{4}-boracyclopenta[*e*]aceanthrylen-7-yl)benzoate (**3.40b**)

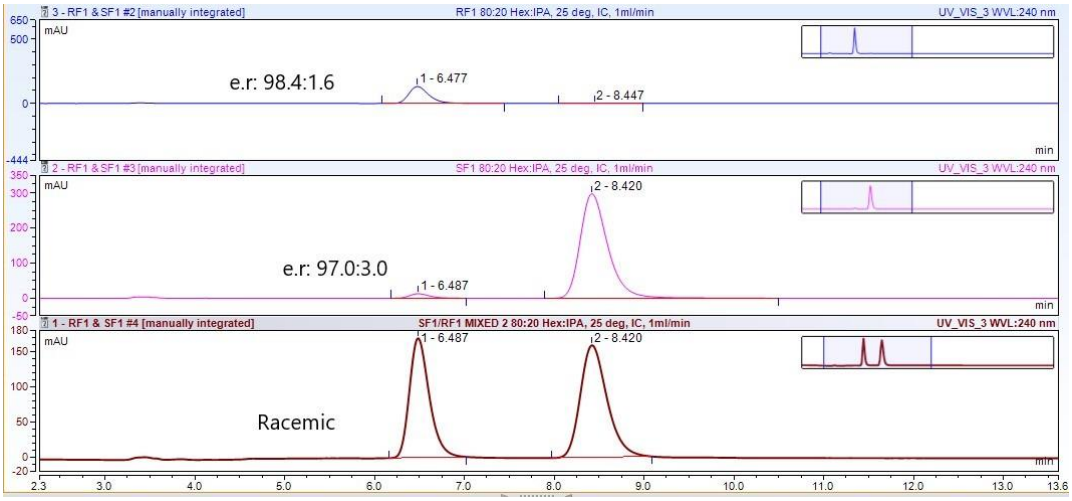

Figure 7.48: Chiral HPLC spectra of BODIPY (**3.7b**) and BODIPY (**3.40b**) using chiral column (CHIRALPAK®IC), Eluent gradient: (hexane: isopropanol 80:20).

7.5 X-Ray Crystallography Data

The following crystal structure data were collected on a Xcalibur, Atlas, Gemini ultra diffractometer equipped with a fine-focus sealed X-ray tube (λ CuKα = 1.54184 Å) and an Oxford Cryosystems CryostreamPlus open-flow N_2 cooling device. The analysis of the X-ray diffraction data of all the following compounds were performed by Dr Paul Waddell.

Chapter 2

7.5.1 Methyl 4-(3,7-dibromo-5,5-difluoro-5*H*-4λ^4,5λ^4-dipyrrolo[1,2-*c*:2',1'-*f*][1,3,2]diazaborinin-10-yl)benzoate (**1.67**)

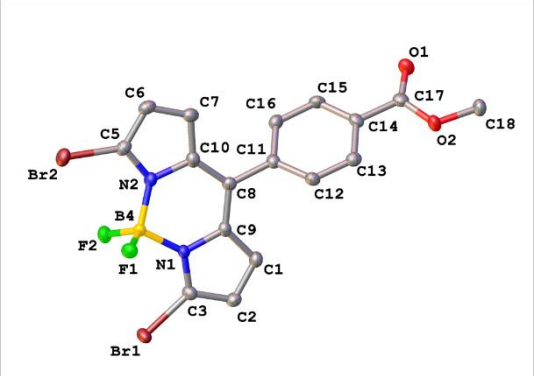

Identification code	mjh190038_fa
Empirical formula	$C_{17}H_{11}BBr_2F_2N_2O_2$
Formula weight	483.91
Temperature/K	150.0(2)
Crystal system	triclinic
Space group	P-1
a/Å	7.8243(5)
b/Å	9.5595(6)
c/Å	12.5695(8)
α/°	73.450(5)
β/°	79.123(5)
γ/°	67.143(6)
Volume/Å^3	827.19(10)
Z	2
ρ_{calc}g/cm^3	1.943
μ/mm^{-1}	6.559
F(000)	472.0
Crystal size/mm^3	0.09 × 0.06 × 0.02
Radiation	CuKα (λ = 1.54184)
2Θ range for data collection/°	7.366 to 133.626

Index ranges	$-9 \leq h \leq 9$, $-11 \leq k \leq 11$, $-14 \leq l \leq 14$
Reflections collected	11710
Independent reflections	2925 [R_{int} = 0.0518, R_{sigma} = 0.0447]
Data/restraints/parameters	2925/0/236
Goodness-of-fit on F^2	1.070
Final R indexes [I>=2σ (I)]	R_1 = 0.0299, wR_2 = 0.0635
Final R indexes [all data]	R_1 = 0.0456, wR_2 = 0.0708
Largest diff. peak/hole / e $Å^{-3}$	0.38/-0.35

7.5.2 Methyl 4-(5,5-difluoro-3,7-diiodo-5*H*-4λ^4,5λ^4-dipyrrolo[1,2-*c*:2',1'-*f*][1,3,2]diazaborinin-10-yl)benzoate (**1.68**)

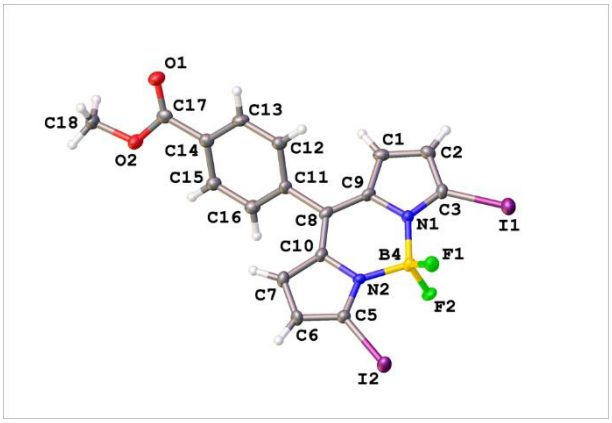

Identification code	mjh220039_tw
Empirical formula	$C_{17}H_{11}BF_2I_2N_2O_2$
Formula weight	577.89
Temperature/K	150.0(2)
Crystal system	triclinic
Space group	P-1
a/Å	8.0299(3)
b/Å	9.9295(3)
c/Å	12.3476(8)
α/°	72.623(4)
β/°	79.742(4)
γ/°	66.157(3)
Volume/Å^3	857.53(7)
Z	2
ρ_{calc}g/cm^3	2.238
μ/mm^{-1}	29.136
F(000)	544.0
Crystal size/mm^3	0.18 × 0.03 × 0.01
Radiation	Cu Kα (λ = 1.54184)
2Θ range for data collection/°	7.518 to 154.172
Index ranges	-8 ≤ h ≤ 9, -12 ≤ k ≤ 12, -14 ≤ l ≤ 14
Reflections collected	5863
Independent reflections	5863 [R_{int} = 0.056, R_{sigma} = 0.0315]
Data/restraints/parameters	5863/0/237
Goodness-of-fit on F^2	1.064
Final R indexes [I>=2σ (I)]	R_1 = 0.0381, wR_2 = 0.1033
Final R indexes [all data]	R_1 = 0.0434, wR_2 = 0.1075
Largest diff. peak/hole / e Å^{-3}	0.81/-1.01

7.5.3 Methyl 4-(3-(((1*S*,2*S*)-2-amino-1,2-diphenylethyl)amino)-7-bromo-5,5-difluoro-5*H*-5λ^4,6λ^4-dipyrrolo[1,2-*c*:2',1'-*f*][1,3,2]diazaborinin-10-yl)benzoate (**2.18**)

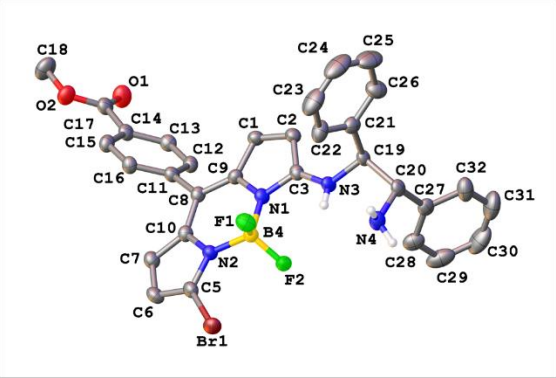

Identification code	mjh220057_fa
Empirical formula	$C_{31}H_{26}BBrF_2N_4O_2$
Formula weight	615.28
Temperature/K	150.0(2)
Crystal system	triclinic
Space group	P1
a/Å	10.12040(10)
b/Å	11.6588(2)
c/Å	13.4218(2)
α/°	106.3360(10)
β/°	101.1190(10)
γ/°	102.0600(10)
Volume/Å^3	1431.77(4)
Z	2
ρ_{calc}g/cm^3	1.427
μ/mm^{-1}	2.367
F(000)	628.0
Crystal size/mm^3	0.24 × 0.08 × 0.02
Radiation	Cu Kα (λ = 1.54184)
2Θ range for data collection/°	7.124 to 153.964
Index ranges	-11 ≤ h ≤ 12, -14 ≤ k ≤ 14, -16 ≤ l ≤ 16
Reflections collected	34357
Independent reflections	10694 [R_{int} = 0.0327, R_{sigma} = 0.0315]
Data/restraints/parameters	10694/3/765
Goodness-of-fit on F^2	1.050
Final R indexes [I>=2σ (I)]	R_1 = 0.0362, wR_2 = 0.0943
Final R indexes [all data]	R_1 = 0.0385, wR_2 = 0.0960
Largest diff. peak/hole / e Å^{-3}	0.94/-0.30
Flack parameter	-0.020(11)

7.5.4 Methyl 4-(3-(((1*S*,2*S*)-2-amino-1,2-diphenylethyl)amino)-5,5-difluoro-7-iodo-5*H*-5λ^4,6λ^4-dipyrrolo[1,2-*c*:2',1'-*f*][1,3,2]diazaborinin-10-yl)benzoate (**2.19**)

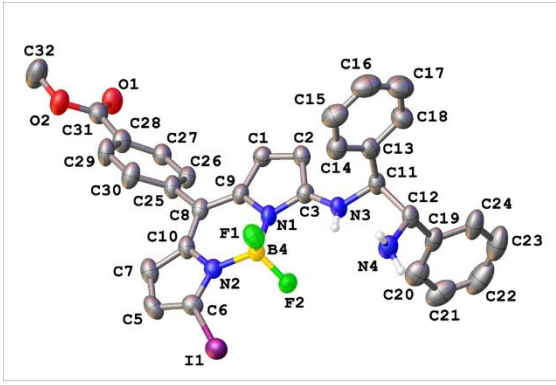

Identification code	mjh220053_fa
Empirical formula	$C_{31}H_{26}BF_2IN_4O_2$
Formula weight	662.27
Temperature/K	150.0(2)
Crystal system	monoclinic
Space group	I2
a/Å	26.7051(11)
b/Å	10.3640(3)
c/Å	22.4215(8)
α/°	90
β/°	111.482(4)
γ/°	90
Volume/Å^3	5774.5(4)
Z	8
ρ_{calc}g/cm^3	1.524
μ/mm^{-1}	9.122
F(000)	2656.0
Crystal size/mm^3	0.2 × 0.02 × 0.01
Radiation	Cu Kα (λ = 1.54184)
2Θ range for data collection/°	7.114 to 154.378
Index ranges	-33 ≤ h ≤ 33, -12 ≤ k ≤ 12, -27 ≤ l ≤ 28
Reflections collected	41195
Independent reflections	11303 [R_{int} = 0.0506, R_{sigma} = 0.0473]
Data/restraints/parameters	11303/2/759
Goodness-of-fit on F^2	1.035
Final R indexes [I>=2σ (I)]	R_1 = 0.0378, wR_2 = 0.0789
Final R indexes [all data]	R_1 = 0.0486, wR_2 = 0.0826
Largest diff. peak/hole / e Å^{-3}	0.75/-0.90
Flack parameter	-0.023(3)

7.5.5 Methyl 4-(3-bromo-7-((4-((7-bromo-5,5-difluoro-10-(4-(methoxycarbonyl)phenyl)-5*H*-4λ^4,5λ^4-dipyrrolo[1,2-c:2',1'-*f*][1,3,2]diazaborinin-3-yl)amino)butyl)amino)-5,5-difluoro-5*H*-4λ^4,5λ^4-dipyrrolo[1,2-*c*:2',1'-*f*][1,3,2]diazaborinin-10-yl)benzoate (**2.28**)

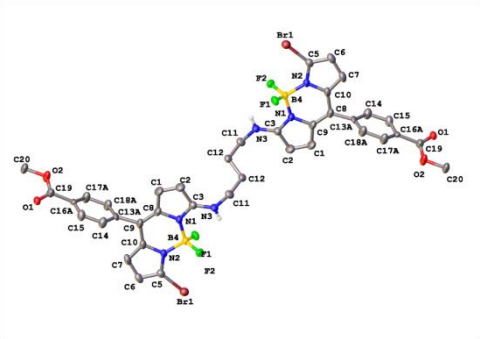

Identification code	mjh230021_fa
Empirical formula	$C_{38}H_{32}B_2Br_2F_4N_6O_4$
Formula weight	894.13
Temperature/K	150.0(2)
Crystal system	monoclinic
Space group	$P2_1/c$
a/Å	11.4987(3)
b/Å	11.2771(3)
c/Å	14.4939(3)
α/°	90
β/°	94.727(2)
γ/°	90
Volume/Å^3	1873.06(8)
Z	2
ρ_{calc}g/cm^3	1.585
μ/mm^{-1}	3.349
F(000)	900.0
Crystal size/mm^3	0.14 × 0.1 × 0.04
Radiation	CuKα (λ = 1.54184)
2Θ range for data collection/°	7.714 to 154.436
Index ranges	-14 ≤ h ≤ 14, -13 ≤ k ≤ 13, -13 ≤ l ≤ 18
Reflections collected	17876
Independent reflections	3709 [R_{int} = 0.0271, R_{sigma} = 0.0217]
Data/restraints/parameters	3709/61/293
Goodness-of-fit on F^2	1.071
Final R indexes [I>=2σ (I)]	R_1 = 0.0312, wR_2 = 0.0842
Final R indexes [all data]	R_1 = 0.0361, wR_2 = 0.0877
Largest diff. peak/hole / e Å^{-3}	0.44/-0.59

7.5.6 Methyl (*S*)-4-(3-bromo-5,5-difluoro-7-((1-hydroxybutan-2-yl)amino)-5*H*-5λ^4,6λ^4-dipyrrolo[1,2-*c*:2',1'-*f*][1,3,2]diazaborinin-10-yl)benzoate (**3.1**)

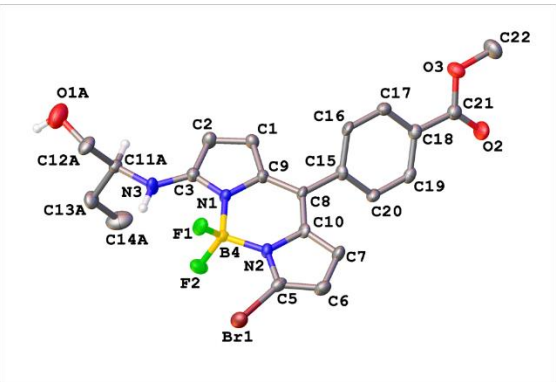

Identification code	mjh220013_fa
Empirical formula	$C_{21}H_{21}BBrF_2N_3O_3$
Formula weight	492.13
Temperature/K	150.0(2)
Crystal system	monoclinic
Space group	C2
a/Å	17.9836(3)
b/Å	7.43580(10)
c/Å	32.5133(5)
α/°	90
β/°	105.552(2)
γ/°	90
Volume/Å^3	4188.58(12)
Z	8
ρ_{calc}g/cm^3	1.561
μ/mm^{-1}	3.088
F(000)	2000.0
Crystal size/mm^3	0.43 × 0.11 × 0.04
Radiation	Cu Kα (λ = 1.54184)
2Θ range for data collection/°	8.468 to 133.106
Index ranges	-21 ≤ h ≤ 21, -8 ≤ k ≤ 7, -38 ≤ l ≤ 38
Reflections collected	18103
Independent reflections	5621 [R_{int} = 0.0482, R_{sigma} = 0.0417]
Data/restraints/parameters	5621/780/656
Goodness-of-fit on F^2	1.101
Final R indexes [I>=2σ (I)]	R_1 = 0.0480, wR_2 = 0.1257
Final R indexes [all data]	R_1 = 0.0493, wR_2 = 0.1268

Largest diff. peak/hole / e $Å^{-3}$	0.95/-0.47
Flack parameter	-0.015(15)

7.5.7 Methyl (*S*)-4-(5,5-difluoro-3-((1-hydroxybutan-2-yl)amino)-7-iodo-5*H*-4λ^4,5λ^4-dipyrrolo[1,2-*c*:2',1'-*f*][1,3,2]diazaborinin-10-yl)benzoate (**3.2**)

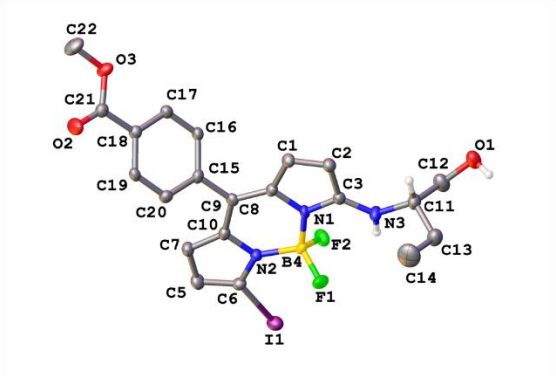

Identification code	mjh220049_fa
Empirical formula	$C_{21}H_{21}BF_2IN_3O_3$
Formula weight	539.12
Temperature/K	150.0(2)
Crystal system	monoclinic
Space group	C2
a/Å	18.5444(3)
b/Å	7.45390(10)
c/Å	32.3877(5)
α/°	90
β/°	106.161(2)
γ/°	90
Volume/Å^3	4299.98(12)
Z	8
ρ_{calc}g/cm^3	1.666
μ/mm^{-1}	12.106
F(000)	2144.0
Crystal size/mm^3	0.16 × 0.04 × 0.02
Radiation	Cu Kα (λ = 1.54184)
2Θ range for data collection/°	8.528 to 154.512
Index ranges	-22 ≤ h ≤ 23, -9 ≤ k ≤ 8, -39 ≤ l ≤ 40
Reflections collected	29732
Independent reflections	6790 [R_{int} = 0.0339, R_{sigma} = 0.0269]
Data/restraints/parameters	6790/519/587
Goodness-of-fit on F^2	1.066
Final R indexes [I>=2σ (I)]	R_1 = 0.0233, wR_2 = 0.0603
Final R indexes [all data]	R_1 = 0.0242, wR_2 = 0.0606
Largest diff. peak/hole / e Å^{-3}	0.43/-0.53
Flack parameter	0.011(4)

7.5.8 Methyl (*R*)-4-(5,5-difluoro-3-((1-hydroxybutan-2-yl)amino)-7-iodo-5*H*-4λ^4,5λ^4-dipyrrolo[1,2-*c*:2',1'-*f*][1,3,2]diazaborinin-10-yl)benzoate (**3.14**)

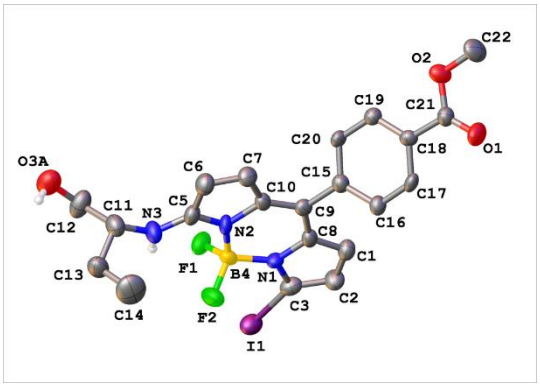

Identification code	mjh230079_2_fa
Empirical formula	$C_{21}H_{21}BF_2IN_3O_3$
Formula weight	539.12
Temperature/K	150.0(2)
Crystal system	monoclinic
Space group	C2
a/Å	18.7179(9)
b/Å	7.4421(2)
c/Å	32.6261(16)
α/°	90
β/°	106.557(5)
γ/°	90
Volume/Å^3	4356.4(3)
Z	8
ρ_{calc}g/cm^3	1.644
μ/mm^{-1}	11.949
F(000)	2144.0
Crystal size/mm^3	0.18 × 0.02 × 0.01
Radiation	CuKα (λ = 1.54184)
2Θ range for data collection/°	5.652 to 155.012
Index ranges	-23 ≤ h ≤ 23, -6 ≤ k ≤ 8, -40 ≤ l ≤ 40
Reflections collected	31876
Independent reflections	7142 [R_{int} = 0.0628, R_{sigma} = 0.0481]
Data/restraints/parameters	7142/12/589
Goodness-of-fit on F^2	1.046
Final R indexes [I>=2σ (I)]	R_1 = 0.0507, wR_2 = 0.1295
Final R indexes [all data]	R_1 = 0.0610, wR_2 = 0.1350
Largest diff. peak/hole / e Å^{-3}	0.60/-0.80
Flack parameter	-0.029(7)

7.5.9 Methyl (*S*)-4-(10b-(4-fluorophenyl)-10-((1-hydroxybutan-2-yl)amino)-10b*H*-11-oxa-4b^{1},10aλ^{4}-diaza-10bλ^{4}-boracyclopenta[*e*]aceanthrylen-7-yl)benzoate (**3.7a**)

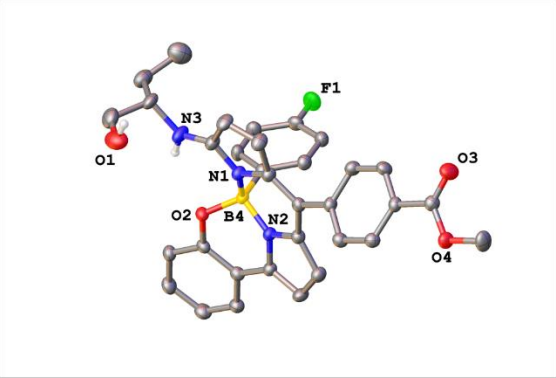

Identification code	mjh220014_1_fa
Empirical formula	$C_{33}H_{29}BFN_3O_4$
Formula weight	561.40
Temperature/K	150.0(2)
Crystal system	Orthorhombic
Space group	$P2_12_12_1$
a/Å	10.8981(3)
b/Å	14.7297(4)
c/Å	17.5838(5)
α/°	90
β/°	90
γ/°	90
Volume/Å^3	2822.65(14)
Z	4
ρ_{calc}g/cm^3	1.321
μ/mm^{-1}	0.745
F(000)	1176.0
Crystal size/mm^3	0.19 × 0.17 × 0.11
Radiation	Cu Kα (λ = 1.54184)
2Θ range for data collection/°	7.83 to 133.222
Index ranges	-11 ≤ h ≤ 12, -17 ≤ k ≤ 17, -20 ≤ l ≤ 17
Reflections collected	12493
Independent reflections	4833 [R_{int} = 0.0604, R_{sigma} = 0.0638]
Data/restraints/parameters	4833/511/433
Goodness-of-fit on F^2	1.031
Final R indexes [I>=2σ (I)]	R_1 = 0.0417, wR_2 = 0.0995
Final R indexes [all data]	R_1 = 0.0557, wR_2 = 0.1141
Largest diff. peak/hole / e Å^{-3}	0.22/-0.22
Flack parameter	0.00(15)

7.5.10 Methyl (*S*)-4-(10b-(4-fluorophenyl)-10-((1-hydroxybutan-2-yl)amino)-10b*H*-11-oxa-4b^{1},10aλ^{4}-diaza-10bλ^{4}-boracyclopenta[*e*]aceanthrylen-7-yl)benzoate (**3.7b**)

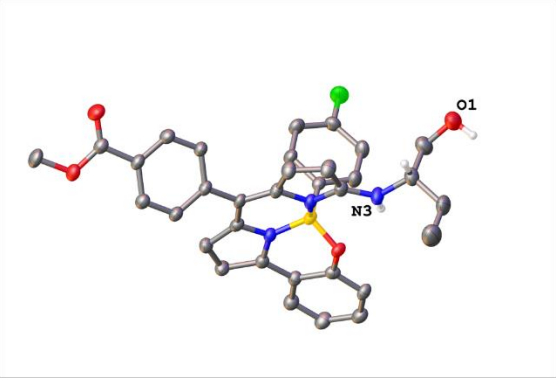

Identification code	mjh220005_fa
Empirical formula	$C_{33}H_{29}BFN_3O_4$
Formula weight	561.40
Temperature/K	150.0(2)
Crystal system	orthorhombic
Space group	$P2_12_12_1$
a/Å	11.0578(6)
b/Å	14.6843(8)
c/Å	17.6365(9)
α/°	90
β/°	90
γ/°	90
Volume/Å^3	2863.7(3)
Z	4
ρ_{calc}g/cm^3	1.302
μ/mm^{-1}	0.735
F(000)	1176.0
Crystal size/mm^3	0.27 × 0.17 × 0.06
Radiation	Cu Kα (λ = 1.54184)
2Θ range for data collection/°	7.834 to 133.188
Index ranges	-13 ≤ h ≤ 13, -17 ≤ k ≤ 17, -20 ≤ l ≤ 20
Reflections collected	14307
Independent reflections	4815 [R_{int} = 0.0900, R_{sigma} = 0.0774]
Data/restraints/parameters	4815/1/387
Goodness-of-fit on F^2	1.050
Final R indexes [I>=2σ (I)]	R_1 = 0.0605, wR_2 = 0.1563
Final R indexes [all data]	R_1 = 0.0764, wR_2 = 0.1808
Largest diff. peak/hole / e Å^{-3}	0.25/-0.25
Flack parameter	-0.1(2)

7.5.11 Methyl (*R*)-4-(10b-(4-fluorophenyl)-10-((1-hydroxybutan-2-yl)amino)-10b*H*-11-oxa-4b^{1},10aλ^{4}-diaza-10bλ^{4}-boracyclopenta[*e*]aceanthrylen-7-yl)benzoate (**3.40a**)

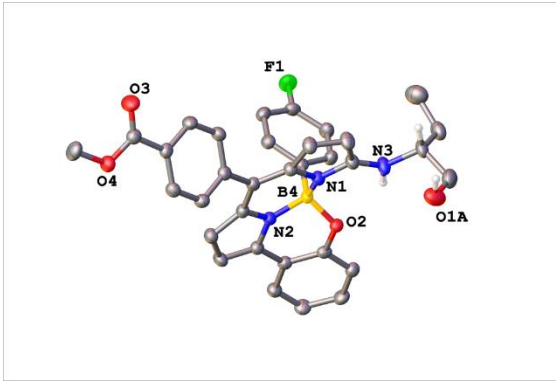

Identification code	mjh220026_fa
Empirical formula	$C_{33}H_{29}BFN_3O_4$
Formula weight	561.40
Temperature/K	150.0(2)
Crystal system	Orthorhombic
Space group	$P2_12_12_1$
a/Å	10.8737(2)
b/Å	14.7221(2)
c/Å	17.5602(3)
α/°	90
β/°	90
γ/°	90
Volume/Å^3	2811.10(8)
Z	4
ρ_{calc}g/cm^3	1.326
μ/mm^{-1}	0.748
F(000)	1176.0
Crystal size/mm^3	0.18 × 0.14 × 0.11
Radiation	Cu Kα (λ = 1.54184)
2Θ range for data collection/°	7.836 to 154.3
Index ranges	-13 ≤ h ≤ 13, -7 ≤ k ≤ 18, -21 ≤ l ≤ 21
Reflections collected	15811
Independent reflections	5470 [R_{int} = 0.0370, R_{sigma} = 0.0389]
Data/restraints/parameters	5470/508/434
Goodness-of-fit on F^2	1.031
Final R indexes [I>=2σ (I)]	R_1 = 0.0380, wR_2 = 0.0988
Final R indexes [all data]	R_1 = 0.0414, wR_2 = 0.1015
Largest diff. peak/hole / e Å^{-3}	0.30/-0.19
Flack parameter	-0.02(12)

7.5.12 Methyl (*R*)-4-(10b-(4-fluorophenyl)-10-((1-hydroxybutan-2-yl)amino)-10b*H*-11-oxa-4b^{1},10aλ^{4}-diaza-10bλ^{4}-boracyclopenta[*e*]aceanthrylen-7-yl)benzoate (**3.40b**)

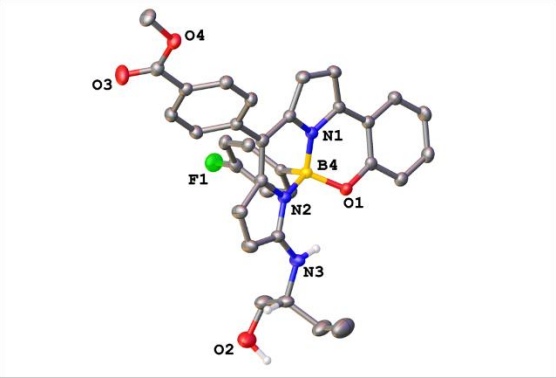

Identification code	mjh220038_fa
Empirical formula	$C_{33}H_{29}BFN_3O_4$
Formula weight	561.40
Temperature/K	150.0(2)
Crystal system	Orthorhombic
Space group	$P2_12_12_1$
a/Å	11.06340(10)
b/Å	14.6656(2)
c/Å	17.6396(2)
α/°	90
β/°	90
γ/°	90
Volume/Å^3	2862.05(6)
Z	4
ρ_{calc}g/cm^3	1.303
μ/mm^{-1}	0.735
F(000)	1176.0
Crystal size/mm^3	0.19 × 0.11 × 0.08
Radiation	Cu Kα (λ = 1.54184)
2Θ range for data collection/°	9.436 to 154.428
Index ranges	-13 ≤ h ≤ 13, -13 ≤ k ≤ 18, -21 ≤ l ≤ 21
Reflections collected	26651
Independent reflections	5599 [R_{int} = 0.0260, R_{sigma} = 0.0195]
Data/restraints/parameters	5599/0/388
Goodness-of-fit on F^2	1.048
Final R indexes [I>=2σ (I)]	R_1 = 0.0322, wR_2 = 0.0846
Final R indexes [all data]	R_1 = 0.0338, wR_2 = 0.0860
Largest diff. peak/hole / e Å^{-3}	0.44/-0.21
Flack parameter	-0.04(4)

7.5.13 Methyl (*S*)-4-(10b-(4-fluorophenyl)-10-((1-hydroxypropan-2-yl)amino)-10b*H*-11-oxa-4b^{1}, 10aλ^{4}-diaza-10bλ^{4}-boracyclopenta[*e*]aceanthrylen-7-yl)benzoate (**3.51a**)

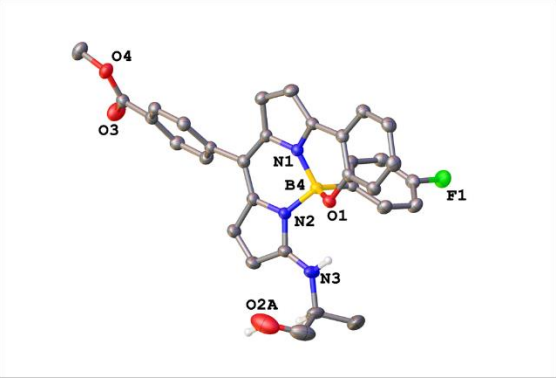

Identification code	mjh220052_fa
Empirical formula	$C_{32}H_{27}BFN_3O_4$
Formula weight	547.37
Temperature/K	150.0(2)
Crystal system	Orthorhombic
Space group	$P2_12_12_1$
a/Å	10.94050(10)
b/Å	14.69500(10)
c/Å	17.4533(2)
α/°	90
β/°	90
γ/°	90
Volume/Å^3	2805.98(5)
Z	4
ρ_{calc}g/cm^3	1.296
μ/mm^{-1}	0.737
F(000)	1144.0
Crystal size/mm^3	0.14 × 0.12 × 0.07
Radiation	Cu Kα (λ = 1.54184)
2Θ range for data collection/°	7.864 to 154.352
Index ranges	-12 ≤ h ≤ 13, -18 ≤ k ≤ 13, -21 ≤ l ≤ 22
Reflections collected	26179
Independent reflections	5552 [R_{int} = 0.0302, R_{sigma} = 0.0228]
Data/restraints/parameters	5552/409/406
Goodness-of-fit on F^2	1.055
Final R indexes [I>=2σ (I)]	R_1 = 0.0298, wR_2 = 0.0767
Final R indexes [all data]	R_1 = 0.0318, wR_2 = 0.0780
Largest diff. peak/hole / e Å^{-3}	0.16/-0.14
Flack parameter	0.08(5)

7.5.14 Methyl (*S*)-4-(10b-(4-fluorophenyl)-10-((1-hydroxypropan-2-yl)amino)-10b*H*-11-oxa-4b^{1}, 10aλ^{4}-diaza-10bλ^{4}-boracyclopenta[*e*]aceanthrylen-7-yl)benzoate (**3.51b**)

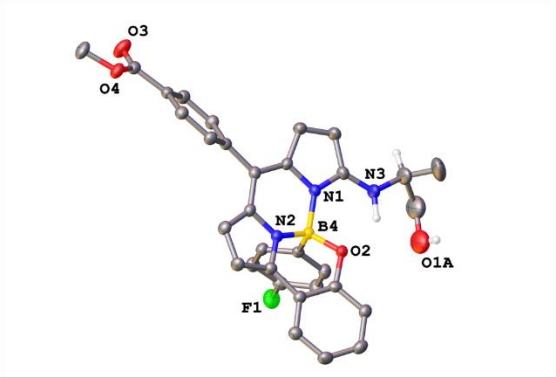

Identification code	mjh220050_fa
Empirical formula	$C_{32}H_{27}BFN_3O_{4.2}$
Formula weight	550.49
Temperature/K	150.0(2)
Crystal system	Orthorhombic
Space group	$P2_12_12_1$
a/Å	11.02850(10)
b/Å	14.6137(2)
c/Å	17.3886(2)
α/°	90
β/°	90
γ/°	90
Volume/Å^3	2802.47(6)
Z	4
ρ_{calc}g/cm^3	1.305
μ/mm^{-1}	0.746
F(000)	1150.0
Crystal size/mm^3	0.25 × 0.16 × 0.02
Radiation	Cu Kα (λ = 1.54184)
2Θ range for data collection/°	7.902 to 154.65
Index ranges	-13 ≤ h ≤ 11, -17 ≤ k ≤ 17, -16 ≤ l ≤ 21
Reflections collected	16059
Independent reflections	5438 [R_{int} = 0.0336, R_{sigma} = 0.0318]
Data/restraints/parameters	5438/32/405
Goodness-of-fit on F^2	1.050
Final R indexes [I>=2σ (I)]	R_1 = 0.0361, wR_2 = 0.0970
Final R indexes [all data]	R_1 = 0.0392, wR_2 = 0.0994
Largest diff. peak/hole / e Å^{-3}	0.43/-0.18
Flack parameter	-0.05(8)

7.5.15 Methyl (*S*)-4-(10b-(4-fluorophenyl)-10-((1-hydroxy-3,3-dimethylbutan-2-yl)amino)-10b*H*-11-oxa-4b^{1},10aλ^{4}-diaza-10bλ^{4}-boracyclopenta[*e*]aceanthrylen-7-yl)benzoate (**3.53b**)

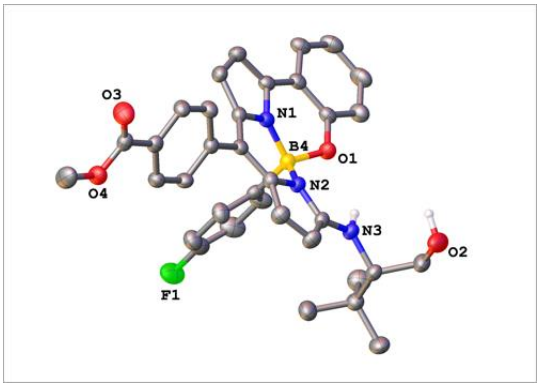

Identification code	mjh230082_fa
Empirical formula	$C_{35}H_{33}BFN_3O_4$
Formula weight	589.45
Temperature/K	150.0(2)
Crystal system	Triclinic
Space group	P1
a/Å	9.94720(10)
b/Å	10.1729(2)
c/Å	16.0690(2)
α/°	101.4190(10)
β/°	91.7480(10)
γ/°	106.4800(10)
Volume/Å^3	1521.88(4)
Z	2
ρ_{calc}g/cm^3	1.286
μ/mm^{-1}	0.715
F(000)	620.0
Crystal size/mm^3	0.13 × 0.1 × 0.02
Radiation	CuKα (λ = 1.54184)
2Θ range for data collection/°	5.634 to 154.466
Index ranges	-12 ≤ h ≤ 12, -12 ≤ k ≤ 12, -19 ≤ l ≤ 20
Reflections collected	43963
Independent reflections	11512 [R_{int} = 0.0305, R_{sigma} = 0.0268]
Data/restraints/parameters	11512/4/814
Goodness-of-fit on F^2	1.033
Final R indexes [I>=2σ (I)]	R_1 = 0.0324, wR_2 = 0.0867
Final R indexes [all data]	R_1 = 0.0343, wR_2 = 0.0878
Largest diff. peak/hole / e Å^{-3}	0.24/-0.17
Flack parameter	0.00(4)

7.5.16 Methyl (*S*)-4-(10b-(4-fluorophenyl)-10-((2-hydroxy-1-phenylethyl)amino)-10b*H*-11-oxa-4b^{1}, 10aλ^{4}-diaza-10bλ^{4}-boracyclopenta[*e*]aceanthrylen-7-yl)benzoate (**3.52b**)

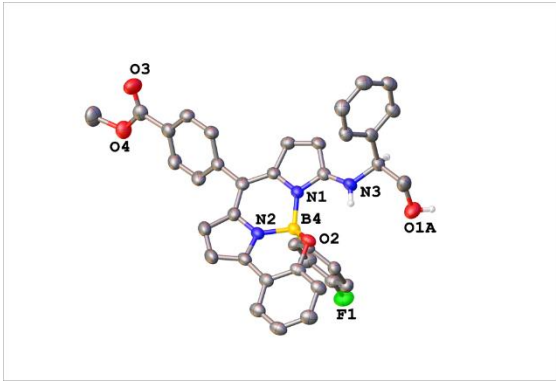

Identification code	mjh220046_fa
Empirical formula	$C_{37}H_{30}BFN_3O_{4.5}$
Formula weight	618.45
Temperature/K	150.0(2)
Crystal system	Orthorhombic
Space group	$P2_12_12$
a/Å	8.8418(2)
b/Å	30.7145(6)
c/Å	11.2997(2)
α/°	90
β/°	90
γ/°	90
Volume/Å^3	3068.68(11)
Z	4
ρ_{calc}g/cm^3	1.339
μ/mm^{-1}	0.752
F(000)	1292.0
Crystal size/mm^3	0.1 × 0.1 × 0.04
Radiation	Cu Kα (λ = 1.54184)
2Θ range for data collection/°	5.754 to 158.69
Index ranges	-10 ≤ h ≤ 5, -38 ≤ k ≤ 39, -13 ≤ l ≤ 13
Reflections collected	16812
Independent reflections	6119 [R_{int} = 0.0220, R_{sigma} = 0.0225]
Data/restraints/parameters	6119/11/436
Goodness-of-fit on F^2	1.112
Final R indexes [I>=2σ (I)]	R_1 = 0.0447, wR_2 = 0.1187
Final R indexes [all data]	R_1 = 0.0468, wR_2 = 0.1198
Largest diff. peak/hole / e Å^{-3}	0.19/-0.24
Flack parameter	0.11(5)

7.5.17 Methyl (*S*)-4-(10-((1-hydroxybutan-2-yl)amino)-10b-(*p*-tolyl)-10b*H*-11-oxa-4b^{1}, 10aλ^{4}-diaza-10bλ^{4}-boracyclopenta[*e*]aceanthrylen-7-yl)benzoate (**3.49a**)

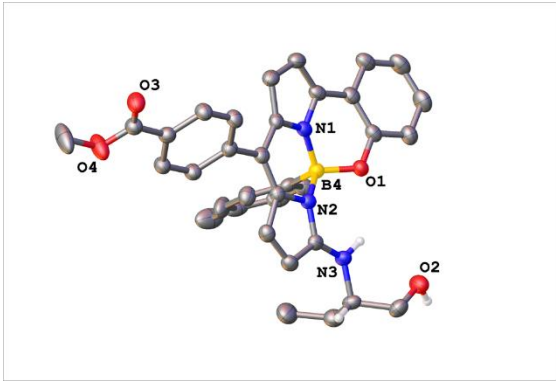

Identification code	mjh220077_fa
Empirical formula	$C_{68}H_{66}B_2N_6O_9$
Formula weight	1132.88
Temperature/K	150.0(2)
Crystal system	monoclinic
Space group	$P2_1$
a/Å	10.2096(2)
b/Å	29.5165(5)
c/Å	10.5846(2)
α/°	90
β/°	112.320(2)
γ/°	90
Volume/Å^3	2950.71(10)
Z	2
ρ_{calc}g/cm^3	1.275
μ/mm^{-1}	0.679
F(000)	1196.0
Crystal size/mm^3	0.21 × 0.12 × 0.01
Radiation	Cu Kα (λ = 1.54184)
2Θ range for data collection/°	5.988 to 157.132
Index ranges	-12 ≤ h ≤ 11, -36 ≤ k ≤ 37, -13 ≤ l ≤ 13
Reflections collected	39214
Independent reflections	11872 [R_{int} = 0.0284, R_{sigma} = 0.0280]
Data/restraints/parameters	11872/6/790
Goodness-of-fit on F^2	1.035
Final R indexes [I>=2σ (I)]	R_1 = 0.0386, wR_2 = 0.0924
Final R indexes [all data]	R_1 = 0.0425, wR_2 = 0.0944
Largest diff. peak/hole / e Å^{-3}	0.31/-0.21
Flack parameter	-0.03(5)

7.5.18 Methyl (*S*)-4-(10-((1-hydroxybutan-2-yl)amino)-10b-(4-methoxyphenyl)-10b*H*-11-oxa-4b^{1}, 10aλ^{4}-diaza-10bλ^{4}-boracyclopenta[*e*]aceanthrylen-7-yl)benzoate (**3.50a**)

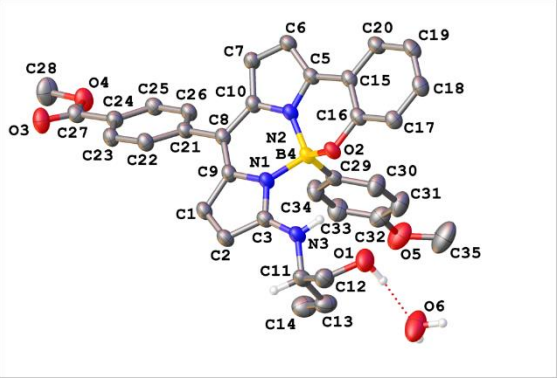

Identification code	mjh220064_fa
Empirical formula	$C_{34}H_{34}BN_3O_6$
Formula weight	591.45
Temperature/K	150.0(2)
Crystal system	triclinic
Space group	P-1
a/Å	10.0994(2)
b/Å	10.9930(2)
c/Å	14.7641(3)
α/°	98.079(2)
β/°	106.894(2)
γ/°	101.953(2)
Volume/Å^3	1498.71(5)
Z	2
ρ_{calc}g/cm^3	1.311
μ/mm^{-1}	0.729
F(000)	624.0
Crystal size/mm^3	0.13 × 0.1 × 0.02
Radiation	Cu Kα (λ = 1.54184)
2Θ range for data collection/°	8.418 to 154.262
Index ranges	-12 ≤ h ≤ 12, -13 ≤ k ≤ 12, -18 ≤ l ≤ 18
Reflections collected	36527
Independent reflections	5868 [R_{int} = 0.0366, R_{sigma} = 0.0244]
Data/restraints/parameters	5868/3/413
Goodness-of-fit on F^2	1.038
Final R indexes [I>=2σ (I)]	R_1 = 0.0437, wR_2 = 0.1181
Final R indexes [all data]	R_1 = 0.0539, wR_2 = 0.1253
Largest diff. peak/hole / e Å^{-3}	0.47/-0.51

7.5.19 Methyl (*S*)-4-(10-((1-hydroxybutan-2-yl)amino)-10b-(4-methoxyphenyl)-10b*H*-11-oxa-4b^{1}, 10aλ^{4}-diaza-10bλ^{4}-boracyclopenta[*e*]aceanthrylen-7-yl)benzoate (**3.50b**)

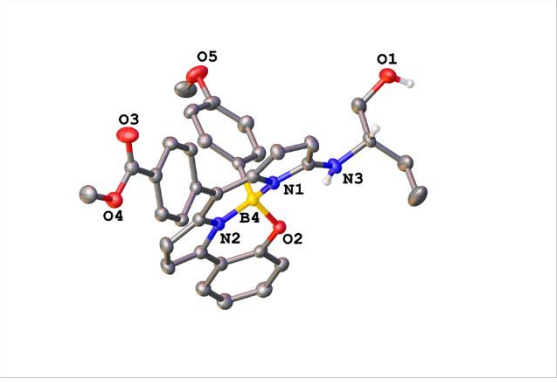

Identification code	mjh220061_fa
Empirical formula	$C_{34}H_{32.4}BN_3O_{5.2}$
Formula weight	577.04
Temperature/K	150.0(2)
Crystal system	orthorhombic
Space group	$P2_12_12_1$
a/Å	11.3634(3)
b/Å	14.6950(4)
c/Å	17.5886(5)
α/°	90
β/°	90
γ/°	90
Volume/Å^3	2937.04(14)
Z	4
ρ_{calc}g/cm^3	1.305
μ/mm^{-1}	0.711
F(000)	1216.0
Crystal size/mm^3	0.17 × 0.09 × 0.02
Radiation	Cu Kα (λ = 1.54184)
2Θ range for data collection/°	7.84 to 154.708
Index ranges	-14 ≤ h ≤ 14, -11 ≤ k ≤ 18, -22 ≤ l ≤ 21
Reflections collected	19020
Independent reflections	5817 [R_{int} = 0.0346, R_{sigma} = 0.0331]
Data/restraints/parameters	5817/1/410
Goodness-of-fit on F^2	1.063
Final R indexes [I>=2σ (I)]	R_1 = 0.0352, wR_2 = 0.0862
Final R indexes [all data]	R_1 = 0.0396, wR_2 = 0.0891
Largest diff. peak/hole / e Å^{-3}	0.22/-0.23
Flack parameter	-0.06(9)

7.5.20 Methyl (*S*)-4-(10-((1-hydroxybutan-2-yl)amino)-10b-(4-nitrophenyl)-10b*H*-11-oxa-4b^{1}, 10aλ^{4}-diaza-10bλ^{4}-boracyclopenta[*e*]aceanthrylen-7-yl)benzoate (**3.47a**)

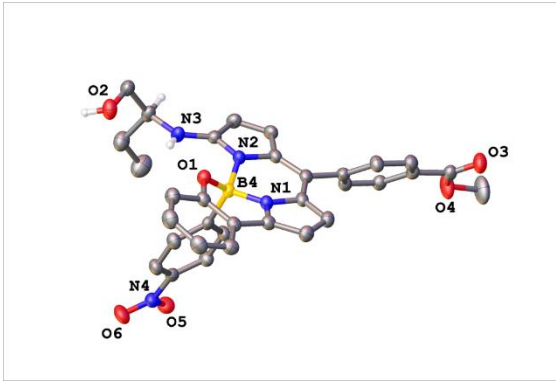

Identification code	mjh220078_fa
Empirical formula	$C_{66}H_{60}B_2N_8O_{13}$
Formula weight	1194.84
Temperature/K	150.0(2)
Crystal system	monoclinic
Space group	$P2_1$
a/Å	10.18400(10)
b/Å	29.3602(3)
c/Å	10.71870(10)
α/°	90
β/°	111.781(2)
γ/°	90
Volume/Å^3	2976.13(6)
Z	2
ρ_{calc}g/cm^3	1.333
μ/mm^{-1}	0.766
F(000)	1252.0
Crystal size/mm^3	0.26 × 0.15 × 0.05
Radiation	Cu Kα (λ = 1.54184)
2Θ range for data collection/°	6.02 to 156.994
Index ranges	-12 ≤ h ≤ 12, -36 ≤ k ≤ 35, -13 ≤ l ≤ 13
Reflections collected	39488
Independent reflections	11698 [R_{int} = 0.0327, R_{sigma} = 0.0310]
Data/restraints/parameters	11698/3/825
Goodness-of-fit on F^2	1.045
Final R indexes [I>=2σ (I)]	R_1 = 0.0341, wR_2 = 0.0854
Final R indexes [all data]	R_1 = 0.0377, wR_2 = 0.0879
Largest diff. peak/hole / e Å^{-3}	0.35/-0.37
Flack parameter	-0.06(6)

7.5.21 Methyl (*S*)-4-(10b-(2,4-difluorophenyl)-10-((1-hydroxybutan-2-yl)amino)-10b*H*-11-oxa-4b^{1}, 10aλ^{4}-diaza-10bλ^{4}-boracyclopenta[*e*]aceanthrylen-7-yl)benzoate (**3.48a**)

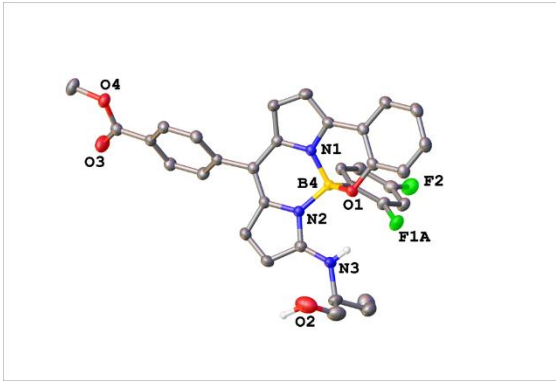

Identification code	mjh220067_fa
Empirical formula	$C_{33}H_{28}BF_2N_3O_4$
Formula weight	579.39
Temperature/K	150.0(2)
Crystal system	orthorhombic
Space group	$P2_12_12_1$
a/Å	11.02510(10)
b/Å	14.7467(2)
c/Å	17.4301(2)
α/°	90
β/°	90
γ/°	90
Volume/Å^3	2833.85(6)
Z	4
ρ_{calc}g/cm^3	1.358
μ/mm^{-1}	0.813
F(000)	1208.0
Crystal size/mm^3	0.22 × 0.11 × 0.06
Radiation	Cu Kα (λ = 1.54184)
2Θ range for data collection/°	7.854 to 154.452
Index ranges	-13 ≤ h ≤ 13, -17 ≤ k ≤ 13, -21 ≤ l ≤ 20
Reflections collected	26543
Independent reflections	5593 [R_{int} = 0.0331, R_{sigma} = 0.0239]
Data/restraints/parameters	5593/1/406
Goodness-of-fit on F^2	1.033
Final R indexes [I>=2σ (I)]	R_1 = 0.0320, wR_2 = 0.0835
Final R indexes [all data]	R_1 = 0.0340, wR_2 = 0.0850
Largest diff. peak/hole / e Å^{-3}	0.27/-0.16
Flack parameter	-0.09(5)

7.5.22 Methyl (*S*)-4-(10b-(2,4-difluorophenyl)-10-((1-hydroxybutan-2-yl)amino)-10b*H*-11-oxa-4b^{1}, 10aλ^{4}-diaza-10bλ^{4}-boracyclopenta[*e*]aceanthrylen-7-yl)benzoate (**3.48b**)

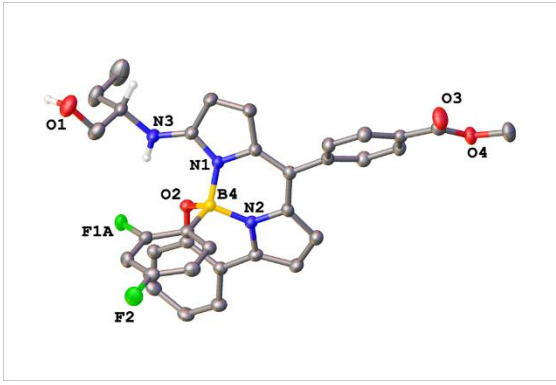

Identification code	mjh220070_fa
Empirical formula	$C_{33}H_{27}BF_2N_3O_4$
Formula weight	578.38
Temperature/K	150.0(2)
Crystal system	orthorhombic
Space group	$P2_12_12_1$
a/Å	11.0806(2)
b/Å	14.6655(2)
c/Å	17.5996(3)
α/°	90
β/°	90
γ/°	90
Volume/Å^3	2859.98(8)
Z	4
ρ_{calc}g/cm^3	1.343
μ/mm^{-1}	0.805
F(000)	1204.0
Crystal size/mm^3	0.17 × 0.14 × 0.03
Radiation	Cu Kα (λ = 1.54184)
2Θ range for data collection/°	7.848 to 156.614
Index ranges	-14 ≤ h ≤ 13, -18 ≤ k ≤ 11, -21 ≤ l ≤ 21
Reflections collected	14517
Independent reflections	5665 [R_{int} = 0.0344, R_{sigma} = 0.0383]
Data/restraints/parameters	5665/2/406
Goodness-of-fit on F^2	1.049
Final R indexes [I>=2σ (I)]	R_1 = 0.0356, wR_2 = 0.0906
Final R indexes [all data]	R_1 = 0.0408, wR_2 = 0.0938
Largest diff. peak/hole / e Å^{-3}	0.23/-0.17
Flack parameter	0.00(8)

7.5.23 Methyl (*R*)-4-(10b-(4-fluorophenyl)-10-((1-hydroxybutan-2-yl)amino)-10b*H*-11-oxa-4b^{1},10aλ^{4}-diaza-10bλ^{4}-boracyclopenta[*e*]aceanthrylen-7-yl)benzoate (**3.40a**) and (**3.40b**)

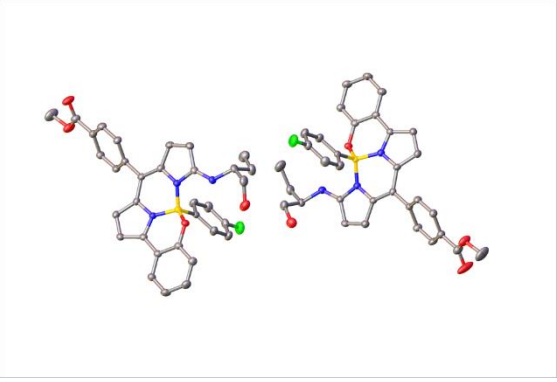

Identification code	mjh220032_fa
Empirical formula	$C_{67}H_{62}B_2F_2N_6O_9$
Formula weight	1154.84
Temperature/K	150.0(2)
Crystal system	triclinic
Space group	P1
a/Å	10.0197(2)
b/Å	10.9264(2)
c/Å	13.6240(3)
α/°	82.712(2)
β/°	80.642(2)
γ/°	78.747(2)
Volume/Å^3	1436.41(5)
Z	1
ρ_{calc}g/cm^3	1.335
μ/mm^{-1}	0.760
F(000)	606.0
Crystal size/mm^3	0.15 × 0.1 × 0.08
Radiation	Cu Kα (λ = 1.54184)
2Θ range for data collection/°	6.608 to 155.822
Index ranges	-11 ≤ h ≤ 12, -13 ≤ k ≤ 13, -16 ≤ l ≤ 16
Reflections collected	33560
Independent reflections	10765 [R_{int} = 0.0189, R_{sigma} = 0.0173]
Data/restraints/parameters	10765/3/794
Goodness-of-fit on F^2	1.089
Final R indexes [I>=2σ (I)]	R_1 = 0.0334, wR_2 = 0.0939
Final R indexes [all data]	R_1 = 0.0345, wR_2 = 0.0950
Largest diff. peak/hole / e Å^{-3}	0.35/-0.23
Flack parameter	0.07(4)

7.5.24 Methyl (*S*)-4-(5,5-difluoro-3-((1-hydroxybutan-2-yl)amino)-7-(4-methoxyphenyl)-5*H*-4λ^4,5λ^4-dipyrrolo[1,2-*c*:2',1'-*f*][1,3,2]diazaborinin-10-yl)benzoate (**4.8**)

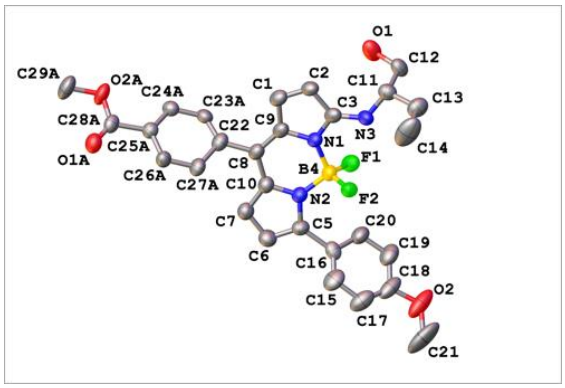

Identification code	mjh220041_fa
Empirical formula	$C_{28}H_{28.01}BF_2N_3O_{4.25}$
Formula weight	523.29
Temperature/K	150.0(2)
Crystal system	monoclinic
Space group	C2
a/Å	32.2839(8)
b/Å	8.0006(2)
c/Å	20.4617(5)
α/°	90
β/°	101.993(2)
γ/°	90
Volume/Å^3	5169.7(2)
Z	8
ρ_{calc}g/cm^3	1.345
μ/mm^{-1}	0.833
F(000)	2191.0
Crystal size/mm^3	0.1 × 0.08 × 0.04
Radiation	CuKα (λ = 1.54184)
2Θ range for data collection/°	7.82 to 154.292
Index ranges	-38 ≤ h ≤ 40, -9 ≤ k ≤ 9, -25 ≤ l ≤ 23
Reflections collected	28063
Independent reflections	9989 [R_{int} = 0.0420, R_{sigma} = 0.0454]
Data/restraints/parameters	9989/1805/976
Goodness-of-fit on F^2	1.033
Final R indexes [I>=2σ (I)]	R_1 = 0.0529, wR_2 = 0.1350
Final R indexes [all data]	R_1 = 0.0769, wR_2 = 0.1511

Largest diff. peak/hole / e $Å^{-3}$	0.32/-0.17
Flack parameter	0.14(13)

7.5.25 Methyl 2-(hydroxy(*p*-tolyl)methyl)acrylate (**4.29**)

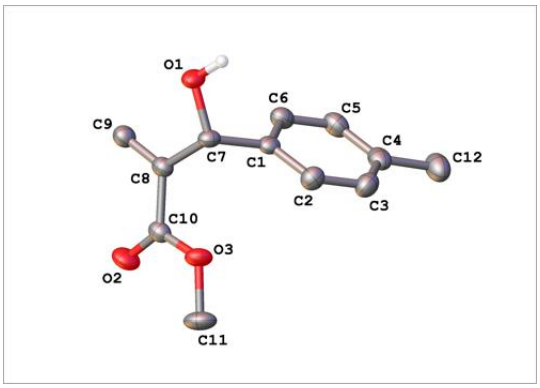

Identification code	mjh230083_fa
Empirical formula	$C_{12}H_{14}O_3$
Formula weight	206.23
Temperature/K	150.0(2)
Crystal system	triclinic
Space group	P-1
a/Å	6.0845(2)
b/Å	7.4058(3)
c/Å	12.6996(4)
α/°	100.766(3)
β/°	92.406(3)
γ/°	104.761(3)
Volume/Å^3	541.20(3)
Z	2
ρ_{calc}g/cm^3	1.266
μ/mm^{-1}	0.739
F(000)	220.0
Crystal size/mm^3	0.23 × 0.15 × 0.1
Radiation	CuKα (λ = 1.54184)
2Θ range for data collection/°	7.118 to 152.952
Index ranges	-7 ≤ h ≤ 7, -9 ≤ k ≤ 9, -15 ≤ l ≤ 16
Reflections collected	15506
Independent reflections	2132 [R_{int} = 0.0869, R_{sigma} = 0.0422]
Data/restraints/parameters	2132/0/142
Goodness-of-fit on F^2	1.052
Final R indexes [I>=2σ (I)]	R_1 = 0.0431, wR_2 = 0.1109
Final R indexes [all data]	R_1 = 0.0524, wR_2 = 0.1216
Largest diff. peak/hole / e Å^{-3}	0.23/-0.19

7.5.26 Methyl 2-(((*tert*-butoxycarbonyl)oxy)(4-chlorophenyl)methyl)acrylate (**4.6**)

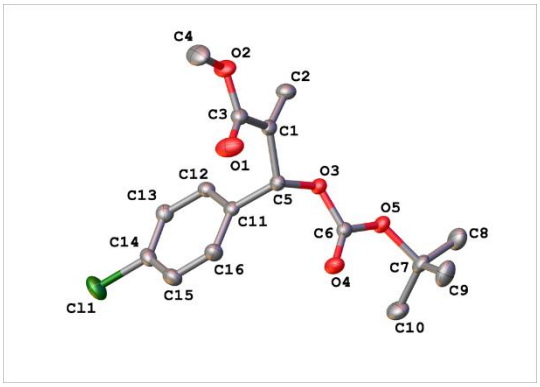

Identification code	mjh230010_fa
Empirical formula	$C_{16}H_{19}ClO_5$
Formula weight	326.76
Temperature/K	150.0(2)
Crystal system	triclinic
Space group	P-1
a/Å	9.1947(4)
b/Å	9.7633(4)
c/Å	10.5852(4)
α/°	69.090(4)
β/°	88.299(3)
γ/°	67.010(4)
Volume/Å^3	810.48(6)
Z	2
ρ_{calc}g/cm^3	1.339
μ/mm^{-1}	2.273
F(000)	344.0
Crystal size/mm^3	0.25 × 0.13 × 0.04
Radiation	CuKα (λ = 1.54184)
2Θ range for data collection/°	9.016 to 156.9
Index ranges	-11 ≤ h ≤ 11, -12 ≤ k ≤ 11, -12 ≤ l ≤ 12
Reflections collected	16548
Independent reflections	3191 [R_{int} = 0.0331, R_{sigma} = 0.0222]
Data/restraints/parameters	3191/0/204
Goodness-of-fit on F^2	1.056
Final R indexes [I>=2σ (I)]	R_1 = 0.0330, wR_2 = 0.0793
Final R indexes [all data]	R_1 = 0.0355, wR_2 = 0.0805
Largest diff. peak/hole / e Å^{-3}	0.26/-0.22

7.5.27 2-(1*H*-pyrrol-2-yl)phenol (**4.35**)

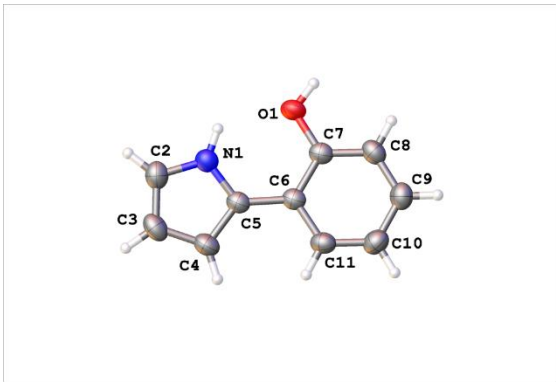

Identification code	mjh230001_fa
Empirical formula	$C_{10}H_9NO$
Formula weight	159.18
Temperature/K	150.0(2)
Crystal system	monoclinic
Space group	$P2_1/c$
a/Å	14.9821(6)
b/Å	5.0617(2)
c/Å	10.5109(4)
α/°	90
β/°	94.473(4)
γ/°	90
Volume/Å^3	794.67(5)
Z	4
ρ_{calc}g/cm^3	1.331
μ/mm^{-1}	0.696
F(000)	336.0
Crystal size/mm^3	0.2 × 0.16 × 0.02
Radiation	Cu Kα (λ = 1.54184)
2Θ range for data collection/°	5.918 to 154.082
Index ranges	-18 ≤ h ≤ 18, -6 ≤ k ≤ 6, -13 ≤ l ≤ 11
Reflections collected	7744
Independent reflections	1582 [R_{int} = 0.0272, R_{sigma} = 0.0239]
Data/restraints/parameters	1582/0/115
Goodness-of-fit on F^2	1.091
Final R indexes [I>=2σ (I)]	R_1 = 0.0412, wR_2 = 0.1118
Final R indexes [all data]	R_1 = 0.0487, wR_2 = 0.1174
Largest diff. peak/hole / e Å^{-3}	0.19/-0.16

7.5.28 2,4,6-triisopropyl-1,1'-biphenyl (**4.36**)

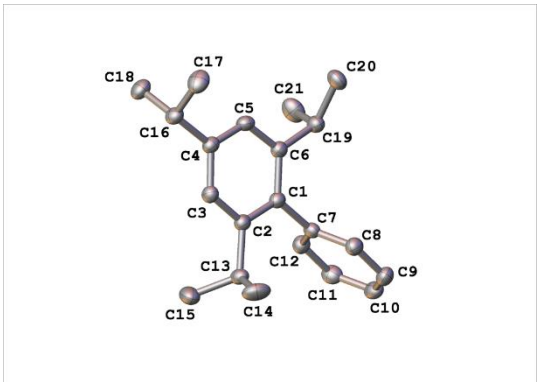

Identification code	mjh230012_fa
Empirical formula	$C_{21}H_{28}$
Formula weight	280.43
Temperature/K	150.0(2)
Crystal system	orthorhombic
Space group	$P2_12_12_1$
a/Å	8.2956(3)
b/Å	9.7795(3)
c/Å	21.4245(7)
α/°	90
β/°	90
γ/°	90
Volume/Å^3	1738.10(10)
Z	4
ρ_{calc}g/cm^3	1.072
μ/mm^{-1}	0.439
F(000)	616.0
Crystal size/mm^3	0.11 × 0.06 × 0.03
Radiation	CuKα (λ = 1.54184)
2Θ range for data collection/°	8.254 to 157.542
Index ranges	-10 ≤ h ≤ 9, -6 ≤ k ≤ 12, -25 ≤ l ≤ 27
Reflections collected	10707
Independent reflections	3416 [R_{int} = 0.0357, R_{sigma} = 0.0353]
Data/restraints/parameters	3416/0/197
Goodness-of-fit on F^2	1.079
Final R indexes [I>=2σ (I)]	R_1 = 0.0313, wR_2 = 0.0816
Final R indexes [all data]	R_1 = 0.0350, wR_2 = 0.0841
Largest diff. peak/hole / e Å^{-3}	0.16/-0.11
Flack parameter	0.3(5)

7.5.29 Racemic Helically chiral *meso*-ethyl- *N*,*N*,*O*,*O*-BODIPY (**4.5**)

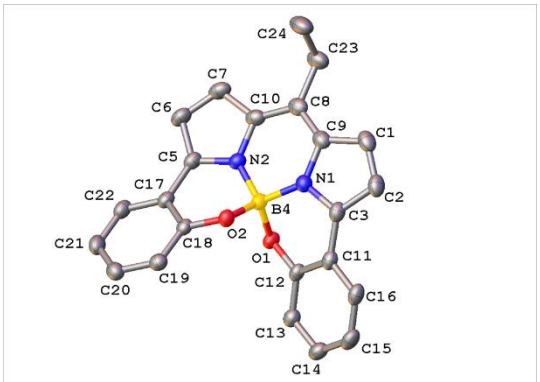

Identification code	mjh230006_fa
Empirical formula	$C_{23}H_{17}BN_2O_2$
Formula weight	364.19
Temperature/K	150.0(2)
Crystal system	monoclinic
Space group	$P2_1/c$
a/Å	11.6374(2)
b/Å	11.0982(2)
c/Å	13.7712(2)
α/°	90
β/°	100.776(2)
γ/°	90
Volume/Å^3	1747.24(5)
Z	4
ρ_{calc}g/cm^3	1.384
μ/mm^{-1}	0.704
F(000)	760.0
Crystal size/mm^3	0.22 × 0.14 × 0.11
Radiation	CuKα (λ = 1.54184)
2Θ range for data collection/°	7.734 to 156.198
Index ranges	-14 ≤ h ≤ 14, -13 ≤ k ≤ 13, -16 ≤ l ≤ 17
Reflections collected	20503
Independent reflections	3463 [R_{int} = 0.0266, R_{sigma} = 0.0191]
Data/restraints/parameters	3463/0/255
Goodness-of-fit on F^2	1.061
Final R indexes [I>=2σ (I)]	R_1 = 0.0322, wR_2 = 0.0883
Final R indexes [all data]	R_1 = 0.0359, wR_2 = 0.0917
Largest diff. peak/hole / e Å^{-3}	0.20/-0.16

7.5.30 Dimethyl 4,4'-(1,4-phenylenebis(10-(((*S*)-1-hydroxybutan-2-yl)amino)-10b*H*-11-oxa-4b^{1},10aλ^{4}-diaza-10bλ^{4}-boracyclopenta[*e*]aceanthrylene-10b,7-diyl))dibenzoate (**5.2a**)

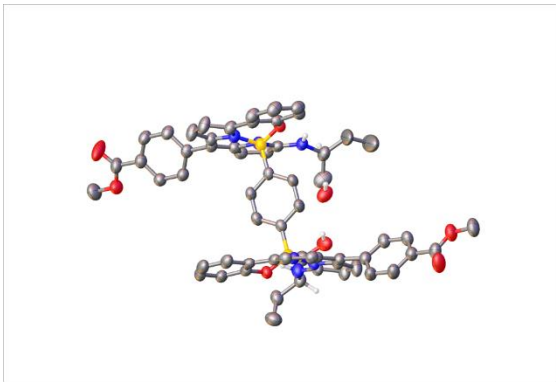

Identification code	mjh220063_fa
Empirical formula	$C_{60.8}H_{55.25}B_2Cl_{1.6}N_6O_8$
Formula weight	1076.30
Temperature/K	150.0(2)
Crystal system	triclinic
Space group	P1
a/Å	9.9760(3)
b/Å	11.1749(4)
c/Å	14.1539(3)
α/°	71.256(3)
β/°	81.529(2)
γ/°	68.628(3)
Volume/Å^3	1390.64(8)
Z	1
ρ_{calc}g/cm^3	1.285
μ/mm^{-1}	1.369
F(000)	563.0
Crystal size/mm^3	0.2 × 0.05 × 0.03
Radiation	Cu Kα (λ = 1.54184)
2Θ range for data collection/°	6.598 to 154.956
Index ranges	-11 ≤ h ≤ 12, -14 ≤ k ≤ 14, -16 ≤ l ≤ 17
Reflections collected	31983
Independent reflections	10336 [R_{int} = 0.0287, R_{sigma} = 0.0291]
Data/restraints/parameters	10336/779/764
Goodness-of-fit on F^2	1.038
Final R indexes [I>=2σ (I)]	R_1 = 0.0597, wR_2 = 0.1684
Final R indexes [all data]	R_1 = 0.0665, wR_2 = 0.1755

Largest diff. peak/hole / e $Å^{-3}$	0.56/-0.26
Flack parameter	0.022(11)

7.5.31 Dimethyl 4,4'-(1,4-phenylenebis(10-(((*S*)-1-hydroxybutan-2-yl)amino)-10b*H*-11-oxa-4b^{1},10aλ^{4}-diaza-10bλ^{4}-boracyclopenta[*e*]aceanthrylene-10b,7-diyl))dibenzoate (**5.2c**)

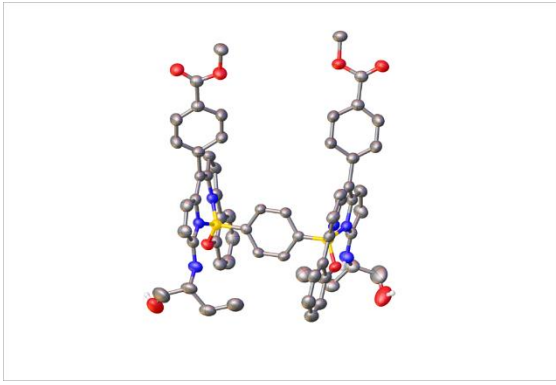

Identification code	mjh220062_fa
Empirical formula	$C_{60}H_{54}B_2N_6O_8$
Formula weight	1008.71
Temperature/K	150.0(2)
Crystal system	tetragonal
Space group	I422
a/Å	16.22770(10)
b/Å	16.22770(10)
c/Å	41.3526(5)
α/°	90
β/°	90
γ/°	90
Volume/Å^3	10889.72(19)
Z	8
ρ_{calc}g/cm^3	1.231
μ/mm^{-1}	0.660
F(000)	4240.0
Crystal size/mm^3	0.16 × 0.11 × 0.06
Radiation	Cu Kα (λ = 1.54184)
2Θ range for data collection/°	5.85 to 142.598
Index ranges	-16 ≤ h ≤ 19, -18 ≤ k ≤ 19, -49 ≤ l ≤ 50
Reflections collected	29700
Independent reflections	5250 [R_{int} = 0.0243, R_{sigma} = 0.0175]
Data/restraints/parameters	5250/467/393
Goodness-of-fit on F^2	1.028
Final R indexes [I>=2σ (I)]	R_1 = 0.0371, wR_2 = 0.1021
Final R indexes [all data]	R_1 = 0.0392, wR_2 = 0.1042
Largest diff. peak/hole / e Å^{-3}	0.51/-0.16
Flack parameter	0.26(8)

7.5.32 Methyl 4-(3-bromo-5,5-difluoro-7-(1*H*-pyrrol-2-yl)-5*H*-5λ^4,6λ^4-dipyrrolo[1,2-*c*:2',1'-*f*][1,3,2]diazaborinin-10-yl)benzoate (**5.13**)

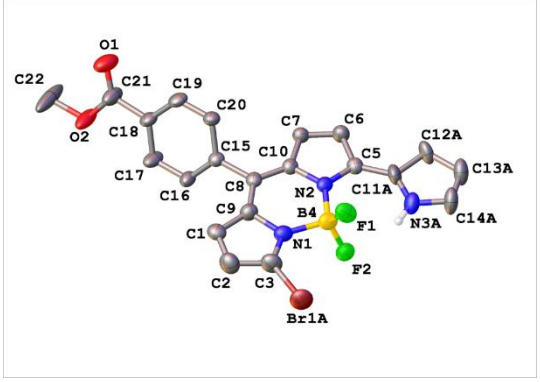

Identification code	mjh230011_2_fa
Empirical formula	$C_{21}H_{15}BBrF_2N_3O_2$
Formula weight	470.08
Temperature/K	150.0(2)
Crystal system	monoclinic
Space group	$P2_1$
a/Å	7.4426(4)
b/Å	19.6225(9)
c/Å	13.9691(7)
α/°	90
β/°	100.496(5)
γ/°	90
Volume/Å^3	2005.95(18)
Z	4
ρ_{calc}g/cm^3	1.557
μ/mm^{-1}	3.163
F(000)	944.0
Crystal size/mm^3	0.25 × 0.03 × 0.02
Radiation	CuKα (λ = 1.54184)
2Θ range for data collection/°	6.436 to 157.472
Index ranges	-7 ≤ h ≤ 9, -23 ≤ k ≤ 24, -17 ≤ l ≤ 17
Reflections collected	21577
Independent reflections	7863 [R_{int} = 0.0317, R_{sigma} = 0.0348]
Data/restraints/parameters	7863/861/646
Goodness-of-fit on F^2	1.130
Final R indexes [I>=2σ (I)]	R_1 = 0.0722, wR_2 = 0.1513
Final R indexes [all data]	R_1 = 0.0766, wR_2 = 0.1535
Largest diff. peak/hole / e Å^{-3}	0.64/-0.51
Flack parameter	0.39(5)

7.5.33 Methyl 4-(5,5-difluoro-3-iodo-7-(1*H*-pyrrol-2-yl)-5*H*-5λ^4,6λ^4-dipyrrolo[1,2-*c*:2',1'-*f*][1,3,2]diazaborinin-10-yl)benzoate (**5.14**)

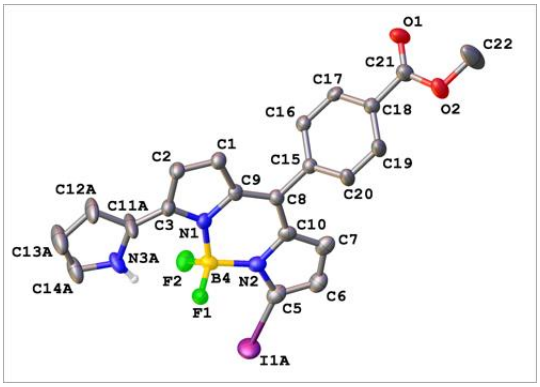

Identification code	mjh230084_fa
Empirical formula	$C_{21}H_{15}BF_2IN_3O_2$
Formula weight	517.07
Temperature/K	150.0(2)
Crystal system	monoclinic
Space group	$P2_1$
a/Å	7.4188(2)
b/Å	19.5722(5)
c/Å	14.1149(3)
α/°	90
β/°	100.552(2)
γ/°	90
Volume/Å^3	2014.86(9)
Z	4
ρ_{calc}g/cm^3	1.705
μ/mm^{-1}	12.857
F(000)	1016.0
Crystal size/mm^3	0.13 × 0.1 × 0.02
Radiation	CuKα (λ = 1.54184)
2Θ range for data collection/°	6.37 to 154.972
Index ranges	-9 ≤ h ≤ 9, -23 ≤ k ≤ 23, -15 ≤ l ≤ 17
Reflections collected	30228
Independent reflections	7922 [R_{int} = 0.0414, R_{sigma} = 0.0358]
Data/restraints/parameters	7922/915/653
Goodness-of-fit on F^2	1.128
Final R indexes [I>=2σ (I)]	R_1 = 0.0696, wR_2 = 0.1645
Final R indexes [all data]	R_1 = 0.0714, wR_2 = 0.1654
Largest diff. peak/hole / e Å^{-3}	1.48/-1.22
Flack parameter	0.233(15)

7.5.34 *N*-(4-(4,4,5,5-tetramethyl-1,3,2-dioxaborolan-2-yl)phenyl)benzamide (**5.20**)

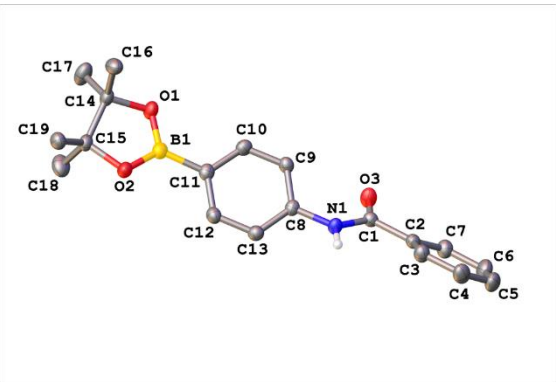

Identification code	mjh230004_tw
Empirical formula	$C_{19}H_{22}BNO_3$
Formula weight	323.18
Temperature/K	150.0(2)
Crystal system	monoclinic
Space group	$P2_1/c$
a/Å	9.9989(2)
b/Å	17.5018(5)
c/Å	10.0579(3)
α/°	90
β/°	96.224(2)
γ/°	90
Volume/Å^3	1749.74(8)
Z	4
ρ_{calc}g/cm^3	1.227
μ/mm^{-1}	0.651
F(000)	688.0
Crystal size/mm^3	0.27 × 0.06 × 0.04
Radiation	Cu Kα (λ = 1.54184)
2Θ range for data collection/°	8.896 to 156.578
Index ranges	-12 ≤ h ≤ 12, -22 ≤ k ≤ 22, -12 ≤ l ≤ 12
Reflections collected	32087
Independent reflections	32087 [R_{int} = ?, R_{sigma} = 0.0287]
Data/restraints/parameters	32087/0/225
Goodness-of-fit on F^2	1.063
Final R indexes [I>=2σ (I)]	R_1 = 0.0442, wR_2 = 0.1201
Final R indexes [all data]	R_1 = 0.0517, wR_2 = 0.1254
Largest diff. peak/hole / e Å^{-3}	0.18/-0.23

7.5.35 N^1,N^3,N^5-tris(4-(4,4,5,5-tetramethyl-1,3,2-dioxaborolan-2-yl)phenyl)benzene-1,3,5-tricarboxamide (**5.3**)

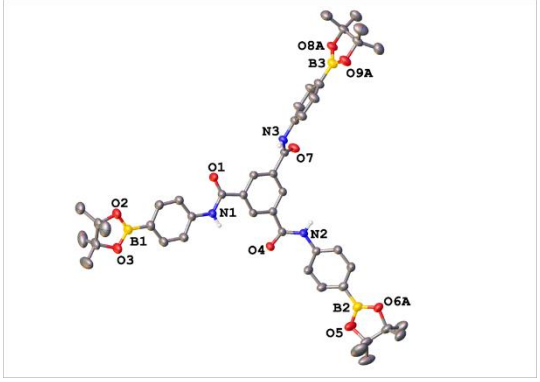

Identification code	mjh230072_3_fa
Empirical formula	$C_{57}H_{82}B_3N_7O_{13}$
Formula weight	1105.72
Temperature/K	150.0(2)
Crystal system	monoclinic
Space group	$P2_1/c$
a/Å	12.2339(3)
b/Å	39.0396(12)
c/Å	12.9414(3)
α/°	90
β/°	90.753(2)
γ/°	90
Volume/Å^3	6180.4(3)
Z	4
ρ_{calc}g/cm^3	1.188
μ/mm^{-1}	0.677
F(000)	2368.0
Crystal size/mm^3	0.21 × 0.04 × 0.02
Radiation	CuKα (λ = 1.54184)
2Θ range for data collection/°	4.526 to 154.762
Index ranges	-15 ≤ h ≤ 15, -47 ≤ k ≤ 47, -12 ≤ l ≤ 15
Reflections collected	56393
Independent reflections	12131 [R_{int} = 0.0428, R_{sigma} = 0.0329]
Data/restraints/parameters	12131/1315/931
Goodness-of-fit on F^2	1.051
Final R indexes [I>=2σ (I)]	R_1 = 0.0564, wR_2 = 0.1563
Final R indexes [all data]	R_1 = 0.0753, wR_2 = 0.1722
Largest diff. peak/hole / e Å^{-3}	0.47/-0.38

7.5.36 Dibenzo[*b*,*d*]furan-4,6-dicarbaldehyde (**5.5**)

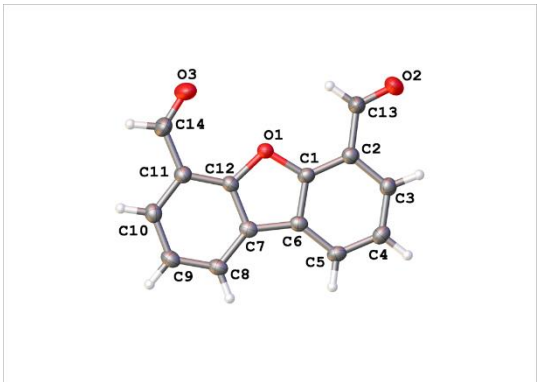

Identification code	mjh230013_fa
Empirical formula	$C_{14}H_8O_3$
Formula weight	224.20
Temperature/K	150.0(2)
Crystal system	orthorhombic
Space group	$Pna2_1$
a/Å	15.2677(7)
b/Å	15.6562(7)
c/Å	4.3071(2)
α/°	90
β/°	90
γ/°	90
Volume/Å^3	1029.54(8)
Z	4
ρ_{calc}g/cm^3	1.446
μ/mm^{-1}	0.845
F(000)	464.0
Crystal size/mm^3	0.15 × 0.06 × 0.04
Radiation	CuKα (λ = 1.54184)
2Θ range for data collection/°	8.088 to 149.52
Index ranges	-18 ≤ h ≤ 18, -17 ≤ k ≤ 18, -5 ≤ l ≤ 2
Reflections collected	4346
Independent reflections	1356 [R_{int} = 0.0295, R_{sigma} = 0.0296]
Data/restraints/parameters	1356/1/154
Goodness-of-fit on F^2	1.052
Final R indexes [I>=2σ (I)]	R_1 = 0.0378, wR_2 = 0.0994
Final R indexes [all data]	R_1 = 0.0419, wR_2 = 0.1039
Largest diff. peak/hole / e Å^{-3}	0.20/-0.22
Flack parameter	0.1(4)

7.5.37 2-(2-Methoxyphenyl)-1*H*-pyrrole (**5.27**)

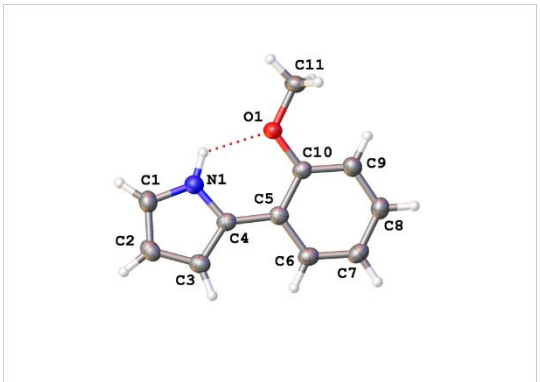

Identification code	mjh230017_fa
Empirical formula	$C_{11}H_{11}NO$
Formula weight	173.21
Temperature/K	150.0(2)
Crystal system	orthorhombic
Space group	$P2_12_12_1$
a/Å	5.1589(3)
b/Å	10.9835(6)
c/Å	15.7592(10)
α/°	90
β/°	90
γ/°	90
Volume/Å^3	892.96(9)
Z	4
ρ_{calc}g/cm^3	1.288
μ/mm^{-1}	0.660
F(000)	368.0
Crystal size/mm^3	0.21 × 0.11 × 0.03
Radiation	CuKα (λ = 1.54184)
2Θ range for data collection/°	9.816 to 154.204
Index ranges	-6 ≤ h ≤ 5, -13 ≤ k ≤ 12, -18 ≤ l ≤ 18
Reflections collected	6941
Independent reflections	1751 [R_{int} = 0.0307, R_{sigma} = 0.0257]
Data/restraints/parameters	1751/0/123
Goodness-of-fit on F^2	1.059
Final R indexes [I>=2σ (I)]	R_1 = 0.0327, wR_2 = 0.0915
Final R indexes [all data]	R_1 = 0.0340, wR_2 = 0.0929
Largest diff. peak/hole / e Å^{-3}	0.13/-0.17
Flack parameter	-0.11(13)

7.5.38 Chiral *meso*-(trifluoromethyl)-*N*,*N*,*O*,*O*-BODIPY (**5.29**)

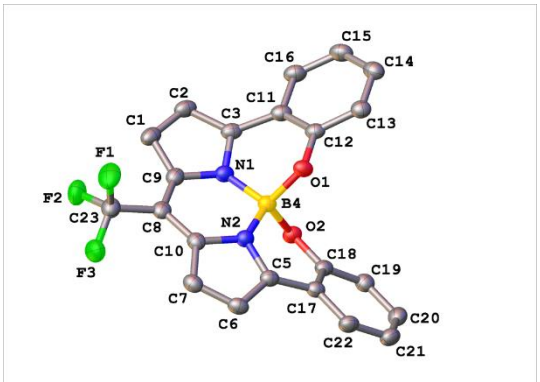

Identification code	mjh230036_fa
Empirical formula	$C_{22}H_{12}BF_3N_2O_2$
Formula weight	404.15
Temperature/K	150.0(2)
Crystal system	monoclinic
Space group	$P2_1/n$
a/Å	13.9144(3)
b/Å	6.4168(2)
c/Å	19.3907(4)
α/°	90
β/°	97.995(2)
γ/°	90
Volume/Å^3	1714.49(7)
Z	4
ρ_{calc}g/cm^3	1.566
μ/mm^{-1}	1.044
F(000)	824.0
Crystal size/mm^3	0.29 × 0.05 × 0.03
Radiation	CuKα (λ = 1.54184)
2Θ range for data collection/°	7.358 to 154.454
Index ranges	-17 ≤ h ≤ 16, -7 ≤ k ≤ 7, -23 ≤ l ≤ 24
Reflections collected	29932
Independent reflections	3425 [R_{int} = 0.0320, R_{sigma} = 0.0178]
Data/restraints/parameters	3425/0/272
Goodness-of-fit on F^2	1.051
Final R indexes [I>=2σ (I)]	R_1 = 0.0327, wR_2 = 0.0872
Final R indexes [all data]	R_1 = 0.0377, wR_2 = 0.0909
Largest diff. peak/hole / e Å^{-3}	0.24/-0.19

References

1 J. R. Lakowicz, *Principles of Fluorescence Spectroscopy Third Edition*, Springer, New York, 3rd ed., 2006.

2 B. Wardle, *Principles and Applications of Photochemistry*, Royal Society of Chemistry, Cambridge, 2009.

3 J. P. Riehl and F. S. Richardson, *Chem. Rev*., 1986, **86**, 1-16.

4 C. Wan, A. Burghart, J. Chen, F. Bergström, L. B. -Å. Johansson, M. F. Wolford, T. G. Kim, M. R. Topp, R. M. Hochstrasser and K. Burgess, *Chem. Eur. J.*, 2003, **9**, 4430–4441.

5 C. Würth, M. Grabolle, J. Pauli, M. Spieles and U. Resch-Genger, *Relative and Absolute Determination of Fluorescence Quantum Yields of Transparent Samples*, *Nature Protocol*, 2013, 8, p 1535 – 1550.

6 J. David and P. Fls, *The distribution of circularly polarized light reflection in the Scarabaeoidea (Coleoptera)*, *Biol. J. Linn. Soc.,* 2010, **100**, 585-596.

7 A. Mendoza-Galván, E. Muñoz-Pineda, K. Järrendahl and H. Arwin, *R Soc Open Sci*, 2018, **5**, 181096.

8 J. D. PYE, *J. Linn. Soc*, 2010, **100**, 585–596.

9 V. Sharma, M. Crne, J. O. Park and M. Srinivasarao, *Science (1979)*, 2009, **325**, 449–451.

10 J. T. Vázquez, *Tetrahedron Asymmetry*, 2017, **28**, 1199–1211.

11 N. Algoazy, R. G. Clarke, T. J. Penfold, P. G. Waddell, M. R. Probert, R. Aerts, W. Herrebout, P. Stachelek, R. Pal, M. J. Hall and J. G. Knight, *ChemPhotoChem*, 2022, **6**, e202200090.

12 R. Clarke, K. L. Ho, A. A. Alsimaree, O. J. Woodford, P. G. Waddell, J. Bogaerts, W. Herrebout, J. G. Knight, R. Pal, T. J. Penfold and M. J. Hall, *ChemPhotoChem*, 2017, **1**, 513–517.

13 L. Arrico, L. Di Bari and F. Zinna, *Chem. Eur. J.*, 2021, **27**, 2920–2934.

14 H. Tanaka, Y. Inoue and T. Mori, *ChemPhotoChem*, 2018, **2**, 386–402.

15 F. Zinna, T. Bruhn, C. A. Guido, J. Ahrens, M. Bröring, L. Di Bari and G. Pescitelli, *Chem. Eur. J.*, 2016, **22**, 16089–16098.

16 C. Ray, E. M. Sánchez-Carnerero, F. Moreno, B. L. Maroto, A. R. Agarrabeitia, M. J. Ortiz, Í. López-Arbeloa, J. Bañuelos, K. D. Cohovi, J. L. Lunkley, G. Muller and S. de la Moya, *Chem. Eur. J.*, 2016, **22**, 8805–8808.

17 X. Li, Y. Xie and Z. Li, *Adv. Photonics Res*., 2021,**2**, 2000136.

18 J. L. Lunkley, D. Shirotani, K. Yamanari, S. Kaizaki and G. Muller, *J. Am. Chem. Soc.,* 2008, **130**, 13814–13815.

19 C. A. Emeis and L. J. Oosterhoff, *Chem. Phys. Lett.*, 1967, **1**, 129–132.

20 H. P. J. M. Dekkers and L. E. Closs, *J. Am. Chem. Soc.*, 1976, **98**, 2210–2219.

21 P. H. Schippers, J. P. M. Van der Ploeg and H. P. J. M. Dekkers, *J. Am. Chem. Soc.,* 1983, **105**, 84–89.

22 E. M. Sánchez-Carnerero, A. R. Agarrabeitia, F. Moreno, B. L. Maroto, G. Muller, M. J. Ortiz and S. de la Moya, *Chem. Eur. J.*, 2015, **21**, 13488–13500.

23 M. J. Hall and S. de la Moya, in *Circularly Polarized Luminescence of Isolated Small Organic Molecules* (Eds.: T. Mori), Springer Singapore, Singapore, 2020, pp. 117–149.

24 A. Gossauer, F. Fehr, F. Nydegger and H. Stöckli-Evans, *J. Am. Chem. Soc.*, 1997, **119**, 1599–1608.

25 A. Loudet and K. Burgess, *Chem. Rev.*, 2007, **107**, 4891–4932.

26 G. Ulrich, R. Ziessel and A. Harriman, *Angew. Chemie - Int. Ed.*, 2008, 47, 1184–1201.

27 J. A. Hendricks, E. J. Keliher, D. Wan, S. A. Hilderbrand, R. Weissleder and R. Mazitschek, *Angew. Chemie - Int. Ed.*, 2012, **51**, 4603–4606.

28 I. Bulut, Q. Huaulmé, A. Mirloup, P. Chávez, S. Fall, A. Hébraud, S. Méry, B. Heinrich, T. Heiser, P. Lévêque and N. Leclerc, *ChemSusChem*, 2017, **10**, 1878–1882.

29 A. Kamkaew, S. H. Lim, H. B. Lee, L. V. Kiew, L. Y. Chung and K. Burgess, *Chem. Soc. Rev.*, 2013, **42**, 77–88.

30 A. Treibs and F. -H Kreuzer, *Justus Liebigs Ann. Chem.*, 1968, **718**, 208–223.

31 R. W. Wagner and J. S. Lindsey, *Pure Appl. Chem.*, 1996, **68**, 1373–1380.

32 P. Rothemund, *J. Am. Chem. Soc.*, 1936, **58**, 625–627.

33 C.-H. Lee and J. S. Lindsey, *Tetrahedron*, 1994, **50**, 11427–11440.

34 T. Rohand, E. Dolusic, T. H. Ngo, W. Maes and W. Dehaen, *Arkivoc*, 2007, **10**, 307–324.

35 V. Leen, E. Braeken, K. Luckermans, C. Jackers, M. Van der Auweraer, N. Boens and W. Dehaen, *Chem. Commun*., 2009, 4515–4517.

36 G. Duran-Sampedro, A. R. Agarrabeitia, I. Garcia-Moreno, A. Costela, J. Bañuelos, T. Arbeloa, I. López Arbeloa, J. L. Chiara and M. J. Ortiz, *European J. Org. Chem.*, 2012, 6335–6350.

37 Y. Hayashi, S. Yamaguchi, W. Y. Cha, D. Kim and H. Shinokubo, *Org. Lett.*, 2011, **13**, 2992–2995.

38 *China Pat*., CN107556333A, 2018.

39 T. Rohand, M. Baruah, W. Qin, N. Boens and W. Dehaen, *Chem. Commun.*, 2006, **0**, 266–268.

40 M. Baruah, W. Qin, N. Basarić, W. M. De Borggraeve and N. Boens, *J. Org. Chem.*, 2005, **70**, 4152–4157.

41 H. Finkelstein, *Berichte der deutschen chemischen Gesellschaft*, 1910, **43**, 1528–1532.

42 G. C. Finger and C. W. Kruse, *J. Am. Chem. Soc.*, 1956, **78**, 6034–6037.

43 R. D. J. Froese, G. T. Whiteker, T. H. Peterson, D. J. Arriola, J. M. Renga and J. W. Shearer, *J. Org. Chem.*, 2016, **81**, 10672–10682.

44 A. V. Agafonova, I. A. Smetanin, N. V. Rostovskii, A. F. Khlebnikov and M. S. Novikov, *Synthesis*, 2019, **51**, 4582–4589.

45 F. J. Frank, P. G. Waddell, M. J. Hall and J. G. Knight, *Org. Lett.*, 2021, **23**, 8595–8599.

46 T. Satoh, K. Fujii, Y. Kimura and Y. Matano, *J. Org. Chem.*, 2018, **83**, 5274–5281.

47 T. Rohand, W. Qin, N. Boens and W. Dehaen, *European J. Org. Chem.*, 2006, **2006**, 4658–4663.

48 S. Rihn, P. Retailleau, N. Bugsaliewicz, A. De Nicola and R. Ziessel, *Tetrahedron Lett.*, 2009, **50**, 7008–7013.

49 L. Jiao, W. Pang, J. Zhou, Y. Wei, X. Mu, G. Bai and E. Hao, *J Org Chem*, 2011, **76**, 9988–9996.

50 L. Gai, J. Mack, H. Lu, H. Yamada, D. Kuzuhara, G. Lai, Z. Li and Z. Shen, *Chem. Eur. J.*, 2014, **20**, 1091–1102.

51 V. Lakshmi and M. Ravikanth, *J Org Chem*, 2011, **76**, 8466–8471.

52 T. Bruhn, G. Pescitelli, S. Jurinovich, A. Schaumlöffel, F. Witterauf, J. Ahrens, M. Bröring and G. Bringmann, *Angew. Chemie - Int. Ed.*, 2014, **53**, 14592–14595.

53 S. Kolemen, Y. Cakmak, Z. Kostereli and E. U. Akkaya, *Org. Lett.*, 2014, **16**, 660–663.

54 E. M. Sánchez-Carnerero, F. Moreno, B. L. Maroto, A. R. Agarrabeitia, M. J. Ortiz, B. G. Vo, G. Muller and S. de la Moya, *J. Am. Chem. Soc.*, 2014, **136**, 3346–3349.

55 R. B. Alnoman, S. Rihn, D. C. O'Connor, F. A. Black, B. Costello, P. G. Waddell, W. Clegg, R. D. Peacock, W. Herrebout, J. G. Knight and M. J. Hall, *Chem. Eur. J.*, 2016, **22**, 93–96.

56 M. Saikawa, T. Nakamura, J. Uchida, M. Yamamura and T. Nabeshima, *Chem. Commun.*, 2016, **52**, 10727–10730.

57 M. Toyoda, Y. Imai and T. Mori, *J. Phys. Chem. Lett*, 2017, **8**, 42–48.

58 Y. Gobo, R. Matsuoka, Y. Chiba, T. Nakamura and T. Nabeshima, *Tetrahedron Lett.*, 2018, **59**, 4149–4152.

59 B. Zu, Y. Guo, L.-Q. Ren, Y. Li and C. He, *Nature Synthesis*, 2023, **2**, 564–571.

60 M. M. Heravi, V. Zadsirjan and B. Farajpour, *RSC Adv.*, 2016, **6**, 30498–30551.

61 G. Diaz-Muñoz, I. L. Miranda, S. K. Sartori, D. C. de Rezende and M. Alves Nogueira Diaz, *Chirality*, 2019, **31**, 776–812.

62 D. A. Evans, J. Bartroli and T. L. Shih, *J. Am. Chem. Soc.*, 1981, **103**, 2127–2129.

63 J. P. Reid, *Commun. Chem.*, 2021, 4.

64 R. J. Armstrong, M. Nandakumar, R. M. P. Dias, A. Noble, E. L. Myers and V. K. Aggarwal, Angew. *Chem. Int. Ed.*, 2018, **57**, 8203-8208

65 M. R. Crittall, N. W. G. Fairhurst and D. R. Carbery, *Chem. Commun.*, 2012, **48**, 11181.

66 M. R. Rao, S. M. Mobin and M. Ravikanth, *Tetrahedron*, 2010, **66**, 1728–1734.

67 R. G. Clarke, PhD thesis, University of Newcastle, 2020.

68 N. Boens, B. Verbelen and W. Dehaen, *European J. Org. Chem.*, 2015, 6577–6595.

69 E. M. Sánchez-Carnerero, F. Moreno, B. L. Maroto, A. R. Agarrabeitia, J. Bañuelos, T. Arbeloa, I. López-Arbeloa, M. J. Ortiz and S. de la Moya, *Chem. Commun*., 2013, **49**, 11641.

70 J. Jiménez, C. Díaz-Norambuena, S. Serrano, S. C. Ma, F. Moreno, B. L. Maroto, J. Bañuelos, G. Muller and S. de la Moya, *Chem. Commun*., 2021, **57**, 5750–5753.

71 F. Diederich, P. J. Stang and R. R. Tykwinski, Eds., *Modern Supramolecular Chemistry*, Wiley, 2008.

72 I. Zalessky, J. M. Wootton, J. K. F. Tam, D. E. Spurling, W. C. Glover-Humphreys, J. R. Donald, W. E. Orukotan, L. C. Duff, B. J. Knapper, A. C. Whitwood, T. F. N. Tanner, A. H. Miah, J. M. Lynam and W. P. Unsworth, *J. Am. Chem. Soc.*, 2024, **146**, 5702–5711.

73 D. Wu, G. Durán-Sampedro, S. Fitzgerald, M. Garre and D. F. O'Shea, *Chem Commun.*, 2023, **59**, 1951–1954.

74 F. J. Frank, PhD thesis, University of Newcastle, 2023.

75 V. Lakshmi, T. Chatterjee and M. Ravikanth, *Eur. J. Org Chem*, 2014, 2105–2110.

76 M. Yu, J. K.-H. Wong, C. Tang, P. Turner, M. H. Todd and P. J. Rutledge, *Beilstein J. Org. Chem.*, 2015, **11**, 37–41.

77 N. C. Bruno, M. T. Tudge and S. L. Buchwald, *Chem. Sci.*, 2013, **4**, 916–920.

78 D. Sirbu, A. C. Benniston and A. Harriman, *Org. Lett.*, 2017, **19**, 1626–1629.

79 R. G. Clarke, J. Weatherston, R. A. Taj-Aldeen, P. G. Waddell, W. McFarlane, T. J. Penfold, J. Bogaerts, W. Herrebout, L. E. Mackenzie, R. Pal and M. J. Hall, *ChemPhotoChem*, 2023, **7**, e20220019.

80 C. Ikeda, T. Maruyama and T. Nabeshima, *Tetrahedron Lett.*, 2009, **50**, 3349–3351.

81 S. Parveen, R. B. Alnoman, M. Hagar, H. A. Ahmed and J. G. Knight, *ChemistrySelect*, 2020, **5**, 13163–13173.

82 A. M. Brouwer, *Pure Appl. Chem.*, 2011, **83**, 2213–2228.

83 J. Sample, Mchem thesis, University of Newcastle, 2022.

84 M. Cracknell, Mchem thesis, University of Newcastle, 2022.

85 R. B. Alnoman, S. Parveen, M. Hagar, H. A. Ahmed and J. G. Knight, *J. Biomol. Struct. Dyn.*, 2020, **38**, 5429–5442.

86 N. Dorh, S. Zhu, K. B. Dhungana, R. Pati, F.-T. Luo, H. Liu and A. Tiwari, *Sci Rep*, 2015, **5**, 18337.

87 X. Zhou, Q. Wu, Y. Feng, Y. Yu, C. Yu, E. Hao, Y. Wei, X. Mu and L. Jiao, *Chem. Asian. J*. 2015, **10**, 1979–1986.

88 F. Paul, J. Patt and J. F. Hartwig, *J. Am. Chem. Soc.*, 1994, **116**, 5969–5970.

89 P. A. Forero-Cortés and A. M. Haydl, *Org. Process. Res. Dev*. 2019, **23**, 1478–1483.

90 A. G. Carpanez, F. Coelho and G. W. Amarante, *J. Mol. Struct*, 2018, **1154**, 83–91.

91 J. T. M. Correia, L. V. Acconcia and F. Coelho, *European J. Org. Chem*. 2016, 1972–1976.

92 N. C. Bruno, N. Niljianskul and S. L. Buchwald, *J. Org. Chem.*, 2014, **79**, 4161–4166.

93 H. L. D. Hayes, R. Wei, M. Assante, K. J. Geogheghan, N. Jin, S. Tomasi, G. Noonan, A. G. Leach and G. C. Lloyd-Jones, *J. Am. Chem. Soc.*, 2021, **143**, 14814–14826.

94 M. Meazza, C. M. Cruz, A. M. Ortuño, J. M. Cuerva, L. Crovetto and R. Rios, *Chem. Sci.*, 2021, **12**, 4503–4508.

95 C. Goze, G. Ulrich and R. Ziessel, *Org. Lett.*, 2006, **8**, 4445–4448.

96 S. Yang, S. Zhang, F. Hu, J. Han and F. Li, *Coord. Chem. Rev*, 2023, **485**, 215116.

97 R. Ziessel, G. Ulrich, A. Haefele and A. Harriman, *J. Am. Chem. Soc*, 2013, **135**, 11330–11344.

98 J. Deschamps, Y. Chang, A. Langlois, N. Desbois, C. P. Gros and P. D. Harvey, *New J. Chem.*, 2016, **40**, 5835–5845.

99 C. Yu, W. Miao, J. Wang, E. Hao and L. Jiao, *ACS Omega*, 2017, **2**, 3551–3561.

100 A. Tyler, PhD thesis, University of Newcastle, 2018.

101 W. G. Skene, V. Berl, H. Risler, R. Khoury and J.-M. Lehn, *Org. Biomol. Chem.*, 2006, **4**, 3652.

102 Y. Wu, J. Mack, X. Xiao, Z. Li, Z. Shen and H. Lu, *Chem. Asian. J*. 2017, **12**, 2216–2220.

103 R. Martin, C. Risacher, A. Barthel, A. Jäger, A. W. Schmidt, S. Richter, M. Böhl, M. Preller, K. Chinthalapudi, D. J. Manstein, H. O. Gutzeit and H.-J. Knölker, *Eur. J. Org. Chem*., 2014, **21**, 4487–4505.

104 L. Copey, L. Jean-Gérard, E. Framery, G. Pilet and B. Andrioletti, *Eur. J. Org. Chem*., 2014, **22**, 4759–4766.